CATALYSIS BY METAL COMPLEXES 33

Series Editors C. Bianchini · D.J. Cole-Hamilton
P.W.N.M. van Leeuwen
Volume Editors P. Barbaro · F. Liguori

Heterogenized Homogeneous Catalysts for Fine Chemicals Production

Materials and Processes

Springer

Heterogenized Homogeneous Catalysts for Fine Chemicals Production

CATALYSIS BY METAL COMPLEXES

This book series covers topics of interest to a wide range of academic and industrial chemists, and biochemists. Catalysis by metal complexes plays a prominent role in many processes. Developments in analytical and synthetic techniques and instrumentation, particularly over the last 30 years, have resulted in an increasingly sophisticated understanding of catalytic processes.
Industrial applications include the production of petrochemicals, fine chemicals and pharmaceuticals (particularly through asymmetric catalysis), hydrometallurgy, and waste-treatment processes. Many life processes are based on metallo-enzyme systems that catalyze redox and acid-base reactions.
Catalysis by metal complexes is an exciting, fast developing and challenging interdisciplinary topic which spans and embraces the three areas of catalysis: heterogeneous, homogeneous, and metallo-enzyme.
Catalysis by Metal Complexes deals with all aspects of catalysis which involve metal complexes and seeks to publish authoritative, state-of-the-art volumes which serve to document the progress being made in this interdisciplinary area of science.

VOLUME 33:
HETEROGENIZED HOMOGENEOUS CATALYSTS FOR FINE CHEMICALS PRODUCTION

Volume Editors

Pierluigi Barbaro Francesca Liguori
Istituto di Chimica dei Composti Organo Metallici
Consiglio Nazionale delle Ricerche
Via Madonna del Piano 10
50019 Sesto Fiorentino, Firenze
Italy

Pierluigi Barbaro · Francesca Liguori
Editors

Heterogenized Homogeneous Catalysts for Fine Chemicals Production

Materials and Processes

Springer

Editors
Pierluigi Barbaro
Istituto di Chimica dei Composti Organo Metallici - Consiglio Nazionale delle Ricerche Via Madonna del Piano 10 50019 Sesto Fiorentino
Firenze
Italy
pierluigi.barbaro@iccom.cnr.it

Francesca Liguori
Istituto di Chimica dei Composti Organo Metallici - Consiglio Nazionale delle Ricerche Via Madonna del Piano 10 50019 Sesto Fiorentino
Firenze
Italy
francesca.liguori@iccom.cnr.it

ISBN 978-90-481-3695-7 e-ISBN 978-90-481-3696-4
DOI 10.1007/978-90-481-3696-4
Springer Dordrecht Heidelberg London New York

Library of Congress Control Number: 2010933790

Foreword: So Why Do We Need Supported Catalysts?

We live in the Oil Age – but not for long. Unlike the Stone Age, Bronze Age or Iron Age, which lasted many thousands of years and, in the case of the Iron Age, is continuing, the Oil Age will extend over only about 150 years. Nehemiah may have discovered oil 2,500 years ago [1], but it was not until the invention of internal combustion engines by Lenoir (1861), Rochas (1860) [2], and especially Otto (1861, 1876 [3]) and their use by Benz and Daimler in cars that oil came to be used as a fuel [4]. Since then, oil has proven to be so useful that massive fortunes have been accumulated by countries where it occurs naturally (even the King in Nehemiah's day saw its potential: "The king, after verifying the facts, had the place (*where the oil was discovered*) enclosed and pronounced sacred. To the people on whom the king bestowed it, he granted a part of the considerable revenue he derived from it" [1]) and even wars have been fought over it. Best estimates indicated that, if usage continues at the present rate, readily extractable (so cheap) oil will only last for another 40 years and this projection has hardly changed, since 25 years ago the estimate was 60 years [5]. Gas does not have a much longer lifetime unless methane hydrate can be exploited cheaply but coal will last for several hundred years.

In many ways the diminishing reserves and availability of fossil fuels are a good thing, because the other major problem is that their use immediately or eventually produces carbon dioxide, the major gas implicated in Global Warming and Climate Change, one of the greatest threats to life on earth if it is allowed to proceed unchecked [6]. Use of all the available reserves of oil, gas and coal would lead to unacceptable warming, but their diminishing supply means that there will be a natural end to this source of overheating of the planet.

Although the main use of fossil fuels is for the production of energy in fixed (power stations) or mobile (vehicles) installations, they also find major uses in the production of a vast array of chemical products that allow us the high standard of living we currently enjoy. The petrochemicals industry manufactures all kinds of important chemicals from building blocks for a wide variety of plastics through lubricating and other oils, the main components of shampoos, detergents, soaps, perfumes etc. to drug precursors and agrochemicals, which allow us to feed an ever increasing world population. Without the petrochemical industry we could not sustain life on the planet. We would be cold, hungry, dirty and ill.

Table 1 *E* factors (tonnes of waste generated per tonne of product manufactured [7]

Industry segment	Annual product tonnage	*E* factor
Oil refining	10^6–10^8	Approx. 0.1
Bulk chemicals	10^4–10^6	<1–5
Fine chemicals	10^2–10^4	5–50+
Pharmaceuticals	10–10^3	25–100+

However, there is another problem. The industries that rely on petrochemicals, as well as those that do not, sometimes use chemistry that produces large amounts of waste, often more than the amount of the desirable material. This waste must be handled and disposed of – often to toxic land-fill sites at great cost in terms of energy and amenity. Soon there will be few sites left for disposal of this kind. The smaller the amounts of product being manufactured, generally the dirtier is the Chemistry. This is well summed up in the table of E-factors (Table 1) developed by Sheldon [7], which represents the tonnes of waste produced per tonne of product manufactured. The pharmaceutical industry produces drugs of enormous benefit to mankind and very high added value, but it does this with little regard to the elimination of waste.

So this is the major challenge facing us today. How do we produce the very many chemical products upon which we have come to rely, cheaply, cleanly and with diminished use of fossil fuel resources?

Much of the answer lies in catalysis. Catalysis allows chemical reactions to be carried out under milder conditions, thus saving energy. There are three main types of catalyst. Enzymes, which nature has engineered over thousands of years to work in water at room temperature and atmospheric pressure to carry out very highly selective reactions, often selecting one feedstock from a vast array of possibilities and producing only one product with 100% selectivity in terms of chemo-, region-, and stereo selectivity. In other words enzymes can modify a particular molecule in one position to give a single product in which even the chirality is controlled. Unfortunately, the products that nature requires are not always the same as those needed for the vast arrays of feedstocks required by the Chemical Industries, so using enzymes for the kinds of products we need is not always possible. Although enzymes are used in some processes even for fairly large volume products such as the synthesis of lactic acid for the synthesis of polylactide [8], which is a biodegradable replacement for polythene or polystyrene, their very high substrate and product selectivity as well as their often low stability under conditions other than those for which they were optimised (water, room temperature, atmospheric pressure) makes them unsuitable at present for use in the wide range of processes required by the chemical industry. Manmade catalysts have therefore been introduced. These come in two forms; those where the catalyst is in a different phase from the reactants and products (heterogeneous) and those where the catalyst is either dissolved in the products or both are in a solvent, usually an organic compound.

Heterogeneous catalysts, usually metals or metal oxides can give dramatic rate accelerations, are stable to high temperature and can easily be separated from the

reaction products. Generally their selectivity is low or cannot be tuned very much, although shape selective tuning can occur using microporous solids such as zeolites. Homogeneous catalysts, which generally consist of metal centres surrounded by a variety of ligands on the, other hand are highly versatile, act under mild conditions and can give very high selectivities [9]. By varying the metal centre and the surrounding ligands, the chemo-, region- and stereo-selectivites can be tuned so that a very wide range of different product can be made available. The power of homogeneous catalysis is reflected in the award of Nobel prizes for asymmetric catalysis (Sharpless, Knowles and Noyori, 2001) and for alkene metathesis (Schrock, Grubbs and Chauvin, 2005) in the last 10 years.

Despite the huge promise offered by homogeneous catalysts, rather few have been commercialised. One of the main reasons for this arises because they *are* homogeneous. This means that the reaction products have to be separated from the catalyst and any solvent. Usually this would be done by fractional distillation, but many of the products have rather low volatility and cannot be distilled below the decomposition temperature of the (often) thermally sensitive catalyst. This separation problem and the need to use organic solvents (often volatile organic compounds, VOCs), which can themselves be pollutants.

The huge potential for using homogeneous catalysis for manufacturing a large range of desirable bulk, commodity, speciality, pharmaceutical and agrochemical products awakened scientists to the separation problem from the very early days of homogeneous catalysis research and very many ingenious approaches are being developed [10–13]. These range from biphasic systems in which the catalyst is present in one phase whilst the product is in another to catalysts that are attached to solid supports. There are hybrid systems where the catalyst is dissolved in a thin film of liquid distributed over a solid support and systems where the catalyst can be switched by a stimulus such as heat [14], light or bubbling CO_2 from a phase where the reaction occurs to an immiscible solvent from which the product can be decanted [15–17]. Sometimes the reaction can be carried out in one phase but the mixture separates into two phases on cooling, bubbling CO_2 etc. When two phase reactions are employed, the separation is usually carried out by taking some of the two phase mixture to a gravity separator where the phase containing the organic product is decanted and the catalyst phase returned to the reactor. Two examples where this approach has been commercialised are the Shell Higher Olefins Process where long chain alkenes are prepared by ethene oligomerisation and separated from the catalyst dissolved in polar 1,4-butanediol [18], and the Ruhr Chemie–Rhône Poulenc process for the hydroformylation of propene with the catalyst dissolved in water with which the product butanal is immiscible [19, 20]. These two processes both involve batch continuous processing where some of the reaction mixture is removed from the reactor and treated under quite different conditions from those in the reactor. It would be more desirable to have continuous flow reactions where the substrates and reacting gases are pumped into the reactor containing the dissolved catalyst whilst the products flow out. All the catalyst is in the reactor all the time and is kept under conditions for which it has been optimised. Continuous flow processing of this kind is possible where the reaction products

are volatile under the reaction conditions (e. g. the rhodium catalysed hydroformylation of propene, where the product butanal (b.p. 75°C) distils from the reactor at the reaction temperature (105°C) [21] or in new systems where the catalyst is dissolved in an ionic liquid [22, 23] or a high molecular mass liquid polymer such as polyethylene glycol with the substrates and products being transported out of the reactor using a supercritical fluid [24]. Although such systems can be used for a much wider range of (less volatile) substrates, they have not so far been commercialised.

For supported catalysts, the possibility exists for flow processing since they can be handled like heterogenenous catalysts and used in simple flow reactors. In principle, they are very simple to use, but none have so far been commercialised. Although the idea of anchoring homogeneous catalysts onto solid supports was first investigatedsoon after the development of the new generation of phosphine liganded catalysts (in the 1960s) [25], usually using a modification of the ligand to provide the attachment, leaching of the liquid was always observed to some extent, either because the metal became detached from the linking ligand at some point during the catalytic cycle and so dissolved, or because the ligand itself was somehow cleaved from the support. Nanoparticle formation can also be a cause of leaching. In one case, a rhodium catalyst supported on an anion exchange resin is used for the carbonylation of methanol. It is accepted that leaching occurs and a guard bed is placed further down the reactor flow system [26]. Leached catalyst is trapped by this guard bed, which is eventually used as a replacement catalyst bed, thus reducing the leaching to manageable proportions even for an expensive rhodium based catalyst. In this system, at least some of the catalysis and possibly the majority occurs through the solubilised rather than the supported catalyst.

A key development occurred in 1999 [27], when the group headed by van Leeuwen, Kamer and Reek reported that a rhodium catalyst involving a bidentate ligand which had been modified to include a remote $–Si(OEt)_3$ group could be incorporated by sol gel processing into silica. A single batch of this catalyst was used for a variety of reactions – mainly hydroformylations in the liquid phase, over a period of 1 year without loss of activity or selective and without observable leaching of rhodium [28]. This development and others have led to a large increase in activity aimed at the development of non-leaching supported catalysts which retain or surpass the activity and selectivity of their homogeneous counterparts [29].

This book brings together contributions from leaders in the field of research into supported homogeneous catalysts. It takes a broad view, covering soluble and insoluble supports, supported liquid phase catalysis and membrane imbedded catalysts. Some Chapters concentrate on the design and synthesis of the supports and on the attachment of the catalysts to the supports, whilst others concentrate on specific types of applications of the supported catalysts or on studies aimed at identifying the exact nature of the supported species. However, the commercialisation of catalysts does not only depend upon the catalyst and the support, but also in the reaction engineering that allows the Chemistry to be carried out to its fully optimised potential. One chapter of the book discusses the challenges and some solutions for the engineering of supported catalysts, whilst another addresses progress made in modelling homogeneous catalysts on supports. Finally, a most important chapter discusses the major

factors that must be taken into account when considering using supported catalysts in commercial processes. The various possible pitfalls are explored and the reasons why a fully homogeneous system was preferred over a supported analogue for the synthesis of the enantiopure herbicide (*S*)-metolachlor are discussed.

The majority of the contributors to the book are members of NANO-HOST an Initial Training Network set up by the European Commission under the auspices of the Marie Curie actions to train young people in the area of supported catalysis and to encourage them to be flexible and mobile within the European Community. Funding for these Networks is extremely competitive so the presence of NANO-HOST indicates the importance placed on the development of supported catalysts by the European Commission. The work of all the authors has been integrated through the European Network of Excellence, IDECAT, which seeks to facilitate integration of scientists working in all branches of catalysis. NANO-HOST sprung from IDECAT, which has also spawned the European Research Institute of Catalysis, for the continued development of catalysis in Europe.

David J. Cole-Hamilton
University of St. Andrews
Fife, KY16 9ST
Scotland
djc@st-and.ac.uk

References

1. 2 Maccabees, Chapter 1, vv 19
2. Beau de Rochas A (1860) French Patent 52593
3. Otto NA (1876) German Patent 365701
4. Benz K (1886) German Patent 37435
5. BP (2009) Statistical Review of Energy. http://bpcom
6. International Panel on Climate Change (2007) 4th assessemnt report. http://ipccch
7. Sheldon RA (1994) Chemtech 24:38
8. Gruber PR, Hall E (1992) US Patent 5142023
9. Cornils B, Herrmann WA (eds) (1996) Applied homogenous catalysis with organometallic compounds. VCH, Weinheim
10. Cole-Hamilton DJ (2003) Science 299:1702
11. Cole-Hamilton DJ, Tooze RP (eds) (2006) Catalyst separation, recovery and recycling; chemistry and process design. Springer, Dordrecht
12. Cornils B, Herrmann WA, Horváth IT, Leitner W, Mecking S, Olivier-Borbigou H, Vogt D (eds) (2005) Multiphase homogeneous catalysis. Wiley, Weinheim
13. Benaglia M (ed) (2009) Recoverable and recyclable catalysts. Wiley-Blackwell, Chichester
14. Zheng XL, Jiang JY, Liu XZ, Jin ZL (1998) Catal Today 44:175
15. Andreetta A, Barberis G, Gregorio G (1978) Chim Ind 60:887
16. Andreetta A, Gregorio G (1978) Can Patent 1023729
17. Desset SL, Cole-Hamilton DJ (2009) Angew Chem Int Ed 48:1472
18. Keim W (1990) Angew Chem Int Edn Engl 29:235
19. Kuntz E (1975) FR 2314910

20. Wiebus E, Cornils B (2006) Biphasic systems: Water – organic. In: Cole-Hamilton DJ, Tooze RP (eds) Catalyst separation, recovery and recycling; chemistry and process design. Springer, Dordrecht
21. Van Leeuwen PWNM, Claver C (eds) (2000) Rhodium catalysed hydroformylation. Kluwer, Dordrecht
22. Cole-Hamilton DJ, Kunene TE, Webb PB (2005) SCFs and Ionic Liquids. In: Cornils B, Herrmann WA, Horváth IT, Leitner W, Mecking S, Olivier-Borbigou H, Vogt D (eds) Multiphase homogeneous catalysis. Wiley, Weinheim
23. Webb PB, Sellin MF, Kunene TE, Williamson S, Slawin AMZ, Cole-Hamilton DJ (2003) J Am Chem Soc 125:15577
24. Heldebrant DJ, Jessop PG (2003) J Am Chem Soc 125:5600
25. Haag WO, Whitehurst DD (1969) German Patent 1800371
26. Sugiyama H, Uemura F, Yoneda N, Minami T, Maejima T, Hamato K (1997) Jap Pat 235250
27. Sandee AJ, van der Veen LA, Reek JNH, Kamer PCJ, Lutz M, Spek AL, van Leeuwen PWNM (1999) Angew Chem Int Ed 38:3231
28. van der Slot SC, Duran J, Luten J, Kamer PCJ, van Leeuwen PWNM (2002) Organometallics 21:3873
29. Reek JNH, van Leeuwen PWNM, van der Ham AGJ, de Haan AB (2006) Supported catalysts In: Cole-Hamilton DJ, Tooze RP (eds) Catalyst separation, recovery and recycling; chemistry and process design. Springer, Dordrecht

Preface

The design of green and economically feasible processes for the production of fine chemicals is certainly one of the major needs and biggest challenges for a sustainable development of our planet. Catalysis contributes substantially to this goal by providing comparatively lower impact technologies and further in the recent years several efforts have been exerted aimed at broadening the scope of the catalysts, increasing their accessibility and efficiency, lowering their costs and ensuring their reuse.

This book collects the contributions of some of the leading scientist working in the field of the heterogenization of homogeneous chemical catalysts. The snapshot we get is a clear evidence of the level of expertise and sophistication reached with this methodology. The fascinating world of "heterogenized catalysis" is perfectly introduced in Chapter 1, where the differences and the advantages of the approach, compared to the two traditional disciplines of homogeneous and heterogeneous catalysis, are illustrated. The following chapters focus on the solid support materials, either inorganic, organic, dendrimer or nanosized, to show their subtle, often determining influence on the catalyst performance and how the mastered elaboration of new materials may be used as a tool to tailor and improve this. Selected examples of application reported in Chapters 9–11 testify the versatility and the potential of the method. No surprise that most processes are carried out in an enantioselective fashion. This is a prerogative of molecular catalysts which, coupled with the easy handling and recycling typical of immobilized systems, favourably differentiate heterogenized catalysts from the conventional heterogeneous ones. To this end, particularly evocative is the possibility to engineer enzyme-mimicking solid catalysts, as properly described in Chapter 2. The contributes dealing with membranes and reactors were purposefully included to provide insights of the technological opportunities and solutions offered by the heterogenization of homogeneous catalysts. Further, clear distinction of immobilized molecular systems is their possibility to enable both a systematic design of new catalysts and an easier characterization of the active sites, compared to the classical heterogeneous catalysts. Chapters 12 and 13 are paradigmatic in this sense.

Nevertheless, despite the above advantageous features and the progresses achieved by academia in this research area, with a few notable exceptions [1], examples of the use of heterogenized catalyst in industrial processes are still rare. This issue is critically analyzed in the "industrial" viewpoint reported in Chapter 7.

In conclusion, the main aim of the book was to provide the reader not only with an update on the state-of-the-art of the heterogenization of molecular catalysts, but also to offer a guide on the basic concepts behind this emerging, multidisciplinary technology which integrates several of the subdivision of chemistry, at the border of physics and chemical engineering; to assess the critical points in the field and, at the same time, to indicate the future perspectives and possible strategies. Our feeling is that the target was fully achieved. Likely, this is the first text in which the subject is treated comprehensively in all its essential facets. Therefore, we are confident that this book will be a helpful companion and deliver key hints to those, in the academia and in the industry, who decide to move their research interests in this direction.

Finally, we wish to thank the Authors of this volume for their enthusiasm and care in drawing up their contribution, all people at Springer's office, London for their precious assistance and the IDECAT (www.idecat.org) and NANO-HOST (www.nano-host.eu) Networks for providing substantial inputs to the topic of the book.

Pierluigi Barbaro and Francesca Liguori

Reference

Yoneda N, Minami T, Weiszmann J, Spehlmann B (1999) In: Hattori H, Otsuka K (eds) Studies in surface science and catalysis, vol 121. Kodansha, Tokyo, pp 93–98

Contents

Contributors

Hans-Ulrich Blaser
Solvias AG, P. O. Box CH-4002, Basel, Switzerland

Dirk De Vos
Centre for Surface Chemistry and Catalysis, Department M2S, Katholieke Universiteit Leuven, Kasteelpark Arenberg 23, 3001, Leuven, Belgium

Enrico Drioli
Institute on Membrane Technology (ITM-CNR), Via P. Bucci, 87030 Arcavacata di Rende, Cosenza, Italy and Department of Chemical Engineering and Materials, University of Calabria, Via P. Bucci, 87030 Arcavacata di Rende, Cosenza, Italy

Joanna Dzierzak
School of Chemistry, University of Southampton, Highfield, Southampton SO17 1BJ, UK

John Evans
School of Chemistry, University of Southampton, Southampton SO17 1BJ, UK

Tomas Floris
Department of Organic Chemistry, University of Szeged, Dóm tér 8, 6720 Szeged, Hungary

Enrica Fontanova
Institute on Membrane Technology (ITM-CNR), Via P. Bucci, 87030 Arcavacata di Rende, Cosenza, Italy and Department of Chemical Engineering and Materials, University of Calabria, Via P. Bucci, 87030 Arcavacata di Rende, Cosenza, Italy

Paulo Forte
Centre for Surface Chemistry and Catalysis, Department M2S, Katholieke Universiteit Leuven, Kasteelpark Arenberg 23, 3001 Leuven, Belgium

José M. Fraile
Departamento de Química Orgánica, Instituto de Ciencia de Materiales de Aragón e Instituto Universitario de Catálisis Homogénea, Facultad de Ciencias, C.S.I.C.-Universidad de Zaragoza, E-50009 Zaragoza, Spain

José I. García
Departamento de Química Orgánica, Instituto de Ciencia de Materiales de Aragón e Instituto Universitario de Catálisis Homogénea, Facultad de Ciencias, C.S.I.C.-Universidad de Zaragoza, E-50009 Zaragoza, Spain

Ciril Jimeno
Institute of Chemical Research of Catalonia (ICIQ), Av. Països Catalans, 16, E-43007 Tarragona, Spain

Matthew D. Jones
Department of Chemistry, University of Bath, Claverton Down Bath BA2 7AY, UK

Robertus J. M. Klein Gebbink
Faculty of Science, Debye Institute for Nanomaterials Science, Organic Chemistry & Catalysis, Utrecht University, Padualaan 8, 3584 CH Utrecht, The Netherlands

Petr Kluson
Department of Organic Chemistry, University of Szeged, Dóm tér 8, 6720 Szeged, Hungary

Duncan Macquarrie
Green Chemistry Centre of Excellence, Department of Chemistry, University of York, Heslington, York YO10 5DD, UK

Kourosh Malek
National Research Council of Canada, Institute for Fuel Cell Innovation, 4250 Wesbrook Mall, V6T 1W5, Vancouver, BC, Canada and Department of Chemistry, Simon Fraser University, 8888 University Drive, V5A 1S6 Burnaby, BC, Canada

José A. Mayoral
Departamento de Química Orgánica, Instituto de Ciencia de Materiales de Aragón e Instituto Universitario de Catálisis Homogénea, Facultad de Ciencias, C.S.I.C.-Universidad de Zaragoza, E-50009 Zaragoza, Spain

Ferenc Notheisz
Department of Organic Chemistry, University of Szeged, Dóm tér 8, 6720 Szeged, Hungary

Miquel A. Pericàs
Institute of Chemical Research of Catalonia (ICIQ), Av. Països Catalans, 16, E-43007 Tarragona, Spain and Departament de Química Orgánica, Universitat de Barcelona, E-08028 Barcelona, Spain

Elisabet Pires
Departamento de Química Orgánica, Instituto de Ciencia de Materiales de Aragón e Instituto Universitario de Catálisis Homogénea, Facultad de Ciencias, C.S.I.C.-Universidad de Zaragoza, E-50009 Zaragoza, Spain

Benoît Pugin
Solvias AG, P. O. Box CH-4002, Basel, Switzerland

Robert Raja
School of Chemistry, University of Southampton, Highfield,
Southampton SO17 1BJ, UK

Albert Renken
Institute of Chemical Sciences and Engineering, Ecole polytechnique fédérale de Lausanne, EPFL-ISIC-Station 6, 1015 Lausanne, Switzerland

Sonia Sayalero
Institute of Chemical Research of Catalonia (ICIQ), Av. Països Catalans,
16, E-43007 Tarragona, Spain

Moniek Tromp
School of Chemistry, University of Southampton, Southampton SO17 1BJ, UK

Rutger A. Van Santen
Schuit Institute of Catalysis, ST/SKA, Eindhoven University of Technology,
Eindhoven, The Netherlands

David Xuereb
School of Chemistry, University of Southampton, Highfield,
Southampton SO17 1BJ, UK

Vital A. Yazerski
Faculty of Science, Debye Institute for Nanomaterials Science, Organic Chemistry & Catalysis, Utrecht University, Padualaan 8, 3584 CH Utrecht, The Netherlands

Agnes Zsigmond
Department of Organic Chemistry, University of Szeged, Dóm tér 8, 6720 Szeged, Hungary

Chapter 1
Fine Chemicals Synthesis Through Heterogenized Catalysts: Scopes, Challenges and Needs

Duncan Macquarrie

Abstract The development of new, highly efficient heterogenized catalysts is an active and important area in fine chemicals production. Many opportunities present themselves in terms of the significant developments in the tailoring of solid supports, which allow a rich variety of surface functionalities and properties, along with unprecedented control of physical features such as porosity, pore connectivity and high surface area. Key challenges include making full use of this palette of materials in the drive towards sustainable manufacturing. The knowledge base in materials chemistry and catalysis, coupled with ever-improving techniques to analyse catalytic materials and the reactions they promote will provide a sound foundation for future research and applications in this area.

1.1 Introductory Remarks

The synthesis of fine chemicals through the use of heterogenized catalysts has been an active research field for several decades Over about the same period, the chemical industry has been enormously reliant on the use of solid catalysts, in particular the zeolites (3D crystalline solids with pore sizes below 1 nm) for the conversion of crude oil into a range of small molecules. These high temperature, gas phase processes run continuously and are amongst the largest volume chemical processes in existence. The enormous thermal stability, robustness and high acidity of the zeolite catalysts employed, combined with their very well defined crystalline nature means that they are extremely effective and highly selective catalysts. Part of this selectivity comes from the fact that, in a crystalline material, active sites are always situated in the same environment and therefore always have the same activity and selectivity (although transport processes taking substrate to, and product from, the

D. Macquarrie (✉)
Green Chemistry Centre of Excellence, Department of Chemistry, University of York, Heslington, York YO10 5DD, UK
e-mail: Djm13@york.ac.uk

P. Barbaro and F. Liguori (eds.), *Heterogenized Homogeneous Catalysts for Fine Chemicals Production*, Catalysis by Metal Complexes 33,
DOI 10.1007/978-90-481-3696-4_1,

active sites may restrict the frequency of their utilisation). A second major contributor to their selectivity comes from the fact that their pore dimensions are often more or less the same size as the substrates/products that are involved in the reaction, leading to the notion of shape selectivity, crucial in the formation of *p*-xylene with a sufficiently high purity (>99.9%) for use in terephthalic acid production. Such selectivity is well beyond normal chemoselectivity. The crystalline nature of the zeolites also means that they can be very well characterised and therefore a thorough understanding of their behaviour is possible.

In stark contrast, there is a distinct lack of solid catalysts or continuous processes in the predominantly solution phase world of fine chemicals. Catalysts are used frequently, but (with the exception of hydrogenation reactions, where e.g. Pd/C or Pt/Al_2O_3 are commonly utilised as catalysts) are almost always homogeneous. This gives them the benefit of being typically discrete, well-characterised molecules (although these molecules may or may not actually be the true catalytic species) where rational modifications can be made and the consequences readily measured. Additionally, diffusion is typically excellent – not always the case with a porous solid, where transport through the (often narrow) pore system can be the rate determining step.

Despite this partial lack of utilisation by the wider community, there has been a considerable amount of research carried out into heterogenized catalysts and catalysis using them. In particular, recent years have seen a resurgence in activity for a range of reasons. These reasons include the increased awareness of clean, efficient processing and the establishment of Green Chemistry as a fundamental part of designing a process [1], with catalysis being very much central to its fundamental principles [2,3], and the very significant breakthroughs in the design and synthesis of very well designed inorganic solids such as the MCM-41 and SBA-15 series of silicas [4,5], both of which have well-defined porosity in the mesoporous range and narrow pore size distributions. The larger pores that these families of materials have allow the conversion of fine chemicals, the vast majority of which are too small to fit into the sub-nanometre pores of the zeolites. Crucially, for heterogenized catalysts, the pores are also large enough to accommodate bound catalytic units. Furthermore, these (or their precursors) can be incorporated during the silica synthesis itself [6,7].

1.2 Scope: What is a Heterogenized Catalyst?

A heterogenized catalyst can be viewed as a homogeneous catalyst attached typically (but not always) via a covalent tether to an insoluble support. Some, such as those based on polymers such as polystyrene or chitosan, can have solubility under some conditions (solvent, pH, etc.), but the majority are based on 3-D inorganic polymers such as silica.

This combination of two species (catalyst plus support) means that the catalyst exists in (usually close) proximity to a solid surface, which may itself have catalytically active groups or groups that can interact with the catalyst in a beneficial or detrimental manner. For example, the slightly acidic nature of the silica surface can be beneficial in acid–base catalysts – the Knoevenagel reaction works unusually well on aminopropyl silicas [8], where the weak acid/weak base combination aids

the reaction. On the other hand, more strongly basic systems such as guanidines have their basicity reduced by interaction with the silica surface, and optimal activity is obtained when the surface is passivated to eliminate acidity [9,10]. Similarly, there may be a requirement to modify the catalyst to provide a binding group which can attach to the surface. This may modify the basic chemistry of the catalyst to a degree and must be taken into account, especially when considering changes to the activity or selectivity which may be noticed in a comparison between the homogeneous and heterogeneous equivalents. Attachment of other catalytic groups to the same surface can lead to bifunctional catalysts; attachment of other, non-catalytic, groups has been shown to lead to rate enhancements in several cases. Behind all this is the requirement to have the correct distribution of groups (uniformly distributed and well spaced out to minimise interactions between groups or, alternatively, to have them clustered together to maximise interactions between groups or to increase the local "concentration" of groups). This is important whether the catalyst is monofunctional or multifunctional, with two or more active different sites – positioning of the sites throughout the material is an important consideration, but is not always straightforward to either measure or to achieve.

1.3 Why Heterogenize a Homogeneous Catalyst?

Given the potentially more complex nature of the heterogenized catalyst, and the likelihood that it may be more difficult to prepare, one must naturally ask why this additional effort is justified. There are several reasons. Firstly, the heterogenized catalyst is almost certainly more easily recovered, and therefore reuse becomes more realistic (although reactivation may be required). Therefore less waste is generated, and expensive, difficult-to-obtain components such as ligands or scarce metals can be effectively recovered and reused. This also has the effect of making the isolation and purification of product easier, as catalyst residues have been easily removed.

As alluded to above, there may be advantages in terms of beneficial chemistry from the support (or indeed shape/size selectivity considerations) which make the catalyst more effective when heterogenized. Catalysts which are deactivated by dimerisation or agglomerisation can be effectively isolated on a surface, maintaining their activity for longer.

More than one catalyst can be present in the reaction mixture at the same time, allowing for multi-stage reactions to be carried out in one pot, simplifying further the processing (so-called telescoped synthesis). These catalysts may be on the same solid support, or on different supports. Examples of these are given later in the chapter.

Solid catalysts can also be fixed in reactors such as fixed or fluidised bed reactors, flow reactors, membrane reactors etc. Here, the reactants are flowed over/through a bed or film of catalyst with reaction and separation being achieved simultaneously. There are many advantages to such technology (which, as stated earlier, is standard practice in gas-phase catalytic chemistry). Examples of such systems are known, and more will be said about them later.

Thus, it can be seen that, with a correctly designed catalyst, excellent rates and selectivities may be achieved, although this may be limited by diffusion constraints

which can make heterogeneously catalysed reactions slower than their homogeneously catalysed counterparts. Nonetheless, the many advantages in terms of product isolation which arise due to the solid nature of the catalyst (easy separations, better recovery and reuse, flow systems, etc.) can outweigh this often slower reaction, making the overall *process* faster. Indeed, one of the major hurdles in the use of heterogenized catalysts by the wider synthetic community is that we, as chemists are very good at thinking in terms of optimising reactions, but rarely think in terms of the process as a whole, meaning that product isolation is often an afterthought. On a larger scale, this then represents a major problem, and many scale-up campaigns are blighted by difficulties in efficiently isolating pure product.

1.4 Methods of Heterogenization

There are several possible routes to heterogenize a catalyst. The most common of these is the covalent attachment of a catalyst to a solid surface (or via co-polymerisation with a suitable non-active monomer), although non-covalent interactions can be used as well. Each route has benefits and disadvantages in terms of generality, complexity and the range of conditions that can be used successfully. The major methodologies for heterogenization are summarised below.

1.4.1 Covalent Binding of Catalyst

Examples of covalent binding of the catalytic group to the support include both organic polymers, such as those formed from the copolymerisation of styrene with a substituted styrene, as well as inorganic polymers formed from the sol-gel polymerisation of e.g. tetraethoxysilane and an organically functionalised trialkoxysilane.

The functional groups introduced via this route may be the catalysts themselves or may be anchor points which are then subsequently reacted with a suitably functionalized catalyst unit. It should be noted that the Y-CAT unit can often be directly attached to the pre-formed polymer. In the case of silicas, this is actually still a far more common route than the sol-gel co-condensation route in Fig. 1.1 and appears to give materials with subtly different properties. Here, the silica is functionalised with $XSi(OMe)_3$ with further reaction on X if required. The direct attachment of Y-CAT units to organic polymers is less common.

What should be borne in mind is that the ratio of the two (or more) monomers is typically far from 1:1. The functional monomer rarely makes up more that 10 mol% of the total, and is often significantly lower than this. In the final product, the distribution (and accessibility) of the functional groups must be defined, and this is often difficult. It is fair to say that more progress has been made for the organic polymers than for the inorganic systems in this respect. A further challenge is often met when X needs to be functionalised. Incomplete functionalisation is often not straightforward, and this means that the loading of catalyst is less than expected and

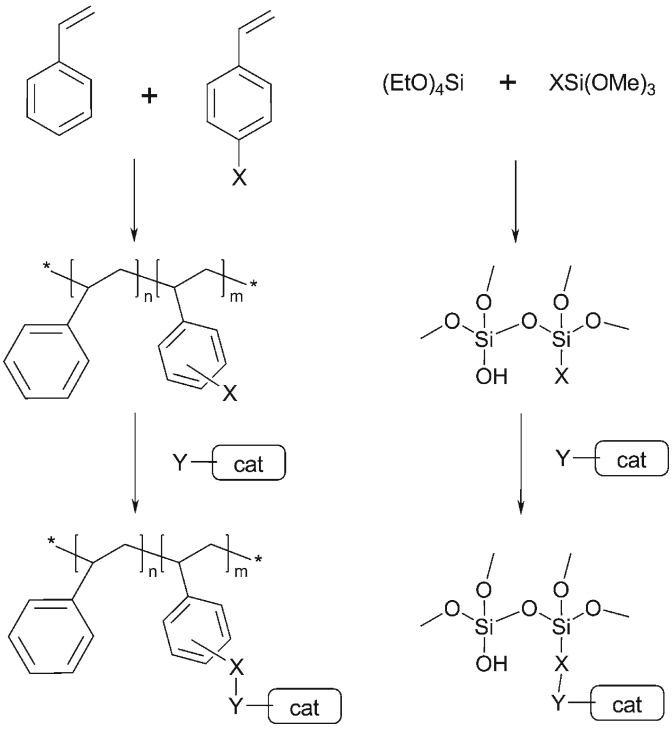

Fig. 1.1 Covalent attachment of catalytic groups to form heterogenized catalysts. Subsequent functionalisation of the X-substituted product of the first step may be necessary if X I itself not catalytically active

there are X groups remaining on the surface which may influence the behaviour of the system. However, incomplete functionalisation is often due, at least in part, to variable accessibility of the functional groups at different parts of the structure, and this probably means that those sites which are readily functionalised are also those which are most likely to be accessible to the substrates during the catalytic reaction itself. Therefore, a partial functionalisation should favour the sites that will play the major part in the process. Nonetheless, there is an argument that the non-accessible sites are wasted, and that improved accessibility by better design of the material/polymer architecture is desirable. Implicit in this is the fact that there are generally a range of different sites in which a catalytic unit might be heterogenized, meaning that there may well be a spread of selectivities and activities.

1.4.2 Ionic Heterogenization

Ionic materials may be readily heterogenized by forming an ion pair with a charged group on the surface of a support. This has been achieved with of the simplest

examples being aminopropyl silica, which can be protonated and used to heterogenize ionic catalytic units. Examples include heteropolyacid salts [11], but other acid functionalised systems could be immobilised too. Clearly, the catalysts should be used and re-isolated/reactivated under conditions where ion exchange is not possible, otherwise leaching and loss of material will be encountered. Augustine's group have demonstrated that heteropolyacids directly adsorbed on alumina can effectively tether a range of organometallic catalysts [12].

1.4.3 Supported Liquid Phase

This technique was introduced in 1989 by the group of Davis and is a cross between liquid–liquid biphasic catalysis and solid–liquid biphasic catalysis [13]. The key concept is the immobilisation of a thin film of liquid (the first examples were water, but others such as ionic liquids have been used [14,15]) on the surface and within the pores of a solid support. A catalyst is then dissolved in the liquid layer. The key requirement for *heterogeneous* catalysis is then that the catalyst does not leach out into the surrounding organic solution, putting restrictions on the nature of the solvent used (it should have very low water miscibility and should not dissolve the catalyst or any intermediates in the catalytic cycle). There can be issues with the synthesis of a catalyst with the correct solubility which may restrict the utility or the green credentials of a system in some cases, but in other instances, where the solubility of the catalyst suits the basic notion, then this may be a very promising avenue to explore.

1.4.4 Ship in a Bottle

A few examples are available for this method whereby a catalyst is prepared inside a cage-like pore such that the dimensions of the catalyst precursors are such that relatively free diffusion in and out of the pore is possible, but the catalyst itself is too large to escape from the pore, and is thus permanently entrapped. Porphyrins and related structures have been prepared within the pores of the larger zeolites and used with some success, but the limitations on diffusion of substrates and products and the constraints of their interaction with the catalyst means that this approach is not particularly common. Nonetheless, good results can be obtained, albeit more slowly than with homogeneous catalysis, as in the example provided by Ferreira et al. where alkenes can be selectively and effectively oxidised to epoxides by a ship in a bottle Ni–Salen complex within zeolite X or Y [16]. While reaction was slower, selectivity and conversion were good, and indeed improved somewhat upon reuse. It was noted that the distribution of active catalytic groups appeared to be mostly centred close to the external surface with less catalyst deep within pores.

1.4.5 Entanglement

This method has been used in the case of nanoparticle catalysts. Nanoparticles are very prone to agglomeration, and heterogenization is one technique that has been used to reduce the prevalence of this phenomenon. While this often takes the form of a covalent tether, a different, non-covalent, approach can sometimes be successful. Many polysaccharides form gels under appropriate conditions, and these can be used to entrap nanoparticles such that the nanoparticles are tangled up in a network of H-bonded polysaccharide strands. This reduces the tendency of the nanoparticles to diffuse and coalesce, meaning that their activity as catalysts is maintained for longer. Indeed, one of the benefits of this approach is that the polysaccharide can effectively reduce the metal salts that are often precursors, meaning that the nanoparticles can be produced in-situ without an additional reductant. This simplifies the procedure enormously, as the reduction takes place without the need for a separate reductant, therefore meaning that there are no side products from the reduction which must be removed [17].

The key features of these different methods of heterogenization are given in Table 1.1 below.

Table 1.1 Summary of the key methodologies for the heterogenization of catalysts

Type of attachment	Key features	Pros/cons
Covalent attachment	One or more covalent bonds between catalyst and support	Generally stable link and more than one route to form catalysts. Requirement for covalent attachment can add complexity and may alter nature of catalyst.
Ionic attachment	Electrostatic attraction between catalyst and support	Ideal for charged catalyst, easily carried out. Catalyst must stay charged throughout catalytic cycle, conditions must not allow ion exchange.
Supported liquid phase (SLP)	Thin film of catalyst on high surface area solid	Relatively simple to carry out with catalyst soluble in SLP. Otherwise modification of catalyst required to make it soluble in SLP but insoluble in bulk liquid medium. Similar requirements for SLP.
Ship in a bottle	Physical constraint	Effective immobilisation but restricted range and diffusion difficult.
Entanglement	Physical restriction on the movement and coalescence of catalyst	Simple to do, and polysaccharides generally inexpensive. Need for interaction between catalyst precursor and polymer. Thermal stability probably limited.

1.5 Nature of the Support

The vast majority of heterogenized catalysts have been prepared either on organic polymeric supports such as modified polystyrenes, or on silicas. Both types of support are widely available and are relatively easily functionalised to give stably bound groups, either by C–X bond formation on e.g. a phenyl ring or by S_N2 reaction of an aryl -CH_2Cl in the case of a functionalised polystyrene, or by the attachment of trialkoxy silanes to the surface of a silica. Several of these are commercially available, and many complex groups can be attached via some of the simpler amine, halide or isocyanate functionalities that can be bought. The Si–O–Si unit is relatively stable under most conditions (especially where all three alkoxy groups are converted to Si–O–Si) and therefore stable catalysts can be produced. Grafting to the surface of a pre-formed silica is the more frequently used route to these materials, but the direct sol-gel synthesis is also an attractive approach. The materials produced by each route are usually broadly similar, but rarely identical, and it is worth using both routes to find which give the better system.

The early 1990s saw an explosion in the area of mesoporous silicas, with unprecedented control over porosity being achieved, along with exceptional surface areas. The templated methods which were developed during this period have led to a great leap in the range of materials available as catalyst supports. About a decade later, there was a second significant jump forward in the choice of highly tunable, regularly structured materials, which has been much less fully exploited in catalysis. This second step forward came about via the findings by Ryoo and co-workers, that carbon replicates of SBA-15 materials could be produced which preserved the structural features of the SBA-15, by filling the pores with carbon precursors, forming the carbon within the pores and then etching the silica away, leaving behind the so-called CMK materials [18]. These mesoporous carbons created great interest, as the vast majority of carbons prepared up to that point had been predominantly microporous.

Following on from this discovery came the finding that these carbons could, in turn, serve as 3-D templates for a range of different oxides, with the same porosity and surface area as the original SBA-15. while some oxides and sulfides can be prepared directly using SBA-15 as a hard template, this is limited to those which are stable to the conditions required to etch away the silica (alkali or HF). For other systems, the use of a CMK material as template can get round this problem, as the removal of carbon requires different conditions. This reverse templating (Fig. 1.2) can be used to provide a range of highly structured mesoporous materials which were previously impossible, or at least very difficult to synthesise by more direct routes [19].

In addition to these systems, other potential solids for functionalisation are available, although currently under-exploited. Two examples are the periodic mesoporous organosilicas (PMOS) pioneered by Inagaki [20], which are prepared from bis-silanes, where the two trialkoxysilane groups are linked by a typically short and non-functionalised organic bridge such as a phenylene or –CH_2CH_2–. Catalytic groups can be subsequently attached, or can be incorporated in the sol-gel synthesis medium, as was done by Sullivan, who prepared a very active base catalyst using this approach [21].

Organically functionalised aluminium phosphonates have been prepared by Vioux's group, using a co-condensation of $M(OR)_3$ and phosphonic acids, leading

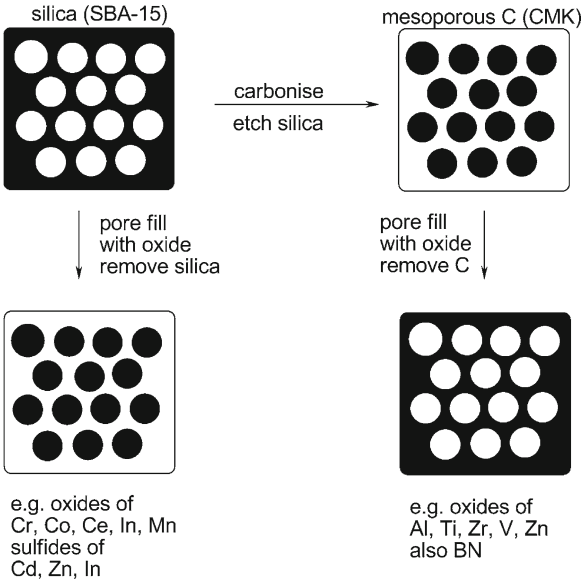

Fig. 1.2 Nanocasting routes to various mesoporous materials

to Ti, Zr, and Al organohybrids [22,23]. Such an approach should be amenable to extension, using the relative simplicity of the three component coupling between phosphites, aldehydes and amines.

It is clear from the examples in this chapter that the surface of the support material can have a significant impact on the chemistry that takes place at the catalytic site, and that controlling/designing this environment is therefore a very important facet of the overall design of an optimal catalyst. Therefore, the choice of support should be made bearing in mind and drawing upon the wide range of possible supports that is now available. The biomass-derived systems described below are also of great interest and further extend the choice of support available.

1.6 Challenges and Needs

There are many challenges to be met and needs to be fulfilled in the area of heterogenized catalysis towards the production of fine chemicals. There is a much wider range of choices available in many ways than there has been before, and some of these, such as the remarkable advances in the synthesis of and structural control over mesoporous solids in particular open up many possibilities to enhance catalysts and their operation. Other challenges are very fundamental, and include the need to move from petrochemical feedstocks to biomass-derived feedstocks.

It is important not to lose sight of the fact that there are likely to be difficulties with the sustainable supply of other elements, and that we need to conserve resources very carefully.

1.6.1 Green Chemistry

The principles of green chemistry highlight very well some of the challenges, opportunities and needs of a good heterogenized catalyst. Green chemistry is a way of looking at chemistry, focussing on developing products and processes which have as little impact on the environment as possible. Of the twelve principles of green chemistry (Table 1.2) several are directly applicable to the concept of heterogenized catalysts. Indeed, catalysis itself is a fundamental aspect, with energy requirements being reduced and the scope for higher selectivity bringing better yields of the desired product (and an increased likelihood of recovering unconverted starting material). Clearly improvements in the separation of the catalyst after reaction has benefits in terms of the recovery of catalyst, reducing catalyst waste and allowing reuse in subsequent reactions. An easily recoverable catalyst will also make the isolation of product (and starting material) easier. All these benefits can help substantially to minimise the waste generated by a process.

However, one aspect of waste reduction must also be borne in mind, and that is the waste generated during catalyst preparation. This is often overlooked

Table 1.2 The 12 principles of green chemistry [1]. The wording has been shortened and the principles (partly) classified in three areas. Those in bold are most inextricably linked to the use of catalysts, but the others are also relevant

Principle	Waste: processing/energy: health/environment
1. **Prevention of waste better than clean-up**	Waste
2. Design of safer chemicals	Health/environment
3. **Less hazardous syntheses**	Health/environment
4. Use renewable feedstocks	Waste, health/environment
5. **Employ catalysis where possible**	Waste, processing/energy
6. **Reduce the use of derivatives and auxiliaries where possible**	Waste, processing/energy
7. Employ atom efficient procedures in the design of synthesis	Waste, processing/energy
8. Use safer solvents and reaction media	Processing/energy, health/environment
9. **Design processes for energy efficiency**	Processing/energy
10. Design processes/products for degradation/ design for end of life	Waste, health/environment
11. Real-time analysis and monitoring of processes	Processing/energy
12. Carry out inherently safer chemistry	Health, processing/energy

(and its impact reduces as catalyst turnover number increases) but it must form a fundamental part of the design and execution of heterogenized catalyst synthesis.

For example, we have demonstrated the potential to recover and reuse template in the synthesis of organically modified mesoporous silicas [24]. Here, the organically modified silica is prepared by a co-condensation of tetraethoxysilane and an organo triethoxysilane in aqueous ethanol at room temperature. 1-Aminododecane is used as a template to direct the pore structure of the material. After reaction, the solid organosilica is filtered and the template removed by ethanol extraction. This gives the product and an ethanol solution of template, which can be used directly (by addition of the appropriate amount of water) in a further synthesis. The more commonly used quaternary ammonium templates can be recovered, but this requires ion exchange and is less straightforward, generating more waste.

A rigorous life-cycle or ecodesign approach is, however, the best way to really define the environmental impact of a given synthesis. However, this is a complex and difficult task, and has rarely been carried out for such systems. A recent paper by Baccile has been published [25], which investigates the synthesis of silica sol-gel materials from an ecodesign perspective. There are a number of suggested routes forward in terms of designing the preparation of silica-based materials covering the source of silica (with TEOS being particularly wasteful due to its synthesis as well as its utilisation – silicates are significantly less of a problem, but are often less amenable to well-controlled syntheses of materials), the nature and conditions of the preparation route, and the use of structure directing agents, all of which can have a significant impact on the overall impact of the preparation. Clearly, the efficiency with which these catalytic materials are used has a similarly significant impact, and therefore design of catalyst synthesis and use must both be considered.

1.6.2 Biomass as Catalyst Support – Towards Sustainable Catalysts

Given the conclusions outlined above, the use of renewable and sustainable raw materials is a major challenge facing the whole of society, and heterogenized catalysts must play a role here too. This means that heterogenized catalysts must be developed that can efficiently convert biomass-derived feedstocks into useful chemicals, but that the catalysts as far as possible should also be derived from renewable and sustainable sources.

1.6.2.1 Biosilica(te)s as Sources of Silica

While silica is thought of as a simple inorganic chemical, it does in fact play an important biological role in many plants, including grasses and related species, as

a structure stabilising agent. Silica therefore forms a considerable proportion of the ash derived from the combustion of biomass. Given that much waste from food processing is burnt to recover energy (e.g. rice hulls, which can have up to 20% by weight silica, [26,27]) and that increasing quantities of biomass is being co-fired in power stations to meet renewable energy targets, it is likely that silica could be obtained from these waste sources and converted into supports for heterogenized catalysts. Examples of such an approach have already started to appear, and some silicas and zeolites have been prepared from bio-silica(te)s. The highly structured mesoporous silica, MCM-41, has been prepared using rice hull ash as a source of silica [28]. Silicas with mesopores have been produced using rice hull ash (rich in silica(te)s) and glycerol as a processing aid [29]. This approach has also been successfully utilised in the synthesis of the zeolite ZSM-5, where Al was obtained from natural clinoptilolite [30].

The varying composition of these bio-derived silica sources is a challenge, as they contain a varying amount of carbon, and also of alkali metal salts such as sodium and potassium. Additionally, the history of the sample is important, in particular whether it has been heated, how long for and to what temperature. All these factors will influence the ease of recovery of the silica in a form suitable for catalyst/support manufacture.

1.6.2.2 Polysaccharide-Derived Support Materials

The use of polysaccharides has been alluded to earlier as a stabilising system for nanoparticles. Almost a decade ago, we developed catalysts heterogenized onto expanded starch, a material with a much higher surface area than native starch, which proved to be useless in this respect. While the expanded catalysts were very active for a series of reactions [31], they suffered from a lack of storage stability. Partial carbonisation of these materials (before attachment of catalyst) led to materials with properties of both starch and carbon, the blend of properties being dependent on the temperature of carbonisation. This led to a series of catalyst supports, which have become known as starbons, and which have much better stability, while maintaining the high surface area and mesoporosity of the initial expanded starches [32]. Recently, this approach has been extended to include other polysaccharides (Fig. 1.3) [33].

Chitosan is a polysaccharide derived from the shells of crustaceans, in which calcium carbonate, proteins and chitin are combined to form the protective shell. Chitin can be converted, by deacetylation, to chitosan, a polysaccharide made up of 2-aminoglucose units. Chitosan has found application in the adsorption of metal ions from water, meaning that it has a natural affinity for such potentially catalytic species. However, the stability of such species is relatively low, and catalytic activity is often poor, meaning that the attachment of ligand systems is preferred to bind the metal more strongly and to enhance its activity. This amine functionality makes it very unusual as a polysaccharide, but is also ideal for attaching catalytic units. Indeed, much of the heterogenization of catalysts on silica employs coupling with aminopropyl-functionalised silicas, and it appears that very similar methods can be directly translated to chitosan (Fig. 1.4).

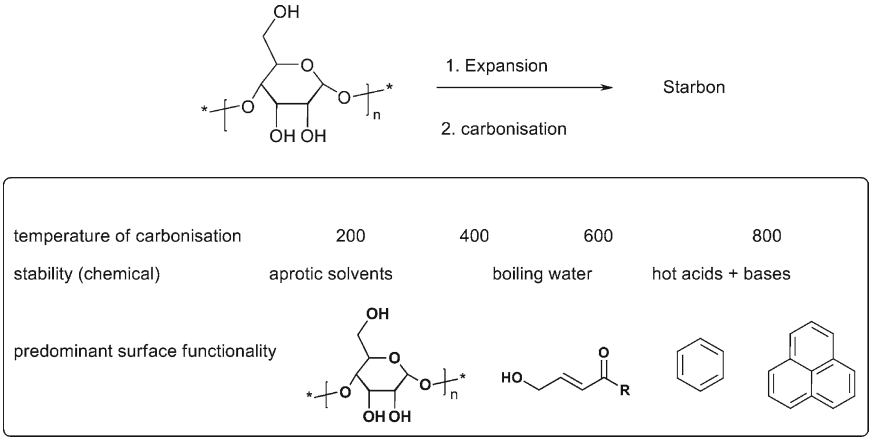

Fig. 1.3 Preparation and characteristics of starbon

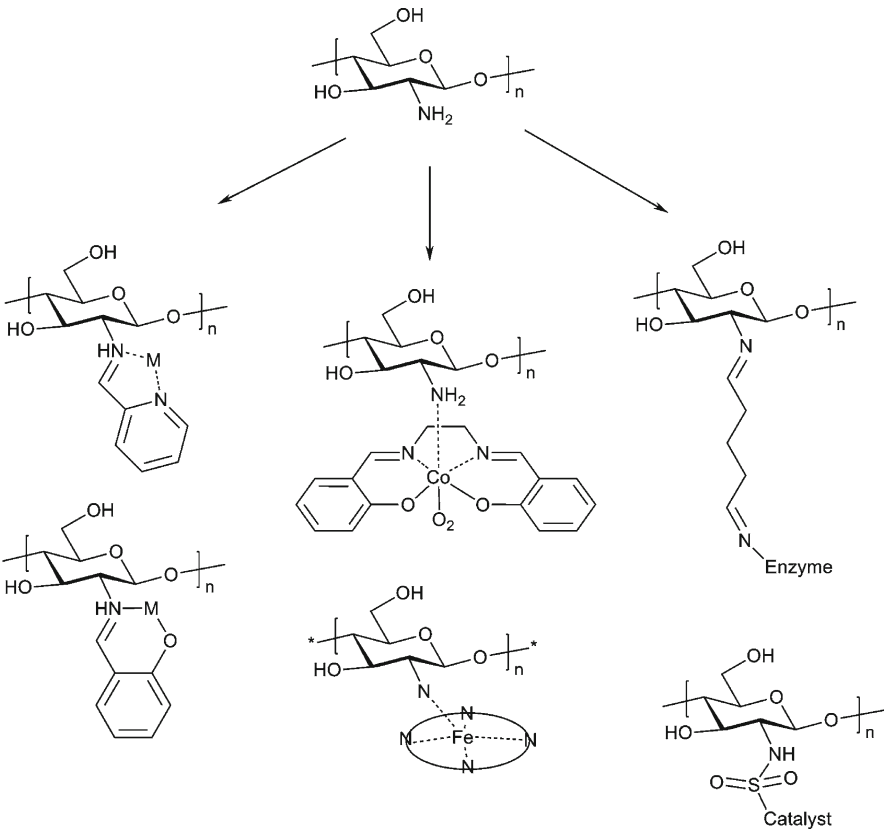

Fig. 1.4 Complexes of chitosan, illustrating strategies for attachment of catalytic units to the polymer backbone

There are many examples of chitosan-based catalysts, summarised in two relatively recent reviews [34]. Chitosan is a low surface area material, which can be expanded using supercritical fluids [35,36], but which can also be converted into a range of forms. This is carried out by dissolving the chitosan in dilute aqueous acid and then precipitating it in various ways. Spraying this solution into alkali leads to beads, the size of which is determined by the fineness of the spray; films and fibres are also readily prepared. Crosslinking, generally using glutaraldehyde, can be used to improve the mechanical properties of these structures if required. Alternative crosslinking can also be achieved by polyvalent anions. Several metal complexes have been attached to chitosan for catalytic applications, and many enzymes have been immobilised on chitosan and used in a range of applications, including catalysis, but also sensing [37].

To this end, salicylaldehyde can be attached readily, as can pyridine-2-aldehyde, leading to N,O– and N,N binding respectively. These have been utilised as bidentate ligands for various metals, and catalytic studies reported. Glutaraldehyde has been used to attach enzymes to chitosan films via imine formation at suitably positioned amine groups on the protein [38]. The amine group has also been used as a covalent linker to $–SO_2Cl$ functionalised phthalocyanin complexes, via sulphonamide formation [39,40]. The amine group has also been utilised as a ligand for the central metal in porphyrins and salen complexes [41,42]. Very little seems to have been done on other complexation routes, despite the rich variety of chemistry available to functionalize the various hydroxyls of chitosan [34].

One of the benefits of using chitosan as a support for such reactions, compared to the more commonly used silica, is that chitosan is stable towards the relatively strongly basic and hard nucleophilic hydroxides and fluoride bases that are ideal especially for the Suzuki reaction. Thus, Barbarella et al. have recently shown that chitosan supported Pd systems (via the pyridylimine route) were particularly good for coupling of thiophenes to give photoactive oligothiophenes (Fig. 1.5) [43]. Microwave activation allowed the reaction to proceed rapidly and in high yield – under conventional heating conditions, the reaction was exceptionally sluggish, with a few percent conversion after 7 days reflux in toluene. In contrast, microwave activation led to the reaction being complete in a few minutes. No leaching was observed, nor was there any solution-phase activity, and the catalysts could be used at least four times with no loss in activity. Longer oligomers (up to 5 thiophenes) were also produced in high yield. The use of

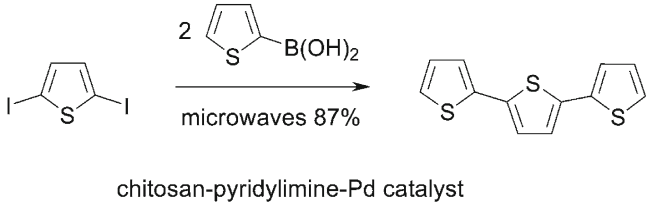

Fig. 1.5 Microwave assisted synthesis of oligothiophenes using a chitosan based catalyst

heterogeneous catalysis for this process resulted in much lower levels of Pd content in films made from the oligothiophenes, something which is very important in their applications. The silica-based equivalents of the catalysts were damaged by the strong nucleophilic bases required.

The use of other polysaccharides as catalyst supports is less well developed, but may also lead to valuable processes. Valentin et al. studied a range of expanded polysaccharides for allylic substitution reactions, catalysed by the water-soluble Pd $(TPPTS)_3$ complex (TPPTS is a sulphonated equivalent of triphenylphosphine) [44]. They found that alginates (which contain carboxylic acid groups) were better than carageenan, which was in turn better than chitosan, in the Pd catalysed allylic substitution reaction. Activity was a function of the electrostatic nature of the support, while relatively low turnover numbers were also ascribed to the relatively basic environment, known to discourage this particular reaction. No enantioselection was observed during the reaction, despite the chiral nature of the support (Fig. 1.6).

1.6.3 Catalytic Conversion of Biomass

The conversion of biomass and biomass-derived raw materials should not be fundamentally different from petrochemical-derived materials, although variability and purity can be a major issue. To minimise waste in the purification and separation of complex biological mixtures, and to cope with subtle (and sometimes not so subtle) differences in composition from one source to another (or even from one time of year to another), biomass derived raw materials present significant challenges to catalysts in terms of reproducibility between different sources of the same raw material, and the lower purity that is often available. The challenge here is to cope well with the variability in feedstocks without compromising product quality or yield. Thomas et al. have published an interesting article which sheds light on the design of solid catalysts for biomass conversion [45].

Fermentation of biomass is a promising route to converting sugars into useful platform molecules, from which a range of other products can be produced.

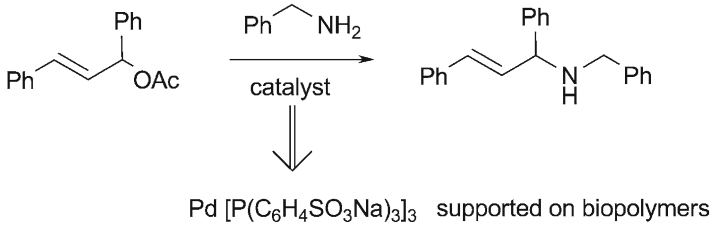

Fig. 1.6 Biomass supports in the allylic substitution reaction

While fermentations typically run in water around ambient temperature, making them safe and relatively environmentally friendly, they suffer from the difficulties in isolation of the products from the complex matrix of cells, nutrients etc. which is present in the mixture. Purification directly form this mixture is difficult and costly, and therefore a big challenge which lies ahead is developing methodologies to improve this situation. One approach which has met with some success is to design catalysts which will operate in fermentation broths, to produce useful products which are more readily separated (e.g. by virtue of their much lower water solubility).

Starbon-sulfonic acid, prepared by direct sulfonation of starbon (discussed above) leads to a heterogenized version of sulfuric acid on the surface of a partially carbonised mesoporous structure. Depending on the temperature of the carbonisation, the surface can be saccharide-like (rich in oxygen functionality such as alcohol, ketone and acid/lactone) or carbon like (rich in aromatics with few oxygen functionalities). Hydrophobicity can be relatively high. Budarin et al. found that these materials were excellent catalysts for carrying out esterifications in water, despite water being the "wrong" solvent for such reactions [46]. Succinic acid was doubly esterified to diethyl succinate effectively in a mixture of water and ethanol using starbon sulfonic acid, whereas other solid acids produced only some monoester, and at best a few percent of diester (Fig. 1.7). Homogeneous acids likewise gave some monoesterification, with the hydrolysis of esters being dominant. It is thought that the hydrophobic nature of the pores in the catalyst provide an environment with much less water than in the bulk, allowing the formation of diester, which subsequently leaves the catalyst to the solution phase (where there is no acid catalyst to hydrolyse it back). Running reactions in water is beneficial as it is a cheap, non-flammable, non-toxic solvent, but also because it allows combination with fermentation processes, in which several valuable platform molecules can be produced [47]. The downside of fermentation is that the isolation of the water soluble products from the complex broth is often exceptionally difficult and consumes considerable quantities of energy and auxiliaries. Converting the product directly in the broth to give a water-insoluble product allows for much easier separation, but requires chemistry that works effectively in water. Given the role of water in esterification is to reverse the reaction, the catalyst must not only be effective in catalysing the reaction, but also be capable of having a relatively water-free environment close to the active sites, so as to push the equilibrium position towards product.

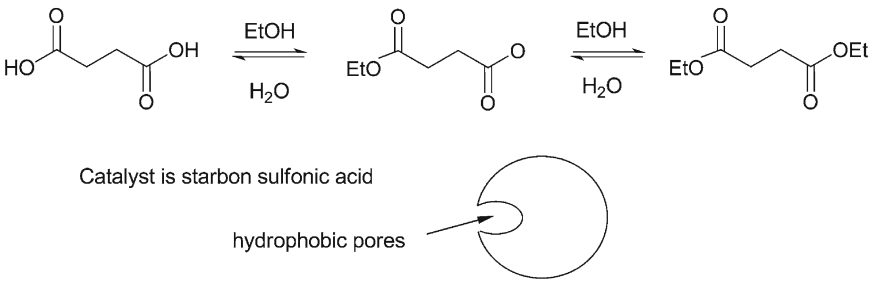

Fig. 1.7 The diesterification of succinic acid in aqueous environments using starbon sulfonic acid

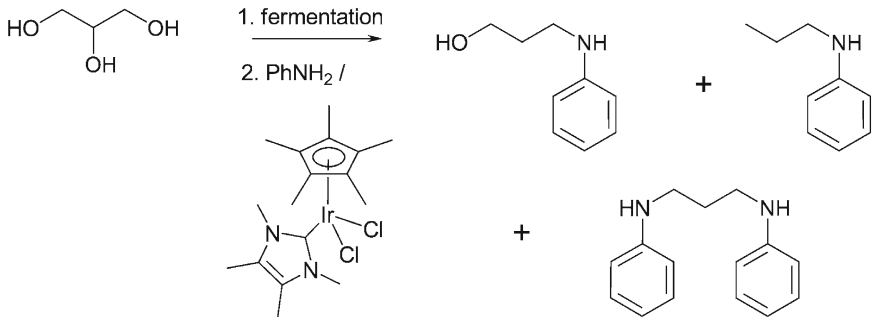

Fig. 1.8 One pot fermentation and catalytic conversion of glycerol to amino alcohols and diamines

Control over surface chemistry as well as over the active site is therefore a clear challenge to allow such processes to function.

The groups of Stephens and Marr have collaborated to provide routes to convert 1,3-propane diol in situ to readily separable products (Fig. 1.8) [48]. They combined a fermentation of glycerol (and this includes crude glycerol waste from biodiesel production) to give 1,3-propanediol with a catalytic hydroamination reaction on the centrifuged fermentation broth. The catalytic conversion, based on oxidation, imine formation and reduction, allowed direct conversion to substituted arylamines. Initial experiments were carried out using toluene, but replacement of this solvent due to cell toxicity with an ionic liquid led to a process that could be carried out in the presence of living cells.

The above examples indicate some of the approaches which are being taken to ensure the sustainability of carbon as a resource for chemistry, and for society in general. However, it is clear, but not always appreciated, that other elements are also "at risk" in terms of sustainability. One very apposite example in the realms of catalytic chemistry is phosphorus, where economically viable supplies are expected to run out this century [49]. "Peak phosphorus" is expected to occur around 2030 with resources dwindling thereafter [50].

1.6.4 Flow Reactors and Continuous Processing

Green Chemistry is also concerned with safe and efficient processes, and the containment of reaction mixtures as well as the development of safer, less environmentally damaging products. One area which addresses both concepts is continuous processing using flow reactors. The added impetus in this area recently along with some of the fundamental concepts of flow chemistry have been well documented in a very recent book [51]. Catalysts can be readily included in the flow unit if heterogenized onto a solid support, although there are additional considerations in terms of particle size which can be critically important (see below).

In terms of process safety, the notion of flow reactors is important, as they allow for the continuous conversion of raw materials to products using a relatively small volume and reaction times of seconds or minutes. As the reactants are only at a high temperature for a short period, then selectivity can be higher than it would be in a batch reactor at the same temperature (due to the longer residence time of the batch reactor). The much smaller reactor size (typically at least one order of magnitude and often 2–4) means that, if a problem does arise, there is far less material affected and any accident is much smaller. The far higher surface to volume ratio of the flow reactor, coupled with often better mixing, means that thermal runaway is far less likely. Indeed, a move towards flow reactors has been the key to solving some serious problems with very exothermic reactions. For example, the thermal cyclisation shown in Fig. 1.9 is very exothermic, and batch processing of this reaction proved to be very challenging. Bristol-Myers Squibb therefore developed a continuous process (non-catalytic) to carry out the reaction. Not only did they manage to achieve excellent temperature control, but they also avoided the need for solvent (present in large quantities in the batch process) and achieved very high yield [52].

1.6.4.1 Flow Reactors and Heterogenized Catalysts

As discussed above, the use of flow reactors can have significant benefits in the processing of fine chemicals, despite there being still relatively few examples of this happening. There are additional benefits that are available from the combination of flow reactors and heterogenized catalysts. Incorporation of the catalyst within the flow reactor means that the reagents flow through the catalyst bed, which remains in the reactor. Therefore, there is a simultaneous reaction and separation, making downstream processing even easier. In addition, some reactor configurations (such as a fluidized bed system) will provide much enhanced mixing, as the catalyst particles help to agitate the liquid phase. An additional feature is that there is a far higher catalyst to substrate ratio at any given time than there would be in a batch process. Short residence times minimise thermal decomposition of starting materials and products, meaning often that reaction temperature can be higher than in batch mode. All these features will help in reducing residence time and allowing for good levels of conversion with very small reactors.

A nice example of what can be done (in this case with a microreactor) has been provided by Fan et al. [53]. Firstly, they carried out a Heck reaction to give 1,2-diphenylethene using Pd on C particles in a compact flow reactor, and then extended this work to add a second stage where they hydrogenated the alkene to

Fig. 1.9 Thermal cyclisation of propargyl ethers carried out in a continuous manner. Excellent control over exotherms was achieved even with no solvent

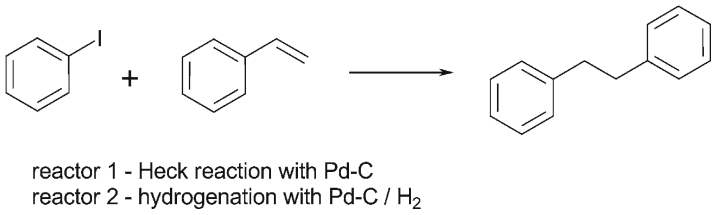

Fig. 1.10 Continuous conversion of styrene and iodobenzene to 1,2-diphenylethane via consecutive Heck reaction and hydrogenation in a flow reactor

give 1,2-diphenylethane, again using Pd on C (Fig. 1.10). This sequence required linked flow reactors with hydrogen being introduced after the first reaction. Excellent results were obtained for the overall reaction sequence, indicating the potential of a direct and very a simple process, avoiding intermediate isolation of the alkene. It was important for the flow system that the particle size of the catalyst support was sufficiently large to allow a reasonable flow – smaller particles led to significant pressure issues. These are not unexpected in a flow system, and this puts an added onus on the design of a heterogenized catalyst in that control over morphological properties is an important consideration. Indeed, the development of a heterogenized catalyst based on a monolithic support is considered to be particularly advantageous for combining high surface area with very low pressure drop (meaning the mixture can be pumped readily through the catalyst bed) and excellent catalytic activity.

As an alternative approach to a particulate or monolithic catalyst bed, it is possible to simply coat the walls of the reactor with catalyst in order to contact the reaction mixture. This is often challenging, particularly for microreactors with very narrow channels, but less so for larger reaction vessels, although residence time here may be significantly longer. For example, Bacheva and Macquarrie prepared a chitosan-subtilisin catalyst immobilised on a reactor wall, which was effective for the formation of peptides (under non-aqueous conditions) and for the hydrolysis of peptides (under aqueous conditions) [54]. This work relied on the ability of chitosan to adhere to surfaces and form a thin film from solution. Subsequent crosslinking and attachment of the enzyme to the film resulted in a stable and active catalytic film, which performed well in both aqueous and non-aqueous environments (Fig. 1.11).

After Merrifield's pioneering work on resin beads for peptide synthesis, it is perhaps not surprising that there are several examples of polymer-supported catalysts operating under flow conditions. Examples include the use of supported borane complexes of amino acids for enantioselective Diels-Alder reactions [55], and the enantioselective addition of diethylzinc to aldehydes [56,57]. Polymer monoliths have also been developed and used (Fig. 1.12) [58].

Supercritical fluids have particularly good diffusion properties, and their combination with solid catalysts has already produced very impressive results, including an industrial process. They are also well-suited to flow processes, and therefore can combine several advantages. Poliakoff and co-workers have developed a continuous

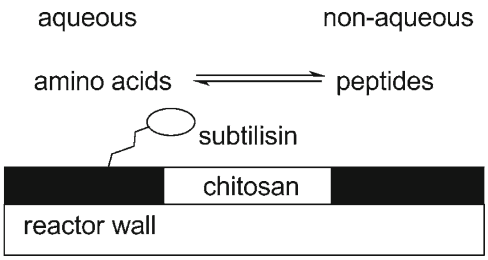

Fig. 1.11 Schematic of a surface coating of chitosan-subtilisin catalyst, and its use in peptide synthesis and hydrolysis

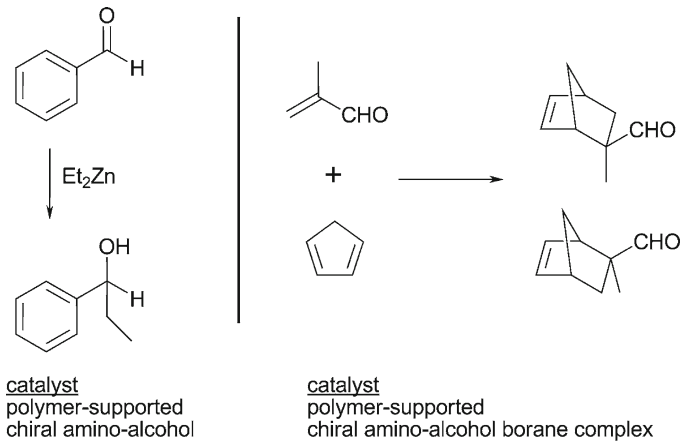

Fig. 1.12 Examples of enantioselective reactions catalysed in flow reactors using polymer bound reagents

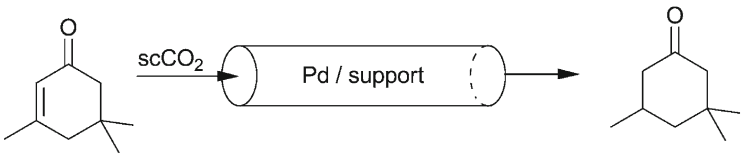

Fig. 1.13 Continuous hydrogenation process utilising supercritical fluid and a flow reactor

hydrogenation process (Fig. 1.13), commercialised by Thomas Swann, based on the use of a supported hydrogenation catalyst and supercritical CO_2 [59].

The same group have also developed a continuous process for the hydroformylation of octene based on a supported rhodium complex of the biphosphine shown in Fig. 1.14. the supercritical fluid provided a reaction medium capable of solubilising

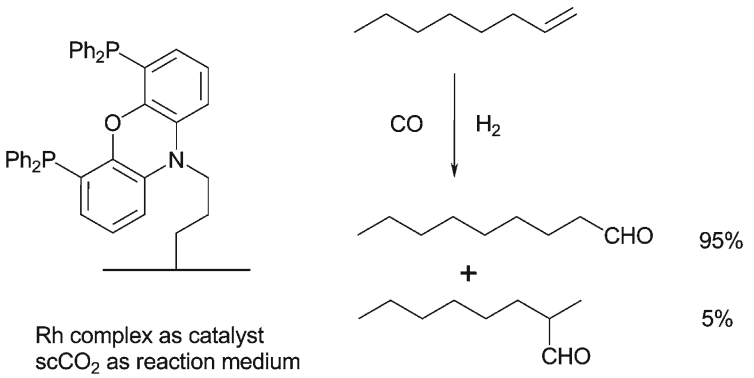

Fig. 1.14 Continuous hydroformylation using supported Rh complex in supercritical carbon dioxide

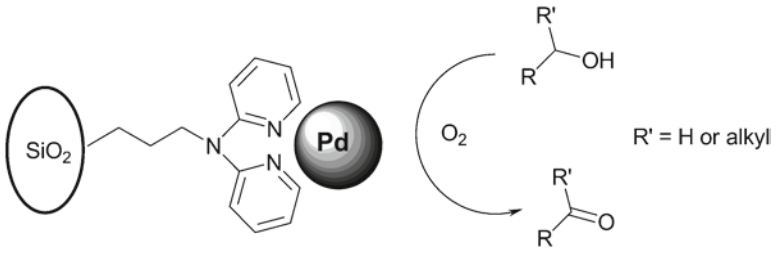

Fig. 1.15 Continuous catalytic oxidation of alcohols to aldehydes and ketones in supercritical CO_2

all the components very well, leading to an excellent reaction, and the catalyst proved to be very robust towards leaching [60].

Hou et al. have developed a supported oxidation catalyst, based on palladium, which has excellent activity in the selective oxidation of alcohols to aldehydes and ketones [61]. A continuous processing mode was shown to be effective with the heterogenized catalyst shown in Fig. 1.15.

All these examples make use of the complete miscibility of gases (CO, hydrogen and oxygen respectively) in supercritical fluids, which is much higher than that found for conventional solvents (where solubility of gases is generally very low indeed), as well as the ability of supercritical fluids to enhance mass transport through porous solids [62,63].

In addition to the flow reactors described above, alternatives such as the spinning disc reactor (to which catalysts can be attached) and membrane reactors are both alternative reactor set-ups which can deliver excellent performance, and often get the most out of catalysts immobilised within them [64,65].

1.7 Optimisation of the Catalyst Support and Support–Catalyst Interaction

The development of a successful heterogenized catalyst depends on close control over the nature of the support and the access to the active sites that is afforded to substrates and escaping products. Pore size, connectivity and surface area can be chosen and controlled more easily than ever before. The surface chemistry is also a very valuable and important feature, and control over the interactions of the surface with the catalyst, and directly with the reagents/products and co-products is also crucial.

1.7.1 Access to Active Sites

One of the key features of a heterogenous catalyst is the influence of mass transport, in particular the issues relating to diffusion into, within and out of the pores of the material. With the ability to tune pore size (and also to be able to choose between different types of pore geometry and connectivity) comes the requirement to be more aware of the influence (positive and negative) that diffusion can play in a reaction, in terms of rate and selectivity.

Diffusion rates have been measured in porous systems using techniques such as pulsed-field NMR, with somewhat surprising results. Generally speaking, one would expect that, for a given pore size, larger molecules would diffuse more slowly than smaller ones, and that diffusion would never be faster than in the bulk liquid that makes up the solvent. This is broadly true, but for small. Relatively volatile molecules, there seems to be an exception.

Hansen and co-workers found than *n*-hexane diffuses faster in small channels than in larger ones, something that they ascribed to the increased influence of surface polarity in smaller pores, where *n*-hexane will have more interaction with the pore walls [66]. The diffusion of benzene in mesoporous channels was found to be even faster than in bulk liquids [67]. Here, the unusual results was considered to be due to a gas-like diffusion within the channels, suggesting that the resistance to movement provided by solvent molecules has diminished significantly within the pores. Larger, analogous molecules with lower vapour pressure behaved more "normally" and diffused more slowly than in bulk liquid.

Within a pore, the radial distribution of molecules could be affected, with more polar molecules being attracted to the polar walls of the solid. This may have an influence on the effect of solvent on reaction progress, which may deviate from that found in the bulk. Such a situation has been documented. A combination of EPR and NMR was used to investigate the distribution of cyclohexane and 2-propanol within the pores of a mesoporous silica. It was found that the polar alcohol was preferentially found close to the walls of the silica, while the non-polar cyclohexane was mainly situated in the centre of the pores [68]. While this stops short of an actual separation of solvents within the pores to the total exclusion of one, it does

indicate that the various components of a reaction mixture may not be distributed ideally, and that the correct choice of solvent may be more critical than in homogeneous situations. Situations with one polar and one much less polar reactant might be especially tricky. The ability to modify surface polarity through spectator groups has already been discussed, as have the PMOS, which have significantly lower wall polarity, although they have had limited use as catalysts so far, there is no reason that catalytic groups could not be attached, either via the usual silane route, or via more sophisticated and functional bis-silanes. There may be much to be gained out of tailoring surface polarity more carefully with reactant and product polarity, although there is likely to be much complexity too, as is found in solvent effects.

Recent developments in fluorescence spectroscopy has allowed unprecedented insights into the activity of zeolites to be obtained [69,70]. The group of De Vos has provided evidence for the distribution of activity within a crystal of ZSM-5. Their findings indicate that the majority of reactions catalyzed by this zeolite occur very close to the external surface of the crystal and that the majority of the pore channels are not utilized effectively. This highlights the strong diffusional constraints arising form the narrow channels of the zeolite, and suggests that activity could be higher if more of the pore structure were accessible.

Such results hint at the potential of hierarchically porous materials, where the micropore structure is connected to a wider mesoporous (or macroporous) network, allowing transport within the larger pores throughout the solid, and allowing access to a greater number of micropores.

In order to preserve the benefits of the micropore-confined catalysis (generally unusual and unusually high selectivity) it is clear that the active sites must be confined within the micropores, and that the interconnecting channels cannot have the same active sites. Control must be exercised over the distribution of active sites (in some cases such as ZSM-5, this is likely to be relatively straightforward), as the particular structure of the acidic centre is partly dependent on the precise geometry around the active site – most mesoporous aluminosilicates (e.g. MCM-41) have much lower acidity. Nonetheless, extending this idea to a wider range of catalysts will require a very well designed material.

Approaches to such hierarchically porous materials typically include the use of a template (such as carbon microspheres) around which the material crystallises. Removal of the template by combustion or by dissolution provides the larger connecting pores. Fine tuning of this approach has been demonstrated whereby selective desilication can tune the mesopore dimensions in a hierarchically porous zeolite beta [71].

1.7.2 Catalyst Robustness

The synthesis of a heterogenized catalyst is not trivial. As has been discussed above, it is very important to provide a catalyst with the correct macroscopic dimensions (monolith vs. particulate) particle size, porosity, surface area, surface chemistry and the correct loading and distribution of sites all must be combined

with the correct reaction conditions, temperature, solvent and nature of reactor (flow, batch, nature of agitation). One crucial aspect remains if any of the preceding is to have genuine value, and that is catalyst robustness. High turnover number (and if at all possible, high turnover frequencies) are very important, so as to maximise the benefit of the extra steps involved in heterogenizing a catalyst and therefore it is vital that the deactivation processes are examined to see whether or not they are reversible, and to develop methods for re-activation where possible. Indeed, part of the strategy for the development of a second generation catalyst should be to avoid the deactivation mechanisms of the first generation catalyst where at all possible, or at least to make regeneration easier and more effective. It is important, having measured reuse to the point where the catalyst has lost significant activity, that steps are taken to decide why the activity has been lost. It may be a simple case of pore blocking, or it may be that an irreversible reaction has taken place which cannot be rectified.

We encountered both examples in the case of silica-supported amine catalysts in the Knoevenagel reaction. For aminopropyl groups grafted onto silica supports, the amine group is basic and is an excellent catalyst for the Knoevenagel reaction. However, the amine is also a good nucleophile and slowly reacts with the ester of the reactant (and of the product) to give the supported amide, which is non-basic and not readily hydrolysed without real damage to the catalyst [72]. Fortunately, when the "same" catalyst is prepared by a direct sol-gel route, the catalyst is still basic, but the amine group is not nucleophilic, and this deactivation mechanism does not operate. This means that the turnover number is much greater [73]. (The provision of phenyl spectator groups decreases surface polarity and minimises the rate of deactivation even further [74]). The spent catalyst suffers from pore blockage due to small amounts of a polar intermediate which can be removed by prolonged solvent extraction, regenerating most of the original activity. Similarly, a supported Pd catalyst for the Heck (check) reaction was found to be deactivated by build up of quaternary ammonium salts (a co-product of the reaction) – these were removed by a simple wash with methanol, and the catalyst activity restored [75]. It was also found with this catalyst that the pre-treatment protocol was crucial in order to avoid leaching (see below). Reflux with three different solvents was required (3x acetonitrile, 3x toluene and 3x ethanol) to eliminate loosely bound Pd species and make the catalyst genuinely heterogeneous. Each solvent appeared to remove a different species from the surface, possibly due to differences in solubility or stability. Such pre-treatment is critically important, and often it may be that the best way is to carry out the desired reaction as a pre-treatment, as any loose material should be removed by conditions as close to reaction conditions as possible.

Particle attrition by physical abrasion (stirring) or chemical decomposition is another factor which can be a problem, and can limit the range of conditions under which the catalyst can be used. Here, the choice of reactor type and solvent/temperature can be critical.

However, perhaps the most crucial aspect of catalyst stability is leaching. Is the catalyst genuinely acting as a heterogeneous catalyst, or does it just function as a source of trace quantities of a homogeneous catalytic species. If the latter is true, is

there any advantage to having heterogenized the catalyst in the first place. If there are unexpected features of the catalysis caused by a gradual leaching of the catalyst, then there may well be advantages, but these will never be appreciated or exploited properly if they are not recognized as being due to a gradual leaching of a (probably) unknown active species.

One of the key difficulties presented by testing for leaching is that tiny quantities of leached species can be responsible for considerable levels of catalytic activity. In the case of homogeneous Pd catalysis, where the oxidation state oscillates between 0 and +II, there is a relatively complex relationship between amount of Pd present and activity/longevity. Higher amounts of Pd will give faster rates initially, but the Pd(0) species are likely to coalesce into bulk Pd, unless there is good reason for this not to happen. The bulk Pd, due in part to its low surface area, is a poor catalyst, and therefore activity is short-lived. However, very low concentrations of Pd are much less prone to coalescence, and therefore remain in an active state for longer. Therefore, trace quantities of Pd coming off a surface could actually give surprisingly "good" results, even though the catalyst would actually not be functioning as desired.

It is for reasons such as the above, that simply analysing for leached species is not sufficient to determine whether there are tiny quantities of leached material causing the catalysis to proceed via a homogeneous route. Alternative methods must be followed in conjunction with careful analysis of the reaction system. However, the analysis of leached species is important in that there may be inactive species being leached from the surface which may impinge on the utility of the final product of the reaction, even when the catalysis itself is entirely heterogeneous.

The first real attempt to define leaching was provided by Sheldon and Lempers and is well known as the hot filtration test [76]. This test requires that the heterogeneous catalyst be removed from the reaction mixture *under reaction conditions* and the reaction continued uninterrupted in the absence of catalyst. If the reaction proceeds, then it can be concluded that at least some of the activity of the catalyst was due to leached species. This test has been broadly accepted, although it suffers from some drawbacks and is not a complete definition of the problem. It can be tricky in a practical sense, to completely separate catalyst from the liquid phase without running the risk of changing reaction conditions (and thereby precipitating solution phase catalytic species) or leaving very small particles in the liquid phase. The former could make the reaction appear heterogeneous when it is not, and the latter homogeneous when it is not. The test does not detect leaching of inactive species, nor does it account for the potential that the catalyst may be acting as an initiator rather than a true catalyst. If this is the case, then the role of the catalyst would be to generate an active species which can lead to product and regenerate itself without the involvement of catalyst. Radical polymerisations and radical oxidations both could potentially fall under this category, and the test should be carried out with such mechanistic considerations in mind. Nonetheless, the test is an important one, and when carried out correctly, and interpreted correctly, can provide important information relating to catalytic activity.

Alternative approaches to the determination of leaching include the incorporation of a supported catalyst poison, such that any leached material is quickly adsorbed from solution, hindering solution phase catalysis, and trapping the leached species for subsequent analysis. This may be useful, but it is essential to ensure that the poison does not become active on adsorption of the soluble catalyst. For example, Webb et al provided a very nice study of catalyst stability and leaching in which they utilised a Pd catalyst supported on a mesoporous silica via mercaptopropyl groups [77]. The mercaptopropyl material was initially developed as a scavenger for soluble Pd, but was found to be an effective catalyst in its own right [78,79]. In addition to the hot filtration test, they carried out the "three phase test" which has been developed for soluble Pd species, but which could be adapted to other systems [80,81]. This test requires that a supported system be prepared where a surface bound group can undergo the same reaction type as that in solution [82]. For example, in the case of the Suzuki–Miyaura reaction, a supported haloarylamide can be prepared on a solid support. If there is leaching of active Pd from the heterogenized catalyst into solution, then the soluble catalyst can migrate to the haloarylamide and carry out the Suzuki–Miyaura reaction on it. Analysis of this solid directly, or cleavage of the surface bound groups will provide evidence for or against products which can only have been formed by homogeneous catalytic routes. A heterogeneous Pd species would not be able to contact the other solid and carry out this reaction, thus proving heterogeneity or not (Fig. 1.16).

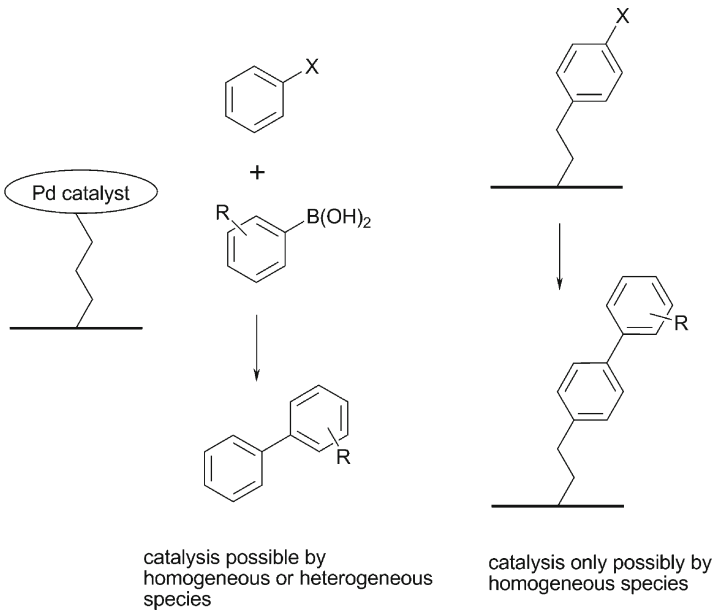

Fig. 1.16 The three phase test for catalyst heterogeneity

1.7.3 Spectator Groups and Control Over Surface Chemistry

The active site of a catalyst is generally carefully designed to ensure optimum activity and selectivity. When attaching this to most surfaces, the catalyst will experience an environment quite different to that in a typical organic solvent (the medium where the catalyst was originally designed to work). While polymer matrices are similar to organic solvents in their nature, inorganic polymeric matrices such as silica are significantly different, being more polar, often very hydrophilic and containing significant amounts of water, as well as a series of different environments, all of which can have an influence on the activity of the catalyst, even before notions of accessibility due to pore structure are taken into account. The influence of these surface features must be considered and controlled wherever necessary.

One approach which is relatively simple, but often quite effective is the attachment of so-called "spectator groups" to the catalysts surface. These groups are typically non-active themselves, and are thought to modify the catalyst surface by reducing polarity, thereby improving adsorption/desorption processes and minimising catalyst – surface interactions. Examples are known for acid, base and metal-centred systems, and the spectator groups can be readily incorporated in a sol-gel synthesis.

Perez-Pariente has demonstrated the use of methyl groups as spectator groups in the sulfonic acid catalysed esterifications. They found that the optimum ratio of methyl to sulfonic acid led to a threefold enhancement in rate [83,84].

The use of propyl functionalities along with short chain perfluorinated sulfonic acids significantly enhanced the rate of Friedel-Crafts acylations and the related Friedel-Crafts reaction between 2-methyl furan and acetone. The smaller methyl spectator group had little if any effect on rate. Selectivity was unaltered [85]. Examples of spectator group enhanced reactions are given in Fig. 1.17

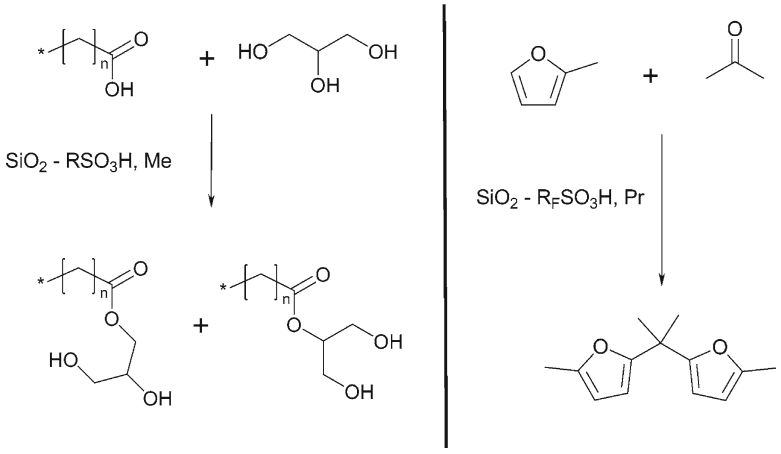

Fig. 1.17 The enhancement of rate in acid catalysed reactions through the use of spectator groups. In both cases significant rate enhancements (6–10×) were seen with the incorporation of the non-active alkyl groups

Pd nanoparticles adsorbed onto a silica surface have been used as catalysts in the Ullmann coupling of halobenzenes to give biphenyls [86]. The inclusion of phenyl groups on the catalyst surface was shown to slightly increase activity, but the major positive effect was to almost completely suppress the reduction of the halobenzenes to benzene (Fig. 1.18).

One of the most challenging areas of catalysis in terms of selectivity (and therefore control over catalyst properties and environment) is enantioselective catalysis. While excellent selectivities are possible using homogeneous systems, the high enantioselectivities are often not reproduced when the catalysts are tethered to an inorganic support. This is perhaps not surprising, as the presence of a very large, extremely polar "ligand" in the form of a silica wall is very different to the environment provided by a typical organic solvent. However, careful work has shown that such high enantioselectivities can indeed be achieved, and can sometimes be better than those obtained under conventional conditions. Thomas et al used a ferrocenyl bisphosphine based catalyst for the allylic amination reaction, and found a number of interesting phenomena [87,88]. Firstly, the regioselectivity of the reaction is significantly different, with the linear product being favoured in the homogeneous case, while the heterogenized version (in MCM-41) gave high levels of the branched product. Enantioselectivity was excellent in the MCM-41 case, but was absent in the homogeneous system (Fig. 1.19). On attachment

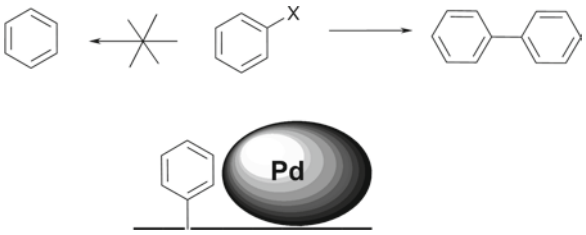

Fig. 1.18 Ullmann coupling using phenyl modified silica. In the absence of the phenyl groups, the reduction to benzene is a significant pathway

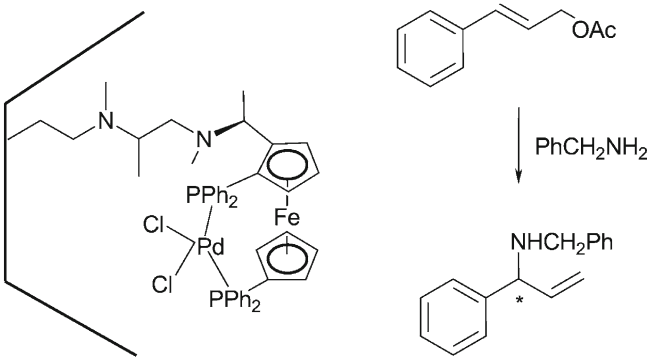

Fig. 1.19 Highly enantioselective heterogeneous catalyst for the allylic amination reaction

to a different, less structured silica, enantioselectivity dropped to 45%. These results indicate that, while the attachment of an enantioselective catalyst to a solid surface can often reduce enantioselection, it can provide excellent and enhanced selectivity if the correct combination of pore structure, surface interactions and spatial confinement are found.

1.8 Telescoped/Multi-step-One Pot Synthesis

An important challenge is to develop syntheses which as are streamlined as possible. Currently, most multi-step procedures are carried out with an isolation stage after each reaction. This is wasteful, although it may be necessary to remove some of the unreacted raw materials and undesired side-products before the next stage. However, this is often not required, and the benefits of integrating (or telescoping) two or more steps into one reaction are significant. Heterogenized catalysts allow an excellent opportunity to do this, as two or more can be added to a reaction sequence, either at the start, or at appropriate points. Used catalysts can be removed by in-line filtration for reuse, or left in the pot if necessary. Two catalytic sites can also be present on the same support, something which may improve transport properties and speed up consecutive conversions. Flow reactors are particularly well suited for such approaches, as a series of flow reactors can be set up, each with the appropriate catalyst present. In batch reactors, strategies can be envisaged where each catalyst could be isolated separately as required – differences in particle size or density could be exploited [89,90], magnetic catalysts can be utilised [91,92]. A recent example of this approach has been provided by Che et al. [93]. They attached the Hoveyda-Grubbs catalyst to monodispersed iron nanoparticles functionalised with aminopropyl trimethoxysilane, and used the resultant catalyst to carry out metathesis reactions (Fig. 1.20). Recovery of catalyst was achieved by simply dipping a magnetic bar into the reaction mixture; reuse was demonstrated for 22 cycles.

Alternatively, a series of catalytic surfaces or membranes could be used. The catalyst in a tea-bag approach where catalysts are held within dialysis membranes would also be amenable to multiple stage reactions [94].

“Switching” catalysts on or off as required is more difficult to envisage, although such a possibility would be useful in minimising cross-catalysis, where the products from one step may be converted by the “wrong” catalyst. Such control over activity would be valuable. Some research into pore opening and closing via external stimuli has been published – e.g. photodimerisation of coumarins [95,96], pH changes [97], and nanoparticle based gates [98], and this may lead to viable routes to switching catalytic activity on and off, given that all catalytic groups exist within the pore network.

Bifunctional catalysts, where the catalytic groups are in close proximity to each other could be particularly valuable where a product is liable to side reactions, and subsequent conversion without isolation is desirable. For example, Goettmann et al have demonstrated a bifunctional catalyst for base catalysis and hydrogenation which addresses such an issue [99]. The Knoevenagel reaction is a well tested

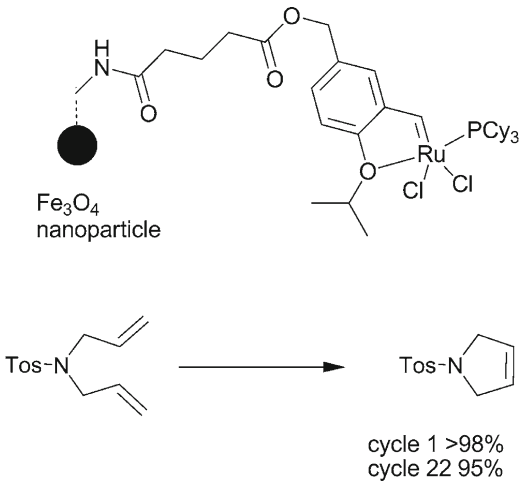

Fig. 1.20 Magnetically separable Hoveyda-Grubbs catalyst for metathesis

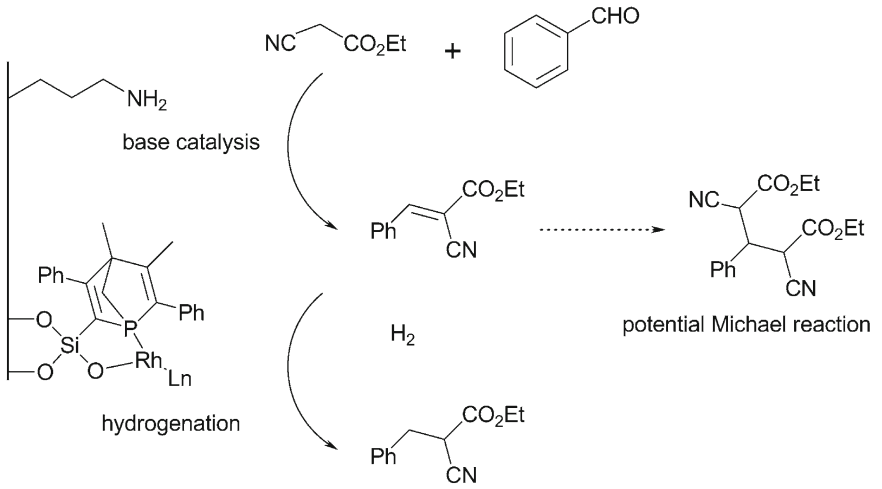

Fig. 1.21 Bifunctional catalyst for the sequential conversion via Knoevenagel condensation and C=C reduction

reaction in base catalysis, but can suffer from selectivity problems, particularly in respect of the potential of the Knoevenagel product undergoing a subsequent Michael addition. The effective base-catalysed condensation forming this product was followed by a direct hydrogenation within the same catalytic material to reduce the double bond, and therefore minimise the likelihood of an undesired further reaction (Fig. 1.21).

The ability to have two mutually incompatible functionalities on the same surface has been demonstrated by several groups. Alauzun et al. prepared a mesoporous silica containing both strongly acidic sulfonic acids and amines, which did not

neutralise each other, giving strong evidence for spatial separation [100]. The precursors to the acid and base groups were the disulfide and the Boc-protected amine respectively, eliminating the possibility for acid–base interaction before materials synthesis. Subsequent oxidation of the disulfide and deprotection of the amine gave the final material, in which the amines were active nucleophiles, adding efficiently to acrylamide (Fig. 1.22).

The Davis group has also synthesised bifunctional catalysts, based on varying strengths of acid and base [101,102]. The common feature in these systems was the amine group, but materials containing this group together with a weak acid (carboxylic) a moderately strong acid (phosphonic) and a very strong (sulfonic acid) were prepared. In each case, the amine and acid sites were independent, and could be selectively neutralised, the amines with added *p*-toluene sulfonic acid, and the acids with propylamine (Fig. 1.23). Catalytic reactions on the condensation of nitrobenzaldehyde with acetone using these systems showed improvements on similar materials with only acidic or basic sites.

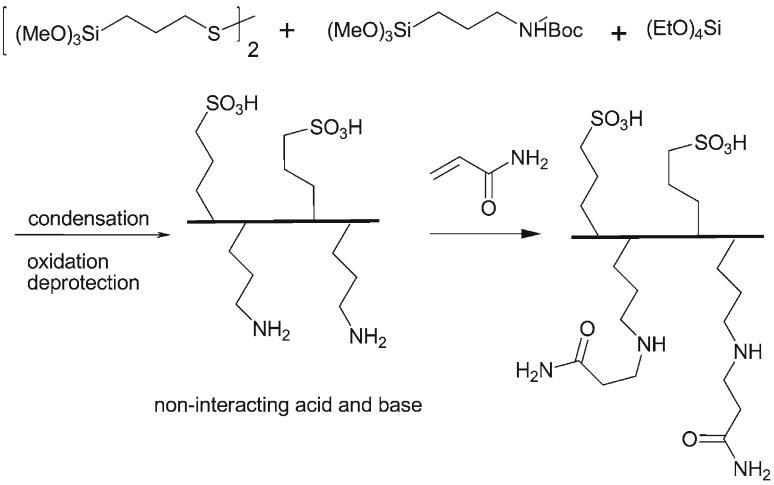

Fig. 1.22 Bifunctional acid/base material with no interaction between acid and basic sites

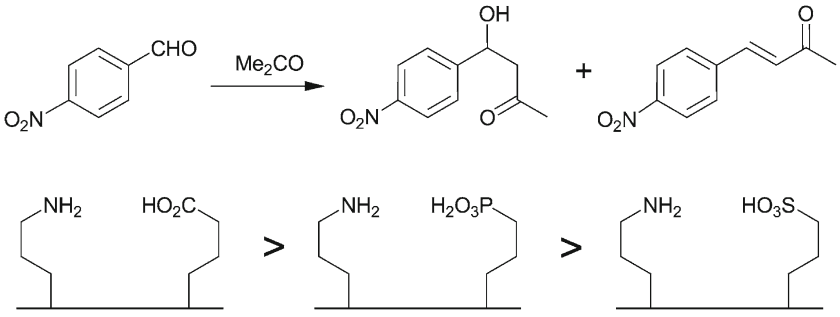

Fig. 1.23 Bifunctional catalysis of the aldol reaction

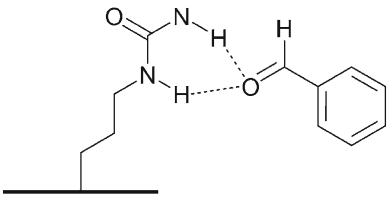

Fig. 1.24 Activation of an aldehyde by a surface bound urea

A related concept has been developed by Huh et al. who combined a basic amine unit (to deprotonate nitromethane) with a surface bound urea in order to provide H-bond activation of aldehydes and showed that the resultant material was an excellent catalyst for the addition of nitromethane to aromatic aldehydes [103]. The catalyst was also active in cyanosilylations and aldol reactions (Fig. 1.24).

1.9 Conclusions

Hopefully, it is clear from the above that there is a great deal that can be achieved by the heterogenization of catalysts onto solid supports. Considerable progress has been made over the last few decades, and much remains to be achieved. There are great opportunities in every direction, from the fundamentals of catalyst design, characterisation right through to their application in fine chemicals synthesis, whether following the traditional petrochemicals routes or taking the challenge of the more complex and variable biomass derived systems and playing a part in the valorisation of this century's raw materials.

Advances in the chemistry of materials have been very rapid over the last couple of decades, and this promises to be a valuable source of inspiration and added levels of control over what is achievable. While the developments in silica chemistry have been grasped enthusiastically by the heterogenization community, there are many more opportunities there in terms of alternative supports, whether they are biomass derived (silicas or carbons) or whether they build on the broader sol-gel field to provide new families of catalysts where the support plays more than just a supporting role. Improving analytical techniques will continue to play a major role in the understanding of the catalysts, something which will grow in value and importance as the ability to design catalytic systems continues to lead us to be able to control the exact nature of the catalyst in increasing detail. In situ monitoring of reactions in-pore or at the surface is still a major challenge, but can lead us to a deeper understanding of what exactly is going on at the active site. Such studies and the increasing body of knowledge they contribute to will allow the development of more active and more selective catalysts for a wider range of processes. Better integration of these catalysts with appropriate engineering solutions are reactor designs will further improve the performance of the catalysts and lead to excellent process options and increasingly sophisticated synthetic opportunities.

The challenge of green chemistry is always there, and we must strive to prepare catalysts that will provide the greatest environmental benefit, and use them to drive chemistry forward through the challenges of changing feedstocks and increasing pressure on existing raw materials. It is important that we focus not only on the sustainability of carbon (as is the case at the moment) but realise that many other elements have serious sustainability difficulties too, and that we must plan how we manage their finite resources.

References

1. Anastas P, Warner J (eds) (1998) Green chemistry: theory and practice. Oxford University Press, Oxford
2. Clark JH, Macquarrie DJ (2002) Handbook of green chemistry and technology. Blackwell, London
3. Sheldon RA, Arends I et al (2007) Green chemistry and catalysis. Wiley, Weinheim
4. Kresge CT, Leonowicz ME et al (1992) Nature 359:710–712
5. Zhao DY, Feng JL et al (1998) Science 279:548–552
6. Burkitt SL, Sims SD, Mann S (1996) Chem Commun 11:1367–1368
7. Richer R, Mercier L (1998) Chem Commun 1775–1777
8. Angeletti E, Canepa C et al (1988) Tetrahedron Lett 29:2261–2264
9. Rao YVS, De Vos DE et al (1997) Angew Chem Int Ed 36:2661–2663
10. Brunel D (1999) Microp Mesop Mater 27:329–344
11. Kamada M, Nishijima H et al (1993) Bull Chem Soc Japan 66:3565–3570
12. Augustine R, Tanielyan S, Anderson S, Yang H (1999) Chem Commun 13:1257–1258
13. Arhancet JP, Davis ME et al (1989) Nature 339:454–455
14. Valkenberg MH, De Castro C et al (2002) Green Chem 4:88–93
15. Virtanen P, Salmi T et al (2009) Ind Eng Chem Res 48:10335–10342
16. Ferreira R, Garcia H et al (2005) Eur J Inorg Chem 21:4272–4279
17. White RJ, Luque R et al (2009) Chem Soc Rev 38:481–494
18. Ryoo R, Joo SH et al (1999) J Phys Chem 103:7743–7746
19. Lu A-H, Schüth F (2006) Adv Mater 18:1793–1805
20. Goto Y, Inagaki S (2006) Microp Mesop Mater 89:103–108
21. Al-Haq N, Ramnauth R et al (2002) Green Chem 4:239–244
22. Guerrero G, Mutin PH et al (2001) J Mater Chem 11:3161–3165
23. Mutin PH, Guerrero G et al (2005) J Mater Chem 15:3761–3768
24. Macquarrie DJ (1999) Green Chem 2:195–198
25. Baccile N, Babonneau F et al (2009) J Mater Chem 19:8537–8559
26. Mitani N, Ma JF (2005) J Exp Botany 56:1255–1261
27. Ma JF, Yamaji N (2006) Trends Plant Sci 11:392–397
28. Chiarakorn S, Arrerob V et al (2007) Sci Technol Adv Mater 8:110–115
29. Sánchez-Flores NA, Pacheco-Malegón G et al (2007) J Chem Technol Biotechnol 82:614–619
30. Pacheco-Malegón G, Sánchez-Flores NA et al (2007) Microp Mesop Mater 100:70–76
31. Doi S, Clark JH et al (2002) Chem Commun 22:2632–2633
32. Budarin V, Clark JH et al (2006) Angew Chem Int Ed 45:3782–3786
33. White RJ, Budarin V et al (2009) Chem Soc Rev 38:3401–3418
34. Hardy JJE, Macquarrie DJ (2005) Ind Eng Chem Res 44:8499–8520
35. Valentin R, Molvinger K et al (2003) New J Chem 27:1690–1692
36. Quignard F, Velentin R et al (2008) New J Chem 32:1300–1310

37. Krajewska B (2004) Enzyme Microbial Technol 35:126–139
38. Zhang YY, Hu X et al (2006) Proc Biochem 41:2410–2416
39. Sorokin AB, Tuel A (1999) New J Chem 23:473–476
40. Sorokin AB, Quignard F et al (2006) App Catal A. General 309:162–168
41. Guo CC, Huang G et al (2003) App Catal A. General 247:261–267
42. Hu DD, Shi QZ et al (2001) Carbohydr Polym 45:385–393
43. Alesi S, Di Maria F et al (2008) Green Chem 10:517–523
44. Valentin R, Molvinger K et al (2005) Biomacromolecules 6:2785–2792
45. Thomas JM, Hernandez-Garrido JC et al (2009) Top Catal 52:1630–1639
46. Budarin V, Clark JH et al (2007) Green Chem 9:992–995
47. Werpy T, Pedersen G (eds) (2004) Top value chemicals from biomass, http://www1.eere.energy.gov/biomass/pdfs/35523.pdf. Accessed 12 January 2010
48. Liu S, Rebros M et al (2009) Chem Commun 2308–2310
49. Oelkers EH, Valsami-Jones E (2008) Elements 4:83–87
50. Cordell D, Drangert JO et al (2009) Global Environ Change 19:292–305
51. Luis SV, Garcia-Verdugo E (2010) Chemical reactions and processes under flow conditions. RSC, Cambridge
52. Bogaert-Alvarez RJ, Demena P et al (2001) Org Proc Res Dev 5:636–645
53. Fan X, Gonzalez Manchon M (2009) J Catal 267:114–120
54. Bacheva A, Macquarrie DJ (2008) Green Chem 10:692–695
55. Kamahori K, Ito K et al (1996) J Org Chem 61:8321–8324
56. Itsuno S, Sakurai Y et al (1990) J Org Chem 55:304–310
57. Hodge P, Sung DWL (1999) J Chem Soc Perkin Trans I:2335–2342
58. Pericàs MA, Herrerías CI et al (2008) Adv Synth Catal 350:927–932
59. Licence P, Ke J et al (2003) Green Chem 5:99–104
60. Meehan NJ, Sandee AJ et al (2000) Chem Commun 1497–1498
61. Hou Z, Theyssen N et al (2008) J Catal 258:315–323
62. Cooper AI (2003) Adv Mater 15:1049–1059
63. Dhepe PL, Fukuoka A, Ichikawa M (2003) Phys Chem Chem Phys 5:5565–5573
64. Oxley P, Brechtelsbauer C et al (2000) Ind Eng Chem Res 39:2175–2182
65. Sirkar KK, Shanbhag PV et al (1999) Ind Eng Chem Res 38:3715–3737
66. Hansen EW, Courivaud F, Karlsson A, Kolboe S, Stöcker M (1998) Microp Mesop Mater 22:309–320
67. Stallmach F, Gräser A et al (2001) Microp Mesop Mater 44–45:745–753
68. Okazaki M, Toriyama K (2003) J Phys Chem B 107:7654–7658
69. Roeffaers MBJ, De Cremer G et al (2007) Proc Natl Acad Sci 104:12603–12609
70. Roeffaers MBJ, Ameloot R et al (2008) J Amer Chem Soc 130:13516–13517
71. Holm MS, Egeblad K et al (2008) Eur J Inorg Chem 33:5185–5189
72. Macquarrie DJ, Clark JH et al (1997) React Funct Polym 35:153–158
73. Macquarrie DJ, Jackson DB (1997) Chem Commun 1781–1782
74. Macquarrie DJ (1996) Chem Commun 1961–1962
75. Mubofu EB, Clark JH et al (2000) Green Chem 2:53–58
76. Lempers HE B, Sheldon RA (1998) J Catal 175:62–69
77. Webb JD, MacQuarrie S et al (2007) J Catal 252:97–109
78. Crudden CM, Sateesh M et al (2005) J Am Chem Soc 127:10045–10050
79. Crudden CM, McEleney K et al (2007) Pure Appl Chem 79:247–260
80. Broadwater SJ, McQuade DT (2006) J Org Chem 71:2131–2134
81. Rebek J, Gavina F (1974) J Am Chem Soc 96:7112–7114
82. Rebek J, Brown D et al (1975) J Am Chem. Soc 97:454–455
83. Diaz I, Marques-Alvarez C et al (2000) J Catal 193:283–294
84. Diaz I, Marques-Alvarez C et al (2000) J Catal 193:295–302
85. Macquarrie DJ, Tavener SJ et al (2005) Chem Commun 2363–2365
86. Li HX, Chen J et al (2007) Green Chem 9:273–280
87. Thomas JM, Raja R (2008) Acc Chem Res 41:708–720

88. Thomas JM, Hernandez-Garrido JC et al (2009) PCCP 11:2799–2825
89. Bednarski MD, Chenault HK et al (1987) J Am Chem Soc 109:1283–1285
90. Houghten RA (1985) Proc Natl Acad Sci USA 82:5131–5135
91. Laska U, Frost CG et al (2009) J Catal 268:318–328
92. Liu W, Li B et al (2009) Chem Lett 39:1110–1111
93. Che C, Li W et al (2009) Chem Commun 5990–5992
94. Gaab M, Bellemin-Lapponaz S et al (2009) Chem Eur J 15:5450–5462
95. Mal NK, Fujiwara M et al (2003) Nature 421:350–353
96. Mal NK, Fujiwara M et al (2003) Chem Mater 15:3385–3394
97. Casasus R, Marcos MD et al (2004) J Am Chem Soc 126:8612–8613
98. Giri S, Trewyn BG et al (2005) Angew Chem Int Ed 44:5038–5044
99. Goettmann F, Grosso D et al (2004) Chem Commun 10:1240–1241
100. Alauzun J, Mehdi A et al (2006) J Am Chem Soc 128:8718–8719
101. Zeidan RK, Hwang SJ et al (2006) Angew Chem Int Ed 45:6332–6335
102. Zeidan RK, Davis ME (2007) J Catal 247:379–382
103. Huh S, Chen H-T et al (2005) Angew Chem Int Ed 44:1826–1830

Chapter 2
Biomimetic Single-Site Heterogeneous Catalysts: Design Strategies and Catalytic Potential

David Xuereb, Joanna Dzierzak, and Robert Raja

Abstract Enzymes catalyze the most fundamental reactions in organic chemistry from simple oxidations of straight chain alkanes to complex C–C bond forming reactions with exceptional selectivity. Mimicking the active site of an enzyme by immobilising a well defined amino acid containing transition-metal centre on a robust inorganic framework, provides a powerful catalyst that can be utilized in the production of fine chemicals and complicated drug molecules. Porous aluminosilicates and mesoporous silicas offer suitable supports for single-site bio-derived catalysts. These materials can be created from a range of methodologies and the different strategies used for immobilisation can greatly affect the nature of the active catalyst. The routes by which these catalysts are immobilised have also given the potential to derivatize inorganic structures with amino acids, not just for complexation to metal centres but for use as organocatalysts as well. These metal free bio-derivatized frameworks offer advantages over their homogeneous counterparts and can carry out stereoselective reactions with great effectiveness. Herein, the routes to heterogenizing biomimetic catalysts will be critically assessed and depending on the methods used, suitable active catalysts for use in chemo- and stereoselective transformations can be developed.

2.1 Metalloenzymes

A metalloenzyme is usually a huge protein that contains a small metal complex in the active site. The metal ion is coordinated by a few amino acids from the protein scaffold that stabilizes and isolates the metal active centre as well as providing a specific binding pocket for a substrate (Fig. 2.1). Proteins coordinate to metal ions with nitrogen, oxygen and sulphur containing ligands. Amino, amido,

D. Xuereb, J. Dzierzak, and R. Raja (✉)
School of Chemistry, University of Southampton, Highfield, Southampton SO17 1BJ, UK
e-mail: R.Raja@soton.ac.uk

P. Barbaro and F. Liguori (eds.), *Heterogenized Homogeneous Catalysts for Fine Chemicals Production*, Catalysis by Metal Complexes 33,
DOI 10.1007/978-90-481-3696-4_2,

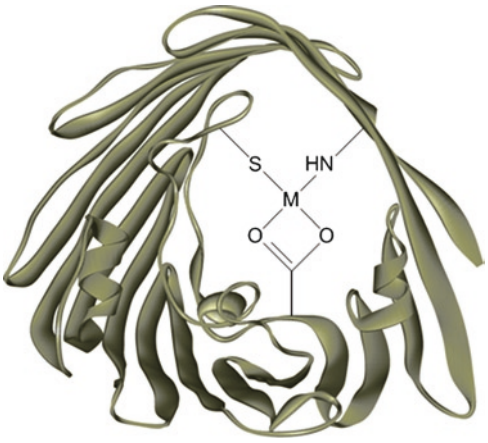

Fig. 2.1 Schematic representation of metalloenzyme active site

amidato, carbonyl and carboxylate ligands can be located at the C- or N-termini of the peptide chain, within the chain itself (expect amino and carboxylate) and in side chain [1].

Iron and copper ions are the most commonly occurring metal centers in biological oxidation systems and play an important role in heterogeneous and homogeneous catalysis, mainly due to their inherent electronic properties and accessible redox potentials. Important examples are haem iron, non-haem iron and copper active sites [2].

2.1.1 Iron Enzymes

Metalloenzymes containing iron active sites comprise a large group of dioxygen activating enzymes that possess potential for functionalizing a wide-range of organic substrates with high efficiency and selectivity [3].

Among heme enzymes activating O_2 cytochrome P450 has received the most attention. P450s play critical roles in the biological hydroxylation of saturated carbon–hydrogen bonds, epoxidation of double bonds, oxidation of heteroatoms and aromatics and dealkylation reactions. The P450 active site consists of an Fe^{III} porphyrin cofactor covalently linked to the protein backbone through coordination of a sulphur atom of cysteine [4].

Mononuclear non-heme iron enzymes comprise a large collection of dioxygen activating enzymes that are very different from their heme counterparts due to electronic and geometric differences arising from ligand environments. These enzymes catalyse oxidative transformations either by involving high-spin ferrous (Fe^{II}) ions or by the utilization of high-spin ferric (Fe^{III}) active centres. The Fe^{III} site is usually utilized to activate substrates for reactions with dioxygen and include intradiol

dioxygenases and lipoxygenases. The Fe^{II} site activates oxygen by direct binding to O_2, resulting in iron-oxygen intermediates that react with the substrate and include Rieske dioxygenases, pterin-dependent hydroxylases or extradiol dioxygenases [5].

Binuclear iron enzymes involved in O_2 activation primarily exist in two oxidation states: the fully reduced bi-ferrous $[Fe^{II}]_2$ and the oxidized bi-ferric $[Fe^{III}]_2$ form. A particular example of a di-iron containing enzyme is soluble methane monooxygenase (sMMO) which consists of a carboxylate-bridged dinuclear iron centre [4] that is capable of producing oxygen species of much superior activity than other monooxygenases. In addition to aromatics and other compounds, MMO exhibits a unique ability to convert even methane, which is known to be the most inert hydrocarbon (C–H bond energy, 104 kcal/mol), into methanol using dioxygen as the oxidant via $[Fe^{III}]_2$-peroxo and $[Fe^{IV}]_2$ intermediates [6]. One oxygen atom is reduced to water, and the second is incorporated into substrate molecule, yielding the alcohol.

2.1.2 Copper Enzymes

Copper active sites play a major role in biological dioxygen activation systems [7]. Copper containing enzymes are involved in hydroxylation reactions (particulate methane monooxygenases pMMO, tyrosinase), reversible dioxygen binding (hymocyanin), two-electron reduction of O_2 to peroxide coupled with oxidation of organic molecules (galactose oxidase GO) and four-electron reduction of H_2O_2 to water while oxidizing the substrate (ascorbate oxidase).

Particulate methane monooxygenase (pMMO) contains copper in the active site, similar to diiron sMMO because it also catalyses the oxidation of methane to methanol. pMMO contains a mononuclear copper active site together with a dinuclear copper site, but the structure, mechanism and actual reaction site for the methane hydroxylation has not be identified due to difficulties in isolation of sMMO [8].

Galactose oxidase (GO) contains one copper atom per active centre. The active site involves residues of four amino acid side chains (two histidine and two tyrosine amino acids) directly coordinated to a mononuclear Cu centre, which is also bound by a solvent molecule to form a distorted five-coordinate metal complex. Galactose oxidase catalyzes the two-electron oxidation of primary alcohols to aldehydes, which in turn can serve as substrates to yield carboxylic acids. During the catalyzed reaction, the enzyme alternates between three different forms: an active, inactive, and fully reduced form. In the active form of GO, the tyrosine is in a radical form and the copper atom with a oxidation state +2 [9,10].

Tyrosinase and catechol oxidase contain a binuclear copper centre as the active site. The dicopper (I) active site in these enzymes react with O_2 to generate a (peroxo) dicopper (II) unit that is responsible for the oxidation of phenols and catechols. Both enzymes can oxidize catechol to quinone, but only tyrosinase can hydroxylate phenol [11,12].

2.2 Amino Acids

Amino acids are highly functional molecules that are protein constituents (Fig. 2.2). An amino acid is composed of a basic amino functional group (-NH_2), acidic carboxyl functional group (-COOH), a hydrogen atom and a characteristic side chain (-R) giving a general formula R-CH-NH_2-COOH.

At high pH the carboxyl group tends to be dissociated, giving the molecule a stronger negative charge. At low pH the amino group is protonated therefore giving the molecule a net positive charge. At the isoelectric point the amino acid in solution has a net charge of zero that contains positively and negatively charged substituents in equal quantities, this state is called a zwitterion (Fig. 2.3).

Amino acids are good metal-complexing agents, forming chelate rings through the amino and carboxylate groups via dissociation of the acidic proton as a bidentate N,O-donor (Fig. 2.4). A side chain e.g. phenol ring of tyrosine, imidazole

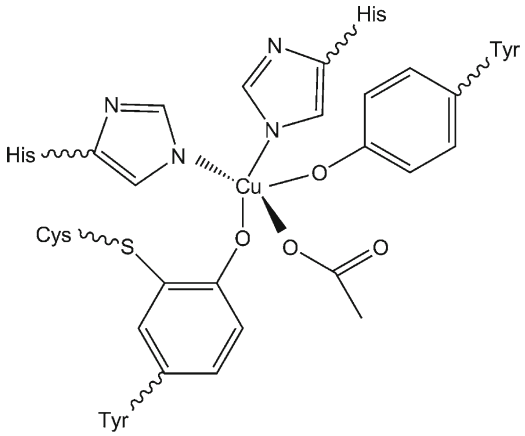

Fig. 2.2 Galactose oxidase active site

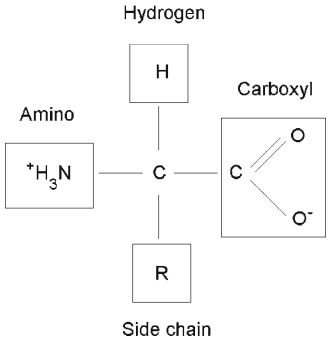

Fig. 2.3 Generalized structure of a typical amino acid

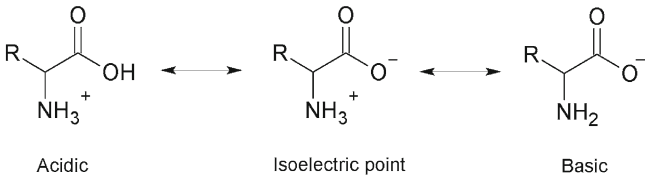

Fig. 2.4 Amino acid dissociation at equilibrium

group of histidine, mercapto group of cysteine or carboxylato groups of aspartate and glutamate can also be involved as a metal binding site [13].

2.3 Bio-inspired Catalysts

Metalloenzyme inspired catalysts have long held the fascination of synthetic chemists. Both structural and functional enzyme mimics have been rationally developed through the interaction of transition-metal complexes containing designed organic ligands [14], natural amino acids [15] or by the utilisation of de-novo designed artificial proteins [16]. Transition-metal complexes containing amino acids can serve as isolated active sites when encapsulated in inorganic host materials such as zeolites and mesoporous silica or polymers, which can serve as substitutes to the protein scaffold of natural enzymes.

Bio-inspired catalysts offer an alternative for conventional biological and chemical processes and have many advantages over natural metalloenzyme systems, allowing development of more robust catalysts at relatively low cost. Such catalysts are pH and thermally more stable, may expand the scope of possible substrates and increase the scale of production. Moreover, their stability and selectivity may be improved by chemical modifications of the active sites by altering the immobilisation procedures.

2.3.1 Metal Amino Acid Complexes Immobilized on Silica

MCM-41 is a porous silica framework that has hexagonally packed arrays of one-dimensional channels with a very large surface area and has potential to encapsulate macromolecules. Mesoporous silica contain a large number of silanol groups at the surface of the channels, which enable it to be organofunctionalised (Fig. 2.5). Introduction of functional groups via silylation is the most reliable method to prepare inorganic–organic hybrids, which can enhance the surface hydrophobicity by decreasing the amount of silanol groups and influencing the catalytic activity [17]. $RSi(OEt)_3$ and $RSiCl_3$ are the most popular silylating agents [18].

The use of primary amine functional groups such as 3-aminopropyl allows attachment of single amino acids and peptides to amino functionalized silica supports by

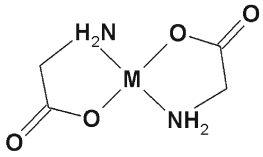

Fig. 2.5 General structural formula proposed for amino acid complexes

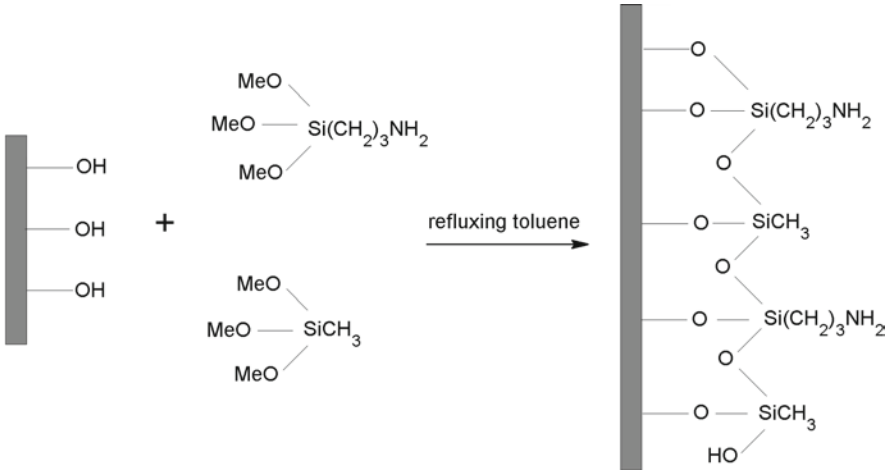

Fig. 2.6 Model of the surface sites in functionalized silica

a methodology called solid phase peptide synthesis (SPPS) (Fig. 2.6). The hydrophobic character inside the pores can be adjusted by co-functionalization with other species e.g. methyl groups [19]. Amino acids can be covalently anchored onto the support by the formation of very stable amide bonds with surface bound amide groups. Amine functionalized materials can be prepared by post synthetic grafting of 3-aminopropyl-trimethoxysilane on a silica surface, or by co-condensation of 3-aminopropyl-trimethoxysilane with a silica precursor [20]. The material with only the 3-aminopropyl moieties shows a poor hydrothermal stability. The reason for this is due to the basicity of the functional groups and the fast hydrolysis of the silica in the presence of an amine. Silica surfaces that are functionalized with a mixture of methyl groups and 3-aminopropyl groups are more stable. The hydrothermal stability improves by decreasing the amount of 3-aminopropyl bound to the silica surface. This is due to a decreasing basic character inside the pores and also because the silica is protected from hydrolysis when hydrophobic methyl groups are present together with 3-aminopropyl groups.

Solid phase peptide synthesis (SPPS), developed by Merrifield et al. [21], was a major breakthrough allowing the chemical synthesis of peptides and small proteins that can be bound to an insoluble support and any unreacted reagents left at the end of the synthetic step can be removed by a simple washing procedure.

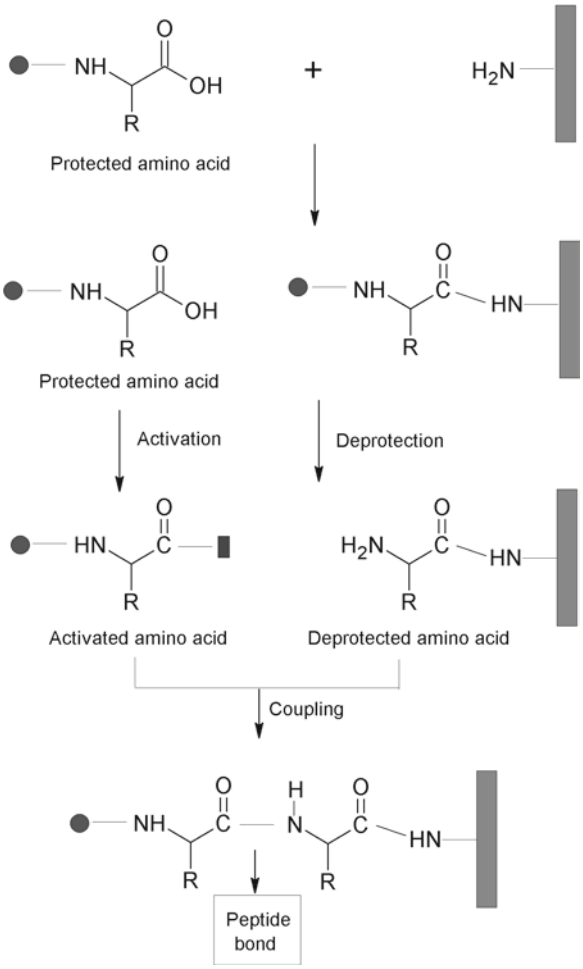

Fig. 2.7 Scheme for solid phase peptide synthesis (SPPS)

SPPS comprises of repeated cycles of coupling and deprotection of successive amino acids (Fig. 2.7). Unlike ribosome protein synthesis, SPPS proceeds in a C → N terminal fashion. The free N-terminal amine of a solid-phase attached peptide is coupled to a single N-protected amino acid (Fig. 2.8). This unit is then deprotected, revealing a new N-terminal amine to which a further amino acid is attached.

There are two major termini used in solid phase peptide synthesis, which are Fmoc (base labile alpha-amino protecting group) and t-Boc (acid labile protecting group). Each method involves different protection, deprotection and cleavage steps. To remove Fmoc from peptide chain, basic conditions are used (usually piperidine in DMF), to remove t-Boc, acidic conditions are used (usually trifluoroacetic acid).

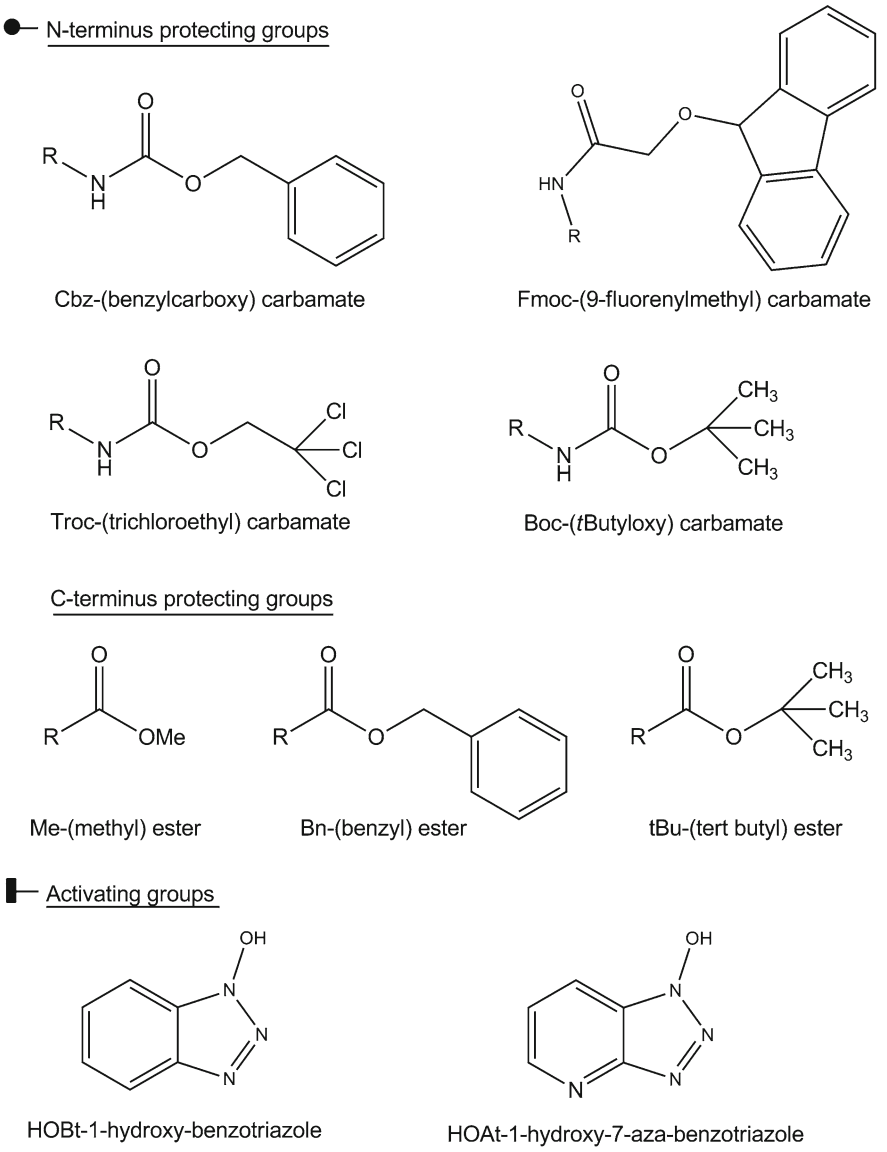

Fig. 2.8 Examples of activating and C-, N-terminus protecting groups in SPPS

When coupling a carboxyl group of an amino acid, it is activated thereby making the reaction proceed at a much faster rate. There are two main types of activating groups: triazolols (HOBt, HOAt) and carbodiimides (DCC, DIC). Fmoc chemistry has many advantages over t-Boc chemistry as it generates peptides of higher quality and in better yield.

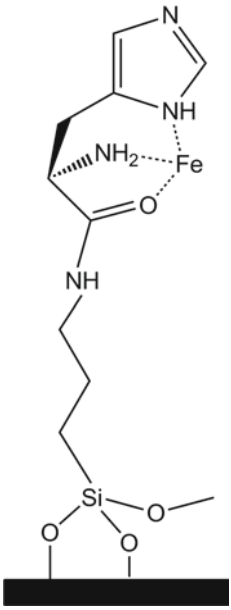

Fig. 2.9 Model of iron complexation by histidine on amino functionalized silica

A number of amino acids and short peptide complexes with iron and copper have been immobilized on mesoporous silica via SPPS and these have shown promising trends in the oxidation of hydrocarbons [22], an example is shown in Fig. 2.9.

2.3.2 Amino Acid Transition Metal Complexes Encapsulated Within Zeolites

Zeolites are crystalline aluminosilicates with a three-dimensionally connected pore structure. The zeolite framework consists exclusively of corner-sharing AlO_4 and SiO_4 tetrahedra. The primary building units are single TO_4 tetrahedra, where the T atom is an aluminium or silicon atom. Each T atom is tetrahedrally bonded to four oxygen atoms forming a bridge to neighbouring T atoms. Silicon surrounded by four oxygen atoms (essentially SiO_2) has no charge. Aluminium has 3^+ charge, thus AlO_2 has a net negative charge. The charge imbalance between Si and Al results in an overall net negative charge on the zeolitic framework. The presence of aluminium produces this negative charge and is balanced by non-framework cations that can be readily exchanged [23].

Zeolites have the ability to act as catalysts for chemical reactions which take place within their internal cavities. They are thermally stable, chemically robust and easy to separate from the reaction products. Zeolites can incorporate and immobilize

various active sites within their structure in the channels and cages. Careful combination of metal complexes immobilized as active sites in an inorganic matrix can result in catalysts that can mimic the functional aspects of enzyme activity [24,25]. Zeolites are ideal supports and by judicious choice of the active site novel single-site heterogeneous catalysts can be designed [26,27]. Such zeolite encapsulated active centres present many advantages. Zeolites have well organized pores and channels, which readily serve as supporting hosts for various molecules. In such systems zeolites can serve as a substitute for the protein mantle of natural enzymes and provide a controlled steric environment, where the catalysis ensues [28,29]. These heterogeneous catalysts are resistant to harsh reaction conditions, more stable at high temperatures, facilitate separation of products from reactants and aid catalyst recyclability.

Several general routes [30] are known for preparation of metal complexes inside zeolites:

- Ion Exchange – Exposing a sodium ion charge balanced zeolite to a solution containing other cations facilitates exchange of the sodium ions. This method has been used for encapsulating metal–amino acid complexes inside a zeolite structure [31].
- Flexible Ligand Method – Synthesis of the metal complex in situ in the zeolite cavity by reaction of the ligand with the exchanged metal cations. Complexes with previously exchanged metal ions are able to diffuse freely through the zeolite pores. This approach is well suited for the encapsulation of metal–salen complexes, as the salen ligand offers the desired flexibility [32].
- Ship in the Bottle – The final molecule is prepared inside the pores by reacting smaller precursors to afford the larger molecule 'mechanically entrapped' inside the cages. This route was employed for metal–phthalocyanine or metal–porphyrin complexes within the zeolite [33].
- Zeolite Synthesis Method – 'Templated' Synthesis Synthesis of the zeolite in the presence of the preformed metal complexes. Transition metal complexes which are stable under the conditions of zeolite synthesis are included in the synthesis mixture. Metal phthalocyanines, porphyrins and amino acids provide examples of such encapsulated catalysts [34].

The first stable and catalytically active example of zeolite immobilized transition metal complex containing amino acid ligands is Cu-Histidine synthesized by the ion exchange method [35]. In the first stage of this method zeolite Y exists in its Na^+ form by successive ion exchanges with NaCl solution. The next step is to ion exchange with a solution of Cu-Histidine at pH 7.3. An AA: Cu^{2+} ratio of 5 is needed because lower ratios give partial hydrolysis of Cu^{2+}, which manifests above pH 6. The ability of the Cu-Histidine to undergo ion exchange is dependent on its charge and stability, which are influenced by the pH. At pH 2 only 0.83% of the Cu^{2+} is coordinated to His. At pH 3, Cu^{2+} forms *mono*-His complexes, whereas in the pH range 6–10, *bis* complexes are formed. In *bis* complexes, four nitrogens, N_{am} and N_{im}, of each molecule as well as carboxylate oxygen can coordinate to the metal. It was found that, in solution, two histidine ligands coordinate to the Cu^{2+} ion

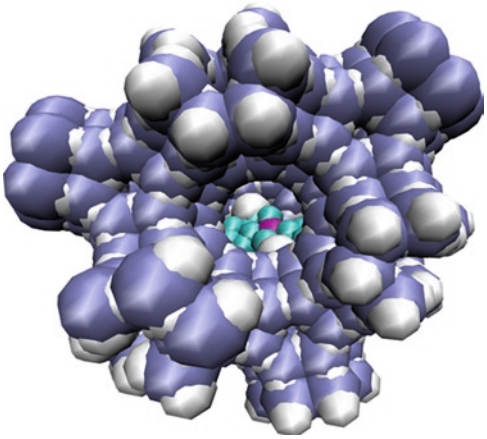

Fig. 2.10 Graphical representation of an Fe–proline complex in its energy-minimized configuration anchored within the supercages of zeolite X

in a square-planar geometry. However, upon encapsulation within the channels and cages of zeolite Y, by the ion-exchange method, a framework oxygen atom replaces one of the histidine ligands.

Another example is an Fe^{3+}-Proline complex that was immobilized within the supercages of the zeolite Faujasite by using zeolite synthesis methodology, in which the zeolite was synthesized in presence of preformed Fe^{3+}-Proline complexes (Fig. 2.10).

Typical XRD patterns of Fe^{3+}-Proline complexes encapsulated within zeolites X and Y reveal identical patterns reported for the neat zeolites [36]. Well-resolved peaks with no phase impurities indicate that the Faujasitic architecture is structurally unaltered after the encapsulation procedure. The absence of additional structural reflections due to the neat complex confirms its dispersion predominantly within the internal cages and not on the external surface.

The FTIR spectra of Fe^{3+}-Proline encapsulated within zeolite X (shown in Fig. 2.11, along with the assignments for the various bands) provides spectroscopic information on the nature and structural integrity of the encapsulated amino acid ligand. The presence of a strong band at 1662 cm^{-1} for Fe^{3+}-Proline-X and neat Fe-Proline, coupled with the absence of signal around 1750 cm^{-1}, which is typical of the COOH species, confirm that the carboxyl group is deprotonated. The carboxylate ions can be readily characterized by an antisymmetric (ν_{as} COO^-) and a symmetric stretching mode (ν_s COO^-), around 1,650 and 1,400 cm^{-1}, respectively [37]. As for the amino group, the $\nu_{N\text{-}H}$ bands of neutral N-H groups can be seen at 3,285 cm^{-1} for Fe^{3+}-Proline-X, and at 3,210 cm^{-1} for neat Fe^{3+}-Proline (corresponding bending $\delta_{N\text{-}H}$ vibration can be observed at 1,375 and 1,345 cm^{-1} respectively). In Fe-$Proline^{3+}$-X, these bands can be readily superimposed to a broad signal in the 3,700–2,800 cm^{-1} interval, which can be attributed to the hydrogen bonding between proline and zeolite. The absence of the δNH_2^+ vibration at 1,550 cm^{-1} is

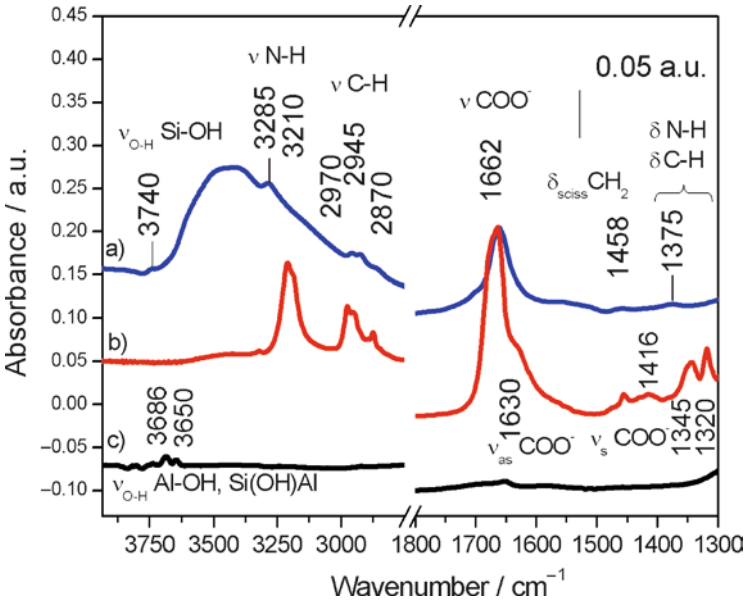

Fig. 2.11 FT-IR spectra of Fe $^{3+}$-Proline-X (**a**), Fe $^{3+}$-Proline (**b**), Zeolite X (**c**)

Table 2.1 Surface area and pore volume measurements for the neat zeolite X and zeolite encapsulated Fe^{3+}-Proline-X catalyst

Catalyst	BET surface area (m^2/g)	Micropore volume (cm^3/g)
Fe^{3+}-proline-X	85.3	0.04
Zeolite X	620.8	0.09

conspicuous, which confirms that the amino group is not protonated and can play a role in complexing with the iron sites.

Significant decrease in the internal pore volume and surface area for the encapsulated materials strongly indicates the presence of the Fe^{3+}-Proline complex within the supercages of the Faujasite structure (Table 2.1).

DR UV–Vis elucidates the nature of Fe species encapsulated within zeolites (Fig. 2.12). The heterogeneous Fe^{3+}-Proline based catalyst showed a band at 37,600 cm^{-1} and a more predominant band at 45,400 cm^{-1}. This component at higher wavenumber (45,400 cm^{-1}) can be assigned to well-dispersed and isolated Fe^{3+} sites [38].

The Electron Paramagnetic Resonance (EPR) spectrum of the Fe^{3+}-Proline-X consist of broad resonance line at $g = 2$ together with a narrow signal at $g = 4.26$. It is highly likely that such signals originate from strongly interacting Fe^{3+}-Proline centers located near the extremities of the cages of zeolite X [39].

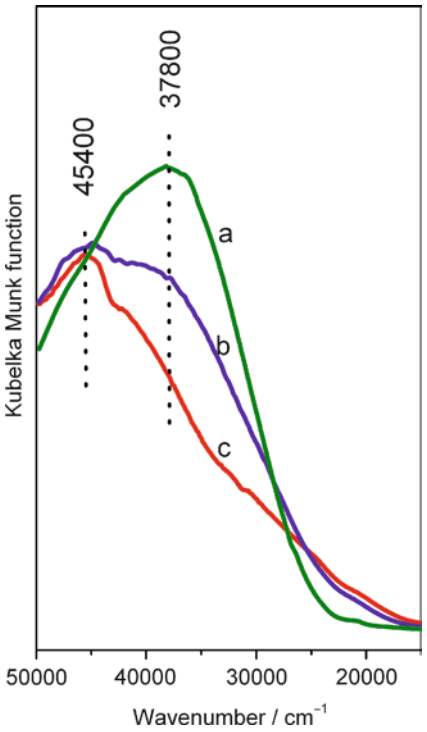

Fig. 2.12 DR UV–Vis spectra of Fe $^{3+}$-Proline (**a**), Fe $^{3+}$-Proline-Y (**b**), Fe $^{3+}$-Proline-X (**c**)

2.3.3 Catalysis

The selective oxidation of hydrocarbons and benzylic alcohols by molecular oxygen continues to pose a major challenge in the synthesis of commodity and fine-chemicals [40,41]. Transition-metal complexes containing amino acids encapsulated within solid supports generate isolated active centers that function as effective selective oxidation catalysts using benign oxidants such as air and display high turnovers and selectivity in industrially significant oxidation reactions (Table 2.2).

Encapsulated Cu-Histidine showed promise as a catalyst for oxidation of cyclohexene and was 89 mol% selective towards 1,2-cyclohexanediol.

The encapsulated Fe^{3+}-Proline showed catalytic potential in the selective oxidation of cyclohexane and benzyl alcohol. The oxidation of cyclohexane revealed interesting changes in activity and selectivity when O_2 was employed as the oxidant. The encapsulated Fe^{3+}-Proline, gives selectivity towards cyclohexanone (99.5 mol%) with O_2, but when tert-butyl hydroperoxide (TBHP) was used as the oxidant cyclohexanol was the major product observed. Fe^{3}+-Proline-X catalyst showed to be 99+ mol% selective towards benzaldehyde. Cyclohexanone, which is an industrially important commodity chemical and a vital precursor in

Table 2.2 Catalytic performances of amino acid based catalysts encapsulated in zeolites

Substrate	Catalyst	Oxidant	Time (h)	TON
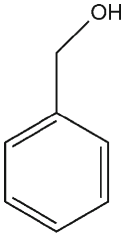	Fe^{3+}-proline	O_2	6	356
	Fe^{3+}-proline	TBHP	6	550
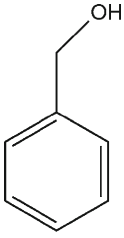	Fe^{3+}-proline	O_2	1	56
	Fe^{3+}-proline	TBHP	1	1,283

the manufacture of ε-caprolactam (for nylon-6) and adipic acid (for nylon 6,6) can be produced in high selectivities using benign oxidants and zeolite-encapsulated amino acid complexes. These benign and green catalysts have shown potential in the oxidation of benzylic alcohols with high selectivities for the corresponding aldehydes. The presence of well-defined and isolated single-sites, coupled with the hydrophobicity/hydrophilicity of the host results in the generation of a powerful functional biomimetic system.

2.3.4 Summary

Bio-molecules such as amino acids immobilized within inorganic host materials attract considerable attention for applications in catalysis. Zeolites and mesoporous silicas are ideal supports for generating single-site heterogeneous catalysts. Transition metal complexes containing natural amino acid ligands can be immobilized as active sites in such supports. The obvious advantages are that such heterogeneous catalysts are highly resistant to harsh reaction conditions, stable at high temperatures, facilitate separation of products from reactants and improve catalyst recyclability. Not only can these heterogenized amino acids serve as ligands that coordinate to metal centres but can individually act as organocatalysts and be active in some of the most fundamental organic transformations.

2.4 Routes to Heterogeneous Organocatalysts Through Amino Acid Immobilization

The use of organic molecules as catalysts has gained much exposure in recent years, so much so that it is now a predominant area in organic chemistry, recognised as *organocatalysis*. Amino acids have been identified as organocatalysts especially that of L-proline, which has been effective in catalysing a range of transformations such as aldol reactions [42], Diels-Alder reactions [43] and Mannich reactions [44]. Employing organocatalysts has many shortcomings due to their homogeneous nature, which necessitates the use of high mol% of catalyst and gives rise to difficulties associated with recovery and reusability. Through immobilisation these downfalls can be suitably overcome and could even lead to increased selectivity. There are various reasons for this increased selectivity accredited to the influence of the steric constraints present in some particular supports or because of the stability the catalyst receives, consequently inducing an affect on the mechanism or the transition state.

Herein, different approaches for immobilisation will be reviewed, with a focus on the methodologies employed for covalent anchoring of amino acids to mesoporous silica. The benefits of heterogenisation will become apparent on evaluation of the catalytic potential.

2.4.1 Choice of Support

Two general concepts used for amino acid immobilisation are by covalent and non-covalent methods (Fig. 2.13). There are a number of support types for each method and the choice of which form is usually based on the inherent properties of the support and the benefits that it can offer.

Careful consideration must be taken regarding the stability of the support, especially that of extreme temperatures and pH, so that a basis of selection can be made.

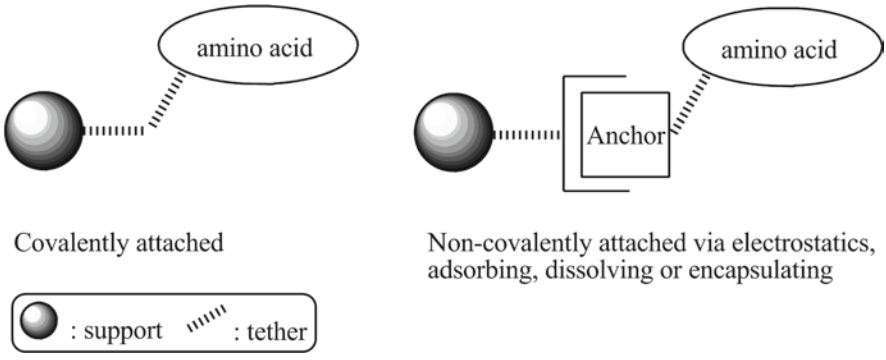

Fig. 2.13 A representation of the two distinct methods of immobilisation

Solubility factors and solvent versatility also play an important role in deciding upon the nature of the support, as these are vital in fulfilling the optimum reaction conditions. Other aspects such as the hydrophobic/hydrophilic nature or steric and electrostatic interactions that may be present must be evaluated to anticipate if this would thwart or assist successful reactions. Immobilised amino acids will serve as active organocatalysts, so the reaction mechanism by which the transformation proceeds must be understood. Specific 'parts' of the supported organic catalyst must be accessible to reactants e.g. when using an amino acid as a catalyst for the asymmetric aldol reaction the amino and carboxylate functionalities must be free for enamine formation and transition state arrangement respectively. In this case, immobilisation by covalent methods must occur through the side-chain so that the reaction mechanism is not hindered in any way.

Covalently anchored catalysts can be separated into two categories based on the solubility: soluble supports, including PEG and dendrimers, and insoluble supports such as silica and polymers. Examples of non-covalently attached catalysts are immobilisation on ionic liquid modified-silica matrices and encapsulation inside the cavities of β-cyclodextrin. These are not the only types of support that are available and supports that have not been mentioned but have had much attention are biphasic catalysts, whereby amino acids are anchored to ionic liquids [45]. The ionic liquid moiety can act as a soluble support and an advantage of using this route is that the catalyst can be recovered simply by the solubility difference with varying solvents. These catalysts, however, are not heterogeneous and will therefore not be discussed here.

2.4.2 Non-covalent Catalysts

These catalysts are not chemically bound to the support but give remarkably strong attachment through attractive interactions between the catalyst and the framework [46].

2.4.2.1 β-Cyclodextrin and Ionic-Liquid Matrices

A striking example of a non-covalently bound catalyst is an L-proline derivative that has been successfully immobilised within β-cyclodextrin [47].

This was achieved by inclusion of the phenol moiety branched from the 4-position on the proline ring (Fig. 2.14). Synthesis of the heterogeneous active catalyst was effortlessly accomplished by heating the phenoxy-amino acid and β-cyclodextrin in a mixture of ethanol and water followed by removal of the solvent. The (4*S*)-phenoxy-(*S*)-proline immobilised catalyst proved to be active in catalysing the asymmetric aldol reaction of various benzaldehydes in good yield and with impressive enantioselectivities. Not only was the catalyst easily recovered by filtration and recycled with no loss of selectivity, but the ease with which the active catalyst was immobilised is

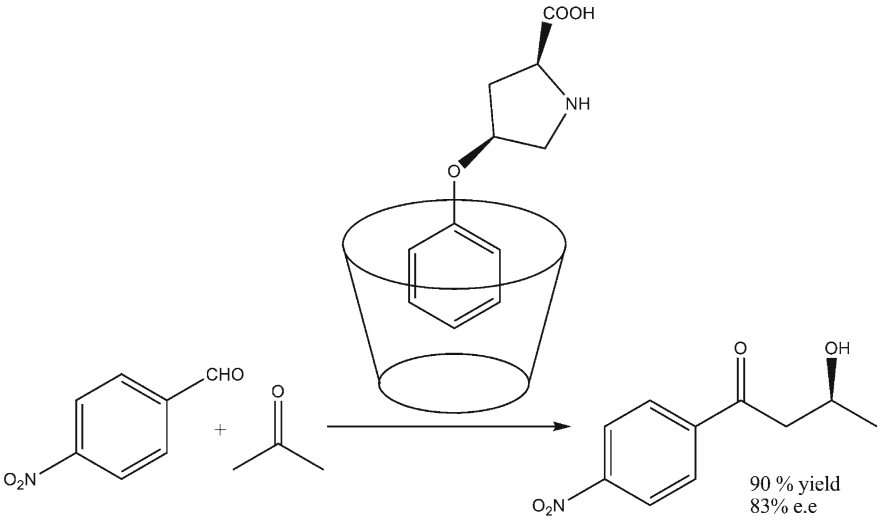

Fig. 2.14 Amino acid immobilised by inclusion into β-cyclodextrin and an example of the asymmetric aldol reaction it catalysed

most noteworthy. This methodology can be applied to other organic moieties used in catalysis, as demonstrated, in the immobilisation of other proline derivatives [48].

A very different route to non-covalent immobilisation is the adsorption of amino acids onto ionic liquid matrices (Fig. 2.15). These are frameworks that consist of a support such as silica gel with anchored ionic liquids at the surface. These layers provide a location for amino acids to adsorb and dissolve. Modified silica gels have been prepared [49,50] and have been successful in catalysing the aldol reaction between acetone and various aldehydes with modest yields.

The choice of support, i.e. the presence and which ionic liquid was immobilised greatly affected the enantiomeric excess. It was also found that the optimum state of the silica gel for catalysis is when the surface is covered entirely with a covalently attached monolayer instead of a mixture of covalently linked and adsorbed ionic liquid fragment. These results demonstrate the consequences of interactions from the support and the active single-site on the transition state in the asymmetric aldol reaction.

2.4.3 Covalently Anchored Catalysts

These catalysts offer advantages over non-covalent analogues such as an increased stability in harsher reaction conditions due to the stronger bonding forces between support and catalyst. Better stability predicts an improved re-usability since in theory, with a stronger attachment, there would be less aggregation and loss of single-site nature.

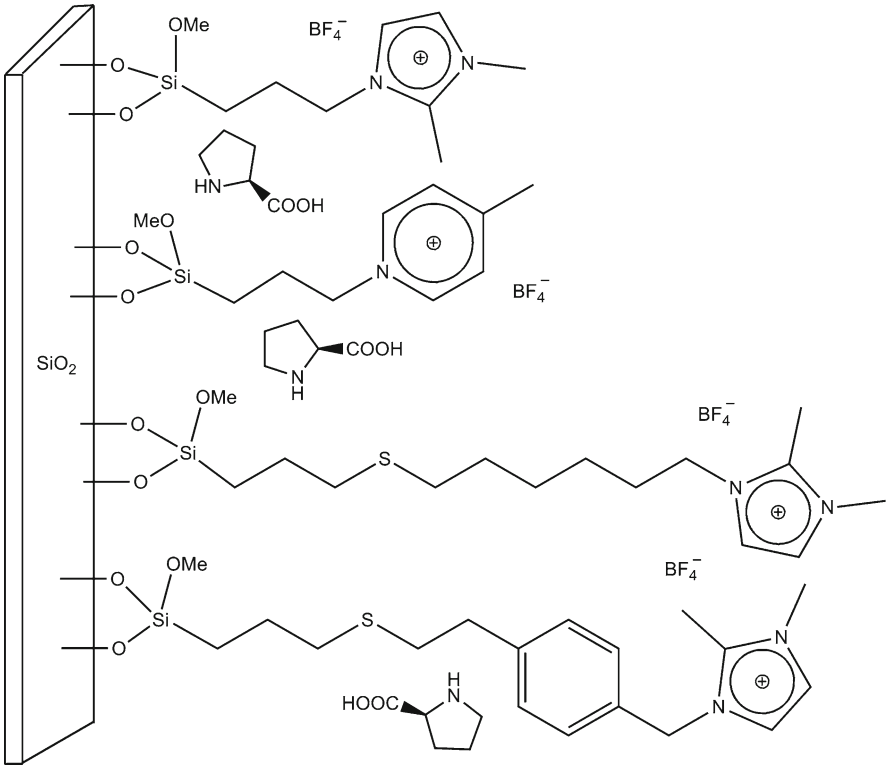

Fig. 2.15 Ionic liquids covalently attached to silica gels as supports for amino acid immobilisation

2.4.3.1 Dendrimers and PEG Supports

As mentioned previously dendrimers are examples of these types of supports and are straight forwardly synthesised using commercially available materials such as diaminobutane poly(propyleneimine) dendrimers DAB(AM)$_n$ containing n = 4, 8, 16, 32 or 64 free amino groups. The surface amine groups are coupled with carboxylic acid functionalised protected amino acids to give the dendrimer-supported amino acid [51]. A varying number of generations can be synthesised and results indicate that shorter reaction times and lower mol% of catalyst used were benefits accredited to immobilisation. Improvements are also observed with amino acid immobilisation on polyethylene glycol (PEG) [52,53]. PEG supports are high molecular weight (in the order of 1,000s) repeating organic chains; these are linked to the amino acid by a spacer to give a bio-derived organocatalyst. Using this support provides an easy way for recovery of the catalyst by precipitation on addition of a non-polar solvent. PEG and dendrimer amino acid supports are soluble and therefore homogeneous. Not only do these catalysts possess disadvantages like

decreasing activity on recycling but their inherent nature presents drawbacks such as the need for treatment steps.

2.4.3.2 Polystyrene

Heterogeneous catalysts offer solutions to problems of recovery and reusability with silica and polystyrene being the most common forms of covalent supports. Amino acids covalently attached to insoluble polystyrene can be recovered by basic filtration. There are numerous strategies for immobilisation; new developments involve 1,3-dipolar cycloaddition of an azide functionalised resin and an *O*-propargyl hydroxy amino acid [54] (Fig. 2.16, e.g. 1) or an even more recent method for synthesising a styrene amino acid derivative that links to a polymer through sulphur via a radical reaction [55] (Fig. 2.16, e.g. 2).

The immobilised proline catalysts were active in the asymmetric aldol reaction for a range of ketones and arylaldehydes and example 2 shown in Fig. 2.16 was also successful in carrying out a variety of α-selenenylation reactions [55].

Apart from just individual amino acids being immobilised, small peptide chains have also been anchored onto insoluble polymer resins. Di- and tripeptides are highly active and selective catalysts for asymmetric aldol reactions [56,57] and have been found to be more active than homogeneous proline [58]. Peptides are appealing catalysts because they are less complex as enzymes and are attractive alternatives to small organocatalysts, as they offer many more sites for structural and functional variations [57]. Solid supports for peptides include polyethylene glycol grafted on cross-linked polystyrene (PEG-PS). PEG-PS is a practical support because of its compatibility with a range of solvents, due to its amphiphilic nature [59], and its wide use in solid-phase peptide synthesis, which is the method of immobilisation employed for these peptides. This resin-anchored catalyst is highly beneficial especially when the peptides are hydrophobic because the hydrophilic PEG branch of the support now makes the peptide soluble and stops aggregation.

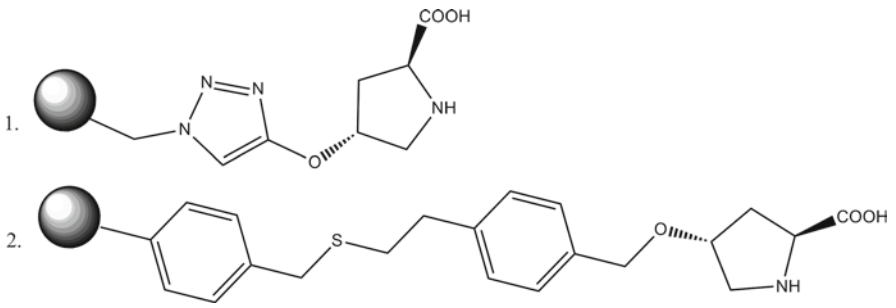

Fig. 2.16 Examples of amino acids covalently immobilised to insoluble resins

2.4.3.3 Porous Silica Supports

More recent work has been concentrated on the synthesis of bio-derived silica frameworks. Metal-based catalysts can be covalently anchored into the pores of mesoporous materials most effectively by the post-grafting method [60,61] through anchoring of the organic ligands present. This strategy can be applied to purely organic moieties where chiral catalysts can be introduced onto the surface via a linkage produced by reaction with the silanol functionalities in the channels. This covalent route to immobilisation of organocatalysts is believed to be the most suitable, since adsorption and ionic methods lead to a decrease in catalyst stability. Amino acids used in catalysis must have the amino and carboxylate groups accessible to fulfill the requirements of the well defined mechanism for each particular reaction that the amino acid is catalyzing. Therefore amino acids are immobilised by reacting the functionalities present on the side chain with a linker that can be covalently attached to the silica surface. This was achieved by Calderon et al. whereby the characteristic amino acid side chain is converted into an amine functionality, which undergoes nucleophilic attack of an isocyanate derivatized silane that can then covalently anchor to a silanol group in the channel of porous silica [62]. Three different methodologies can be followed to covalently anchor amino acids on a silica surface, each approach having its own advantages and disadvantages. The two routes shown in Fig. 2.17 are very similar; comprising of the same

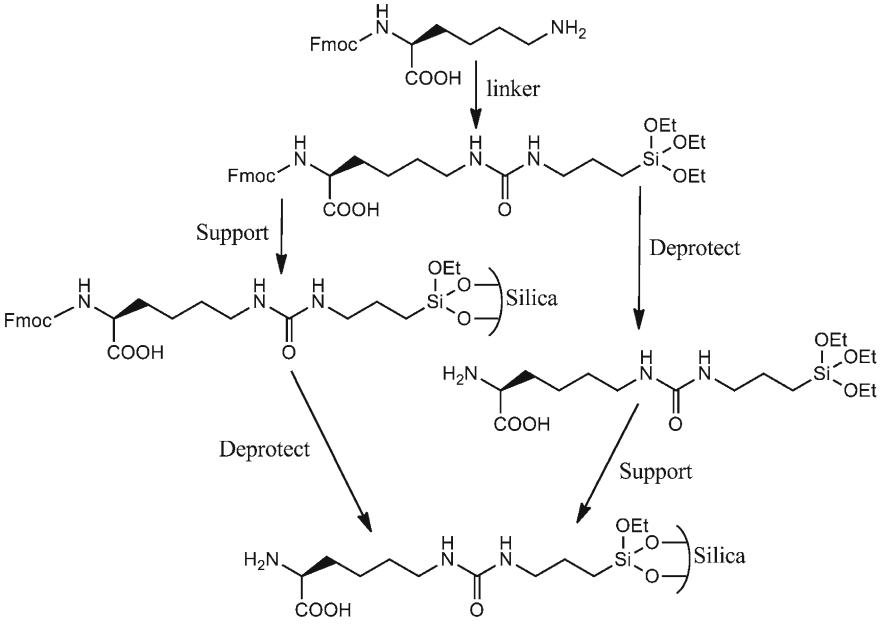

Fig. 2.17 Route (i) and (ii) for the immobilisation of the amino acid L-lysine on porous silica from the starting material Fmoc-Lys-OH

first step of producing an amino acid coupled to an oxy-silane through a urea linkage. The other method couples the amino acid to the linker after the silica has been derivatized with the tether.

(i) In the first route, the protected amino acid is reacted with a linker; in this case an isocyanate silane. The isolated product is attached to the silica surface under reflux and purified via soxhlet extraction and numerous washings. The amino acid undergoes Fmoc cleavage to leave an accessible amino acid derivatized silica framework ready for catalysis.
(ii) The second route repeats the first step in method one by reacting the protected amino acid with the linker. After this step the amino acid is deprotected in solution before immobilisation. The product from this stage is anchored to give the single-site heterogeneous catalyst.
(iii) The third method of heterogenization begins with the attachment of the linker to the framework to construct a functionalized silica surface. The protected amino acid couples with the fixed linker and transfers from being dissolved in solution to being connected to the solid phase. Lastly the immobilised amino acid is deprotected by Fmoc cleavage to leave available amino and carboxylate groups for catalysis.

The first route (i), appears to be more employable than the second (ii), because of the need for less separation and work up steps. This can be problematic when dealing with the silane groups because of the reactivity towards water and the affinity to react with one another to form Si–O–Si bonds. The less work done in solution the better, so by anchoring the product formed in the first step before deprotection, means that only one product has to be isolated in solution. The products in other steps can be isolated by simple filtration because of the solid phase. In this instance the first route is also more appropriate than the third method mentioned above because amino acids are difficult to dissolve. If the linker is already attached inside a pore then the amino acid will not couple to it since it is not in solution and therefore cannot diffuse throughout the framework. To help characterise the reaction between Fmoc-Lys-OH (protected amino acid) and 3-(triethoxysilyl)propyl isocyanate (linker) numerous reactions were carried out with varying primary amines such as benzylamine and propylamine to help give a handle on the shifting of the CH_2 environment neighbouring the urea linkage. The shift was measured at around 0.5 ppm down field. This outcome matches the shift noticed in the ^{1}H NMR spectrum of the product of the first step which is the reacted Fmoc-Lys-OH. There was a possibility that the acid functionality of the protected amino acid could also undertake nucleophilic attack of the isocyanate linker, but this was not considered after a reaction with the isocyanate tether and γ-aminobutyric acid showed only one product formed. This was proven by the detection of only two inequivalent carbonyl ^{13}C environments in the NMR spectrum.

Various silica frameworks can be used as supports and these give differing results on enantiomeric excesses and yields. Silica supports can have high or low surface areas, be porous or non-porous and have individual surface properties

such as convex pockets where the catalysts resides, such as in Cab-osil®. All these different properties have an effect on the catalyst loading, steric constraints on reactant diffusion, transition states and intermediates, consequently altering the selectivity and activity from one catalyst to another. This can be observed in differences of selectivity when pore diameters are varied from 30 to 150 Å [46]. Not only does this affect the active site isolation when synthesizing the heterogeneous catalyst but also has an effect on reactant diffusion and the mechanistic course because of the spatial restrictions. Selectivity can be influenced by the constriction of space around the active site. In order to ascertain whether the catalyst is encapsulated inside the channels of the framework or on the outer surface, it is essential to understand the effect of the support. To ensure most of the active sites are located within the framework, a capping agent is introduced before attaching the amino acid. The capping agent is a bulky group, usually dichlorodiphenylsilane, which is added in a very small quantity. The bulky group binds to the outer surface of the silica framework by coupling to the easily accessible silanol groups on the outside. These silanol groups are now 'deactivated' so the amino acid can preferentially bind to the inside walls of the structure. Instead of using a capping agent to make sure the catalyst is incorporated, one can assume that the inner surface area is much greater than the outer surface, so the majority of the catalyst is immobilised inside the channels of the network. This is an adequate deduction, but if the support has a greater effect on the stereoselectivity of the product then having a minute amount of catalyst on the outer surface could have a great significance on the ee.

2.4.3.4 Characterisation

Considering that the bulk of the material is the silica support, it is understandable that characterising the active catalyst is more difficult than previously perceived. Even more so since there is no metal present; this reduces the number of techniques that can be used. Structural information cannot be deduced from EPR and UV–Vis spectroscopy that can give a high-quality insight into the active site but reveal very little useful information in this case. A further difficulty for characterisation is that the catalyst is immobilised in the channels of the silica structure. Several techniques are surface sensitive so the fact that the catalyst is encapsulated and not on the outer surface renders these methods unusually unhelpful.

Basic experiments such as the Kaiser test can be used to detect if there is deprotected amino acid in the sample [63]. This is a simple colour change observation on addition of the two Kaiser reagents with heating at 120°C. The solution will turn deep blue in colour if there are free primary amines present. A quantitative value can be taken by measuring the absorbance of cleaved Fmoc adducts after the deprotection step. The intensity of the absorbance measured at λ_{max} 302 nm depends on the concentration of Fmoc adduct in solution. By working out the concentration of Fmoc-adducts using the Beer-Lambert law, the

amino acid concentration in the sample can be indirectly calculated, since for every cleaved Fmoc there must be one deprotected amino acid. As a result the amino acid/catalyst loading can be calculated and in turn gives the necessary quantities for turnover number (TON) and turnover frequency (TOF) to be derived when catalysis is carried out.

Another informative technique is to carry out elemental analysis. This gives the % mass of the varying elements contained in the sample; therefore an empirical formula can be deduced by working out the ratios between different elements. This is useful as it gives an insight into the catalyst loading and confirms the presence of the amino acid derivative but it does not offer proof that the organic moiety is incorporated in the channels of the framework. One way of substantiating this claim is by Brunauer–Emmett–Teller (BET) adsorption isotherms. Measuring the concentration of adsorbed probe molecules on a non-derivatized porous silica framework provides a specific surface area for the support before catalyst impregnation. Covalent attachment of the catalyst should give a smaller surface area, because now the surface available for the adsorption of small gaseous molecules has decreased due to the amino acid occupying significant space in the pores.

Further evidence for amino acid immobilisation can be sought by means of solid state NMR spectroscopy. ^{13}C MAS NMR is a principal technique that confirms the presence of the specific amino acid by matching the corresponding peaks to that of the pure amino acid (Fig. 2.18). NMR is a valuable asset in characterisation methods, but in this case because the sample has only around 1% carbon content and only 1.1% of that is the spin active ^{13}C isotope, this means that the amino acid is actually quite difficult to detect. From the spectra it is just possible to distinguish the peaks due to inequivalent carbon environments over the background noise. Using solid state NMR spectroscopy one can also determine if the organocatalyst is covalently attached to the silica surface or just adsorbed. This is achieved by measuring the spectrum of ^{27}Si. If covalently attached, the NMR spectrum should show several peaks that indicate the presence of different silicon environments. A peak at around –100 ppm is characteristic of $(Si(O\text{-})_4)$ silicates, which are of the bulk material. Further peaks around –60 ppm are typical of the silicon in the tether which is bound to the framework. Numerous peaks in the region of this chemical shift can be detected due to the varying number of ethoxy groups that have been grafted onto the support from each tether. These peaks are a clear indication of covalent immobilisation and are due to $(RSi(OEt)_2O\text{-})$ and $(RSi(O\text{-})_2OEt)$.

Powder infrared (IR) spectroscopy is another powerful tool to characterise the immobilised catalyst. Again the absorbances identified are extremely weak due to the catalyst residing inside the channels but, nevertheless, absorbances are noticed though they are very weak. Typical absorbances are found at around 3,300 cm^{-1} for O–H and N–H stretches and along with carbonyl stretching frequencies at ~1,700 cm^{-1}, C–H stretches are also detected just below 3,000 cm^{-1} to confirm presence of the amino acid. IR spectroscopy can also give an insight as to whether the amino acid is covalently bound to the silica support or not. This is achieved by interpreting the absorbances ~1,000 cm^{-1} in the fingerprint region where Si–O

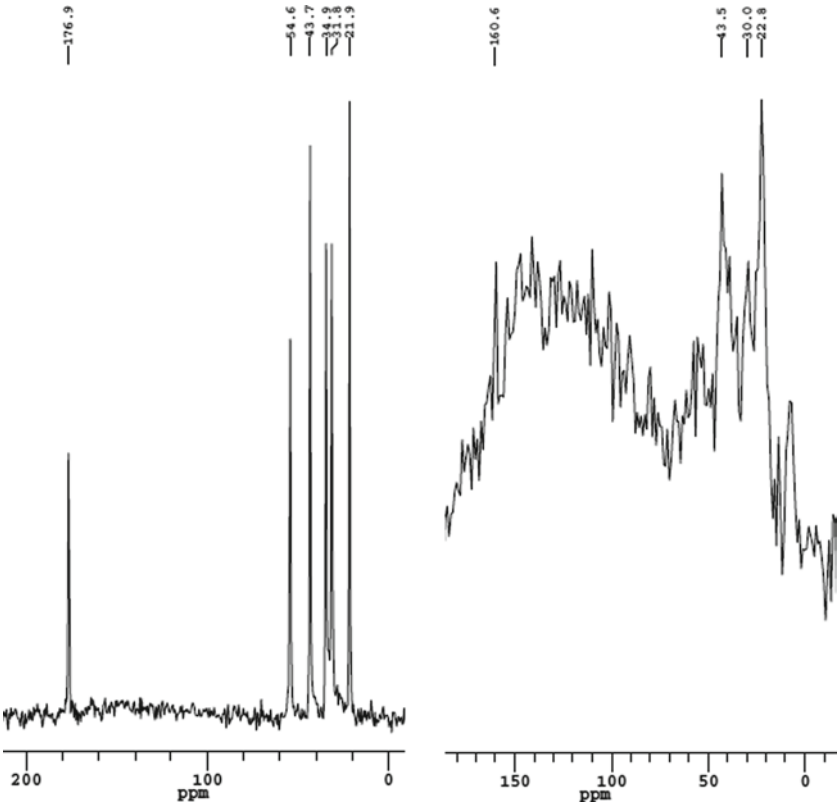

Fig. 2.18 ^{13}C MAS CP NMR of pure lysine (*left*) and immobilised lysine on porous 60 Å silica (*right*)

bonds absorb. Noticing extra peaks in this region suggests other Si–O environments. This can be accounted for the presence of Si in the tether that is bonded to different substituents when compared to the typical Si of the framework. The bulk Si of the support are all in a tetrahedral environment with four Si–O bonds whereas the Si of the tether either exists as $RCH_2Si(OSi)_2(OEt)$ or $RCH_2Si(OSi)_3$, confirming to varying Si–O bond strengths that will absorb at differing frequencies.

Collectively using these characterisation methods a conclusion can be adequately drawn regarding not only the presence of the amino acid, but its covalently attached heterogeneous nature.

2.4.4 Heterogenised Amino Acids as Single-Site Catalysts

Immobilising amino acids in this way produces covalently anchored single-site heterogeneous catalysts for utilisation in asymmetric enamine catalysis. Enamine

catalysis is the reversible generation of an enamine, from a catalytic amount of amine and a carbonyl compound, as an intermediate step in addition and substitution reactions [64]. All amino acids follow this mode of catalysis because of the free amine group, with the additional benefit of the close proximity carboxylate group. The carboxylate functionality influences the configuration of the transition state and therefore gives rise to stereoselectivity in the final product. An example of enamine catalysis is in the asymmetric aldol reaction and this is why amino acids, especially that of proline, have been employed as catalysts for this type of reaction [42] (Fig. 2.19). The aldol reaction is a fundamental C–C bond forming reaction and is used for the synthesis of complex natural products and drug molecules.

Many reports of different aldehydes have been used in the catalysed aldol reaction along with specific aldolizations such as Hajos-Parrish reactions [65,66] and intermolecular aldolizations with cyclic ketone donors [67]. The scope for these bio-derived supports is extensive. Any reaction that uses an organocatalyst that goes via an enamine intermediate has the potential to be catalysed by these amino acid derivatized frameworks. Intermolecular and intramolecular Michael reactions have been catalysed by amino acids in the homogeneous state [68,69] so these heterogeneous catalysts have great potential in replicating and improving these results. Reactions that include the α-amination, α-oxygenation and α-halogenation of carbonyl compounds have also been catalysed by amino acids [70–72] in solution so these can potentially

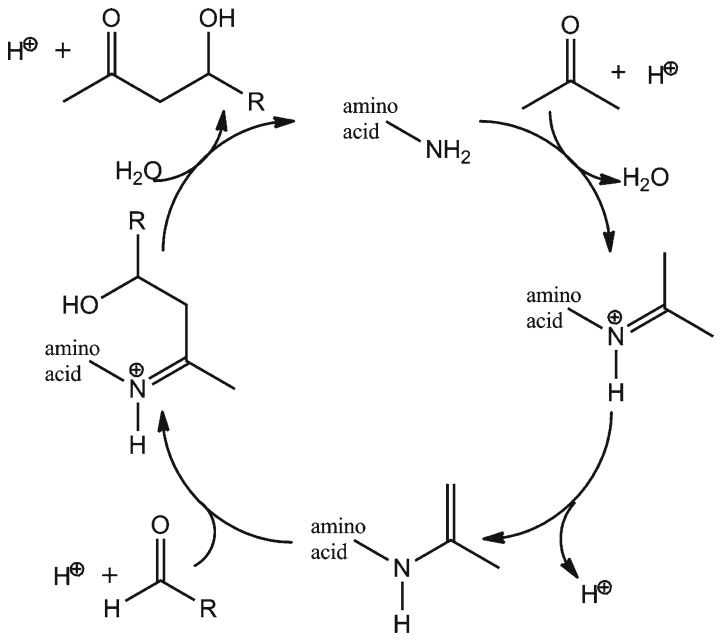

Fig. 2.19 Catalytic cycle of an asymmetric aldol reaction via an enamine intermediate

undergo the transformations assisted by the bio-derived frameworks with greater efficiency.

2.4.5 Summary

The use of amino acids as organocatalysts has generated widespread interest in recent years. They have been used to catalyse some of the most fundamental C–C bond forming reactions, such as the aldol and Mannich reactions, with high stereoselectivity and yields. These organocatalysts still suffer drawbacks in the homogeneous state and through suitable immobilisation techniques these disadvantages can be overcome with complimentary yields and selectivities. Covalently anchoring amino acids to silica through the side chain functionalities, offers accomplished routes to bio-derived frameworks that can be utilized as catalysts for specific transformations in fine chemical production.

References

1. Holm RH, Kennepohl P, Solomon EI (1996) Chem Rev 96:2239–2314
2. Que L, Tolman WB (2008) Nature 455:333–340
3. Shan X, Que L (2006) J Inorg Biochem 100:421–433
4. Meunier B, de Visser SP, Shaik S (2004) Chem Rev 104:3947–3980
5. Neidig ML, Solomon EI (2005) Chem Commun 47:5843–5863
6. Zhang J, Zheng H, Groce SL, Lipscomb JD (2006) J Mol Catal A Chem 251:54–65
7. Solomon EI, Chen P, Metz M, Lee SK, Palmer AE (2001) Angew Chem Int Ed 40:4570–4590
8. Lieberman RL, Rosenzweig AC (2005) Dalton Trans 21:3390–3396
9. Klinman JP (1996) Chem Rev 96:2541–2561
10. Whittaker JW (2003) Chem Rev 103:2347–2363
11. Matoba Y, Kumagai T, Yamamoto A, Yoshitsu H, Sugiyama M (2006) J Biol Chem 281:8981–8990
12. Eicken C, Krebs B, Sacchettini JC (1999) Curr Opin Struct Biol 9:677–683
13. Yamauchi O, Odani A, Takani M (2002) Dalton Trans 18:3411–3421
14. Suzuki K, Oldenburg PD, Que L Jr (2008) Angew Chem Int Ed Engl 47:1887–1889
15. Luechinger M, Kienhöfer A, Pirngruber GD (2006) Chem Mater 18:1330–1336
16. Kerman K, Kraatz HB (2008) Angew Chem Int Ed 47:6522–6524
17. Wight AP, Davis ME (2002) Chem Rev 102:3589–3614
18. Yang H, Zhang G, Hong X, Zhu Y (2004) Micropor Mesopor Mater 68:119–125
19. Luechinger M, Prins R, Pirngruber GD (2005) Micropor Mesopor Mater 85:111–118
20. Walcarius A, Etienne M, Lebeau B (2003) Chem Mater 15:2174–2180
21. Merrifield RB (1963) J Am Chem Soc 85:2149–2154
22. Pirngruber GD, Frunz L, Lüchinger M (2009) Phys Chem Chem Phys 11:2928–2938
23. Derouane EG (2002) Cat Tech 6:11–13
24. Raja R, Thomas JM (2002) J Mol Catal 181:3–14
25. Raja R, Ratnasamy P (1997) J Catal 170:244–253
26. Raja R, Ratnasamy P (1997) Catal Lett 48:1–10
27. De Vos DE, Sels BF, Jacobs PA (2002) Cat Tech 6:14–29

28. Raja R, Ratnasamy P (1996) Applied Catal A 143:145–158
29. Raja R, Ratnasamy P (1996) Applied Catal A 158:L7–L15
30. Raja R, Thomas JM (2001) Chem Record 1:448–466
31. Weckhuysen BM, Verberckmoes AA, Fu L, Schoonheydt RA (1996) J Phys Chem 100:9456–9461
32. Fan B, Li H, Fan W, Jin Ch, Li R (2008) Appl Catal A Gen 340:67–75
33. Balkus KJ Jr, Eissa M, Levado R (1995) J Am Chem Soc 117:10753–10754
34. Dzierzak J, Lefenfeld M, Raja R (2009) Top Catal 52:1669–1676
35. Grommen R, Manikandan P, Gao Y, Shane T, Shane JJ, Schoonheydt RA, Weckhuysen BM, Goldfarb D (2000) J Am Chem Soc 122:11488–11496
36. http://www.iza-structure.org/databases/
37. Mateo Marti E, Barlow SM, Haq S, Raval R (2002) Surface Sci 501:191–202
38. Bordiga S, Buzzoni R, Geobaldo F, Lamberti C, Giamello E, Zecchina A, Leofanti G, Petrini G, Tozzola G, Vlaic G (1996) J Catal 158:486–501
39. Zhilinskaya EA, Delahay G, Mauvezin M, Coq B, Aboukais A (2003) Langmuir 19:3596–3602
40. Raja R, Thomas JM, Greenhill-Hooper M, Doukova V (2007) Chem Comm 1924–1926
41. Raja R (2009) Top Catal 52:322–332
42. List B, Lerner RA, Barbas CF (2000) J Am Chem Soc 122:2395–2396
43. Ramachary DB, Chowdari NS, Barbas CF (2000) Tet Lett 43:6743–6746
44. List B (2000) J Am Chem Soc 122:9336–9337
45. Miao WS, Chan TH (2006) Adv Synt Catal 348:1711–1718
46. Raja R, Thomas JM, Jones MD, Johnson BFG, Vaughan DEW (2003) J Am Chem Soc 125:14982–14983
47. Shen ZX, Ma JM, Liu YH, Jia CJ, Li M, Zhang YW (2005) Chirality 17:556–558
48. Liu K, Haeussinger D, Woggon WD (2007) Synlett 14:2298–2300
49. Gruttadauria M, Riela S, Aprile C, Lo Meo P, D'Anna F, Noto R (2006) Adv Syn Catal 348:82–92
50. Aprile C, Giacalone F, Gruttadauria M, Marculescu AM, Noto R, Revell JD, Wennemers H (2007) Green Chem 9:1328–1334
51. Bellis E, Kokotos G (2005) J Mol Catal Chem 241:166–174
52. Benaglia M, Celentano G, Cozzi F (2001) Adv Syn Catal 343:171–173
53. Gu LQ, Wu YY, Zhang YZ, Zhao G (2007) J Mol Catal A Chem 263:186–194
54. Font D, Jimeno C, Pericas MA (2006) Org Lett 8:4653–4655
55. Giacalone F, Gruttadauria M, Marculescu AM, Noto R (2007) Tet Lett 48:255–259
56. Akagawa K, Sakamoto S, Kudo K (2005) Tet Lett 46:8185–8187
57. Revell JD, Gantenbein D, Krattiger P, Wennemers H (2006) Biopolymers 84:105–113
58. Krattiger P, Kovasy R, Revell JD, Ivan S, Wennemers H (2005) Org Lett 7:1101–1103
59. Bayer E (1991) Angew Chem Int Ed Engl 30:113–129
60. Jones MD, Raja R, Thomas JM, Johnson BFG (2003) Top Catal 25:71–79
61. Jones MD, Raja R, Thomas JM, Johnson BFG, Lewis DW, Rouzaud JM, Harris KD (2003) Angew Chem Int Ed 42:4326–4331
62. Calderon F, Fernandez R, Sanchez F, Fernandez-Mayoralas A (2005) Adv Syn Catal 347:1395–1403
63. Kaiser K, Colescott RL, Bossinger CD, Cook PI (1970) Anal Biochem 34:595
64. Mukherjee S, Yang JW, Hoffmann S, List B (2007) Chem Rev 107:5471–5569
65. Hoang L, Bahmanyar S, Houk KN, List B (2003) J Amer Chem Soc 125:16–17
66. Northrup AB, MacMillan DWC (2002) J Amer Chem Soc 124:6798–6799
67. List B, Pojarliev P, Castell C (2001) Org Lett 3:573–575
68. Kozikowski AP, Mugrage BB (1989) J Org Chem 54:2274–2275
69. List B, Pojarliev P, Martin HJ (2001) Org Lett 3:2423–2425
70. List B (2002) J Amer Chem Soc 124:5656–5657
71. Zhong GF (2003) Angew Chem Int Ed 42:4247–4250
72. Enders D, Hüttl MRM (2005) Synlett 6:991–993

Chapter 3
Heterogenization on Inorganic Supports: Methods and Applications

José M. Fraile, José I. García, José A. Mayoral, and Elisabet Pires

Abstract Inorganic supports offer interesting properties for immobilization of metal complexes, such as mechanical strength and developed surface area and porosity. The different composition and structure of the inorganic supports allow the immobilization through a large variety of methods, including those using weak support–complex interactions, such as van der Waals forces or hydrogen bonds, and those in which strong support–complex interactions are formed, electrostatic or covalent, taking into account the part of the complex participating in the interaction, either the metal or one of the ligands. In this chapter those methods will be reviewed in a critical way to show the advantages and disadvantages of each one and its applicability.

3.1 Inorganic Supports: Types and Properties

The immobilization of metal catalysts has different objectives. The most evident is the possibility of recovery and reuse, made easier by filtration or centrifugation due to the solid nature of the immobilized catalyst. For this purpose solids with a determined particle size and mechanically stable are necessary, requirements fulfilled by inorganic solids of different nature. As high catalytic activity is desirable and, in the case of solid catalysts, it is related with accessibility to sites, it is necessary that the support has a developed surface area, with pores large enough to allow the molecules of reagents and products reaching the sites and leaving the solid respectively.

The other objective, and probably the most important one, is to improve the catalytic performance of the metal complex, either by preventing deactivation thanks to the phenomenon of *site isolation* or by improving selectivity. This last

J.M. Fraile (✉), J.I. García, J.A. Mayoral, and E. Pires
Departamento de Química Orgánica, Instituto de Ciencia de Materiales de Aragón e Instituto Universitario de Catálisis Homogénea, Facultad de Ciencias, C.S.I.C.-Universidad de Zaragoza, E-50009 Zaragoza, Spain
e-mail: jmfraile@unizar.es

P. Barbaro and F. Liguori (eds.), *Heterogenized Homogeneous Catalysts for Fine Chemicals Production*, Catalysis by Metal Complexes 33,
DOI 10.1007/978-90-481-3696-4_3,

objective is very important in fine chemicals synthesis, as selectivity is one of its main issues, and one of the important requirements for this is the preparation of *single-site heterogeneous catalysts* [1]. Such single sites are spatially and chemically isolated from one another, and each site has the same energy of interaction between it and a reactant as every other single site. In order to obtain single-sites it is necessary to have defined regular immobilization positions, which is easier with rigid inorganic solids than with flexible organic polymers. Moreover, the rigidity is interesting with respect to porosity, as it is not dependent on the reaction solvent.

Inorganic supports can be classified by their composition. Most of supports are metal oxides, either single (silica, alumina) or mixed oxides, including all types of silicates and phosphates. However in many cases the most relevant properties as supports for metal complexes come from their structure and morphology, which condition the presence of either one type or several types of immobilization sites, leading to truly single-site catalysts or to solids with different kinds of sites. The structural criterion has been used to classify the solids [2].

3.1.1 Amorphous Solids

Amorphous solids are those lacking long-range crystalline order. However they may possess some short-range order, or even microcrystalline solids are considered. In general most of their properties, such as pore size or particle size, are not well-defined but they present a distribution.

3.1.1.1 Silica

Silica is a general term used to name the different forms of silicon dioxide (SiO_2), composed by SiO_4 tetrahedrons sharing corners in a disordered manner. It is without any doubt the amorphous solid most used as support due to its availability with tailored properties, due also to the extensive use as chromatography adsorbent [3]. Amorphous silica can be classified into three main types:

(a) *Silica Gel* Formed by polymerization of primary silicate particles prepared from precursors such as $Si(OEt)_4$ or $SiCl_4$, although in industry the method of choice is the reaction of sodium silicate with a mineral acid. The conditions of the reaction, gel ageing, and drying allow tailoring the final properties of the silica gel. Hydrogels present the pores filled with water. Drying by heating produces the partial collapse of the pore system, leading to xerogels with lower surface area and pore volume. The pore structure can be kept by drying under mild conditions, such as $scCO_2$ extraction, forming aerogels with high porosity and surface area. In general silica gels can be prepared with narrow pore size distribution in

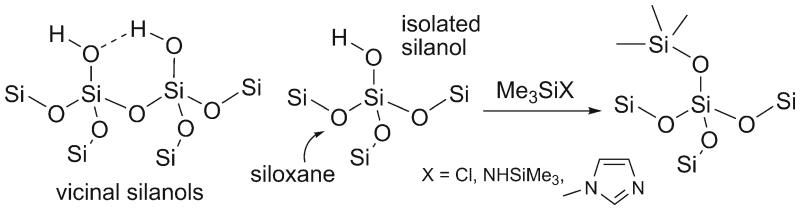

Fig. 3.1 Types of silanol groups in silica surface

the range of 0.5–200 nm, although values between 2.5 and 15 nm are the most common.

(b) *Precipitated Silica* Obtained by acidic precipitation of silicate solutions under conditions preventing the formation of gels. Primary particles are then larger, and silica presents a wide pore size distribution, in contrast with silica gel, although properties can be tailored by controlling the precipitation and drying conditions.

(c) *Fumed (Pyrogenic) Silica* Prepared from aerosols at high-temperature, which confers it higher purity. In general fumed silica is non-porous, with moderate to low surface area (50–300 $m^2\ g^{-1}$) and small particle size. Silica surface is composed by Si–O–Si siloxane groups and Si–OH silanol groups (Fig. 3.1) which confer hydrophilic character to the surface and slight acidity. Although double (geminal, $(–SiO)_2–Si–(OH)_2$) and even triple ($–SiO–Si–(OH)_3$) hydroxyls are possible, the vast majority of the surface hydroxyls are single $(–SiO)_3–Si–OH$. The arrangement of them greatly depends on the type of silica, and they can be either isolated or vicinal forming hydrogen bonds (Fig. 3.1), and hence their reactivity is different. Vicinal silanols can be eliminated by dehydration at high temperature (around 600°C), forming hydrolysable strained siloxane groups. Silanols are crucial for the support role of silica, as they can be used as anchoring points for covalent immobilization, for surface organometallic chemistry, or for adsorption by formation of hydrogen bonds with the complex. The hydrophilic character of silica surface can be modified by anchoring of silanes bearing hydrophobic chains. The most commonly used group is trimethylsilyl (Fig. 3.1), anchored from different precursors, such as trimethylsilyl chloride, hexamethyldisilazane or N-trimethylsilylimidazole.

3.1.1.2 Alumina

Alumina is also a general term to design different forms of aluminum oxide, including trihydrated ($Al_2O_3·3H_2O$), monohydrated ($Al_2O_3·H_2O$), and anhydrous forms (Al_2O_3). Structurally, alumina is composed by AlO_6 octahedra sharing edges in a layered arrangement, such as in gibbsite (Fig. 3.2) the trihydrated α form, whose layers are condensed by heating at high temperature, being converted into boehmite (monohydrated) and corundum (anhydrous) forms, although meta-stable

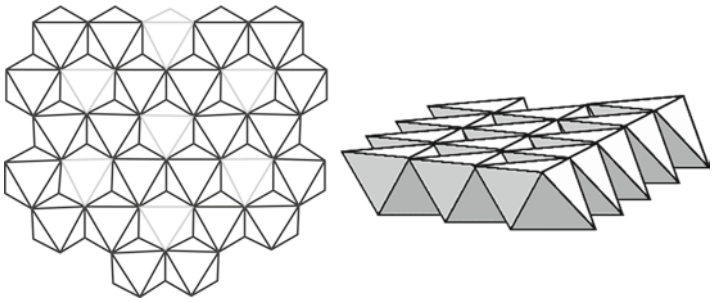

Fig. 3.2 *Left*: gibbsite (Al_2O_3, black octahedra) and brucite (MgO, all octahedra) structures. *Right*: side view of the layered arrangement

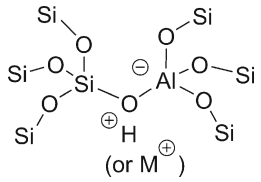

Fig. 3.3 Acid/cationic exchange sites in mixed oxides

forms (γ, δ, θ, κ…) with applications as metal supports (e.g. Pt/γ-alumina) can be obtained. The two most important amorphous alumina types are:

(a) *Alumina Gel* Amorphous or microcrystalline alumina gels can be prepared from aluminum salts or alkoxides in the same way as silica gels, and xerogels and aerogels can be obtained depending on the drying method. Rather high surface area (up to 500 $m^2\ g^{-1}$) and mesoporosity can be easily obtained.
(b) *Activated Alumina* Flash calcination of hydrated aluminas results in large pores formation by steam release from inside the solid particles.

Alumina is amphoteric, and acidic and basic forms can be obtained depending on the treatment. The presence of hydroxyl (Al–OH) groups on the surface is also one the main features to immobilize organometallic complexes, although the examples reported in literature are by far scarcer than in the case of silica.

3.1.1.3 Other Single and Mixed Oxides

Metal oxides, such as MgO, ZnO, ZrO_2, B_2O_3, or TiO_2, are materials commonly used as heterogeneous catalysts or supports for metals or other inorganic species, but very scarcely used as supports for organometallic complexes. Mixed oxides have interesting properties, and silica-alumina is probably the most used due to their acidic properties. The acidity comes from the isomorphous substitution of silicon by aluminum in tetrahedral sites (Fig. 3.3), leading to an excess

of negative charge that must be compensated by a cation, either a metal or a proton, which can be exchanged by a cationic organometallic compound. This is also the origin of the charge in other silicates, such as clays and zeolites as described below.

3.1.2 Layered Solids

Layered solids are formed by piled up sheets with short- and long-range two-dimensional order.

3.1.2.1 Clays

Clays are sheet silicates (phyllosilicates), in which each sheet is formed by one or two layers of silica (SiO_4 tetrahedra) sharing corners with one octahedral layer of either alumina (brucite) or magnesia (gibbsite, Fig. 3.2). The most common clays are 1:1 (one tetrahedral and one octahedral layers, TO) and 2:1 (one octahedral layer between two tetrahedral ones, TOT, Fig. 3.4). 2:1 clays can be classified into dioctahedral (magnesiosilicates) and trioctahedral (aluminosilicates), whose names come from the occupancy of the octahedral layer, 2/3 or 3/3 respectively.

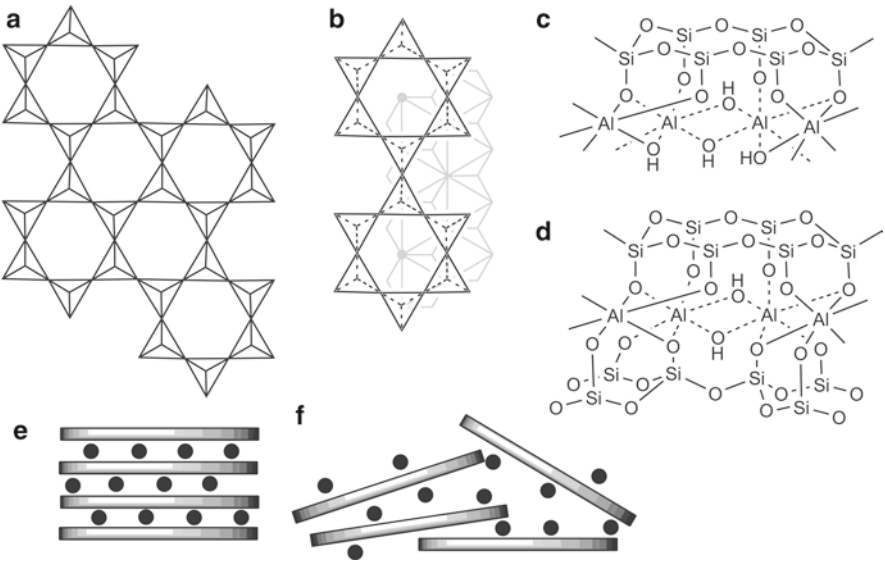

Fig. 3.4 Structure of clays: (**a**) arrangement of silica tetrahedra in phyllosilicates; (**b**) overlayered tetrahedral and octahedral layers; (**c**) side view of a dioctahedral 1:1 clay; (**d**) side view of a dioctahedral 2:1 clay; (**e**) piled up structure; (**f**) disordered "house of cards" structure

The most important feature of clays to act as supports for organometallic complexes is the cation exchange capacity. This capacity, as in the case of mixed oxides, comes from isomorphous substitutions either in the tetrahedral layers, where silicon is substituted by Al^{3+} or Fe^{3+}, or in the octahedral one, in which aluminum of trioctahedral clays is substituted by Mg^{2+} or Fe^{2+} or magnesium of dioctahedral clays is substituted by Li^{+}. Those substitutions generate an excess of negative charge in the sheets which is compensated with cations in the interlamellar zone, usually alkaline or alkaline-earth cations.

For cationic exchange to take place, it is necessary either to generate void space in the interlamellar zone by separation of the sheets or to delaminate the clay to obtain a disordered (house of cards) structure (Fig. 3.4). 2:1 clays present a large variety in number of substitutions (layer charge). Talc has very low number of substitutions, and hence it has almost no exchange capacity. Micas present a very high layer charge, which makes difficult to separate the layers and exchange is then improbable. Smectites are the clays most typically used as supports, as they show moderate layer charge, having moderate exchange capacity and swelling ability to allow the complexes entering in the interlamellar space. Montmorillonite is a dioctahedral smectite with substitutions mainly in the octahedral layer, corresponding to a general formula $(M^{+})_x[Si_8Al_{4-x}M(II)_xO_{20}(OH)_4]^{x-}$. Hectorite and saponite are trioctahedral smectites with substitutions in the octahedral and tetrahedral layers, respectively. Laponite is a synthetic hectorite with small particle size and especially suitable for cationic exchange. Delaminated clays (e.g. K10 and KSF montmorillonites) are prepared by acid treatment, which confers to them higher acidity, and they present higher accessible surface area.

3.1.2.2 Layered Double Hydroxides

Layered double hydroxides (LDH) [4] are composed by brucite-like sheets (Fig. 3.2) in which part of the divalent cations are substituted by trivalent ones, generating an excess of positive charge in the sheets which is compensated by interlamellar anions (Fig. 3.5). The most typical example is hydrotalcite, a Mg-Al mixed hydroxide with general formula $[Mg_{1-x}Al_x(OH)_2]^{x+}(CO_3^{2-})_{x/2}$. The main interest of LDH as supports is the anion exchange capacity. As described above for clays, the sheets must be separated for the exchange to take place. Moreover the high affinity of LDH for carbonate makes it difficult to exchange it and the support must be prepared with other type of anions, such as chloride or nitrate, and in the absence of CO_2.

3.1.3 Crystalline Solids

Crystalline solids have short- and long-range order along a three-dimensional network, with a regular pore system.

3.1.3.1 Zeolites

Zeolites [5] are crystalline microporous aluminosilicates. The three-dimensional structure is formed by a framework of corner-sharing SiO_4 tetrahedra and the different arrangements of those tetrahedra give rise to the large variety of structures described in the literature [6], which are represented as by lines joining the silicon atoms ignoring the oxygen atoms between them. Purely siliceous zeolites present defects only on the external surface of the crystals, and hence the amount of silanols is very low and of minor importance for immobilization purposes. The two main properties of zeolites as supports are porosity and cationic exchange capacity.

The dimensions and morphology of the zeolites pore systems (Fig. 3.6) depend on the arrangement of the silicon tetrahedra. Straight channels of 0.3–0.74 nm can be arranged in 1D (e.g. linde L, 0.71 nm Ø), 2D (e.g. ferrierite, 0.42 × 0.54 nm and 0.48 × 0.35 nm)

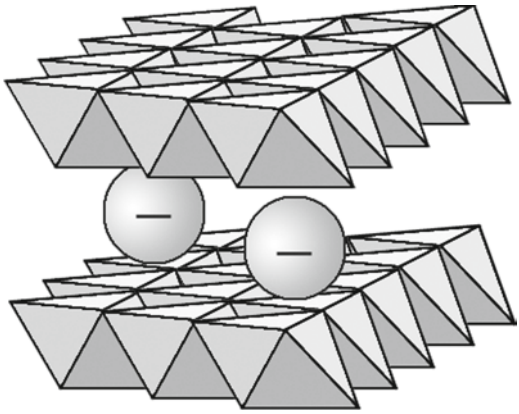

Fig. 3.5 Structure of layered double hydroxides

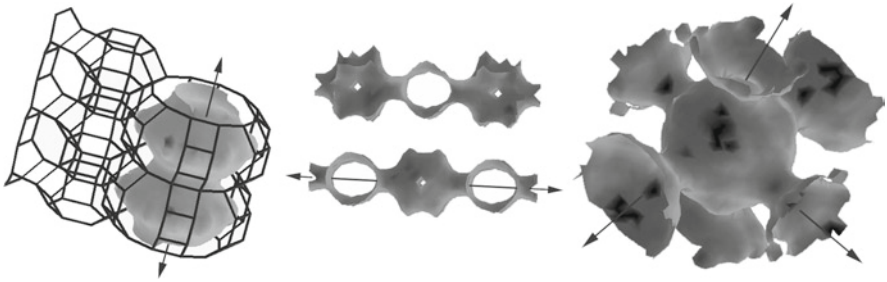

Fig. 3.6 Pore systems of zeolites: 1D in linde L (*left*), 2D in ferrierite (*center*), and 3D in linde A (*right*)

or 3D (e.g. linde A, 0.41 nm Ø) pore systems. The intersection of those channels may generate larger cavities, often called supercages, with diameters up to 1.2 nm (e.g. 1.14 nm in linde A). This feature is extremely important in the case of encapsulated complexes, as the narrower diameter of the channels prevents the loss of catalyst by diffusion. Faujasite-type zeolites (X and Y zeolites, with spherical supercages of 1.18 nm Ø connected by channels of 0.74 nm Ø, are among the most used for this purpose.

The origin of cationic exchange capacity is the same outlined for mixed oxides (Fig. 3.3). The isomorphous substitution of some silicon atoms by aluminum in tetrahedral sites generates an excess of negative charge, compensated by the presence of exchangeable cations.

Depending on the size of the complexes to be immobilized, the microporosity of zeolites may be an important limitation. Because of that, zeolites have been modified to allow large molecules entering inside the pore system. For this purpose dealumination has been carried out by different methods, such as hydrothermal treatment, chemical (EDTA, $SiCl_4$ vapor, etc.) treatment or both, leading to the so-called ultrastable zeolites with a partial loss of crystallinity and the formation of mesopores. The ultrastable Y zeolite (USY) is probably the most used both as catalyst and support. Microporous solids with different composition, namely aluminum phosphates, are not usually employed as supports for metal complexes.

3.1.3.2 Mesoporous Crystalline Materials

An alternative to overcome the pore size limitation of zeolites is the synthesis of mesoporous crystalline materials [7]. These solids show long-range order in the mesopores systems but not short-range order, given that the pore walls are composed by amorphous silica. This means that these solids are only partially crystalline and, in contrast with zeolites, show similar features to amorphous silica regarding anchoring of organometallic complexes. The pore size can be tailored by changing the preparation conditions, which include the use of some kind of surfactant. On the other hand, isomorphous substitutions of Si by Al have been described in some cases, introducing in this way the possibility of cationic exchange. The four main types of mesoporous materials are:

(a) *M41S* It is the generic name of the first materials of this type described in the literature, called MCM (Mobil Composition of Matter). The two best known examples are MCM-41, with hexagonal structure and straight channels in the range of 1.5–20 nm (Fig. 3.7), and MCM-48, with cubic structure and a 3D pore system. Pore walls are quite thin and hence (hydro)thermal stability is limited.
(b) *SBA (Santa Barbara Acids)* These materials possess mesopores with thick microporous silica walls, which confers higher (hydro)thermal stability. SBA-15 is a hexagonal material with curved mesopores in the range of 4–14 nm and 0.5–3 nm micropores. SBA-16 is a cubic material with mesopores of around 6 nm in a 3D system with larger cages in the intersections of channels.

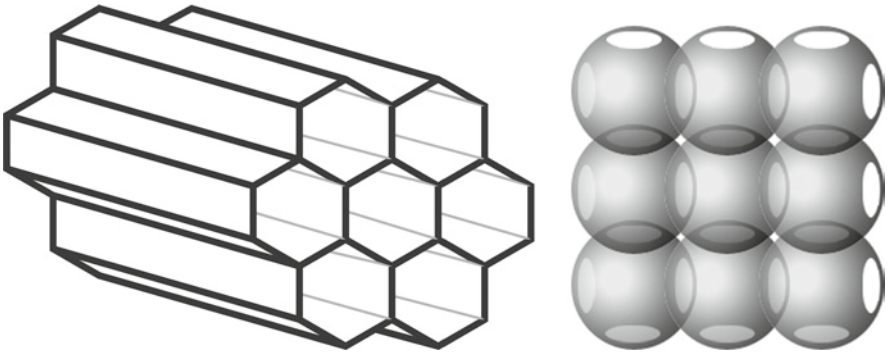

Fig. 3.7 Structure of mesoporous crystalline materials. *Left*: hexagonal arrangement of 1D pores (MCM-41). *Right*: schematic representation of a silica mesocelular foam (MCF)

(c) *MCF (Mesostructured Cellular Foam)* These materials are similar to SBA with expanded pores, which gives rise to sponge-like solids with large spherical cells (15–50 nm) connected with large windows (5–20 nm) (Fig. 3.7). In spite of this, walls are again thick enough to confer high stability.
(d) *MSU (Michigan State University)* This acronym corresponds to a large variety of structures, from poorly ordered wormhole structures to quite ordered hexagonal materials with tailored properties.

3.1.4 New (Alternative) Supports

3.1.4.1 Metal and Metal Oxide Nanoparticles

Nanoparticles have sizes between 1 and 100 nm and they constitute a growing research field given that in many cases their properties are different from those of the bulk analogous solids. In some cases, such as gold nanoparticles [8], they can act as efficient catalysts for a variety of reactions. With regard to their role as support for organometallic complexes, two main applications have been envisaged: the immobilization of thiol-functionalized complexes on gold nanoparticles and the immobilization on magnetic nanoparticles to facilitate the recovery of the catalytic complex using a magnet.

3.1.4.2 Carbon: Graphite, Nanotubes and Related Supports

Graphite is a layered material formed by sheets of sp^2 carbon atoms. However it has been seldom used as support for organometallic catalysts. For this purpose, oxidized forms of graphite (Fig. 3.8) or most commonly activated carbon are used. The presence of carboxylic groups allows the formation of bonds with either ligands (esters, amides) or with the metal (carboxylates). The same type of strategy can be

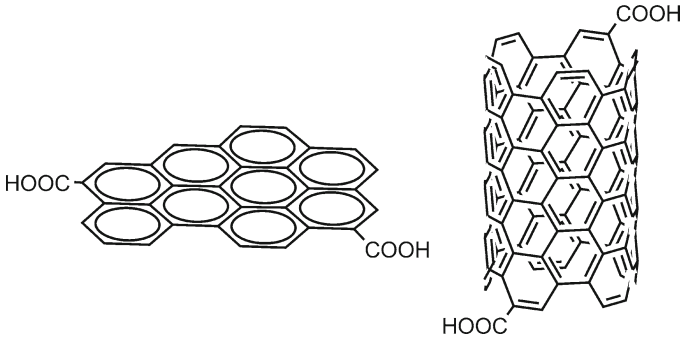

Fig. 3.8 Structure of a functionalized graphite (*left*) and a carbon nanotube (*right*)

also applied to carbon nanotubes (Fig. 3.8) [9] and nanowires, promising materials with interesting additional properties.

3.1.4.3 Composite Materials

The interest of composite materials as supports for organometallic complexes is increasing due to the possibility of tailoring the properties of the material, including the addition of new functionalities. Some examples are nanoparticles supported on silica or mesoporous crystalline materials, magnetic nanoparticles covered by silica and heteropolyanions supported on silica.

Each support can be used in several ways to immobilize organometallic complexes, and this chapter has been classified in three main sections according to the part of the complex having an interaction with the support. Section 3.2 deals with methods including a support–metal interaction. In Section 3.3 the methods based on a support–ligand interaction are revised. Finally the methods without any specific support–complex interaction are reviewed in Section 3.4.

3.2 Immobilization by Support–Metal Interactions

Immobilization of organometallic catalysts through direct interaction between the metal and the support is one of the most attractive alternatives, given that in this way the nature of the support may play a role in the catalytic performance. This type of immobilization can be carried out by means of two strategies, depending on the type of interaction. In the case of electrostatic interaction, the most frequently used, a cationic complex interacts with an anionic support, acting as the counterion. Obviously this immobilization is not efficient when the complex becomes neutral along the catalytic process. In the second strategy the support acts as a ligand included into the coordination sphere of the metal.

3.2.1 Support–Metal Electrostatic Interactions

Cationic complexes can be immobilized on anionic solids by three methods (Fig. 3.9). In the first one the cationic complex is previously formed in solution and then exchanged by the compensating cation of the solid. The main advantage of this method is that the complex can be well-characterized before immobilization, and the main drawback is the compatibility of the complex with the solvent of high dielectric constant necessary to carry out the cation exchange. Furthermore some of the original cations of the solid may remain on it, mainly if they are placed on sites non accessible to the bulkier complex, which reduces the degree of functionalization. This circumstance is not a major problem if it does not interfere with the catalytic process. The second method includes the exchange of the metal cation and the formation of the complex around it on the solid. The main advantage of this approach is that the exchange is carried out in the absence of the ligand, which solves the problem of solvent compatibility. Moreover it is possible to add an excess of ligand to force complexation in the case of complexes with low formation constant. However the main disadvantage is that some exchanged cations may be located in hindered sites, remaining uncomplexed and interfering in the catalytic process. Finally the third method tries to overcome the solvent limitation of the direct

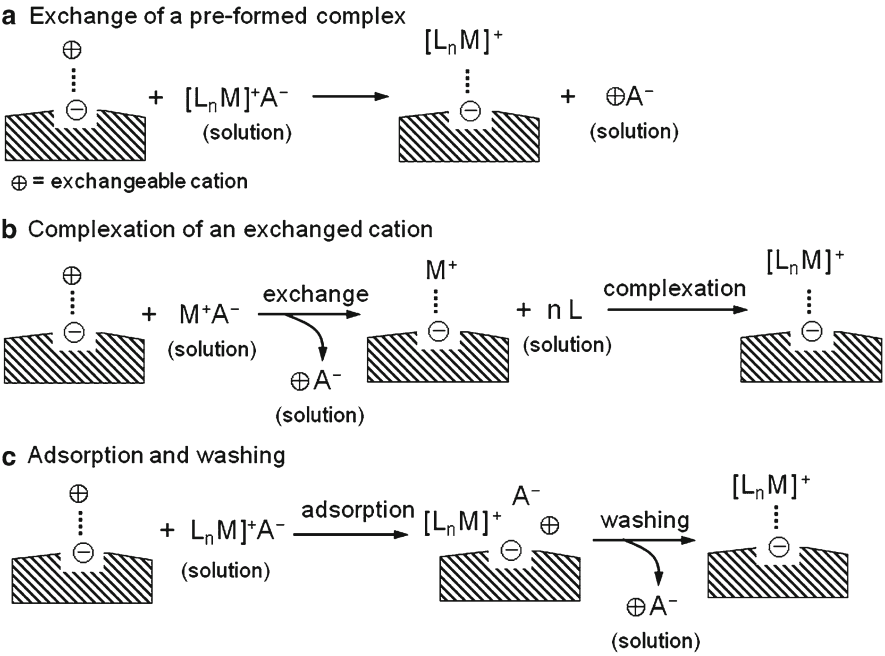

Fig. 3.9 Immobilization methods including a support–metal interaction: (**a**) direct exchange; (**b**) complex formation with an exchanged cation; (**c**) adsorption of the complex and washing of the resulting salt

exchange by adsorption of the complex from a solution in a solvent of low dielectric constant and then washing out the resulting salt with a different solvent.

Enantioselective hydrogenation is a very important process related to the synthesis of fine chemicals. Given that cationic Rh-diphosphine catalysts are highly efficient for this reaction, the immobilization of many different complexes of this type (Fig. 3.10) by electrostatic interactions has been studied using all the available strategies [10].

The direct exchange method (Fig. 3.9a) has been the most used, both with clays [11, 12] and mesoporous solids [13, 14]. The chosen exchange solvent with high dielectric constant is usually methanol [11, 14] or another alcohol [13], although water/acetonitrile mixtures have also been used [12]. Regarding ionic species, the starting complex bears a non-coordinating anion such as ClO_4^- [11, 12] or BF_4^- [13, 14], whereas the exchangeable cation on the solid may be sodium [11, 12] or even the exchange is carried out on the acidic form of the support [13, 14]. The cationic exchange was confirmed in some cases by the disappearance of the IR bands corresponding to the starting anion (ClO_4^-) in the final solid [12]. The different solids have been tested in the enantioselective hydrogenation of itaconates (Fig. 3.11a) and/or dehydroamino acid derivatives (Fig. 3.11b) and several interesting effects have been described.

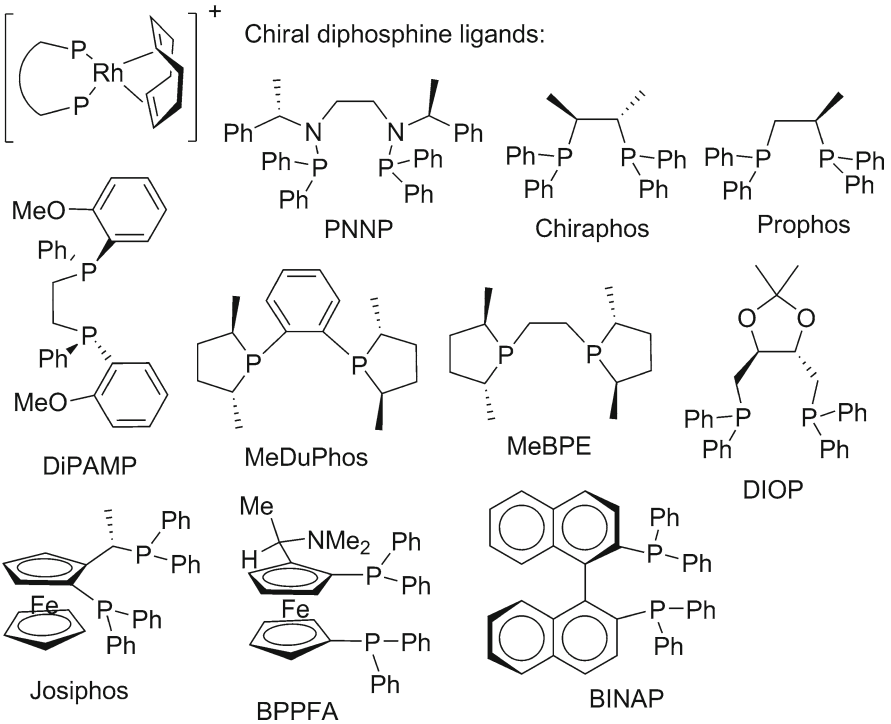

Fig. 3.10 Chiral cationic Rh–diphosphine complexes immobilized by support–metal electrostatic interactions

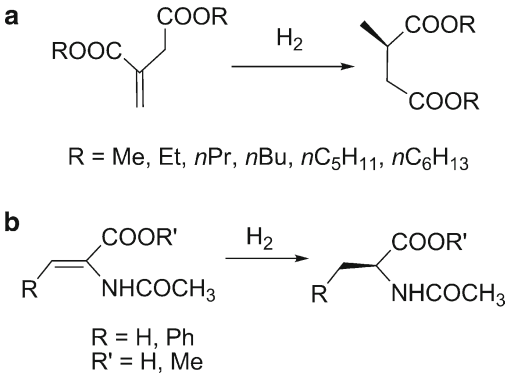

Fig. 3.11 Enantioselective hydrogenation of itaconates and dehydroamino acid derivatives

In the case of using different clays [11], hectorite (trioctahedral 2:1) was shown to be more efficient than bentonite (dioctahedral 2:1), nontronite (dioctahedral 2:1), and halloysite (dioctahedral 1:1) for the immobilization of $[(PNNP)Rh(cod)]^+$ and its use in the hydrogenation of several dehydroamino acid derivatives (Fig. 3.11b). Although the reason for this behavior is not clear, it shows the importance in the support choice for this kind of immobilization. The type of support is also important in the case of mesoporous materials [14], as Al-MCM-41 was shown to be a more suitable support than Al-SBA-15 for the immobilization of $[(MeDuPhos)Rh(cod)]^+$. The authors proposed an explanation based the different structure of both solids, with lack of accessibility to exchange sites in Al-SBA-15 due to the thickness of the pore walls. As a result the immobilized complex was less stable, as shown by the extensive leaching of Rh.

The existence of leaching was also detected in the case of Al-TUD1, a mesoporous support [13], for $[(MeDuPhos)Rh(cod)]^+$ and $[(DiPAMP)Rh(cod)]^+$. In the hydrogenation of methyl itaconate, the effect of the reaction solvent was crucial for the leaching level, but always in inactive form. This seems to indicate the formation of neutral species of Rh^0 that loss the electrostatic interaction with the support. This is the main limitation of this kind of immobilization.

Complexation method (Fig. 3.9b) has been very seldom used for Rh-diphosphine complexes immobilized by electrostatic interactions. Only in one case [14] the chiral diphosphine was added to $[Rh(cod)_2]^+$-exchanged Al-MCM-41, to obtain the immobilized $[(Josiphos)Rh(cod)]^+$ complex. This catalyst was used in the hydrogenation of dimethyl itaconate with 98–99% conversion and 90–94% ee along 10 consecutive runs.

Adsorption method (Fig. 3.9c) has been only applied on mesoporous materials [15]. Initial adsorption of complexes from a CH_2Cl_2 solution was followed by Soxhlet extraction with methanol to eliminate the adsorbed species, leaving only the truly exchanged species. This was demonstrated by the complete elimination of the complex in the case of purely siliceous materials. It was remarkable the amount of exchanged complex much lower than the theoretical one. The difficulty for the exchange of the sites in the inner part of the pore systems when the most external sites are already (kinetically favored) exchanged may explain this result. Again

SBA-15 showed consistently worse results than MCM solids, both in catalytic activity and enantioselectivity, and in this case the different method of Al insertion in the support, in-synthesis for MCM solids and post-synthesis for SBA-15, was proposed as an explanation. The best results were obtained with [(MeDuPhos)Rh(cod)]$^+$ in the hydrogenation of dimethyl itaconate.

Mn(III)(salen) complexes (Fig. 3.12) are extremely useful catalysts for epoxidation of alkenes, and their cationic nature makes them suitable for electrostatic immobilization. Both direct exchange and complexation methods (Fig. 3.9) were tested in the immobilization of the non-chiral Mn(salen) complex on clays [16]. Complexation method requires in this case an oxidation step from a Mn(II)-exchanged support to a Mn(III) complex (Fig. 3.13), in which the formation of neutral species such as Mn(III)(salen)Cl and Mn(II)(salen) (not shown) is possible and in agreement with the leaching of Mn in the complexation process. Direct exchange in methanol is then a more suitable immobilization method, in this case, and several factors such as the nature of the clay and the complex loading affect the catalytic performance. Higher TOF and TON in the cyclohexene epoxidation with iodosylbenzene (Fig. 3.14a) were obtained with low complex loading on laponite. Intercalation of the complex between the clay sheets is observed at high complex loading, but migration during the reaction and/or delamination of the clay produce a reduction in (001) basal spacing after recovery.

The best method was applied to Jacobsen's complex (Fig. 3.12) [16]. Very low catalyst loading was obtained due to the large size of the complex, preventing intercalation. The catalyst led to moderate enantioselectivity (34% ee) in the epoxidation of dihydronaphthalene with iodosylbenzene (Fig. 3.14b), consistent with an additional role of the clay sheets as axial ligands. One relevant point was the demonstration by IR spectroscopy of the degradation of the ligand under the reaction conditions, responsible for the lost in catalytic activity and selectivity of this Mn(salen) immobilized catalysts.

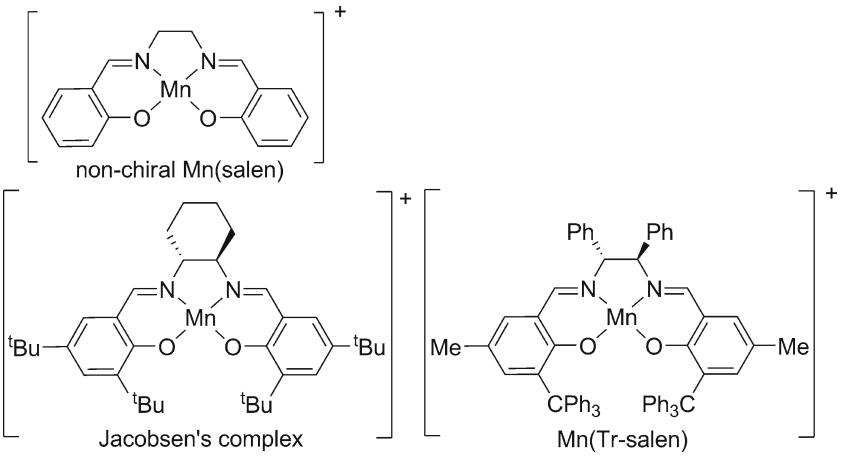

Fig. 3.12 Mn(salen) complexes immobilized by electrostatic interactions

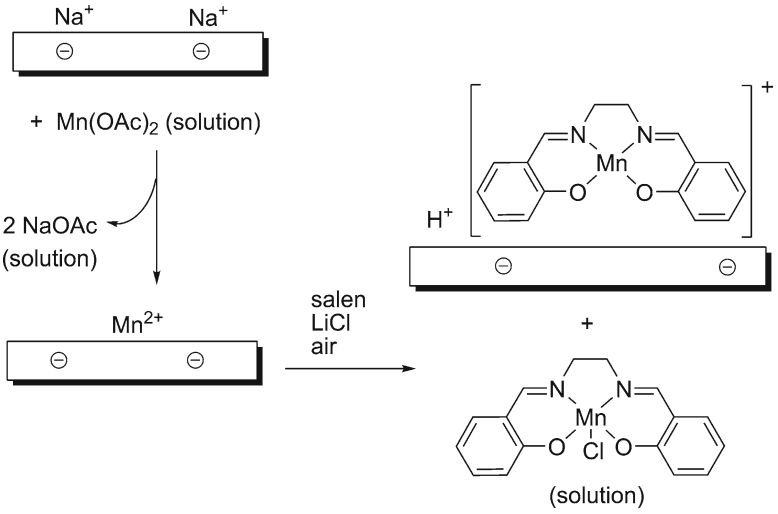

Fig. 3.13 Complexation method for immobilization of Mn(salen) complexes

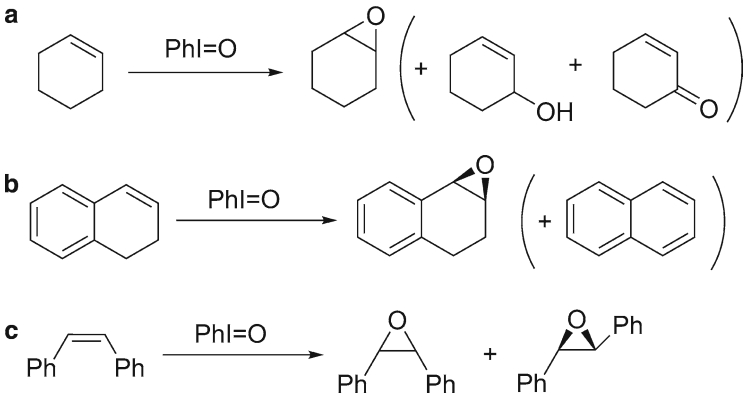

Fig. 3.14 Epoxidation reactions catalyzed by Mn(salen) complexes

The complexation method was also used to immobilize Jacobsen's complex on Al-MCM-41 [17]. By refluxing the ligand in CH_2Cl_2 with Mn^{2+}-exchanged Al-MCM-41, only 10–30% of the cation was complexed, showing the difficult accessibility to the inner exchange sites. However the low catalytic activity of the uncomplexed cation allowed obtaining good results in the epoxidation of (*Z*)-stilbene with iodosylbenzene (Fig. 3.14c). A mixture of *cis* (non chiral) and *trans*-epoxides, with 70% ee, was obtained, but reuse of the catalyst led to a noticeable loss of activity and enantioselectivity, probably due again to ligand degradation.

The immobilization of a sterically hindered trityl–salen complex (Mn(Tr-salen) Fig. 3.12) on Al-MCM-41 was tested by direct exchange from Mn(Tr-salen)PF_6 in ethanol and by treatment of Mn(II)-Al-MCM-41 with the chiral ligand and

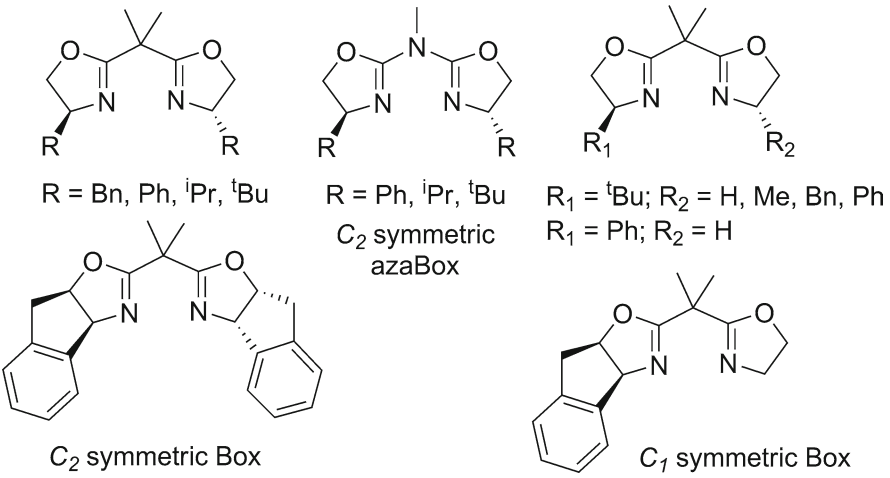

Fig. 3.15 Oxazoline-containing chiral ligands

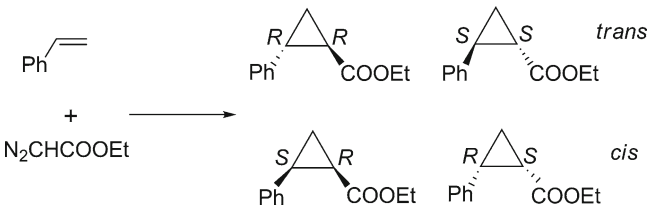

Fig. 3.16 Cyclopropanation reaction of styrene with ethyl diazoacetate

subsequent in situ oxidation [18]. Both types of catalyst led to similar results in epoxidations with m-CPBA, although the one obtained by direct exchange showed slightly higher activity and selectivity, with efficient recovery and reuse in three runs.

The electrostatic immobilization of copper complexes with oxazoline-containing chiral ligands (Fig. 3.15) has been also studied in depth. Clays were the first type of supports used to immobilize C_2 symmetric bis(oxazoline)–Cu complexes, (Box)–Cu-complexes, that were used as catalysts in cyclopropanation of styrene (Fig. 3.16). Immobilization was carried out by direct exchange of the (Box)$CuCl_2$ or (Box)$Cu(OTf)_2$ complexes in either methanol or nitroethane. Slight differences in catalytic performance depending on the clay and the exchange solvent were observed [19].

The integrity of the ligand was shown by FTIR spectroscopy whereas the geometry and the environment of Cu were studied by EPR and EXAFS, comparing in all cases the original (Box)$CuCl_2$ complex and the clay-immobilized one (Fig. 3.17) [20]. These experiments demonstrated that the whole complex was supported without modification of its chemical nature and that the starting chloride was lost during the exchange process, so that the complex was electrostatically bonded to the support acting as the counterion of the complex. This was not a trivial question,

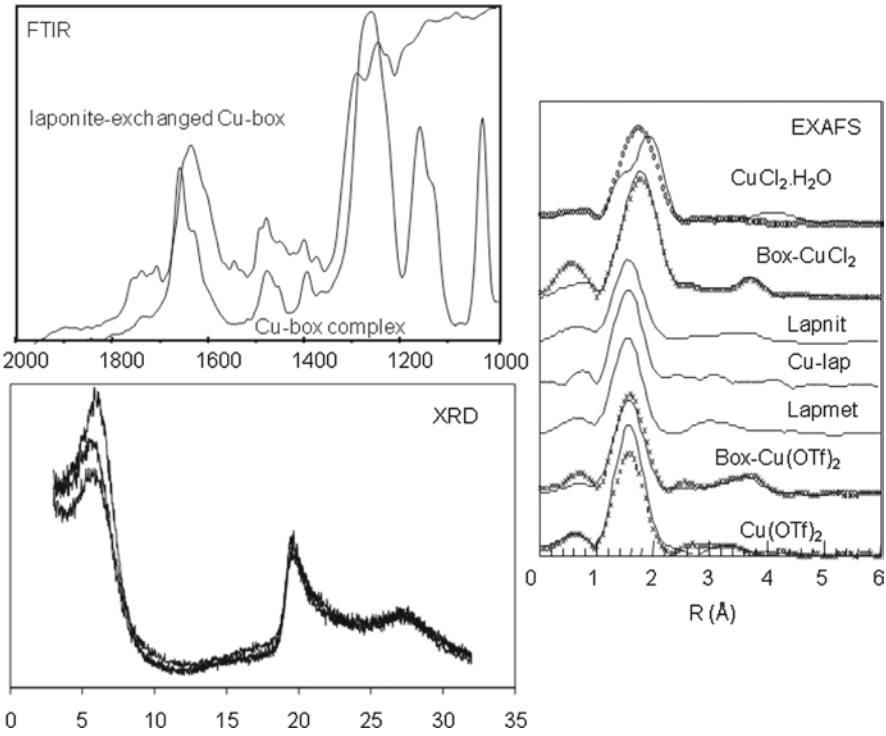

Fig. 3.17 Characterization of exchanged Box–Cu complexes

given that in this case the exchanged complex is dicationic, in contrast with (diphosphine)Rh and (salen)Mn.

In the case of BoxPh the increase in basal spacing determined by XRD indicates that, at least in part, the catalyst is intercalated between the clay sheets, behavior not observed with the larger Box^{t}Bu. The broadening and loss of intensity of the 001 diffraction line (Fig. 3.17) indicates that the clay is partially delaminated.

Important differences were observed between the behavior of BoxPh and Box^{t}Bu in the catalytic tests. The immobilized $[(BoxPh)Cu]^{2+}$ catalyst led to results very close to those obtained in solution with $(BoxPh)Cu(OTf)_2$, and the catalyst was recoverable. However the immobilized $[(Box^tBu)Cu]^{2+}$ catalyst was less enantioselective than its homogeneous counterpart and the enantioselectivity decreased upon recovery. In an attempt to improve the results with $[(Box^tBu)Cu]^{2+}$, some parameters of the exchange process were changed, such as the solvent and the outcoming cation, and even the complexation method (Fig. 3.9b) was used, with only minor improvements of the results [21]. The origin of this behavior lies on the loss of chiral ligand by decomplexation during the exchange process (Fig. 3.18) and upon recovery, due to the low stability of the complex.

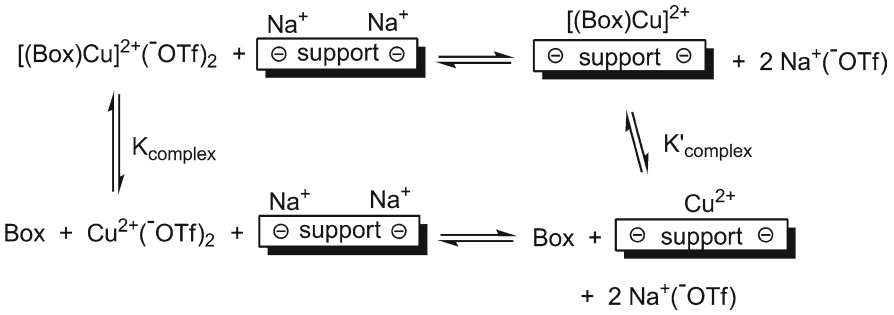

Fig. 3.18 Role of complexation constant on the exchange process

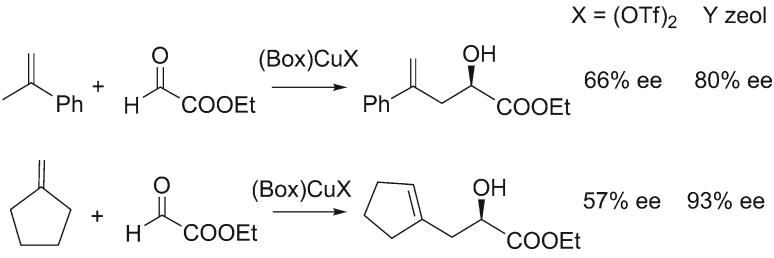

Fig. 3.19 Carbonyl-ene reactions catalyzed by (Box)Cu complexes

Azabis(oxazoline) ligands (azaBox, Fig. 3.15) posses a higher coordinating ability with regard to the analogous box ligands, as shown by theoretical calculations and competitive catalytic experiments [22]. This property was exploited to prepare more stable immobilized chiral catalysts, in which the loss of chiral ligand by decomplexation was minimized. Hence laponite immobilized [(azaBox^{t}Bu)Cu]$^{2+}$ led to better results than the Box counterpart, with enantioselectivities (up to 83% ee) close to those obtained in solution and good recoverability.

(Box)Cu complexes are also able to act as chiral Lewis acids, and the electrostatic immobilization with this purpose presents particular features. Carbonyl- (Fig. 3.19) and imino-ene reactions were promoted by [(BoxPh)Cu]$^{2+}$ exchanged in Y-zeolite [23]. The catalyst was prepared by the complexation method, with a previous exchange of Cu^{2+} in water, followed by calcination of Cu-Y, and treatment with Box in CH_2Cl_2. In this way only a minor part of Cu is under complex form, but the uncomplexed centres must be located in the inaccessible parts of the zeolite. Enantioselectivities obtained with the heterogeneous catalysts were similar to or better than those obtained in solution (Fig. 3.19) and the catalyst was reused up to three times in a different reaction each run.

Box and azaBox copper complexes can also act as Lewis acids in enantioselective Mukaiyama aldol reactions (Fig. 3.20) [24]. With enolsilanes of low reactivity (Fig. 3.20a) the donor character of the chiral ligand and the solvent of the exchange process play an important role on the catalytic activity of the complexes electrostatically immobilized on laponite. In the case of catalysts prepared by direct

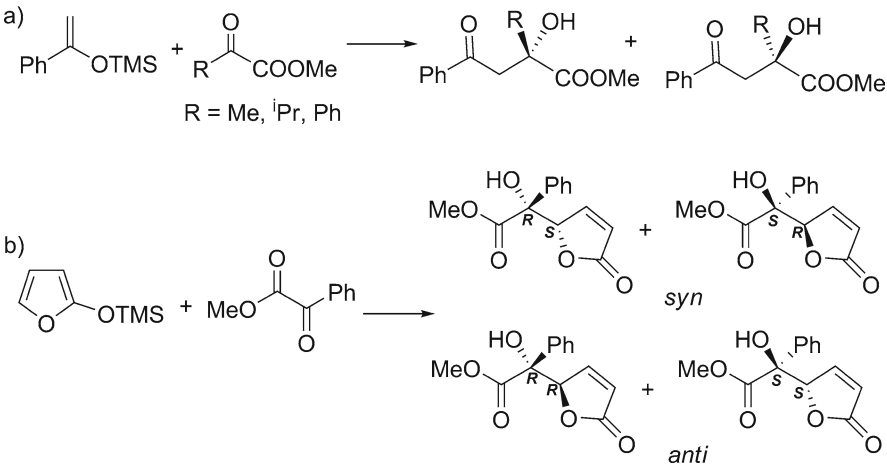

Fig. 3.20 Mukaiyama aldol reactions

exchange, $[(azaBox)Cu]^{2+}$ complexes were not active at all. The role of methanol as deactivating agent was demonstrated by the activity of the catalyst prepared by the adsorption procedure (Fig. 3.9c). On the contrary $[(BoxPh)Cu]^{2+}$ was active even in the case of the catalyst prepared by direct exchange.

One interesting additional feature of the electrostatic immobilization on clays is the existence of surface effects on the diastereo- and enantioselectivities [25]. This effect is the result of a combination of the presence of a layered cationic material (clay) and the use of a solvent with low dielectric constant. Under such conditions a tight ion pair is formed between the (Box)Cu complex and the layered support, leading to a change in the environment symmetry of the complex (Fig. 3.21), which modifies the stereochemical course of the reactions, although at the moment in a difficult to predict way.

The largest effects have been observed with BoxPh in three different reactions [25], namely cyclopropanation, C-H insertion, and Mukaiyama aldol (Fig. 3.22). In the case of the enantioselective C-H carbene insertion of ethyl 2-phenyldiazoacetate on THF an improvement in diastereo- and enantioselectivity was observed, reaching up to 88% ee in the major *syn* product. A more dramatic effect was observed in the cyclopropanation of styrene with ethyl diazoacetate, in which a complete reversion of the *trans/cis* diastereoselectivity (31:69) was observed, as well as a reversal in the sense of the chiral induction. As a result of those reversals, the major product obtained with the heterogeneous catalyst is the (1*S*)-*cis*-cyclopropane instead of the (1*R*)-*trans*-cyclopropane obtained in solution (Fig. 3.22). The role of the angle formed by the Box plane and the support sheet was demonstrated by the use of C_1-symmetric ligands (Fig. 3.15) that allow enhancing the surface effect [26].

Probably the most spectacular result was obtained in Mukaiyama aldol reactions. An incipient effect was observed in the reaction of methyl pyruvate with 1-phenyl-1-trimethylsilyloxyethene (Fig. 3.20a, R = Me), with a positive effect of immobilization on the enantioselectivity (86% ee vs. 45% ee in solution) [24]. However, the most important effect has been observed in the reaction between

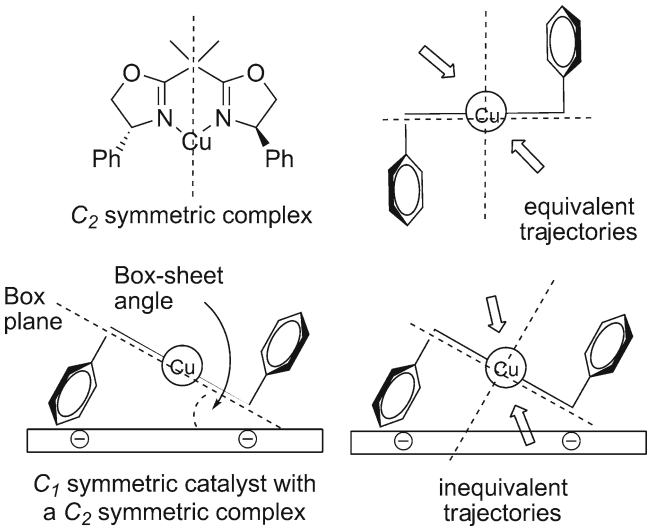

Fig. 3.21 Modification of the (Box)Cu symmetry upon immobilization on a layered material

2-trimethylsilyloxyfuran and methyl 2-oxo-2-phenylacetate (Fig. 3.20b) [27]. In this case the surface effect is able to modify the selectivities from *anti/syn* 38:62 and 16% ee for the *anti* isomer in solution to 86:14 and 90% ee with the supported catalyst, enabling in this way the separation and determination of the absolute configuration of the major *anti* compound.

In some cases the support acts as an anion with high coordinating ability, in a similar way to carboxylates or phenoxides in solution, and this immobilization cannot be considered as fully electrostatic, given the important covalent character of the metal-oxygen bond. However this method cannot be considered either as SOMC (see Section 3.2.2) as the nature of the complex is not modified with respect to the homogeneous one. For this reason this immobilization method has been included here. Oxygenated groups (carboxylic and/or phenolic) in active carbon may play the role of coordinating anions in the immobilization of different complexes, such as (diphosphine)Rh [28]. In fact the immobilization was carried out in the same way as an cationic exchange, by treatment of a solution of [(diphosphine)Rh(nbd)]BF_4 in methanol with active carbon and washing with the same solvent to eliminate the loosely adsorbed complex.

This type of anionic groups can be also immobilized on silica supports, either amorphous or crystalline mesoporous. In fact those supports can be considered as hybrid materials, because they take advantage of the properties of the inorganic support, such as surface area and porosity, as well as of those of the organic anion, such as modulation of the activity and selectivity. One example is the immobilization of Mn(salen) complexes on mesoporous silicas (MCM-41, SBA-15, amorphous silica) functionalized with phenoxide or sulfonic groups (Fig. 3.23). The immobilization was also carried out by treatment of the support with an ethanolic solution of (salen)MnCl, as in a cationic exchange process [29].

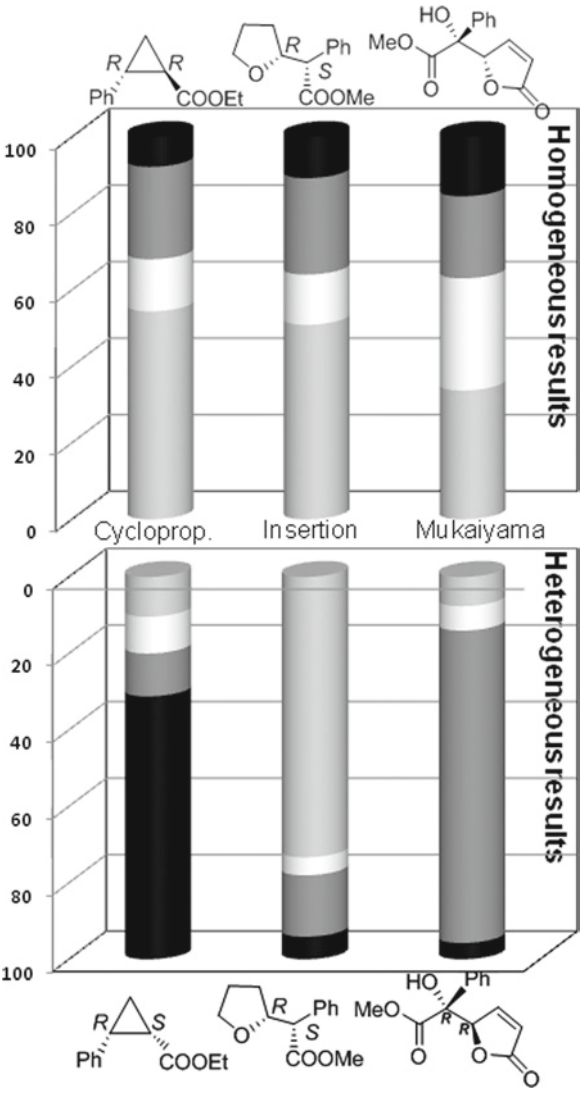

Fig. 3.22 Surface effect on the products distribution of three different enantioselective reactions

3.2.2 Participation of the Support in the Metal Coordination Sphere

One of the most interesting possibilities of inorganic materials to immobilize organometallic catalysts is by formation of one or several bonds between the support and the metal, using the strategy known as *surface organometallic chemistry* (*SOMC*) [30]. The base of most of SOMC reactions is the substitution of a ligand

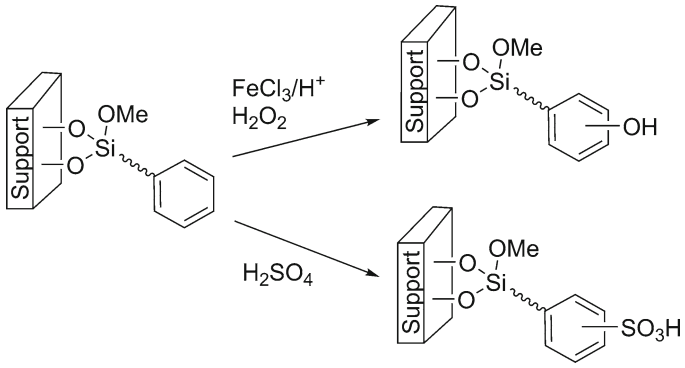

Fig. 3.23 Modification of inorganic supports with organic anions

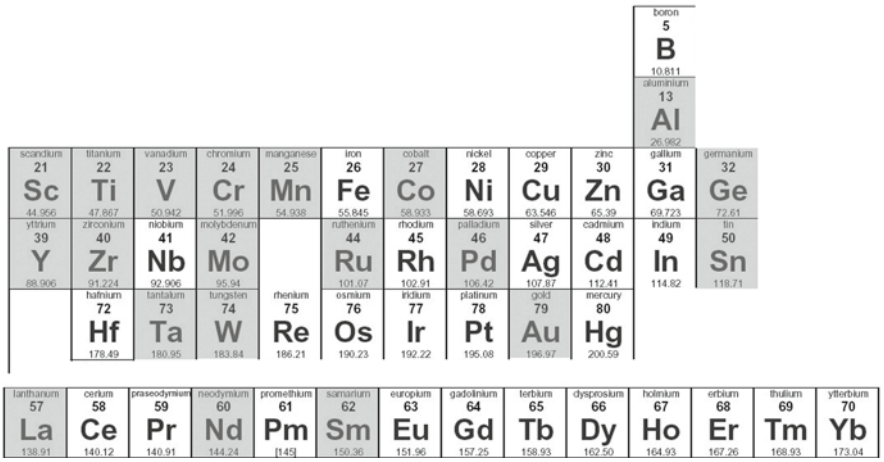

Fig. 3.24 Suitable metals for surface organometallic chemistry (in grey those used for the preparation of catalysts)

present in the metal precursor by the silanol group of the surface of a silica, either amorphous or mesoporous crystalline. Precursors such as alkoxides ($Ti(O^iPr)_4$), alkyls ($AlMe_3$), carbonyls ($Mn_2(CO)_{10}$), or amides ($Nd[N(SiHMe_2)_2]_3$) can be used for this purpose. In fact many metals can react with silanols (Fig. 3.24), and a good number of them (in grey) have been used as catalysts or catalyst precursors after SOMC reactions. Several advantages can arise from the immobilization of organometallic compounds on silica surface, for example the change in nuclearity with respect to the species obtained in solution, thanks to the site isolation effect, and the modulation of the catalytic properties due to electronic effects, from coordination to silica, and/or steric effects, from constrains imposed by the type of binding to the surface. In this regard three main species can be envisaged, monopodal, bipodal, and tripodal, with one, two, and three M–O–Si bonds respectively (Fig. 3.25).

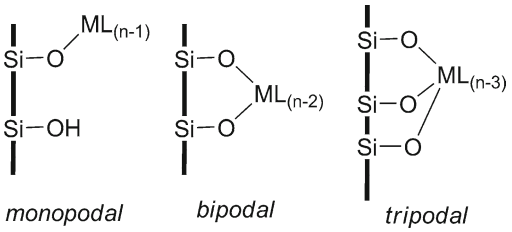

Fig. 3.25 Types of species according to the number of M-O-Si bonds

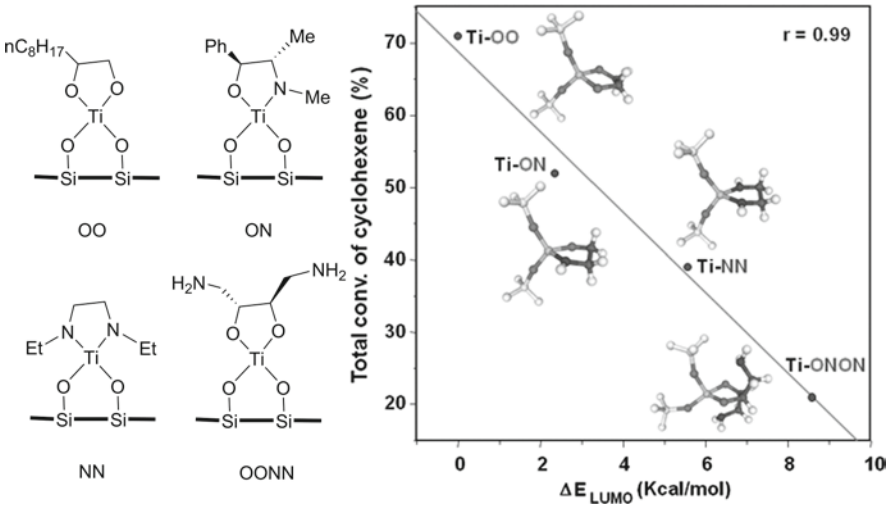

Fig. 3.26 Effect of ligand exchange in activity of Ti-supported catalysts for cyclohexene epoxidation with H_2O_2

This strategy has been frequently used to immobilize single-site olefin polymerization catalysts, such as zirconocene derivatives, and/or Al cocatalysts [31]. However there are not many examples regarding the use of this strategy to immobilize catalysts to be used in the synthesis of fine chemicals

Grafting Ti-species onto different supports is a well known strategy to prepare oxidation catalysts. Calcination is usually the last step in the catalyst preparation, removing any organic ligand, and forming a fully inorganic supported Ti catalyst. However, the organic part can be retained and subsequently substituted by alternative ligands, which allow modulating the catalytic activity of the solid. This is the case of silica treated with $Ti(O^iPr)_4$, whose activity and selectivity in the epoxidation of cyclohexene with hydrogen peroxide was modulated by introduction of more donor nitrogenated ligands (Fig. 3.26). In this way the LUMO energy of the Ti center increases and this reduction of the Lewis acidity modifies both catalytic activity and

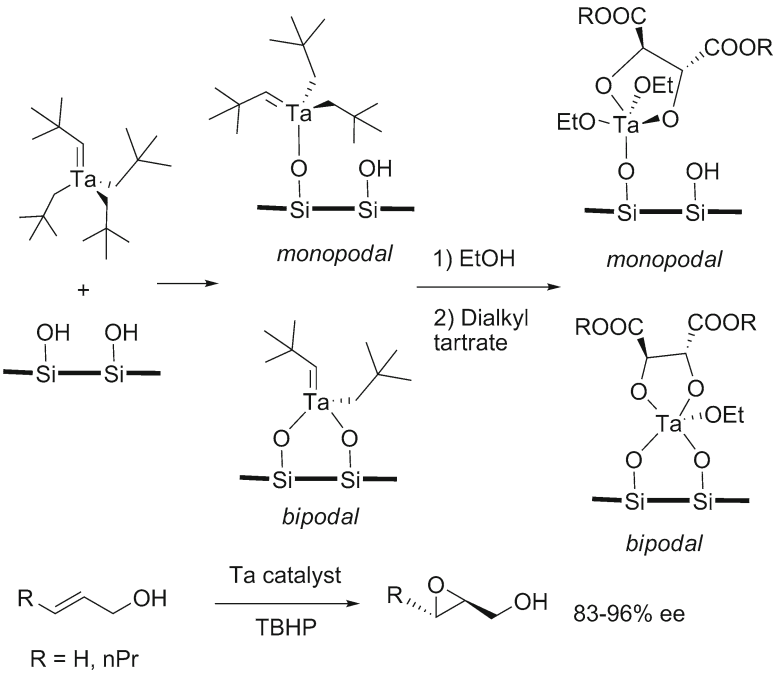

Fig. 3.27 Supported tantalum species for epoxidation reactions

selectivity. Unfortunately the activity for direct epoxidation is correlated with Lewis acidity, and its reduction produces an increase in the percentage of the reaction taking place through the radical pathway, leading to allylic oxidation products [32].

Sharpless asymmetric epoxidation of allylic alcohols has become a benchmark classic in asymmetric catalysis, in spite of the very low TON obtained. The development of a recoverable heterogeneous catalyst remains a challenge difficult to accomplish due to the dimeric nature of the active (DET)Ti(O^iPr)$_4$ catalyst in solution, incompatible with the site isolation character of the immobilized catalysts.

One possible method to overcome this limitation would be the use of a metal with a higher coordination number, such as tantalum. Ta-catalysts were prepared in three steps by grafting Ta(=CH^{t}Bu)(CH$_2{}^t$Bu)$_3$ onto silica, exchange of the alkyl/alkylidene ligands with EtOH, and final treatment with tartrate (Fig. 3.27) [33]. These catalysts consisted in monopodal and bipodal species in 1/1 ratio, and they showed excellent enantioselectivity in the epoxidation of allylic alcohols, whereas the analogous Ti catalyst, prepared from Ti(O^iPr)$_4$ showed very poor activity and enantioselectivity. The different behavior may be due to the fact that Ti-grafted species cannot accommodate at the same time the support (one on two σ-bonded silanols), the tartrate chelating ligand (two σ-bonded oxygen atoms), one σ/π coordinated *tert*-butylperoxy group, and the σ-bonded allylic alcohol. Furthermore the supported catalyst is more active

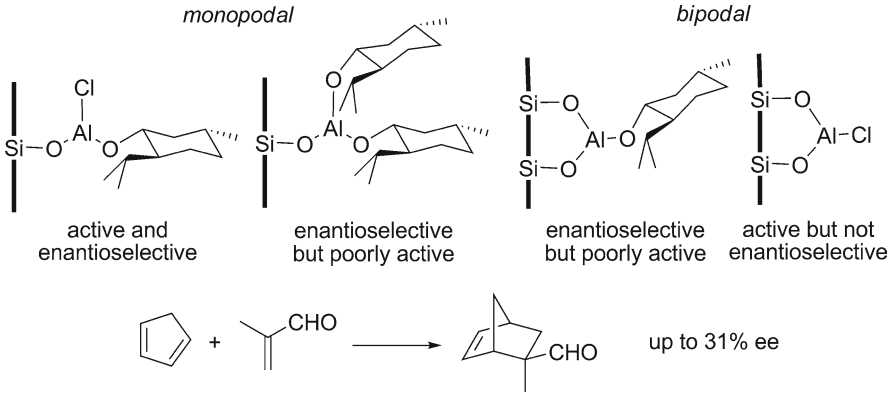

Fig. 3.28 Menthol-Al species on silica

that a homogeneous analogous, which may be due to the dispersion of Ta-species onto silica, leading to the formation of monomeric active sites.

Lewis acids can also be immobilized by reaction with surface hydroxyl groups. (–)-Menthol-aluminium Lewis acids were supported on silica and alumina (Fig. 3.28) [34]. Different species are possible, but the optimal one should bear one chlorine, to increase Lewis acidity, and one menthol to induce enantioselectivity. Up to 31% ee was obtained in the Diels-Alder reaction between methacrolein and cyclopentadiene, analogous to the homogeneous (menthol)$AlCl_2$ species, but lower than the maximum described for $(menthol)_2AlCl$, impossible to immobilize by this method.

The "silylamide route" has been used for functionalization of the MCM-41 surface with organolanthanides (Fig. 3.29) [35]. In a first step, isolated silanol groups react with silylamide complexes $[Ln(N(SiHMe_2)_2)_3(thf)x]$ (Ln= La, Sc, or Y), forming stable linkages between the metal and the support. Simultaneously, the released silylamines perform an end-capping with formation of hydrophobic $-OSiHMe_2$ sites. In a second step the silylamide ligand can be exchanged with different ligands. The resulting materials contains 0.2 mol% Ln and catalyze the asymmetric hetero-Diels-Alder reaction of Danishefsky's diene with benzaldehyde (Fig. 3.29). The surface-grafted complexes did not show metal leaching and displayed a more stable activity than the homogeneous complexes, such as La $(fod)_3$, which may be due to the high-dispersion of well-defined surface complexes.

SOMC also allows the preparation of immobilized Re-, W-, and Mo-based olefin metathesis catalysts. It has been shown that grafting on rigid oxide supports produces asymmetry at the metal centre, increasing the catalytic activity, and site isolation, which enhances the stability of these catalysts. The catalysts are prepared by direct substitution of one amido group of the homogeneous catalyst by one silanol of the support surface, although a minor surface species is also obtained in 20%. The fine tuning of the ligands on the metal environment allows

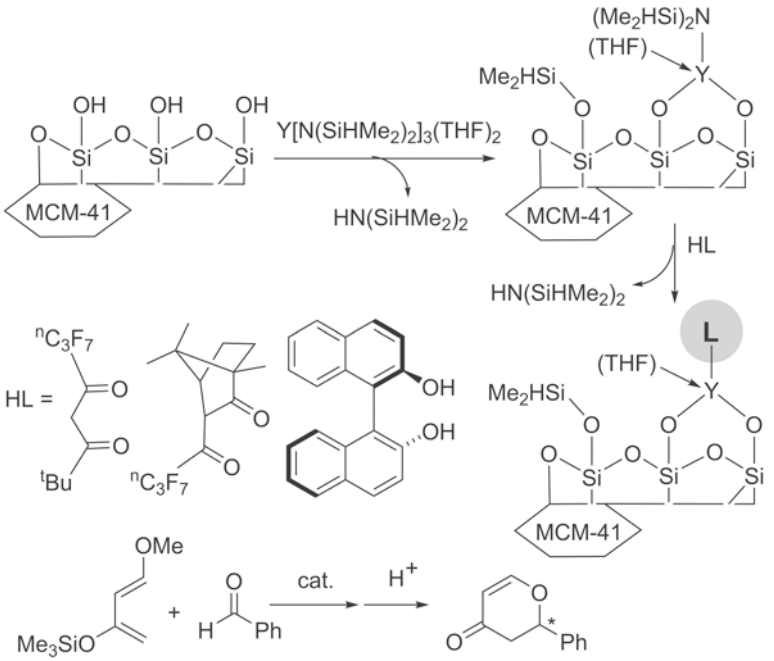

Fig. 3.29 Rare-earth species on MCM-41

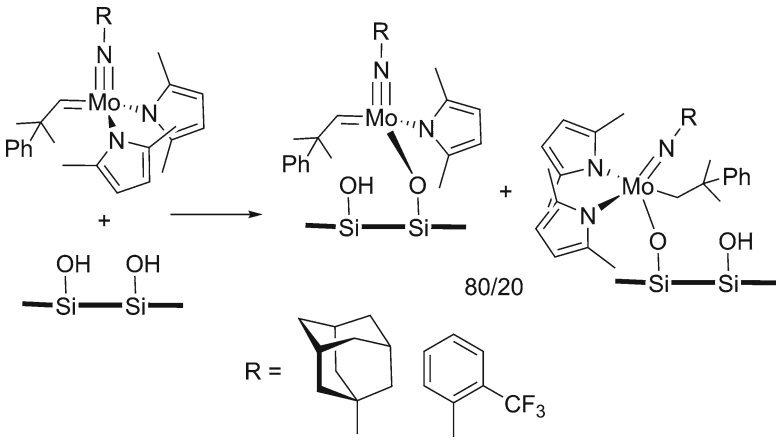

Fig. 3.30 Optimized silica-supported Mo catalysts for self-metathesis of olefins

the optimization of the catalyst [36]. As an example, the 2,5-dimethylpyrrolyl derivatives (Fig. 3.30) are able to catalyze self-metathesis of propene with up 231,000 TON in 1,500 min (adamantylimido) and that of ethyl oleate with TOF 1.2 s^{-1} (2-trifluoromethylphenylimido).

3.3 Immobilization by Support–Ligand Interactions

When immobilizing catalysts on inorganic supports, the alternative strategy to the metal–support interaction, reviewed in the previous section, is the linking of the metal complex to the support by interactions with one or several of the ligands. These interactions can be either covalent or electrostatic.

Obviously this strategy implies the suitable modification of the ligand, to be able to link the support, and hence additional synthetic steps in the preparation of the catalyst. On the other hand, it has the great advantage of not being affected by changes in the oxidation state of the metal during the reaction that would cause the leaching of the catalyst in other cases. Another feature of this approach is that the support does not directly affect the coordination sphere of the metal, although subtle modifications may be produced by electronic or steric effects of the additional functionalization.

3.3.1 Support–Ligand Covalent Bond Formation

Binding a ligand to a solid support via a covalent bond has become the most often employed method for immobilization of homogeneous catalysts. Even if this strategy is synthetically more demanding than others, it gives the strongest complex-support binding, and at least ensures the retention of the ligand, very important in the case of valuable chiral ligands.

When anchoring a metal complex to a solid through a covalent bond with the ligand, several possibilities can be foreseen (Fig. 3.31): linking the ligand or the complex to

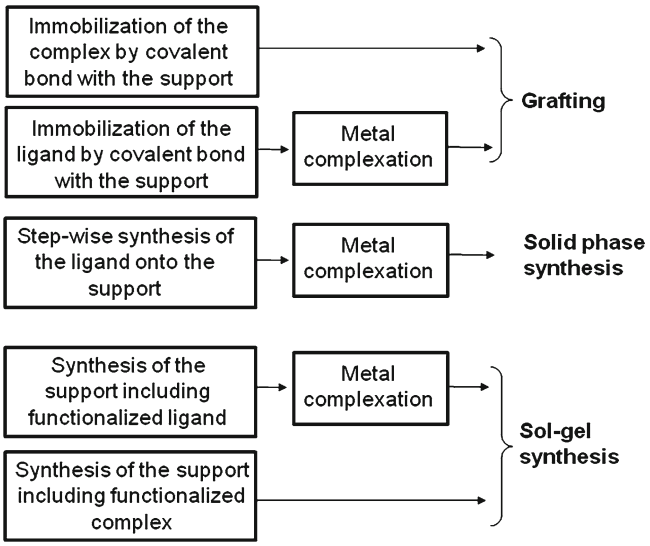

Fig. 3.31 Different strategies for immobilization through support-ligand covalent bonding

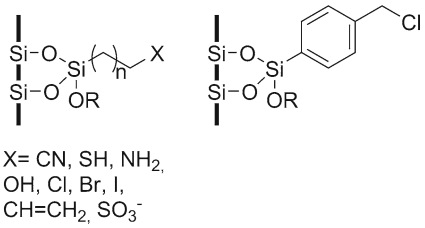

Fig. 3.32 Functionalization of inorganic supports

the solid (*grafting methods*), synthesis of the ligand onto the support (*solid phase synthesis*) or synthesis of the support using precursors containing the ligand or the complex (*sol-gel processes*).

3.3.1.1 Grafting Methods

In order to link a catalyst to a support by means of covalent bond with the ligand, the support and the ligand must be functionalized in such a way to be able to carry out immobilization.

There is a large variety of functional groups that can be attached to the surface of inorganic supports (Fig. 3.32). These groups can react with the suitable functionalized ligand in such a way that a new covalent bond between the solid and the ligand is created.

When grafting metal complexes to an inorganic support through the ligand two different strategies can been considered: (a) initial covalent anchoring of the ligand and further incorporation of the metal with final formation of the complex or (b) anchoring the preformed complex.

Initial Covalent Anchoring of the Ligand

The strategy of anchoring the ligand on the solid support instead of the preformed complex shows the advantage of its versatility to prepare a library of different complexes, starting from the same anchored ligand, which can be used in different reactions. A good example is the anchoring of vinyl-functionalized salen ligands onto mercaptopropyl modified silica, using AIBN as radical initiator [37]. In this way, two types of supported salen–metal complexes were prepared: a Mn catalyst used for asymmetric epoxidation of alkenes and a Cr catalyst used for the hetero Diels-Alder reaction of aldehydes. Both catalysts showed a good behavior leading to high enantioselectivities and good recovery, four runs with Mn catalyst and up to ten runs with the Cr complex.

When using this approach the introduction of the metal must be carefully controlled, either choosing the right metal precursor or protecting free silanol groups in order to avoid the coordination of the metal to the support, creating non selective catalytic sites. This effect was observed when immobilizing Box ligands onto silica [38]. Hydroxymethylene-functionalized indaBox was immobilized onto silica through a carbamate spacer (Fig. 3.33). Different copper catalysts, prepared from

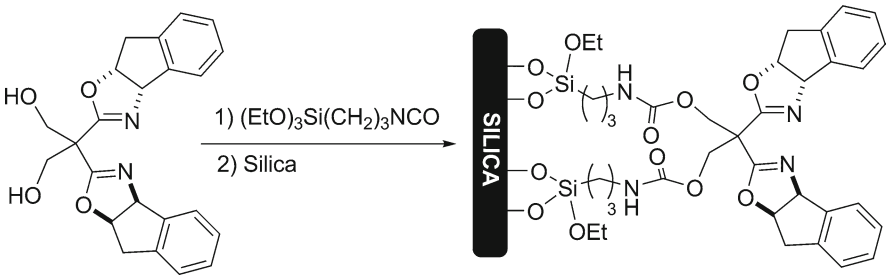

Fig. 3.33 Covalent immobilization of Box–Cu complexes

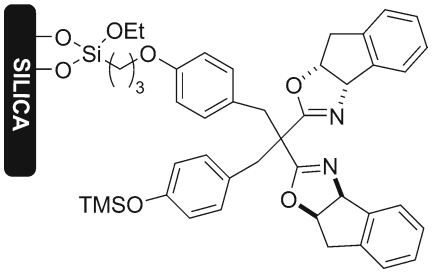

Fig. 3.34 Covalent immobilization of indaBox–Cu complexes on MCF silica

$Cu(OTf)_2$ and $Cu(ClO_4)_2 \cdot 6H_2O$, were tested in Diels-Alder reaction of 3-acryloyl-2-oxazolidinone and cyclopentadiene. When $Cu(OTf)_2$ was used as the metal precursor good enantioselectivities were obtained in the first reaction but conversion and selectivities (endo diastereoselectivity and enantioselectivity) slowly dropped off upon recycling. This was attributed to a major sensitivity of the complex to water. Using a less sensitive metal precursor such as $Cu(ClO_4)_2 \cdot 6H_2O$ good conversions and selectivities were achieved and the catalyst was reusable up to four times. Protection of silanol groups with trimethylsilyl moieties also improved enantioselectivities. This result reveals the importance of controlling the presence of those groups for a right coordination of the metal to the ligand.

The same type of ligand was immobilized on a MCF (mesocellular foam) silica (Fig. 3.34) using an ether linker [39]. In this case, it was assumed that the ligand was grafted just through one arm of the bridge. Results in Diels-Alder reactions did not differ from those obtained with amorphous silica, indicating that the support morphology does not influence the catalytic results in this reaction.

Anchoring a Preformed Complex

The direct immobilization of the metal complex by covalent binding through the ligand reduces the possibility of formation of non selective catalytic sites due to uncomplexed metal ions or metal oxide clusters. This strategy allows fully characterization of the complex just before immobilization, guaranteeing the integrity of the catalyst.

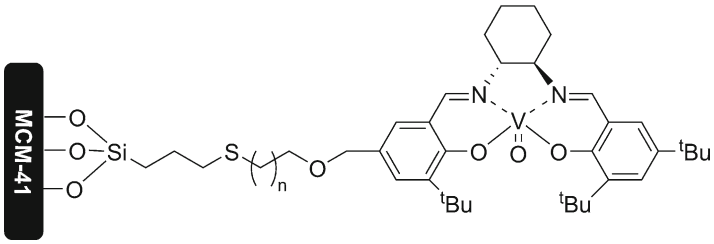

Fig. 3.35 Covalent immobilization of VO–salen complex

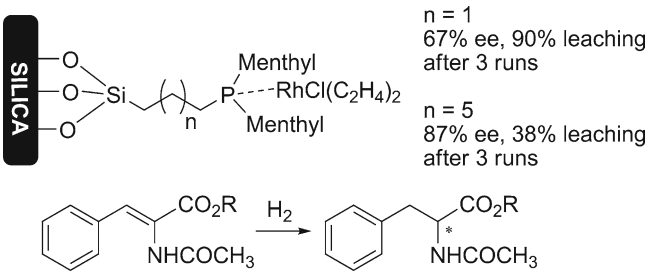

Fig. 3.36 Influence of the tether length of immobilized chiral Rh-complexes

Several factors may affect the properties of the final catalyst: namely the length of the tether, the nature and the position of the linker in the modified ligand, or the support nature.

The *influence of tether length* has been described in vanadyl-salen complexes bonded to MCM-41 (Fig. 3.35). These catalysts were used in the cyanosilylation of aldehydes [40]. Catalysts with longer tethers provided higher enantioselectivity, up to values almost comparable to those obtained in homogeneous phase. It was assumed that long tethers place the chiral complex far from the solid surface leading to a solution-like behavior.

The same type of effect was also observed in the enantioselective hydrogenation of 2-acetamidocinnamic derivatives catalyzed by chiral Rh complexes immobilized on silica (Fig. 3.36) [41]. As the tether length increased, the enantioselectivity increased (from 67% ee with n = 1 to 87% ee with n = 5) and the leaching of catalyst decreased (from 90% leaching after 3 runs with n = 1 to only 38% with n = 5). However, longer linkers are not always positive due to the possible formation of inactive dimeric species, as it happens in solution.

The influence of the *anchoring position in the ligand* and the *nature of the linker* has been reported for the immobilization of (salen)Mn complexes. Their catalytic activity in asymmetric epoxidation of alkenes can be modified by the introduction of groups in the aldehyde fragment and the diimine bridge. That is why the effect of the position in which the complex is attached to the support should be carefully studied.

In the case of amorphous silica as support, (salen)Mn complexes were immobilized by functionalization in different positions (Fig. 3.37) and the resulting catalysts were tested in the epoxidation of styrene [42]. Yields and selectivities were comparable

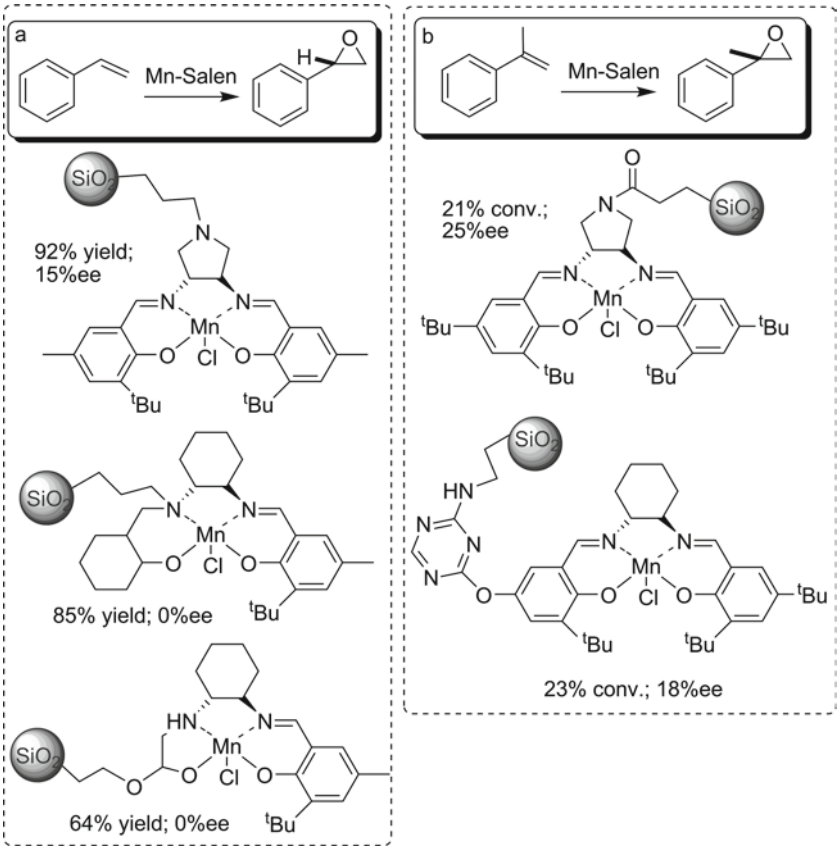

Fig. 3.37 Immobilization of (salen)Mn complexes through different positions

to the homogeneous counterpart when the complex was bonded through the diimine bridge, albeit poor enantioselectivity results were obtained with the rest of the catalysts. This behavior was attributed to electronic factors. In fact, ligands bearing the linker in the amino group have amino alcohol moieties instead of imine groups, which negatively affected the asymmetric induction. The same effect was observed in the case of complexes immobilized on HMS silica (Fig. 3.37) tested for epoxidation of α-methylstyrene [43]. Again the immobilization through the diimine group improves the enantioselectivities while the catalyst linked through a phenolic group exhibits lower % ee than its homogeneous counterpart. These results indicate that the covalent attachment of the Jacobsen's catalyst to any type of silica through the diimine bridge leads to improved % ee, whereas bonding through one of the aldehyde fragments results in a negative effect on the enantioselectivity. As can be seen, (salen)Mn complexes have been immobilized using tethers of different nature, but its influence has not been systematically studied. In addition to the tethers shown in Fig. 3.37, sulfur groups were formed by reaction of vinyl-functionalized (salen)Mn

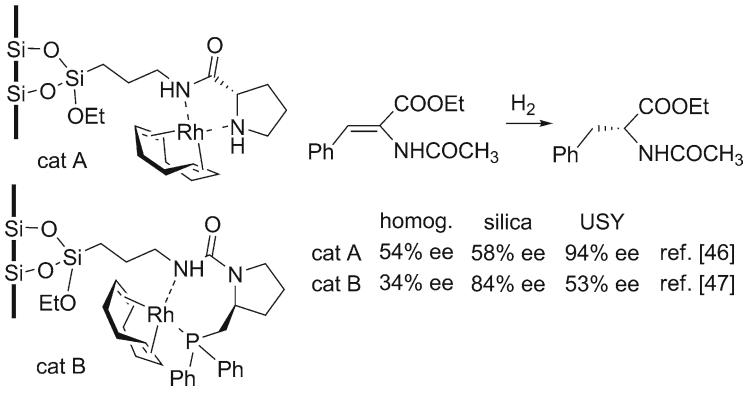

Fig. 3.38 Immobilization of Rh complexes with proline-derived ligands onto USY

and mercaptopropyl silica [44]. The catalytic activity on epoxidation of alkenes was only moderate, but it is not clear if this is an effect of either the nature of the linker or the position, again in the aldehyde moiety.

Finally, the influence of the *nature of the support* may be important in the covalent grafting of catalysts. Sometimes large pore sizes may be required to prevent diffusion limitations, improving the catalytic activity. In other cases, the proximity of the complex to the support may be favorable.

Chloromethyl mono-functionalized (salen)Mn complexes were covalently immobilized onto supports with hexagonal structure but different pore size [MCM-41 (50 Å) and SBA-15 (75 Å)] [45]. Excellent results were obtained with these catalysts in alkene epoxidation. An effect of the pore size of the support was observed, as the catalyst immobilized on SBA-15 was found to be more active, in agreement with the larger pore size. Moreover, the heterogenized catalyst was more stable than the homogeneous one and recoverable four times with the same enantioselectivity.

In other cases, a support effect on stereoselectivity has been observed. As an example, Rh complexes with chiral proline derivatives were immobilized on silica and USY zeolites (Fig. 3.38) and tested in the hydrogenation of various (Z)-α-N-acylcinnamic acid derivatives. Increased enantioselectivity was obtained using zeolite support compared with homogeneous phase or silica supported catalysts [46]. This effect was attributed to steric constraints imposed by the highly ordered zeolite support but an opposite effect was obtained for similar complexes, in which the positive effect was obtained with amorphous silica [47], showing that the nature of this effect is not fully understood.

A confinement effect was observed when using an immobilized (ferrocenyl-diphosphine)Pd complex in the allylic amination of cinnamyl acetate (Fig. 3.39) [48]. In this case the complex immobilized on a mesoporous crystalline support (MCM-41) exhibited superior catalytic properties (50% branched selectivity, 95% ee) compared to the same complex anchored on non porous high surface silica or the homogeneous catalyst, which lead almost completely the linear product. This

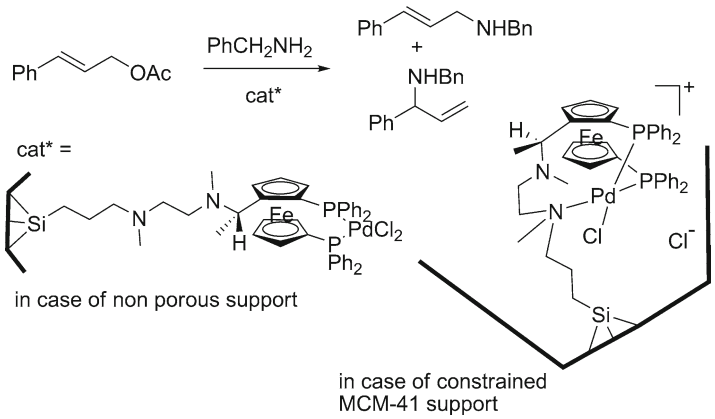

Fig. 3.39 Confinement effect on immobilizing (ferrocenyl-diphosphine)Pd complex

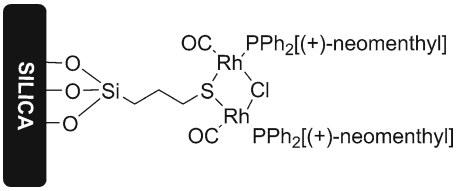

Fig. 3.40 Chiral dimeric Rh catalyst immobilized onto silica

effect was explained by a change in the coordination of Pd induced by the steric constrains of the mesoporous support.

Besides improving yields and selectivities, in some cases the presence of the support can induce a reversal in enantioselectivity, as it happened in the case of cationic exchange in clays (see Section 3.2.1). One example is the covalent immobilization of a dimeric chiral Rh complex on silica (Fig. 3.40) and its application in the hydrogenation of (Z)-α-acetamidocinnamate. The levorotatory product was obtained with the immobilized catalysts in contrast with the dextrorotatory product obtained in solution [49]. This effect was associated with the different orientations of the phosphine ligands in the homogeneous and the immobilized catalysts.

As can be seen, due to the versatility of the grafting method, most of the catalysts successfully used in homogeneous phase have been immobilized using this strategy.

3.3.1.2 Solid Phase Synthesis

Solid phase synthesis of immobilized catalysts implies the immobilization of a ligand precursor and the building of the ligand on the support in several reaction steps. The advantage of this strategy is the easy separation of the solid-linked

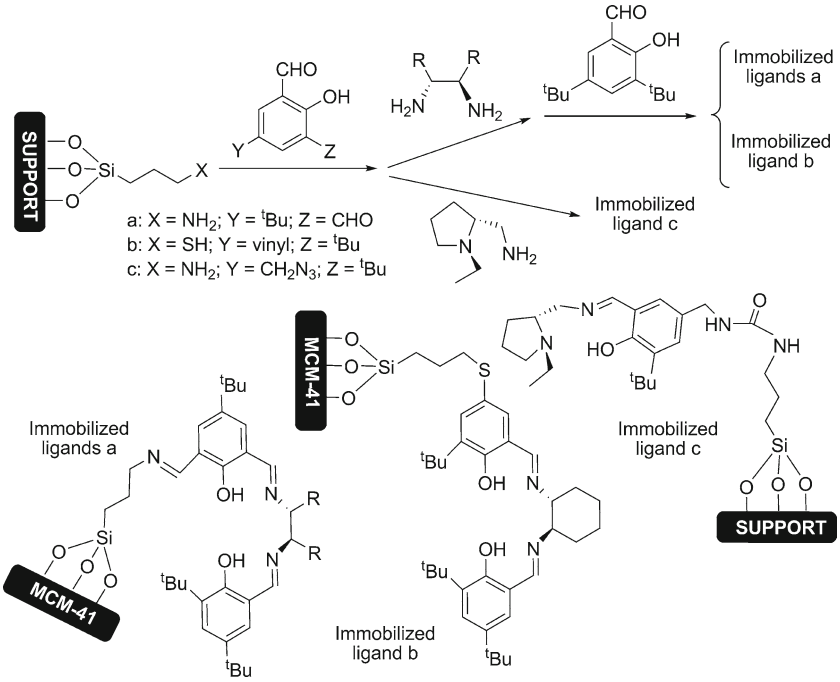

Fig. 3.41 Solid phase synthesis of salen complexes onto inorganic supports

products from the reaction mixture, but on the other hand characterization of the species formed onto the solid may be difficult, and the presence of incompletely formed ligand molecules cannot be excluded.

A representative example of this strategy is the immobilization of salen ligands. Non-symmetric salen-type ligands were synthesized on MCM-41 in three steps (Fig. 3.41a), with better yields than the homogeneous reaction due to the statistical distribution of condensed products. At the end the ligand was bonded to the support by the *ortho* position of the phenolic group [50]. This position was crucial for the asymmetric induction of the complex. Mn, Co(II) and Co(III) complexes of the immobilized ligand were prepared and tried on several reactions such as styrene epoxidation, asymmetric reduction or epoxide hydrolysis, with variable results.

The anchoring of the ligand through the *para* position of the phenolic group was achieved via reaction of mercaptopropyl modified support and a vinyl functionalized salicylaldehyde with AIBN as initiator and subsequent condensation reactions (Fig. 3.41b) [51]. This catalyst was tested in asymmetric epoxidation of styrene. Moderate enantioselectivity was observed but the catalyst was reused in three cycles without any loss of activity or metal leaching.

The influence of the nature of the support was studied for complexes of salen-like ligands immobilized by solid phase synthesis using an isocyanate linker (Fig. 3.41c) and different supports (amorphous silica, MCM-41 and ITQ-2) [52]. Pd and Ni complexes of those ligands were tested in the hydrogenation of imines.

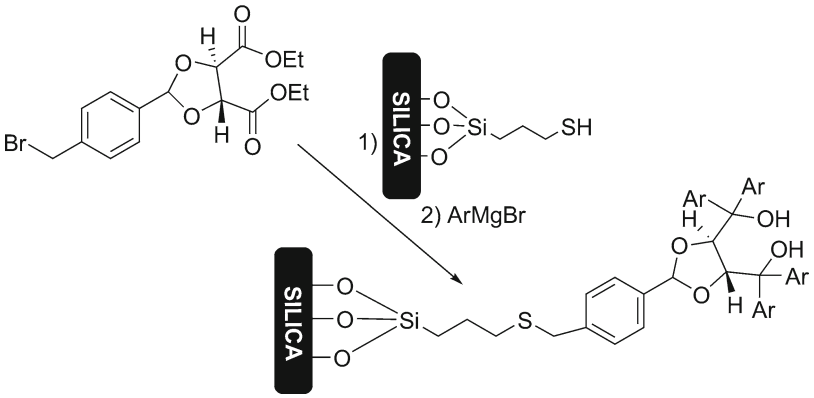

Fig. 3.42 Solid phase synthesis of immobilized TADDOLs

The complex anchored on mesoestructured silicates or delaminated zeolite increases its activity compared to the homogeneous one or the one immobilized on amorphous silica. This fact has been attributed to a preferential adsorption of hydrogen and reactants on this solid.

The ligand solid phase synthesis has also been applied to the immobilization of TADDOLs over a high porous silica gel (CPG). Thiol groups of mercaptopropyl functionalized CPG silica were benzylated with 4-bromomethylbenzaldehyde acetal of diethyl tartrate. Diaryl moieties were created by addition of phenyl or naphthyl magnesium bromide on the supported tartrate derivative. Finally the ligands were titaned to give $(^{i}PrO)_2Ti$-, Cl_2Ti- or $(TosO)_2Ti$-TADDOLates (Fig. 3.42) [53]. Those catalysts were tested in two different reactions, Et_2Zn addition to benzaldehyde and 1,3-dipolar cycloaddition of N-crotonyloxazolidin-2-one and diphenyl nitrone. In both cases, results were comparable to the homogeneous ones and to the ones obtained with grafted TADDOLs. In this case, solid phase synthesis of immobilized TADDOLs shows the advantage of easier purification after each synthetic step, in comparison with the difficult purification of the functionalized ligand before grafting.

3.3.1.3 Sol-Gel Methods

Although grafting is the most commonly used strategy for immobilization through the ligand, it suffers from some drawbacks such as inhomogeneity of the reactive centers or difficulties in controlling the density of the catalytic centers on the surface. This is due to the kinetics of the grafting, favoring the functionalization of the outer grafting sites, that may block the access of the ligand to the inner part of the support.

The sol-gel method is based in the co-condensation of silyl-functionalized metal complexes or ligands with various alkoxysilanes, providing materials in which the catalytic centers are homogeneously distributed on the support. This method would be analogous to the polymerization in organic supports. The way in which the material is prepared can strongly influence the performance of the final catalyst.

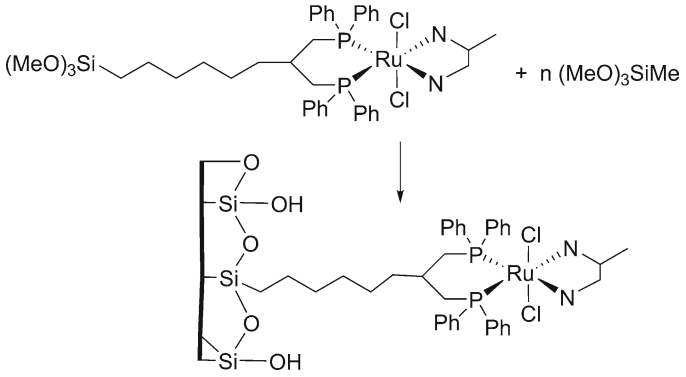

Fig. 3.43 Sol-gel synthesis of immobilized (diamino)(diphosphine)Ru complexes

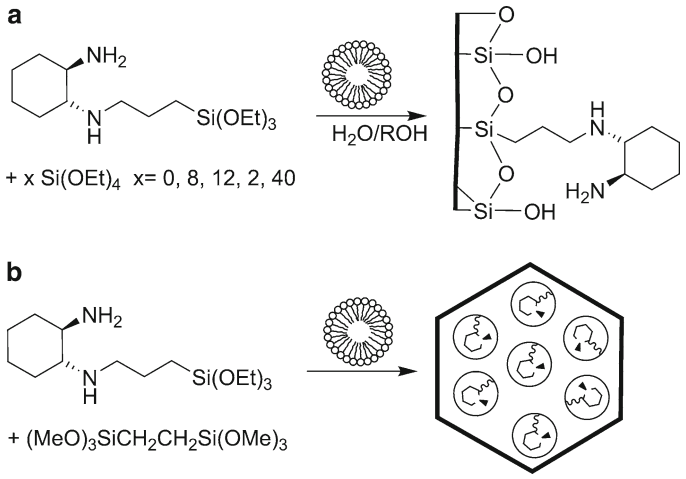

Fig. 3.44 Sol-gel synthesis of immobilized chiral diamine–Rh complexes

A good example is the preparation of immobilized (diamine)(diphosphine) ruthenium(II) complexes (Fig. 3.43) for the catalytic hydrogenation of ketones [54]. The use of different ratios of silylated ligand and $(MeO)_3SiMe$ led to catalysts with different activity, indicating that the density of catalytic centers within the solid plays an important role.

A similar behavior was observed in the immobilization of silylated chiral diamine–Rh complexes [55]. In this case, the best enantioselectivity in acetophenone reduction was obtained with the solid prepared without $Si(OEt)_4$ (Fig. 3.44a, x = 0), whose network consisted only in chiral ligands units linked by siloxane groups. This was attributed to the poor organization in mixed solids due to the different hydrolysis and/or condensation rates of silylated ligand and $Si(OEt)_4$, as it happens in immobilization by polymerization with monomers and functionalized co-monomers.

As this factor plays an important role in the formation of well-ordered highly porous materials, a new hybrid material was prepared using bis(trimethylsilyl)ethane and N-[(triethoxysilyl)propyl]-(–)-(1*R*,2*R*)-diaminocyclohexane as precursors (Fig. 3.44b) [56]. A solid with 2D hexagonal mesostructure was obtained. This material exhibited an improved catalytic activity compared to the grafted catalyst in the corresponding mesoporous silica, attributed to the hydrophobic character of the solid due to the presence of ethane bridges in the framework. The described synthesis demonstrates the possibility of modulate the surface properties of the solid at a molecular level by tuning the organic group in the silylated precursors.

The length of the spacer, the density of active sites, the physical properties (surface area and porosity) of the final hybrid material, as well as the sol-gel synthetic process have a strong influence in catalytic results [57]. Those parameters should be optimized for each catalytic system, which would difficult the development of those systems However, given that it is possible to tune the catalyst properties in the synthetic process, and there are examples of sol-gel processed catalysts that improve the results of their homogeneous counterparts, a great number of opportunities, challenges and applications are to be expected to this kind of heterogeneous catalyst. However, the main limitation is the sensitivity of many chiral ligands to the hydrolytic conditions required for sol-gel synthesis.

3.3.2 Support–Ligand Electrostatic Interactions

A different strategy for the immobilization of complexes through the ligand is by electrostatic interactions. This approach implies the functionalization of the ligand with charged substituents and subsequent exchange onto a support of opposite charge (Fig. 3.45). This approach is comparable with the analogous metal–support electrostatic interaction, in which the complex with charge on the metal is supported by ion exchange (Section 3.2.1). Some advantages of the electrostatic immobilization through the ligand would be that it can be applied to complexes neutral on the metal, and that the leaching of the ligand is avoided, as in the case of covalent support–ligand bond.

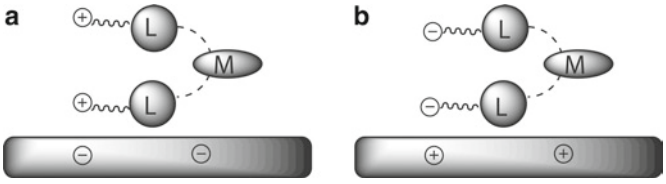

Fig. 3.45 Immobilization by support–ligand electrostatic interactions: (**a**) cation exchange (**b**) anion exchange

3.3.2.1 Immobilization of Complexes with Cationic Ligands

Cationic groups on ligands are usually ammonium moieties, that must be introduced in the ligand synthesis process, and because of that the number of examples is quite limited. Metalloporphyrins, mainly iron(III) and Mn (III), represent versatile oxidation catalysts and they have been designed as models for monooxygenases based on cytochrome P-450. Tetracationic Mn–porphyrin complexes have been immobilized on montmorillonite (Fig. 3.46) [58] and tested in linear alkane hydroxylation reactions. Those catalysts were easily prepared, easily reused without loss of activity and exhibited a particular ability to oxidize poorly reactive short linear alkanes compared to their homogeneous counterpart and to silica immobilized catalysts.

In another example positive charges were introduced on salen ligands in the form of quaternary ammonium salts and the corresponding Mn complex was exchanged on montmorillonite clay from an ethanolic solution (Fig. 3.47) [59]. Due to the large size of the complex the catalyst loading was very low, and exchange mainly took place on the outer surface of the clay. This catalyst was highly active in the epoxidation of alkenes with NaOCl using pyridine N-oxide as an additive. The catalyst was recoverable up to five times in styrene epoxidation without loss of enantioselectivity.

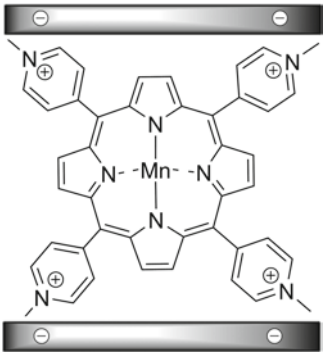

Fig. 3.46 Immobilization of tetracationic Mn–porphyrin complexes

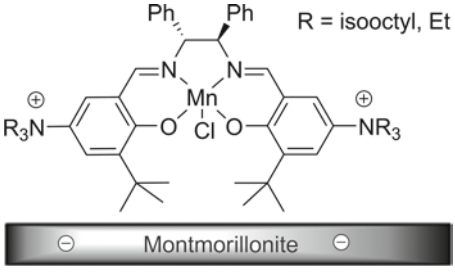

Fig. 3.47 Immobilization of Mn complexes with cationic salen ligand

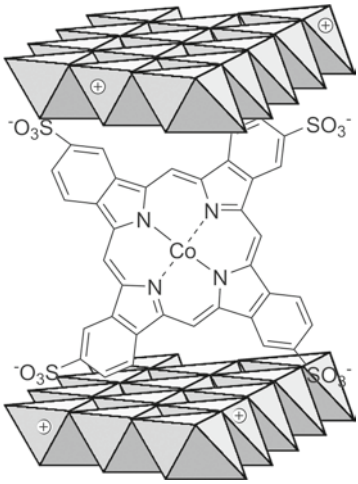

Fig. 3.48 Immobilization of a Co-phthalocyaninetetrasulfonate complex on LDH

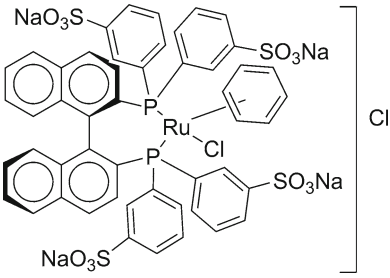

Fig. 3.49 Anionic (BINAP) Ru complex

3.3.2.2 Immobilization of Complexes with Anionic Ligands

In the same way as cationic groups, anions can be introduced in the ligands and the corresponding complexes can be immobilized by electrostatic interaction with cationic supports. The inorganic supports for this immobilization are usually layered double hydroxides (LDH).

A Co-phthalocyaninetetrasulfonate complex (Fig. 3.48) was immobilized on Mg/Al LDH [60]. This catalyst was tested for the aqueous autoxidation of 1-decanethiol showing an improved catalytic activity compared to its homogeneous counterpart. Moreover, the catalyst was recovered up to five times with a total TOF of 770 whereas the homogeneous one was deactivated after one cycle with a TON of 150.

A sulfonated Ru–BINAP complex (Fig. 3.49) was also immobilized on Mg-Al/Cl and Zn-Al/NO_3 layered double hydroxides (LDHs) and the catalysts were tested in the hydrogenation of dimethyl itaconate and geraniol [61]. An influence of the nature of the support on the catalytic results was observed. In the case of

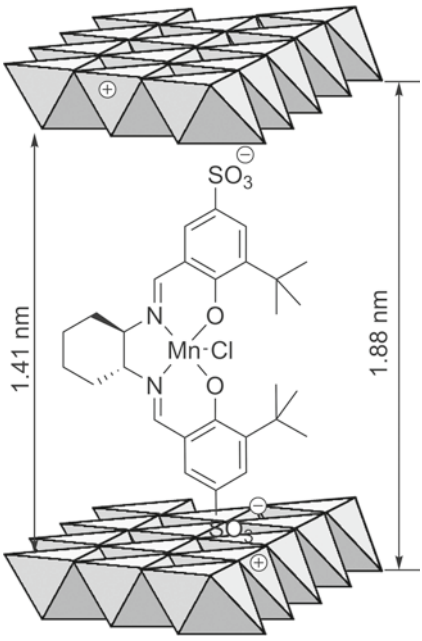

Fig. 3.50 Immobilized anionic Mn(salen) complex

dimethyl itaconate, the activity and enantioselectivity of the complex remained practically unchanged after immobilization on Mg-Al/Cl LDH, whereas on Zn-Al/NO_3 LDH a decrease in enantioselectivity was observed. Although that effect was not easy to explain, it was suggested that the different acid-base character of the supports, Mg-Al/Cl LDH basic and Zn-Al/NO_3 acidic, might be the origin for this behavior. Another interesting observation was the lack of activity of the anionic complex supported on an organic anion exchanger.

The same strategy was applied for the electrostatic immobilization of sulfonated Mn(salen) complexes (Fig. 3.50) onto Zn-Al LDH [62]. TGA analysis was consistent with the presence of the complex and XRD study showed an increase of basal spacing (from 15.22 to 18.78 Å), but those values were not high enough to certificate an orientation of the complex perpendicular to the layers. The catalyst was tested in the oxidation of several alkenes with molecular oxygen showing a good performance. No evidence for leaching or catalyst decomposition was observed. The authors emphasized the fact that this catalyst can readily be prepared from aqueous medium without using organic solvents, whereas a large number of salen catalysts are prepared in chlorinated solvents, and the use of the molecular oxygen/pivalaldehyde system avoids salt formation.

The examples of electrostatic immobilization of complexes through electrostatic ligand–support interactions show that this is a simple immobilization method, very useful when complexes have formation constant high enough to be stable under the exchange conditions, in order to avoid metal leaching. Due to the need for a ligand modification, when possible the immobilization through electrostatic metal–support interactions (Section 3.2.1) is normally preferred.

3.4 Other Types of Immobilization

Immobilization strategies based on strong interactions between support and either ligand or metal may have some disadvantages, such as the need for ligand or support chemical modification, the inclusion of additional synthetic steps, or the interference of the support in the chemical course of the reaction. In this section we will review some "soft" immobilization strategies sharing the feature of not requiring modification neither of the catalytic complex nor of the support, as well as not requiring strong catalyst–support interactions [10]. As discussed below, this last feature does not necessarily means that the catalyst is easily lost form the support.

We can classify this rather heterogeneous set of strategies attending the order of support synthesis, catalyst synthesis, and immobilization steps. The different possibilities are schematized in Fig. 3.51. In some cases, different strategies may lead to the same kind of final catalyst, as in the case of encapsulation.

3.4.1 Building the Support Around the Catalyst: Entrapment

The entrapment strategy consists in synthesizing the inorganic support from a solution that contains the homogeneous catalyst. Part of the solution with the catalyst get occluded within the pores of the resulting solid, and cannot diffuse out. Reagents and products of the target catalytic reaction however can, leading to the desired immobilized catalytic system.

Inorganic solid synthesis is usually accomplished by traditional sol-gel methods, which can lead to amorphous, ordered mesoporous and crystalline materials. In the latter case, the resulting immobilized catalyst may be identical to those

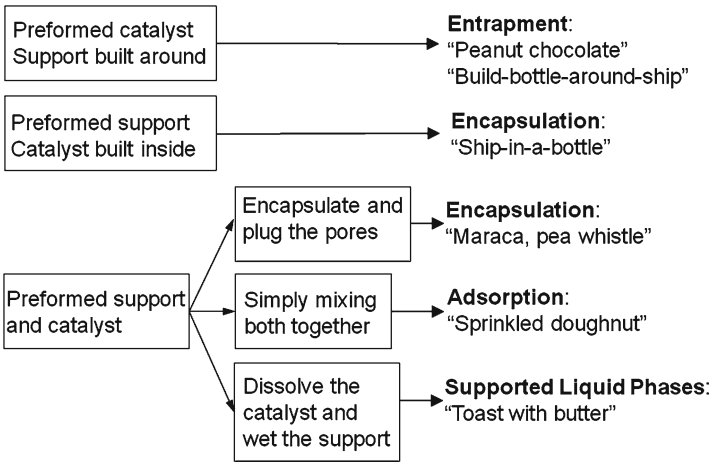

Fig. 3.51 Different strategies for catalyst immobilization without strong binding forces between support and catalyst

obtained by the "ship-in-a-bottle" methodology, as we will see in the next section. Inorganic and hybrid flexible membranes can also be used with catalyst entrapment purposes, and pure organic polymers have also been used as flexible matrices for entrapment, but their use is out of the scope of this chapter, and will not be further considered.

Anyway, the use of rigid supports is usually preferred over the flexible matrices, which present severe leaching problems. Given that the pore size is constant, the entrapped catalyst must be retained within the solid matrix, provided the pore and catalyst sizes are adequate. The common strategy, consisting in synthesizing an amorphous solid (either silica or alumina), has been applied to the entrapment of Ru and Mn catalysts. However, leaching problems, as well as reduced catalytic activity upon immobilization are usually observed.

A variant on this methodology is the use of an ionic liquid in the sol-gel procedure [63]. The entrapment of Wilkinson's catalyst ($[RhCl(PPh_3)_3]$) was carried out in conventional and ionic liquid mediated sol-gel glasses. Selectivity in the benchmark hydrogenation reaction of ethyl benzene was higher than that obtained with Rh/C catalyst. Besides, the ionogel phase method led to an entrapped catalyst more active than the conventional sol-gel synthesis. In fact, the Rh catalyst was activated during entrapment and the resultant material was more active than the homogeneous Wilkinson's catalyst. Material characterization studies indicate that the solid consists of amorphous silica with the metal complex and ionic liquid imprisoned within its pores.

The inorganic support built around a catalytic complex can also be crystalline. This strategy is particularly useful when the size of the complex is too big to apply the "ship-in-a-bottle" strategy (Section 3.4.2). In those cases, a zeolite gel can be

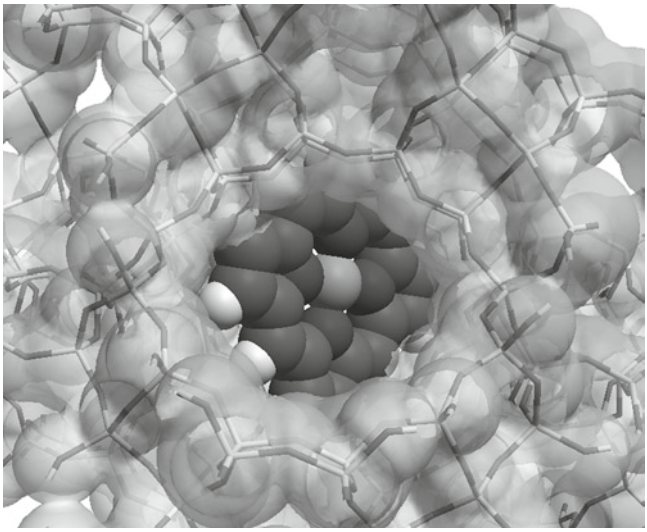

Fig. 3.52 Structure of a metalloporphyrin entrapped into a supercage of zeolite Y

crystallized in a solution containing the complex. This strategy has been applied, for instance, to metalloporphyrins (Fig. 3.52) [64], and larger metallophthalocyanines, which have been entrapped within the supercages of zeolite Y. This strategy often receive the name of "build-bottle-around-ship" and is particularly useful in the case of faujasites (as zeolite Y), because no structure-directing agent is required.

3.4.2 *Building the Catalyst Within a Capsule: the "Ship-in-a-Bottle" Strategy*

This immobilization method consists in the introduction of portions of the catalyst, small enough to enter through the pore aperture of a zeolite or zeotype structure, with subsequent formation of the complex inside the supercages. As the resulting complex is larger than the pore aperture, it remains retained inside the pore system. The first example of the "ship-in-a-bottle" strategy (as the very name for the method) was described in 1986 [65] and consisted in the Co(II) ion exchange in zeolites A and Y, with subsequent treatment with salen ligand. The neutral Co(salen) complex is then formed within the zeolite supercages, where remains entrapped, due to its rigidity. Other metal–salen complexes have also been encapsulated following the same methodology, as those of V=O, Fe or Rh [66]. The first examples of application of this methodology to chiral complexes were also devoted to salen complexes. Other kinds of complexes that have been encapsulated in zeolites through the "ship-in-a-bottle" strategy are the metallophthalocyanines, starting from o-phthalodinitrile and a metal-exchanged zeolite (Fig. 3.53).

There are two critical issues in the immobilization by the "ship-in-a-bottle" strategy, namely the identity and purity of the encapsulated species, on the one hand, and the location of the guests with respect to the zeolite particle, on the other. The first aspect requires the combined use of different spectroscopic techniques. Once the nature of the species is known, the location (internal vs. external) of the guests requires specific techniques to be answered, as the formation of the product in a zeolite cannot be taken as evidence of its internal location of the catalyst. When the guests are heavy metal atoms, direct evidence of their internal location can be

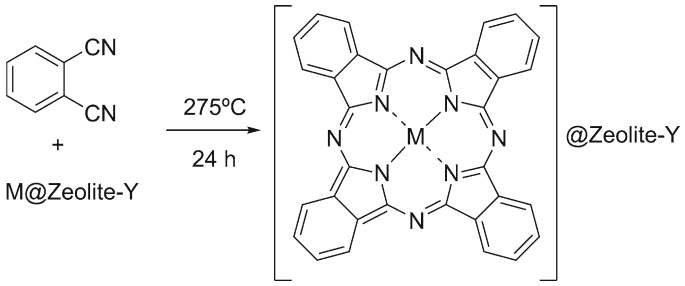

Fig. 3.53 General scheme for metallophthalocyanine encapsulation within zeolite Y

obtained by high-resolution XRD, neutron scattering or high-resolution TEM. An indirect technique used to address the location of a guest in a zeolite is isothermal gas adsorption. Surface area and pore volume measurements should reflect a decrease in the specific values due to the presence of the guest occupying the internal void. Finally, XPS provides an elemental analysis of a shallow layer (approx. 20 nm depth for soft X-rays) of the zeolite particle, allowing to determine if the host is really inside the zeolitic structure.

The encapsulated metal complexes into the supercages of zeolites have been named *zeozymes* [66], since the encapsulated complex may constitutes a "single site" catalytic species with well-defined geometrical constraints, which is supposed to behave like the active center of an enzyme. For instance, encapsulated Pd(II)–salen complexes have been used as carbonyl hydrogenation catalysts for methyl pyruvate and methyl acetoacetate, with high selectivities and conversions [67]. Also, [Rh(I)(cod)(N-*tert*-butylprolinamide)] complex has been prepared inside the zeolite, and the immobilized catalyst has been used in the hydrogenation of alkenes. In the case of the N-acetyldehydrophenylalanine, the enantiomeric excess obtained in much higher than that obtained with the homogeneous complex [68].

Encapsulated chiral Mn–salen complexes have been used as catalysts in the epoxidation of alkenes [66]. The enantiomeric excesses obtained were only modest (about 60%), particularly compared to those achieved in solution with Jacobsen's catalyst (Fig. 3.12). It has to be noted, however, that due to steric restrictions the actual chiral salen ligand encapsulated within the Y zeolite cages lacks the some of the bulky *tert*-butyl substituents. Molecular modeling predicts that Jacobsen's ligand is too large to be accommodated inside the zeolite Y supercage.

The "ship-in-a-bottle" strategy is a simple yet elegant idea, but suffers from several drawbacks, not always acknowledged in the literature covering this topic. Some of the most relevant are: (i) the formation of the whole catalytic complex on the external surface of the support and not inside the supercage, already mentioned; (ii) problems in the diffusion of reagents and products through the support pores and channels; (iii) the presence of uncomplexed metal, that may act as a competing catalytic species; and (iv) the suitability of the support cages to host reaction intermediates and the corresponding transition states, as illustrated in the case of the chiral Mn–salen complexes, which severely limits the scope of application to Fine Chemicals synthesis.

3.4.3 Building Catalytic Maracas Through Encapsulation

One possibility to overcome the limitation in pore and supercage size of zeolites is the use of ordered mesoporous silicas (OMS). However, the cylinder-like pores of some of these materials such as MCM-41 or SBA-15 cannot prevent the leaching of the encapsulated metal complexes, as described in the case of copper phthalocyanine and porphyrin [69]. On the other hand, mesoporous silicas with cagelike structures, such as SBA-1, SBA-16, FDU-12, and

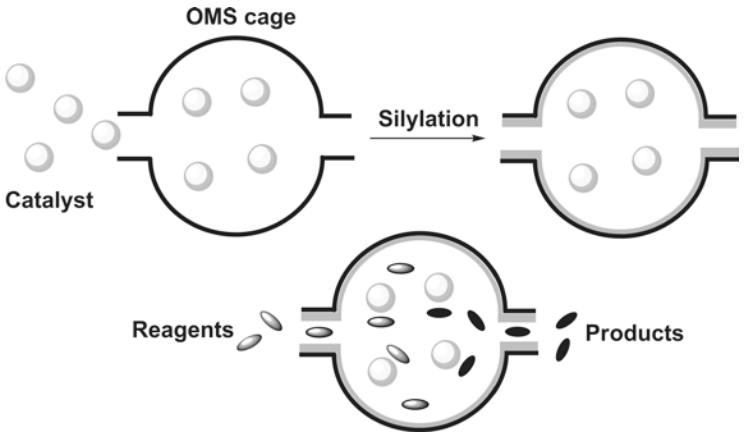

Fig. 3.54 General scheme for catalyst encapsulation within an ordered mesoporous silica followed by tailored pore entrance through silylation

FDU-1, are more suitable as host materials for the encapsulation. These mesoporous cagelike silicas have tunable cage sizes (4–8 nm for SBA-16; 10–22 nm for FDU-12) interconnected three-dimensionally by tunable pore entrances. Additionally, the existence of plentiful hydroxyl groups in the mesoporous silicas provides the possibility of tailoring the pore entrance size by a simple silylation method [69].

Although the "ship-in-a-bottle" strategy can also be used with OMS, together with post-synthesis silylation of the support pores, the most successful method for immobilization in OMS is the direct encapsulation of the whole catalytic complex (Fig. 3.54). A preformed metal complex catalyst is first introduced into the cagelike pore of SBA-16 by impregnation or adsorption. The pore entrance size is then finely tailored by a silylation method according to the molecular size of the catalyst, reactants, and products. Thereby the metal complexes can be encapsulated in the mesoporous cages while the reactants and products can still diffuse freely through the pore entrance.

For example, chiral catalysts Co(salen) and Ru(tsdpen) were encapsulated in SBA-16 by this strategy. The encapsulated catalysts showed enantioselectivity and activity as good as the homogeneous analogues in the hydrolytic kinetic resolution of epoxides and asymmetric transfer hydrogenation of ketones, respectively. Furthermore these catalysts could be recycled for more than ten times without significant loss of catalytic performance.

The use or the large cages present in the OMS offers additional possibilities, as is the boosting of catalytic activity and/or selectivity by the cooperative activation by two or more catalytic centers with proper proximity. For instance, two or more than two chiral Co(salen) catalyst molecules could be confined in a single nanocage of SBA-16. Catalysts with ≥2 Co complexes per cage show a significantly enhanced cooperative activation effect and exhibit much higher

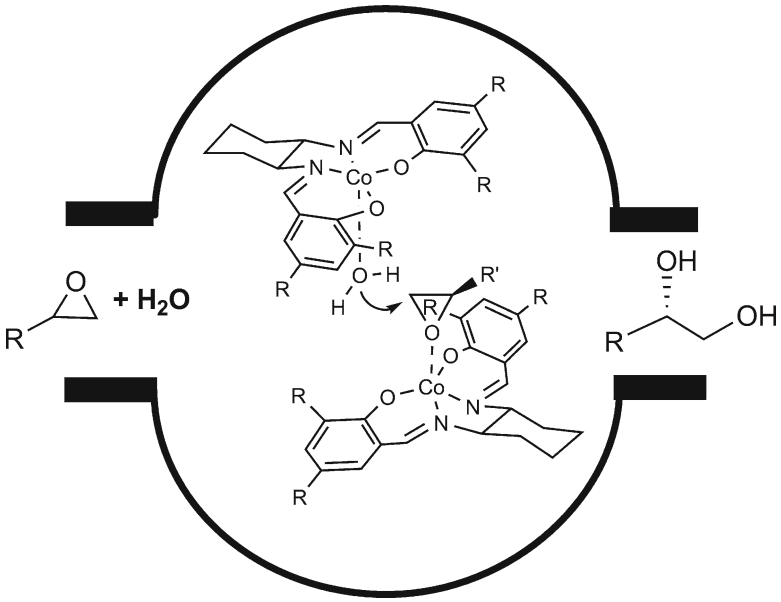

Fig. 3.55 Hydrolytic kinetic resolution of epoxides on Co(salen) complexes confined in the nanocages of SBA-16

activity than the homogeneous catalyst for the hydrolytic kinetic resolution of epoxides (Fig. 3.55).

The enhanced cooperative activation effect by confinement of several catalysts molecules in the nanocage of the support is better appreciated when the substrate/catalysts ratio is increased. When the S/C ratio is increased up to 12,000:1, the conversion for the homogeneous catalyst sharply decreases from 34% to 7% even though the reaction time is prolonged to 24 h. The enantioselectivity simultaneously decreases from 98% ee to 89% ee. In contrast, under similar conditions, Co(salen)/SBA-16 can still afford 50% conversion with 98% ee of the diol.

It is clear that this encapsulation strategy constitutes a real breakthrough in the field of homogeneous catalyst immobilization, and it is expected that new applications of this methodology will appear in the near future.

3.4.4 Sprinkling the Catalyst over the Support: Adsorption

Immobilizing homogeneous catalysts by mere physisorption onto a solid support may be considered as the most straightforward strategy available, since, in principle, neither catalyst nor support have to be modified. The main drawback associated to this strategy, however, is the weak van de Waals forces associated to the physisorption phenomenon, so leaching of catalyst to the solution becomes almost unavoidable. In order to overcome this problem,

immobilization by catalyst adsorption usually takes advantage from other, stronger, interactions, such as hydrogen bonding or hydrophobic effect. The use of either charged species or ion pairs leads to a supplementary strength in the metal complex-support interaction, facilitating the recovery and reuse of the immobilized catalyst.

The possibility of immobilizing homogeneous chiral catalysts by means of weak interactions was explored as early as in 1983 [70]. Chiral [(diphosphine)Rh(cod)Cl] neutral complexes were adsorbed on pretreated charcoal from ethanolic solutions. Enantioselectivities in the hydrogenation of (*Z*)-2-acetamidocinnamic acid were even better than those obtained in solution (87% ee vs 79% ee). Solvent was crucial for recovery, probably due to the solubility of the complex. Leaching of Rh was detected, although 85% of the initial amount was still present on the catalyst after four runs.

The use of the hydrophobic effect to immobilize neutral [(BPPM)Rh(cod)Cl] and cationic [(BPPM)Rh(cod)]ClO_4 complexes was attempted on methylated silica [71]. Good results (≥85% ee) in the hydrogenation of a DOPA precursor were obtained, but activity and enantioselectivity decreased significantly upon recycling. Cationic complexes were more efficiently recovered under the same conditions. Adsorption was carried out from methanol/water mixtures, showing that the maximum was reached at high water content. Hydrophobic character of the immobilization was invoked due to the lower adsorption observed for non-methylated silica.

In a recent example of this strategy a hydrophobic rhodium catalyst precursor, $[Rh(cod)Cl]_2$ was immobilized in the hydrophobic pores of a OMS modified via post-synthesis trimethylsilylation [72]. This immobilized catalyst was used in the 1,4-conjugate addition reaction between the water-soluble reactants *p*-carboxyphenylboronic acid and methyl acrylate in aqueous basic conditions (Fig. 3.56). Solid-supported catalyst showed improved recyclability over liquid–liquid biphasic systems, with stable yields (78%) for three cycles. However, filtration experiments demonstrated that catalyst leaching is also an issue for these systems.

A comparative study of different supports for catalyst adsorption was carried out for $[(diphosphine)Rh(cod)Cl]_2$ catalysts, used for the hydrogenation of the C_2=N bonds in the pyrazine ring of the folic acid (Fig. 3.57) [73]. Silica was found to be the best support. Catalysts immobilized on $BaSO_4$, TiO_2, MgO, molecular sieves, sephadex and cellulose were inactive. The best stereoselectivity was obtained using a silica gel with medium particle size (40 μm), whereas other silicas, alumina, celite or charcoal led to worse results. Unfortunately, both yield and, above all, stereoselectivity decreased

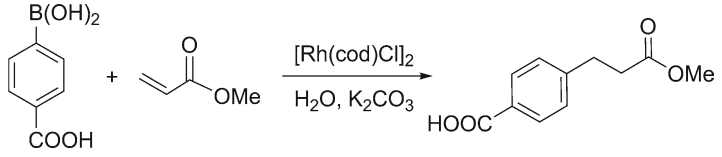

Fig. 3.56 Rh-catalyzed 1,4-conjugate addition of *p*-carboxyphenylboronic acid to methyl acrylate in water

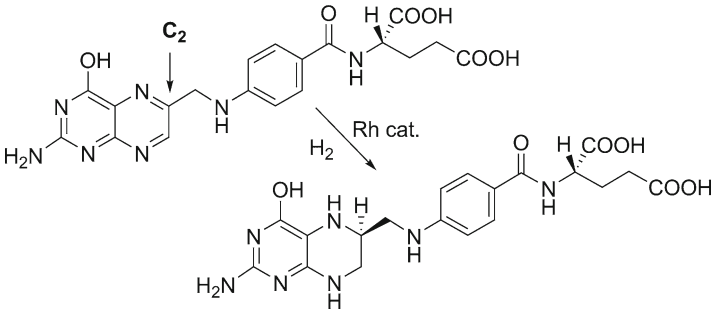

Fig. 3.57 Hydrogenation of folic acid by Rh catalyst adsorbed on different supports

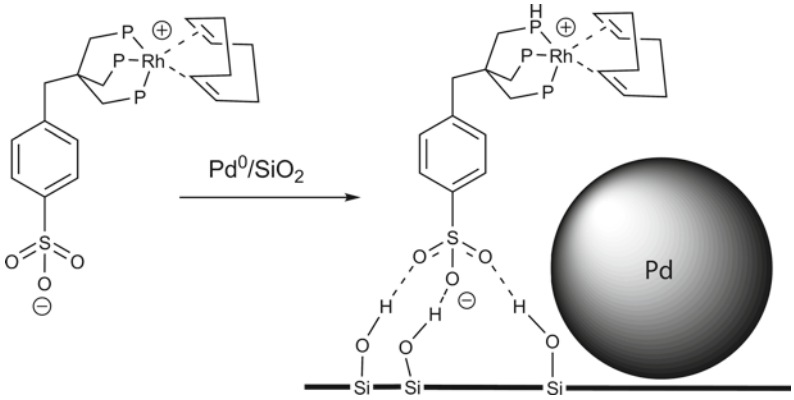

Fig. 3.58 Rh catalyst immobilized by hydrogen bonding with the ligand

upon reuse. The nature of the catalyst–support interaction was not clear, although it probably involves the superficial silanol groups, but the retention on the surface was probably related to the low solubility of the complex in the reaction medium.

More defined and stable support–catalyst interactions are established through hydrogen bonding when the inorganic supports present different types of OH groups. 2:1 complexes of (*S*,*S*)-1,2-diphenylethylenediamine with $[Rh(C_6H_{10})Cl]_2$ were adsorbed onto different supports and used in the hydride transfer reduction of the ketones in a continuous flow reactor [74]. Good immobilization was observed only with silica, indicating better hydrogen bonding with the surface silanols.

Enhanced hydrogen bonding between catalyst and support can be obtained when charged groups participate in the hydrogen bond. Two main variants of this strategy are used in catalyst immobilization. On the one hand, the charged group can belong to one of the catalyst ligands, and on the other, the charged group can be the counteranion of a cationic complex.

Examples of the first strategy are rather scarce. In one of them a neutral [Rh(cod)(sulphos)] complex, but of zwitterionic nature (Fig. 3.58), was immobilized through

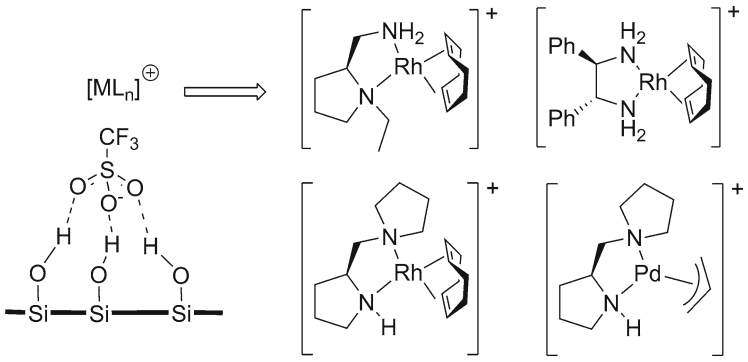

Fig. 3.59 Cationic Rh and Pd catalysts immobilized through support–counterion interaction

hydrogen bonding on silica [75]. This catalyst was combined with palladium nanoparticles and it was tested in the hydrogenation of benzene to cyclohexane. The Rh single-site and the Pd nanoparticle form a unique, stable heterobimetallic catalyst in which Pd adsorbs and activates benzene so as to allow its η^4-coordination to Rh, followed by reduction to cyclohexa-1,3-diene. Fast hydrogenation of cyclohexa-1,3-diene takes place at the Rh site, and the resulting cyclohexene is hydrogenated to cyclohexane by either metal.

There are comparatively more examples where hydrogen bonding serves to fix the counterion of the cationic catalytic complex, which gets subsequently immobilized through electrostatic forces. In one of the pioneering works in this field [(MeDuPhos)Rh(cod)]OTf was immobilized on MCM-41 [76]. The catalyst showed to be highly active and selective in the hydrogenation of several enamides, with results (>99% conversion, 98–99% ee) better than in solution. Leaching of active species was not observed and the catalyst was recovered by decantation leaving the solid with a small amount of solvent. The reaction was repeated four times without loss of conversion or selectivity.

In several cases, confinement effects have been described with this immobilization strategy, for example in the case of Rh(I) and Pd(II) of chiral diamines immobilized on a series of commercially available silicas of narrow pore size distribution (Fig. 3.59) [77]. The catalytic results in the hydrogenation of methyl 2-oxo-2-phenylacetate clearly showed the influence of the spatial restrictions imposed by the support on enantioselectivity. This influence declined as the pore diameter of the silica support increased. Although some of the catalysts exhibited noticeable enantioselectivity in solution, these values were significantly increased upon immobilization. No leaching was observed when catalysts were recycled.

Similar immobilization strategy has been used with Rh-phosphinoxazoline, Rh–DIOP and Rh–BINAP complexes, and with Cu–Box and Cu–Pybox complexes. In most cases, triflate and silica are the anion and support used to accomplish the immobilization through hydrogen bonding.

3.4.5 *Spreading the Catalytic Solution over the Support: Supported Liquid Phases*

Supported liquid phases constitute an interesting solution for immobilization of homogeneous catalysts. In most cases, this strategy consists in dissolving the catalytic species in a small quantity of a liquid phase. The resulting solution is then dispersed over the solid support, leading to the supported liquid phase catalyst (SLPC). In the SLPC system, although the final material is a solid, with a free-flowing solid material aspect, the active species in the liquid phase, acting as a genuine homogeneous catalyst, is expected to preserve the high activity and selectivity displayed in solution, or even to improve it. Figure 3.60 schematizes the structure of a SLPC.

Silica is the solid of choice in the vast majority of cases, due to its easy availability, low price and high surface area. Furthermore, silica surface can be easily modified in a variety of forms to tailor its properties (hydrophobicity or ionic liquid affinity, for instance), so it becomes more suitable for its use as support of a SLPC. However, the use of other solid supports with specific applications is a matter of current research.

Concerning the liquid phase, there are two main classes of liquids that have been successfully applied in the preparation and use of SLPC, namely water and ionic liquids.

The preparation of supported aqueous phase catalysts (SAPC) uses the hydrophilic nature of a silica surface to adhere a layer of water in which a hydrophilic

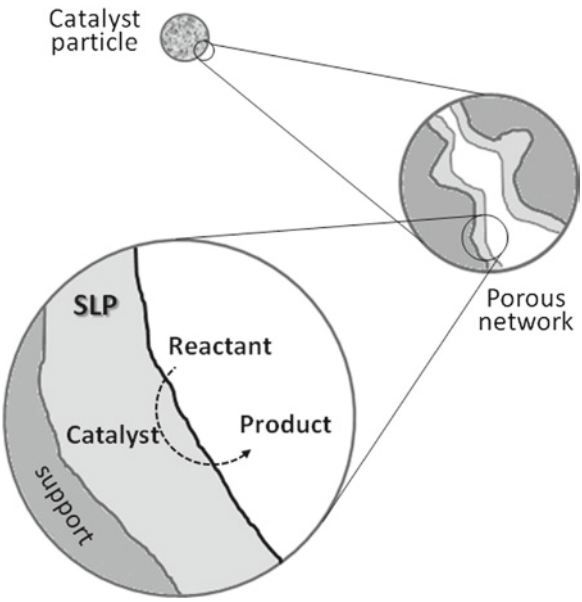

Fig. 3.60 Schematic representation of a supported liquid phase catalyst (SLPC)

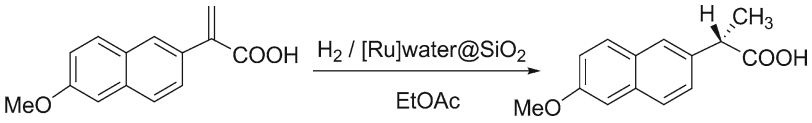

Fig. 3.61 Hydrogenation of 2-(6′-methoxy-2′-naphthyl)acrylic acid with SLPC

catalyst can be dissolved [78]. Aqueous phase impregnation results in a large area of surface contact. In general, reactants diffuse from the bulk organic phase (either the own reactants or a solution in a water-immiscible solvent) into the wet silica and react at the water-organic interphase. One of the first examples described the hydroformylation of oleyl alcohol catalyzed by $[HRh(CO)(TPPTS)_3]$ [79]. The corresponding aldehydes were obtained in almost quantitative yield, and the SAPC was recyclable without loss of catalytic activity. Rhodium leaching from the SAPC to the organic phase was discarded through Maitlis' filtration experiments. A similar approach was used in the asymmetric synthesis of naproxen by hydrogenation of 2-(6′-methoxy-2′-naphthyl)acrylic acid (Fig. 3.61) catalyzed by Ru-BINAP-$4SO_3Na$ [80]. SLPC was 50 times more active than the liquid-liquid biphasic system and no leaching of ruthenium was observed.

This catalytic system also serves to illustrate the use of liquids phases different from water in the preparation of hydrophilic SLPC. In order to avoid the hydrolytic cleavage of the Ru–Cl bond, which leads to reduced enantioselectivity, water was substituted by ethylene glycol supported on CPG-240. Up to 96% ee was obtained, and no leaching of Ru was observed, leading to a recovered catalyst with almost the same performance.

Another interesting effect is the role of liquid loading (water or polyalcohols) in the catalytic activity of the SLPC [81]. In many cases, the maximum catalytic activity is obtained at a support pore filling around unity, irrespective of the surface area and pore volume. The inverse behavior (i.e. maximum activity at pore filling below unity) is observed when highly hydrophobic substrates (long-chain olefins, cinnamaldehyde) are used in hydroformylation or hydrogenation reactions. In the case of the hydrogenation of cinnamaldehyde, not only the catalytic activity increases with the water content up to a certain limit, but also the selectivity, which has been explained assuming that water is dispersed in the form of small islets of a certain thickness on the support. Increasing the water content leads to a grow in size, but not in thickness, of the islets. This results in less free support surface, which difficults the hydrogenation of the C=C double bond (Fig. 3.62).

Applications of SLPC using water or polyalcohols as the liquid phase have been described for a variety of organic transformations, and using different metals, such as hydroformylation (Rh), hydrogenation (Ru, Pd), allylic alkylation (Pd), Heck reactions (Pd, Ni), or Tsuji–Trost reactions (Pd) [81].

However these successful applications, the main drawback of SAPC is the relatively high volatility of water, so there is a significant loss during the use, handling and recovery. In some cases, as the silica support is hydrophilic, it is able to retain the water-soluble catalyst by hydrogen bonding of the hydrated sulfonate groups on

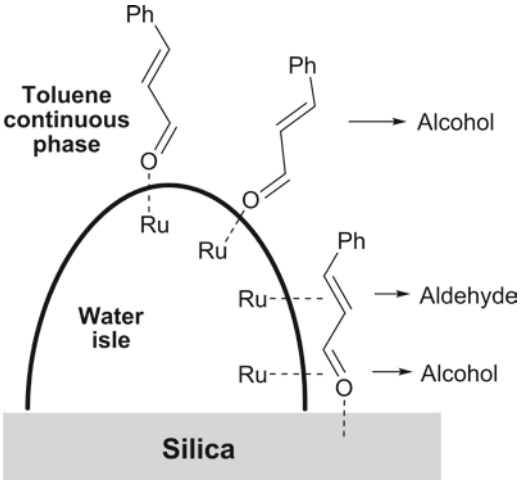

Fig. 3.62 An explanation of the effect of water content on the selectivity of the hydrogenation of cinnamaldehyde

the surface, even if most of initial water is lost [81]. In most cases, however, deactivation of the SAPC occurs.

Ionic liquids constitute a new class of solvents that display interesting properties and that are increasingly used as reaction media for homogeneous catalysis. Some properties of ILs such as low volatility and good solubility for many organic and inorganic complexes perfectly fit the requirements of the liquid component in the supported ionic liquid phase catalysts (SILPC). An additional advantage of using SILP over bulk liquid phases is the low volume of the usually expensive ionic liquids, necessary to prepare the SILPC.

In spite of the relatively recent development of SILPC, there are many catalytic applications already known in different organic reactions and using different metals as, for instance, hydroformylation (Rh), carbonylation (Rh), hydrogenation (Rh), Heck reactions (Pd), hydroaminations (Rh, Pd, Zn), epoxidation (W, Mn), epoxide ring-opening (Cr), Grubbs' olefin metathesis (Ru), Mukaiyama aldol (Cu), olefin cyclopropanation (Cu), among others [82].

One of the particular advantages of SILPC systems is that the mass transport limitation from the gas to a liquid phase can be circumvented because of the high interfacial area in these SILP catalysts. This advantage allows the SILPC system to be applicable in a fixed-bed reactor for simple continuous processes. Especially advantageous is the use of SILPC in conjunction with gaseous substrates, whereby product separation and catalyst recycling could be avoided. The main drawback is that even a minor ionic liquid solubility in a liquid feedstock/product mixture can be sufficient to remove the catalyst from the carrier over time in both continuously operated or batch processes upon catalyst recycling (due to the very small amount of ionic liquid on the support). Even worse, the thin immobilized catalyst layer can physically be removed from the support by mechanical forces, for example, by a convective liquid flow.

An example of such kind of process is the hydroformylation of propene with the combination of 2,7-bis-(SO_3Na)-4,5-bis(diphenylphosphino)-9,9-dimethyl-xanthene (sulfoxantphos) modified rhodium complexes and [BMIm] [n-$C_8H_{17}OSO_3$] dispersed on silica [83]. In a fixed-bed reactor, the resultant SILPC showed very high activity and good selectivity. Particularly, the lifetime of the SILPC system reached up to 200 h time-on-stream although a slight decrease in activity was observed at the end. Interestingly, treatment of the catalyst under vacuum can extend the lifetime to 700 h.

Sometimes, the use of SILPC displays additional advantages over those already pointed out. For instance, an imidazolium-tagged bis(oxazoline)–Cu(II) complex was found to be an effective and enantioselective catalyst for the Mukaiyama-aldol reaction between methyl pyruvate and 1-methoxy-1-trimethylsilyloxypropene in a biphasic system composed of diethyl ether and IL [84]. However, the decomposition of the silyl enol ether generates a by-product (Fig. 3.63), which is completely suppressed by supporting the Cu(II) complex on silica or an imidazolium-modified silica with the SILPC strategy without reducing the enantioselectivity. The system could be reused up to five times without a significant loss in conversion or enantioselectivity.

Comparative studies of the use of different supports in the preparation of SILPC are scarce. In one example concerning cyclopropanation reactions using bisoxazoline-Cu catalysts [85] [bmim][PF_6] was supported on different solids (three different clays, graphite, Y zeolite, silica and hydrotalcite). Using decreasing amounts of IL, the average thickness of the IL film in the SILPC was reduced. When a small amount of IL was supported on clays (laponite, bentonite, K10 montmorillonite) confinement effects were observed (Fig. 3.64), pointing to a strong interaction of the catalytic complex with the charged surface of the clay. Other lamellar solids, such as graphite or hydrotalcite did not exhibit this effect, the catalytic results being identical to those obtained in homogeneous IL phase.

Immobilization of homogeneous catalyst through SLPC has reached in a short time the maturity status. The increasing use of aqueous and ionic liquid phases in

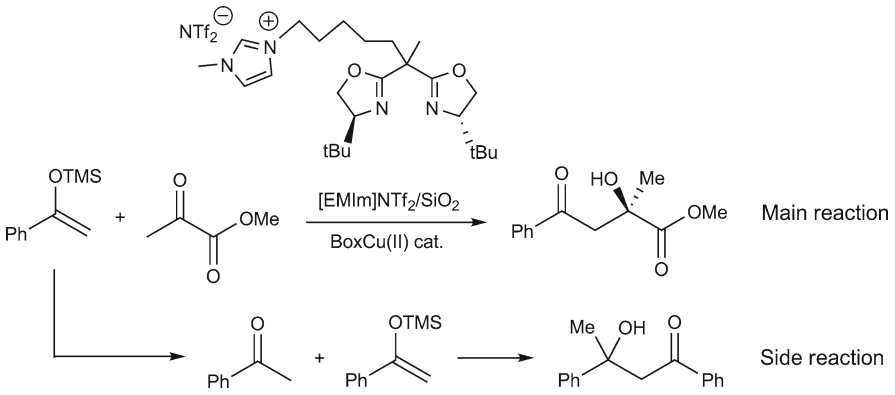

Fig. 3.63 Mukaiyama-aldol reaction of methyl pyruvate over SILP-Cu(II) system

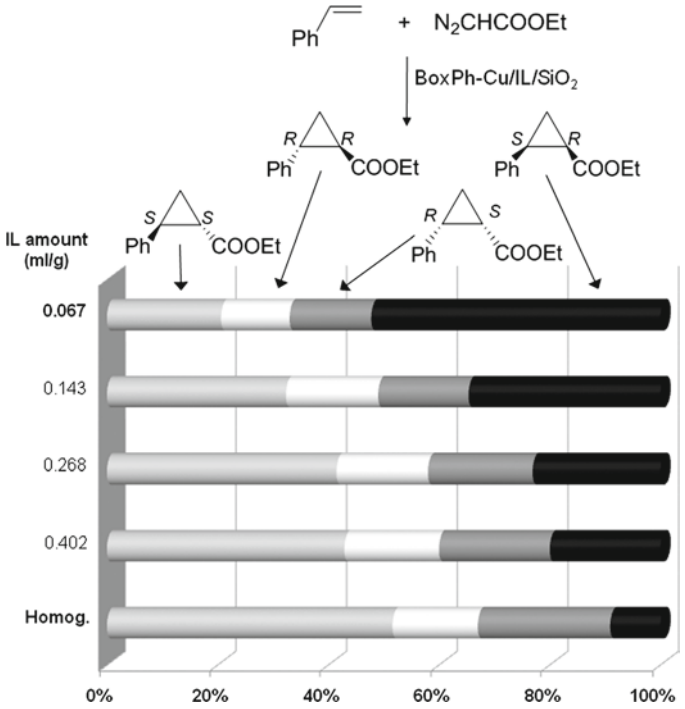

Fig. 3.64 Effect of ionic liquid phase thickness on selectivity results of cyclopropanation reaction between styrene and ethyl diazoacetate

liquid–liquid biphasic catalysis allows developing the SLPC counterparts in a straightforward manner, so a continuous growth in this field is to be expected in the near future.

3.5 Conclusions and Future Perspectives

Regarding inorganic supports, new materials and new immobilization approaches are currently being explored, which may help to expand the applicability of immobilized catalysts. One of them is the use of nanoparticles as supports to increase the accessibility and density of catalytic sites as to improve separation. In this regard the use of gold nanoparticles decorated by thiol terminated ligands [86] or the use of magnetic nanoparticles to allow the recycling by using an external magnet [87] are two attractive alternatives.

Heteropolyacids, leading to weakly coordinating anions, may be considered as alternative to other frequently used counterions, such as ClO_4^-, BF_4^-, TfO^-, or PF_6^-. Immobilized heteropolyacids can be considered as interesting alternative supports for metal complexes [88], although still scarcely explored.

Some metal-organic frameworks (MOF) are topologically analogous to pure inorganic zeolites (ZMOF), possess extra-large cavities, and are stable in aqueous media, which offer a great potential for their application in the immobilization of homogeneous catalysts by encapsulation by self-assembly around the complex [89]. However, these supports are not purely inorganic materials.

In the field of SILPC, new materials are emerging as potential supports for the heterogenization of homogeneous catalysts. In particular, carbon nanotubes [90] and carbon/metal hybrid fibers [91] have also been recently used as supports for SILPC in conjunction with Rh catalysts for hydrogenation reactions.

The use of inorganic solids to support catalytic metal complexes has increased over the last years motivated by the practical advantages of these solids and the possibility of using supports with well-defined morphology. The use of the geometrical regularity of these solids allows increasing not only the activity and stability but also the different types of selectivity. Achieving selectivities complementary from those obtained in solution is one of the ways to increase the applicability of immobilized catalysts in the field of Fine Chemicals synthesis.

However, the large variety of possible immobilization methods and the lack of accurate information about the nature of the catalyst or its purity, make in some cases difficult to draw general conclusions on the role of factors such as the catalyst preparation procedure or the support morphology in the catalytic performance. Although still a challenging objective, the full understanding of the effect of those factors seems to be the only way to design, in the near future, the immobilized catalysts “à la carte”.

References

1. Thomas JM, Raja R, Lewis DW (2005) Angew Chem Int Ed 44:6456–6482
2. Diddams P (1992) Inorganic supports and catalysts – an overview. In: Smith K (ed) Solid supports and catalysts in organic synthesis. Chichester, Ellis Horwood and Prentice Hall
3. Scott RPW (1993) Silica gel and bonded phases. Wiley, Chichester
4. Cavani F, Trifirò F, Vaccari A (1991) Catal Today 11:173–301
5. Van Bekkum H, Flanigen EM, Jansen JC, ed (1991) Introduction to zeolite science and practice, Studies in Surface Science and Catalysis, vol 58. Elsevier, Amsterdam
6. Baerlocher C, McCusker LB, Database of zeolite structures: http://www.iza-structure.org/databases/
7. Meynen V, Cool P, Vansant EF (2009) Micropor Mesopor Mater 125:170–223
8. Daniel MC, Astruc D (2004) Chem Rev 104:293–346
9. Tasis D, Tagmatarchis N, Bianco A, Prato M (2006) Chem Rev 106:1105–1136
10. Fraile JM, García JI, Mayoral JA (2009) Chem Rev 109:360–417
11. Mazzei M, Marconi W, Riocci M (1980) J Mol Catal 9:381–387
12. Shimazu S, Ro K, Sento T, Ichikuni N, Uematsu T (1996) J Mol Catal A 107:297–303
13. Simons C, Hanefeld U, Arends IWCE, Sheldon RA, Maschmeyer T (2004) Chem Eur J 10:5829–5835
14. Hems WP, McMorn P, Riddel S, Watson S, Hancock FE, Hutchings GJ (2005) Org Biomol Chem 3:1547–1550
15. Crosman A, Hoelderich WF (2007) Catal Today 121:130–139
16. Fraile JM, García JI, Massam J, Mayoral JA (1998) J Mol Catal A 136:47–57

17. Piaggio P, Langham C, McMorn P, Bethell D, Bullman-Page PC, Hancock FE, Sly C, Hutchings GJ (2000) J Chem Soc Perkin Trans 2:143–148
18. Kim GJ, Kim SH (1999) Catal Lett 57:139–143
19. Fraile JM, García JI, Mayoral JA, Tarnai T (1998) Tetrahed Asym 9:3997–4008
20. Alonso PJ, Fraile JM, García J, García JI, Martínez JI, Mayoral JA, Sánchez MC (2000) Langmuir 16:5607–5612
21. Fraile JM, García JI, Herrerías CI, Mayoral JA, Harmer MA (2004) J Catal 221:532–540
22. Fraile JM, García JI, Herrerías CI, Mayoral JA, Reiser O, Socuéllamos A, Werner H (2004) Chem Eur J 10:2997–3005
23. Caplan NA, Hancock FE, Bulman Page PC, Hutchings GJ (2004) Angew Chem Int Ed 43:1685–1688
24. Fraile JM, Pérez I, Mayoral JA (2007) J Catal 252:303–311
25. Fraile JM, García JI, Herrerías CI, Mayoral JA, Pires E (2009) Chem Soc Rev 38:695–706
26. García JI, López-Sánchez B, Mayoral JA, Pires E, Villalba I (2008) J Catal 258:378–385
27. Fabra MJ, Fraile JM, Herrerías CI, Lahoz FJ, Mayoral JA, Pérez I (2008) Chem Commun 5402–5404
28. Barnard CFJ, Rouzaud J, Stevenson SH (2005) Org Proc Res Devel 9:164–167
29. Zhang H, Li C (2006) Tetrahedron 62:6640–6649
30. Anwander R (2001) Chem Mater 13:4419–4438
31. Severn JR, Chadwick JC, Duchateau R, Friedrichs N (2005) Chem Rev 105:4073–4147
32. Fraile JM, García JI, Mayoral JA, Salvatella L, Vispe E, Brown DR, Fuller G (2003) J Phys Chem B 17:519–526
33. Meunier D, Piechaczyk A, de Mallmann A, Basset JM (1999) Angew Chem Int Ed 38:3540–3542
34. Fraile JM, García JI, Mayoral JA, Royo AJ (1996) Tetrahed Asym 7:2263–2276
35. Gerstberger G, Anwander R (2001) Micropor Mesopor Mater 44–45:303–310
36. Blanc F, Berthoud R, Salameh A, Basset JM, Copéret C, Singh R, Schrock R (2007) J Am Chem Soc 129:8434–8435
37. Heckel A, Seebach D (2002) Helv Chim Acta 85:913–926
38. Rechavi D, Lemaire M (2001) Org Lett 3:2493–2496
39. Park JK, Kim SW, Hyeon T, Kim BM (2001) Tetrahed Asym 12:2931–2935
40. Baleizao C, Gigante B, Sabater MJ, García H, Corma A (2003) J Catal 215:199–207
41. Kinting A, Krause H, Capka M (1985) J Mol Catal 33:215–223
42. Choudary BM, Chowdari NS, Kantam ML, Santhi PL (2001) Catal Lett 76:213–218
43. Silva AR, Wilson K, Clark JH, Freire C (2006) Micropor Mesopor Mater 91:128–138
44. Pini D, Mandoli A, Orlandi S, Salvadori P (1999) Tetrahed Asym 10:3883–3886
45. Kureshy RI, Ahmad I, Khan NH, Abdi SHR, Pathak Jasra RV (2005) Tetrahed Asym 16:3562–3569
46. Corma A, Iglesias M, del Pino C, Sánchez F (1991) J Chem Soc Chem Commun 1253–1255
47. Carmona A, Corma A, Iglesias M, San José A, Sánchez F (1995) J Organometal Chem 492:11–21
48. Johnson BFG, Raynor SA, Shephard DS, Mashmeyer T, Thomas JM, Sankar G, Bromley S, Oldroyd R, Gladden L, Mantle MD (1999) Chem Commun 1167–1168
49. Eisen M, Blum J (1989) J Mol Catal 56:329–337
50. Kim GJ, Shin JH (1999) Tetrahed Lett 40:6827–6830
51. Park DW, Choi SD, Choi SJ, Lee CY, Kim GJ (2002) Catal Lett 78:145–151
52. González-Arellano C, Corma A, Iglesias M, Sánchez F (2004) Adv Synth Catal 346:1316–1328
53. Heckel A, Seebach D (2002) Chem Eur J 8:560–572
54. Wu DY, Lindner E, Mayer HA, Jiang ZJ, Krishnan V, Bertagnolli H (2005) Chem Mater 17:3951–3959
55. Bied C, Gauthier D, Moreau JJE, Man MWC (2001) J Sol-Gel Sci Technol 20:313–320
56. Jiang D, Yang Q, Yang J, Zhang L, Zhu G, Su W, Li C (2005) Chem Mater 17:6154–6160

57. Lu ZL, Lindner E, Mayer HA (2002) Chem Rev 102:3543–3578
58. Barloy L, Battioni P, Mansuy D (1990) J Chem Soc Chem Commun 1365–1367
59. Kureshy RI, Khan NH, Abdi SHR, Ahmad I, Singh S, Jasra RV (2003) Catal Lett 91:207–210
60. Pérez-Bernal ME, Ruano-Casero R, Pinnavaia TJ (1991) Catal Lett 11:55–62
61. Tas D, Jeanmart D, Parton RF, Jacobs P (1997) Stud Surf Sci Catal 108:493–500
62. Bhattacharjee S, Anderson JA (2006) Adv Synth Catal 348:151–158
63. Craythorne SJ, Anderson K, Lorenzini F, McCausland C, Smith EF, Licence P, Marr AC, Marr PC (2009) Chem Eur J 15:7094–7100
64. Zhan BZ, Li XY (1998) Chem Commun 349–350
65. Herron N (1986) Inorg Chem 25:4714–4717
66. Corma A, Garcia H (2004) Eur J Inorg Chem 1143–1164
67. Kahlen W, Janssen A, Holderich WF (1997) Stud Surf Sci Catal 108:469–476
68. Zsigmond A, Bogar K, Notheisz F (2002) Catal Lett 83:55–58
69. Yang QH, Han DF, Yang HQ, Li C (2008) Chem Asian J 3:1214–1229
70. Inoue M, Ohta K, Ishizuka N, Enomoto S (1983) Chem Pharm Bull 31:3371–3376
71. Ishizuka N, Togashi M, Inoue M, Enomoto S (1987) Chem Pharm Bull 35:1686–1690
72. Handa P, Holmberg K, Sauthier M, Castanet Y, Mortreux A (2008) Micropor Mesopor Mater 116:424–431
73. Brunner H, Bublak P, Helget M (1997) Chem Ber 130:55–61
74. Gamez P, Fache F, Lemaire M (1994) Bull Soc Chim Fr 131:600–602
75. Barbaro P, Bianchini C, Dal Santo V, Meli A, Moneti S, Psaro R, Scaffidi A, Sordelli L, Vizza F (2006) J Am Chem Soc 128:7065–7076
76. de Rege FM, Morita DK, Ott KC, Tumas W, Broene RD (2000) Chem Commun 1797–1798
77. Thomas JM, Raja R (2004) J Organometal Chem 689:4110–4124
78. Minakata S, Komatsu M (2009) Chem Rev 109:711–724
79. Arhancet JP, Davis ME, Merola JS, Hanson BE (1989) Nature 339:454–455
80. Wan KT, Davis ME (1995) J Catal 152:25–30
81. Zhao FY, Fujita SI, Arai M (2006) Curr Org Chem 10:1681–1695
82. Gu YL, Li GX (2009) Adv Synth Catal 351:817–847
83. Riisager A, Fehrmann R, Flicker S, van Hal R, Haumann M, Wasserscheid P (2005) Angew Chem Int Ed 44:815–819
84. Doherty S, Goodrich P, Hardacre C, Parvulescu V, Paun C (2008) Adv Synth Catal 350:295–302
85. Castillo MR, Fousse L, Fraile JM, Garcia JI, Mayoral JA (2007) Chem Eur J 13:287–291
86. Belser R, Stöhr M, Pfaltz A (2005) J Am Chem Soc 127:8720–8731
87. Hu A, Yee GT, Lin W (2005) J Am Chem Soc 127:12486–12487
88. Augustine R, Tanielyan S, Anderson S, Yang H (1999) Chem Commun 1257–1258
89. Alkordi MH, Liu Y, Larsen RW, Eubank JF, Eddaoudi M (2008) J Am Chem Soc 130:12639–12641
90. Rodriguez-Perez L, Teuma E, Falqui A, Gomez M, Serp P (2008) Chem Commun 4201–4203
91. Ruta M, Yuranov I, Dyson PJ, Laurenczy G, Kiwi-Minsker L (2007) J Catal 247:269–276

Chapter 4
Covalent Heterogenization of Asymmetric Catalysts on Polymers and Nanoparticles

Ciril Jimeno, Sonia Sayalero, and Miquel A. Pericàs

Abstract The development of enantioselective processes involving the use of catalytic species covalently bonded onto polymers and nanoparticles has gained a considerable importance over the last decade, as sustainability concerns have deeply influenced the practice of chemistry. In this review, an overview is given of the different strategies followed for the covalent immobilization of ligand–metal assemblies (for metal catalysis) and catalytic organic molecules (for organocatalysis) onto organic polymers and nanoparticles, paying special attention to the factors that control catalytic activity and enantioselectivity. Efforts devoted to the development of continuous flow processes with immobilized catalysts of these types are also reviewed.

4.1 Introduction

While many catalytic industrial processes are carried out in flow systems, enantioselective catalytic processes have been traditionally performed in a batch manner using homogeneous catalysts. This obviously involves important advantages, such as high turnover numbers and ready access to selectivity control, either by modification of experimental parameters or through structural fine-tuning. However, batch processing has also negative consequences both from the economic and the environmental points of view; it is characterized by normally wasteful workup treatments, and usually requires specific treatments for catalyst recovery and separation (metal traces) from reaction products.

C. Jimeno, S. Sayalero, and M.A. Pericàs (✉)
Institute of Chemical Research of Catalonia (ICIQ), Av. Països Catalans, 16, E-43007 Tarragona, Spain

M.A. Pericàs
Departament de Química Orgànica, Universitat de Barcelona, E-08028 Barcelona, Spain
e-mail:mapericas@iciq.es

P. Barbaro and F. Liguori (eds.), *Heterogenized Homogeneous Catalysts for Fine Chemicals Production*, Catalysis by Metal Complexes 33,
DOI 10.1007/978-90-481-3696-4_4,

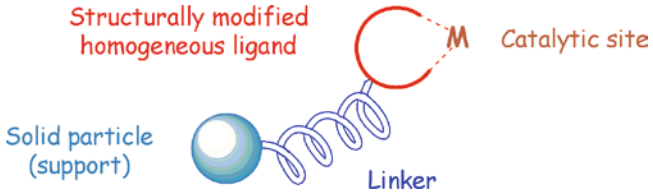

Fig. 4.1 Schematic representation of a covalently supported catalytic species, showing the different parts that are relevant to catalytic activity

In recent times, the idea of covalently bonding homogeneous catalysts onto supports (Fig. 4.1) as a strategy that combines the advantages of homogeneous and heterogeneous catalysis has gained wide acceptation [1, 2]. In this approach, if the chemically modified homogeneous ligand has been properly designed (in such a way that the supporting process does not perturb the reaction site) and an appropriate linker has been selected, the target catalytic process can take place in an essentially homogeneous environment, providing the same opportunities for selectivity control than homogeneous catalysis.

As additional advantages inherent to this approach, catalyst separation and recycling can be readily performed (usually by simple filtration). As an ultimate goal, continuous flow operation can be implemented provided that the supported catalytic species are sufficiently robust and stable under the reaction conditions.

In the present review, emphasis will be put on the design of the different parts of the supported catalytic species for optimal catalytic activity and enantioselectivity. Materials will be classified and presented according to the nature of the support (organic polymers and functional nanoparticles).

For the more abundant, polymer-supported species, examples have been classified into organocatalyzed and metal-catalyzed processes.

All over the review, the still rare examples of enantioselective, continuous flow processes have been highlighted.

4.2 Organocatalytic Reactions on Polymeric Supports

During the last few years, the development of new catalysts, novel methodologies and the invention or identification of generic modes of catalyst activation, induction and reactivity have given rise to an impressive growth in the field of asymmetric organocatalysis. As a result of this effort, conditions have been developed for many types of reactions, such as cycloadditions, Michael additions, aldol reactions, nucleophilic substitutions and many other reactions to take place mediated by organic catalysts with excellent enantioselectivities under mild conditions [3].

Organocatalysis incorporates important characteristics of sustainability through the suppression of complex workup operations for catalyst separation and the removal of metal-containing by-products. Even so, the possibility of separating the catalyst by

simple physical methods and even recovering and reusing it would represent an additional bonus. Actually, from an economical point of view, immobilization would be clearly convenient in case of expensive or difficultly available enantiomerically pure catalysts, or for catalytic species employed in a relatively large amount. Another significant advantage comes from the unique microenvironment created for the reactants within the polymer support. Improved catalyst stability, increased regioselectivity and chemioselectivity due to steric hindrance, and the superior activity of some supported chiral organocatalysts due to site cooperation have all been reported [4]. Most remarkably, the behavior of some of these catalytic species is reminiscent of polypeptides with enzyme activity and can be considered as macromolecular enzyme mimics [5].

Several factors must be considered in the design of a successful immobilization since the final goal can be different from recovering or recycling the catalyst. For instance, the development of polymer-supported chiral organocatalysts suitable for work in a broad variety of solvents could be sometimes considered a more desirable achievement than the development of a supported system exceptionally active in a specific process.

4.2.1 Immobilization Strategies for Organocatalysts

There are three general strategies for organic catalysts immobilization depending on the nature of both the catalyst to be anchored and the support (Fig. 4.2) [1].

(a) **Covalently Supported Catalysts** In this case the ligand or catalyst is covalently anchored to a soluble or insoluble support. The immobilization process involves either reaction of a functional resin with a suitably functionalized catalytic species or copolymerization of a derivative of the organocatalyst with other monomers [6].
(b) **Non-covalently-Supported Catalysts** This approach implies the immobilization of catalysts through adsorption, hydrogen bond, electrostatic interactions or entrapment within several supports [7].
(c) **Biphasic Catalysis** In this case the catalyst is dissolved or anchored into ionic liquids and the product extracted using an immiscible solvent [8].

Covalent binding of catalysts to solid supports implies, in general, a more stable interaction and therefore a broader applicability of the immobilized catalysts. However, it usually requires higher synthetic effort due to the chemical modifications of the catalyst typically needed for linking it to the support. On the contrary, although immobilization of catalysts through adsorption, hydrogen bond or electrostatic interactions is simple, the weak nature of these interactions generally makes the resulting catalysts less robust. With regard to entrapment of homogeneous catalysts within solids, the applicability of this approach is limited basically due to the restricted diffusion of substrates and products. On the other hand, the use of functionalized polymers to provide an effective reagent or catalyst recycling system in multiphase catalysis has gained attention as an efficient alternative that avoids the use of expensive ionic liquids or fluorous solvents [9].

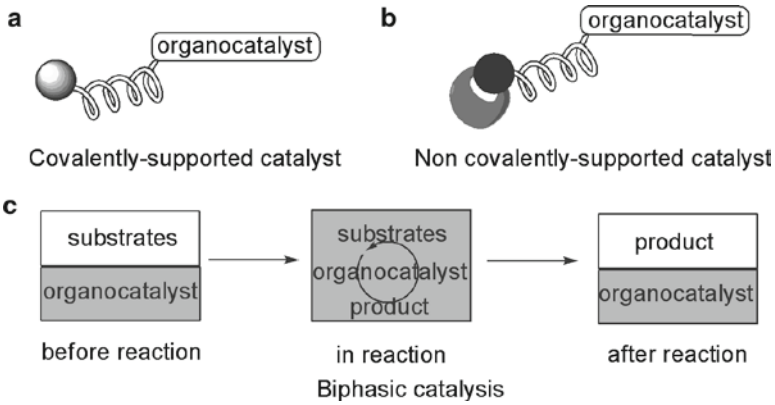

Fig. 4.2 General strategies for organic catalysts immobilization

In the following sections representative examples of polymer-supported chiral organocatalysts will be presented. Comparison between the behavior of different catalytic species will be focused on both the catalytic efficiency and catalyst stability, since generally the ultimate goal of the immobilization process is the recovery and recycling of the catalytic species.

4.2.2 Immobilized Proline and Proline Derivatives

Many of the enantioselective organocatalysts identified in recent years have been also immobilized on different supports [4]. Among them, proline and its derivatives occupy a relevant position [10]. Since the first asymmetric reaction using L-proline, reported in the early 1970s [11], and the initial works of List, Lerner and Barbas 30 years later [12], proline and proline-derivatives have been extensively applied, especially in asymmetric organocatalyzed aldol-type reactions [3]. It should be noted that the immobilization approach requires the use of synthetic derivatives that are more expensive than proline. This amino acid is commercially available at low cost but often employed at high catalyst loading. However, attempts of improving or modifying its catalytic behaviour, taking advantage of specific properties of the support, would justify the immobilization in many instances.

4.2.2.1 Soluble Polymers

Since the immobilization of L-4-hydroxyproline on $MeOPEG_{5000}$ reported in 2001 by Benaglia and Cozzi [13], poly(ethylene glycol) (PEG) has been suggested as the support of choice by its favorable solubility profile besides

other important considerations, including the polymer's low cost, commercial availability and easy functionalization. As a soluble support, PEG allows running catalyzed reactions under homogeneous conditions and to isolate and efficiently recover the catalyst by precipitation and filtration. Proline was anchored by means of a succinate spacer affording a recyclable catalyst (**1**) able to promote aldol reactions of acetone and hydroxyacetone with various aldehydes in an aprotic dipolar solvent (Scheme 4.1) [14]. The level of stereocontrol and yield achieved (45–81% yield, 59–≥98% ee) were comparable to those reported with non-supported proline derivatives at the same catalyst loading. The polymer was re-used three times showing unchanged enantioselectivity but certain loss on its catalytic activity.

Catalyst **1** also performed nicely in Mannich reactions between acetone or hydroxyacetone and preformed or in situ generated aldimines (48–81% yield, 78–97% ee) [14]. Recycling experiments in this case displayed the same trend previously observed in the direct aldol condensations. A similar behavior was described later for enantioselective Michael-type additions catalyzed by **1** [15]. In the conjugate additions reported, this PEG-supported catalyst was less efficient than native proline. For instance, in the addition of cyclohexanone to β-nitrostyrene in the presence of 15 mol% of **1**, the γ-nitroketone was obtained in up to 60% yield and good stereoselectivity (95/5 *syn/anti*) but the ee observed (40%) were lower than that observed with proline as the catalyst (up to 57%).

More effective PEG-supported proline-based catalysts, in terms of both enantioselectivity and substrate scope, for the asymmetric Michael addition of ketones to nitrostyrenes were developed by Zhao *et al*. (Scheme 4.2) [16]. Using 5 mol% of the best catalyst in the prepared series (**2**), the addition products were obtained in good yields (39–94%), moderate to good enantioselectivity (23–86%) and high diastereoselectivities (>98/2, *syn/anti* ratios). However, the problem of a dramatic decrease of chemical yield after the first cycle of recycling remained unsolved.

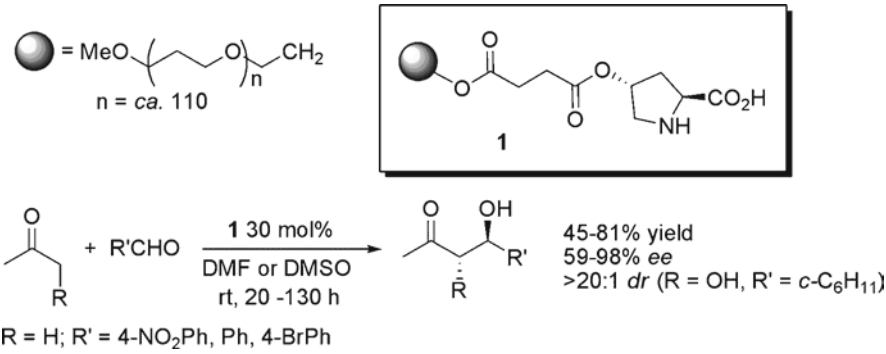

Scheme 4.1 Enantioselective aldol reactions mediated by PEG-supported catalyst **1**

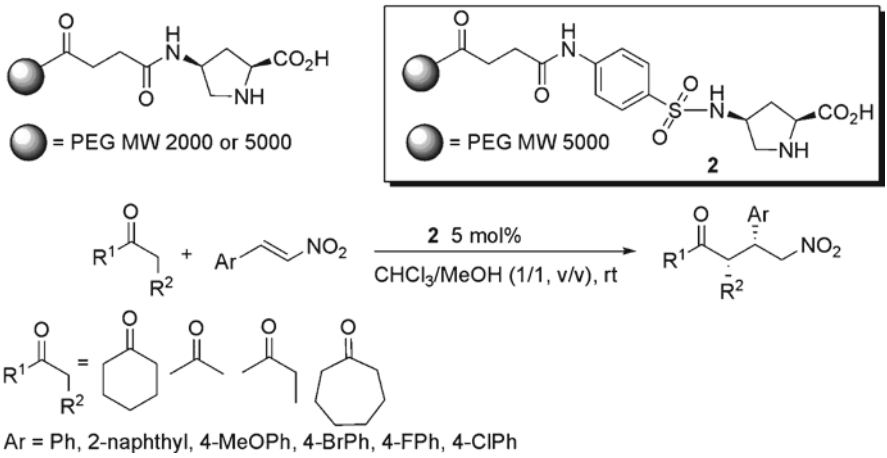

Scheme 4.2 Enantioselective Michael addition of ketones to nitrostyrenes mediated by PEG-supported catalyst

4.2.2.2 Insoluble Polymers

Important advantages have been obtained from the use of insoluble polymer-supported proline-based catalysts, which can be recovered by simple filtration, recycled and re-used and furthermore, efficiently employed in continuous flow processing. In addition, new developments in this field confirm that the high hydrophobicity of the polymer backbone can favor stereocontrol in organocatalyzed reactions performed in aqueous medium. This is of relevant interest considering the environmental benefits of using water as a reaction solvent [17].

For optimal performance, the proline-based catalyst must be anchored through positions remote from the catalytically active α-amino acid moiety to avoid interference by the bulky polymer backbone. In 1985 Takemoto reported the preparation of polymer-bound L-proline by direct anchoring of hydroxyproline via a spacer onto polystyrene (PS) resins with different degrees of cross-linking. Those functionalized resins provided poor values of yield and ee in the aldol step of a Robinson annulation (29% yield, 39% ee) [18].

In 2006 Pericàs and coworkers reported the immobilization of *trans*-4-hydroxyproline onto Merrifield-type polymers through a copper-mediated 1,3-dipolar cycloaddition between alkynes and azides. The resulting resins exhibited improved catalytic properties over homogeneous counterparts in the direct aldol reaction in water (Scheme 4.3) [19]. Under optimal conditions, aromatic aldehydes reacted with cyclohexanone with good to excellent yield and diastereoselectivity, and with 93–97% ee for the *anti* isomer. Quite interestingly, no decrease in performance (catalytic activity or stereoselectivity) was observed after three consecutive cycles of the same reaction. Moreover samples of the resin could be repeatedly used in different aldol reactions without noticeable deterioration of catalytic properties.

The scope of applicability of catalyst **3** was later extended to enantioselective α-aminoxylation of aldehydes and ketones (Scheme 4.4) [20]. Using optimal

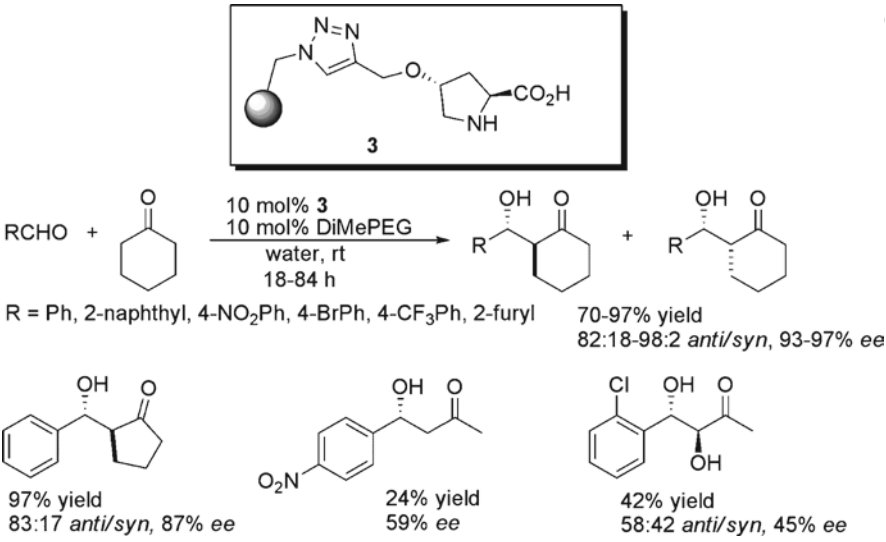

Scheme 4.3 Enantioselective direct aldol reactions in water catalyzed by resin **3**

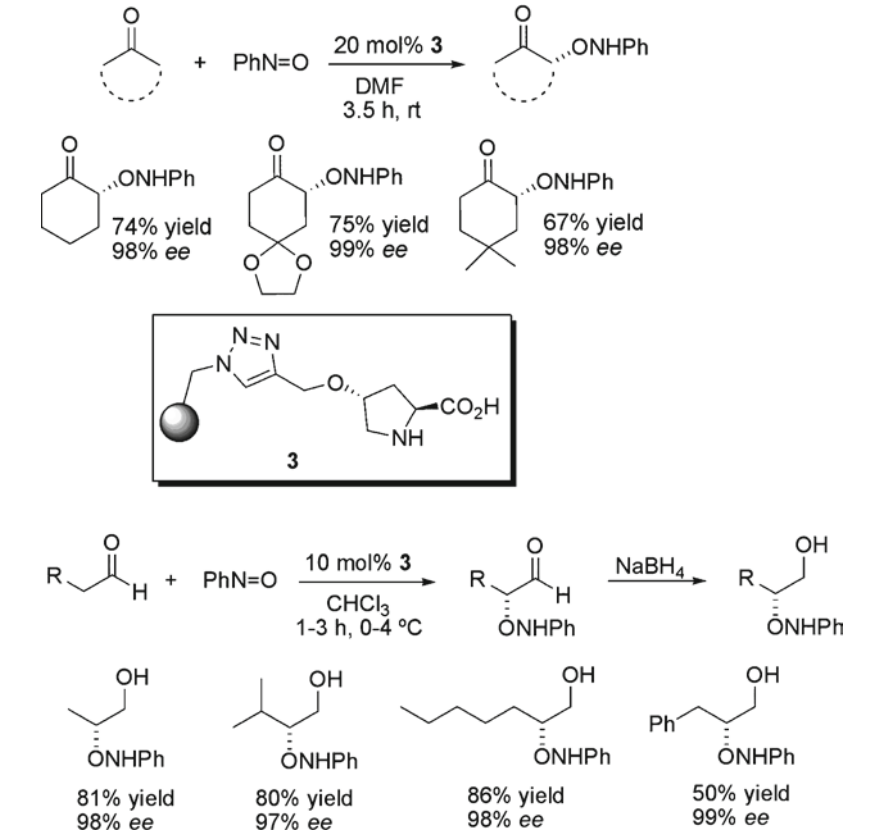

Scheme 4.4 Enantioselective α-aminoxylation of ketones and aldehydes with catalyst **3**. Some selected examples

conditions, different six-membered ring cyclic ketones reacted with nitrosobenzene affording α-aminoxylated ketones in 97–99% ee and 49–75% yield and with improved reaction rates compared to native proline. In a similar way, aldehydes were selectively converted within 1–3 h to the corresponding aminoxylated products in good yield (35–86%) and excellent ee (96–99%). The heterogeneous nature of the catalyst allowed for significantly simplified workup conditions. The product was isolated in some cases after simple filtration and solvent removal. Recycling experiments showed similar values of yield and ee for the aminoxylation of propanal after three cycles.

The role of the polymeric support has been thoroughly investigated by Pericàs' group in further studies on stereoselective reactions in water mediated by different polystyrene-supported proline resins obtained using the same click-chemistry strategy as for **3** or following a complementary approach (resin **4**) (Fig. 4.3) [21]. Grafted resin **4** exhibits an optimal catalytic performance in the aldol reaction between cyclohexanone and benzaldehyde in water (74% yield, 96:4 *anti/syn* ratio, 98% ee for the *anti* isomer, room temperature, 24 h), with a notable rate acceleration and improved stereoselectivity over those of catalyst **3**, polystyrene-supported hydroxyproline **5**, macroporous ArgoPore resin **6** and amphiphilic PS-PEG NovaBioSyn resin **7**. Remarkably, and in sharp contrast with other PS-resins, resin **4** perfectly swells in water with building of an aqueous microenvironment, and depicts characteristics targeted for an artificial aldolase. Indeed, it could be demonstrated that the small amount of water required to swell the resin is sufficient to impart optimal catalytic properties to this material. Theoretical calculations showed that the 1,2,3-triazole linker is connected with the amino and carboxy groups through a water-mediated hydrogen-bond network. It was suggested that this fact importantly contributes to the catalytic behavior of **4**, which efficiently promotes the condensation of cylohexanone or cyclopentanone with several aromatic aldehydes affording excellent yields, diastereoselectivities and enantioselectivities. Noticeably, 1 mol% of catalyst **4** is enough to induce the complete self-condensation of propanal in 24 h with 97% ee. Finally, the resin could be recycled and reused for at least five times without any appreciable loss in yield or in stereoselectivity.

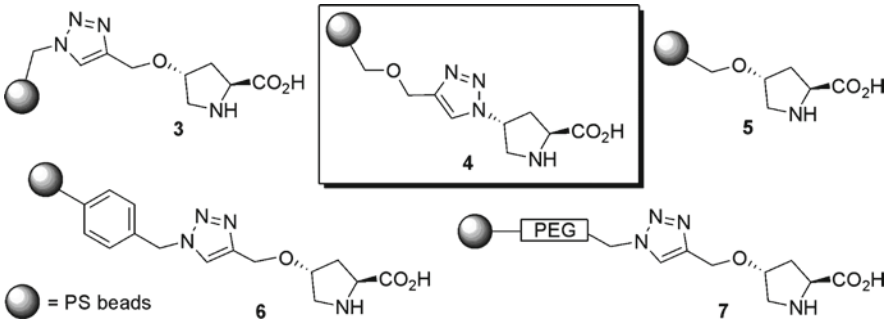

Fig. 4.3 Polymer-supported proline-derivative catalysts for enantioselective aldol reactions in water

Catalysts **3**, **4** and **5** have been also recently tested in asymmetric Mannich reaction of aldehydes with preformed *N*-(*p*-methoxyphenyl)ethyl glyoxylate imine [22]. The results replicate those recorded with the same catalyst set for aldol reactions in water, thus confirming the beneficial effect of the 1,2,3-triazole linker connecting proline with the polymeric backbone, which turns out to be crucial for catalytic activity and enantioselectivity. The more readily available resin **3** was eventually used as the catalyst in a systematic study (Scheme 4.5). Whereas complete conversion was recorded in only 1–3 h with aldehydes (45–79% yield, 88:12–97:3 *syn/anti* ratio, 96–99% ee), with ketones the reactions were slower (24–48 h). Nevertheless, they could be efficiently accelerated (3–4 h for six-membered ring cycloalkanones) by low-power microwave irradiation (40–95% yield, 87:13–97:3 *syn/anti* ratio, 76–99% ee). The robustness of the catalyst is illustrated by the results obtained in three consecutive runs with isovaleraldehyde, since the excellent stereochemical performance of resin **3** remains intact while catalytic activity shows only marginal erosion. This approach allowed to perform the reactions of aldehydes under single-pass, continuous-flow conditions. In this manner, the continuous synthesis of the enantiomerically and diastereomerically pure Mannich adducts of isovaleraldehyde and propanal (*syn/anti* > 97:3, ee > 99%) has been achieved at room temperature with residence times of 6.0 min, in a greatly simplified experimental protocol that avoids any purification step (Scheme 4.6).

Gruttadauria *et al*. described in 2007 the preparation of catalysts **8** [23] by means of a thiol-ene click-coupling procedure [24]. Proline was anchored to a polystyrene resin through a radical reaction between a styrene derivative of *trans*-*N*-Boc-4-hydroxy-L-proline and mercaptomethyl polystyrene (1% cross-linked with DVB). The aldol reaction of cyclohexanone with some aromatic aldehydes took place in water in the presence of **8** with high conversion, 96:4–92:8 *anti/syn* ratio, and 90–98% ee for the *anti* isomer.

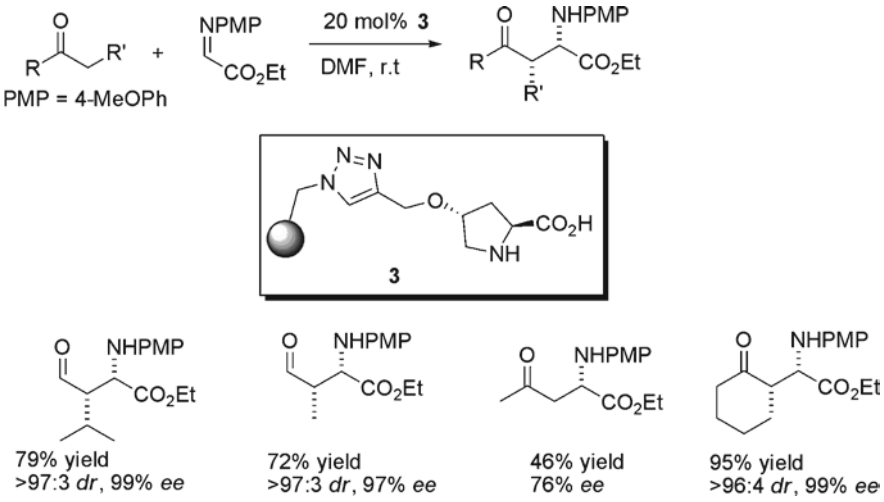

Scheme 4.5 Enantioselective Mannich reactions catalyzed by **3**

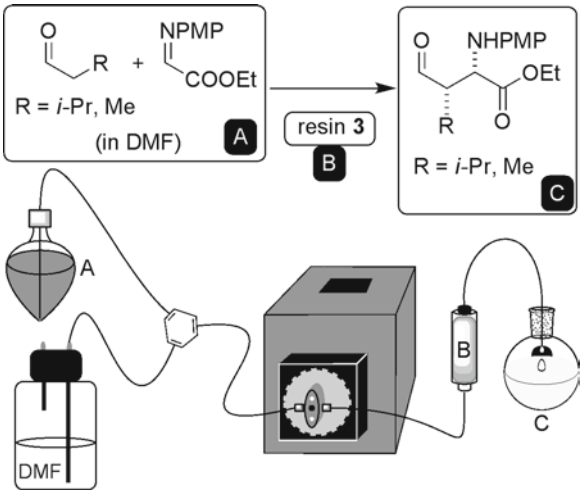

Scheme 4.6 Continuous flow production of Mannich adducts of aldehydes

In a subsequent paper, the same authors studied the effect of solvents and the scope of applicability of resin **8** in the asymmetric aldol reaction in the presence of water [25]. This catalyst performs efficiently in the standard addition of acyclic and cyclic ketones to benzaldehydes, providing the aldol products in general with high yield and excellent *anti/syn* ratios and ee values (Scheme 4.7). The resins can be recovered by simple filtration and recycled without decrease of performance after five cycles. The catalytic activity and the observed stereoselectivity has been explained in terms of the formation of a hydrophobic core in the inner surface of the resin, whereas the hydrophilic proline moiety lies at the resin/water interface.

Dendrons have been used as spacers in an elaborated approach to polymer-supported proline-based catalysts (Fig. 4.4) [26]. A family of polystyrene resins was prepared by immobilization of a hydroxyproline derivative onto dendronized polymeric supports via click-chemistry. The effect of the dendritic architecture of the spacers in the catalytic activity of the resins was evaluated in the aldol reactions of benzaldehyde and *p*-nitrobenzaldehyde with acetone. Under optimal reaction conditions, and using the most structurally complex (third generation) catalyst, it was possible to obtain the aldol product with 35% yield and 71% ee. However, the catalytic activity of the resins rapidly decreased in a second cycle in the recycling experiments performed.

The traditional approach to immobilization starting from Merrifield resins has certain limitations mainly associated with the difficulty of monitoring reactions on cross-linked supports during a multistep synthesis of the polymeric catalysts. Solid-supported organocatalysts might be efficiently prepared through copolymerization. Controlled free-radical co-polymerization of unsaturated monomers is a promising route to prepare an unlimited number of polymer compounds with highly controlled

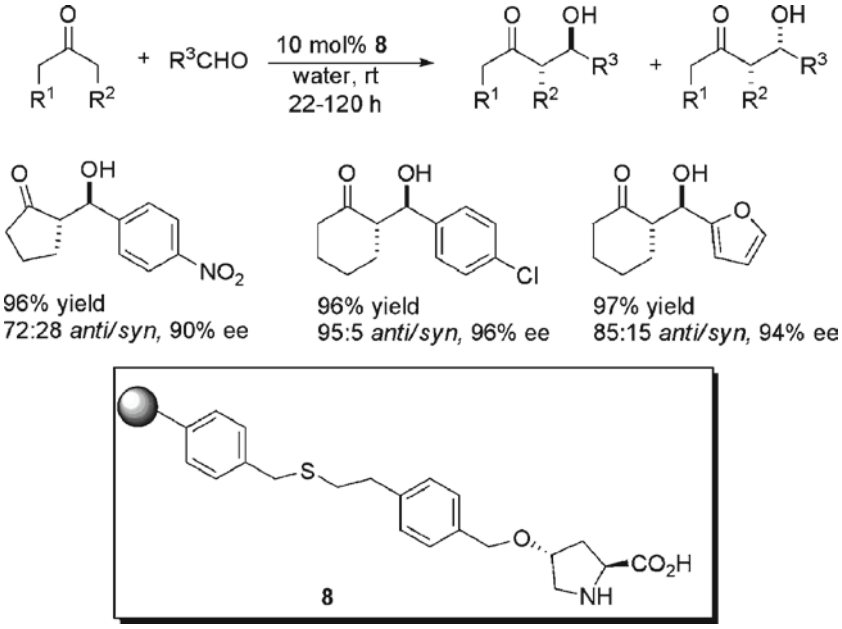

Scheme 4.7 Enantioselective direct aldol reactions in the presence of water catalyzed by **8**. Some selected examples

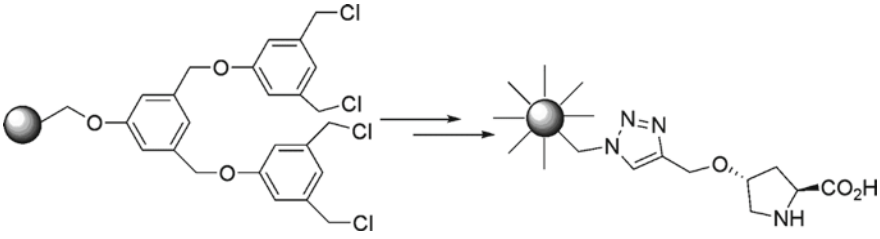

Fig. 4.4 Polymer-supported proline-decorated dendrons

microstructure by properly changing the nature and relative proportions of monomers in the reaction medium [27].

From this point of view, Hansen and coworkers have described a new and efficient approach to synthesizing acrylic polymer beads containing proline and prolinamides to be used in organocatalysis [28]. This method has given access to reusable solid-supported proline derivatives on a preparative scale (Fig. 4.5). Since it is possible to adjust the catalyst loading and structure by simply changing the ratios of the co-monomers used, this strategy opens an easy access to modular, immobilized organo-catalysts. The two-step procedure involves the synthesis of monomeric proline methacrylates from hydroxyproline followed by a free-radical copolymerization. Either suspension or dispersion copolymerized catalysts performed nicely in the aldol

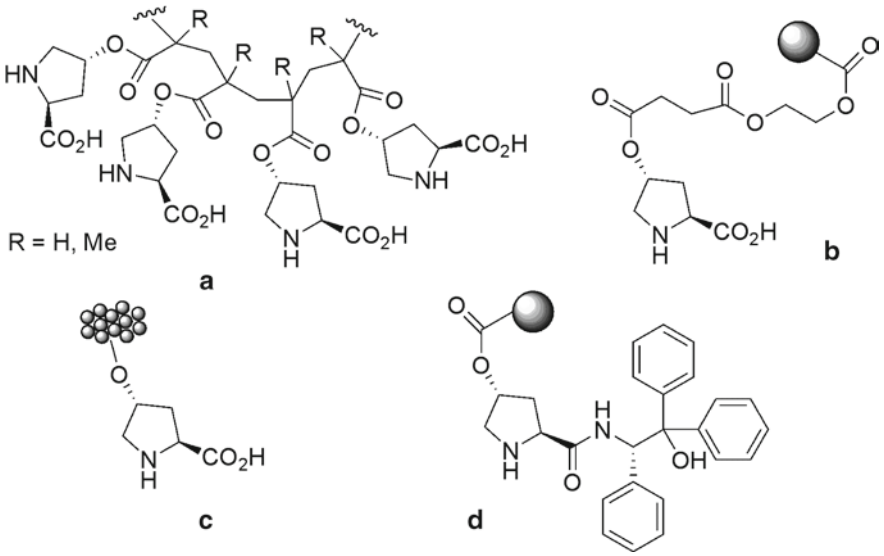

Fig. 4.5 Polymer-supported proline-derived organocatalyst prepared from acrylic polymer beads: (**a**) High-load linear proline polymers; (**b**) Polymer beads obtained by suspension copolymerization; (**c**) Agglomerated polymer microspheres by dispersion copolymerization; (**d**) Prolinamide beads

reaction of *p*-nitrobenzaldehyde with cyclohexanone, giving quantitative conversions and excellent enantioselectivities after 24 h in water.

Substituted prolinamides have attracted a considerable degree of attention over the last years due to their notable activity and stereoselectivity as bifunctional organocatalysts in many kinds of asymmetric transformations [3]. In many approaches proline is covalently supported through its carboxylate group making the choice of a suitable spacer to be essential in order to retain the activity and stereoselectivity of the immobilized catalyst. Dipeptides and tripeptides frequently have been chosen to act as spacer and both soluble and insoluble polymer-supported proline-terminated short chain peptides have been developed for enamine-mediated organocatalytic reactions [29].

Following their thiol-ene coupling method, Gruttadauria *et al*. recently reported the preparation of several polystyrene-supported prolinamide-based catalysts for the asymmetric aldol reaction (Fig. 4.6) [30]. Catalyst **9a** successfully worked in the direct aldol reaction of various aromatic aldehydes with both cyclic and acyclic ketones. In addition, it could be recovered and re-used, after regeneration with formic acid, at least for twelve cycles without loss of activity. Remarkably, under the optimal reaction conditions (1:2 (v/v) water/chloroform mixture) the aldol reactions between acetone and substituted benzaldehydes gave in general excellent yield (30–98%) and enantioselectivities (89–97%) after several cycles of recycling [30a].

Especially good results have been recorded in the catalytic enantioselective 1,4-addition of ketones to nitrostyrenes with insoluble polymer-supported pyrrolidine derivatives. In the Michael transformations mediated by 2-substituted cyclic amines (mostly pyrrolidines) the side chain of the amine is believed to act as a steric controller

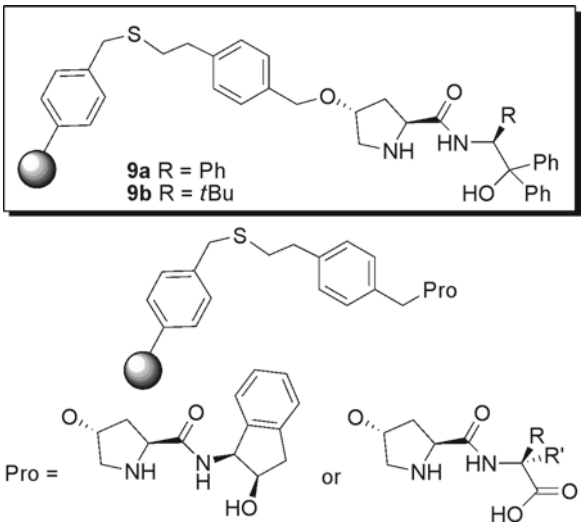

Fig. 4.6 Polystyrene-supported prolinamide-based organocatalysts tested in aldol reactions

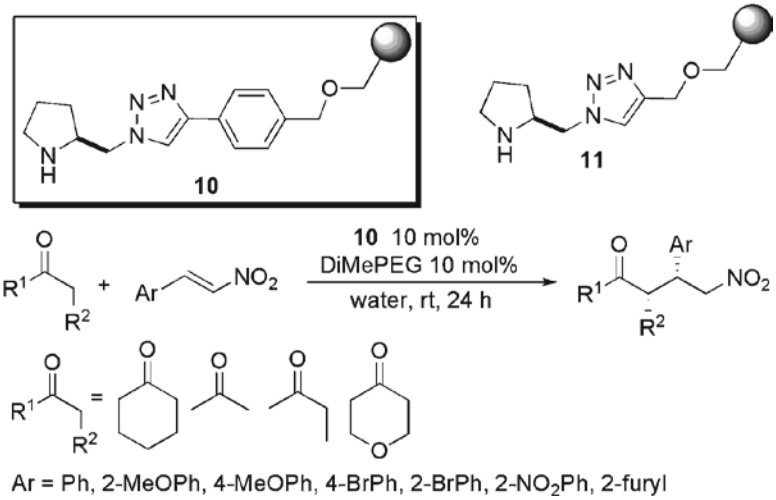

Scheme 4.8 Polystyrene-supported pyrrolidine-based organocatalysts developed for enantioselective Michael additions in water

that directs the reactivity toward the less hindered diastereotopic face of the intermediate enamine. According to this consideration, systems bearing highly nitrogen-rich substituents such as tetrazoles and 1,2,3-triazoles have shown promising activity-selectivity profiles [31]. Catalyst **10**, developed by Pericàs and coworkers, is a highly efficient polymer-supported organocatalyst for the enantioselective Michael addition of ketones to nitroolefines (Scheme 4.8) [32]. The triazole ring, constructed via 1,3-dipolar cycloaddition between an azidomethylpyrrolidine and an alkyne-functionalized resin, plays the double role of grafting the chiral pyrrolidine monomer

onto the polystyrene backbone and of providing a structural element, complementary to pyrrolidine, key to high catalytic activity and enantioselectivity. In addition, resin **10** showed optimal operation in water and full recyclability. Thus, cyclohexanone reacted with different nitrostyrene in water giving the addition products with total conversion, high yields (76–85%), excellent diastereoselectivities (90:10–99:1 *syn/anti* ratio) and enantioselectivities up to >99% ee.

The nature of the linker connecting the pyrrolidine-triazole system with the polymer backbone appears to have an important effect on the efficiency of the catalyst. In fact, polymer-supported pyrrolidine **11** was more active but less enantioselective than **10** in the studied processes, suggesting that the balance between hydrophobic and hydrophilic regions in the catalytic resins could play an important role in determining the performance of these catalysts.

The same pyrrolidine-triazole catalyst was later immobilized onto Merrifield resin 2% cross-linked with DVB following the same procedure and similarly applied in Michael additions of cyclohexanone to various nitrostyrenes [33]. The catalyst behaved similarly than the less reticulated resin **11** in terms of yield and enantioselectivity, and also as **11**, it could be recovered and recycled by a simple filtration, and re-used in several cycles without significant loss of its catalytic activity.

Among the diversity of pyrrolidines bearing a bulky C-2 substituent developed as organocatalysts for asymmetric Michael additions, α,α-disubstituted prolinols exhibit optimal performance for a variety of donors and acceptors [34]. Nevertheless, work within polymer supported silylated diarylprolinols has not been as common as with proline and prolinamides [35]. Very recently, a PS-supported version of enantiopure (*S*)-α,α-diphenylprolinol trimethylsilyl ether has been reported by the Pericàs laboratory [36]. It is worth noting that under optimal conditions resin **12** displays catalytic activity and enantioselectivity comparable to the best homogeneous catalyst in the Michael addition of aldehydes to nitroolefins. Furthermore, it represents the first example of an insoluble catalyst successfully dealing with aldehydes in water [32]. For instance, the addition of propanal to (*E*)-β-nitrostyrene took place in water with 97% conversion, 96:4 *syn/anti* ratio, and 99% ee. In addition, this catalyst exhibits unprecedented substrate selectivity that allows, in practice, inducing the completely selective reaction of a linear short-chain aldehyde in the presence of its α-branched regioisomer or a ketone (Scheme 4.9). Finally, re-conditioning of deactivated resin by a short treatment with trimethylsilyl *N*,*N*-dimethylcarbamate in order to regenerate the silyl ether, leads to complete preservation of its catalytic activity and stereoselectivity, thus allowing effective reuse over six consecutive runs.

4.2.2.3 Amphiphilic Supports

The beneficial role of water to improve the reactivity and stereoselectivity in the aldol reaction catalyzed by polymer-supported L-proline was also pointed out with the amphiphilic catalysts developed by Tao *et al*. (Scheme 4.10) [37]. In 2007, this group reported the synthesis of catalysts **13** anchoring *cis*-4-aminoproline onto linear

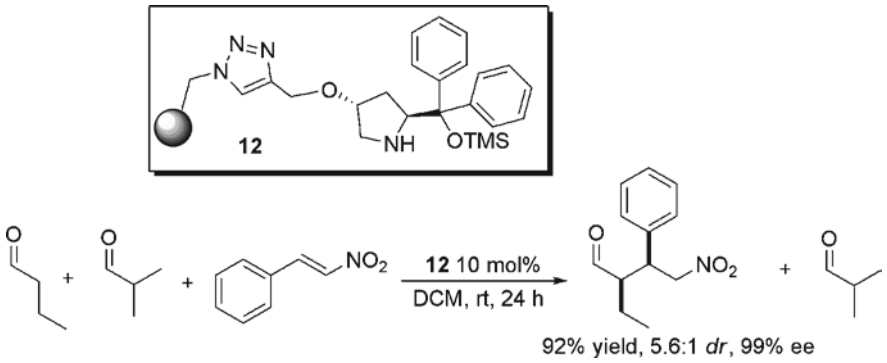

Scheme 4.9 Selective Michael addition of butanal to β-nitrostyrene in the presence of 2-methylpropanal catalyzed by polymer-supported organocatalyst **12**

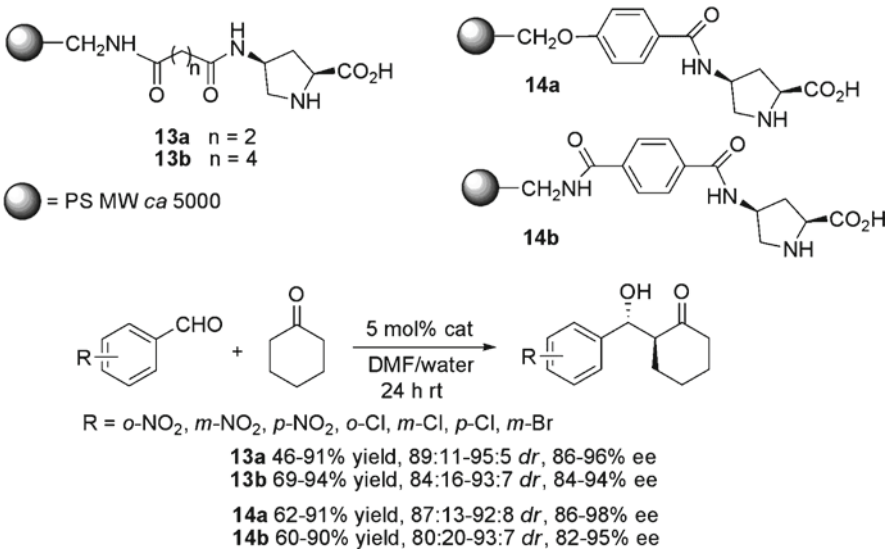

Scheme 4.10 Linear polystyrene-anchored catalysts **13** and **14** for enantioselective aldol reactions

aminomethyl polystyrene through flexible spacers. The resulting catalysts, which were soluble in the reaction medium, promoted efficiently the aldol reaction between aromatic aldehydes and ketones in wet DMF and ketone/water mixtures, and could be recovered and re-used at least four times maintaining their stereoselectivity and giving acceptable levels of yield [37a]. In a subsequent work, the same authors described the preparation of catalysts **14** by the same approach but using rigid spacers to connect the proline moiety with the polystyrene chains. Such polymers were used in the same reactions and conditions previously reported providing similar results [37b].

4.2.3 Non-covalent Immobilization of Catalytic Amines

Luo and Cheng described a new noncovalent procedure for the immobilization of chiral diamines [38]. By combining in situ PS-sulfonic resins with chiral diamines, amine catalysts supported in a noncovalent manner through acid–base interactions were developed. These catalysts, which were insoluble in most organic solvents, were used for the asymmetric direct aldol and Michael addition reactions (Fig. 4.7). The structure and the density of the sulfonic acid groups were found to have an important effect on the activity and stereoselectivity of the catalysts. Direct aldol reactions for a range of ketone donors and aromatic aldehyde acceptors were conducted in dichloromethane with 10 mol% of the heterogeneous catalyst **15**, providing in general the aldol products in high yield (72–87% for acetone, 67–99% for cyclohexanone) with good *anti* diastereoselectivity, and good to excellent ee (76–83% for acetone, 91–99% for cyclohexanone). On the other hand, Michael addition reactions of cyclohexanone to several nitrostyrenes performed well in toluene with catalyst **16** (70–97% yield, 93:7–96:4 *syn/anti* ratio, 68–90% ee). In all cases, the catalyst could be recovered by filtration, re-used several times with similar catalytic behaviour and then reactivated by an acidic washing/recharging treatment to recover its activity.

4.2.4 Imidazolidinone Derivatives

The concept of iminium ion catalysis mediated by chiral secondary amines was developed by MacMillan in 2000 [39]. Since then, constant contributions in this field allow to encompass a wide range of cycloaddition and conjugate addition

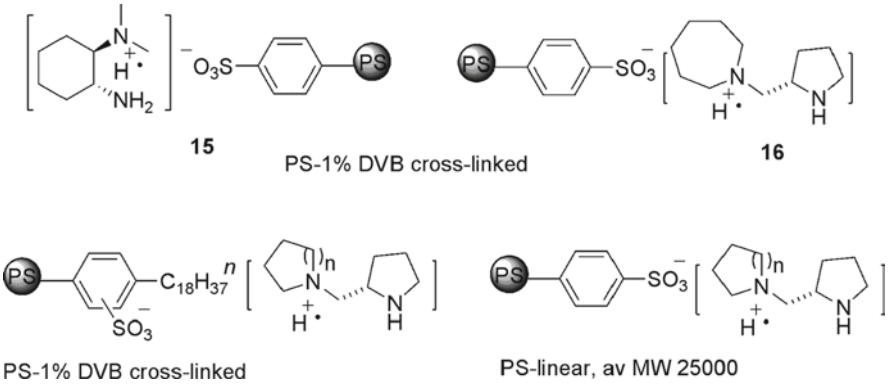

Fig. 4.7 Some examples of noncovalently supported heterogeneous chiral diamine catalysts

reactions that proceed in high yield and with exceptional levels of asymmetric induction [40]. MacMillan's imidazolidinone has been elegantly applied in a number of target processes, but in contrast to proline derivatives, catalytic transformations with supported chiral imidazolidin-4-ones are more scattered.

The first polymer-supported version of the MacMillan catalyst was described in 2002 by Benaglia and Cozzi. The soluble PEG_{5000}-supported catalyst **17** (Scheme 4.11) was prepared in the traditional way, anchoring a tyrosine-derived imidazolidin-4-one by means of a spacer to MeOPEG [41]. Different ammonium salts of **17** were tested in the enantioselective Diels–Alder cycloaddition between acrolein and 1,3-cyclohexadiene (67% yield, 94:6 *endo/exo*, 92% ee *endo*) and 2,3-dimethyl-1,3-butadiene (75% yield, 73% ee). The catalyst was recovered and reused, although chemical efficiency decreased after the second cycle.

Catalyst **17** was later employed in 1,3-dipolar cycloadditions involving acrolein or crotonaldehyde and some nitrones (Scheme 4.11) [42]. The products were obtained in enantiomeric excesses very similar to those observed with the non-supported catalyst, but in lower chemical yields. On the other hand, although the catalyst was readily recovered, it could not be efficiently recycled. Authors ascribe the observed erosion in the catalytic activity to the intrinsic instability of the catalyst under the reaction conditions.

Insoluble JandaJel™-bounded catalyst **18** (Fig. 4.8) [43] was obtained in a complementary approach from JandaJel™-NH_2 and *N*-Fmoc-protected (*S*)-phehylalanine.

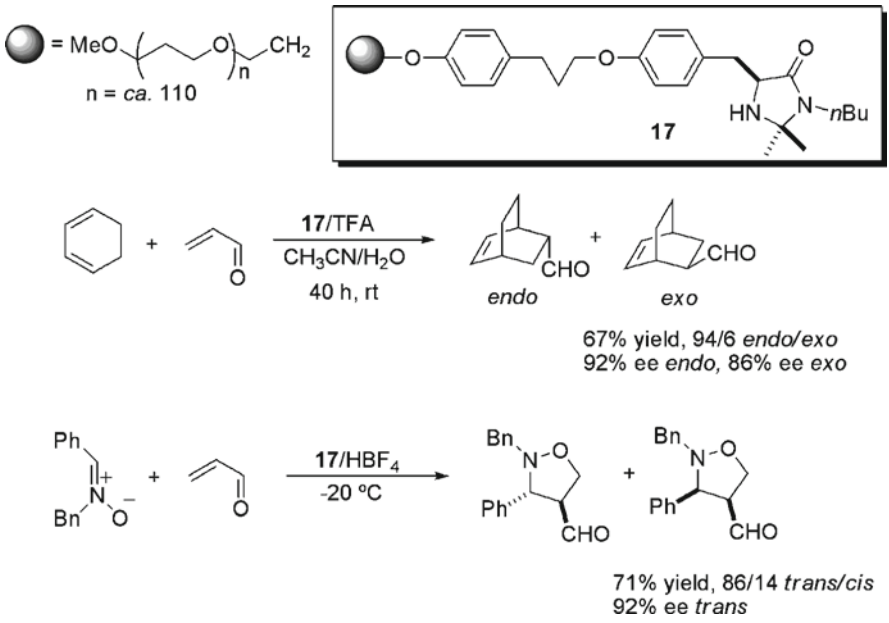

Scheme 4.11 Enantioselective Diels–Alder and 1,3-dipolar cycloadditions catalyzed by **17**

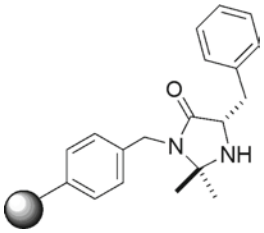

Fig. 4.8 Insoluble JandaJel™-bounded catalyst **18**

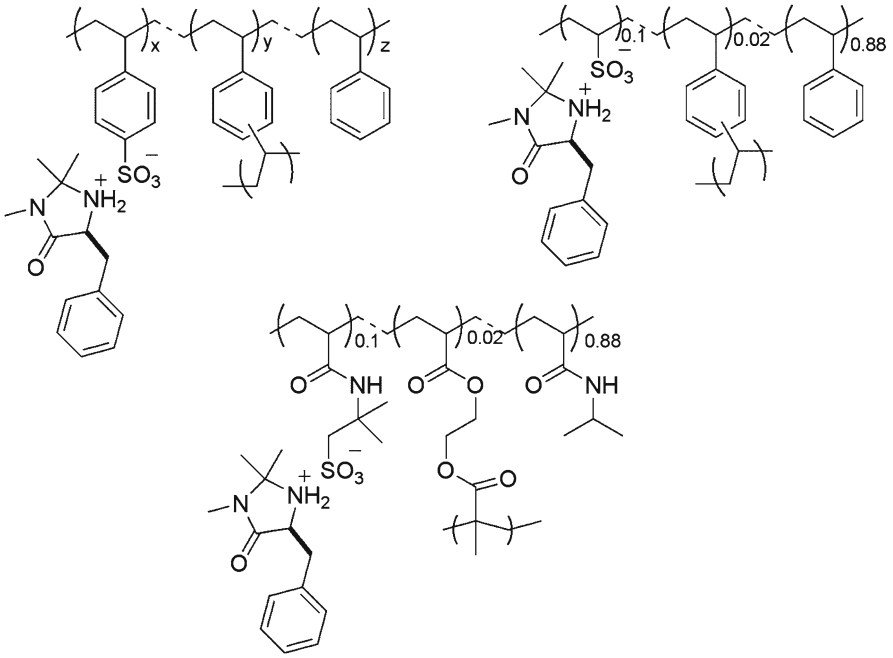

Fig. 4.9 Polymer-supported MacMillan's catalysts obtained via ion exchange reaction

Using cyclopentadiene as diene, the Diels–Alder adducts of different α,β-insaturated aldehydes were obtained in good yield (60–73%), excellent enantioselectivity (83–99%) and with variable *endo/exo* selectivity (1:1.2–5.1:1). These values are comparable to those obtained with the corresponding solution phase catalysts [39]. Furthermore, the catalyst was easy to recover and reuse.

A noncovalent strategy for the immobilization of MacMillan type catalysts has been recently reported by Haraguchi and coworkers [44]. The polymer-supported organocatalyst was obtained via ion exchange reaction of MacMillan's iminium catalyst with polymer-based sulfonic acids prepared by copolymerization (Fig. 4.9). The resulting polymeric catalyst was effective for Diels–Alder reaction of

1,3-cyclopentadiene and *trans*-cinnamaldehyde (methanol/water, 10 mol% catalyst loading, room temperature), affording quantitative conversion, good enantioselectivity and showing high reusability.

4.3 Asymmetric Metal Catalysis on Polymeric Supports

Homogeneous metal complexes are widespread in catalysis because their catalytic properties can be fine-tuned by modifying the stereoelectronics of the ligands around the metal centre. Many powerful and selective asymmetric catalysts have been discovered in this way [45]. However, metal salts are expensive, and sometimes the organic ligands can be even more costly. Moreover, regulations in pharmaceuticals and food additives (some of the main industrial users of homogeneous catalysts) require only trace amounts of metal impurities, which could be highly toxic contaminants otherwise. Therefore, supporting metal catalysts in order to make their recovery and reuse easy, as well as to avoid contamination of the catalyst into the final product, is a real demand [1, 2]. Finally it is currently possible to develop flow methods using polymer-supported asymmetric catalysts, which permits the continuous production of enantioenriched chemicals.

4.3.1 Immobilization Strategies

There are three general classes of polymer-immobilized asymmetric metal complexes [46, 47]. They are shown schematically in Fig. 4.10.

Type 1. Grafted Polymers Formed by a polymeric backbone with pendant ligands where the metal salt is coordinated. This is the classical and most common approach, which implies functionalization of a pre-existing polymer.

Type 2. Copolymers Obtained by copolymerization of a ligand with other monomers. The metal will be bound afterwards. Although the preparation of the functional polymer is quite different from Type 1, the resulting material is very similar in practice.

Type 3. Self-supported Catalysts A polymeric network of metal complexes, usually through coordination and self-assembly, is formed. The metal-organic framework thus contains the metal centres and the stereochemical information needed for the catalytic reaction.

Next, we will briefly give particular examples of all three types of supported catalysts for illustration. Several types of asymmetric reduction of ketones have been chosen as leitmotiv due to the availability of examples.

Lemaire and coworkers immobilized a BINAP derivative into a polymer by using a bis-urea linker. This polymer was successfully used in the asymmetric hydrogenation of acetylacetates under 40 atm of hydrogen and a substrate/catalyst ratio of 1,000/1, achieving 99% ee. This supported catalyst was recycled three times without

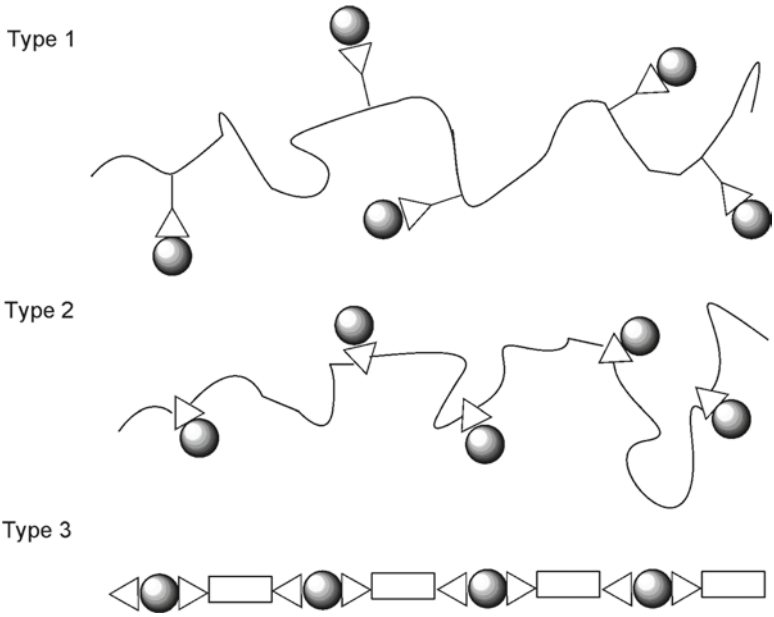

Fig. 4.10 Types of polymer-immobilized asymmetric catalysts. *Triangle*: ligand; *shaded circle*: metal

changes in its performance (Scheme 4.12, top) [48]. Another example includes a TsDPEN derivative grafted on polystyrene. This material was developed by Wang *et al.* who showed that the ruthenium-catalyzed hydrogen transfer reaction of 2-cyanoacetophenone proceeded in 98% yield and 97% ee using formic acid/triethylamine as reducing agent (Scheme 4.12, bottom) [49]. Both polymers are examples of the first type of immobilized catalyst (Type 1).

An example of Type 2 immobilized catalyst is discussed next. A TsDPEN monomer was copolymerized with a *p*-vinylbenzene sulfonate and a cross-linker by Itsuno *et al.* The resulting polymers were tested in the asymmetric reduction of acetophenone with sodium formate in water. The sulfonate groups allowed the resin to swell in water, and therefore were key to its efficiency. The ammonium counterion also showed influence in the reaction outcome. The optimal catalyst, which achieved full conversion and 98% ee, is depicted in Scheme 4.13 [50].

Finally, as an example of self-supported catalyst (Type 3), the work by Ding and coworkers will be briefly discussed. A bis(diphosphine) and a bis(diamine) were heated in the presence of a ruthenium salt to yield the polymeric material shown in Scheme 4.13. Analyses showed that the material was formed by non-crystalline, micrometer size particles, which were insoluble in the reaction mixture. Indeed, the set of ketones tested was hydrogenated in full conversion and with an enantioselectivity in the range 95–97% ee, and the catalyst could be filtered off and reused without loss of activity or enantioselectivity for more than five cycles (Scheme 4.14) [51, 52].

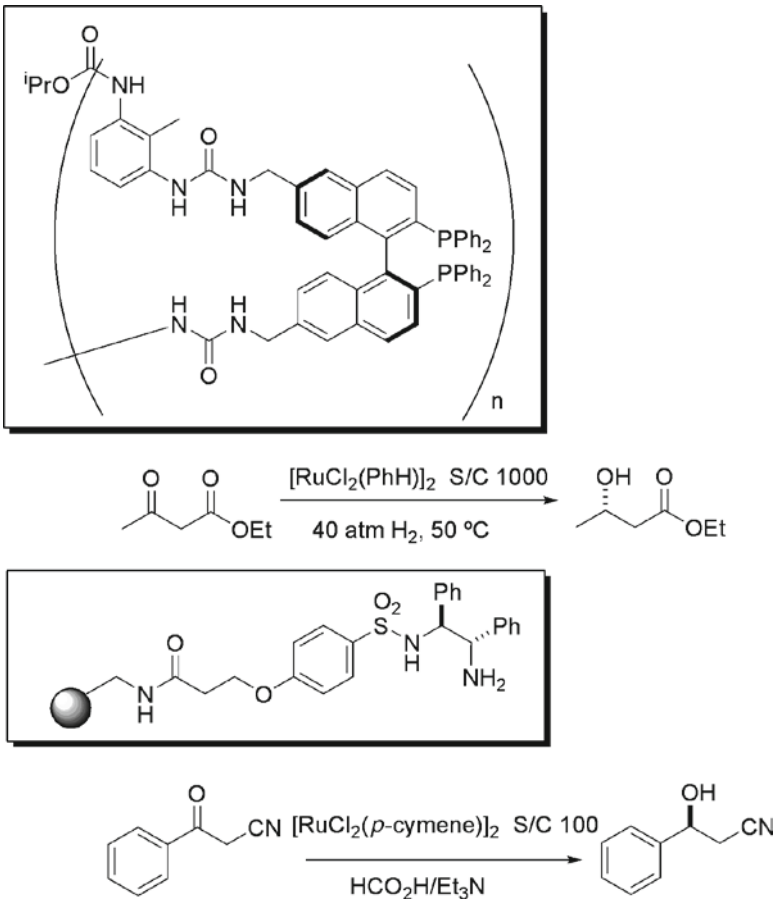

Scheme 4.12 Grafted polymers for asymmetric reduction of ketones

At this point, it must be noted that the catalytic systems presented above have efficiencies totally comparable with that of Noyori's homogeneous catalyst, with the advantage of recyclability.

In the following sections we will limit mostly (but not always) to polymer-supported asymmetric complexes (grafted polymers) since the chemical literature is full of examples for many different reactions. These immobilized catalysts are readily available, since they can be prepared from commercial resins and polymers. Furthermore, it is in principle easier to translate the properties of a homogeneous catalyst into a grafted polymer by optimizing a few key points, such as the nature of the polymer backbone, the nature of potential linkers connecting the ligand with the polymer, and the structural modifications introduced in the ligand molecule to allow covalent supporting onto the resin.

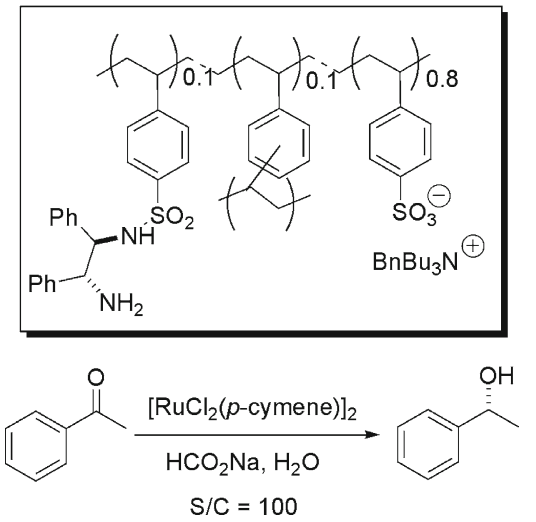

Scheme 4.13 Co-polymerized ligand for the asymmetric reduction of ketones

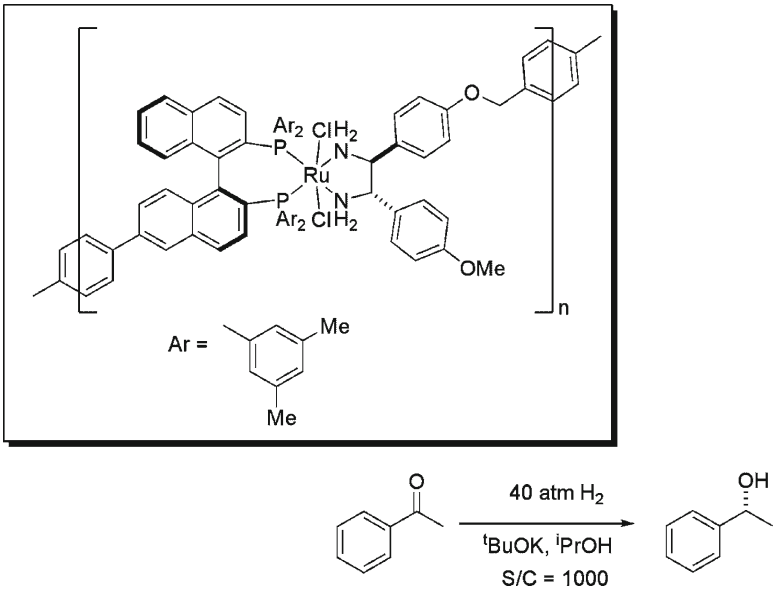

Scheme 4.14 Self-supported catalyst for the asymmetric reduction of ketones

4.3.2 Effect of the Polymer Backbone on Catalytic Performance

The polymer backbone is in direct contact with the solvent and reaction environment. This interaction must allow the diffusion of reagents into the active sites, and products out into the bulk solution. Therefore the polymer backbone not only

immobilizes the catalyst for recycling, but also controls the mass transport in the catalytic reaction.

Both *soluble and insoluble polymers* can be used. Soluble polymers facilitate diffusion, but are slightly more difficult to separate from the reaction mixture (typically a precipitation step is needed before filtration). On the other hand, insoluble resins can be separated by simple filtration, and are better suited to develop flow methods thanks to their higher rigidity. In this case, swelling is the essential property to allow diffusion of the reactants and products. This means that a previous, in situ conditioning of the polymer into the suitable solvent (both for swelling and for the reaction) is necessary. Typically, low cross-linked polystyrene (1–2% divinylbenzene-DVB) has a microporous structure and enough flexibility as to allow swelling. These polymers are also known as gel-type resins. Merrifield resins, originally developed for solid-phase peptide synthesis, are still likely the most popular insoluble resins of this type. Their major drawback is that they usually do not swell in protic solvents such as water or alcohols, and thus reactions in these media cannot be conducted efficiently. Amphiphilic polystyrene-poly(ethyleneglycol) resins (PS-PEG) have been introduced to solve these problems.

Highly cross-linked polystyrene (>5% DVB) forms macroporous, rigid resins with a permanent pore structure that do not swell. Reagents simply diffuse into the pores, and thus a wider variety of solvents can be used. Unfortunately, these materials suffer from lower reactivity, and brittleness.

4.3.2.1 Steric Effects Exerted by the Polymer Backbone

A clear example of the steric effect of the polymer on the reaction outcome is shown below (Scheme 4.15). Polystyrene resins with identical cross-linking degree but with different functionalization types were used to support an amino alcohol ligand for the

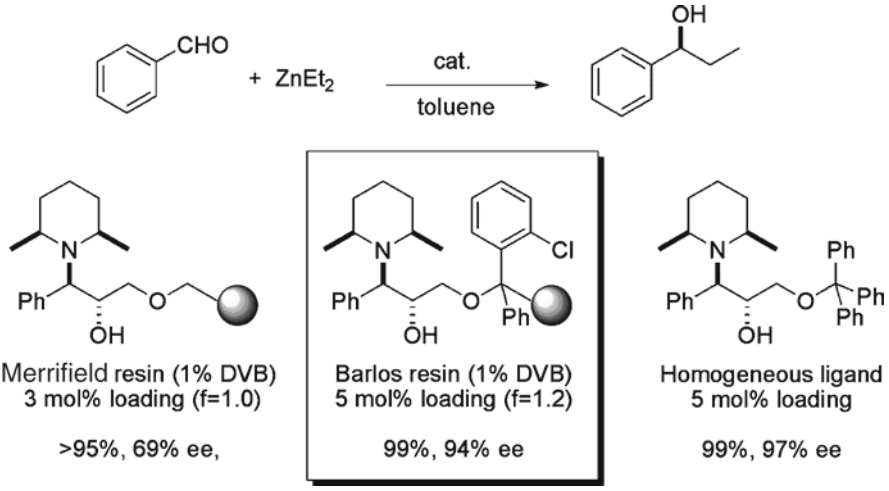

Scheme 4.15 Effect of Merrifield vs. Barlos resins on the asymmetric diethylzinc addition to aldehydes

asymmetric diethylzinc addition to aldehydes. The chloromethyl moiety of the Merrifield resin compares poorly with the 2-chlorotritylchloride group in the Barlos resin [53]. This makes sense once it is known that the trityl group in the homogeneous ligand is essential to achieve high rates and enantioselectivities [54]. It could be argued that the polymeric backbone is itself a sterically demanding group, however it turns out that a fine tuning of the structural requirements of the anchoring moiety to match the optimal ligand is needed, and achieved by using a Barlos resin. It must be noted that this situation is commonly solved by testing different linkers which are usually much easier to modify than the polymeric backbone.

4.3.2.2 Grafting vs. Copolymerization vs. Self-supporting

A less precise type of steric interactions that can be the key for a high catalytic activity involves the whole polymeric material and the method employed to prepare it. The three general types of polymeric catalysts shown above (Section 4.3.1) can have, and usually have, completely different properties (catalytic activity, enantioselectivity, rate, etc.) even though the same metal complex is present in the material. These differences are attributed to diffuse steric hindrance, different pore sizes, and in general, to the ease of access (or lack thereof) to the catalytic site, which might vary enormously depending on the structure of the polymer.

This section will be illustrated by analyzing immobilized Jacobsen catalysts for the asymmetric epoxidation of unfunctionalized olefins. Besides the possibility of recycling, supporting salen complexes on polymeric materials is the easiest route to achieve site isolation, and therefore to avoid some of the typical problems of salen-based homogeneous catalysts such as degradation by oxidation. However, as we will see below, both activity and enantioselectivity of these otherwise identical supported complexes is highly dependent on the polymeric support. For best comparison, only examples of catalysts fully resembling the Jacobsen catalyst **19** (Fig. 4.11) will be shown: those containing a cyclohexanediamine unit and 2-*tert*-butyl-1-phenol salicylaldehydes (Fig. 4.12).

Salvadori *et al*. prepared several chiral salen–manganese complexes containing vinyl units and co-polymerized them with styrene and divinylbenzene. It was necessary to use a long chain vinyl linker in the manganese complex, but still the highly cross-linked polymer **20** was not very efficient as asymmetric catalyst neither for the epoxidation of *cis* olefins nor trisubstituted alkenes (see Table 4.1, entries 1 vs. 2, and 4 vs. 5) [55].

In view of these results, Sherrington identified the key points to develop and efficient, highly enantioselctive version of Jacobsen catalyst: (1) The local structure of

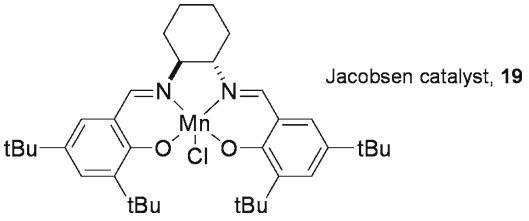

Fig. 4.11 Jacobsen salen–manganese epoxidation catalyst

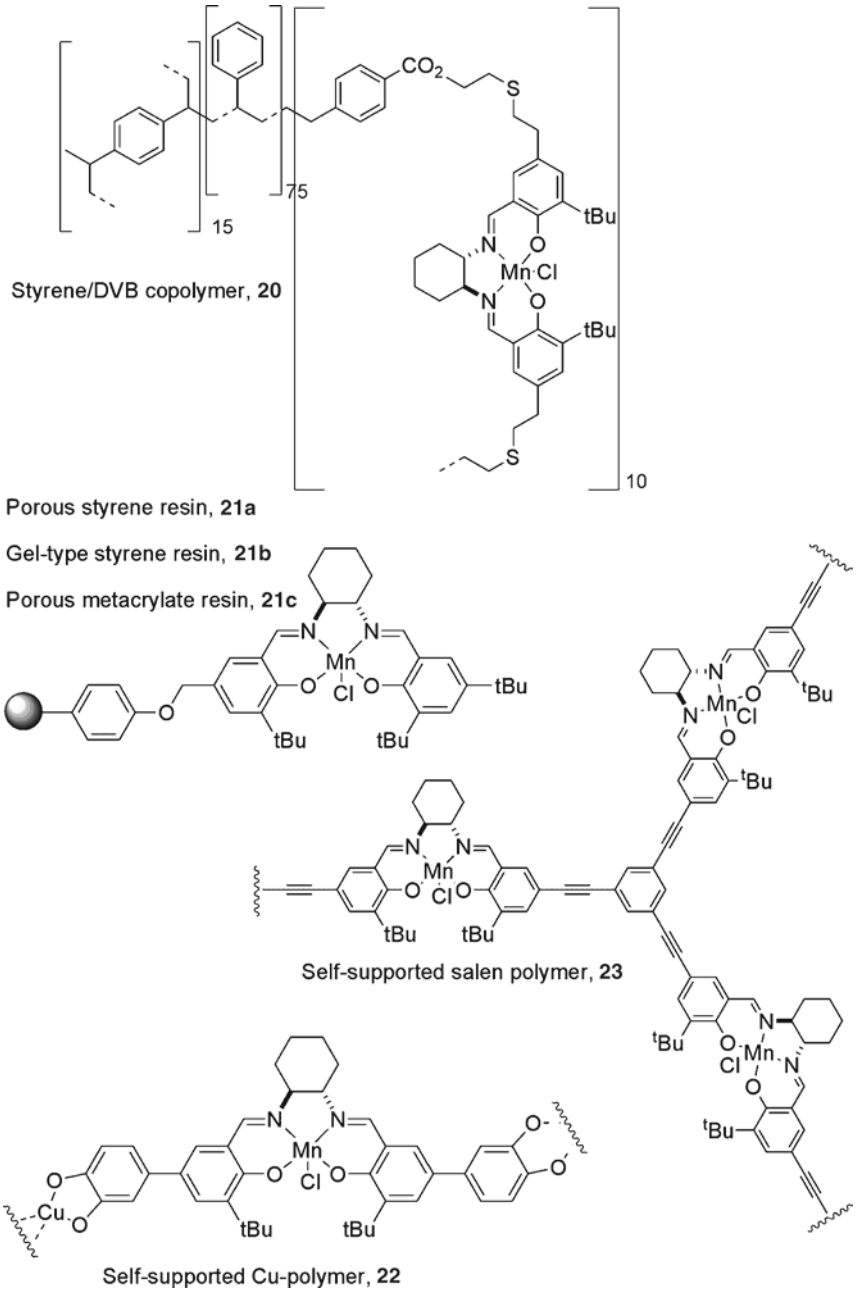

Fig. 4.12 Supported Jacobsen epoxidation catalysts

Table 4.1 Epoxidation of olefins with supported salen–Mn complexes

Entry	Substrate	Catalyst	Conditions	Yield (%)	ee (%)
1	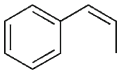	**19**	NaOCl	–	90
2		**20**	MCPBA/NMO	97[a]	62[b]
3		**23**	MCPBA/NMO	56[c]	46[d]
4	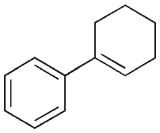	**19**	MCPBA/NMO	72	92
5		**20**	MCPBA/NMO	25	38
6		**21a**	MCPBA/NMO	36	61
7		**21b**	MCPBA/NMO	47	66
8		**21c**	MCPBA/NMO	49	91
9	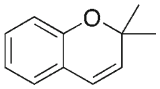	**19**	NaOCl	–	97
10		**22**	2-(*t*-BuSO$_2$)C$_6$H$_4$IO	79	76

[a] *cis/trans* 85/15
[b] ee of the *cis* isomer
[c] *cis/trans* 86/14
[d] ee of the *cis* isomer

the Mn complex should mimic precisely that of Jacobsen's optimal catalyst. (2) The complex should be attached through a single flexible linkage to the polymer to minimize local steric hindrance. (3) Low catalyst loading should guarantee site isolation, hence minimizing deactivation pathways. (4) The morphology of the support should not create mass transfer limitations, leaving active sites freely accessible. After studying several polymers grafted with Mn complexes, they found that a porous methacrylate resin **21c** afforded enantioselectivities comparable to those achieved with the homogeneous Jacobsen catalyst **19**, although in lower yields [56]. A detailed comparison can be found in Table 4.1, entries 4–8.

Self-supported Jacobsen catalysts have not proven until now more efficient. For example, a Cu linked polymer of salen–Mn complexes, **22**, achieved a reasonable yield and ee in the epoxidation of 2,2-dimethyl-2-*H*-chromene (Table 4.1, entries 9–10) [57], but the higher cross-linked self-supported catalyst **23** behaved poorly (entries 1 vs. 3) [58]. These examples tell in favour of the importance of diminished steric hindrance in the vicinity of the active site to mimic the original homogeneous catalyst, and to avoid diffusion or mass transfer restrictions.

4.3.2.3 Influence of Resin Swellability

When a polymer swells in contact with a liquid, the molecules of liquid interpenetrate the polymeric chains, and expand the structure of the resin. This means that the interactions of the material with the liquid are stronger than with itself. This also means that molecules dissolved in that liquid will diffuse better into the polymeric structure,

and that a ligand anchored on that polymer will be in a solution-like environment, with more degrees of freedom. Hence this seems the ideal situation for the development of a supported catalyst starting from a homogeneous one.

A clear example is shown next. When working in palladium-catalyzed asymmetric allylic substitutions, two research groups independently reached the same conclusions on the polymer backbone requirements. Song, Han, *et al*. developed a supported version of Trost catalyst by using a pyrrolidino moiety instead of the typical cyclohexane. The JandaJel version **25b** was clearly more effective than the polystyrene-based one (Scheme 4.16). The authors stated: The JandaJel resin is a

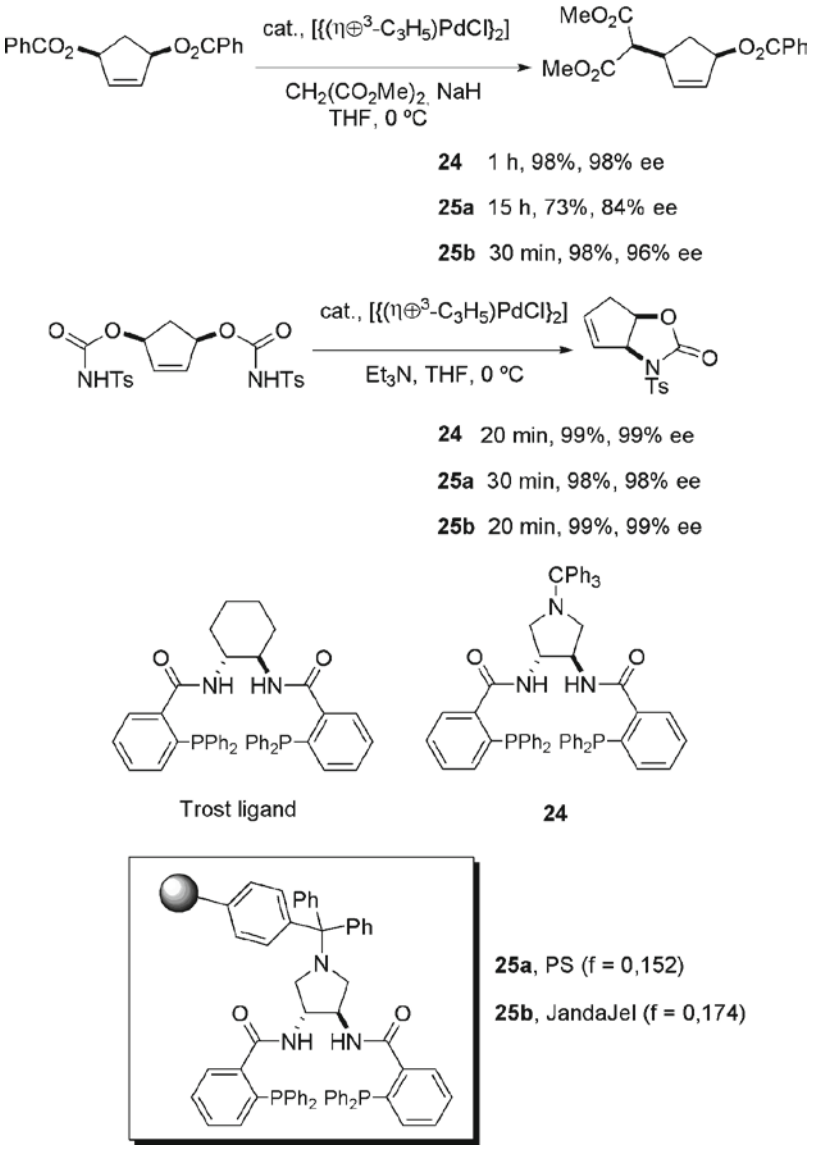

Scheme 4.16 Supported Trost ligands for allylic substitution

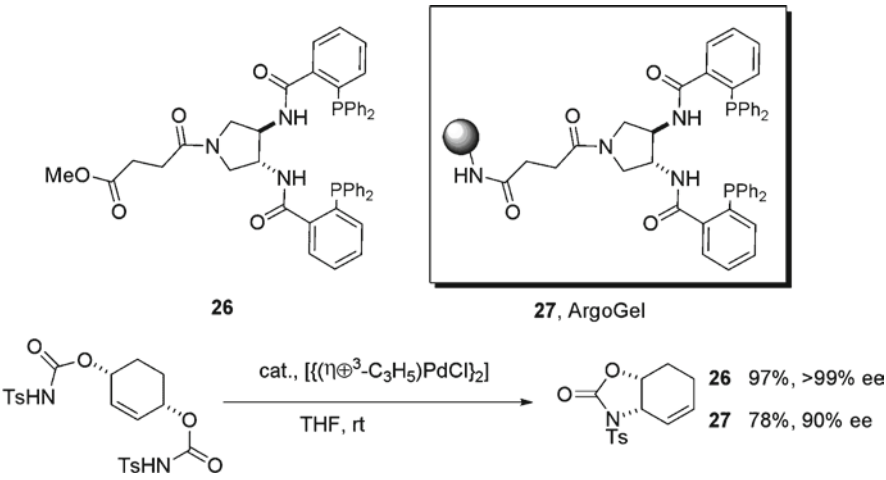

Scheme 4.17 ArgoGel supported Trost ligand for Pd catalyzed allylic substitution

polystyrene resin containing flexible tetrahydrofuran-derived cross-linkers, and is is therefore reported to swell much better than the Merrifield resin. This characteristic of the JandaJel support is envisaged to give the bulky ligand greater degrees of freedom and, as a result, to act more like a homogeneous catalyst [59]. Shortly afterwards, the Trost group published a similar approach (Scheme 4.17). In this case, an ArgoGel resin (PS-PEG) **27** was key for the success. These authors concluded: The more solution-like environment of the ArgoGel resins make them more efficacious than the other polymeric supports such as the Merrifield or ArgoPore resins. Nevertheless, the choice of the scaffold and the bond tethering is critical. While reactivities were normally not an issue, the impact of the solid support on enantiomeric excess was significant [60].

Both supported catalysts were successfully recycled for several cycles without loss of activity or enantioselectivity.

4.3.3 Influence of the Linker and of the Linking Point on the Ligand Molecule

Besides the polymeric material chosen to act as support for a particular catalyst, the way this catalyst is anchored can have a profound impact on its performance. Indeed, it is quite common to do a straight selection of a polymeric support compatible with the reaction conditions used (solvent and temperature) to facilitate swelling or solubility, or to ensure that its mechanical properties will remain stable. Then, the linker and the anchoring point of the catalyst are optimized against a model reaction.

For example, the Pericàs research group developed a simple yet highly efficient β-amino alcohol for the asymmetric addition of alkylzincs to aldehydes [61]. When attention was paid to the immobilization of such ligand on a polymeric support, several possibilities arose. The leading idea was to keep untouched the catalytic properties of the homogeneous ligand. To do so, several *tail-tied* ligands were developed. This is, ligands that could be anchored to a polystyrene resin by a position far away from the catalytic centre in a manner that their catalytic properties remained the same as the free ligand. This idea is shown in Scheme 4.18.

The highly efficient homogeneous ligand **28** was initially supported through a modified aromatic ring. Polymer **29** was highly active and enantioselective, but its synthesis was lengthy [62]. Therefore, a simplified version was developed by attaching the ligand through the piperidino group (by using piperazine) [63]. Indeed the resulting polystyrene supported ligand, **30**, was highly active as well. In view of its ready availability and high catalytic activity, **30** has been employed in a flow process

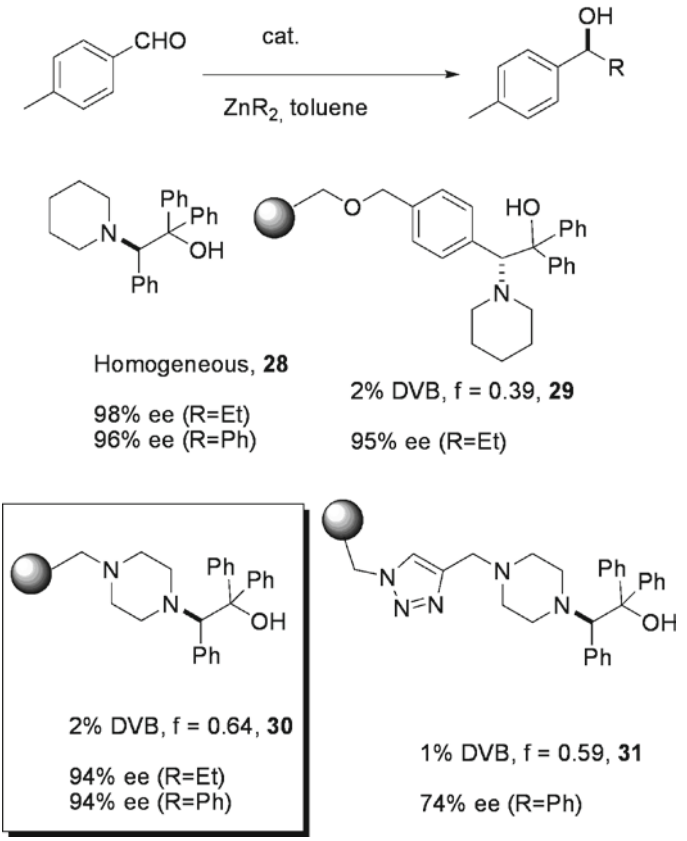

Scheme 4.18 Tail-tied ligands for the asymmetric alkylation of aldehydes

for the asymmetric alkylation of aldehydes: benzaldehyde was ethylated with full conversion and 93% ee using a flow of 0.24 ml min^{-1}. The catalytic resin is so active that a residence time of less than 10 min was enough to complete the reaction [64]. A silica-supported version was developed too, but poorer results were obtained [65].

A different anchoring strategy was attempted later. A propargyl derivatized ligand was clicked with an azido substituted Merrifield resin to yield catalyst **31**, following the strategy that had been so successful for anchoring organocatalysts [19–22, 32, 36]. Unfortunately, arylations of aldehydes using organozinc reagents gave poor results. Diminished ee's were attributed to the participation of the triazole moiety in non-asymmetric catalytic pathways. The triazole can coordinate zinc to form active complexes that deliver the aryl group to the aldehyde without any selectivity [66].

Another interesting example of the effect of the anchoring point of the ligand is found in the asymmetric cyclopropanation of olefins. Initial attempts to mimic bis(oxazoline) **32** led to the polymerization of a disubstituted styrene derivative, **33**. However, as shown in Table 4.2, neither the isomer ratios nor the ee's resembled the ones of the original catalyst [67]. Based on this results, Salvadori *et al*. realized that the general lack of efficiency of supported bis(oxazolines) in this reaction could be simply due to the failure to replicate the homogeneous ligand structure. Therefore, they prepared a highly cross-linked polymer, **34**, where the bis(oxazoline) contained a fragment mimicking the key dimethylmethylene unit bridging the two oxazoline groups. Furthermore, the linker placed the ligand at a reasonable distance from the polymer backbone in order to avoid undesired steric hindrance. This material was effectively acting as an asymmetric catalyst for the cyclopropanation of styrene, with nearly equal performance as the homogeneous parent ligand (Table 4.2) [68].

Aza bis(oxazoline) **35** (Fig. 4.13) is also a good ligand for the same reaction, and a very interesting starting point for the immobilization on a polymer. It was anchored into a Tentagel resin (PS-PEG) using a carboxylate linker (**36**), and directly grafted onto a Merrifield resin (**37a**). Another version of this catalyst was made by copolymerization of a monomer with styrene/divinylbenbeze (**37b**). When tested in the benchmark reaction, the PS-PEG catalyst showed a poor performance in all aspects, as the copolymerized resin **37b** also did. However, even though the reaction was considerably slower, grafted resin **37a** gave excellent stereochemical results, very close to those obtained with the free ligand (Table 4.2) [69].

Table 4.2 Epoxidation of olefins with supported salen–Mn complexes

Catalyst	Yield (%)	Time (h)	*Trans/cis*	ee (%)
32	61	3	71/29	94/92
33	51	24	35/65	75/72
34	60	3	67/33	93/90
35	82	8	73/27	92[a]
36	35	48	64/36	47[a]
37a	28	96	70/30	88[a]
37b	28	96	67/33	58[a]

[a]ee of the *trans* isomer

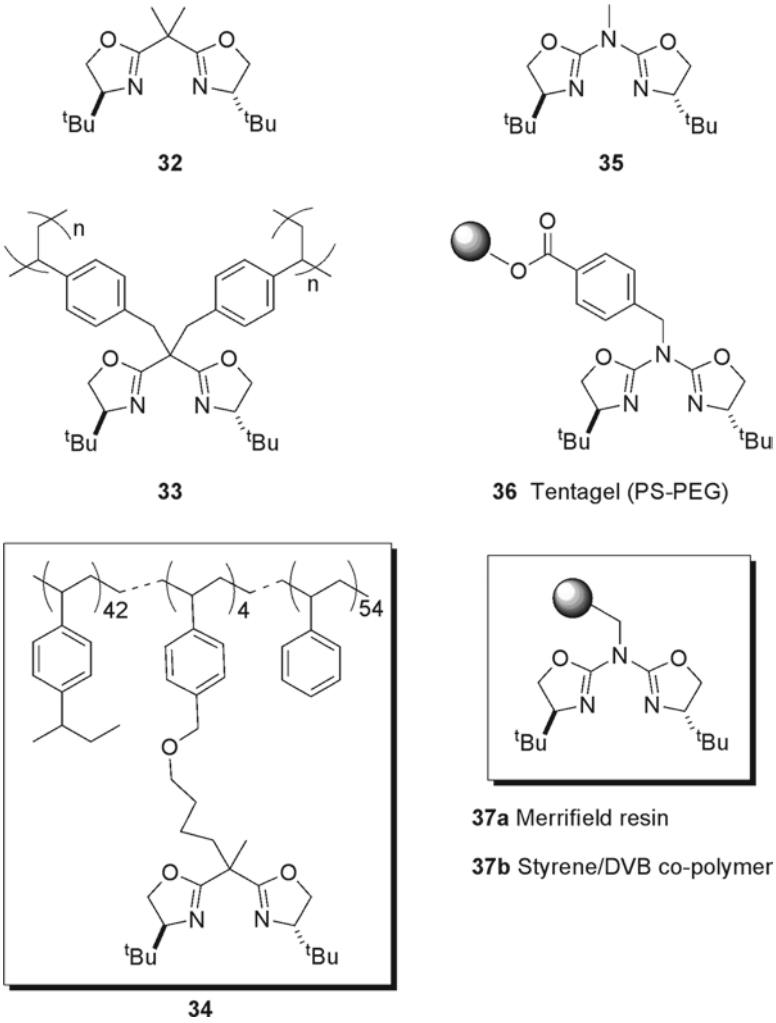

Fig. 4.13 Supported catalysts for the asymmetric cyclopropanation of olefins

4.3.4 Miscellaneous Performance Enhancing Effects

The usual approach to supported ligands and metal complexes is based on designs looking for maximal similarity between the homogeneous and the supported species, with the hypothesis that this will lead to close similarity between the activity and stereoselectivity of the two species. As we have seen, this is not always an easy task, and many parameters (polymer backbone, linker, structural modifications of

the ligand) must be taken into account. Indeed they are all important to achieve an efficient supported catalyst that can be eventually separated from the reaction media and recycled. Sometimes, however, the immobilized catalyst has new properties that make it very different from the homogeneous, free catalyst. These properties might be designed on purpose or appear serendipitously, but in any case, they offer new opportunities for catalysis.

Uozumi *et al*. have investigated for years the use of supported chiral palladium complexes for asymmetric allylic substitution. They found that biphenyl based phosphine–palladium complexes could be effectively supported and stabilized on PS-PEG polymers. It is interesting to note how catalyst **38** can perform an asymmetric reduction in organic media, and the closely related polymer **39** an asymmetric allylic alkylation *in water*. The possibility of this catalyst to operate in water is totally attributed to the effect of the polymeric backbone, which overcomes the hydrophobic interactions of the binaphtyl ligand (Scheme 4.19) [70].

The same research group has developed other supported chiral phosphines able to operate *in water*. These catalysts turn out to be extremely efficient in a large variety of palladium catalyzed reactions (Scheme 4.20) [71]. Indeed, the combination of water and the PS-PEG supported catalyst turned out to be essential: in the allylic amination of 2-cycloheptenol methylcarbonate, the product was isolated in 91% yield and 98% ee in water, whereas no reaction took place in dichloromethane. Furthermore, and homogeneous ligand operating in CH_2Cl_2 gave the expected product in only 6%, and 85% ee. The authors suggested that the hydrophobic organic substrates must diffuse into the polymer matrix thanks to water, and therefore a highly concentrated organic phase is reacting fast and efficiently [72].

An example where the supported ligand is more enantioselective than the homogeneous one will be discussed too. In another study on palladium-catalyzed asymmetric allylic substitutions, Ding *et al*. prepared a diphosphine with a cyclobutane backbone supported on PEG. In the allylic amination reaction, this catalyst was clearly more enantioselective than its unsupported counterpart. The reasons for this synergistic effect between the polymer and the ligand remained unexplained (Scheme 4.21) [73].

A continuous flow allylic amination was developed very recently by Pericàs, Vidal-Ferran, and coworkers. A phosphinooxazoline ligand was anchored to an azide substituted Merrifield resin *via* click chemistry. After loading with palladium, the system was optimized for the test reaction using microwaves irradiation. Noticeably, only 1 W power was needed to reach significant levels of conversion. The effect of the microwaves on the reaction outcome could not be explained satisfactorily, since the low power used was insufficient to produce any macroscopic thermal effect. Under continuous flow conditions, conversion decreased slowly with time (from a maximum of 86%). However enantioselectivity was kept constant, and even increased slightly with time, from 81% to 86% ee. Using a flow rate of 0.12 ml min^{-1}, the system achieved a production of 9.2 mmol h^{-1} g^{-1} of resin (Scheme 4.22) [74].

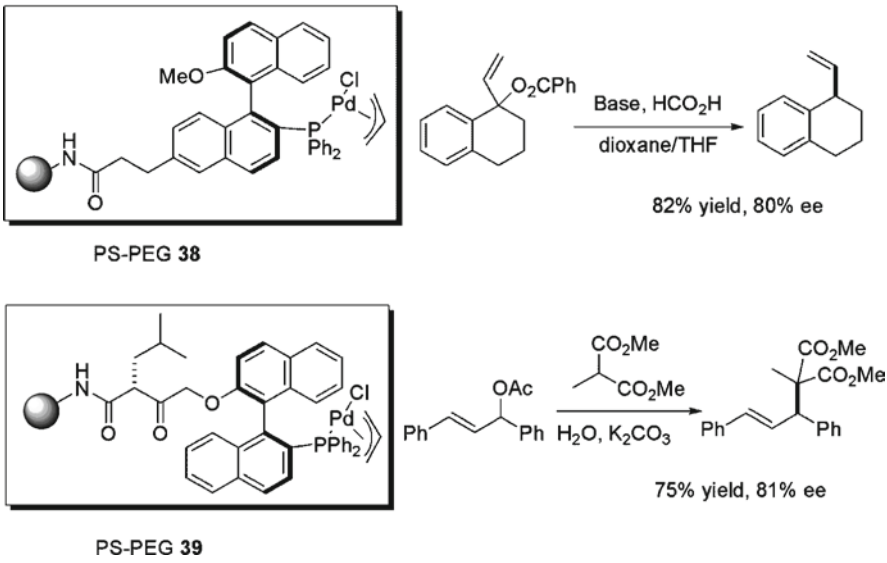

Scheme 4.19 *Top*, asymmetric allylic reduction in organic media. *Bottom*, asymmetric allylic alkylation in water

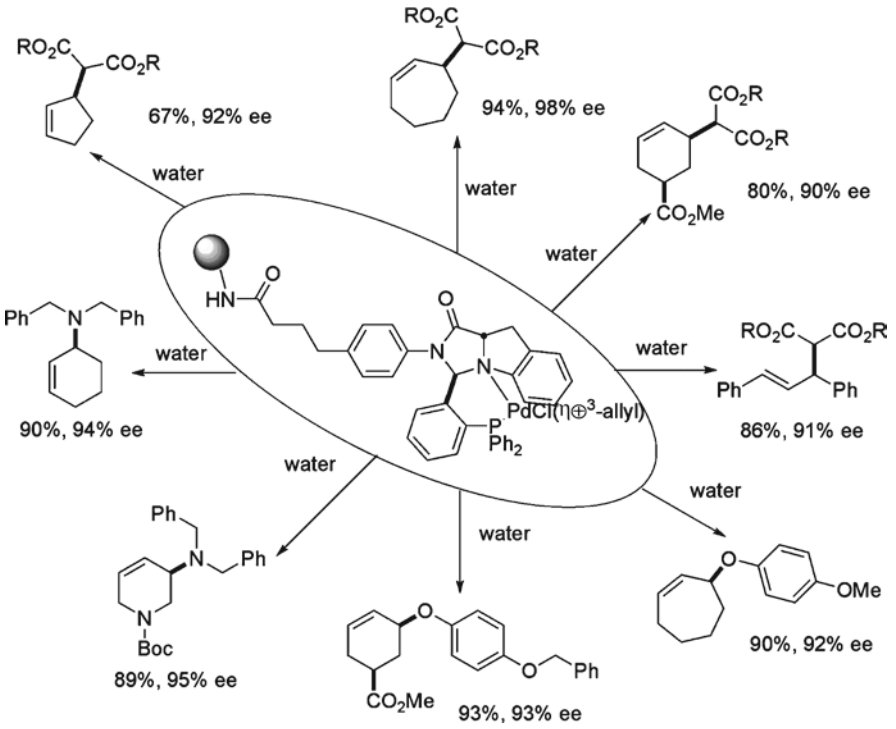

Scheme 4.20 Asymmetric allylic substitutions in water with PS-PEG supported palladium complexes

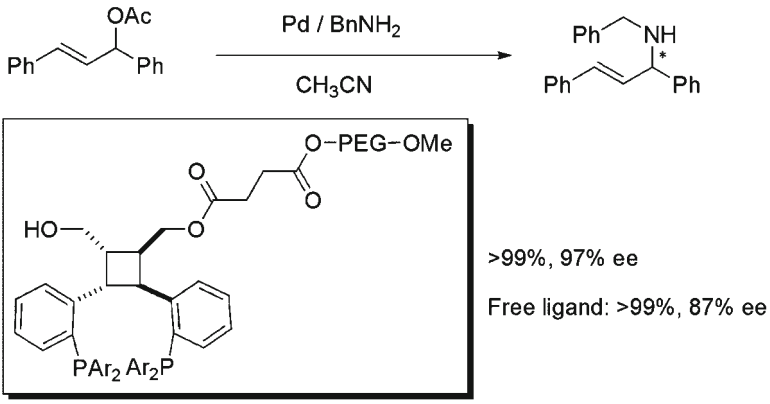

Scheme 4.21 Enhanced supported diphosphine for aymmetric allylic amination

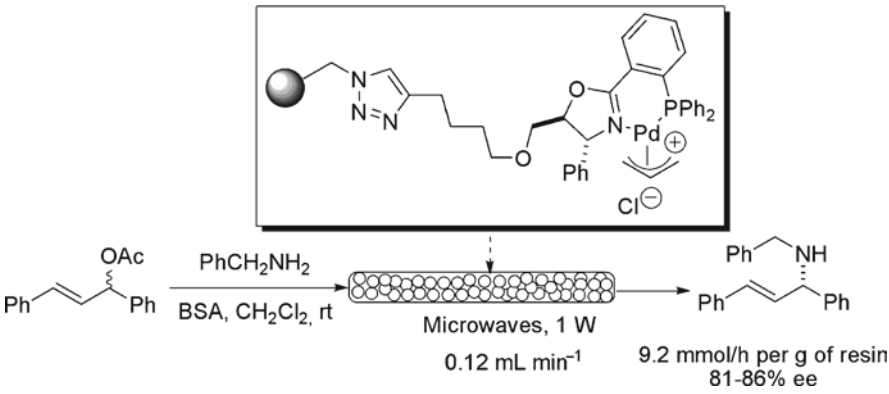

Scheme 4.22 Continuous flow allylic amination

4.4 Covalent Immobilization of Enantiopure Catalytic Species on Nanoparticles

The application of nanoparticles in catalysis has attracted considerable attention in recent times, since the very high specific surface of these materials could in principle lead to catalytic activities approaching those of homogeneous, molecular systems [75]. This feature is complemented by the availability of highly efficient methods for their separation and recovery, which makes nanoparticles highly valuable supports for catalytic species.

It is worth mentioning that non-functional nanoparticles have been used as catalytic materials for the formation of carbon–carbon [76], carbon–nitrogen [77] carbon–sulfur [78], and carbon–oxygen bonds [79], as well as in oxidation [75a], and

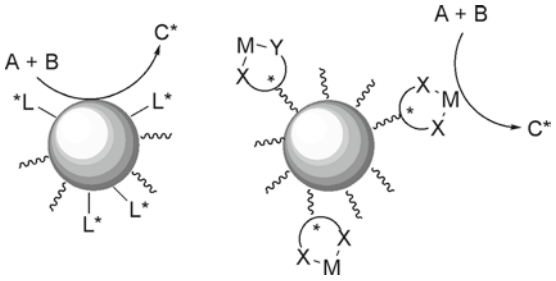

Fig. 4.14 General approaches to functional nanoparticles as catalysts for enantioselective processes

reduction [80, 81] processes. Material reviewed herein, however, will restrict to work involving the use of well-defined functional nanoparticles in catalytic asymmetric processes.

In these applications, two general approaches can be followed depending on the role exerted by the nanoparticle and the location of the chiral ligand with respect to the particle (Fig. 4.14). In one approach, the involved nanoparticles must also act as catalytic materials (Fig. 4.14, left). This normally involves the use of systems where the ligand is adsorbed to the metal surface through some of its chelating atoms. Therefore, the catalytic process takes place on the surface of the nanoparticle, and the achievement of enantiocontrol depends on how the ligands and capping agents employed to stabilize the particles are able to convey their influence to substrate molecules adsorbed in their vicinity. Functional nanoparticles operating according to this scheme are analogous to asymmetric heterogeneous catalysts, except that they can form stable suspensions. While this approach has led in some instances to spectacular results [82], the present section will restrict to the alternative approach (Fig. 4.14, right) where the nanoparticles act as structuring elements for an assembly of ligands, which are bonded to the particle through some additional function, different from the chelating functional groups defining the catalytic centre.

In these cases, the catalytic activity arises from a metal complex. The main advantages expected from this approach range from increased catalytic activity due to the accumulation of active centres on the nanoparticle periphery to the possibility of enhanced enantiocontrol due to the close similarity with purely homogeneous processes, or to the ease of separation and recycling of the catalyst through the application of a magnetic field whenever the nanoparticles possess a magnetic core [83].

4.4.1 Gold Nanoparticles as Supports

Gold nanoparticles, because of their capacity to strongly interact with thiol groups leading to the formation of self-assembled monolayers (SAM), have played a central

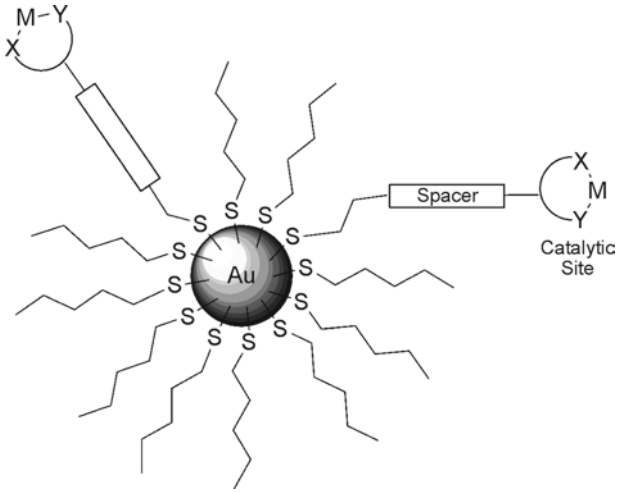

Fig. 4.15 Schematic representation of a thiol-functionalised ligand anchored on a thiol-stabilised gold nanoparticle

role in this approach. Within this strategy, the structures of ligands to be supported on gold nanoparticles are modified as to include additional thiol group(s). Best results are normally obtained when the thiol-modified ligands are diluted on the nanoparticle surface among non-functional thiols acting as mere nanoparticle stabilizers. To ensure the efficient exposure of the catalytic sites to the reagents, the thiol-modified ligands normally incorporate spacers so that the chain connecting the ligand with the nanoparticle is longer than that of the non-functional, stabilizing thiols (Fig. 4.15).

Catalyst separation and recycling is one of the relevant issues in catalytic processes mediated by functional nanoparticles. Functional gold nanoparticles stabilized by alkanethiol SAM's exhibit in many cases an agglomeration behavior that is highly responsive to solvent polarity. In this manner, it is possible to shift from the optimal situation in catalysis (maximal dispersion) to the optimal situation for catalyst separation (maximal agglomeration) by the simple addition of the appropriate solvent to the reaction mixture.

In an early attempt to use this strategy, Mrksich *et al*. reported the synthesis of gold nanoparticles protected with a mixture of alkanethiolate and an alkanethiolate-functionalized dihydroquinidine ligand (3:1 ratio) through a ligand exchange approach, and used them in the asymmetric Sharpless dihydroxylation of *trans*-olefins containing an aryl substituent (Scheme 4.23) [84]. Yields comparable to those obtained with monomeric ligands were recorded while enantioselectivities (84–90% ee) were slightly lower when using the gold nanoparticle supported ligand. The ligand-functionalized colloids were easily separated by gel permeation chromatography and could be reused once with only a modest decrease in enantioselectivity. As pointed out by these authors, the interest of these particles stems from two important features. First, as the structure of the chemisorbed monolayer of alkanethiolates is reasonably well ordered, it is possible to control the density and environments of functional molecules present on the nanoparticle

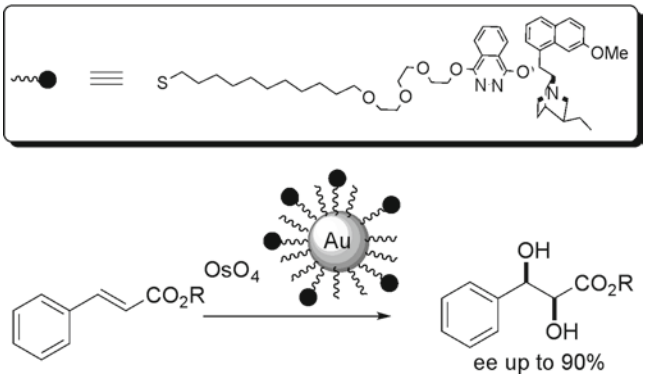

Scheme 4.23 Functional gold nanoparticles as ligands for the Sharpless dihydroxylation of olefins

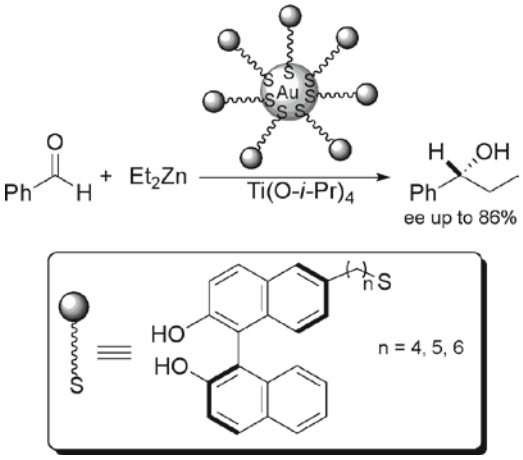

Scheme 4.24 Functional gold nanoparticles as ligands for the catalytic enantioselective diethylzinc addition to aldehydes

surface. Second, the preparation of the modified colloids is straightforward and allows wide flexibility in tailoring both the size and the chemical functionality of the particles.

Sasai *et al*. reported a practical synthesis of a thiol-modified 1,1′-bi-2-naphthol (BINOL) supported on gold nanoparticles, and used this nanostructured ligand for the asymmetric alkylation of aldehydes with diethylzinc (Scheme 4.24) [85]. The asymmetric induction exerted by the supported ligand depends on the length of the spacer connecting by BINOL moiety with the nanoparticle, and in the optimal case led to results almost comparable with those obtained with BINOL itself. Very interestingly, these gold-supported ligands were stable to the acidic workup of the alkylation reaction and could be reused without deterioration of their properties.

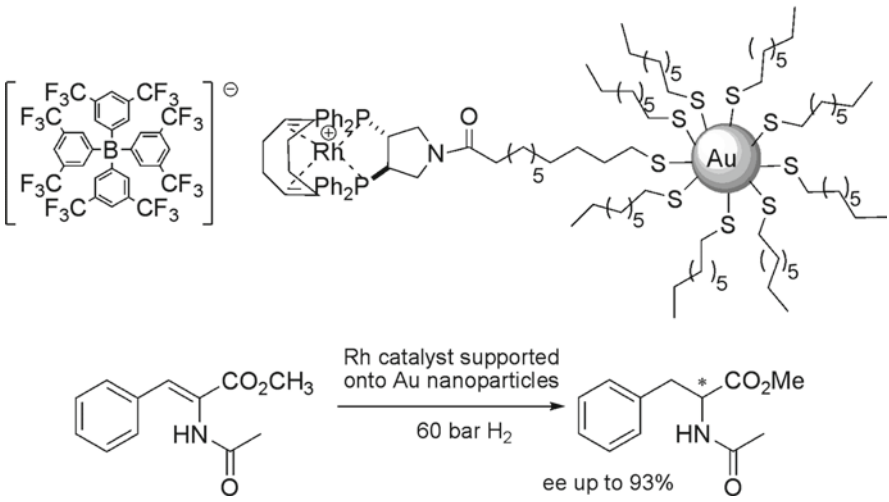

Scheme 4.25 A rhodium catalyst for the asymmetric hydrogenation of olefins supported onto Au nanoparticles

Pfaltz and co-workers performed a very detailed study on the rhodium catalyzed asymmetric hydrogenation of methyl α-acetamidocinnamate mediated by functional gold nanoparticles (Scheme 4.25) [86]. In this study, *ca*. 3 nm gold nanoparticles stabilized by a self-assembled octanethiolate monolayer were submitted to ligand exchange with a thiol-functionalised Rh(COD)(PYRPHOS) catalyst. The resulting gold nanoparticles modified with chiral ligands were tested as hydrogenation catalysts. With methyl α-acetamidocinnamate as the substrate, the functional gold NPs led to the same enantioselectivity that the homogeneous catalytic system; i.e., [Rh(COD)(PYRPHOS)]BArF. The nanocatalysts could be easily separated by filtration and used for three consecutive runs without losses in enantioselectivity. However, catalytic activity importantly decreased in recycled catalyst samples. To understand the structure and dynamics of mixed thiol monolayers, as those present on these gold nanoparticles, STM studies of analogous SAMs on Au(111) were performed. The STM images showed that the catalyst-bearing thiolates are distributed statistically on the nanoparticle surface and that the ordered structure of the *n*-octanethiolate SAM can be retained during incorporation of the catalyst-bearing thiols using the place-exchange methodology.

Kanemasa *et al*. reported another interesting application of gold nanoparticles in asymmetric catalysis by supporting bisoxazoline (BOX) type ligands on their surface [87]. They prepared by ligand exchange gold nanoparticle-supported BOX ligands containing thiol-terminated spacers of different length (4, 6, 8, and 10 carbons) and applied them in the asymmetric ene type reaction between 2-phenylpropene and ethyl glyoxylate in the presence of $Cu(OTf)_2$ (Scheme 4.26). While all four ligands depicted essentially identical enantioselectivities approaching that of the homogeneous Ph-BOX/$Cu(OTf)_2$ system, the nanoparticles containing the BOX ligand attached to the gold nanoparticles through the shortest four carbon spacer showed the best activity profile during recycling. The authors attributed this behavior to the fact that this particular ligand presented the polar Cu-BOX moiety buried in

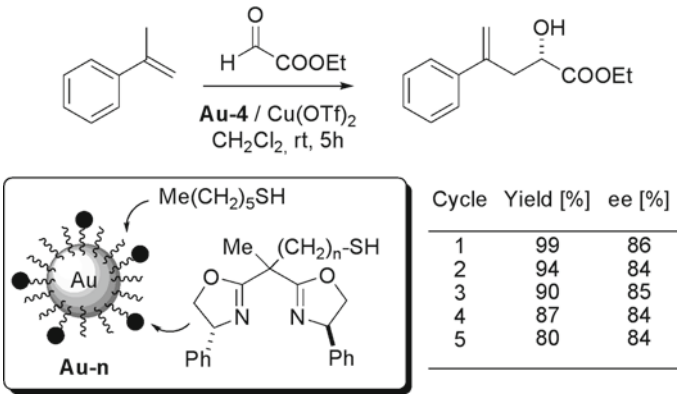

Cycle	Yield [%]	ee [%]
1	99	86
2	94	84
3	90	85
4	87	84
5	80	84

Scheme 4.26 A Cu-BOX catalyst for the asymmetric ene reaction supported onto Au nanoparticle

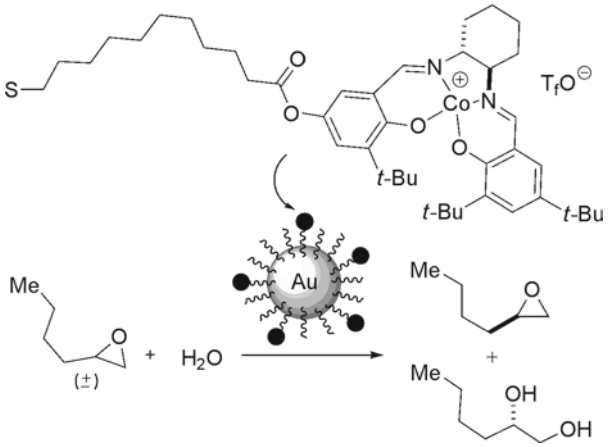

Scheme 4.27 Hydrolytic kinetic resolution of epoxides with a Co–Salen catalyst supported onto gold nanoparticles

an array of neighboring hexanethiolate ligands, and that this leaded to an optimal dispersion of the nanoparticles in the reaction media. However, since the differences in catalytic activity increase as the recycling proceeds, the existence of more important leaching levels in the nanoparticles with longer spacers can probably not be excluded. The catalyst was separated by precipitation and reused for five cycles with a moderate decrease in its activity, but with the same enantioselectivity.

A highly efficient hydrolytic kinetic resolution of epoxides by chiral[(salen) Co(III)] complexes immobilized on gold nanoparticles was reported by Belser and Jacobsen (Scheme 4.27) [88]. The nanoparticle-supported catalyst showed significantly higher activity than the homogeneous ones, while showing similarly high selectivity factor values, k_{rel}. This turned out to be the first example of cooperative behavior in catalysts supported on gold nanoparticles. The catalyst maintained its

high reactivity as well as excellent enantioselectivity for up to six recycles. It could be established that this decrease in activity was due to reduction of the Co(III) centre and not to leaching, since oxidation of the catalyst restored its initial activity.

4.4.2 Magnetic Nanoparticles as Supports

Besides gold nanoparticles, the use of functional magnetic nanoparticles for enantioselective catalytic applications is attracting an increasing interest. Given the manifold applications of these materials, there are many reliable procedures for their production and stabilization. In fact, the same methodologies that have been developed for anchoring organic molecules on magnetic nanoparticles for many different applications can also be used to support a catalytic ligand. In catalytic applications, the possibility of controlling the motion of these species by application of a magnetic field is translated into the opportunity for catalyst separation and recycling by magnetic decantation. Until now, most applications in this field have been based on readily available iron oxide nanocolloids. Other magnetic nanomaterials, such as ε-cobalt, have recently demonstrated its suitability for the same purposes.

In a pioneer development, Gao and coworkers reported the kinetic resolution of racemic carboxylates catalyzed by a magnetic nanoparticle-supported lipase from *Candida rugosa* (Scheme 4.28) [89]. Following what has become an almost universal approach for the functionalization of nanoparticles made of iron oxides, highly crystalline 11 nm maghemite nanocrystals were first functionalized with 3-aminopropyltriethoxysilane. Then, glutaraldehyde was used as a linker to tether the lipase to the surface of the magnetic nanoparticles leading to an iron oxide–lipase assembly (MNP-Lipase). The MNP-Lipase biocatalyst exhibited high stereoselectivity in the kinetic resolution of racemic carboxylates and improved long-term stability over its parent free enzyme, allowing the supported enzyme to be repeatedly used for a series of chiral resolution reactions. Immobilization of the lipase onto the magnetic nanoparticle has the advantages of facile recovery and excellent stability of the expensive enzyme catalyst over several cycles.

A phosphonic acid substituted BINAP–ruthenium complex was immobilized by Lin and coworkers onto magnetite (Fe_3O_4) nanoparticles prepared either by thermal decomposition (8.9 nm mean diameter) or by co-precipitation (6.6 nm mean diameter). The functional particles were used for the enantioselective hydrogenation of aromatic ketones (Scheme 4.29) [90]. When these nanocatalysts were tested in the hydrogenation of a broad family of ketone substrates, the larger magnetite particles led to the corresponding secondary alcohols with enantioselectivities higher than those recorded with the homogeneous Noyori catalyst, Ru(BINAP)(DPEN)Cl_2. Interestingly, when the catalyst involving the smaller particles prepared by co-precipitation was recovered by magnetic decantation and reused, no decrease in catalytic activity or in enantioselectivity was observed over 14 consecutive runs. Most likely, the three-point binding provided by the phosphonic acid group plays a fundamental role in preventing leaching of the catalytic species into solution, thus contributing to the preservation of the catalytic activity. This study nicely illustrated the tremendous potential of magnetic nanoparticles in asymmetric catalysis.

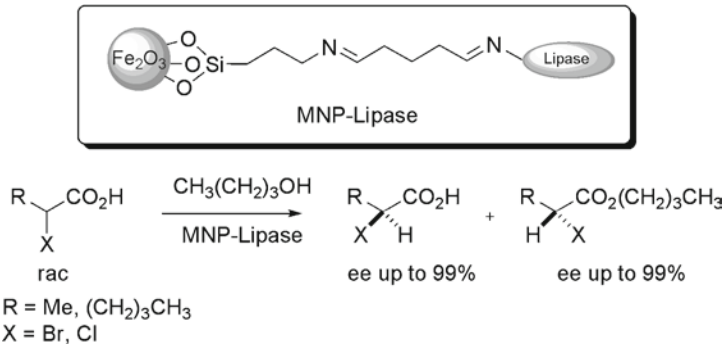

Scheme 4.28 Kinetic resolution of α-halocarboxylic acids using a lipase immobilized on magnetic nanoparticles

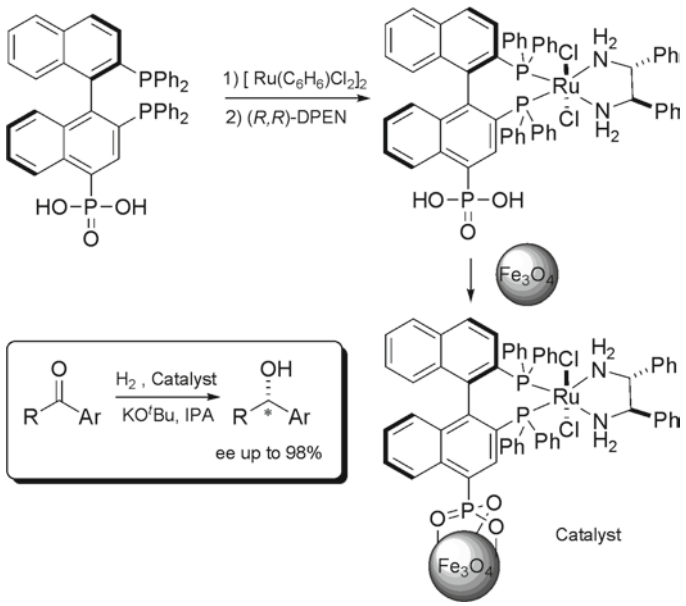

Scheme 4.29 Asymmetric hydrogenation of ketones mediated by a Noyori type catalyst immobilized onto magnetic Fe_3O_4 nanoparticles

Very recently, Pericàs and coworkers have reported the first application of magnetic ε-cobalt nanoparticles in asymmetric catalysis. Cobalt NPs are usually stabilized by long chain carboxylic acids such as oleic acid. When the preparation of the particles is performed in the presence of modular, enantiopure amino alcohol ligands modified with long chain carboxylic acids, they are also incorporated at the surface (Scheme 4.30) [91]. These nanoparticles have been then used as magnetically decantable ligands in the Ru-catalyzed asymmetric transfer hydrogenation of alkyl aryl ketones with enantioselectivities generally higher than those observed with structurally related, monomeric amino alcohols [92]. This fact confirms the

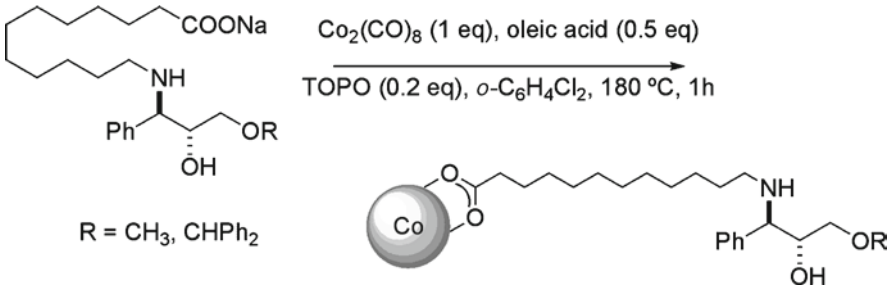

Scheme 4.30 Preparation of functional ε-cobalt nanoparticles for asymmetric transfer hydrogenation of ketones

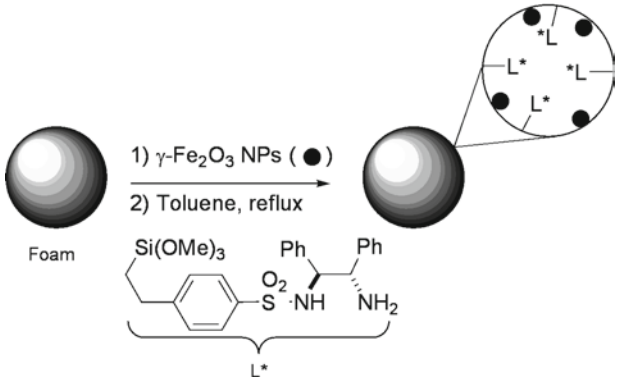

Scheme 4.31 Functionalization of a siliceous mesocellular foam for Ru-mediated asymmetric transfer hydrogenation

advantages derived from supporting the ligand on nanosized particles for this particular application. The main drawback associated to this approach is the poor reusability of the functional cobalt nanoparticles. Thus, a significant decrease in catalytic activity detected upon magnetic recovery and reuse appears to obey to leaching of the carboxylate ligands. The differences of stability between nanoparticle-ligand assemblies involving three-point (Scheme 4.29) and two-point binding become evident from these examples.

Quite recently, magnetic γ-Fe_2O_3 nanoparticles trapped inside a siliceous mesocellular foam have been used to impart magnetic mobility to Ru-TsDPEN (TsDPEN = *N*-(*p*-toluenesulfonyl)-1,2-diphenylethylenediamine) complexes grafted on the siliceous matrix (Scheme 4.31). This material has been used as a catalyst for the transfer hydrogenation of imines and ketones. Very high yields and enantioselectivities were noticed for at least nine consecutive uses of the catalyst, thus demonstrating the robustness of this approach [93].

An asymmetric aldol reaction catalyzed by primary amines supported on magnetic nanoparticles and on silica has been reported by Luo and coworkers (Scheme 4.32)

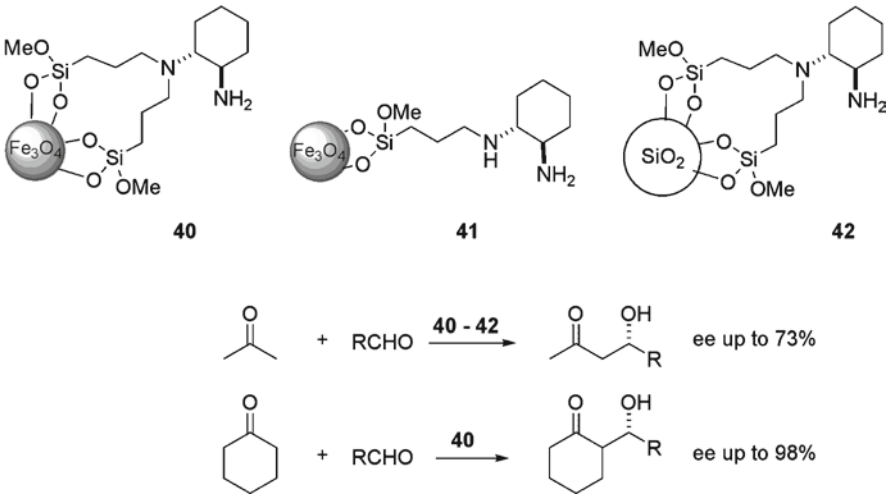

Scheme 4.32 Chiral amines supported on magnetic nanoparticles for asymmetric, amine-catalyzed aldol reactions

[94]. It was observed that the tertiary–primary amine catalyst supported on magnetic NPs (**40**) was better than the secondary–primary amine catalyst on the same support (**41**). The same tertiary–primary diamine catalyst supported on chromatographic silica (**42**) showed less activity than **40**, thus highlighting the effect of the nanometric size of the particles. The optimal catalyst (**40**) was recycled for 11 times with consistent activity and enantioselectivity. Another interesting example of asymmetric aldol reaction was reported by Liu *et al*. using an oligopeptide supported onto magnetic NPs through an ionic liquid spacer [95].

4.5 Summary and Outlook

The present literature survey illustrates the potential of the covalent immobilization of enantiopure catalytic species on polymers and functional nanoparticles for asymmetric catalysis. This fast growing field still presents many areas to be explored and important problems to be satisfactorily solved. In any case, it holds the promise of providing the chemical community with highly active, fully recoverable and reusable catalytic systems leading to enantioselectivities similar or even better to those depicted by referable homogeneous systems.

For polymer-supported catalytic species the nature of the technique employed for catalyst preparation [grafting, (co)polymerization, or self-supporting] has an important impact on the performance of the material. More active and enantioselective materials have been traditionally obtained by grafting suitably modified ligands and catalysts onto functional resins of different types. However, the number of systems prepared by copolymerization techniques is growing very fast.

While grafting approaches benefit from a ready implementation, they suffer from the limitation that functionalization is conditioned by the commercial resins used as starting materials. Furthermore, the origin and functionalization of commercial resins of different brands change rather often, and this can pose difficulties to the reproducibility of published procedures. In principle, all of these difficulties could be overcome with the implementation of copolymerization approaches.

With respect to the nature of the chemical process that can be performed with polymer-supported catalysts, almost every important catalyst has one or more polymer-supported version. It is, however, still rare that practicing chemists decide to use polymer-supported catalysts for their enantioselective transformations, in spite of potential benefits. Poor catalytic activity and enantioselectivity in comparison with referable homogeneous catalysts is a plausible explanation for this fact. Substantial effort has still to be devoted to the formulation of the design principles for supported catalytic species in order to achieve useful levels of performance.

A further step in the application of enantioselective, polymer-supported catalysts consists in their implementation for continuous-flow processes. The number of available examples, some of them discussed in this review, is still very low. Ligands or catalysts developed with this purpose should exhibit, besides high catalytic activity and enantioselectivity, high chemical stability to ensure an extended life cycle. To achieve this goal, attention has to be paid to the development of analytical methods to track the evolution of polymer-supported species under specific reaction conditions.

For nanoparticle-supported catalysts, much effort has been put until now on gold. This is probably due to the existence of a generally valid approach to the self assembly of monolayers around the particles. Moreover, the solvent dependent dispersion/agglomeration behavior of these particles can be readily controlled. Magnetic materials (mostly iron oxides) offer great promise in view of magnetic decantation. Many other materials are thus still awaiting evaluation for this purpose.

With respect to the strategy for anchoring the ligand on the nanoparticle, it seems clear that either covalent grafting (via alkoxysilanes) or multipoint ionic binding are important to prevent leaching and, thus, deterioration of activity. The development of new supporting strategies characterized by robustness and flexibility will open in the near future important opportunities in this field.

The promise for high catalytic activity with functional nanoparticles due to a high concentration of active sites in the periphery of the nanoparticle plus ligand assembly, as it happens with dendrimers (dendrimer effects) [96] still awaits definitive confirmation. Aspects such as functional dilution (i.e. the molar ratio between ligand and stabilizing agent molecules), chain length ratio between the ligand and stabilizing agent molecules, and agglomeration control still require a substantial and systematic research effort.

Finally, enantioselectivity heavily depends on ligand design. In the available examples, whenever the ligand molecules to be supported on nanoparticles have been modified in such a way that neither the linker nor the nanoparticle bulk perturbs the catalytically active site, enantioselectivities comparable to those recorded in homogeneous phase have been achieved.

Work along the lines outlined here will lead with high probability to a new generation of highly active and enantioselective, fully recyclable catalysts for metal-catalyzed and organo-catalyzed reactions.

References

1. (a) De Vos DE, Vankelecom IFJ, Jacobs PA (eds) (2000) Chiral catalyst immobilization and recycling. Wiley, Weinheim; (b) Buchmeiser MR (ed) (2003) Polymeric materials in organic synthesis and catalysis. Wiley, Weinheim; (c) Ding K, Uozumi Y (eds) Handbook of asymmetric heterogeneous catalysis. Wiley, Weinheim; (d) Benaglia M (ed) (2008) Recoverable and recyclable catalysts. Wiley, Chichester
2. For relevant reviews, see: (a) Fan QH, Li YM, Chan ASC (2002) Chem Rev 102: 3385–3466; (b) Bräse S, Lauterwasser F, Ziegert RE (2003) Adv Synth Catal 345:869–929; (c) Trindade AF, Gois PMP, Afonso CAM (2009) Chem Rev 109:418–514
3. (a) Houk KN, List B (eds) (2004) Acc Chem Res 37:631–847; (b) Dalko PI, Moisan L (2004) Angew Chem Int Ed 43:5138–5175; (c) Berkessel A, Gröger H, MacMillan D (eds) (2005) Asymmetric organocatalysis. In: Biomimetic concepts to applications in asymmetric synthesis. Wiley, Weinheim; (d) Koćovský P, Malkov AV (eds) (2006) Tetrahedron 62:243–502; (e) Pellissier H (2007) Tetrahedron 63:9267–9331; (f) List B (ed) (2007) Chem Rev 107:5413–5883; (g) Dondoni A, Massi A (2008) Angew Chem Int Ed 47:4638–4660; (h) MacMillan DWC (2008) Nature 455:304–308
4. Reviews on supported organocatalysts: (a) Benaglia M, Puglisi A, Cozzi F (2003) Chem Rev 103:3401–3429; (b) Cozzi F (2006) Adv Synth Catal 348:1367–1390; (c) Benaglia M (2006) New J Chem 30:1525–1533; (d) Altava B, Burguete I, Luis SV (2008) Polymer-supported organocatalysts. In: Tulla-Puche J, Albericio F (eds) The power of functional resins in organic synthesis. Wiley, Weinheim
5. (a) Breslow R (1995) Acc Chem Res 28:146–153; (b) Murakami Y, Kikuchi JI, Hisaeda Y, Hayashida O (1996) Chem Rev 96:721–758; (c) Motherwell WB, Bingham MJ, Six Y (2001) Tetrahedron 57:4663–4686; (d) Breslow R (ed) (2005) Artificial enzymes. Wiley, Weinheim
6. Lu J, Toy PH (2009) Chem Rev 109:815–838
7. Fraile JM, García JI, Mayoral JA (2009) Chem Rev 109:360–417
8. Baker RT, Kobayashi S, Leitner W (2006) Adv Synth Catal 348:1317–1771
9. Ikegami S, Hamamoto H (2009) Chem Rev 109:583–593
10. Gruttadauria M, Giacalone F, Noto R (2008) Chem Soc Rev 37:1666–1688
11. (a) Eder U, Sauer G, Wiechert R (1971) Angew Chem Int Ed Engl 10:496–497; (b) Hajos ZG, Parrish DR (1974) J Org Chem 39:1612–1615
12. (a) List B, Lerner RA, Barbas III CF (2000) J Am Chem Soc 122:2395–2396; (b) Sakthivel K, Notz W, Bui T, Barbas III CF (2001) J Am Chem Soc 121:5260–5267
13. Benaglia M, Celentano G, Cozzi F (2001) Adv Synth Catal 343:171–17
14. Benaglia M, Cinquini M, Cozzi F, Puglisi A, Celentano G (2002) Adv Synth Catal 344:533–542
15. Benaglia M, Cinquini M, Cozzi F, Puglisi A, Celentano G (2003) J Mol Catal A Chem 204–205:157–163
16. Gu L, Wu Y, Zhang Y, Zhao G (2007) J Mol Catal A Chem 263(1–2):186–194
17. Gruttadauria M, Giacalone F, Noto R (2009) Adv Synth Catal 351:33–57
18. Kondo K, Yamano T, Takemoto K (1985) Makromol Chem 186:1781–1785
19. Font D, Jimeno C, Pericàs MA (2006) Org Lett 8:4653–4655
20. Font D, Bastero A, Sayalero S, Jimeno C, Pericàs MA (2007) Org Lett 9:1943–1946
21. Font D, Sayalero S, Bastero A, Jimeno C, Pericàs MA (2008) Org Lett 10:337–340
22. Alza E, Rodríguez-Escrich C, Sayalero S, Bastero A, Pericàs MA (2009) Chem Eur J 15:10167–10172
23. Giacalone F, Gruttadauria M, Marculescu AM, Noto R (2007) Tetrahedron Lett 48:255–259
24. Dondoni A (2008) Angew Chem Int Ed 47:8995–8997
25. Gruttadauria M, Giacalone F, Marculescu AM, Lo Meo P, Riela S, Noto R (2007) Eur J Org Chem 4688–4698
26. Kehat T, Portnoy M (2007) Chem Commun 2823–2825
27. Moad G, Solomon DH (2006) The chemistry of radical polymerization, 2nd edn. Elsevier, Amsterdam, Boston

28. Kristensen TE, Vestli K, Fredriksen FK, Hansen FK, Hansen T (2009) Org Lett 11:2968–2971
29. (a) Andreae MRM, Davis AP (2005) Tetrahedron Aymmetry 16:2487–2492; (b) Akagawa K, Sakamoto S, Kudo K (2005) Tetrahedron Lett 46:8185–8187; (c) Revell JD, Gantenbein D, Krattiger P, Wennemers H (2006) Biopolymers (Pept Sci) 84:105–113; (d) Yan J, Wang L (2008) Synthesis 2065–2072; (e) Carpenter RD, Fettinger JC, Lam KS, Kurth MJ (2008) Angew Chem Int Ed 47:6407–6410
30. (a) Gruttadauria M, Giacalone F, Marculescu AM, Noto R (2008) Adv Synth Catal 350:1397–1405; (b) Gruttadauria M, Salvo AMP, Giacalone F, Agrigento P, Noto R (2009) Eur J Org Chem 5437–5444
31. (a) Cobb AJA, Longbottom DA, Shaw DM, Ley SV (2004) Chem Commun 1808–1809; (b) Mitchell CET, Cobb AJA, Ley SV (2005) Synlett 611–614; (c) Luo S, Xu H, Mi X, Li J, Zheng X, Cheng, JP (2006) J Org Chem 71:9244–9247
32. Alza E, Cambeiro XC, Jimeno C, Pericàs MA (2007) Org Lett 9:3717–3720
33. Miao T, Wang L (2008) Tetrahedron Lett 49:2173–2176
34. (a) Palomo C, Mielgo A (2006) Angew Chem Int Ed 45:7876–7880; (b) Lattanzi A (2009) Chem Commun 1452–1463
35. (a) Varela MC, Dixon SM, Lam KZ, Schore NE (2008) Tetrahedron 64:10087–10090; (b) Röben C, Stasiak M, Janza B, Greiner A, Wendorff JH, Studer A (2008) Synthesis 2163–2168
36. Alza E, Pericàs MA (2009) Adv Synth Catal 351:3051–3056
37. (a) Liu YX, Sun YN, Tan HH, Wei L, Tao JC (2007) Tetrahedron Asym 18:2649–2656; (b) Liu Y-X, Sun Y-N, Tan H-H, Tao J-C (2008) Catal Lett 120(3–4):281–287
38. Luo S, Li J, Zhang L, Xu H, Cheng J-P (2008) Chem Eur J 14:1273–1281
39. Ahrendt KA, Borths CJ, MacMillan DWC (2000) J Am Chem Soc 122:4243–4244
40. (a) Lelais G, MacMillan DWC (2006) Aldrichimica Acta 39:79–87; (b) Erkkilä A, Majander I, Pihko PM (2007) Chem Rev 107:5416–5470
41. Benaglia M, Celentano G, Cinquini M, Puglisi A, Cozzi F (2002) Adv Synth Catal 344: 149–152
42. Puglisi A, Benaglia M, Cinquini M, Cozzi F, Celentano G (2004) Eur J Org Chem 567–573
43. Selkälä SA, Tois J, Pihko PM, Koskinen AMP (2002) Adv Synth Catal 344:941–945
44. Haraguchi N, Takemura Y, Itsuno S (2010) Tetrahedron Lett 51:1205–1208
45. (a) Jacobsen EN, Pfaltz A, Yamamoto H (eds) (1999) Comprehensive asymmetric catalysis, vols I–III. Springer, Berlin; (b) Mikami K, Lautens M (eds) (2007) New frontiers in asymmetric catalysis. Wiley, Hoboken
46. Dai LX (2004) Angew Chem Int Ed 43:5726–5729
47. Dioos BML, Vankelecom IVF, Jacobs PA (2006) Adv Synth Catal 348:1413–1446
48. Saluzzo C, Lamouille T, Hérault D, Lemaire M (2002) Bioorg Med Chem Lett 12:1841–1844
49. Li Y, Li Z, Li F, Wang Q, Tao F (2005) Org Biomol Chem 3:2513–2518
50. Arakawa Y, Haraguchi N, Itsuno S (2006) Tetrahedron Lett 47:3229–3243
51. Liang Y, Jing Q, Li X, Shi L, Ding K (2005) J Am Chem Soc 127:7694–7695
52. Liang Y, Wang Z, Ding K (2006) Adv Synth Catal 348:1533–1538
53. Vidal-Ferran A, Bampos N, Moyano A, Pericàs MA, Riera A, Sanders JKM (1998) J Org Chem 63:6309–6318
54. Vidal-Ferran A, Moyano A, Pericàs MA, Riera A (1997) J Org Chem 62:4970–4982
55. Minutolo F, Pini D, Petri A, Salvadori P (1996) Tetrahedron Asymmetry 7:2293–2302
56. Canali L, Cowan E, Deleuze H, Gibson CL, Sherrington DC (1998) Chem Commun 2561–2562
57. Cho SH, Gadzikwa T, Afshari M, Nguyen ST, Hupp JT (2007) Eur J Inorg Chem 4863–4867
58. Nielsen M, Thomsen AH, Jensen TR, Jakobsen HJ, Skibsted J, Gothelf KV (2005) Eur J Org Chem 342–347
59. Song CE, Yang JW, Roh EJ, Lee SG, Ahn JH, Han H (2002) Angew Chem Int Ed 41:3852–3854
60. Trost BM, Pan Z, Zambrano J, Kujat C (2002) Angew Chem Int Ed 41:4691–4693

61. (a) Solà L, Reddy KS, Vidal-Ferran A, Moyano A, Pericàs MA, Riera A, Alvarez-Larena A, Piniella JF (1998) J Org Chem 63:7078–7082; (b) Fontes M, Verdaguer X, Solà L, Pericàs MA, Riera A (2004) J Org Chem 69:2532–2543
62. Pericàs MA, Castellnou D, Rodríguez I, Riera A, Solà L (2003) Adv Synth Catal 345:1305–1313
63. (a) Castellnou D, Solà L, Jimeno C, Fraile JM, Mayoral JA, Riera A, Pericàs MA (2005) J Org Chem 70:433–438; (b) Castellnou D, Fontes M, Jimeno C, Font D, Solà L, Verdaguer X, Pericàs MA (2005) Tetrahedron 61:12111–12120
64. (a) Pericàs MA, Herrerías CI, Solà L (2008) Adv Synth Catal 350:927–932; (b) Rolland J, Cambeiro XC, Rodríguez-Escrich C, Pericàs MA (2009) Beilstein J Org Chem 5:56
65. Fraile JM, Mayoral JA, Serrano J, Pericàs MA, Solà L, Castellnou D (2003) Org Lett 5:4333–4335
66. Bastero A, Font D, Pericàs MA (2007) J Org Chem 72:2460–2468
67. (a) Burguete MI, Díez-Barra E, Fraile JM, García JI, García-Verdugo E, González R, Herrerías CI, Luis SV, Mayoral JA (2002) Bioorg Med Chem Lett 12:1821–1824; (b) Díez-Barra E, Fraile JM, García JI, Garcia-Verdugo E, Herrerías CI, Luis SV, Mayoral JA, Sánchez-Verdú P, Tolosa J (2003) Tetrahedron Asymmetry 14:773–778; (c) Burguete MI, Fraile JM, García JI, García-Verdugo E, Luis SV, Mayoral JA (2000) Org Lett 2:3905–3908
68. Mandoli A, Orlandi S, Pini D, Salvadori P (2003) Chem Commun 2466–2467
69. Werner H, Herrerías CI, Glos M, Gissibl A, Fraile JM, Pérez I, Mayoral JA, Reiser O (2006) Adv Synth Catal 348:125–132
70. (a) Uozumi Y, Danjo H, Hayashi T (1998) Tetrahedron Lett 39:8303–8306; (b) Hocke H, Uozumi Y (2004) Tetrahedron 60:9297–9306
71. (a) Uozumi Y, Shibatomi K (2001) J Am Chem Soc 123:2919–2920; (b) Nakai Y, Uozumi Y (2005) Org Lett 7:291–293; (c) Uozumi Y, Kimura M (2006) Tetrahedron: Asymmetry 17:161–166
72. Uozumi Y, Tanaka H, Shibatomi K (2004) Org Lett 6:281–283
73. Zhao D, Sun J, Ding K (2004) Chem Eur J 10:5952–5963
74. Popa D, Marcos R, Sayalero S, Vidal-Ferran A, Pericàs MA (2009) Adv Synth Catal 351:1539–1556
75. (a) Astruc D (ed) (2007) Nanoparticles and catalysis, Wiley, Weinheim; (b) Abbet S, Heiz U (2004) In: Rao CNR, Müller A, Cheetham AK (eds) The chemistry of nanomaterials, vol 2, ch. 17. Wiley, Weinheim; (c) Klabunde KJ, Mulukutla RS (2001) In: Klabunde KJ (ed) Nanoscale materials in chemistry, ch. 7. Wiley, New York
76. (a) Somorjai GA, Park JY (2008) Angew Chem Int Ed 47:9212–9228; (b) Somorjai GA, Contreras AM, Montano M, Rioux RM (2006) Clusters, surfaces, and catalysis. PNAS 103:10577–10583; (c) Astruc D, Lu F, Aranzaes JR (2005) Angew Chem Int Ed 44:7852–7872; (d) Park KH, Chung YK (2005) Synlett 545–559; (e) Grunes J, Zhu J, Somorjai GA (2003) Chem Commun 2257–2260; (f) Pasquato L, Pengo P, Scrimin P (2004) J Mater Chem 14:3481–3487; (g) Moreno-Mañas M, Pleixats R (2003) Acc Chem Res 36:638–643
77. (a) Tang BX, Guo SM, Zhang MB, Li JH (2008) Synthesis 1707–1716; (b) Kantam ML, Yadav J, Laha S, Sreedhar B, Jha S (2007) Adv Synth Catal 349:1938–1942; (c) Rout L, Jammi S, Punniyamurthy T (2007) Org Lett 9:3397–3399
78. (a) Rout L, Sen TK, Punniyamurthy T (2007) Angew Chem Int Ed 46:5583–5586; (b) Ranu BC, Saha A, Jana R (2007) Adv Synth Catal 349:2690–2696
79. Zhang J, Zhang Z, Wang Y, Zheng X, Wang Z (2008) Eur J Org Chem 5112–5116
80. (a) Rossi LM, Machado G (2009) J Mol Cat A Chem 298:69–73; (b) Maity P, Basu S, Bhaduri S, Lahiri GK (2007) Adv Synth Catal 349:1955–1962
81. Studer M, Blaser HU, Exner C (2003) Adv Synth Catal 345:45–65
82. (a) Tamura M, Fujihara H (2003) J Am Chem Soc 125:15742–15743; (b) Jansat S, Gómez M, Philippot K, Muller G, Guiu E, Claver C, Castillon S, Chaudret B (2004) J Am Chem Soc 126:1592–1593; (c) Sawai K, Tatumi R, Nakahodo T, Fujihara H (2008) Angew Chem Int Ed 47:6917–6919; (d) Park KH, Chung YK (2005) Adv Synth Catal 347:854–866;

(e) Choudary BM, Ranganath KVS, Pal U, Kantam ML, Sreedhar B (2005), J Am Chem Soc 127:13167–13171
83. For a recent review, see: Roy S, Pericàs MA (2009) Org Biomol Chem 7:2669–2677
84. Li H, Luk YY, Mrksich M (1999) Langmuir 15:4957–4959
85. Marubayashi K, Takizawa S, Kawakusu T, Arai T, Sasai H (2003) Org Lett 5:4409–4412
86. Belser T, Stohr M, Pfaltz A (2005) J Am Chem Soc 127:8720–8731
87. Ono F, Kanemasa S, Tanaka J (2005) Tetrahedron Lett 46:7623–7626
88. Belser T, Jacobsen EN (2008) Adv Synth Catal 350:967–971
89. Gardimalla HMR, Mandal D, Stevens PD, Yen M, Gao Y (2005) Chem Commun 4432–4434
90. Hu A, Yee GT, Lin W (2005) J Am Chem Soc 127:12486–12487
91. Michalek F, Lagunas A, Jimeno C, Pericàs MA (2008) J Mater Chem 18:4692–4697
92. (a) Pastó M, Riera A, Pericàs MA (2002) Eur J Org Chem 2337–2341; (b) Alza E, Bastero A, Jansat S, Pericàs MA (2008) Tetrahedron Asymmetry 19:374–378
93. Li J, Zhang Y, Han D, Gao Q, Li C (2009) J Mol Cat A Chem 298:31–35
94. Luo S, Zheng X, Cheng JP (2008) Chem Commun 5719–5721
95. Jiang Y, Guo C, Xia H, Mahmood I, Liu H (2008) Ind Eng Chem Res 47:9628–9635
96. Helms B, Fréchet JMJ (2006) Adv Synth Catal 348:1125–1148

Chapter 5
Heterogenization of Homogeneous Catalysts on Dendrimers

Vital A. Yazerski and Robertus J.M. Klein Gebbink

Abstract The functionalizing of dendrimers with homogeneous catalyst moieties either to the dendrimer periphery or to the dendrimer core yields macromolecular homogeneous catalysts. These polymeric materials are characterized by a high level of molecular integrity and usually retain a comparable activity and selectivity as the parent monomeric catalyst. Moreover, such size-enlarged catalysts can be easily separated from homogeneous reaction mixtures by means of any size-discriminative technique. In this chapter, modern as well as classical examples of dendrimer-heterogenized catalysts will be highlighted in detail with respect to their preparation, properties, and catalytic application with specific emphasis on the role of the dendritic support.

5.1 Introduction

The vivid consumption of limited natural resources in combination with the widespread environmental exposure to human activities is an evident problem of humanity for the twenty-first century. For the modern chemical industry this first of all indicates an urge for the development and application of ultimately atom-efficient and environmental friendly technologies, rather than the simplification and acceleration of already existing chemical processes to economic profits only. A high selectivity is the inherent requirement for any "green" chemical transformation. In turn, a selective process can be realized only on well-defined reaction sites, i.e. catalyst with a molecularly defined structure. Indeed, molecular catalyst design allows for the adjustment of properties of already existing homogeneous catalysts in a predictable manner and allows for the discovery of new ones. However, a major hurdle to implement molecularly defined catalysts, or homogeneous catalysts, in

V.A. Yazerski and R.J.M.K. Gebbink (✉)
Faculty of Science, Debye Institute for Nanomaterials Science, Organic Chemistry & Catalysis, Utrecht University, Padualaan 8, 3584 CH Utrecht, The Netherlands
e-mail: r.j.m.kleingebbink@uu.nl

P. Barbaro and F. Liguori (eds.), *Heterogenized Homogeneous Catalysts for Fine Chemicals Production*, Catalysis by Metal Complexes 33,
DOI 10.1007/978-90-481-3696-4_5,

large-scale operations originates from the solubilized nature of these catalysts and in particular from issues concerning catalyst separation and reuse.

While the immobilization of homogeneous catalysts onto insoluble solid supports such as silica, alumina or cross-linked polymeric materials may solve part of these problems, there are a number of soft spots in this approach that usually suppress their wide application in sustainable technological processes. Molecular catalysts that are heterogenized in this manner typically loose a part of their uniformity in a structural and especially micro-environmental sense, much like typical heterogeneous catalysts, and can no longer be regarded as single site catalysts. These apparent drawbacks along with the possibility of catalyst leaching dramatically influence the overall activity and selectivity of the prepared 'heterogenized' catalysts [1].

The usage of well-known chemical reactions to connect a homogeneous catalyst to a soluble polymeric support has clear benefits over the rather unpredictable immobilization onto insoluble solid supports with their complicated surface morphology. This alternative approach is based on the idea of a significant size enlargement of a molecular catalyst without a differentiation of its molecular and single site properties. The soluble, yet macromolecular nature of the heterogenized catalyst in this case allows for its separation from reaction mixtures using filtration and precipitation techniques and in the end for its recycling for reuse, which includes continuous catalyst operations [2].

Various linear and branched organic polymers have been successfully tested as soluble supports for catalysts, reagents, and substrates [3]. The loading capacity of polymers depends on their branching degree, i.e. branched polymers are potentially superior supports in terms of the amount of supported units per amount of supporting material. For instance, linear monomethoxypoly(ethylene glycol) (MeO-PEG_{5000}) is able to carry only 0.2 mmol catalyst per gram of support, while branched polymers with a branching degree of 50% typically carry at least a tenfold amount of catalyst or even more [4].

Dendrimers are highly symmetrical, hyperbranched organic macromolecules with superb solubility profiles and large sizes and seem ideal supports of choice to arrive at soluble, yet supported homogeneous catalysts. In the case of dendrimers, the degree of branching is close to 100% and, accordingly, a very high theoretical loading can be achieved while maintaining a good solubility.

This chapter focuses on the potential of dendrimers as soluble supports for molecular catalysts. Specifically, we review the different dendrimer families that are used as homogeneous catalyst support, their preparation, the methods for loading and incorporation of catalytic agents onto the dendritic supports, as well as the associated activity. Instead of being comprehensive, we have tried to illustrate the development in the field of dendritic catalysts by presenting selected, yet typical examples.

5.2 Dendrimers

Dendrimers are nanosized, three-dimensional macromolecules that are characterized by a unique tree-like branching structure and compact globular shape in solution (Fig. 5.1) [5–7]. The word "dendrimer" comes from the Greek "δενδρον"/dendron,

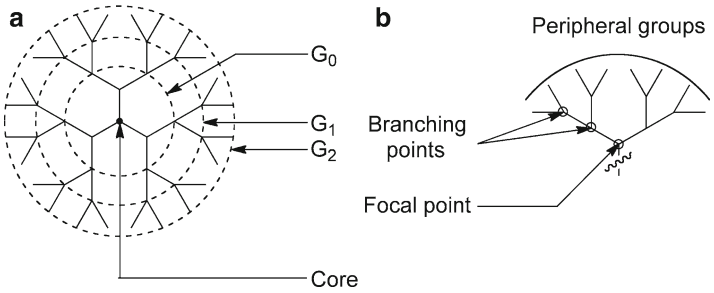

Fig. 5.1 Schematic drawing of a G_2 dendrimer (**a**) and a single dendritic wedge (**b**). Each dashed layer relates to a new generation (G). Peripheral groups form the second generation

meaning "tree" and refers to the singular organization of molecular fragments. Synonymous terms are arborols and cascade molecules.

In 1922 Ingold and Nickolls reported the synthesis of the branched small molecule "methanetetraacetic acid" [8]. This is probably the first example of a directly prepared symmetrically substituted dendritic molecule. Vögtle proposed an iterative methodology toward the synthesis of higher generation dendrimers in 1978 in his paper "Cascade and Nonskid-Chain-like Syntheses of Molecular Cavity Topologies" [9]. In this paper the study and preparation of polymeric branching units with large molecular cavities via repetitive reactions, i.e. exhausted alkylation of amines with acrylonitrile and reduction of newly formed nitriles to primary amines, was described. Only in the middle of 1980s, Tomalia and co-workers reported the first preparation of entire series of dendritic macromolecules, which they called "starburst dendrimers" [10].

Dendrimers are composed of identical "wedges" or dendrons that radiate from a central core in space, forming functional layers of dendritic surfaces. The branching level of dendrons is known as the generation number of a dendrimer (G_n) (Fig. 5.1). This tree-like architecture leads to a predictable geometrical growth of the number of surface groups. Over the past 3 decades, several synthetic strategies were developed to generate multiple dendrimer families with versatile chemical compositions that are useful for a variety of applications in chemistry, biology, and medicine [11].

5.2.1 Properties of Dendrimers

As was described above dendrimers have a well-defined and highly symmetrical molecular structure and a large size. The architectural perfection of such compounds makes them potentially superior supports for homogeneous catalysts, and allows a dispersionless translation of the single-sited nature of molecular catalysts to a heterogenized, dendritic catalyst system with a predefined number of uniform active centers. Hence, this type of dendritic agglomeration of catalytic sites maintains the properties of the single unit at a constant level, while the number of

these units can be tuned in a controllable manner by variation of the nature and architecture of the dendritic support (see also peripheral-functionalized dendrimers, section 5.3.1). The second dendritic strategy of catalyst heterogenization on soluble supports is based on the size-enlargement of a single active site only, via its anchoring to the focal point of a dendron (a single wedge of a dendrimer). This strategy enables the design and synthesis of a defined micro-environment around a catalytic active site (see core-functionalized dendrimers, section 5.3.2).

Both of these concepts toward the immobilization of molecular catalytic sites on dendritic supports are aimed at the creation of continuously active and recyclable catalysts that are easy separable by size-discrimination methods. As for any nanoscaled object, the properties of dendrimes are mostly determined by their surface. This means that the solubility and in particular the hydrophilicity or hydrophobicity of this dendritic material can be adjusted by the mere modification of only the surface terminal groups. This variety and flexibility of dendrimer characteristics is important in the fine-tuning of the retention of dendritic catalysts in membrane reactor technology. In this regard, the heterogenization of molecular catalysts on well-defined soluble supports has become an important research field in homogeneous catalysis. To date several filtration techniques were investigated and optimized at high efficacy for the operation and separation of dendritic catalysts [12–14] (see Chapter 8).

According to these recycling studies, many but not all dendrimer catalysts demonstrate a high stability of their active sites in these processes. In several cases, a predictive additive behavior of the catalytic ensemble of uniform monomolecular units confirms the initial hypothesis about the single-sited nature of the catalysts connected to the dendrimer (neutral dendritic effect). In other cases did the immobilization of a multiple number of catalysts onto a dendrimer provide an alteration of the activity, stability, selectivity etc. of the dendritic catalyst over the (cumulative) properties of its monomeric molecular counter part in either a positive or a negative sense (positive and negative dendritic effects). These findings have pointed out the importance of the choice of the type of dendritic support for particular catalytic reactions. Together, the support and the catalyst connectivity determine the micro-environment of active sites and their isolation or proximity, which in turn is translated on to the catalytic behavior of these sites and explains the observed synergism.

5.2.2 Divergent Dendrimer Synthesis

Divergent dendrimer synthesis represents the assembly of the complete target dendrimer structure from the multivalent core to the periphery by the sequential addition of monomer units (Scheme 5.1) [5].

Starburst dendrimers (the commercial name of PAMAM, polyamidoamine) are the first class of dendrimers that were synthesized using the divergent synthesis strategy [10, 15]. The preparation of each new generation of a PAMAM dendrimer

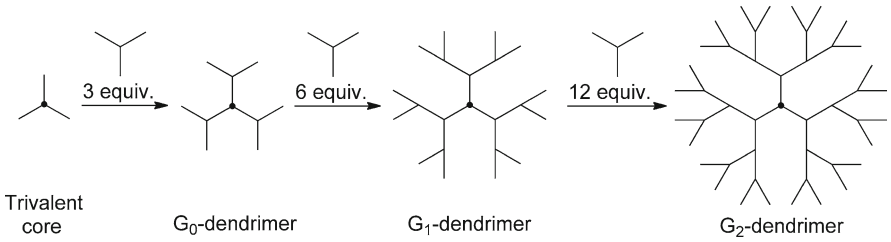

Scheme 5.1 Schematic depiction of the divergent method for the synthesis of dendrimers

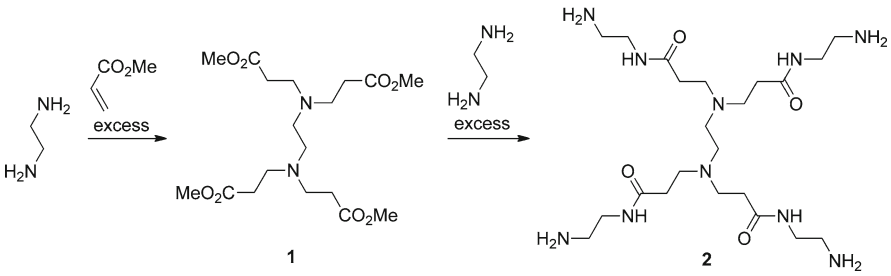

Scheme 5.2 Synthesis of G_0-NH_2 as an example of the divergent synthesis of PAMAM dendrimers

is a two-step process. In the very first step ethylene diamine (EDA) as a tetravalent core is subjected to exhaustive Michael addition of methylacrylate monomers. The resulting aliphatic tetra-ester intermediate **1** subsequently undergoes aminolysis with excess of EDA in the second step to give G_0-PAMAM **2** (Scheme 5.2), which in its own turn serves as a multivalent core for the synthesis of the next generation of PAMAM dendrimer and so on.

Yet, no single chemical process possesses an absolute efficiency due to side reactions and/or the existence of thermodynamic equilibria. In the case of dendrimer synthesis it signifies an inescapable presence of a certain amount of defects in the real dendrimer structure. For instance, amino groups that have not reacted in the Michael addition with methylacrylate, as well as EDA molecules, can participate in a further aminolysis step leading to the formation of intra- or intermolecular links. Even the statistical elimination of whole dendrons is allowed thermodynamically via retro-Michael addition. Large molar excesses of reagents and thorough purification after each step, along with careful thermal control of synthetic processes are used to limit these undesirable side reactions.

The main inherent drawback of any divergent synthesis is a serious reduction of the product yield after a large number of required reaction steps. In the case of dendrimers it also introduces statistically distributed and progressive defects in their structure from generation to generation, that strongly affects the dispersity of the product material.

5.2.3 *Convergent Dendrimer Synthesis*

The convergent schemes in organic synthesis are characterized by usually higher yields of the target product and seem to be superior over divergent schemes in dendrimer assembly [5]. In convergent synthesis, complete dendrimer wedges (dendrons) are prepared prior to their connection to a multivalent core in the last step (Scheme 5.3).

Hawker and Fréchet applied this approach in 1990 for the preparation of poly(aryl benzyl ether) dendrimers. The first step of their dendron synthesis is the regioselective base-catalyzed reaction between 5-(hydroxymethyl)benzene-1,3-diol **3** and bromomethylbenzene [16]. Nucleophilic transformation of the unreacted hydroxymethyl group of the product into the corresponding bromomethyl derivative gives a G_1-dendron **4a** that is able to react with a next portion of 5-(hydroxymethyl) benzene-1,3-diol (Scheme 5.4). This procedure can be repeated until the desired generation is reached, while generating all smaller dendron generations along the line (Fig. 5.2). Finally in the last step of this convergent dendrimer synthesis, G_n-dendrons are attached to 4,4′,4″-(ethane-1,1,1-triyl)triphenol that serves as a trivalent core forming dendrimers **5** (Fig. 5.2).

According to the described strategy, dendrimers up to G_6 were synthesized as almost monodisperse macromolecules (polydispersity index 1.01–1.02). The achieved high purity of the dendrimers is a result of the significant size difference between the target dendrimer and any possible byproduct in the last synthetic step, which facilitates a size-discriminative separation.

In the case of dendrimer synthesis, the last step of the assembly is associated with the reaction of several bulky dendrons with a relatively small core. As a result of the increasing steric hindrance around the dendrimer core after each subsequent introduction of a new wedge, the yields of the target dendrimers are usually moderate or even low. For instance, the chemical yield of the last step of the considered poly(aryl benzyl ether) dendrimers drops from 84% for G_4 to 51% for G_6.

Summarizing, while the divergent approach is convenient for assembling relatively small dendrimers or dendrons, the synthesis of monodisperse, higher generation analogues is an unfeasible task using this approach. The more elaborate convergent approach, on the other hand, is intended for the preparation of dendritic molecules of high purity, but suffers from unsatisfactory yields once applied in the synthesis of higher generation dendrimers due to steric obstacles in the last synthetic step.

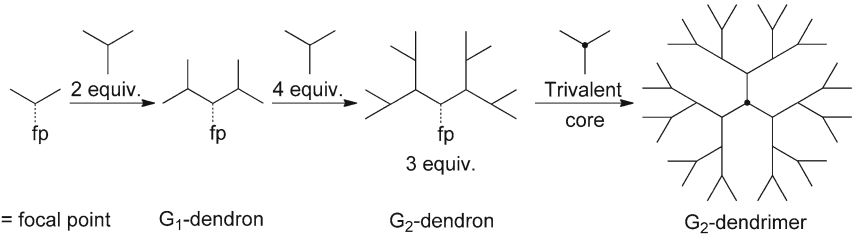

Scheme 5.3 Schematic depiction of the convergent method for the synthesis of dendrimers

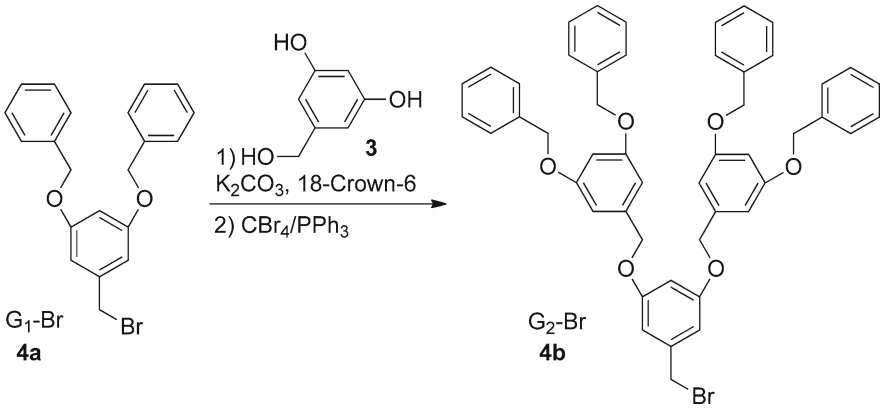

Scheme 5.4 Synthesis of Fréchet-type G_2-dendron

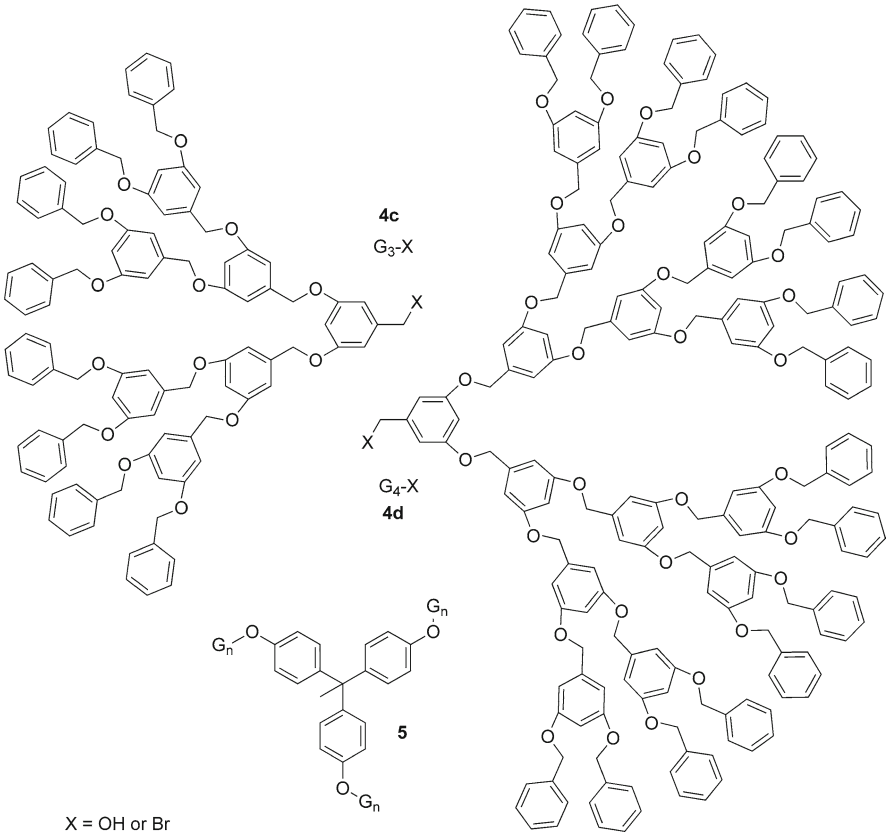

Fig. 5.2 Fréchet dendrons and dendrimer

5.3 Functionalization of Dendrimers

5.3.1 Peripheral-Functionalized Dendrimers

Periphery-modified dendrimers bear numerous catalytic sites at their surface that are directly available to the substrates. In a first approximation any deviation in catalyst behavior after immobilization in this manner is determined by the proximity of elemental sites on a dendrimer. From this point of view the manifestation of a positive dendritic effects can be expected in systems where two or more elemental sites form an active ensemble, i.e. when the kinetic order in catalyst is larger than one. If such agglomeration is undesired and enables side reactions or leads to catalyst deactivation, the prudent choice of support and level of peripheral catalyst loading are crucial to minimize the potential negative impact of peripheral active site accumulation. One of the first published examples of a dendrimer-immobilized catalyst with transition metal active sites was developed and exhaustively studied by the Van Koten group [17]. In particular, NCN-pincer nickel complexes were supported on G_0 and G_1 carbosilane dendrimers.

The selected mononuclear pincer nickel complex demonstrates good results in the regioselective Kharasch addition of polyhalogenoalkanes to terminal alkenes (Scheme 5.5) and is remarkably robust toward self-degradation. The latter stability factor is a prerequisite feature for continuous catalyst usage – the final purpose of immobilization. The highly energetic character of the active high-valent metal species and radicals participating in the Kharasch reaction, furthermore, puts some serious limitations on the nature of the supporting material and asks for a supporting material of very high chemical integrity. In this light carbosilane dendrimers are excellent supports for the chosen catalysts as these are highly resistant toward radical cleavage and have a generally high chemical integrity.

The synthesis of dendritic carbosilane supports is straightforward and includes only two repetitive and quantitative steps: (a) Grignard reaction between a slight excess of freshly prepared allylmagnesium bromide and a chlorosilane compound ($SiCl_4$ or various dendrimers with "$SiCl_n$" end-groups) and (b) hydrosilylation reaction of previously introduced allylic fragments with an appropriate hydrosilane ($HSiCl_3$, $HSiMeCl_2$ or $HSiMe_2Cl$) using a Pt-catalyst (Scheme 5.6).

The immobilization of NCN-pincer nickel complexes on G_0 and G_1 dendrimers was carried out in two steps. First, a special derivative of the prototypical NCN-pincer ligand furnished with a tethered hydroxyl group (OH~NCN) was attached to the carbosilane dendrimer periphery by a stoichiometric alcoholysis reaction with peripheral dimethylsilylchloride groups. The subsequent oxidative addition of

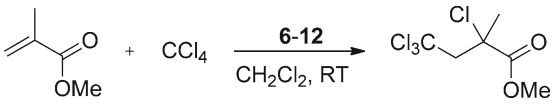

Scheme 5.5 Kharasch addition catalyzed by a metallodendrimer

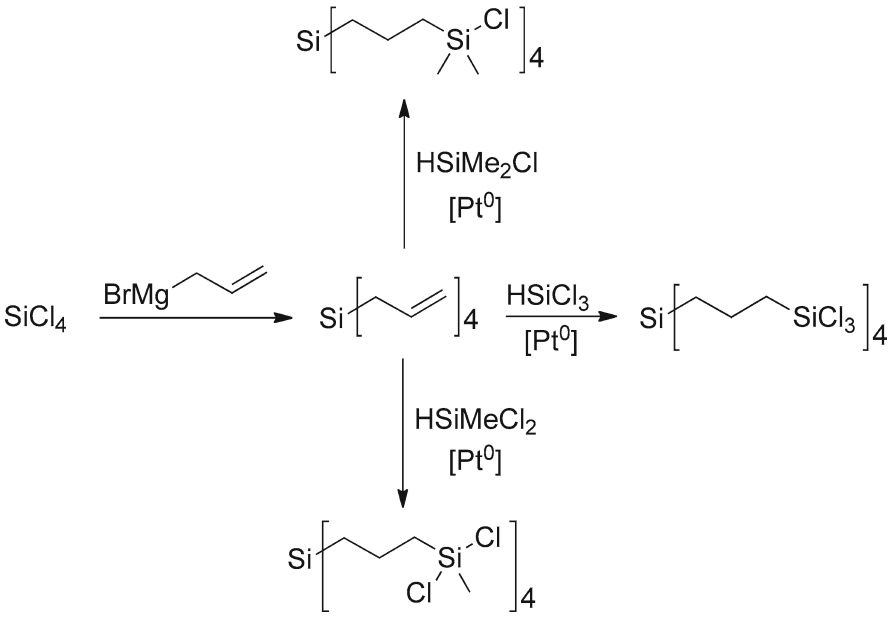

Scheme 5.6 Synthesis of carbosilane dendrimers

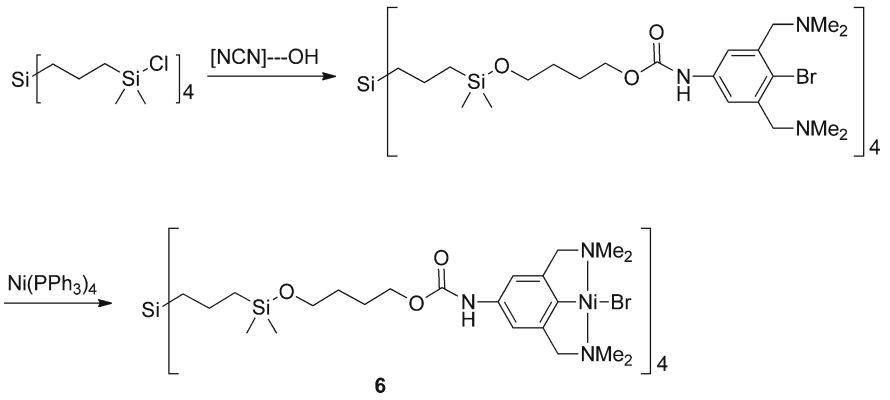

Scheme 5.7 Synthesis of Van Koten's G_0 metallodendrimer

$Ni(PPh_3)_4$ to the immobilized ligand in the second step provided the target metallodendrimers **6** and **7** (Scheme 5.7 and Fig. 5.3).

These Ni-containing dendrimers are active catalysts for the Kharasch reaction much like the monomeric catalyst. The neutral dendritic effect observed in this reaction confirms that a high level of isolation and uniformity of active sites was achieved upon catalyst immobilization. Moreover, the metallodendritic catalysts are nanosized and highly soluble; these physical properties along with the absence of nickel leaching

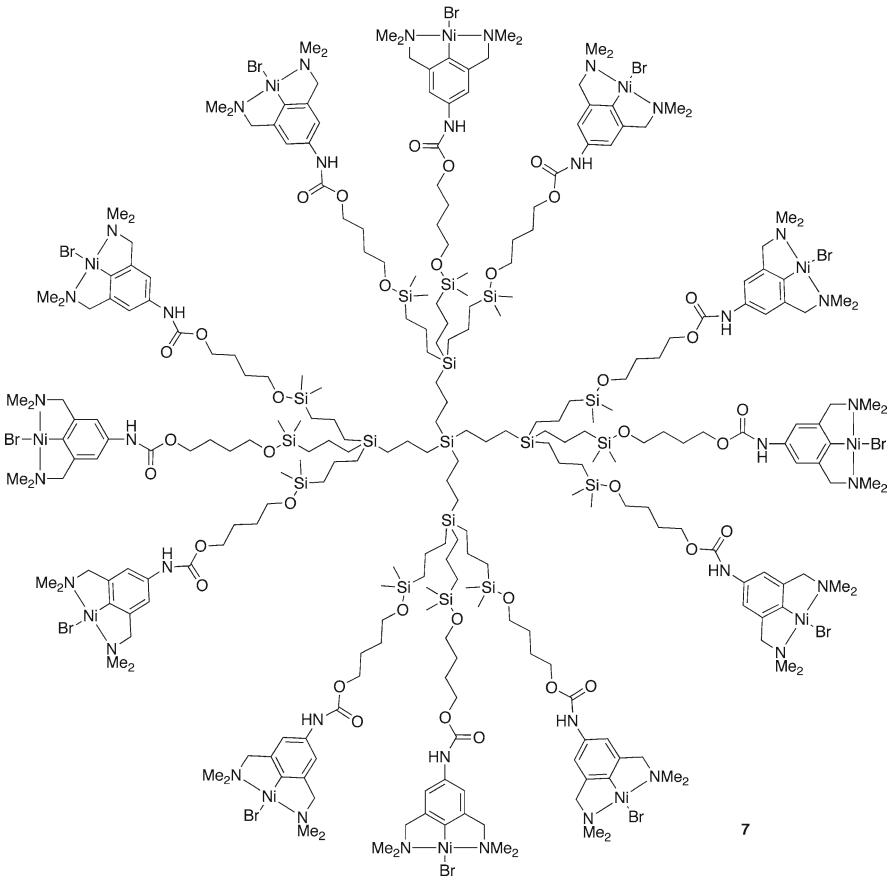

Fig. 5.3 Van Koten's carbosilane G_1 metallodendrimer

make them amenable for homogeneous catalytic applications in nanofiltration membrane reactor set-ups. Overall, this first report on dendrimer-supported catalysts stimulated the development of a new research area in catalysis, i.e. heterogenization of homogeneous catalysts on nanosized, well-defined soluble supports.

Based on these preliminary results, a small library of nickel containing dendrimers (Fig. 5.4) was prepared by Van Koten et al. to estimate the influence of active site proximity – the main factor affecting the catalyst performance in the Kharasch reaction [18, 19]. Also the applicability of the new dendritic catalysts in nanofiltration membrane reactors was comprehensively studied.

The concentration of active sites was tuned through the introduction of different "spacers" in the dendritic framework by changing the substitution patterns at the branching points.

In this study, the metallodendrimers were synthesized starting from a carbosilane dendrimer with terminal $–SiMe_2$-Cl groups via quenching with a para-lithiated

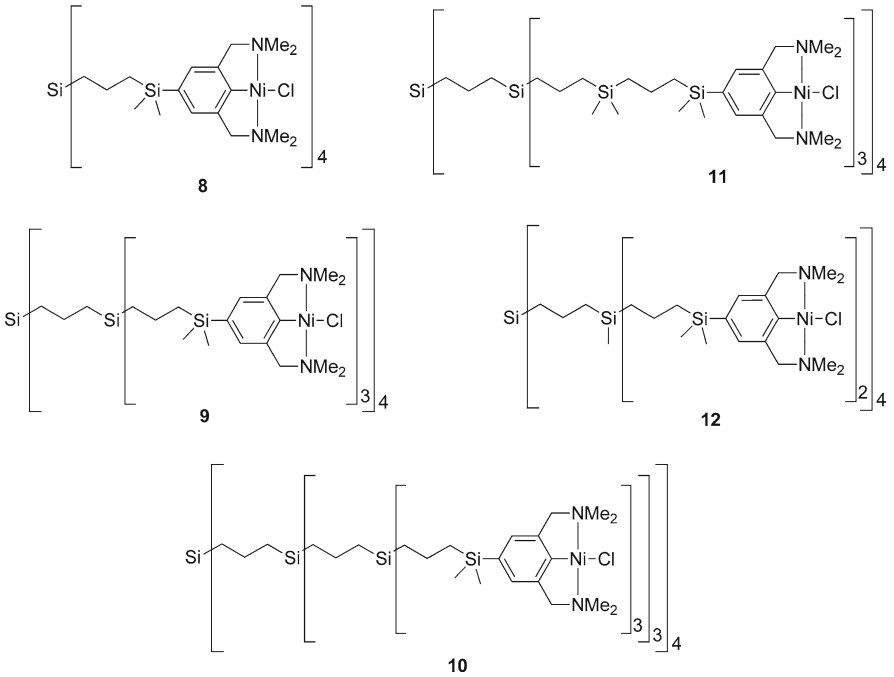

Fig. 5.4 Structure of Van Koten's carbosilane-based catalysts

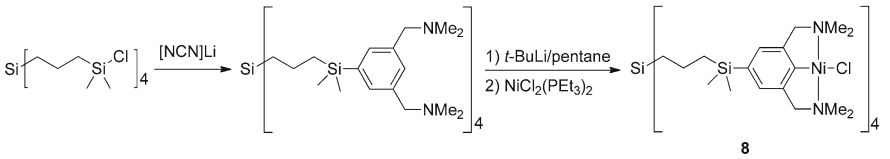

Scheme 5.8 Synthetic pathway for Van Kotens's Ni-based carbosilane metalodendrimers as shown for G_0

NCN-pincer ligand. Subsequent selective deprotonation between the NMe_2-arms of the NCN-pincer ligand with *t*-BuLi and transmetallation with $NiCl_2(PEt_3)_2$ afforded the Ni-containing catalysts (Scheme 5.8). Spectroscopic and elemental analysis indicated that a high level of nickellation (80–90%) was achieved, which corresponds to quite good yields of 90–95% for the last two, synthetically challenging steps.

These dendritic catalysts were examined in the Kharasch addition reaction for which a remarkable degree of variation in activity was observed. The zeroth-generation metallodendrimer G_0-**8** (4 Ni sites) exhibited a similar catalytic activity per Ni-site as its monomeric counterpart. The activity of the first-generation metallodendrimer G_1-**9** (12 Ni sites) was two times less active than G_0-**8** and exhibited significant catalyst deactivation after 1 h (characterized by the formation of a purple precipitate), whereas

the second-generation metallodendrimer G_2-**10** (36 Ni sites) was almost inert. The alternative metallodendrimers G_1-**11** and G_1-**12**, in which the branches are enlarged or the number of peripheral nickel sites is smaller compared to the standard first generation metallodendrimer G_1-**8**, respectively, did not show any sign of catalyst degradation and full substrate conversion was achieved within 22 h.

To explain the observed catalyst deactivation, the authors considered the mechanism of the Ni(II)-catalyzed Kharash addition (Scheme 5.9): in the first step Ni(II) reacts with CCl_4 and forms a Ni(III) species (persistent radical) and a $^{\bullet}CCl_3$ transient radical (initiation of radical chain). The transient radical reacts with a molecule of methylmethacrylate (growth of radical chain) and the newly formed adduct subsequently reduces Ni(III) back to Ni(II), to form the desired addition product (termination of radical chain). In principal, all radical reactions suffer through statistical recombination of active radical species. In this case, the irreversible coupling of two $^{\bullet}CCl_3$ units results in a "half-way" reaction interruption and in the unproductive consumption of CCl_4. The probability of this undesired radical recombination is second order in the transient radical concentration, which makes this process dominant over the Kharash addition (first order in radical concentration) at higher concentrations of $^{\bullet}CCl_3$ species. By extending the spacer length or decreasing the number of peripheral Ni-sites (as is the case for G_1-**11** and G_1-**12**, respectively), the local peripheral radical concentration under the reaction conditions is drastically reduced, along with the rate of catalyst deactivation, to yield metallodendrimers that indeed behave as single-site catalysts in the Kharasch Addition.

Evidently, the non-productive reaction conditions correspond to dendrimers with a high peripheral concentration of active sites (the amount of $^{\bullet}CCl_3$ radicals depends linearly on catalyst concentration) and correlates well with the experimentally

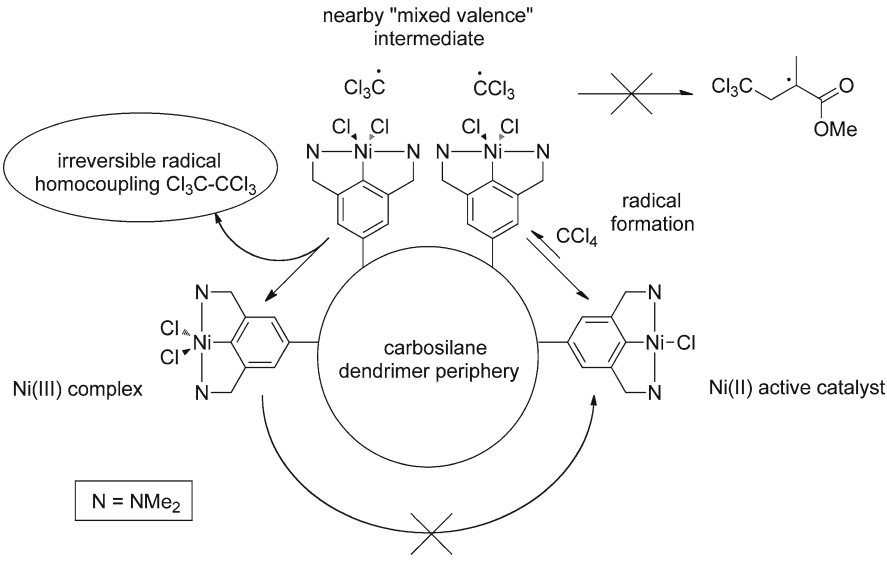

Scheme 5.9 Proposed deactivation pathway for Van Koten's catalysts in the Kharasch addition

observed deactivation trend. These model catalysts, therefore, demonstrate how peripheral catalyst accumulation can lead to negative effects on catalyst activity, and how catalyst activity can be 'restored' by peripheral catalyst 'dilution'.

The pincer-based carbosilane dendrimers G_0-**8** and G_1-**9** were tested for their degree of retention in a membrane reactor equipped with a SelROMPF- 50 nanofiltration membrane. Their retentions are 97.4% for G_0 -**8** and 99.75% for G_1-**9**, indicating that the larger dendrimer (G_1-**9**) is sufficiently retained. Applying the G_1-**9** dendrimer in a continuous flow membrane reactor (CFMR), a significant loss of catalytic activity was observed over 33 h. After continuous membrane reactions (after the reactor volume was replaced 64 times), tests of the retained and filtered fractions indicated that the membrane retained the catalyst at 98.6% (which closely resembled the measured retention found earlier in batch-wise processes for this catalyst). Although this degree of retention leads to some loss of catalytic material in the continuous membrane reactor, it could not solely explain the observed deactivation of G_1-**9** in the reactor. It was, therefore, proposed that the reactive radical intermediates might be interacting with the functional groups of the membrane material and thus influencing the overall reactivity. While the catalyst was effectively retained, it was concluded at that time that new membranes compatible with the reaction conditions used were needed to successfully construct a useful system for continuous operation.

Opposed to the negative dendritic effect observed by Van Koten and co-workers, a positive dendritic effect on the catalytic activity of metallodendrimers was shown in an elegant study by Jacobsen et al. on the hydrolytic kinetic resolution (HKR) of terminal epoxides [20] (Scheme 5.10). This reaction is catalyzed by cobalt(salen) complexes and involves substrate and nucleophile activation by two different catalyst moieties [21]. Theoretically, the proximity of catalyst moieties might result in increased reaction rates in this case due to the bimetallic structure of the transition state, i.e. the second order kinetic dependence on catalyst concentration.

The chiral [Co(II)salen] units were attached to several generations of PAMAM dendrimers through an amide linker via the reaction with activated ester **14** (Scheme 5.11). The obtained crude metallodendrimers were purified by precipitation from a saturated THF solution with hexane and subsequently subjected to size-exclusion chromatography with Sephadex. The final step of the preparation of the active dendritic [Co(III)salen] catalysts was the stoichiometric oxidation of the immobilized [Co(II)salen] groups with molecular iodine in THF.

The activity for HKR of **13** using 0.027 mol% of G_1-PAMAM dendrimer **16** with 8 Co units (Fig. 5.5) was firstly studied. Complete resolution of the racemic epoxide occurred after 20 h, whereas the monomeric catalyst was almost inactive at such low concentrations. This observation can be rationalized by the relatively high local

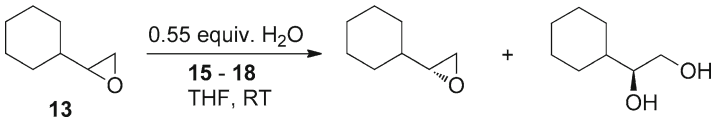

Scheme 5.10 The HKR reaction of epoxide isomers

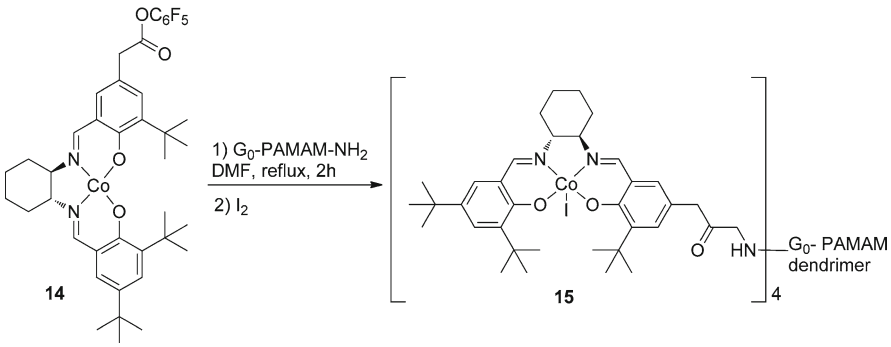

Scheme 5.11 Synthesis of PAMAM-immobilized Co-catalysts for the HKR reaction of terminal epoxides

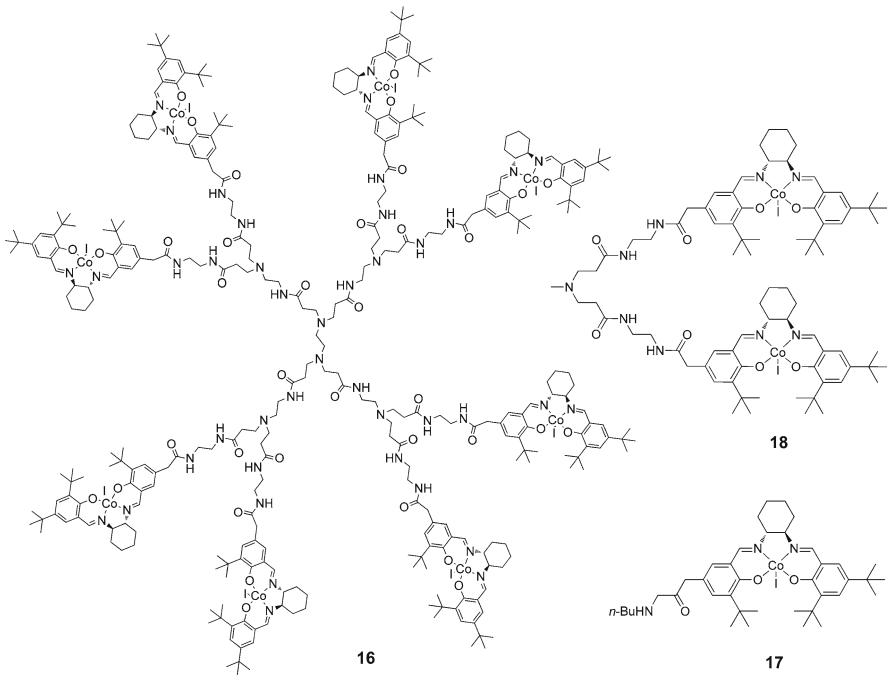

Fig. 5.5 Structures of a G_1 [Co(salen)] dendritic catalyst and model compounds

concentration of active sites connected to one and the same dendrimer. A comparison of the catalytic activity of the monomeric complex and compound **17** also showed a positive electronic influence of the amide linker on the catalyst activity. Nevertheless, this effect is much smaller than the accelerating effect found with the dendritic catalysts, and the close proximity of a second complex moiety is the determinant condition for the increased resolution rate as exemplified by the enhanced resolution rate of the simple bimetallic compound **18**.

The optimal reaction rate was found for G_0-**15** catalyst (Scheme 5.11) where only four salen molecules are conjugated to the dendrimer. It therefore seems that a particular molecular geometry is required for the HKR reaction, which for this series of macromolecules is best obtained in the G_0 dendrimer generation.

Sometimes positive dendritic effects are not only displayed by an increased kinetic behavior of the dendritic catalyst relatively to the monomeric activity of catalyst, but also by the improved characteristics of target products. Such a positive influence of catalyst microenvironment (steric and dielectric tuning of the active site) was observed in an ethylene polymerization study using carbosilane-immobilized bis(imino)pyridyl iron(II) catalysts, carried out by Zheng and coworkers [22]. In this study, zeroth- and first-generation iron metallodendrimers were synthesized in a divergent manner: the ligand **19** furnished with an allylic fragment was anchored to G_0 or G_1 carbosilane dendrimers via a Pt-catalyzed hydrosilylation reaction in 68% and 43% yield, respectively, and was subsequently treated with a stoichiometric amount of $FeCl_2{\cdot}4H_2O$ to furnish the desired metallodendritic compounds (Scheme 5.12 and Fig. 5.6).

The polymerization of ethylene were carried out in toluene under 1 bar pressure of ethylene using the iron metallodendrimers and the parent mononuclear complex as a benchmark catalyst in the presence of activator-modified methylaluminoxane (MMAO). At Al/Fe molar ratios above 1,200, the catalytic activities of the dendritic and mononuclear catalysts are comparable. Yet, both metallodendrimers **20** and **21** yielded polyethylenes (PE) of much higher molecular weights and with higher melting temperatures. At lower Al/Fe ratios, the difference in activity of the immobilized catalysts from the benchmark catalyst becomes significant. For instance at Al/Fe = 500, the iron metallodendrimers are more than two times more active than the corresponding monomolecular complex ($2.5{\cdot}10^3$ kg PE/$mol_{Fe}{\cdot}h{\cdot}bar$ vs. $1.14{\cdot}10^3$ kg PE/$mol_{Fe}{\cdot}h{\cdot}bar$) and produce heavier polymers (M_w~137 kg/mol vs. 62.5 kg/mol) with higher melting temperature (T_m~134°C vs. 128°C).

The noticeable lowering of monomolecular catalyst activity is the predictable response on a decrease of activator (MMAO) content in this reaction. At the same time, the activity of the dendritic catalysts does change slightly over the broad range of Al/Fe ratios that were studies. These results indicate that the catalytic iron

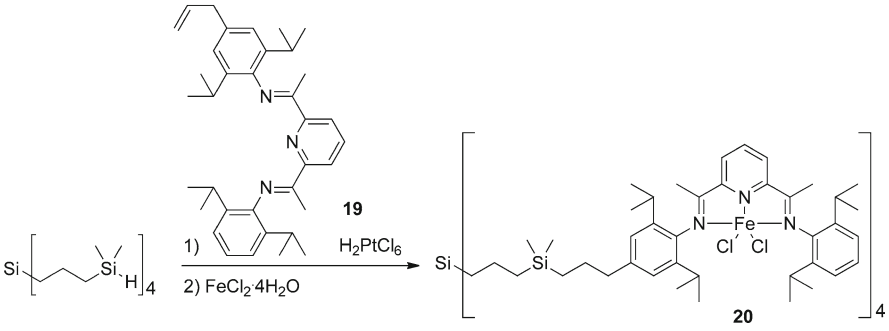

Scheme 5.12 Synthesis of carbosilane-immobilized Fe-catalyst **20** for ethylene polymerization

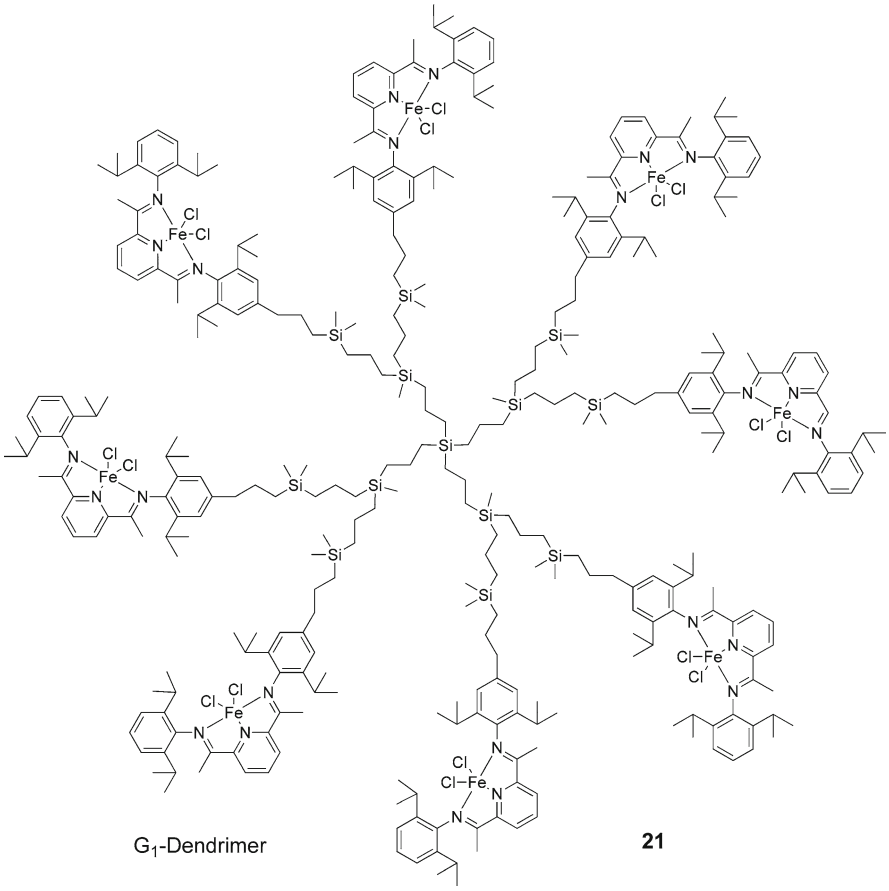

Fig. 5.6 Zheng's G_1 catalyst for ethylene polymerization

site is sterical hindered and therefore stabilized by both dendrimer support moieties as well as by MMAO. Moreover, enforced steric crowding around the active center can decrease the probability of chain transfer reactions during ethylene polymerization to a certain extent and can create favorable conditions for the production of mostly linear PE with higher M_w.

Gade et al. have reported on the immobilization of BINAP ligands on polypropylene imine (PPI) dendrimers (Scheme 5.13) and hyperbranched polymers [23]. Up to the fifth generation dendrimers were successfully synthesized and the corresponding dendritic BINAP-copper(I) complexes were used in the enantioselective hydrosilylation of acetophenone (Scheme 5.14).

The enantioselectivities and activities of the dendritic AMINAP-based catalysts **22** remained almost unchanged upon immobilisation and do not depend on the dendrimer generation. A considerable variation of stereoinduction was observed for G_0–G_5 dendrimers **23** with 4–64 immobilized catalyst units without linker moieties. The first

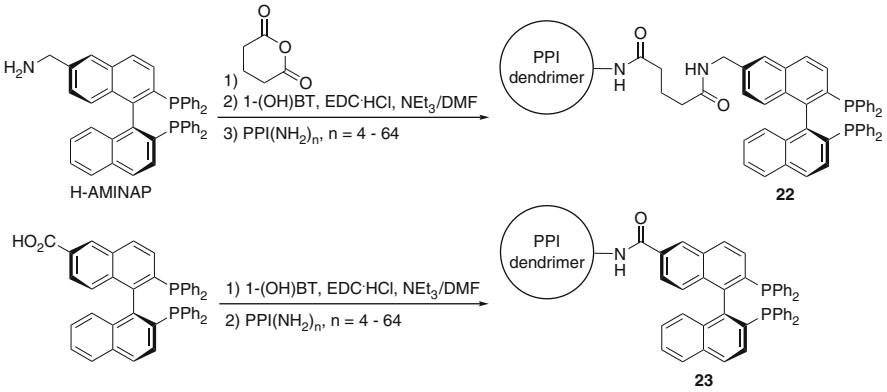

Scheme 5.13 Immobilization of BINAP on PPI dendrimers

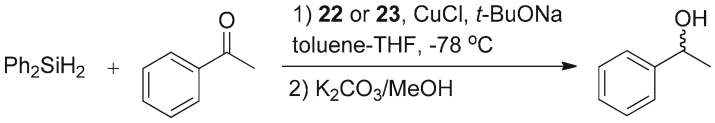

Scheme 5.14 Copper-catalyzed hydrosilylation of acetophenone

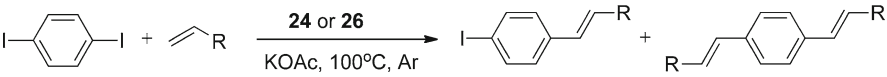

Scheme 5.15 Heck reaction of p-diiodobenzene with olefins using Pd complexes

generation system catalyzed the reaction with a selectivity of only 34% ee and the fifth generation dendrimer reached 90% ee. On the other hand, the reaction time required for complete conversion increased from 24 to 96 h upon going from the mononuclear catalyst to the lower generation dendritic catalysts, whilst decreasing again for the higher generation dendrimers. Decreasing of the CuCl amount from 1 to 0.5 equiv. per BINAP led to an increase in enantioselectivity to 93–95% ee for catalysts **23**.

The G_5-**23** catalyst was removed from the reaction mixture via precipitation and then reused in three successive catalytic runs without loss of activity (TOFs at 50% conversion of 4.7 h^{-1}) or enantioselectivity.

Remarkably, the catalytic characteristics of the hyperbranched polyethyleneimine (PEI)-immobilized BINAP system in this reaction remained unaltered within the range of 9–138 BINAP units per polymer molecule.

Kaneda and co-workers have reported on the control of product selectivity in Pd-catalyzed Heck reactions (Scheme 5.15) and allylic aminations (Scheme 5.16) through the tuning of the dendrimer microenvironment [24].

In this study, the catalysts were assembled by a novel non-covalent approach from decanoyl-terminated polypropylene imine (PPI) dendrimers, (G_2-**24**, G_3 and

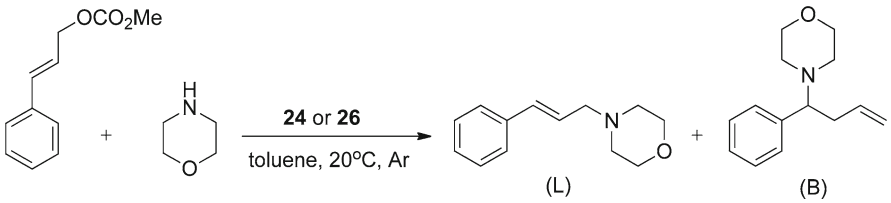

Scheme 5.16 Allylic amination using dendrimer-encapsulated Pd complexes

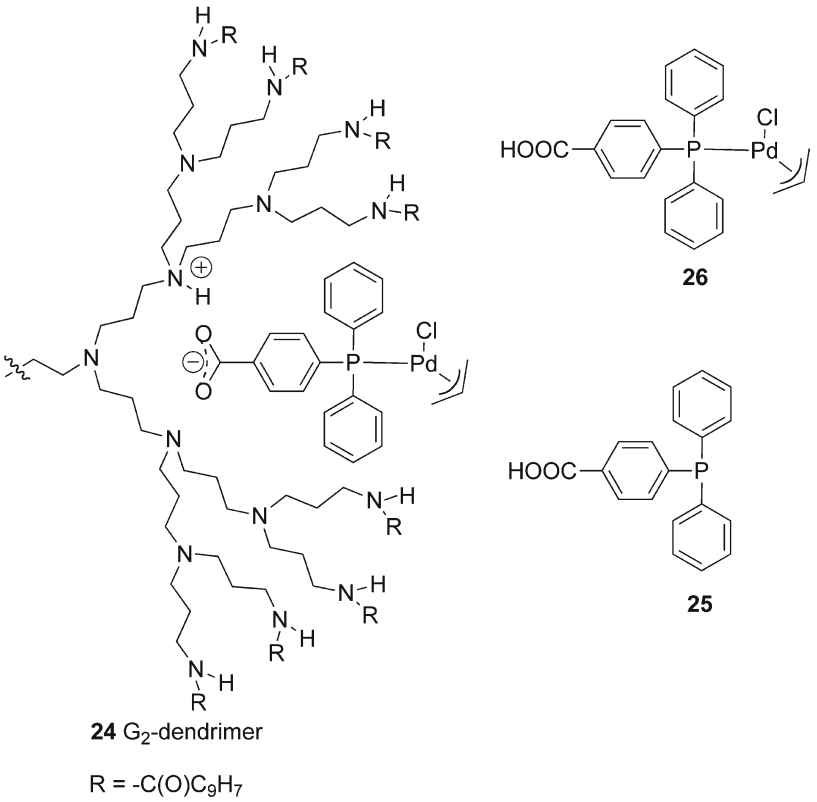

Fig. 5.7 Non-covalent immobilization of anionic Pd-phosphane complexes on PPI dendrimers

G_4) and 4-diphenylphosphinobenzoic acid **25** as the phosphine ligand to locate the Pd complex inside the dendrimers (Fig. 5.7). The formation of ionic bonds between the benzoic acid-derived phosphine ligand and internal tertiary amine moieties of the dendrimer was confirmed by means of ^{31}P, ^{13}C, and ^{1}H-NMR. In this way, the dendrimer encapsulates the Pd complexes and acts as a unique nanoreactor for these versatile catalytic moieties.

In fact, the Heck reaction between iodobenzene and n-butyl acrylate is accelerated with each new generation of dendritic catalyst (Pd/P ratio is 1:1), while in the absence

of the dendrimer no catalytic activity was observed. A similar reaction between 1,4-diiodobenzene and n-butyl acrylate (Scheme 5.15) using the G_4 dendritic catalyst shows a high selectivity toward the mono-Heck coupling product (mono:di=92:8), while the monomeric catalyst **26** possesses a poor selectivity (mono:di=45:55). These experiments strongly suggest that catalysis occurs inside the dendrimers.

In contrast to the case of Heck reactions, the rate of the allylic amination reaction of cinnamyl methyl carbonate with morpholine decreases with increasing dendrimer generation (Scheme 5.16). The same dependence characterizes the rate of olefin hydrogenation by these immobilized catalysts [25]. Probably, the surface overcrowding of the higher-generation dendrimers suppresses the penetration of substrates inside the dendritic nanoreactors. However, such a discrimination effect on the reaction rates was not observed in the above Heck reactions [26].

The predominant formation of linear (L) against branched (B) product in the allylic amination reaction usually occurs in more polar media [27]. The observed L/B rates in the amination reaction carried out with the non-covalently immobilized catalysts in toluene were higher than for the monomolecular catalyst. This fact can be considered as an additional evidence of the influence of the molecular support microenvironment on the active site of the embedded Pd catalyst.

Recycling of the immobilized catalysts derived from decanoyl-terminated dendrimers via precipitation or membrane filtration resulted in some loses of catalytic activity. Modification of the PPI dendrimer with 3,4,5-triethoxybenzoyl chloride instead of decanoyl chloride afforded dendrimers that are amenable for continuous usage and recycling. These dendrimers are well soluble in polar DMF and insoluble in heptane. In the allylic amination of cinnamyl methyl carbonate with piperidine, the thermomorphic phases of DMF and heptane became homogeneous during the reaction at elevated temperature and could be readily separated by cooling the reaction mixtures, where the DMF-phase containing the dendritic material was recycled after decantation from the heptane phase containing the product. This procedure was repeated four times without any catalyst deactivation.

Similar non-covalent approaches to catalyst immobilization on dendrimers were also described by Van Leeuwen [28], Van Koten [29] and Klein Gebbink [30] and have been put forward as facile procedures for dendrimer modification and alteration.

5.3.2 Core-Functionalized Dendrimers

Dendritic effects in core-functionalised dendrimers mainly arise from the site isolation created by the dendritic microenvironment. The steric crowding of a dendritic catalytic core can enhance the stability of the “immobilized” catalyst. At the same time, core immobilization generally suffers from a significantly reduced reaction rate by the catalyst due to the decreased accessibility of the active site. However, in cases where stability determines the overall catalyst activity, dendronization becomes an attractive solution to reach the maximum performance of an expensive catalyst.

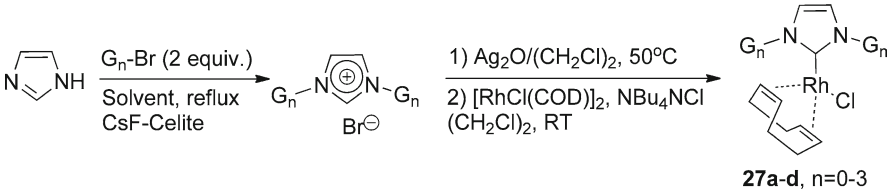

Scheme 5.17 Synthesis of a dendronized Rh-catalyst for the hydrosilylation of ketones

Tsuji et al. applied this concept for the functionalization of rhodium (I) centers with dendritic N-heterocyclic carbenes (NHC) [31]. The straightforward synthesis of these dendritic complexes includes the preparation of G_0–G_3 Fréchet-type dendrons (Scheme 5.4 and Fig. 5.2) and anchoring two equivalents of these to one molecule of imidazole via N-alkylation reactions (Scheme 5.17). Subsequently, silver adducts of the corresponding carbenes were generated from the imidazolium salts by typical treatment with Ag_2O [32]. Finally, these Ag-bis-carbene complexes were subjected to transmetallation with dimeric $[RhCl(COD)]_2$, forming the target metallodendrimers **27a–d**.

These dendritic compounds were employed as catalysts for the hydrosilylation of ketones (acetophenone and cyclohexanone). A positive dendritic effect was observed through an increase in product yield with increasing dendrimer generation. In the hydrosilylation of acetophenone, the product yield was not sensitive toward moderate dilution of the reaction mixture for the G_1–G_3 complexes **27b–d**; however, it dropped from 62% to 44% at 0.41 and 0.29 M substrate concentration in case of the smallest **27a** G_0 metallodendrimer. These observations suggest that the reported dendronized catalysts suffer from mass transfer limitations at the experimental reaction concentrations, except for the G_0-catalyst **27a**.

Cyclic voltammograms of these complexes were recorded in CH_2Cl_2 with *n*-Bu_4NClO_4 as the supporting electrolyte and showed similar irreversible metal-centered oxidation peaks for **27a–c**. In turn, the G_3-**27d** dendrimer does not exhibit a distinguishable oxidation peak, which confirms the essential shielding of the metal core by the bulky dendritic wedges. Based on these observations the authors proposed that for these dendritic Rh-complexes the total turnover number of the monomolecular catalyst increases after the immobilization because the created microenvironment of the metal core suppresses deactivation processes rather than the main catalytic reaction.

In 1999 the group of Van Leeuwen reported the synthesis of a family of core-functionalized carbosilane dendrimers derived from bis(diphenylphosphanyl)ferrocene (dppf) [33]. These macromolecules (G_0–G_2) were assembled from four carbosilane dendrons with an aryl lithium focal point, derived from the corresponding aryl bromide, and ferrocenyl bisphosphonite (Scheme 5.18). Dendrimers with allylsilane moieties at their periphery (R = allyl) were tested as ligands in the palladium-catalyzed allylic alkylation reaction (Scheme 5.19). The complexation of the dendritic dppf ligands with $[PdCl_2(MeCN)_2]$ was monitored by ^{31}P NMR spectroscopy, which confirmed a similar ligand coordination as in monomeric dppf complexes, i.e. one

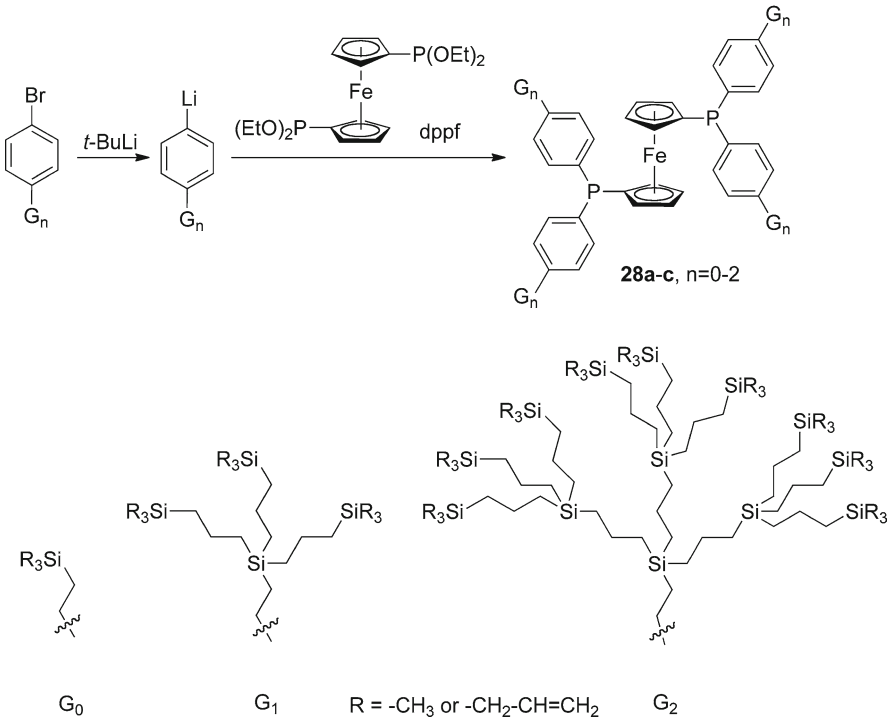

Scheme 5.18 Synthesis of Van Leeuwen's core functionalized ferrocenyl-phosphine carbosilane dendrimers and the structure of their dendrons

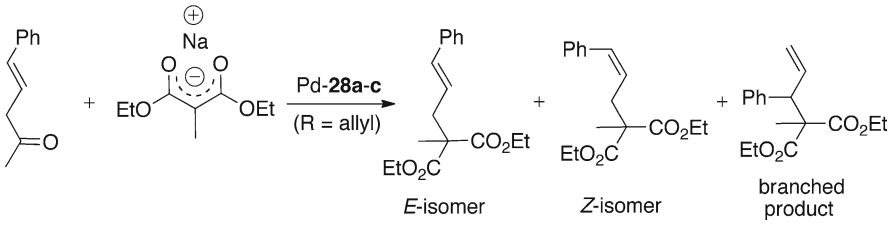

Scheme 5.19 Pd-catalyzed allylic alkylation reaction

bidentate phosphine ligand chelates palladium in a *cis* fashion. In order to perform the catalytic reactions, the active palladium catalysts were generated *in situ*, mixing the selected phosphine ligand and crotylpalladium chloride $[(\eta^3\text{-}C_4H_7)PdCl]_2$ (molar ratio P/Pd = 2:1) in THF followed by addition of the reaction substrates and a base.

Similar substrate conversions were detected for the dendrimers **28a–c** and the monomeric dppf complex, indicating that the peripheral allylic end groups do not participate in the catalytic reaction. The activity and regioselectivity of the alkylation reaction changed with the dendron generation. An increase in the size of the ligand resulted in a decrease in reaction rate, as expected for a restricted

accessibility of the metal centre. Larger dendritic ligands also favoured the formation of the minor, branched product. A change in the local microenvironment caused by the apolar dendritic shell was proposed as one of the possible origins of the modified product selectivity.

The applicability of this type of dendritic catalyst in a CFMR was tested for G_2-**28c**. It was observed that the catalytic activity remained almost constant for up to 8 h of reaction time. Although resulting in an overall lower activity per catalytic center, the location of the catalytic site within the dendritic sphere seems to protect the active species against deactivation via interaction with the membrane or with other metallodendritic species.

Diphosphine core-functionalized dendrimers with a methyl group on the periphery (R = Me, Scheme 5.18) were applied as ligands in the rhodium-catalyzed hydroformylation and hydrogenation of alkenes [34]. For the hydrogenation of dimethyl itaconate (Scheme 5.20), the rhodium catalyst was formed *in situ* via the reaction of $[Rh(nbd)_2]_2(ClO_4)$ (nbd = 2,5- norbornadiene) with the diphosphine dendritic ligand (molar ratio P/Rh = 2). All dendritic dppf-type ligands gave active hydrogenation catalysts with activities similar to the monomeric dppf ligand under the same reaction conditions. In a CFMR, however, the reaction applying the rhodium catalyst of dendrimer G_1-**28b** (R = Me) gave a higher maximum conversion and was more stable over time (77–85% of conversion for 35 reactor volumes) than dppf itself (15–70% of conversion for 35 reactor volumes). The lower conversion observed with dppf was attributed to its lower rate of hydrogenation compared to G_1-**28b** and to leaching of the active Rh–dppf complex.

ICP–AES analysis (induced coupled plasma atomic emission spectroscopy) was performed on the reactor permeate, which showed that the amount of metal leaching is similar to that of the phosphine ligand, i.e. the molar ratio P/Rh is 2 in the permeate. This indicated that the ligand–metal interaction was sufficiently strong under the applied reaction conditions. In addition, measurements on the parent ligands in the membrane reactor showed a retention of 87.5% for dppf and 99.4% for G_1-**28b**, indicating a significantly enhanced retention behavior of the "dendronized" dppf ligands.

The steric crowding of a Mn(III) porphyrin core increases the regioselectivity of the catalyzed olefin epoxidation reaction as was shown by Suslick et al [35]. Within this study a family of oxidatively robust poly(phenylesters) dendrimers was convergently synthesized via anchoring of 8 equiv. of G_1 or G_2 dendrons at the phenolic groups of meso-5,10,15,20-tetrakis(3,5-dihydroxy-phenyl) porphyrinatomanganese-(III) chloride (Mn[T(3′,5′-OHPh)P]Cl) using a DCC coupling reaction in the presence of 4-dimethylaminopyridinium 4-toluenesulfonate (DPTS) as the catalyst (Scheme 5.21).

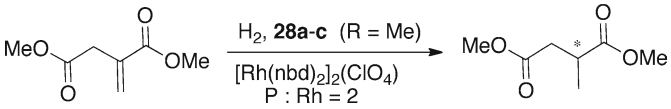

Scheme 5.20 Rh-catalyzed asymmetric hydrogenation

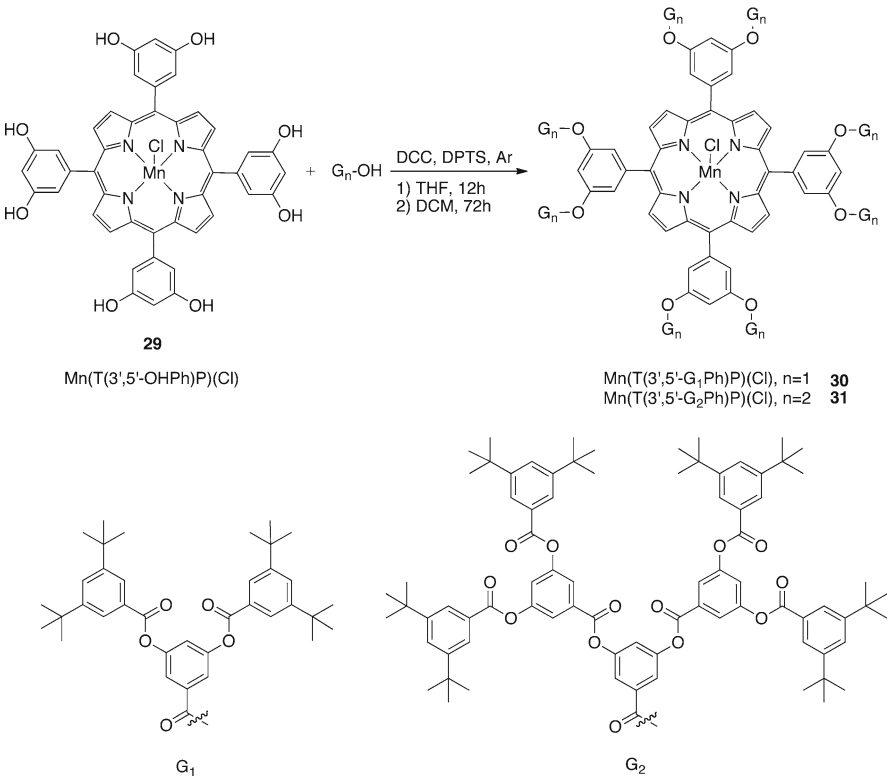

Scheme 5.21 Synthesis of Mn(III) complexes of dendrimer-porphyrins and the molecular structure of the monodendrons

The purity and integrity of the obtained compounds were confirmed by HPLC and MALDI-TOF MS data. The mass spectra contain exclusively the molecular ion peak $[M\text{-}Cl]^+$ (m/z = 5,344.0 (calcd. [M-Cl] 5,346.2) and 10,980 (calcd. 10,985)), respectively for the G_1-**30** and G_2-**31** metallodendrimers. In the latter, two minor peaks were observed at m/z = 9,724 and 8,462, which is possibly due to the successive loss of one and two G_2 dendrons from the parent molecular ion (calcd. m/z = 9,694 and 8,437, respectively).

The catalytic epoxidation reactions using these dendronized Mn-porphyrins were carried out under oxidant limiting conditions using iodosylbenzene as the oxygen donor. In the epoxidation of nonconjugated dienes and 1:1 mixtures of linear and cyclic alkenes under competitive conditions, the dendritic catalysts selectively epoxidize the less hindered double bond and this regioselectivity increases with increasing dendrimer generation.

Sterically demanding dendrons tethered to the meta-positions of meso-tetraphenyl porphyrin (TPP), extremely limit the access to the catalytic metal core. This is the clue to the origin of discrimination of more hindered double bonds in a substrate

with increasing dendrimer generation, i.e. the preferred oxidation of sterically available double bonds.

A competition experiment between cyclohexene and cyclooctene also indicated the presence of a certain positive electronic effect of the dendron substituents. While the G_1-**30** outperforms the parent molecular catalyst Mn(TPP)(Cl) in selectivity more than twice, the selectivity of the G_2-**31** metallodendrimer equals that of the G_1-**30** metallodendrimer. Interestingly, the "immobilization" of the manganese porphyrin complex does not influence the overall catalyst activity. The turnover frequency values obtained for dendronized complexes (2-4 s^{-1}) are similar to that of Mn(TPP)(Cl) (3–4 s^{-1}). Moreover, a fair resistance toward selfoxidation during catalysis was observed for the dendritic metalloporphyrins. Even after 1,000 turnovers (of oxidant) less than 10% degradation occurred (according to UV–Vis data).

Recently, the group of Tsuji has designed novel NHC ligands that are furnished with tetraethylene glycol (TEG) and *n*-C_{12} alkyl chains (Fig. 5.8) [36]. Both of these compounds were tested in the palladium-catalyzed Suzuki–Miyaura coupling of aryl bromides. It was found the TEG moieties of **32a** considerably enhance the catalytic activity in this reaction, whereas the *n*-C_{12} alkyl chains of **32b** do not influence the catalysis. The observed positive dendritic effect arises from the stabilization of the active centers by changes in the dielectric properties of their microenvironment through the TEG moieties. However, these NHC ligands failed to catalyze more challenging reactions, e.g. the activation of the less reactive aryl chlorides for Pd-mediated cross-coupling reactions.

Site-isolation may also lead to the formation of low-coordination number metal complexes, which in turn may have enhanced catalytic properties [37]. Two independent examples that illustrate this concept were recently reported by the groups of Tsuji [38] and Klein Gebbink [39].

On the base of bulky phosphane analogues of their NHC ligands, highly active catalytic systems were developed by Tsuji et al. for the Suzuki-Miyaura coupling of aryl chlorides [38]. In particular, a family of new triarylphosphanes in which the TEG (**33a**, **34a**) or *n*-C_{12} (**33b**, **34b**) moieties are arranged radially around the phosphanes was designed and prepared (Fig. 5.8). The high yielding and straightforward synthesis of these ligands includes the reaction of tri(4-hydroxyphenyl) phosphane oxide with the corresponding benzyl chlorides followed the reduction of the phosphane oxides with $PhSiH_3$ (Scheme 5.22). Amongst these dendritic phosphanes, the second-generation dendritic derivative with TEG chains is distinctly effective as a ligand and provides a highly active Pd catalyst system for the Suzuki–Miyaura cross-coupling reactions.

The dendrimers were tested as ligands in the Suzuki–Miyaura coupling of 4-chlorotoluene with phenylboronic acid (2 equiv.) in combination with $PdCl_2(PhCN)_2$ (0.1 mol% Pd, 0.2 mol% ligand) with K_2CO_3 in THF at 60°C (Scheme 5.23). While the application of **33a** with the TEG moieties afforded 4-phenyltoluene in 36% yield, the next generation dendrimer **34a** afforded the product in 93% yield (a positive dendritic effect). In contrast, phosphane dendrimers with *n*-C_{12} alkyl chains (**33b**, **34b**) do not exhibit any dendritic effect [40] being almost unactive catalysts for this coupling, which parallels the use of the parent ligand PPh_3 in this reaction.

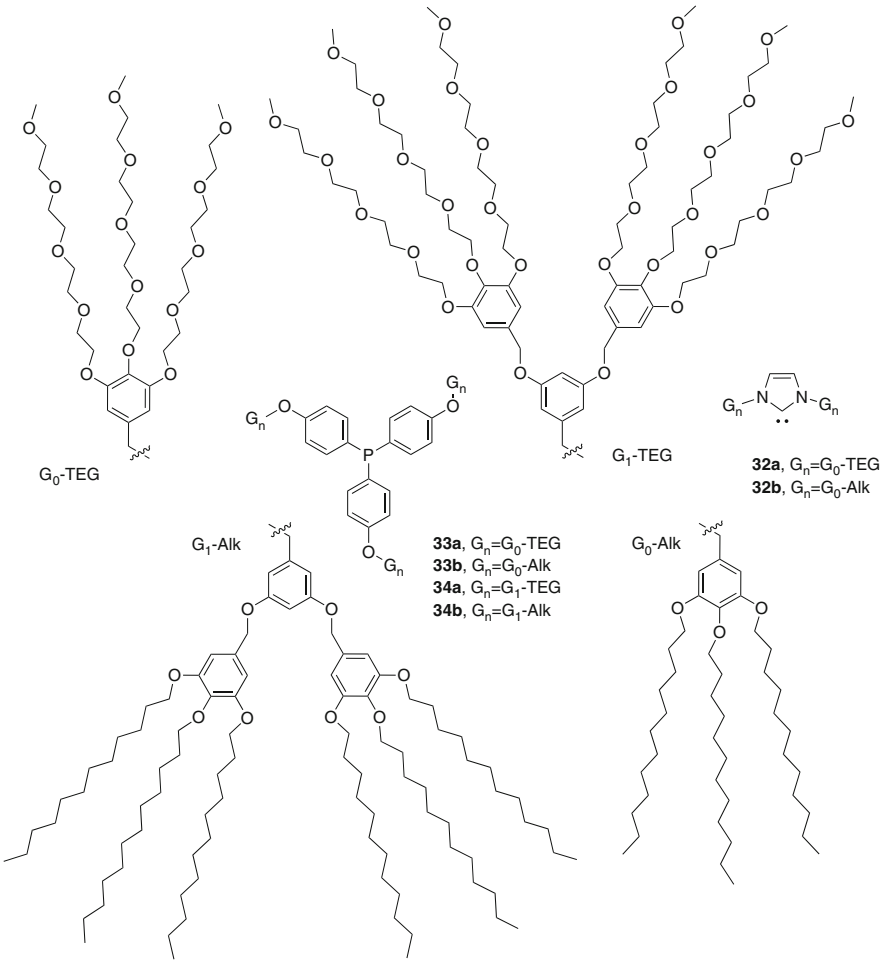

Fig. 5.8 *N*-Heterocyclic carbene and phosphane ligands bearing tetraethylene glycol or n-C_{12} moieties

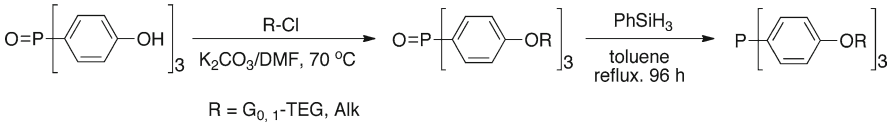

Scheme 5.22 Synthesis of phospane dendrimers

The efficiency of **34a** as the ligand essentially depends on the type of solvent and base used in the reaction. For instance, the highest yield of cross-coupling products was achieved in THF. In the solvents DME, DMF, 2-propanol, and water the products were obtained in only low to moderate yields and 1,4-dioxane and toluene, very common solvents for the Suzuki–Miyaura coupling reaction, were not suitable for the present system

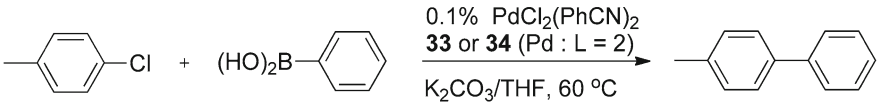

Scheme 5.23 Pd-catalyzed Suzuki-Miyaura reaction in the presence of phosphane dendrimers

at all. Among the bases, potassium and rubidium salts are more favorable for catalysis; in the presence of sodium, cesium and lithium salts only low yields were obtained.

The special role of the dendritic TEG moieties of **34a** in catalysis was confirmed by several control experiments. Under identical catalytic conditions a mixture of PPh_3 and tetraethylene glycol dimethyl ether (molar ratio = 1:18) instead of ligand **34a** did not afford any product.

Because dendrimers are known to stabilize nanoparticles [41], a mercury test [42] was performed in order to examine the possibility of zero-valent nanoparticles to act as active catalyst species. In this experiment the cross-coupling product was obtained in a significant yield (55%), even in the presence of 25 mol% mercury. The authors, therefore, concluded that it is unlikely that nanoparticles act as the active catalyst species in this system.

Interestingly, both **34a** with TEG moieties and its alkyl analogue **34b** possess identical basicities based on the ^{31}P-Se coupling constants [43] of the corresponding phosphane selenides ($^1J_{P,Se}$ = 715 Hz). This value is close to the one for PPh_3 ($J_{P,Se}$ = 730 Hz) and much larger than P(*t*-Bu)$_3$ ($J_{P,Se}$ = 686 Hz) and PCy_3 ($J_{P,Se}$ = 674 Hz), which are known to be strong π-bases.

From a steric point of view, bulky phosphanes facilitate the formation of coordinatively unsaturated and highly reactive catalyst species that can participate in the oxidative addition step of strong aryl–Cl bonds. In an experiment with a double amount of the phosphane ligand **34a** (molar ratio P/Pd = 4:1), the initial reaction rate decreased to one-thirtieth of the rate for a normal amount of phosphane (molar ratio P/Pd = 2:1). This observation is in line with the assumption shown above, as the existence of unsaturated complexes becomes more unfavorable at higher ligand concentration.

The group of Klein Gebbink designed a related type of dendritic phospine ligands "Dendriphos" (Fig. 5.9) [39, 44, 45]. These behave as very bulky phosphine ligands and, hence, can stabilize coordinatively unsaturated and catalytically active Pd(0) species that are crucial for the activation of relatively inert substrates such as aryl chlorides in cross-coupling reactions.

Dendriphos ligands were successfully employed in the palladium-catalyzed Suzuki–Miyaura cross-coupling of aryl halides. While this reaction in case of aryl bromides occurs pretty smoothly and without any visible dendritic effect, the behavior of aryl chlorides is quite interesting and was investigated in detail.

Following a standard alkylation procedure the Fréchet-type G_0-G_2 dendrons were tethered to the triphenylphosphine core furnished with six dimethylamino groups. All synthesized hexacationic Dendriphos macromolecules were used as ligands in the palladium-catalyzed Suzuki–Miyaura cross-coupling of 4-nitrochlorobenzene and phenylboronic acid in combination with $Pd_2(dba)_3{\cdot}CHCl_3$ (0.1 mol% Pd, 0.25 mol%

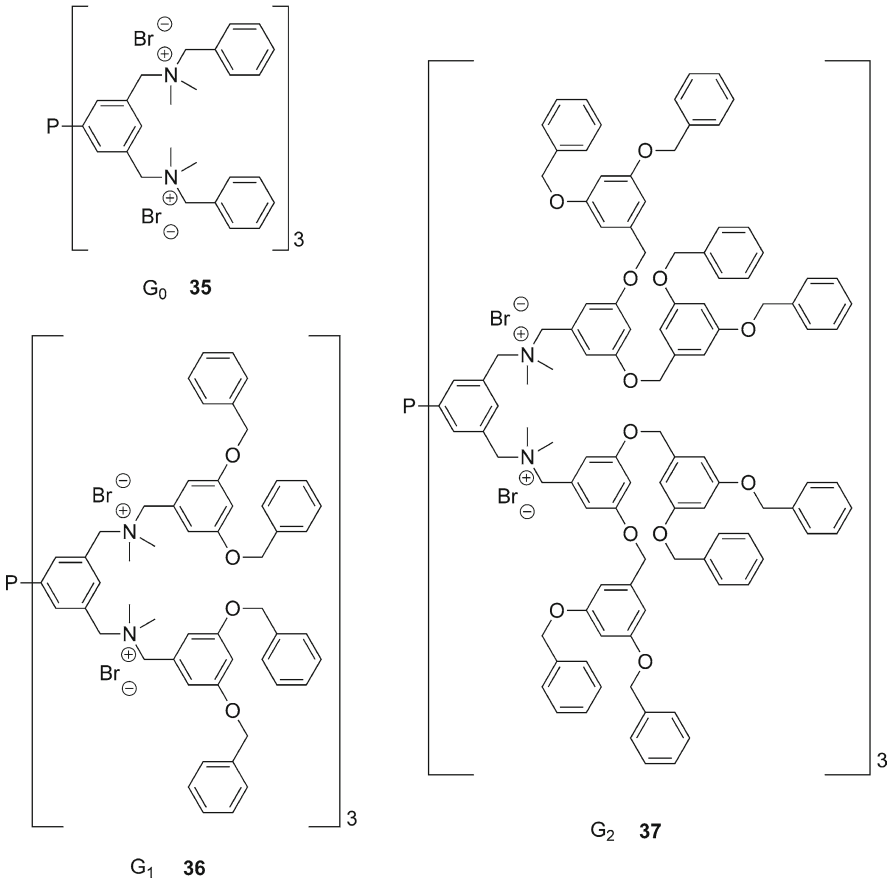

Fig. 5.9 Dendriphos ligands for Suzuki-Miyamura couplings

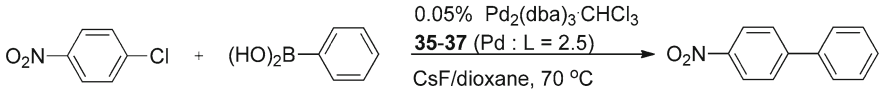

Scheme 5.24 Pd-catalyzed Suzuki-Miyaura reaction in the presence of Dendriphos ligands

ligand) and a base (CsF) in dioxane at 70 °C (optimized conditions) (Scheme 5.24). The kinetic data of these reactions confirmed a strong positive dendritic effect. In the presence of the most active G_2-**37** Dendriphos ligand, the yield of 4-nitrobiphenyl was 80% after 3 h, while in case of G_1-**36** and G_0-**35** phosphanes about 40% and 30% yields, respectively, were determined. However, at 95 °C thermal decomposition of G_1-**36** and G_2-**37** ligands was observed, while the activity of G_0 increased.

Several experiments were carried out to reveal the nature of the active species in these reactions. Blank reactions with PPh_3 in combination with a bis(tetra-alkyl)ammonium dendron did not produce a serious amount of cross-products. This observation confirms the special role of the Dendriphos architecture in the activation of aryl halides and the acceleration of cross-coupling reactions with increasing dendrimer generation.

Poly(4-vinylpyridine) (PVPy) is known to act as a selective trap for homogeneous, ligandless Pd(0) species [46]. Addition of PVPy to the catalytic system Pd_2dba_3 $CHCl_3$/**35** did not have any effect on the catalytic activity. This is a strong indication that, in the present system, the observed activity cannot be attributed to ligandless Pd(0) species, but to a homogeneous Pd-Dendriphos complex of the type $Pd(0)L_n$.

Rothenberg et al. reported on the immobilization of Ru(II) complex with (*S,S*)-*N*-arenesulfonyl-1,2-diphenylethylenediamine ligands (Ts-DPEN) on a third-generation Fréchet-type dendron [14]. Previously, this complex was developed by Noyori and Ikariya as an asymmetric transfer hydrogenation catalyst [47]. The core functionalized dendritic ligand **40** was synthesized by condensing the Boc-protected amino derivative of (*S,S*)-DPEN **39** with the G_3-**38** polyether dendron (Scheme 5.25). Subsequently the Boc group was removed and the dendritic ruthenium complex was prepared by mixing the dendrimer ligand with $(RuCl_2(cymene))_2$ at 25 °C in THF.

This metallodendritic catalyst was used in the asymmetric transfer hydrogenation of acetophenone with *i*PrOH in the presence of *i*PrOK as a base (Scheme 5.26).

After 48 h a substrate conversion of 65% was achieved, yielding predominantly (*S*)-1-phenylethanol (95% ee). Neither the reverse reaction nor significant catalyst deactivation was observed.

After these encouraging results the catalyst was tested in a specially designed ceramic membrane reactor. This reactor has a cylindrical shape (15 × 7 mm) and walls made of a thin nanoporous γ-alumina layer, covering a macroporous α-alumina

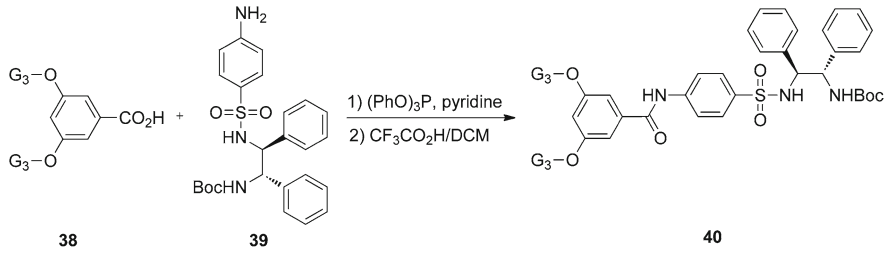

Scheme 5.25 Synthesis of a Ts-DPEN ligand with a third generation Fréchet dendron

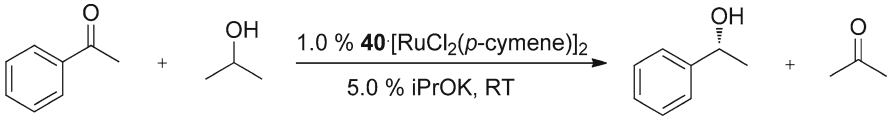

Scheme 5.26 Asymmetric transfer hydrogenation in the presence of a dendronized Ru-catalyst

membrane [13]. The reactor is closed with teflon caps on both sides. In this way, a macromolecular dendritic catalyst can be placed inside this small reactor and subsequently introduced into the reaction mixture. At the end of the reaction, catalysts retained inside of the cap can be easily separated, purified from the reaction mixture, and recycled. The molecular-weight cutoff of the γ-alumina layer is 1,000 Da. The reaction permeate was analyzed via inductively coupled plasma mass spectrometry (ICP-MS) analysis and it was found that less than 0.3% of the Ru leached into the permeate solution after 48 h.

A series of control experiments were run to determine the background reaction level. No reaction was observed in the absence of catalyst or when only the dendritic ligand was present. Reactions run with the Ru precursor salt, the Ru non-dendritic complex, and the Ru–dendrimer complex are characterized by similar conversion values, however only the latter two catalysts act in an enantioselective manner (93–95% ee in both cases). Finally, the same catalyst was used in two subsequent runs and gave practically identical conversions, selectivities, and reaction rates. These data clearly confirm that the Ru catalyst retains inside the membrane reactor in the form of the dendrimer-supported complex.

Related 'cat-in-a-cup' or 'tea bag' approaches have been reported by Van Koten [48] and by Vogt [49].

5.4 Conclusions and Outlook

The application of homogeneous catalysts undoubtedly has a superior potential over heterogeneous catalysts in synthetic organic operations where both reaction selectivities in terms of the regio- and stereo-selectivity of product formation, as well as a total predictability of the overall process are mandatory. Moreover, molecular catalysts possess an incomparable higher activity and occur almost without additional thermal activation, which allows for shorter operation times and decreases the overall energy costs of production. These inherent irreprehensible properties of homogeneous catalysts lay a foundation for a "green" chemical technology using environmentally friendly processes. However, homogeneous catalysts also have one, albeit extremely undesirable consequence of their molecular nature: the self-contamination of reaction products, which are often not easily separated from even tiny amounts of metal-containing catalysts. Consequently, the molecular nature of homogeneous catalysts also imparts the ability to regenerate and recycle either the ligand or metal component, and ultimately both components of homogeneous catalysts.

Elaborated approaches for homogeneous catalyst separation from product streams based on size-discrimination concepts have found considerable attention in recent years and allow for the previously unfeasible separation of molecular components within one phase according to their size. According to these approaches, the artificial size-extension of catalyst molecules might be

applied to facilitate their discrimination, i.e. separation, among reaction product molecules. The task of homogeneous catalyst 'immobilization' via molecular size enlargement brings new challenges to the development of homogeneous catalyst. These challenges mainly deal with the maintenance of particular molecular catalyst properties like activity and selectivity at the same level as those of the 'non-immobilized' parent catalysts.

Within this chapter we have combined a brief historical description with selected recent examples of the contemporary scientific progress in the relatively young and developing field of homogeneous catalyst heterogenization on dendritic supports, as a most promising way toward the flawless transfer of molecular catalyst properties on the macromolecular level. We have discussed the main problems that may be associated with this approach, next to its anticipated and appreciable benefits, and by doing so have tried to highlight the unique features of the dendrimer supports.

Although the field has gone through a rapid progression phase, several hurdles remain for the commercialized use of dendritic and dendronized molecular catalysts. Clearly, the specialty, i.e. expensive, nature of dendrimer materials needs to be addressed. While alternative molecular supports such as hyper-branched polymers have been put forward, the development of novel high-definition dendrimer and dendron classes needs further attention. In addition, the further technological development of practical filtration set-ups, which has been advocated since the early days of the field, has yet to result in applicable and affordable 'molecular' filtration protocols. In our opinion, these aspects are prerequisites for the development of economically viable synthesis protocols based on size-enlarged homogeneous catalysts.

References

1. Frenzel T, Solodenko W, Kirschning A (2003) Solid-phase bound catalysts: properties and applications. In: Buchmeiser MR (ed) Polymeric materials in organic synthesis and catalysis. Wiley, Weinheim
2. Berger A, Klein Gebbink RJM, van Koten G (2006) Top Organomet Chem 20:1–38
3. Dickerson TJ, Reed NN, Janda KD (2002) Chem Rev 102:3325–3344
4. Haag R, Roller S (2003) Dendritic polymers as high-loading supports for organic synthesis and catalysis. In: Buchmeiser MR (ed) Polymeric materials in organic synthesis and catalysis. Wiley, Weinheim
5. Newkome GR, Moorefield CN, Vögtle F (2001) Dendrimers and dendrons: concepts, syntheses, applications. Wiley, Weinheim
6. Vögtle F, Richardt G, Werner N (2009) Dendrimer chemistry: concepts, syntheses, properties applications. Wiley, Weinheim
7. Bosman AW, Janssen HM, Meijer EW (1999) Chem Rev 99:1665–1688
8. Ingold CK, Nickolls LC (1922) J Chem Soc 121:1638–1648
9. Buhleier E, Wehner W, Vogtle F (1978) Synthesis 1978:155–158
10. Tomalia DA, Baker H, Dewald J et al (1985) Polymer J 17:117–132
11. (a) Gillies ER, Frechet JM (2005) J Drug Discovery Today 10:35–43; (b) Boas U, Heegaard PMH (2004) Chem Soc Rev 33:35–43; (c) Chase PA, Klein Gebbink RJM, van Koten G (2004)

J Organomet Chem 689:4016–4054; (d) Peng X, Pan Q, Rempel GL (2008) Chem Soc Rev 37:1619–1628; (e) Helms B, Fréchet JMJ (2006) Adv Synth Cat 348:1125–1148
12. (a) Dijkstra HP, van Klink GPM, van Koten G (2002) Acc Chem Res 35:798–810; (b) Vankelecom IFG (2002) Chem Rev 102:3779–3810
13. (a) Benes N, Nijmeijer A, Verweij H (2000) Microporous silica membranes. In: Kanellopoulos NK (ed) Recent advances in gas separation by microporous ceramic membranes. Elsevier, Amsterdam; (b) van Gestel T, Vandecasteele C, Buekenhoudt A et al (2003) J Membr Sci 214:21–29
14. Gaikwad AV, Boffa V, ten Elshof JE et al (2008) Angew Chem Int Ed 47:5407–5410
15. Tomalia DA, Naylor AM, Goddard WA III (1990) Angew Chem Int Ed 29:138–175
16. Hawker CJ, Frechet JMJ (1990) J Am Chem Soc 112:7638–7647
17. Knapen JWJ, van der Made AW, de Wilde JC et al (1994) Nature 372:659–663
18. Kleij AW, Gossage RA, Jastrzebski JTBH et al (2000) Angew Chem Int Ed 39:176–178
19. Kleij AW, Gossage RA, Klein Gebbink RJM et al (2000) J Am Chem Soc 122:12112–12124
20. Breinbauer R, Jacobsen EN (2000) Angew Chem Int Ed 39:3604–3607
21. Konsler R, Karl J, Jacobsen EN (1998) J Am Chem Soc 120:10780–10781
22. Zheng ZJ, Chen J, Li Y-S (2004) J Organomet Chem 689:3040–3045
23. Kassube JK, Wadepohl H, Gade LH (2009) Adv Synth Catal 35:607–616
24. Ooe M, Murata M, Mizugaki T et al (2004) J Am Chem Soc 126:1604–1605
25. (a) Ooe M, Murata M, Mizugaki et al (2002) Nano Lett 2:999–1002; (b) Scott RWJ, Datye AK, Crooks RM (2003) J Am Chem Soc 125:3708–3709
26. Yeung LK, Crooks RM (2001) Nano Lett 1:14–17
27. Reichardt C (1988) Solvents and solvent effects in organic chemistry, 2nd edn. Wiley, Weinheim
28. de Groot D, de Waal BFM, Reek JNH et al (2001) J Am Chem Soc 123:8453–8458
29. van de Coevering R, Alfers AP, Meeldijk JD et al (2006) J Am Chem Soc 128:12700–12713
30. Virboul MAN, Lutz M, Siegler MA et al (2009) Eur J Chem 15:9981–9986
31. Fujihara T, Obora Y, Tokunaga M et al (2005) Chem Commun 4526–4528
32. Wang HMJ, Lin IJB (1998) Organometallics 17:972–975
33. Oosterom GE, van Haaren RJ, Reek JNH et al (1999) Chem Commun 1119–1120
34. Oosterom GE, Steffens S, Reek JNH et al (2002) Top Catal 19:61–73
35. Bhyrappa P, Young JK, Moore JS et al (1996) J Am Chem Soc 118:5708–5711
36. Ohta H, Fujihara T, Tsuji Y (2008) Dalton Trans 379–385
37. Muller C, Ackerman LJ, Reek JNH et al (2004) J Am Chem Soc 126:14960–14963
38. Fujihara T, Yoshida S, Ohta H et al (2008) Angew Chem Int Ed 47:8310–8314
39. Snelders DJM, van Koten G, Klein Gebbink RJM (2009) J Am Chem Soc 131:11407–11416
40. Yamamoto K, Kawana Y, Tsuji M et al (2007) J Am Chem Soc 129:9256–9257
41. (a) Astruc D, Lu F, Azanzaes JR (2005) Angew Chem 117:8062–8083; (b) Wu L, Li Z-W, Zhang F et al (2008) Adv Synth Catal 350:846–862
42. Phan NTS, van der Sluys M, Jones CW (2006) Adv Synth Catal 348:609–679
43. (a) Allen DW, Taylor BF (1982) J Chem Soc Dalton Trans 51–54; (b) Andersen NG, Keay BA (2001) Chem Rev 101:997–1030
44. Kreiter R, Klein Gebbink RJM, van Koten G (2003) Tetrahedron 59:3989–3997
45. Snelders DJM, Kreiter R, Firet JJ et al (2008) Adv Synth Catal 350:262–266
46. (a) Weck M, Jones CW (2007) Inorg Chem 6:1865–1875; (b) Chen J, Vasiliev AN, Panarello AP et al (2007) Appl Catal A 325:76–86
47. (a) Hashiguchi S, Fujii A, Takehara J et al (1995) J Am Chem Soc 117:7562–7563; (b) Haack KJ, Hashiguchi Fujii A et al (1997) Angew Chem 109:297–300
48. Albrecht M, Hovestad NJ, Boersma J (2001) Eur J Chem 7:1289–1294
49. Janssen M, Müller C, Vogt D (2009) Adv Synth Cat 351:313–318

Chapter 6
Catalytic Membranes Embedding Selective Catalysts: Preparation and Applications

Enrico Drioli and Enrica Fontananova

Abstract The embedding of a catalyst in membranes is today recognized as a promising strategy to develop highly efficient and eco-friendly heterogeneous catalytic chemical processes. When a catalyst is heterogenized within or on the surface of a membrane, the membrane composition (characteristics of the membrane material: hydrophobic or hydrophilic, presence of chemical groups with specific functionality, etc.) and the membrane structure (dense or porous, symmetric or asymmetric), can positively influence the catalyst performance, not only by the selective sorption and diffusion of reagents and/or products, but also influencing the catalyst activity by electronic and conformational effect. These effects are similar to those occurring in biological membranes. In this chapter, after a preliminary presentation of the basic principles of membrane reactors and polymer membranes, the preparation, characterization and applications of polymeric catalytic membranes, will be discussed.

6.1 Introduction

Catalytic reactions are today intensively used in chemical industry, wastewater treatments and many other fields; however the reduction of energy demand and environmental impact of these processes are challenges that must be faced to realize a sustainable growth.

To deal with this objective, a shift is required in the industrial catalysis towards novel intensified processes that are expected to bring substantial improvements in manufacturing and processing, decreasing production costs, equipment size, energy consumption, waste generation, and improving remote control, information fluxes and process flexibility [1].

E. Drioli (✉) and E. Fontananova
Institute on Membrane Technology (ITM-CNR), Via P. Bucci,
87030 Arcavacata di Rende, Cosenza, Italy
e-mail: e.drioli@itm.cnr.it

P. Barbaro and F. Liguori (eds.), *Heterogenized Homogeneous Catalysts for Fine Chemicals Production*, Catalysis by Metal Complexes 33,
DOI 10.1007/978-90-481-3696-4_6,

Reactive separations well respond to the requirements of this strategy combining a reaction with a separation process, not only at equipment level, but also introducing functional interrelations between the operations involved, resulting in improved processes [2].

Membrane reactors (MRs) are examples of reactive separations which, in comparison with other systems (reactive distillation, reactive adsorption, reactive crystallization/precipitation), present the advantages to use intrinsically more clean and energy-efficient separation.

MRs can allow to achieve many advantages: lower energy requirements, increased productivity, easier down- and up-stream processing, reduced by-products formation, possibility of heat recovery, compact process equipment, catalyst recycling.

In numerous cases, membrane separation processes operate at much lower temperature, especially when compared with thermal processes such as reactive distillation [3]. As a consequence they might provide a solution in the case of limited thermal stability of either catalyst and products. Furthermore, by membrane separation processes it is possible also to separate non volatile components.

If the membrane is used to embedding an homogenous catalyst, the catalyst recovery, regeneration and reuse in successive catalytic runs, is generally easier in comparison with other heterogeneous catalytic systems [4].

Moreover in classical heterogeneous catalysis the conversion and selectivity of the catalytic process is often limited by the diffusion of the reagents to the catalytic sites and of the product from them.

On the contrary, an easy control of the contact time reactants/products with the catalyst can be generally achieved in a MR by the control of the convective flux [5].

The catalyst entrapment in the functional micro-structured environment constituted by the membrane, can also have a positive influence on the transition states and reaction kinetics by electronic and weak interactions, as well as by spatial restriction and transport dynamics [6].

In the following sections, after a short presentation of the basic principles of MRs, the preparation, characterization and applications of catalytic membranes to reactions of interest, will be presented.

6.2 Membranes and Membrane Reactors

Membrane reactors are multifunctional reactors combining a chemical reaction (generally catalytically promoted) with a membrane-based separation. MRs have been investigated since 1970s employing primarily polymer membranes in enzymatic reactions or metal membranes for high temperature reactions.

MRs are today accepted as proven technology for many biotechnological applications; however there is a huge potential for these integrated systems in various industrial sectors.

Their large scale applications is still limited by problems related to the manufacturing costs of the membranes and membrane modules, and their limited durability.

Key issues to be addresses in the near future is the development of advanced membranes and modules with acceptable costs, stable in a wide range of solvents and conditions, and showing high and reproducible performance over long times.

The combination of advanced separation and chemical conversion realized in a MR, allows to achieve many advantages in comparison to traditional reactors depending on the specific functions performed by the membrane [7].

However in order to have a synergic combination of the separation and reaction processes that allows to obtain optimal performances, a multidisciplinary approach in the membrane reactor design, is necessary.

Because there are different ways to combine a catalyst with a membrane in a MR, there are numerous possible categorizations of these systems [3].

The most general is based on the transport function of the membrane; it is possible to have extractor, distributor and contactor type MRs (Fig. 6.1).

The nature of the membrane material (organic or inorganic) is a criteria used to distinguish between the organic MRs from the inorganic [8].

Another possible classification is based on the role of the membrane in the catalytic process [9]. If the membrane is itself catalytically active because the membrane is made of a catalytic material (e.g. metal membranes) or a catalyst is immobilized within or on the membrane, the MR is indicated as a Catalytic Membrane Reactor (CMR).

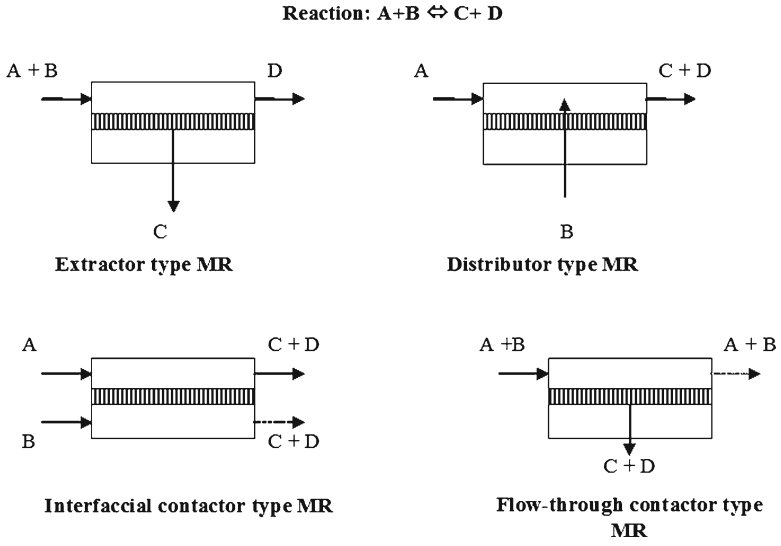

Fig. 6.1 Schematic representation of extractor, distributor and contactor type membrane reactors (MRs)

If the membrane provides only a separation function and the catalyst is in solution, in the packed-bed or fluidized-bed configuration, the system is indicated as inert or membrane assisted reactor.

The nature of the catalyst, biological or artificial, is also used as classification tool.

The variety in the MRs classification reflects the diversity of the functions that the membrane can serve in the reactor. Typical examples are the separation of products from the reaction mixture, the separation of a reactant from a mixed stream for introduction into the reactor and the controlled addition of reactants.

In a membrane extractor the removal of one or more products can allow the enhancement of the conversion of thermodynamically controlled reactions. Typical examples are esterification and de-hydrogenation reactions in which the removal respectively of water or hydrogen, has been used to increase the reaction yield [10].

The extraction of an instable intermediate product by a membrane, represents a possible method to increase the selectivity of reactions in which the desired product is more reactive than the reagents and usually give secondary product [11].

The membrane can also work as a distributor in the MR by dosing of the reactants and increasing the selectivity of kinetically controlled reactions like hydrogenation and selective oxidation preventing hot spots and side reactions.

The controlled addition of the reactants by the membrane can reduce possible dangerous interactions (e.g. with flammable or explosive mixtures) by the control of the local reactants composition.

The membrane can be also used as upstream separation unit, selectively dosing (and distributing) one component from a mixture [12–14].

The membrane can define the reaction volume facilitating the contact between the reactants. An interfacial membrane contactor can provide a contacting zone for two immiscible phases excluding polluting solvents and reducing the environmental impact of the process [15].

When the membrane is catalytically active, the control of the contact time reactants-catalyst by the control of the convective flux in the flow-through CMR, can improve the reaction selectivity [5]. This represents a fundamental advantage of MRs in comparison with traditional heterogeneous reactors.

In classical heterogeneous catalysis (catalyst absorbed or linked in porous polymeric or inorganic solids) the conversion and selectivity of the catalytic process is often limited by the diffusion of the reagents to the catalytic sites and the product from them.

On the contrary, the convective flux in a catalytic membrane reactor is easier to control and to adjust to the reaction kinetic, by the control of the driving force and/or the membrane structure.

In a membrane separation process, the transport rate of a component can be activated by various driving forces such as gradients in concentration, pressure, temperature or electrical potential. In numerous membrane processes more than one driving force is involved (e.g. pressure and concentration in gas separation,

concentration and electrical potential in electrodialysis, etc.), but all these parameters can be included in one thermodynamic function, the electrochemical potential (η). For a single component i transported, the flux (J_i) can be described by a semi-empirical equation:

$$J_i = -L \cdot \frac{d\eta_i}{dx} \tag{6.1}$$

where $\frac{d\eta_i}{dx}$ is the gradient in electrochemical potential of the component i and L is a phenomenological coefficient.

In multi-component systems, driving forces and fluxes are interdependent, giving rise to more complex interactions [16].

The transport depends, of course, from the membrane structure and, for a dense membrane in which the transport occur by a solution-diffusion mechanism, also from the membrane material.

The contact time (τ) between the catalytic membrane and the reactant can be estimated by the following equation:

$$\tau = \frac{\delta}{J_i} \tag{6.2}$$

where δ is the membrane thickness.

In some specific cases, the mass transport can be coupled, at least in principle, with the heat transport through a metal membrane for reactions occurring at the two opposite sides of the membrane. For example the heat dissipated in an exothermic reaction (like hydrogenation) can be used in an endothermic reaction (dehydrogenation reactions), taking place at the opposite side of a membrane (palladium membrane selective for hydrogen) [17, 18].

The membrane can also be used for the retention of the catalyst in the reactor by using membrane with appropriate molecular weight cut off (MWCO), i.e. the molecular weight of the solute (generally globular protein) that is 90% retained by the membrane. However in the selection of the membrane to be used for this aim, it is necessary to consider that the MWCO depends on the solvent; moreover the solution composition (and polarity) can change relevantly during the reaction [4].

In some cases the catalyst retention can be optimized by enlargement of the catalyst in the form of: dendrimers, hyperbrached polymers, catalyst bound to a soluble polymer [19]. New possibilities have been recently opened by the coupling of solvent resistant nanofiltration (SRNF) with homogeneous reactions [20].

SRNF compared to traditional separation techniques (distillation, chromatography, extraction), allows to reduce energy cost and waste production in the recovery of homogeneous catalysts.

The process is carried out in continuous or in batch-wise filtration-reaction cycles. The second one operative mode is usually employed if the operative conditions (solvent, temperature, pressure, etc.) are not adequate for the membrane.

The catalyst can be also immobilized inside or on the membrane surface allowing generally an easy catalyst recovery, reuse and regenerations in successive catalytic runs. The basic principles of catalyst entrapment in a polymeric membranes will be presented in Section 6.4.

6.3 Polymer Membranes

Synthetic membranes show a large variety in their physical structure and the materials they are made from.

Based on the materials used for their preparation it is possible to distinguish them in inorganic membranes (made of ceramics, glass, or metals) and organic membranes (made of organic polymers).

Inorganic membranes are widely used in the field of high temperature (>200°C) reactions because of their high chemical and thermal stability.

Table 6.1 Examples of polymer material used for membrane preparation for application in various membrane separation processes

Polymer	Membrane process
Cellulose acetates	GS, RO, UF, MF
Cellulose nitrate	MF
Cellulose, regenerated	UF, D
Perfluorosulfonic acid polymer	ED, fuel cells
Polyacrylonitrile	UF
Polyetherimides	UF
Polyethersulfones	UF, MF
Polyarylethersulfones sulfonated	ED, fuel cells
Polyetherketone	MF, UF
Polyaryletherketones sulfonated	ED, fuel cells
Polyethylene terephthalate	MF
Polyphenylene oxide	GS
Poly(styrene-co-divinylbenzene), sulfonated or aminated	ED
Polytetrafluoroethylene	MF, GS
Polyamide, aliphatic	MF
Polyamide, aromatic	UF
Polyamide, aromatic	RO, NF
Polycarbonates, aromatic	GS, MF
Polyether, aliphatic crosslinked	RO, NF
Polyethylene	MF
Polyimides	GS, NF
Polypropylene	MF, MC
Polydimethylsiloxane	GS PV, NF
Polysulfones	GS, UF
Polyvinyl alcohol	PV
Polyvinylidene fluoride	UF, MF

Codes of membrane processes: MF, microfiltration; UF, ultrafiltration; NF, nanofiltration; RO, reverse osmosis; GS, gas separation; PV, pervaporation; D, dialysis; ED, electrodialysis; MC, membrane contactor

Organic membranes are usually employed when the reaction temperatures are lower, such as in the field of fine chemicals or when biocatalysts are present.

The use of organic membranes in MRs has a lot of interest because a much wider choice of polymeric materials is available as compared with inorganic membranes; the cost of the polymer membranes is generally lower and the preparation protocols allow a better reproducibility (Table 6.1).

The relatively low operating temperatures of the polymeric membranes, are also associated with less stringent demands for materials used in the reactor construction.

Despite polymeric membranes are generally less resistant to high temperatures and aggressive chemicals than inorganic ones, polymeric materials resistant under rather harsh conditions are available like polydimethylsiloxane (PDMS), polyvinylidene fluoride (PVDF), Hyflon (a perfluoro amorphous polymer), Nafion (a perfluorosulfonic acid polymer) and polyimides (PI) [21].

Some selected examples of polymer CMRs and polymer catalytically inert MRs, are listed in Tables 6.2 and 6.3.

Table 6.2 Selected examples of polymeric catalytically active membrane reactors (CMRs)

Selected examples	Applications	References
Metal or bimetals nanoparticles in/on porous membranes:		
- Pd in PAA[a,b]	[a]Selective hydrogenation in gas	[59][a]
	[b]Selective hydrogenation in liquid phase	[53][b]
- Au-Pd/PVP in PI[c]	[c]Oxidation of alcohols	[51][c]
Catalyst embedded in dense membranes		
- FePcY in PDMS[d]	[d]Cyclohexane oxidation	[15][d]
- Rh–MeDuPHOS in PDMS[e]	[e]Enantioselective hydrogenation of methyl-2-acetamidoacrylate	[57][e]
Enzymes immobilized in UF membrane:		
- Lipase from Candida rugosa in PA capillary membranes[f]	[f](S)-Naproxen esters hydrolysis	[48][f]
- Lipase from Serratia marcescens in hollow fibers hydrophilic membranes[g]	[g](–)-MPGM resolution by Sepracor reactor*	[54][g]
Acid membrane and/or functionalized with solid acid catalysts:		
- PVA/sulfosuccinic acid[h]	[h]Transesterification of soybean oil	[49][h]
- Nafion[h]		
- Supported acid catalysts mixed with a polymeric binder on PAN/PDMS[i,j]	[i]Esterification reaction	[45][i]
	[i,j]Dimerisation of isobutene	[47][j]

*Industrial application

Polyacrylic Acid (PAA); iron phthalocyanine in zeolite Y (FePcY); Polyamide (PA); polyvinyl alcohol (PVA); (3-(4-methoxyphenyl)glycidic acid methyl ester), (MPGM)Polyvinylpyrrolidone (PVP); Polyacrylonitrile (PAN)

Table 6.3 Selected examples of catalytically passive membrane reactors

Selected examples	Membranes	Applications	References
PV assisted reactor for products removal	PVA, Nafion[a] PEI, Chitosan[b]	Esterification reaction	[52][a][46][b]
SRNF for catalyst retention in organic solvent	MPF-60, KOCH[a] COK M2 (silicon based membrane with an inorganic filler)[b]	Enantioselective hydrogenation in methanol[a] Hydrolytic kinetic resolution of epoxides[b]	[20][a][44][b]
UF for enzyme retention in EMR	Hydrophilic hollow fibers	Acylase process for the hydrolyses of N-acetyl-(L) amino acids	[58]*
UF in (s)MBRs for wastewater treatments	Submerged PVDF hollow fibers	Municipal wastewaters treatments	[50]**
PEM for electrochemical processes	Nafion, SPEEK, PBI	Solid electrolyte in H_2 and DM-PEMFCs	[55, 56]

PEI, polyether Imide; EMR, enzymatic membrane reactors; (s)MBR, submerged membrane bioreactor; PEM, polymer electrolyte membrane; PEMFC, polymer electrolyte membrane fuel cell; DM-PEMFC, direct methanol-PEMFC.
*Industrial application
**Large scale sMBR

The development of polymer membranes having advanced or novel functions is a key issue to be addressed in order to better exploit the potentialities of polymer membranes in MRs. Important approaches toward this aim have been presented by Ulbricht in a recent review [22], including:

(a) Development of polymers membranes in the form of composite or mixed matrix membranes in which an organic and an inorganic phase coexist in order to have synergistic effect on transport properties, mechanic and thermal stability, as well as, to introduce new functionalities
(b) Advanced functionalization by coating of functional layer or grafting of functional groups on the membrane surface or inside the pores
(c) Development of organic solvent resistant (OSR) membranes (in particular nanofiltration membranes – SRNF)
(d) Use of templates for realizing molecular imprinted (MIP) membranes
(e) Synthesis of novel polymers with controlled architecture like polymers of intrinsic microporosity (PIMs)

Of course the strategies devoted to obtain advanced membrane materials, have to be combined with novel processing technologies of polymers in order to obtain tailored structures controlling the density, size, size distribution, shape and alignment of membrane pores.

The driving idea is to obtain ordered structures similar to track-etched polymer and anodically oxidized alumina membranes, and tailored surface properties, like biological membranes, but prepared by simple, reliable, reproducible and economical methods.

Micro-fabrication, self-assembling, phase separation micro moulding, are tentative towards this direction but more work is necessary to obtain systems commercially competitive and available on large scale [23–25].

6.4 Immobilization of Catalyst in/on Polymer Membranes

The main requirements that must be considered to produce an "ideal catalyst" are: low costs, high selectivity, high stability under reaction conditions, non-toxicity, "green properties", first of all recoverability, i.e. the possibility to recover and reuse the catalyst [26, 27].

In this perspective, the heterogenization of catalysts has interesting implications because it allows the reuse several time of the same catalyst. Among the different heterogenization methods, the entrapping of a catalyst in/on a membrane offers new possibility for the design of new catalytic processes.

The main membrane selection criteria that have to be considered in a membrane assisted reactor, are:

- Stability (mechanical, thermal and chemical)
- Rejection
- Permeability and selectivity
- Fouling tendency
- Cost (capital and operating)

Additional technical complexities in the design and realization of catalytic membranes by the immobilization of catalyst in/on the membrane, need do be considered:

- Catalyst stability during the immobilization procedure
- Influence of the catalyst particles on the membrane properties (mechanical, transport, etc.)
- Effect of the catalyst loading, dimensions and distribution, on the catalytic efficiency
- Leaching of the catalyst in liquid phase

However catalytic membranes deserve special advantages that in many cases justify these additional efforts.

In the design of a catalytic membrane major issues in the polymer selection are the mechanical, thermal and chemical stability under reaction conditions.

Fundamental is to realize a stable catalyst immobilization in order to avoid its leaching out from the membrane. Different immobilization strategies can be used

in order to achieve this goals: covalent bindings, electrostatic interactions, weak interactions (Van del Waals or hydrogen bonds) of the catalyst with the membrane, or catalyst encapsulation.

A good affinity for the catalyst is desirable in order to avoid catalyst leaching and to have a good adhesion between the polymer and the catalyst, with an optimal dispersion of the second one.

The affinity between a compound and the membrane polymer can be often anticipated by the calculation of the *affinity parameters* [21, 28]. These parameters reflects the ability to form hydrogen bond, polar and Van der Waals interactions in condensed phase.

The polymer/catalyst affinity can be also improved by an appropriate chemical functionalization of one or both components.

Ideally the solvent used for the reaction need to be a non-solvent for the catalyst, and the membrane doesn't have to excessively in it.

It also possible in some cases to improve the catalyst retention in the membrane by the catalyst enlargement as: dendrimers, hyperbrached polymers, catalyst bound to a soluble polymer [19].

Mass transfer of the reagents to the catalytic sites, and of the product away from them, should be fast enough in order to not limit the reaction but, in the same time, the contact time catalyst/reagent should be also appropriate.

For a porous membrane, the choice of the polymer material is of less importance for transport properties in comparison with a dense membrane, because permeation does not take place through the polymer matrix, but through the membrane pores [4].

However the membrane material is relevant for the membrane stability and surface properties, such as wettability and fouling tendency.

The membrane preparation conditions depend from the membrane material and desired structure and morphology. In the case of a polymer catalytic membrane, the incorporation of the catalyst complicates the process because the catalyst should be firmly entrapped in the membrane and the catalyst structure and activity has to be preserved during the membrane preparation procedure.

Moreover, the properties (including transport properties) of a catalytic membrane are usually different than those of a pure polymer membrane prepared in the same conditions.

Different techniques for polymeric membrane preparation are today available and can be opportunely employed also to prepare catalytic membranes: phase inversion, coating, sintering, stretching, track-etching, are some examples [29].

The most versatile is the phase inversion technique, in which a polymer is transformed, in a controlled mode, from a liquid to a solid state (the membrane).

In some cases the catalyst is entrapped in/on the membrane already formed, by covalent bonds, electrostatic interaction, absorption by weak interactions or physical entrapment. In alternative, the catalyst immobilization can be carried out in the same time of the membrane formation, for example by dispersing the catalyst in the polymer casting solution and successive phase inversion.

Phase inversion can be induced by different ways, the most used are: phase separation induced by solvent evaporation (to obtain dense membrane) and phase separation induced by immersion in a non-solvent (to obtain porous membrane) (Fig. 6.2).

In the phase inversion process induced by solvent evaporation the polymer is dissolved in a solvent having appropriate volatility, the solution is cast in an environment with controlled temperature and humidity. The solvent evaporation causes the polymer precipitation with the concomitant formation of a dense membrane.

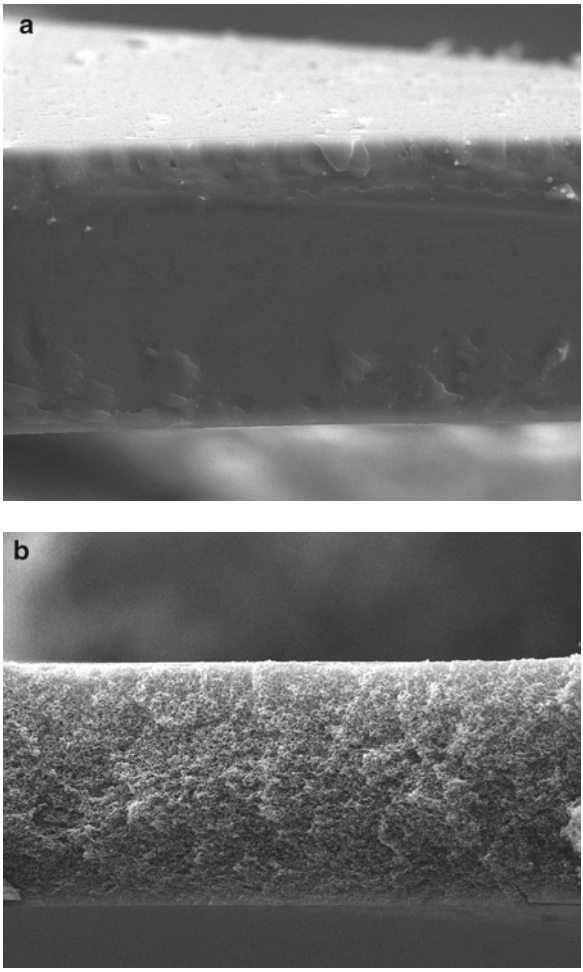

Fig. 6.2 Scanning electron microscopy images of the cross section of a dense membrane prepared by phase inversion induced by solvent evaporation (**a**) and a porous membrane prepared by phase inversion induced by immersion in a non-solvent (**b**)

In the phase inversion process induced by a non-solvent, a film of the homogeneous polymeric solution is cast on a support and immersed in a coagulation bath (a solvent or solvent mixture, in which the polymer is not soluble, but the solvent of the casting solution, is mixable). The polymer solution is initially demixed in two liquid phases because of the exchange of the solvent and non-solvent. The phase with the higher polymer concentration will form the solid membrane, the phase with the lower polymer concentration will form the membrane pores. During the process, the exchange of solvent and non-solvent in the demixed phases continues to cause an increase of the polymer concentration in the concentrated phase surrounding the pores. The polymer molecules may rearrange their structure until the solidification (vitrification or crystallization) of the concentrated phase occurs.

6.5 Preparation of Catalytic Membrane and Their Applications in Catalytic Membrane Reactors (CMRs)

An interesting example of catalyst immobilization is the heterogenization of the decatungstate ($W_{10}O_{32}^{4-}$), a photocatalytic polyoxometalalte (POM, polyanionic metal oxide cluster of early transition metals) widely applied in oxidation catalysis for fine chemistry and wastewater treatments.

The proposed mechanism for decatungstate based photocatalysis involves the absorption of light by the complex ground state forming a charge-transfer excited state ($W_{10}O_{32}^{4-}$) with strong oxidazing properties (photoactivation) (Fig. 6.3) [30].

This is the primary photoreactant, which is able to undergo multi-electron reduction without structural rearrangement, leading to the well-known "blue" reduced form (heteropolyblue). In the presence of aliphatic hydrocarbons, the oxidative step occurs mainly through hydrogen atom abstraction (RH), generating in solution a

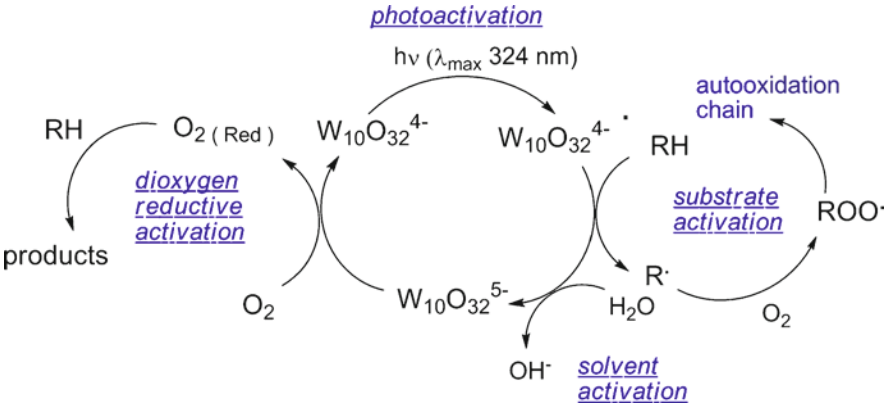

Fig. 6.3 Composite reaction mechanism in the photocatalytic oxidation cycle by decatungstate

reactive radical intermediate (*substrate activation*). Therefore, in the catalytic cycle, dioxygen plays a multifaceted role: by intercepting the organic radicals giving rise to an autooxidation chain, and providing to the re-oxidation of the reduced $W_{10}O_{32}^{5-}$ thus closing the cycle and generating reduced oxygenating species (*dioxygen reductive activation*). Furthermore, in aqueous solution, the photooxidation performance can be strongly enhanced by the production of highly reactive hydroxyl radicals $OH^{\bullet}$ formed through the direct reaction of water with the excited decatungstate (*solvent activation*).

Decatungstate exhibits especially interesting properties for the photocatalytic detoxification of wastewater since its absorption spectrum (λ_{max} = 324 nm) partially overlaps the UV solar emission spectrum opening the potential route for an environmentally benign solar-photoassisted application [31].

However, decatungstate has also some relevant limitations: it is characterized by low quantum yields, small surface area, poor selectivity and limited stability at pH higher than 2.5 [32].

Membrane technology can offer interesting possibilities in order to overcome these limitations by: the multi-turnover recycling associated to heterogeneous supports, the selectivity tuning as a function of the substrate affinity towards the membrane phase, the effect of the polymeric micro-environment on catalyst stability and activity.

In this respect, the design of alternative heterogeneous photooxygenation systems able to employ visible light, oxygen, mild temperatures and solvent with a low environmental impact (water or neat reaction), have been investigated by the immobilization of the decatungstate in polymer membranes [33, 34].

The successfully heterogenization has been guaranteed by a proper choice of both, the catalyst and the polymer material.

Considering the interest towards the photo-oxidation reactions of organic substrates, principally in aqueous phase, hydrophobic polymer materials have been selected for membrane preparations: the PDMS, the partially fluorinated PVDF and the perfluorinated polymer Hyflon AD60X (Fig. 6.4).

These polymers do not absorb in the region of interest of the catalyst and are characterized by a high chemical, thermal and UV stability.

In order to improve the catalyst/polymer interactions, and to avoid catalyst leaching out from the membrane, liphophilic and insoluble in water derivatives of the decatungstate have been employed: the tetrabutilamonium salt ($(n\text{-}C_4H_9N)_4W_{10}O_{32}$; indicated as TBAW10) and a fluorous-tagged decatungstate, ($[CF_3(CF_2)_7(CH_2)_3]_3CH_3N)_4W_{10}O_{32}$; indicated as R_fN_4W10) (Fig. 6.5).

A membrane-induced structure-reactivity trend that may be exploited to achieve selective processes, was observed in polymeric catalytic membranes prepared embedding decatungstate within porous membranes made of PVDF (PVDF-W10) or dense PDMS membranes (PDMS-W10).

The PDMS catalytic membranes were prepared by dispersing the TBAW10 in a solution in dichloromethane (DCM) of a PDMS vinyl terminated prepolymer with high molecular weight and a cross-linker containing several hydride groups on shorter polydimethylsiloxane chains prepolymer (prepolymer:crosslinker = 10:1).

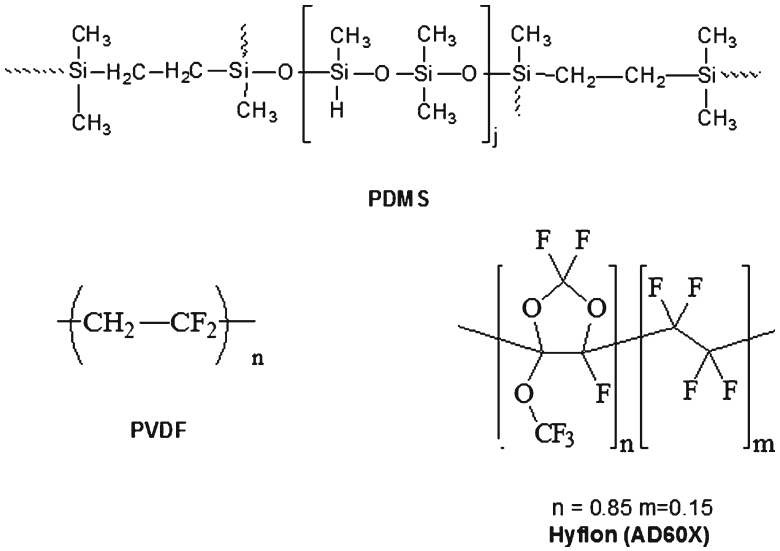

Fig. 6.4 Polymers used as membrane materials for decatungstate immobilization

The catalyst was entrapped in the polymer matrix during the phase inversion by solvent evaporation. The catalytic membranes were finally cured via a Pt-catalysed hydrosilylation reaction at 150°C to form a densely crosslinked polymer network.

However, because the catalyst is not soluble in DCM and it does not well interact with the PDMS matrix, a poor dispersion of the catalyst has been obtained as evident from the scanning electron micrographs (SEM) in back scattered electrons mode (BSE) and energy dispersive X-ray (EDS) analyses (Fig. 6.6a,b).

On the contrary the TBAW10 is soluble in the solvent used for the PVDF membranes preparation.

The TBAW10 heterogenization has been carried out by solubilisation of the catalyst into the polymer solution using a common solvent (dimethylacetamide) to prepare hybrid membranes by the phase inversion technique induced by a non solvent (water). The catalytic membranes obtained are characterized by an homogeneous distribution of the catalyst in membrane, as evident from SEM in BSE and linear EDS maps on the cross sections (Fig. 6.6c,d).

One of the crucial aspect during catalyst heterogenization is the maintaining of its structural integrity. Solid state characterization techniques (Fourier transform infrared (FT-IR) analysis; Uv–Vis spectroscopy in diffuse reflectance (DR-UV-Vis)) confirmed that the catalyst structure and spectroscopic properties have been preserved within the membranes.

The presence of the charge transfer band at 324 nm, typical of the decatungstate, was evident in the DR-UV-Vis spectra of the PVDF-W10 catalytic membranes surface (Fig. 6.7). The intensity of the CT band increase with the increase of the catalyst loading. The DR–UV–Vis spectra carried out on the PVDF reference membrane confirmed that the polymer does not absorb in the region of interest of the catalyst.

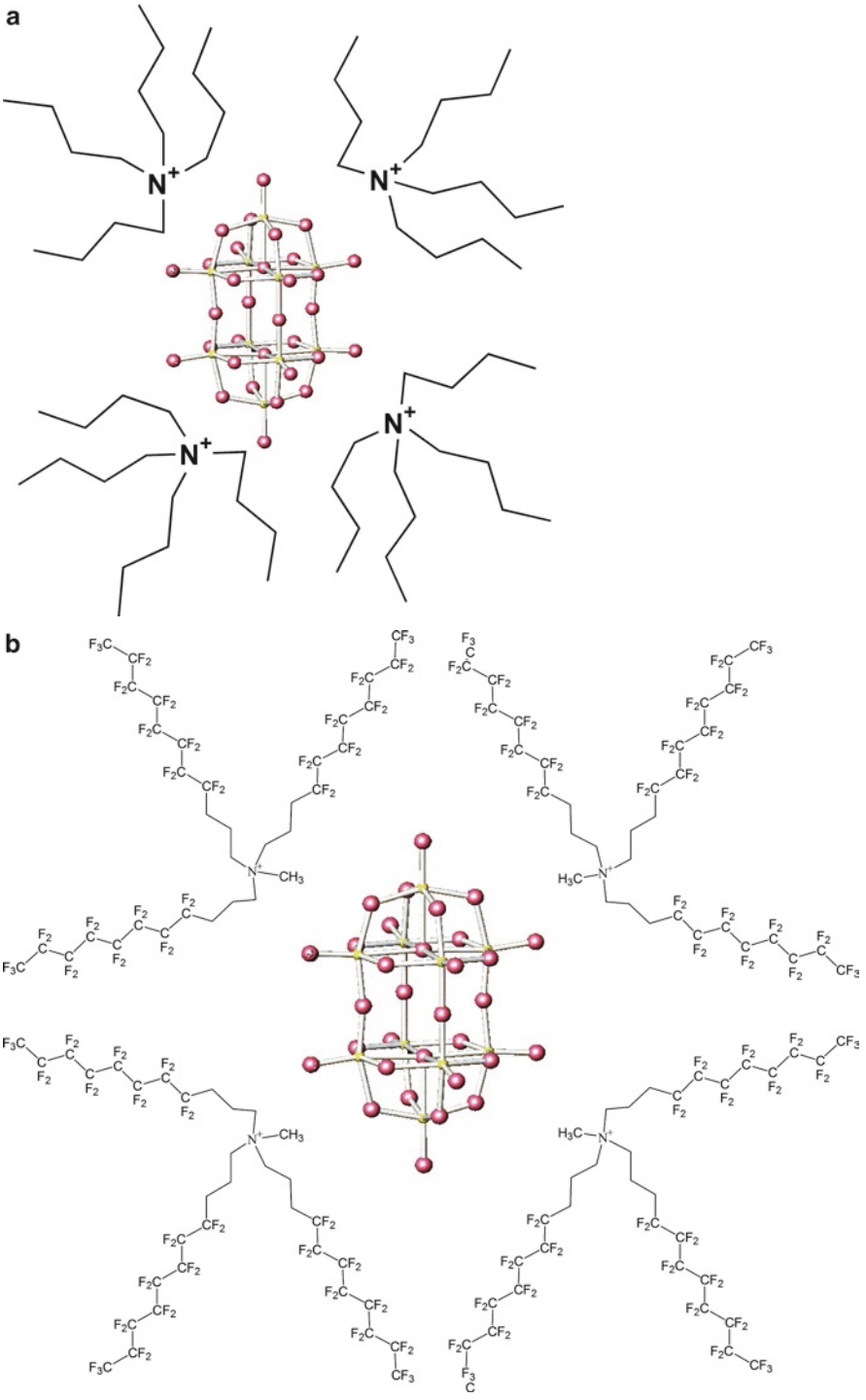

Fig. 6.5 Decatungstate in the form of the tetrabutilamonium salt ($(n\text{-}C_4H_9N)_4W_{10}O_{32}$) (**a**) and fluorous-tagged decatungstate, ($[CF_3(CF_2)_7(CH_2)_3]_3CH_3N)_4W_{10}O_{32}$)

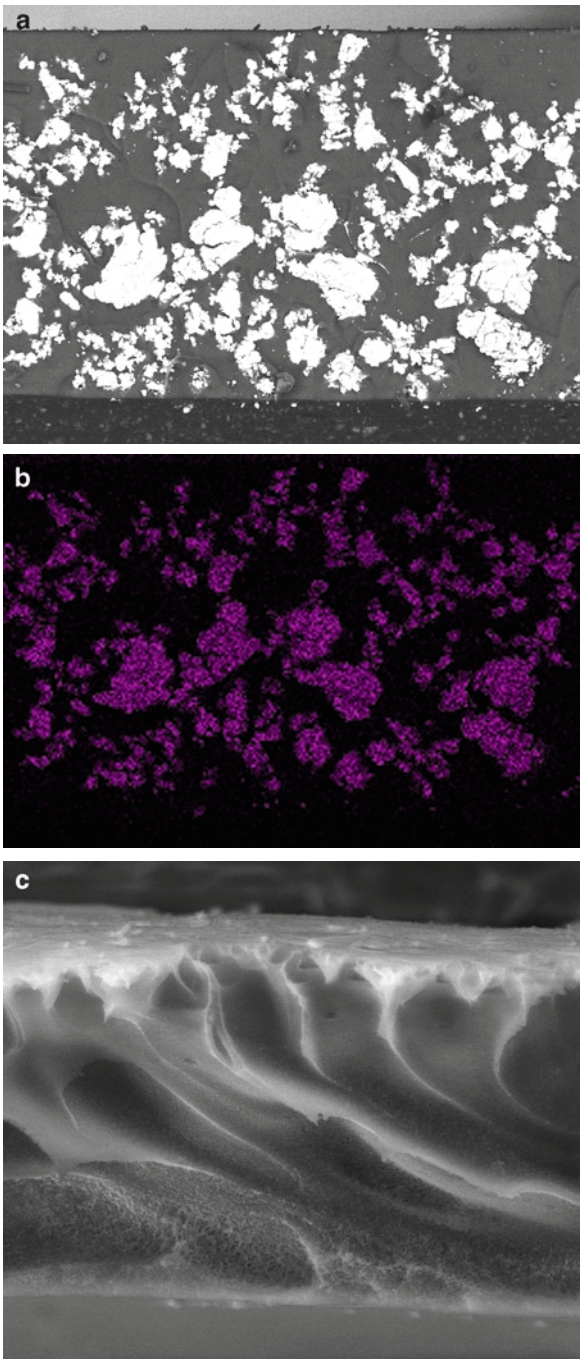

Fig. 6.6 SEM images in BSE of the cross section of a PDMS dense membrane containing the TBAW10 catalyst (loading 12.8 wt%) (**a**) and EDS maps for the W atoms (**b**). SEM images in BSE of the cross section of a PVDF porous membrane containing the same catalyst (25 wt%) (**c**) and with superimposed EDS analyses for W, F, O and C atoms (**d**)

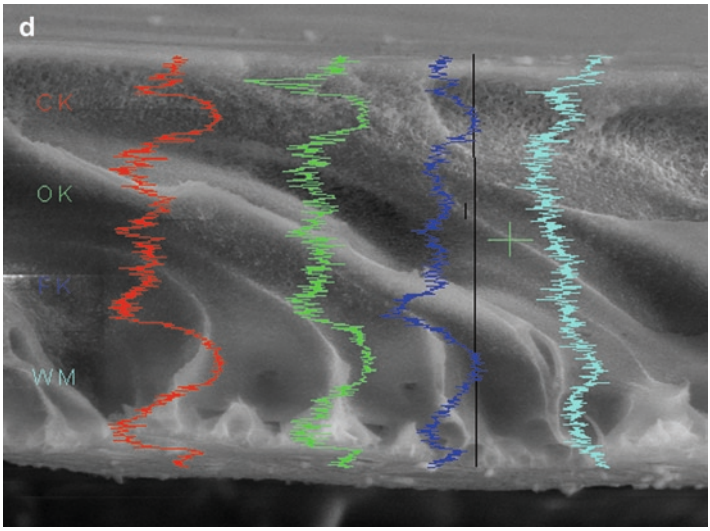

Fig. 6.6 (continued)

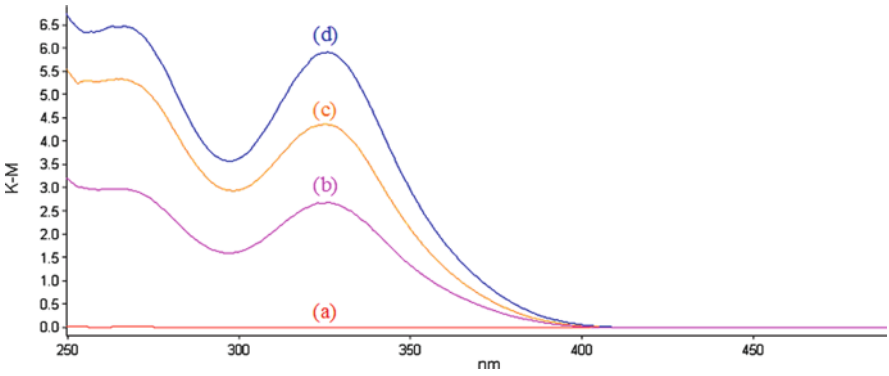

Fig. 6.7 UV–Vis spectra in diffuse reflectance of the PVDF polymer membrane (**a**) and the catalytic membranes prepared with different tetrabutilamonium decatungstate loading (14.3% (**b**); 25.0% (**c**) and 33.3% (**d**))

Also FT-IR analyses confirmed that the catalyst structure is preserved within the polymeric membrane. The infrared spectra of the catalytic membranes (Fig. 6.8) show the characteristic bands of $W_{10}O_{32}^{4-}$ units as well as those typical of the employed alkylammonium cation [35].

The PVDF-W10 and PDMS-W10 photocatalytic systems are characterized by different and tuneable properties depending on the nature of the polymeric micro-environment [33]. These polymer catalytic membranes were used for the selective photooxidation of water-soluble alcohols. The photocatalytic experiments

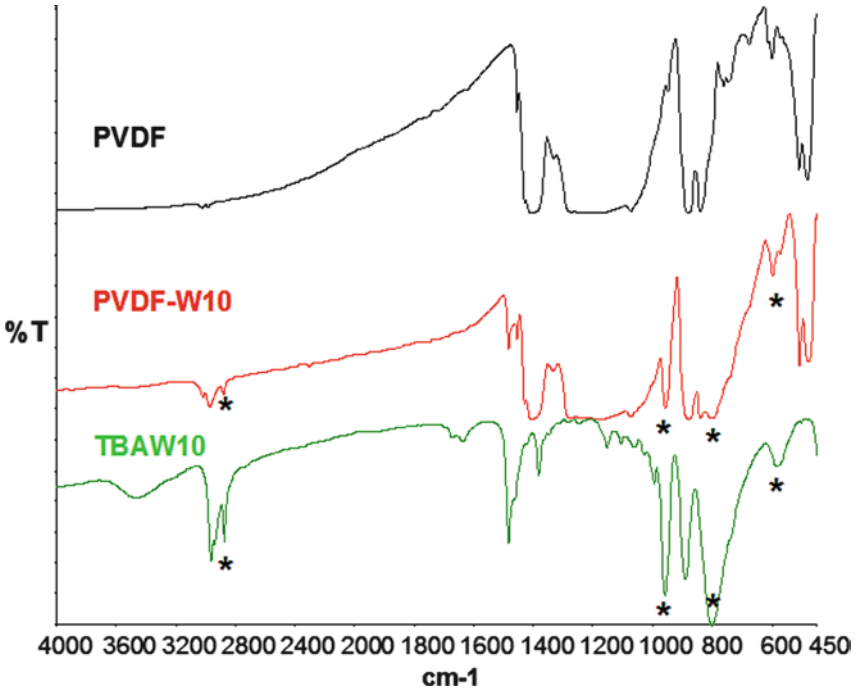

Fig. 6.8 FT-IR spectra of the PVDF polymer membrane, the catalytic PVDF-W10 membrane and the TBAW10 (the asterisks indicate the main absorption bands of the catalyst)

were carried out in a batch setup employing a quartz cell hosted in a thermostatted holder. A single piece of membrane (size: 1.1 × 1.6 cm) was placed on the one internal wall of the cell opposite to the light source, to collect all the focused radiation. The reaction solution (H_2O, 2 ml) containing the substrate (0.04 mmol) was placed in the cell, under magnetic stirring, and oxygen was supplied through a small teflon tube connected with a tank [33].

Membrane induced discrimination of the substrate results from the oxidations of a series of alcohols with different polarity, through comparison with the homogeneous reactions (Fig. 6.9).

The catalyst activity is influenced by the selective sorption and diffusion of the substrate in membrane. Generally, substrates that are preferentially adsorbed, and therefore are more concentrated around the catalytic sites, increase the reaction rate; on the other hand, also diffusion is an important factor for the catalytic reactions, particularly in dense membranes. Cycloheptanol is the more hydrophobic alcohols in this series, and consequently can better interact with the PDMS by Van der Waals interactions; however it is also the more sterically constrained and the reaction rates is lower than for *n*-cyclopentanol.

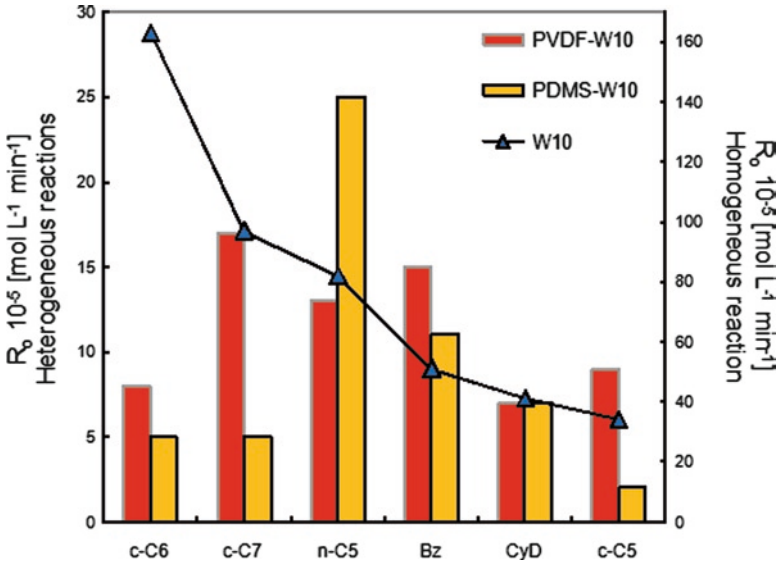

Fig. 6.9 Structure-reactivity trend observed in the photoxidation of alcohols in water by heterogeneous PDMS-W10, PVDF-W10 and homogeneous $Na_4W_{10}O_{32}$ (W10). In all reactions: substrate (0.04 mmol), H_2O (2 ml, pH = 7), pO_2 = 1 atm, $\lambda > 345$ nm, T = 25°C. W10 (0.6 μmol), PDMS-W10 (6.3% loading, 0.6 μmoli); PVDF-W10 (25% loading, 0.6 μmol). Substrate: cis-1,2-cyclohexandiol (CyD); cycloheptanol (c-C7); cyclohexanol (c-C6); cyclopentanol (c-C5); n-pentanol (n-C5); benzyl alcohol (Bz). (Data from [33])

In all cases, the alcohols oxidation occurs following a degradation pathway in which the aldehyde is formed as an intermediate. This reactivity behaviour is known for photooxidations promoted by POMs in water, where an efficient flow of hydroxyl radicals is generated from the solvent.

The PVDF-W10 membranes have been also employed in the aerobic photooxidation of phenol in water carried out in a membrane reactor operating with flow through the membrane [36].

This reaction has been chosen because phenol and its derivatives constituted one of the main organic pollutants present in wastewater, and the development of new effective and environmental benign methods for its degradation is an important research area [37].

The dependence of the phenol degradation rate by the catalyst loading in membrane and the transmembrane pressure has been investigated, allowing to identify the catalytic membrane with catalyst loading 25.0 wt% and operating at 1 bar (contact time 22 s), as the more efficient conditions [36].

The rates of phenol degradation catalysed by homogenous $Na_4W_{10}O_{32}$ and heterogeneous PVDF-W10 (25.0 wt%) has been compared in similar operative conditions. The amount of phenol degraded in the homogeneous and heterogeneous reaction was similar. In both cases, after 5 h of reaction about 50% of the phenol is converted

(starting from 150 ml of a 0.002 M phenol solution). However in the case of the homogenous reaction several persistent intermediate were observed and only the 34.0% of mineralization to CO_2 and water, has been obtained. On the contrary, during photodegradation performed by PVDF catalytic membrane, the phenol converted is also mineralized to CO_2 and H_2O, as confirmed by a similar (49%) percentage of total organic carbon loss.

The high catalytic activity of thePVDF-W10 membranes, in comparison to the homogeneous catalyst, can be ascribed to the selective absorption of the organic substrate from water on the hydrophobic PVDF polymer membrane that increases the effective phenol concentration around the catalytic sites, allowing and intensive contact in the flow-through CMR.

Moreover, the polymeric hydrophobic environment protect the decatungstate from the conversion to an isomer which absorb only light under 280 nm, which instead occurs in homogeneous solution at pH > 2.5.

Polymeric catalytic membranes have also prepared by immobilizing photocatalytic POMs, sodium deacatungstate ($Na_4W_{10}O_{32}$; W10) [38, 39] and phosphotungstic acid ($H_3PW_{12}O_{40}$; W12) [40], on the surface of PVDF membranes modified by Ar/NH_3 plasma discharges (PVDF-NH_2) (Fig. 6.10).

Polar chemical groups (principally NH_2, together with OH, CN, NH and CO) have been grafted, by a NH_3 plasma discharge on the upper surface of PVDF membranes, pre-treated with Ar in order to control hydrophobic recovery [41].

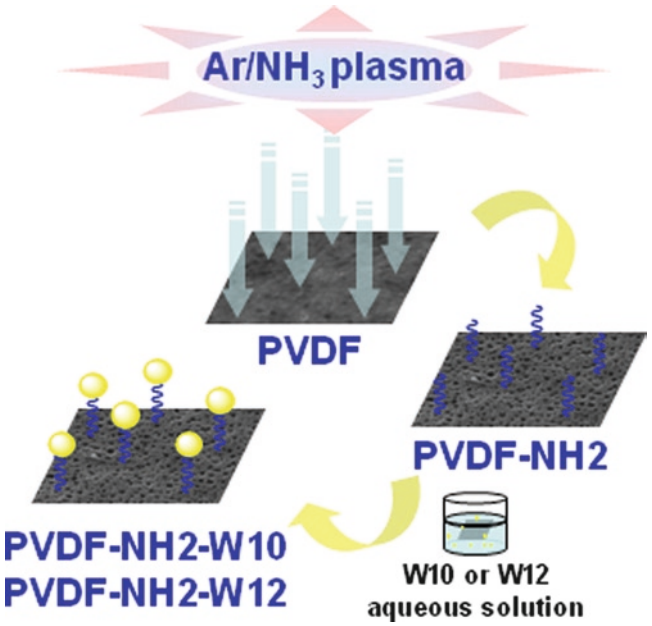

Fig. 6.10 Heterogenization of catalysts on the surface of plasma functionalized PVDF *membranes*

Table 6.4 XPS analysis carried out on the up surface of the PVDF pure membrane, of the membrane treated with Ar/NH_3 plasma (PVDF-NH_2) and the catalytic membranes containing W10 or W12 catalysts (respectively PVDF-NH_2-W10 and PVDF-NH_2-W12) (Data from [38–40])

Membrane	C%	O%	W4f%	P2p%	F%	N%
PVDF	54.2	1.9	–	–	43.8	/
PVDF-NH_2	57.6	4.7	–	–	28.0	9.4
PVDF-NH_2-W10	58.9	19.1	3.3	–	12.1	6.2
PVDF-NH_2-W12	53.1	18.3	3.5	0.4	19.3	5.1

The groups grafted on the surface are able to bind the W10 or W12 catalysts dissolved in aqueous solution, forming charge transfer complexes.

Surface-diagnostics techniques such as X-ray photoelectron spectroscopy (XPS; Table 6.4), contact angle measurements (CA) and RX maps, have been used to attest the surface modification.

The XPS N% value can be taken as a measure of the efficiency of the grafting of N-groups after the NH_3 plasma treatments.

The N content is lowered from 9.4 for PVDF-NH_2, to 6.2 for the PVDF-NH_2-W10 and 5.1 for PVDF-NH_2-W12 surfaces, since W10 or W12 is added to the surface, and W%, O% (and P% for the second one) XPS value increase.

The catalytic membranes (PVDF-NH_2-W10 and PVDF-NH_2-W10), showed superior performances (higher reaction rates) compared to the corresponding homogeneous catalysts, in the aerobic phenol degradation reaction carried out the flow-through CMR [39, 40].

The decatungstate in the form TBAW10 has been also heteorogenized in Hyflon membranes by dispersing it in a polymer solution in Galden HT55 (a mixture of perfluoro-hydrocarbons). However the insolubility of catalyst in this solvent and the low affinity between the catalyst and the polymeric matrix, induced the formation of irregular catalyst aggregates, not well dispersed in the polymeric matrix, which tend to precipitate towards the down surface (Fig. 6.11).

On the contrary, in the case of the fluorus-tagged decatungstate, SEM images of the membrane surface and cross-section highlight an homogeneous distribution of the catalyst domains which appear as spherical particles with uniform size (Fig. 6.12).

Catalytic membranes were prepared by mixing a solution of Hyflon in Galden (2.4 wt%, *sol. 1*) with a solution of $(R_fN)_4W_{10}O_{32}$ in hexafluoroisopropanol (6.8 wt%, *sol. 2*) in an appropriate ratio in order to have the desired loading of catalyst in membrane.

Galden is a good solvent for the Hyflon, but not for the $(R_fN)_4W_{10;}$ on the contrary hexafluoroisopropanol is a good solvent for the catalyst but not for the polymer. However we have found that when the ratio *sol. 1* : *sol 2* is in the range 14.2–7.9 (g:g), an homogeneous solution can be obtained.

Hy-R_fN_4W10 membranes with catalyst loading up to 26% and different thickness 7–94 μm have been prepared by phase inversion induced by solvent evaporation in an environment with temperature and relative humidity controlled (Hy-R_fN_4W10).

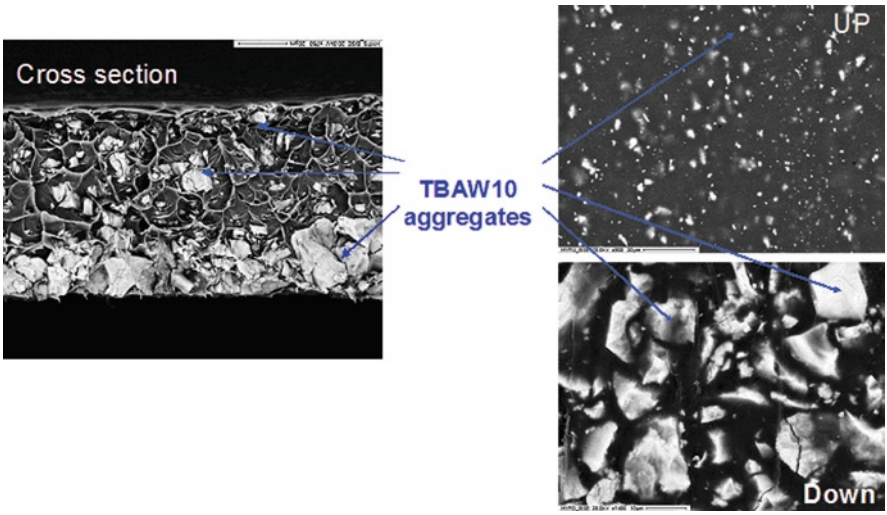

Fig. 6.11 SEM images in BSE of an hyflon membrane conatining TBAW10 catalyst

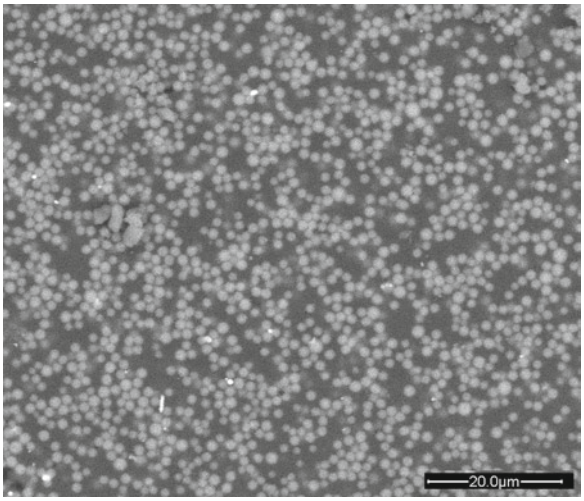

Fig. 6.12 SEM images in BSE of the down surface of an Hyflon membrane immobilizing the R_fN_4W10 catalyst (20 wt%)

DR-UV analyses carried out on the membrane surfaces confirmed that the catalyst did not suffered any modification during the membrane preparation process. The presence of the charge transfer band at 324 nm typical of the decatungstate was evident in the DR-UV spectra of the catalytic membranes surface (Fig. 6.13).

The cationic amphiphiles R_fN^+ groups induce the self-assembly of the surfactant-encapsulated clusters (R_fN^+ groups capped on $W_{10}O_{32}^{4-}$) which, during membrane formation process, give supramolecular assemblies of the catalyst, stabilized by the polymeric matrix [42, 43].

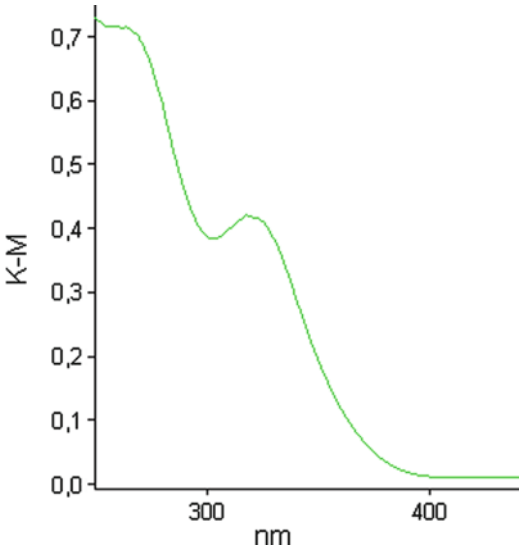

Fig. 6.13 UV spectra in diffuse reflectance of an Hy-R_fN_4W10 (20 wt%)

The dimensions of these clusters and, as a consequence, the surface area and catalytic activity of the decatungstate, can be modulated acting on the membrane preparation conditions. Increasing the membrane formation time by an increase of the membrane thickness (increase of the casting solution initial thickness) the mean dimensions of the R_fN_4W10 clusters became larger because they have more time for aggregate before the solidification of the membrane (Fig. 6.14). Also the increase of the catalyst loading contribute to increase the mean dimension of the clusters.

The catalytic Hyflon-based membranes have been tested in batch solvent-free oxygenation of benzylic C–H bonds of the ethylbenzene (Fig. 6.15) at 25°C under O_2 atmosphere.

The key observation was provided by an increase of the selectivity towards the alcohol (product of interest) when the catalyst is heterogenised in Hyflon membrane (Table 6.5 entries 4–7) in comparison with homogeneous catalysts (entries 1–2) or the catalyst heterogenized in PVDF (entry 3). Moreover, the use of the fluorus-tagged decatungstate well dispersed in Hyflon membrane (entries 5,6) improve the turnover number (TON) in comparison with the TBAW10 only physically entrapped in Hyflon (entry 4).

Only with the thicker Hyflon membrane (entry 7) the TON resulted lower because in the operative condition used the reagent can only diffuse inside the membrane and mass transfer limitations reduce the process efficiency.

Better performance are expected using these membranes in a CMR operating with flow through.

The catalytic membranes with smaller catalyst cluster are characterized by an higher activity in the photooxygenation of ethylbenzene (entries 5–7).

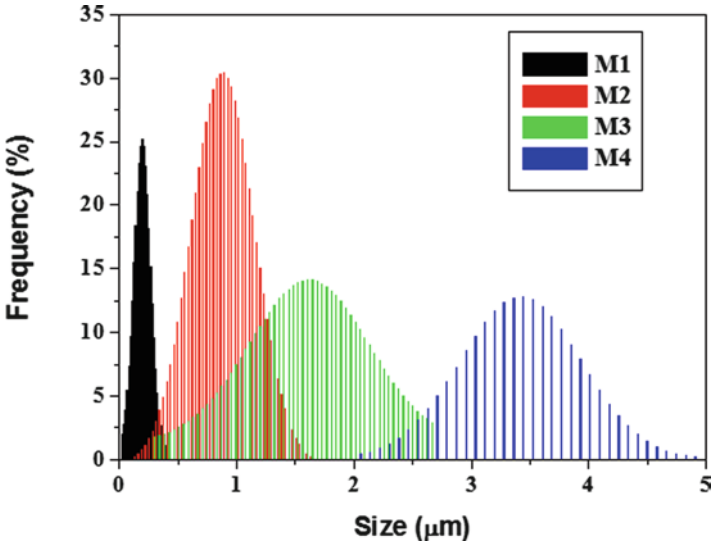

Fig. 6.14 R_fN_4W10 cluster dimensions distribution in the Hyflon membranes for different catalyst loading and membrane thickness (M1: catalyst loading 17%, thickness 8 ± 1 μm; M2: catalyst loading 17%, thickness 44 ± 4 μm; M3: catalyst loading 20%, thickness 45 ± 5 μm; M4: catalyst loading 25%, thickness 94 ± 12 μm)

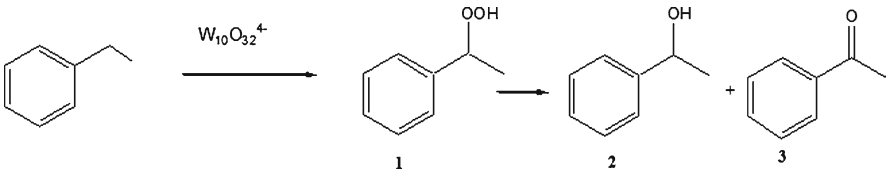

Fig. 6.15 Photooxygenation of ethylbenzene. The products are: hydroperoxide (1), alcohol (2) and acetophenone (3)

Table 6.5 Photocatalytic oxygenation of ethylbenzene by homogeneous decatungstate or heterogeneous catalytic membranes made of PVDF or Hyflon (Data from [34])

Catalyst		Solvent	Cat.μmol	Products (mM)(% 1:2:3)	TON
1	[a]TBAW10	CH_3CN	0.20	64(36:32:32)	351
2	[a]R_fN_4W10	HFP	0.18	95(56:23:21)	581
3	PVDF-TBAW10	Neat	0.32	23(45:23:32)	78
4	Hy- TBAW10	Neat	0.20	81(14:66:20)	443
5	Hy-R_fN_4W10(thickness 7 μm)	Neat	0.03	94(16:46:38)	3,447
6	Hy-R_fN_4W10(thickness 50 μm)	Neat	0.18	196(25:41:34)	1,198
7	Hy-R_fN_4W10(thickness 94 μm)	Neat	0.70	270(15:48:37)	424

1, peroxide; 2, alcohol ; 3, keton. Reaction conditions: ethylbenzene, 1.1 ml; pO_2, 1 atm; $\lambda > 345$ nm; T = 25°C; 4 h irradiation time. Turnover number calculated as: products (mol)/catalyst (mol). [a]Pseudo-neat conditions by addition of 20 μl of solvent; HFP, hesafluoroisopropanol).

6.6 Conclusions

Membrane reactors, in particular catalytic membrane reactors (CMRs) employing polymer catalytic membranes, have a large growth potential for the competitiveness and sustainability of the chemical production.

Key issue to be addresses in the near future is the development of advanced catalytic polymer membranes and modules with acceptable costs, stable in a wide range of solvents and conditions, and showing high and reproducible performance on long terms.

The design of an efficient polymeric catalytic membranes has to be derived from an application-based multidisciplinary approach.

Tailored functionalizations of the catalysts and/or the polymeric membranes are useful tools for the realization of smart membranes with more functions than just to be a selective barrier.

In our research group, novel polymer catalytic membranes have been designed and developed by the heterogenization of photocatalytic POMs (principally decatungstate) in polymeric membranes.

We have demonstrated the possibility to improve the affinity between the polymer and the catalyst by an appropriate functionalizations of the catalyst or the polymer membranes.

Structural and spectroscopic integrity of the catalyst has been confirmed by solid state characterization techniques.

The new functional catalytic membranes prepared have been successfully used to catalyze photooxidation reactions demonstrating as an appropriate choice of the polymeric material used for catalyst heterogenization can allow, not only to recycle the catalysts, but also to improve the catalytic performances.

References

1. Charpentier JC (2007) Ind Eng Chem Res 46:3465–3485
2. Stankiewicz A (2003) Chem Eng Process 42:137–144
3. Drioli E, Fontananova E (2010) Membrane reactors. In: Ullmann's encyclopedia of industrial chemistry, 7th Edition (Article Online Posting Date: January 15, 2010 http://www.interscience.wiley.com/ullmanns). Wiley-VCH Verlag GmbH & Co. KGaA, Weinheim. DOI: 0.1002/14356007.d16_d01.pub
4. Vankelecom IFJ (2002) Chem Rev 102:3779–3810
5. Westermann T, Melin T (2009) Chem Eng Process 48:17–28
6. Fontananova E, Drioli E (2010). Catalytic membranes and membrane reactors. In: Comprehensive membrane science and engineering, chapter 3.05. Elsevier B.V., Amsterdam (The Netherlands)
7. Sirkar KK, Shanbhag PV, Kovvali AS (1999) Ind Eng Chem Res 38:3715–3737
8. Drioli E, Fontananova E (2008) Membrane reactors. In: Advanced membrane technology and applications, Chap. 27. Wiley, Weinheim
9. Sanchez Marcano JG, Tsotsis TT (2005) Membrane reactor. In: Ullmann's encyclopedia of industrial chemistry. Wiley, Weinheim
10. Heinzel A, Vogel B, Hubner P (2002) J Power Sources 105:202–207

11. Molinari R, Caruso A, Poerio T (2009) Catal Today 144:81–86
12. Wang HH, Cong Y, Yang W (2002) Catal Lett 84:101–106
13. Cruz-Lopez A, Guilhaume N, Miachon S, Dalmon JA (2005) Catal Today 107–108:949–956
14. Sundmacher K, Rihko-Struckmann LK, Galvita V (2005) Catal Today 104:185–199
15. Vankelecom IFJ, Parton RF, Casselman MJA, Uytterhoeven JB, Jacobset PA (1996) J Catal 163:457–464
16. Drioli E, Curcio E, Fontananova E (2006) Mass transfer operation−membrane separations. In: Bridgwater J, Molzahn M, Pohorecki R (eds) Chemical engineering, encyclopedia of life support systems (EOLSS). Eolss Publishers, Oxford, UK
17. Gryaznov V (1999) Catal Today 51:391–395
18. Itoh N, Godvind R (1989) Ind Eng Chem Res 28:1554–1557
19. Dioos BML, Vankelecom IFJ, Jacobs PA (2006) Adv Synth Catal 348:1413–1446
20. De Smet K, Aerts S, Ceulemans E, Vankelecom IFJ, Jacobs PA (2001) Chem Commun 7:597–598
21. Van Krevelen DW (1990) Properties of polymers, 3rd edn. Elsevier, Amsterdam
22. Ulbricht M (2006) Polymer 47:2217–2262
23. Ma M, Hill RM (2006) Curr Opin Colloid Interface Sci 11:193–20
24. Vogelaar L, Lammertink RGH, Wessling M (2006) Langmuir 22:3125–3130
25. Clapper JD, Sievens-Figuero L, Guymon CA (2008) Chem Mater 20:768–781
26. Gladysz JA (2001) Pure and Appl Chem 73:1319–1324
27. Hill CL (1999) Nature 401:436–437
28. Barton AFM (1990) Handbook of polymer-liquid interaction parameters and solubility parameters. CRC, Boca Raton, FL
29. Strathmann H, Giorno L, Drioli E (2006) An introduction to membrane science and technology. CNR Roma, ISBN 88-8080-063-9
30. Hill CL, Prosser-McCartha CM (1997) In: Kalyanasundaram K, Gratzel M, Kalyanasundaram K, Gratzel M (eds) Photosensitization and photocatalysis using inorganic and organometallic compounds. Kluwer, Dordrecht, The Netherlands
31. Texier I, Giannotti C, Malato S, Richter C, Delaire J (1999) Catal Today 54:297–307
32. Mylonas A, Roussis V, Papaconstantinou E (1996) Polyhedron 15:3211–3217
33. Bonchio M, Carraro M, Scorrano G, Fontananova E, Drioli E (2003) Adv Synth Catal 345:1119–1126
34. Bonchio M, Carraro M, Gardan M, Scorrano G, Drioli E, Fontananova E (2006) Top Catal 40:133–140
35. Chemseddine A, Sanchez C, Livage J, Launay JP, Fournieric M (1984) Inorg Chem 23:2609–2613
36. Drioli E, Fontananova E, Bonchio M, Carraro M, Gardan M, Scorrano G (2008) Chin J Catal 29(11):1152
37. Kormali P, Dimoticali D, Tsipi D, Hiskia A, Papaconstantinou E (2004) Appl Catal B-Environ 48:175–183
38. Lopez LC, Buonomenna MG, Fontananova E, Iacoviello G, Drioli E, D'Agostino R, Favia P (2006) Adv FuncT Mater 16:1417–1424
39. Lopez LC, Buonomenna MG, Fontananova E, Drioli E, Favia P, d'Agostino R (2007) Plasma Processes Polym 4:326–333
40. Fontananova E, Donato L, Drioli E, Lopez L, Favia P, d'Agostino R (2006) Chem Mater 18:1561–1568
41. Favia P, Sardella P, Gristina E, d'Agostino R (2003) Surf Coat Tech 707:169–170–707–711
42. Bu W, Li H, Sun H, Yin S, Wu L (2005) J Am Chem Soc 127:8016–8017
43. Li H, Sun H, Qi W, Xu M, Wu L (2007) Angew Chem Int Ed 46:1300–1303
44. Aerts S, Weyten H, Buekenhoudt A, Gevers LEM, Vankelecom IFJ, Jacobs PA (2004) Chem Comm 6:710–711
45. Bagnell L, Cavell K, Hodges AM, Mau AWH, Seen AJ (1993) J Membr Sci 85:1291–299
46. De Souza Figueiredo KC, Martins Salim VM, Piacsek Borges C (2008) Catal Today 133–135:809–814

47. Fritsch D, Randjelovic I, Keil F (2004) Catal Today 98:295–308
48. Giorno L, D'Amore E, Mazzei R, Piacentini E, Zhang J, Drioli E, Cassano R, Picci R (2007) J Membr Sci 295:95–101
49. Guerreiro L, Castanheiro JE, Fonseca IM, Martin-Aranda RM, Ramos AM, Vital J (2006) Catal Today 118:166–171
50. Lyko S, Wintgens T, Al-Halbouni D, Baumgarten S, Tacke D, Drensla K, Janot A, Dott W, Pinnekamp J, Melin T (2008) J Membr Sc 317:78–87
51. Mertens PGN (2008) Adv Synth Catal 350:1241–1247
52. Parulekar SJ (2007) Ind Eng Chem Res 46:8490–8504
53. Schmidt A, Haidar R, Schomäcker R (2005) Catal Today 104:305–312
54. Shibatani T, Omori K, Akatsuka H, Kawai E, Matsumae H (2000) J Mol Catal B Enzym 10:141–149
55. Smitha B, Sridhar S, Khan AA (2005) J Membrane Sci 259:10–26
56. Thampan T, Malhotra S, Zhang J, Datta R (2001) Catal Today 67:15–32
57. Wolfson A, Geresh S, Gottlieb M, Herskowitz M (2002) Chem Commun 4:388–390
58. Woltinger J et al (2005) Adv Biochem Engin/Biotechnol 92:289–316
59. Gröschel L, Haidar R, Beyer A, Cölfen H, Frank B, Schomäcker R (2005) Ind Eng Res 44:9064–9070

Chapter 7
Immobilized Complexes for Enantioselective Catalysis: the Industrial Perspective

Benoît Pugin and Hans-Ulrich Blaser

Abstract Work carried out during the development of a production process for (*S*)-Metolachlor, an important herbicide now produced on a >10,000 t/year scale with a homogeneous catalyst, is used as an example to describe the design and preparation of immobilized catalysts in an industrial environment. In the course of this work, a modular approach for the covalent immobilization of catalysts was developed. It is shown that immobilized catalysts with industrially relevant properties can indeed be prepared but that these catalysts tend to be substantially more complex and expensive than their homogeneous counterparts. The second part addresses the question of which requirements an immobilized catalyst must meet to be of industrial interest. Different methods for the preparation of catalysts that can be separated by filtration or extraction are discussed and assessed from our personal point of view and experience. It is shown, that to be accepted, immobilized catalysts must have a clear advantage over their homogeneous counterparts and that the immobilization strategy has to be tailored to the type of product as well as to limitations in time and money to be spent. It is concluded that the most feasible method for the immobilization of chiral catalysts is adsorption on suitable solid supports.

7.1 Introduction

There is no doubt that the trend towards the application of single enantiomers of chiral compounds is increasing. This is especially the case for pharmaceuticals but also for agrochemicals, flavors and fragrances [1, 2]. Among the various methods to selectively produce one single enantiomer of a chiral compound, enantioselective catalysis is arguably the most attractive method. With a minute quantity of a

B. Pugin (✉) and H.-U. Blaser
Solvias AG, P.O. Box CH-4002, Basel, Switzerland
e-mail: benoit.pugin@solvias.com

P. Barbaro and F. Liguori (eds.), *Heterogenized Homogeneous Catalysts for Fine Chemicals Production*, Catalysis by Metal Complexes 33,
DOI 10.1007/978-90-481-3696-4_7,

(usually expensive) chiral auxiliary, large amounts of the desired product can be produced. At this time, biocatalysts [3] and molecular, i.e. homogeneous, metal complexes with chiral ligands [4] are the most widely used and versatile enantioselective catalysts. From an industrial point of view, however, solid catalysts which are not soluble in the same phase as the organic reactant could have attractive new properties such as easy separation and in some cases a heterogeneous nature might be decisive for the use of a catalytic method. Such catalysts can be truly heterogeneous, i.e., insoluble solids or they can be soluble in a second phase that is not miscible with the organic one [5].

We will start this contribution with a case study. One approach during the development of a production process for the grass herbicide (*S*)-metolachlor [6] was the preparation of immobilized Ir diphosphine complexes [7]. We will first describe how we developed a concept based on a modular ligand – linker – support combination with covalent attachment and how we finally found a very efficient iridium Josiphos complex tethered to silica gel. We will then explain why this catalyst finally could not compete with the homogeneous analog and what lessons we learned from these efforts. In the second part we try to generalize these lessons and discuss criteria which are important for any potential industrial application of (immobilized) catalysts.

7.2 The Development of a Catalytic Process for (*S*)-Metolachlor

For about 20 years, metolachlor, Ciba Geigy's most important herbicide was produced as a racemic mixture in a volume of > 20,000 t/year via a Pt/C catalyzed hydrogenation of the sterically hindered imine followed by chloroacetylation as shown in Fig. 7.1. Since both a stereogenic center as well as axial chirality due to inhibited rotation around the C–N bond are present in the molecule, four stereoisomers are produced when a non-chiral catalyst is used. Since independent investigations had shown that the (*S*)-enantiomers carry most of the biological activity a method allowing to produce the (*S*)-enantiomers with 80% ee would result in approx. 30% reduction of environmental load. However, in order to be competitive, a very active and productive catalytic system had to be found and the following

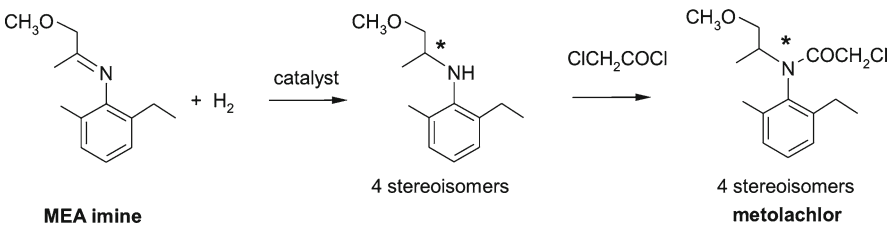

Fig. 7.1 Process for preparing metolachlor

minimum requirements were defined: ee ≥ 80%, a productivity of >50,000 turnovers (TO) and an activity of >10,000 TO/h.

When our project was started in 1983, the only useful state of the art for the hydrogenation of imines was a paper from the Marko group [8] who described the use of Rh diphosphine catalysts but with rather low ee and activity which were improved by Kang et al. [9] in a collaboration with Ciba-Geigy. Very soon we could show that Ir diphosphine complexes were superior to the Rh complexes applied up to this time. However, while several Ir diphosphine complexes were identified with improved enantioselectivities, the more difficult problem turned out to be reaching the required productivity. We achieved up 3,000 TO, however, this seemed to be the limit. Further investigations showed, that a gradual deactivation of the catalyst took place and that this prevented higher productivities [10]. NMR-measurements of the hydride region of spent Ir-catalysts indicated that the cause for deactivation was due to the irreversible formation of catalytically inactive hydride-bridged di- or trinuclear Ir clusters as described by Crabtree for achiral Ir complexes [11]. This hint led to the idea to fix the Ir complexes on a solid support in order to prevent the Ir-centers to interact with each other. Since we hoped that we could also improve catalyst separation with this strategy, we decided to start a program to study the immobilization of chiral metal complexes.

Since a first survey of the literature showed that with few exceptions, most immobilized catalysts were significantly less active and productive than their homogeneous analogs [12], we developed a new approach to solve this problem [13, 14].

Our approach is based on the functionalization of known effective diphosphine ligands. In this strategy an additional OH or NH function is introduced that can react with commercial isocyanate linkers which in turn can be attached to various supports (see Fig. 7.2). To immobilize ligands on inorganic supports, trialkoxysilane-alkyl-isocyanate linkers were used [13]. In a similar way, the same ligands were attached to organic polymers via OH or NH functions by the use of diisocyanate linkers [14]. The metal complex catalysts can be prepared in situ by adding a

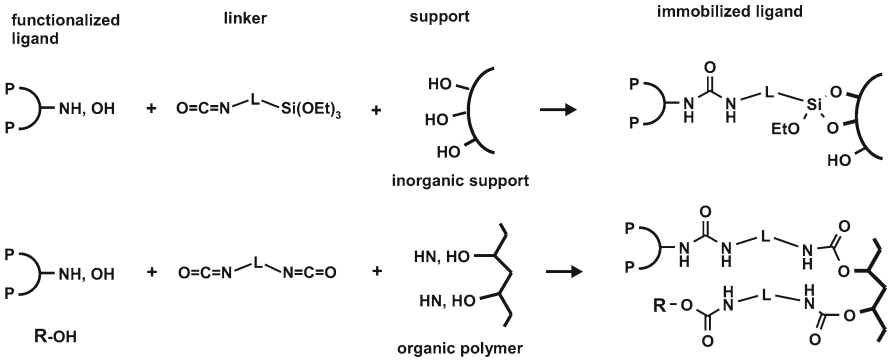

Fig. 7.2 Modular approach for the immobilization of ligands

suitable metal complex such as $[Rh(NBD)_2]BF_4$, $[Rh(COD)Cl]_2$ or $[Ir(COD)Cl]_2$ to the immobilized ligands. To identify suitable support types, we prepared a series of immobilized ligands and tested these in the Rh catalyzed hydrogenation of methyl acetamido cinnamate (MAC), a standard test in enantioselective hydrogenation.

In these studies, we found that with our immobilization strategy silica gels were the supports of choice, especially since a large variety of silica gels with different pore size distributions and specific surfaces are commercially available. In many cases the immobilized Rh diphosphine catalysts were at least as efficient as their homogeneous counterparts. The catalyst attached to a soluble polyphenoxy-resin performed as the free catalyst, but its separation was tedious. Catalysts on aminomethylated polystyrene crosslinked with 1% of divinylbenzene (DVB) could easily be separated by filtration, but a solvent like THF which swells the polymer is required and the immobilized catalyst was significantly less active.

With these excellent silica gel bound diphosphine ligands in hand we set out to study the effects of site isolation with several Ir catalysts. We immobilized several ligands on silica gel with varying ligand loading (μmol of ligand/m^2 support surface) and determined their catalytic activity for the Ir catalyzed hydrogenation of the DMA imine (see Fig. 7.3). Our working hypothesis was indeed confirmed since the catalytic activity increased with decreasing ligand loading if the same s/c ratio was used. However, in spite of intense optimization work, it was not possible to achieve more than 10,000–15,000 turnovers and the ee values could also not improved sufficiently.

Fortunately, just at that time a new class of diphosphine ligands, the ferrocene based Josiphos ligand family was developed in our laboratories [15]. These ligands are highly modular and easily accessible in two synthetic steps starting from Ugi amine. It was soon found that their Ir complexes exhibit unprecedented activity and productivity for the MEA imine hydrogenation and yielded the desired chiral amine with ee's around 80%.

Very soon it looked quite probable that a Josiphos type ligand would be chosen for the production of (*S*)-metolachlor. In order to have a solution for catalyst separation at hand, if needed, we set out to develop synthetic routes to functionalized Josiphos ligands. A chiral dibromo ferrocene scaffold proved to be highly versatile and allowed preparation and attachment of ferrocene based diphosphines to solid

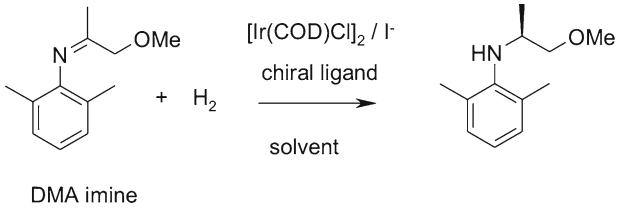

Fig. 7.3 Stereoselective hydrogenation of DMA imine with free and immobilized Ir-catalysts

supports or vehicles to render them soluble in water or ionic liquids [16, 17]. However, it is important to realize, that compared to the preparation of soluble Josiphos ligands, at least two additional synthetic steps have to be carried out to access these functionalized analogs.

Meanwhile, the catalytic system that is now used for the production of (*S*)-metolachlor was developed. It is based on an Ir complex containing a Josiphos derivative with R = 3,5-xylyl and we prepared the corresponding functionalized Josiphos derivative. This ligand was then immobilized on silica gel and also made water soluble and the results of the hydrogenation reaction of MEA imine are summarized in Fig. 7.4.

The good news was that 120,000 TON and good selectivity could be obtained with the silica gel bound catalyst – indeed a very remarkable result. However, the immobilized catalyst is significantly less active than the free catalyst which has an unprecedented activity and productivity (in production, complete conversion is obtained in a few hours with s/c of up to two million). As before, the polystyrene bound catalyst was less active than the silica gel bound analog. Estimates based on models suggest that the lower activities obtained with both immobilized catalysts result from mass transport problems within the supports. The extractable catalyst also showed excellent performance similar to the free catalyst and catalyst separation via extraction was efficient. However, since it was decided to purify the product by distillation there was no need for such a sophisticated and more expensive extractable catalyst.

In the process of developing a comprehensive immobilization strategy and its implementation on a concrete chemical process we learned several lessons which might be of general importance. These points will be discussed more generally in the next section.

	free		**extractable**	**immobilized, silica gel**		**immobilized, polystyrene**
	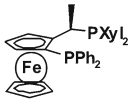		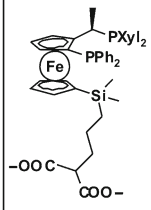	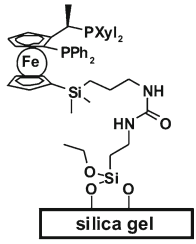		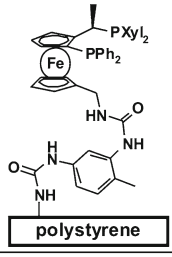
S/C	50,000	120,000	120,000	50,000	120,000	50,000
time	1h	2.1h	3h	8h	10h	30h
ee	79%	80%	79%	78%	78%	74%
separation			extraction > 90%	filtration 95%		filtration 95%

Fig. 7.4 Hydrogenation of MEA imine with free, extractable and immobilized Josiphos

7.3 Requirements for an Immobilized Catalysts to be of Industrial Interest

The major reasons that none of the immobilized catalysts were competitive in the (*S*)-metolachlor process are obvious: The immobilized catalysts were more expensive than their unmodified analogs, activity and selectivity were in most cases inferior and they did not offer any advantage in the chemical processing. Generally speaking, immobilized catalysts should meet the following requirements in order to make them competitive in an industrial setting:

1. The immobilized catalysts must have a significant chemical and or operational advantage over the homogeneous system.
2. The catalysts must be available within an acceptable time in the requested amounts at competitive costs.
3. Their scope and limitations concerning catalytic performance should be well known.

In the following, the first two points are discussed on the basis of what is often claimed in the literature with comments from our own experience and illustrated with a few examples.

7.3.1 Chemical or Operational Advantages

The advantages most often claimed in the literature are catalyst separation, catalyst re-use, new opportunities in process engineering and improved catalytic performance.

7.3.1.1 Catalyst Separation

It is correct that many catalysts immobilized on solid supports can easily be separated by a simple filtration. It must however be realized that there are gel like or soluble polymer based catalysts which require more sophisticated (and expensive) methods such as microfiltration. There are also some very convincing cases where separation via extraction works well.

However, some words of caution should be added. There are many cases in the literature where immobilization leads to a decline of the catalytic performance (see below), sometimes due to mass transport problems, sometimes due to chemical interactions. Furthermore, while filtration will be able to remove the bulk of the catalyst, trace metal impurities might still require an additional purification step (especially for pharma products). For this purpose a number of effective adsorbents or scavengers are now commercially available.

Of course, immobilized catalysts can be very handy. However, their importance is often overestimated. In our own experience with chiral pharmaceutical intermediates, classical work up and purification methods such as extraction, crystallization or distillation of the product allow to separate the homogeneous catalysts in a majority of cases [1].

7.3.1.2 Catalyst Re-use

Obviously, catalyst recycling is a valuable strategy to improve catalyst productivity (TON) and this is much better possible with a heterogeneous catalyst. Indeed most papers on catalyst immobilization demonstrate some sort of recycling. Unfortunately, this is very often done with much lower s/c ratios than typically applied with homogeneous catalysts and a comparison of the maximal attainable TONs is often missing. Furthermore, we would like to stress that the catalyst must be very stable and not too sensitive to deactivation. This will be demonstrated with two examples from our laboratory.

The first example concerns Rh diphosphine catalysts typically used in asymmetric hydrogenation. We found that not only homogeneous but also the corresponding immobilized catalysts can be rather air sensitive. This is illustrated for the catalyst depicted in Fig. 7.5 for the hydrogenation of MAC. As can be seen, already traces of air are sufficient to almost completely deactivate the catalyst. Since this also occurred with the immobilized catalyst, handling of this catalyst is very demanding and recycling will be very difficult and not trivial.

The second example shows a very positive case: A Ru biphep immobilized on silicagel was found to be extremely stable and recycling over 11 cycles proved to be unproblematic at s/c ratios between 400 and 1,000 as depicted in Fig. 7.6 [18]. After eight cycles the catalyst was even stored in the fridge for about 2 weeks before it was used again. While there are variations in ee and turnover frequency (TOF), the values are comparable to those of the soluble analog.

In conclusion it can be stated that a recycling strategy to reach high TON is usually only the second best solution and that it should be considered when very stable catalysts with relatively low activity are involved. In such case, higher catalyst

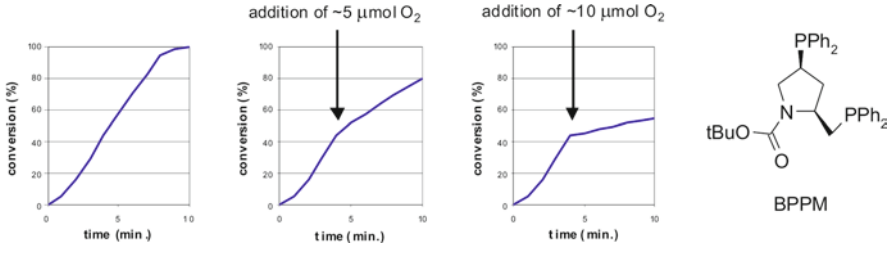

Fig. 7.5 Effect of oxygen addition on the H_2-up take in the hydrogenation of MAC in presence of 10 µmol $[Rh(BPPM)]BF_4$

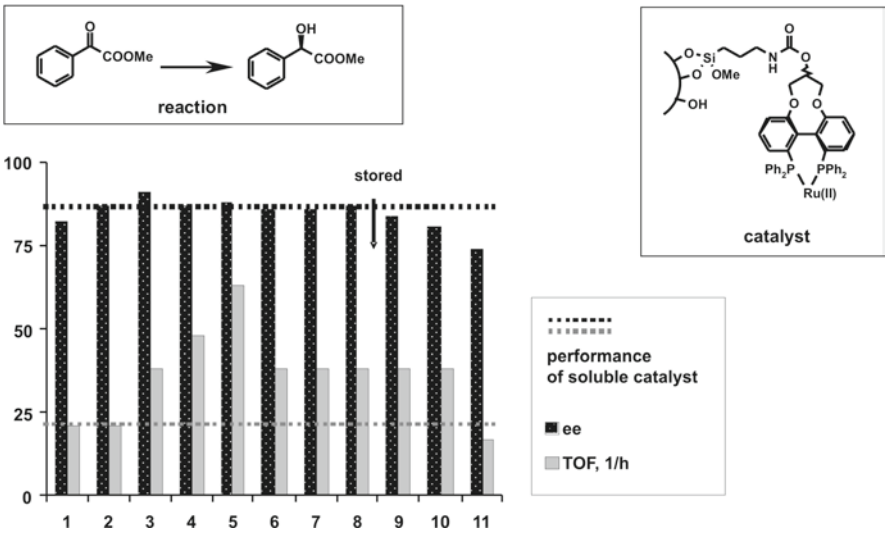

Fig. 7.6 Ee and TOF (at high conversion) for the recycling of an immobilized Ru biphep catalyst

loadings allow to improve the space/time yields and sometimes inhibition by product or starting material might be alleviated.

7.3.1.3 New Opportunities in Process Engineering

Working in different phases also presents new opportunities for process engineers such as working in a continuous mode which can have significant advantages over batch operations. At the moment this technique is considerably more complex and is mainly applied in dedicated production plants for the manufacture of large scale products or due to safety considerations when dangerous chemicals are involved. This situation might change when the upcoming micro reactor technology is more broadly established. Several elegant examples have been published where immobilized solid catalysts have been used to prepare chiral products in a continuous fashion, however as far as we know there are no industrial applications in the fine chemicals industry up to now. Here we briefly summarize results reported by Kragl and coworkers for the reduction of acetophenone with BH_3-SMe_2 in presence of an immobilized amino alcohol which is well known to accelerate the otherwise very slow reduction and to render it enantioselective [19] (see Fig. 7.7). There are two beneficial effects of using membrane reactor with a high catalyst loading. On the one hand, the very high local concentration of the ligand suppresses the slow background reaction and the catalyst must not be removed from the product. Indeed using a quite small reactor allows the production of appreciable amounts of chiral product since the ligand is quite stable.

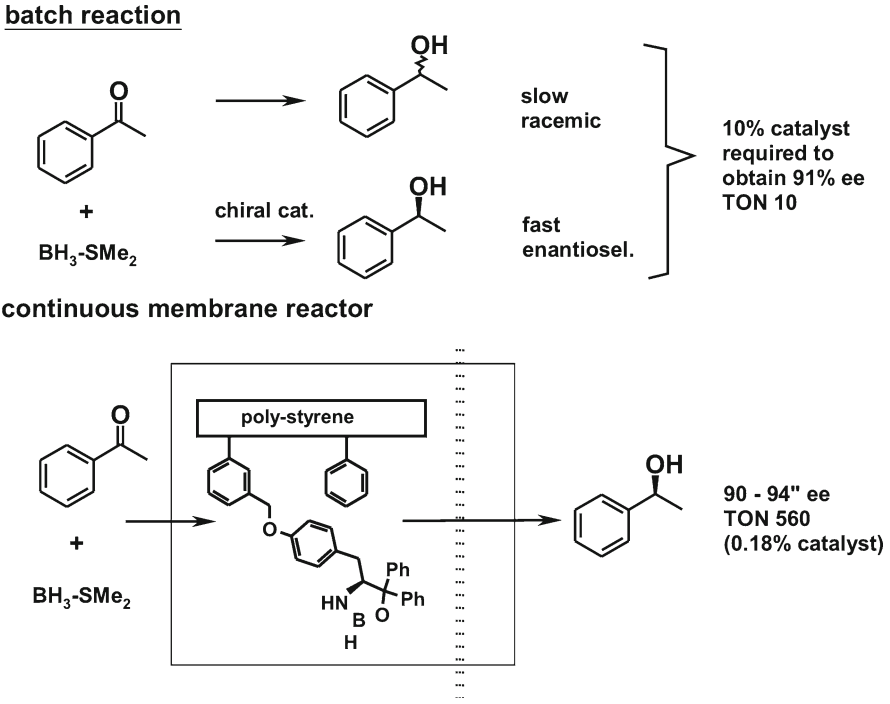

Fig. 7.7 Use of an immobilized organocatalyst in a continuous flow membrane reactor

7.3.1.4 Improved Catalytic Performance

As described in the introduction, most immobilized catalysts of the first generation showed inferior catalyst performance (ee, TON and TOF). This must of course not be the case and there are some proponents which claim just the opposite, especially for catalysts confined in defined cages due spatial confinement [20]. While such effects are hard to predict, there are two cases where immobilization can predictably lead to improved catalytic performance. The first case has been described above, when site isolation prevented the formation of inactive di- and trinuclear Ir species in for the hydrogenation of MEA imine. It is also immediately clear that there is a price to pay for this strategy. In order to achieve site isolation, very low ligand loadings have to be applied and this means that the highest activity is obtained with the most voluminous catalysts. In the case described above this means that the average weight per mole of catalyst increase from 5 to 62 kg when changing the ligand loading form 190 to 16 μmol/g.

The second case of a beneficial effect of immobilization is when metal centers have to cooperate to give an active species (cooperative effect). A prominent example is Jacobsen's epoxide opening using Co salen catalysts [21]. He showed that the two Co centers have to cooperate and achieved site cooperation by catalyst immobilization as depicted in Fig. 7.8 (similar effects were observed with a

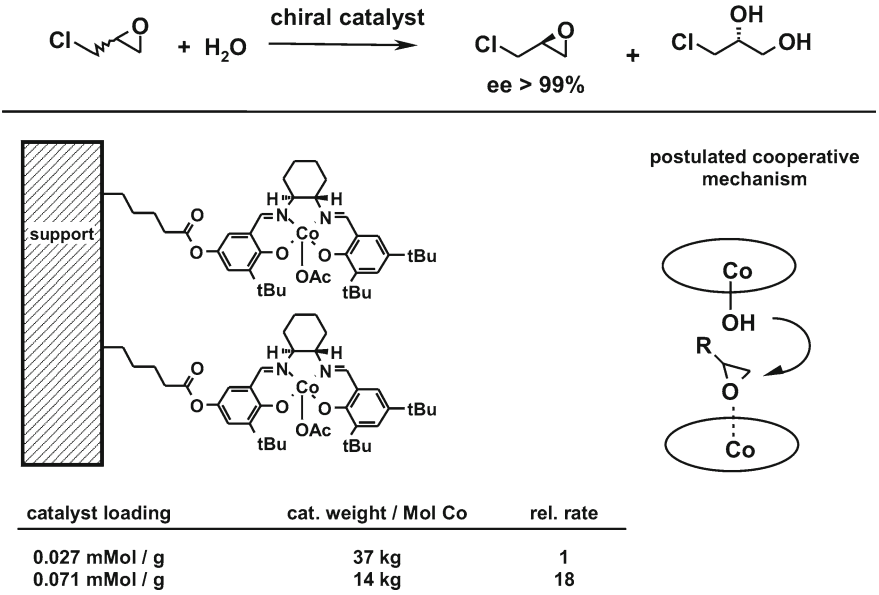

catalyst loading	cat. weight / Mol Co	rel. rate
0.027 mMol / g	37 kg	1
0.071 mMol / g	14 kg	18

Fig. 7.8 The effect of site cooperation in the Co catalyzed resolution of epoxides

soluble dimeric catalysts obtained by coupling via an organic linker). It is also apparent that this case is inherently more advantageous since the most active immobilized catalysts are those with the highest ligand loading and hence the least voluminous ones.

Finally, there are rare cases where the catalyst solubility has to be adapted to the solubility of the substrate. A case in point is hydrogenation of folic acid which is only soluble in water which necessitates the use of water soluble complexes which can be achieved e.g. by tethering ligands to a water soluble vehicle [16].

7.3.2 Catalyst Availability, Development Time, Catalyst Costs: The Rules of the Game

In order to make our point, we will first give some background information on typical industrial situations. It is important to realize that the relative importance of these factors differ according to the type of chiral product which should be manufactured. This means that the rules of the game are very different depending on whether new chemical entities (i.e., new drug candidates, NCE) in the pharmaceutical industry or relatively large scale intermediates or products are produced. The following factors are crucial:

For new chemical entities	For large scale chemicals
– Patent protection for the compound – Short development time essential (time to market might be decisive) – Relatively low development costs (high attrition rate) – The process must be competitive but not the best (high priced products, performance driven, cost of goods not so important)	– Patent protection for the process – It is worthwhile to invest in the development of the catalyst and the process (low attrition rate – the product is established) – The process (and the catalyst) must be the best (low priced products, cost driven, cost of goods very important)

7.3.2.1 Catalysts for NCEs and Similar Fine Chemicals

These are usually rather complex molecules with many functionalities which are produced in relatively small scale of typically 100 kg to maybe 10–20 t/year. Most of these chemicals are high added value products which are bought for their superior performance and therefore tolerate relatively high production costs. This allows applying alternative methods such as chiral pool synthesis, optical resolution or even separation of enantiomers by preparative chiral HPLC. On the other hand, a catalytic method has not to be optimal, it just has to be competitive compared with the alternative methods. Finally, since most of these compounds are patent protected, time to market is a crucial. Typically, the development of a catalytic system from the first experiments to an optimized scalable process should be achievable within less than half a year. Very often such a development is carried out in parallel with alternative (usually non-catalytic) synthetic routes.

Typically, the development of a catalytic system includes the following steps: (a) catalyst screening, (b) catalyst optimization, (c) scale up, catalyst separation.

Catalyst screening is now routinely done in a high through put mode [22]. The ligands and metal complexes must be available within a few days on the 100 mg scale. Since it is not possible to predict which catalytic system is optimal for a desired transformation, many candidates must be tested. This is especially true for the chiral ligands which are structurally very diverse. Today, several commercial suppliers offer a considerable number of chiral phosphine ligands for screening purposes. In contrast, the commercial availability of immobilized ligands/catalysts is restricted to a few simple achiral monodentate phosphines. To the best of our knowledge, no immobilized chiral phosphine ligand is commercially available today. Once a suitable ligand/catalyst system has been identified and optimized, catalyst separation is studied. First, the classical methods such as distillation or crystallization of the product or extraction methods are tested. Only when these do not allow separation of the catalyst, immobilization strategies for the optimized ligand are being considered.

This leads then to the question, which of the several known immobilization methods depicted and assessed in Table 7.1 are suitable for this purpose. In order to covalently

Table 7.1 Overview and assessment of immobilization methods

	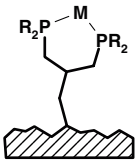	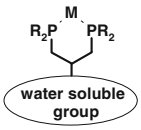	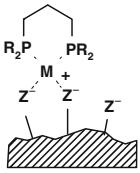	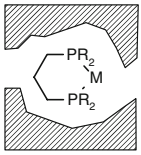
Immobilization method	Covalent binding	Solubility	Adsorption	Entrapment
Applicability	Broad	Restricted	Restricted	Very restricted
Problems	Cost, time	Cost, time, solvent choice	Competition with ions, solvent	Access of substrate, mass transport

bind the chosen ligand to a solid support the ligand has to be modified as described above. While this often leads to a catalyst with few restrictions concerning solvent or operating mode, covalent binding goes along with higher ligand costs and longer development times. Binding to a water soluble vesicle has similar consequences. In contrast, immobilization by adsorption or entrapment can be performed with the unchanged ligand and is therefore much more straightforward and less costly. However, for larger multifunctional substrates entrapment is not feasible since the required small pores will usually not allow easy access to the catalyst. For these reasons, adsorption seems to be the most promising approach since it can be applied with unmodified commercial ligands and it is not limited to supports with small pores.

Many adsorbed catalysts have already been described in the literature and the field has recently been reviewed [23–26]. The most successful approaches for hydrogenation catalysts are the adsorption of the metal/ligand complexes on various alumina-silicates [23, 26, 28], on heteropolyacids attached to alumina [27], and on ion exchange resins [25]. The results of these studies can be summarized as follows:

- With the possible exception of the heteropolyacids attached to alumina supports which are being commercialized by Johnson Matthey and Engelhard [27, 30], none of the publications indicate any industrial application of an immobilized catalyst.
- Enantioselectivities with all three supports are in many cases very close to their homogeneous counterparts, even for recycling experiments.
- In contrast, activity seems to be the more difficult problem to solve. Typical turnover frequencies for adsorbed catalysts are in the range of 50–5,000/h, which is considerably lower than those reported for the homogeneous catalysts under similar conditions (TOF's up to 50,000/h can be reached). Unfortunately, it was not always clear, whether stirring was efficient enough to avoid gas–liquid transport limitations but in many cases it is quite likely that slow mass transport within the supports is responsible for the lower rates. This leaves much room for the development of better supports with improved mass transport properties

(small particle size, uniform large pores). It must also be noted that the TOF can depend on the optimal solvent/support combination [29].

- With most support types, acceptable leaching (<1% Rh) can be achieved, however, no recipe for success can be given. The extent of leaching seems to depend mostly on the combination of adsorbent type and solvent used. As expected, polar, protic solvent such as MeOH give higher leaching than less polar solvents such a *i*-propanol or TBME.
- As mentioned earlier, another important factor is the "molecular weight", respectively the volume of immobilized catalysts. For reasons of handling large catalyst volumes and also of costs (many supports are expensive) there is interest to attach a large number of metal complexes on a small amount of support. The typical molecular weight of a chiral Rh-diphosphine catalyst is in the range of 500–1,000 Da. It seems that for most methods, immobilized catalysts with ~10 kDa/mol can be obtained (which is close to ideal), but this aspect has not received much attention and many examples for higher weights (up to over 100 kDa) have been reported.

7.3.2.2 Catalysts for Larger Scale Chemicals

Typical bulk chemicals are simple, low added value molecules which are produced on large scale, very often in highly optimized single purpose plants. At the moment, there are not very many such chiral products. Typical examples are (*S*)-metolachlor or several amino acids which are produced on >10,000 t/year scale. Usually there are no viable alternatives to catalysis for their production and to be competitive, the catalytic process should at least match or better outperform the state of art process. Quite often, these products are produced in continuous processes. Therefore, efficient catalyst immobilization/separation is an important issue. Under these conditions, any catalyst separation method can be envisaged, even if it has to be developed from scratch and with a significant effort in time and manpower. While we are not aware of any case where a chiral bulk intermediate is being produced with such an immobilized catalyst, several industrial applications have been reported for the production of achiral bulk chemicals.

The first example is the well known Ruhrchemie/Rhone Pôulenc oxo process. In this process, propylene and syngas are reacted to yield *n*-butanal as the desired product besides 4% *i*-butanal. The catalyst is a water soluble Rh/triphenylphosphine trisulfonate (TPPTS) [31] complex which allows to carry out the reaction in a two phase (water/organic product) system. The catalytic species in this process is $[HRh(CO)(TPPTS)_3]$ which is separated from the organic product by continuous decantation. The separation is highly efficient, the Rh content in butanal being as low as 10^{-9} g/kg product. Important R&D and engineering efforts had to be invested to develop this sophisticated system to a stable and optimized process. The first plant with a capacity of 330,000 t/year went on stream in 1984 [32].

The same principal of immobilization of a catalyst in an aqueous phase was extended by Rhône Poulenc to the synthesis of geranylacetone, an important intermediate for the

manufacturing of vitamin E, by Rh/TPPTS catalyzed addition of acetoacetate to myrcene [33].

A second example is the Acetica process developed by Chiyoda and UOP for the production of acetic acid from methanol and carbon monoxide using an Rh complex immobilized via adsorption on a polyvinylpyridine resin [34]. The reaction is carried out in a three phase, continuous bubble reactor which prevents attrition of the polymer beads which might be a problem in a classical stirred reactor. It has been shown that the catalyst is stable over >7,000 h.

These examples demonstrate that immobilized catalysts can indeed be applied on a technical level but it is also clear that considerable development efforts are needed in order to achieve a competitive process.

7.4 Conclusions

The case study of (*S*)-metolachlor illustrates that immobilized metal complex catalysts are much more complicated than the corresponding homogeneous systems, especially when solid supports are involved. Factors such as the influence of the functionalization of the ligand, the type of linkers, the type of support, mass transport or compatibility with solvents have to be studied and understood before production chemists and engineers will use such catalysts. The situation will only gradually improve with increasing insight and experience in this highly exciting and complex interdisciplinary field.

Looking back, the development of the (*S*)-metolachlor process was untypical. (*S*)-Metolachlor is a chiral product but due to its large size (>10,000 t/year) and relatively low added value (the costs for a comparable herbicidal effect had to be in same range as those for (*rac*)-metolachlor) it can be regarded as a bulk chemical. Untypical for a bioactive compound, there was no real alternative to the asymmetric catalytic hydrogenation to access (*S*)-metolachlor and because the racemic product was already commercial, market acceptance was guaranteed. For this reason management was ready to make this large investment in R&D over several years, which among other things allowed the development of immobilized catalysts.

Our modular approach was very helpful since it allowed to quickly test and assess a large variety of supports and to adapt these systems for different ligands. However, covalent binding called for functionalization of the ligands which proved to be time consuming and costly. Nevertheless, the metolachlor project allowed us to acquire the experience and to establish a tool box that today allows us to develop covalently bound chiral catalysts within useful time.

The fact that several processes use water soluble or adsorbed catalysts for the manufacture of bulk chemicals demonstrates that these technologies can be used in an industrial environment and that they can indeed compete with more conventional alternatives. However, it is also evident that the development efforts required to achieve

good results exceeds what can usually be tolerated in the Fine Chemicals industry for their lower volume products.

References

1. Blaser HU, Schmidt E (eds) (2003) Large scale asymmetric catalysis. Wiley, Weinheim
2. Ager DJ (ed) (2005) Handbook of chiral chemicals, 2nd edn. Boca Raton, CRC Press
3. For e recent overview see: Pantaleone DP (2005) Biotransformations: "green" processes for the synthesis of chiral fine chemical. In: Ager DJ (ed) Handbook of chiral chemicals, 2nd edn. CRC, Boca Raton
4. Jacobsen EN, Hayashi T, Pfaltz A (eds) (1999) Comprehensive asymmetric catalysis. Springer, Berlin
5. For a recent review see: Blaser HU, Pugin B (2008) In: Ertl G, Knözinger H, Schüth F, Weitkamp J (eds) Handbook of heterogeneous catalysis, 2nd edn. Wiley, Weinheim, p. 3603
6. For a detailed case history see: Blaser HU (2002) Adv Synth Catal 344:17
7. Pugin B, Landert H, Spindler F, Blaser HU (2002) Adv Synth Catal 344:974
8. Vastag S, Bakos J, Torös S, Takach N, King RB, Heil B, Marko L (1984) J Mol Catal 22:283
9. Kang GJ, Cullen WR, Fryzuk MD, James BR, Kutney JP (1988) Chem Comm 22:1466
10. Blaser HU, Pugin B, Spindler F, Togni A (2002) C R Chimie 5:1
11. Cadosh D, Crabtree R, Felkin H, Morehouse S, Morris G (1982) Inorg Chem 21:1307, and references cited therein
12. See literature cited in: Vilim J, Hetfleijs J (1978) Collect Czech Chem Commun 43:122
13. Pugin B, Müller M (1993) Stud Surf Sci Catal 78:107
14. Pugin B, Blaser HU (2006) Adv Synth Catal 348:1742
15. Blaser HU, Brieden W, Pugin B, Spindler F, Studer M, Togni A (2002) Topics Catal 19:3
16. Pugin B, Groehn V, Moser R, Blaser HU (2006) Tetrahedron Asym 17:544
17. Feng X, Pugin B, Küsters E, Sedelmeier G, Blaser HU (2007) Adv Synth Catal 349:1803
18. Steiner I, Aufdenblatten R, Togni A, Blaser HU, Pugin B (2004) Tetrahedron Asym 15:2307
19. Giffels G, Beliczey J, Felder M, Kragl U (1998) Tetrahedron Asym 9:691
20. For a recent review see: Thomas JM, Raja R (2008) Acc Chem Res 41:708
21. Allen DA, Jacobsen EN (1999) J Am Chem Soc 121:4147
22. Blaser HU, Hoge G, Lotz M, Nettekoven U, Schnyder A, Spindler F (2008) Chimia 62:476
23. Fraile JM, Garcia JI, Mayoral JA (2009) Chem Rev 109:360
24. Masters AF, Ward AJ, Maschmeyer T (2008) Noncovalently anchored catalysts based on chiral P-ligands. In: Boerner A (ed) Phosphorus ligands in asymmetric catalysis. Weinheim, Wiley
25. Barbaro P, Liguori F (2009) Chem Rev 109:515
26. Crosman A, Schuster C, Wagner HH, Batorfi M, Cubillos J, Hoelderich W (2007) Immobilization of transition metal complexes and their application to enantioselective catalysis. In: Enders D, Jaeger KE (eds) Asymmetric synthesis with chemical and biological methods. Weinheim, Wiley
27. Brandts JAM, Berben PH (2003) Org Process Res Dev 7:393
28. Hems WP, McMorn P, Riddel S, Watson S, Hancock FE, Hutchings GJ (2005) Org Biomol Chem 3:1547
29. Simons C, Hanefeld U, Arends IWCE, Maschmeyer T, Sheldon RA (2006) J Catal 239:212
30. Augustine R (2004) Special Chem Mag 24:19, and references cited
31. Kuntz EG (1987) Chemtech 17:570
32. Cornils B, Kuntz EG (1995) J Organomet Chem 502:177
33. Mercier C, Chabardes P (1994) Pure Appl Chem 66:1509
34. Yoneda N, Kusano S, Yasui M, Pujado P, Wilcher S (2001) Appl Catal A 221:253

Chapter 8
Chemical Reaction Engineering Aspects for Heterogenized Molecular Catalysts

Albert Renken

Abstract Homogeneous catalysts are characterized by high selectivity and reactivity under mild operating conditions. But the separation of the molecular catalysts from the reaction medium is a serious drawback and hampers industrial applications. A promising way to facilitate the separation and the reuse of the catalysts is its immobilization in a second liquid phase or on a solid support. In any case a mass transfer step is introduced in addition to the catalytic reaction. Transport phenomena may modify the effective reaction kinetics and harm the high product selectivity and activity observed in homogeneous systems. In the present chapter the impact of transport phenomena on the effective reaction rate, product selectivity, and observed reaction kinetics will be discussed in detail. The main parameters influencing the catalytic transformation will be presented. Besides heterogeneous fluid/solid systems biphasic liquid/liquid systems will be treated. Finally transport phenomena in supported liquid phase catalysts will be described. The latter regain lately actuality with the introduction of ionic liquids as supported liquid phase.

8.1 Introduction

In homogeneously catalyzed systems the selectivity of the reaction can be controlled by the appropriate choice of ligands on the catalytic metallic center. Combining a catalytic active metal with ligands often allows the synthesis of organic compounds that are otherwise only accessible through complex multistep synthesis. In addition, enantioselective reactions with high optical yields can be carried out in the presence of homogeneous catalysts, thus avoiding the costly separation of enantiomeric products. Homogeneously catalyzed reactions normally proceed at moderate temperatures. A drawback of homogeneously catalyzed processes is often the complex and

A. Renken (✉)
Institute of Chemical Sciences and Engineering, Ecole polytechnique fédérale de Lausanne, EPFL-ISIC-Station 6, 1015 Lausanne, Switzerland
e-mail: albert.renken@epfl.ch

P. Barbaro and F. Liguori (eds.), *Heterogenized Homogeneous Catalysts for Fine Chemicals Production*, Catalysis by Metal Complexes 33,
DOI 10.1007/978-90-481-3696-4_8,

costly separation and recycling of the catalyst. Therefore, considerable efforts are made to combine the easy separation of heterogeneous catalysts with the high potential reactivity and selectivity of homogeneous molecular catalysts.

Different methods are proposed to facilitate the recovery of the catalyst. A very successful way is to use biphasic systems of two immiscible liquids. The catalyst should be soluble only in one phase, in which the transformation takes place, while the products and sometimes the reactants should be preferentially soluble in the second. The catalyst is thus "immobilized" in a "liquid support". The liquid supports may be water, supercritical fluids, ionic liquids, organic liquids, or fluorous liquids [1]. The Oxo synthesis and the Shell Higher Olefin Process (SHOP) are important industrial processes based on the biphasic catalytic system.

Tremendous attempts were made to immobilize the molecular catalyst in a solid matrix. As supports polymers as well as inorganic materials were used. Polystyrene as a support has the advantage of being cheap and commercially available in various qualities. Compared to inorganic supports the swelling property and the plasticity leading to high pressure drop in conventional packed bed reactors are serious disadvantages.

Different immobilization methods are described in the open literature like covalent binding, binding by ion pair formation, adsorption or entrapment in the organic or inorganic matrix (ship in the bottle). A particular concept to immobilize homogeneous catalysts on solid supports concerns the so called Supported Liquid Phase catalysts (SLP catalyst). These catalysts consist of a porous material, whose surface is covered with a thin liquid layer. The layer finally contains the molecular catalyst. Examples are Supported Aqueous Phase (SAP) catalyst with water as reacting liquid phase or Supported Ionic Liquid Phase (SILP) catalysts. The generality of the concept is particularly important.

The immobilization of the molecular catalyst on a second phase involves transport processes in addition to the chemical reaction, since the reactants must be first transferred from the bulk of the fluid phase to the catalyst surface, where the reaction occurs. Depending on the relative rate of the chemical and the transport processes the observed overall transformation rate and the product selectivity will be influenced. This will be discussed in detail in the following sections.

8.2 Biphasic Liquid/Liquid System

In a biphasic system two immiscible liquids are used, one containing the catalyst and the other containing the non converted reactant and the products [2, 3]. Both liquids can be easily separated after the reaction and the catalyst is recycled in the reactor. This can be done without any thermal or chemical treatment. As the reaction is carried out in presence of the homogeneously dissolved catalyst the advantages of homogeneous catalysis are fully preserved. In addition, eventual consecutive reactions of the product are avoided or diminished since the reaction products are preferentially present in the second inert phase.

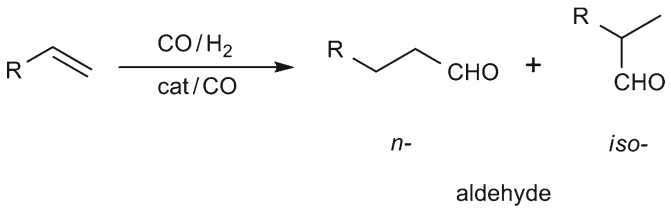

Scheme 8.1 Hydroformylation of olefins

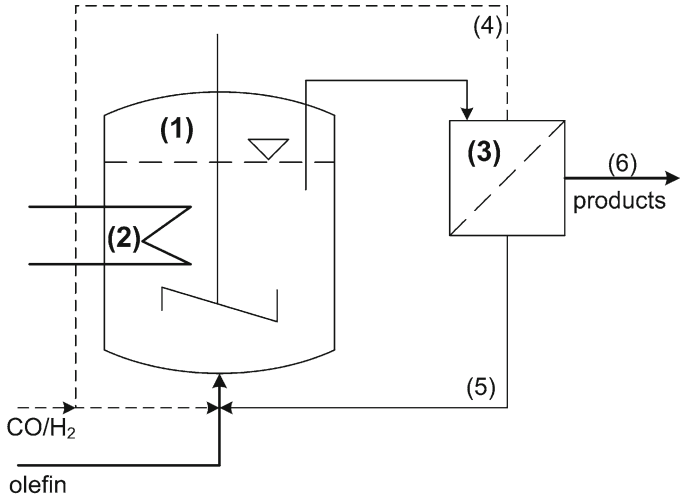

Fig. 8.1 Basic flow sheet of the oxo process. (1) Reactor, (2) heat exchanger, (3)separator, (4) gas recycle, (5) catalyst recycle, and (5) product stream

An important example for the use of a biphasic system to immobilize a metal complex is the hydroformylation of olefins (oxo synthesis) developed by Roelen in 1938 at Ruhrchemie [4] (Scheme 8.1).

The most important oxo products are in the range of C3–C19; with a share of ca. 75%, butanal is the most important [4]. The basic flow sheet of the oxo process is shown in Fig. 8.1 [5]. The reactor (1) brings in contact the two liquid phases with the synthesis gas. As the hydroformylation is a highly exothermic reaction, heat evacuation is an important issue to avoid overheating and reactor runaway. Conventionally, a stirred tank equipped with a gas distributor and heat exchanger (2) is used. The reaction mixture is separated in a decanter (3), the unreacted gas (4) and the catalyst phase (5) are recycled to the reactor, whereas the product stream (6) is discharged and purified in further steps by stripping and distillation.

A special attention has to be paid to the mixing and mass transfer efficiency in the reactor. Because the reaction takes place in the catalyst containing phase, the reactants must be firstly transferred from the second and the gas phase to the reaction phase.

The mass transfer rate between the different phases depends on the area of the interface and the mass transfer coefficient. Whether the reaction will take place in the bulk of the reaction phase or near the interface depends on the ratio between the characteristic reaction time (t_r) to the characteristic time for mass transfer (t_m). This ratio is known as the Hatta number (Ha).

$$Ha = \sqrt{\frac{t_m}{t_r}} \tag{8.1}$$

The discussion can be facilitated on the basis of the film model and by supposing a first order irreversible reaction in the reaction phase [6–8]. Under these conditions the following relationships result:

$$Ha = \delta_{II} \sqrt{\frac{k_r'}{D_{i,II}}} = \frac{\sqrt{k_r' D_{i,II}}}{k_{L,II}} \tag{8.2}$$

With δ_{II}, the thickness of the boundary layer; k_r', the reaction rate constant, which is a function of the catalyst concentration ($k_r' = k_r \cdot c_{cat}$), $D_{1,II}$; the diffusion coefficient for the compound 1 in the second liquid phase, and $k_{L,II}$ the mass transfer coefficient in this liquid phase.

Depending on the value of Ha, different regimes can be distinguished:

For Ha ≤ 0.3 the reaction rate is slow compared to the mass transfer and the reaction takes place in the bulk phase and the mass transfer can be considered as an additional resistance in series to the reaction. The effective (observed) reaction rate is given by (Fig. 8.2a):

$$r_{ov} = \left(\frac{1}{k_{L,II} a} + \frac{1}{k_r'} \right)^{-1} c_{1,II} \tag{8.3}$$

For values of the Hatta number of 0.3 ≤ Ha ≤ 3 the reaction takes place partially in the boundary layer. This leads to deformation of the concentration profile as indicated in Fig. 8.2b. The overall rate of reaction is given by the reaction in the bulk at reactant concentration $c_{1,L}$ and in the boundary layer. This leads to the following expression for the observable effective rate:

$$r_{ov} = \frac{Ha}{\tanh(Ha)} \left[1 - \frac{c_{1,II}}{c_1^*} \cdot \frac{1}{\cosh(Ha)} \right] \cdot k_L a \cdot c_1^* \tag{8.4}$$

The bulk concentration $c_{1,II}$ is a rather complex function of the intrinsic reaction rate, the mass transfer coefficient, and the area of the interface [6].

A further increase of the intrinsic reaction rate at constant volumetric mass transfer coefficient ($k_{L,II}$·a) results in Hatta numbers greater than 3 (Ha ≥ 3). The reaction rate can be considered as very fast compared to the mass transfer rate. As a consequence, the reactants do not reach the bulk phase ($c_{1,II} \approx 0$), the reaction takes place only in the boundary layer (Fig. 8.2c). Under these conditions, the

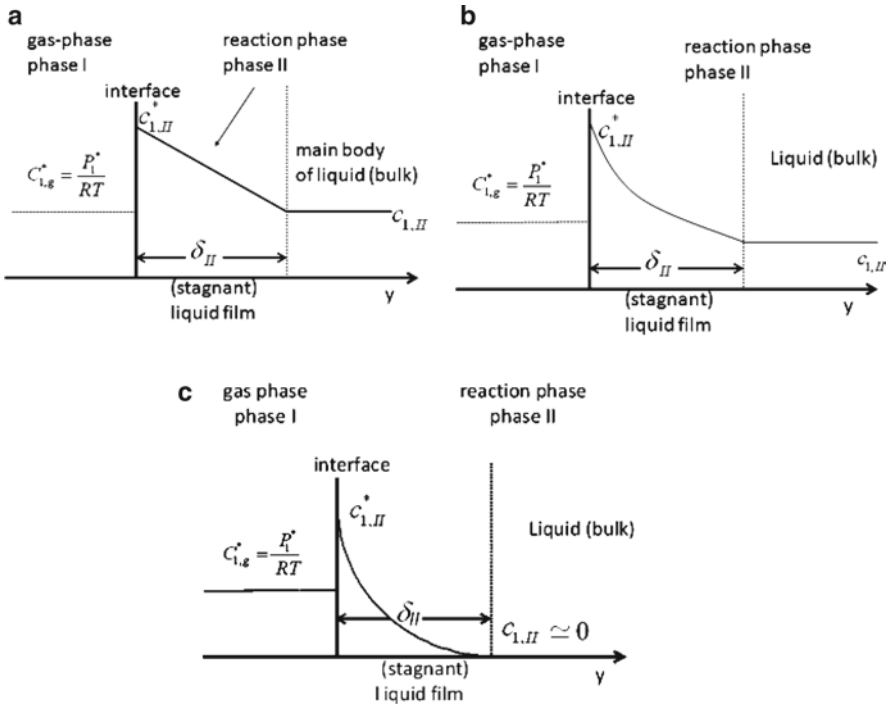

Fig. 8.2 Concentration profiles for mass transfer with pseudo first order chemical reaction (film model) (**a**) slow chemical reaction: Ha ≤ 0.3; (**b**) moderate chemical reaction: 0.3 ≤ Ha ≤ 3.0; (**c**) fast chemical reaction: Ha ≥ 3.0

reaction rate increases proportional with the specific area between the phases (a), and the square root of the reaction rate constant, respectively of the catalyst concentration as indicated in Eq. 8.5.

$$r_{eff} = k_{L,II} \cdot a \cdot Ha \cdot c_1^* = \sqrt{k_r' \cdot D_{1,II}} \cdot a \cdot c_1^* = \sqrt{k_r \cdot c_{cat} \cdot D_{1,II}} \cdot a \cdot c_1^* \tag{8.5}$$

In summary, increasing values of Ha leads to a decreasing reactant concentration in the reacting phase and as a consequence, the available volume of the reacting phase is less and less utilized. This situation can be characterized by introducing an efficiency factor η. The efficiency factor is defined as the ratio between the observed, effective rate and the maximal production rate referred to the reactor volume (V_R) corresponding to the maximum concentration in the reacting phase ($c_{1,II} = c_{1,II}^*$).

$$\eta = \frac{r_{eff}}{r_{\max}};\ r_{\max} = k_r' \frac{V_{II}}{V_R} c_{1,II}^* \tag{8.6}$$

The reactor efficiency depends on the Ha number and the specific interfacial area. For a first order irreversible reaction the following relationship is obtained

$$\eta = \frac{B}{Ha}\left[\frac{\tanh(Ha) + \left(B^{-1} - 1\right)Ha}{1 + \left(B^{-1} - 1\right)Ha\tanh(Ha)}\right] \tag{8.7}$$

with $B = \dfrac{a \cdot V_R \cdot D_{1,II}}{V_{II} \cdot k_{L,II}}$.

The parameter B can be interpreted as the ratio between the film volume (V_f) and the volume of the reacting phase (V_{II}). In Fig. 8.3 the efficiency factor as function of *Ha* and *B* is shown. The figure clearly demonstrates that the reactor efficiency decreases with increasing *Ha* and with decreasing specific interfacial area *a*.

The presented relations above are strictly valid only for simple irreversible first order reactions, but appropriate models for more complex kinetics can accordingly be developed based on the film model.

Wachsen et al. [9] studied the industrially important hydroformylation of propene (PR) in the presence of a rhodium catalyst with the water soluble ligand triphenyphosphine trisulfonate (TPPTS). The reaction was carried out in a stirred autoclave at different reaction temperatures and stirrer speeds. The authors suggested the following formal kinetic power law model (Eq. 8.8):

$$r = k_r c_{Rh}^{n1} c_{TPPTS}^{n2} c_{CO}^{n3} c_{H2}^{n4} c_{PR}^{n5}; \quad k_r = k_{r0} \exp\left(-\frac{E_a}{RT}\right) \tag{8.8}$$

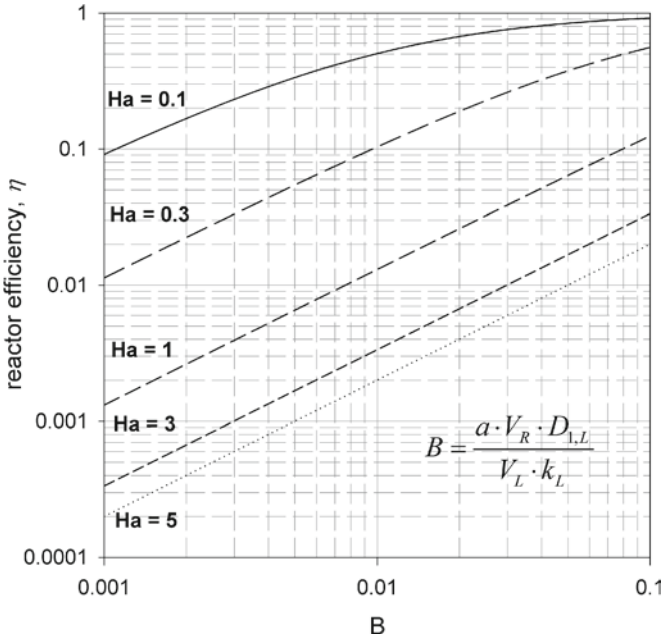

Fig. 8.3 Effectiveness factor for fluid/fluid reactions as function of *Ha* and *B*

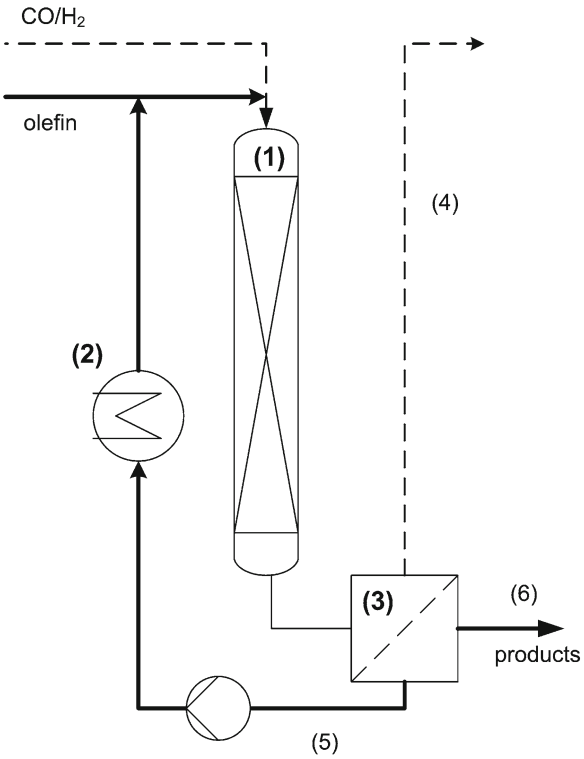

Fig. 8.4 Scheme of the aqueous hydroformylation process with integrated static mixer as gas/liquid/liquid contactor. (1) Reactor column packed with static mixing elements, (2) heat exchanger, (3) phase separator, (4) off gas, (5) catalyst recycling, and (6) product stream to work up units (redrawn based on [10])

Where n_i indicates the corresponding reaction order for the individual compound. Based on a systematic analysis of the experimental results for the propene hydroformylation, and application of the methodology discussed above, the authors came to the conclusion that the hydroformylation reaction takes place near the interface within the boundary layer (Ha > 3).

A similar result was found by Wiese et al. [10] for the same reaction. Since the reactant concentration in the reacting phase is negligible ($c_{1,II} \approx 0$), only the film volume ($V_f = A \cdot \delta_{II}$) contributes to the reactor performance. Or, in other words the degree of reactor utilization is very poor.

As a logical consequence, the reaction has to be carried out in reactors ensuring a high interfacial area and high mass transfer coefficient. Wiese et al. replaced the commonly used stirred tank reactor by a column reactor filled with static mixers as contact units for the gas/liquid/liquid system (Fig. 8.4). Static mixers are known for significant higher interfacial areas [11–14] compared to conventional stirred tank reactors [15, 16]. This allowed increasing the specific interfacial area and the mass transfer rate, thus decreasing Ha. The consequence is a better utilization of the reactor

volume. In addition, reactor columns show a narrower residence time distribution (see [7, 8]) compared to continuous stirred tank reactors. Both effects may explain the observed increase of the reactor performance of a factor 10 compared to conventional stirred tanks.

8.3 Solid Catalysts

An attractive way to combine the advantages of homogeneous and heterogeneous catalysis is the immobilization of molecular catalysts on solid supports to obtain tailor made catalysts that can be applied in packed bed, trickle bed or slurry reactors. No wonder that for more than 30 years the immobilization of homogeneous catalysts is under investigation as it is evident from the numerous papers, reviews, and books published on this topic. In spite of these efforts and the many patents on immobilized catalysts, their industrial use is very rare. This indicates that there is still a strong interest in the immobilization of molecular catalysts on solid supports, but that several problems are not overcome yet. These problems are related to metal leaching, insufficient mechanical resistance, particle swelling, and reduced activity and selectivity. Since heterogeneous catalytic reactions involve by their nature a combination of reaction and transport processes, the intrinsic catalytic activity and selectivity may be disguised by physical phenomena. Hence, the relationship between physical and chemical processes must be known for an efficient and correct catalyst development.

The transport processes combined with catalytic reactions are shown schematically in Fig. 8.5.

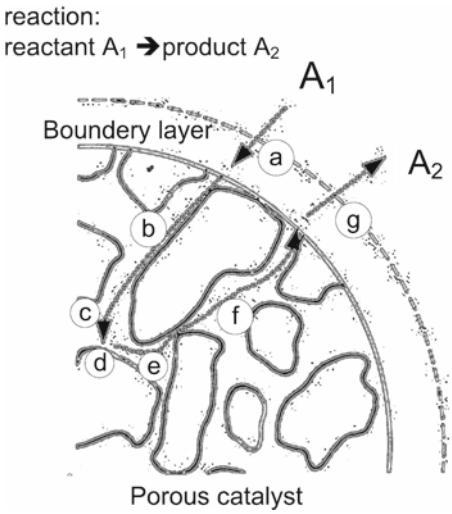

Fig. 8.5 Steps involved in heterogeneous catalytic reactions

Supposing a porous catalyst particle with a large specific surface area surrounded by a fluid (gas or liquid) containing the reactant A_1. For the transformation to take place the following steps are necessary:

(a) Transfer from the fluid bulk to the outer surface
(b) Diffusion through the porous material to active site
(c) Adsorption
(d) Transformation of A_1 to the product A_2
(e) Diffusion of the product to the outer surface
(f) Transfer of the product to the bulk of the fluid

In the following sections the influence of the internal diffusion (steps (b) and (e)) and the external transfer (steps (a) and (f)) on the observed (overall) activity and selectivity will be discussed.

8.3.1 Internal Mass and Heat Transfer

8.3.1.1 Isothermal Pellet

In general, porous supports are used to immobilize a high amount of molecular catalysts in the particle. Therefore, the reactant has to be transported through the pores to the active centers inside the particle. In parallel to the diffusion process the chemical transformation occurs in the pellet. As a consequence of these two processes a concentration profile will develop inside the particle as shown in Fig. 8.6. The final concentration profile depends on the ratio between the characteristic reaction time t_r and the diffusion time t_D. This ratio is called "Thiele modulus":

$$\phi_s^2 = \frac{t_D}{t_r};\ t_D = \frac{r_p^2}{D_{1,e}};\ \frac{1}{t_r} = k_r c_{1,s}^{n-1} \tag{8.9}$$

In Eq. 8.9 the definition for the squared Thiele modulus is given for a spherical pellet. The diffusion time is inversely proportional of the effective diffusion coefficient in the pellet and increases with the square of the particle radius.

With increasing Thiele modulus corresponding to decreasing reaction time, and/or increasing diffusion time, the concentration profile becomes steeper and the concentration in the particle center finally tends to zero. As a result, the effective reaction rate in the particle diminishes for reactions with positive reaction order. This is illustrated in Fig. 8.7. A quantitative relation is given for a first order reaction in Eq. 8.10.

$$r_{eff} = \frac{3}{\phi_S}\left(\frac{1}{\tanh(\phi_S)} - \frac{1}{\phi_S}\right) k_r c_{1,s} \tag{8.10}$$

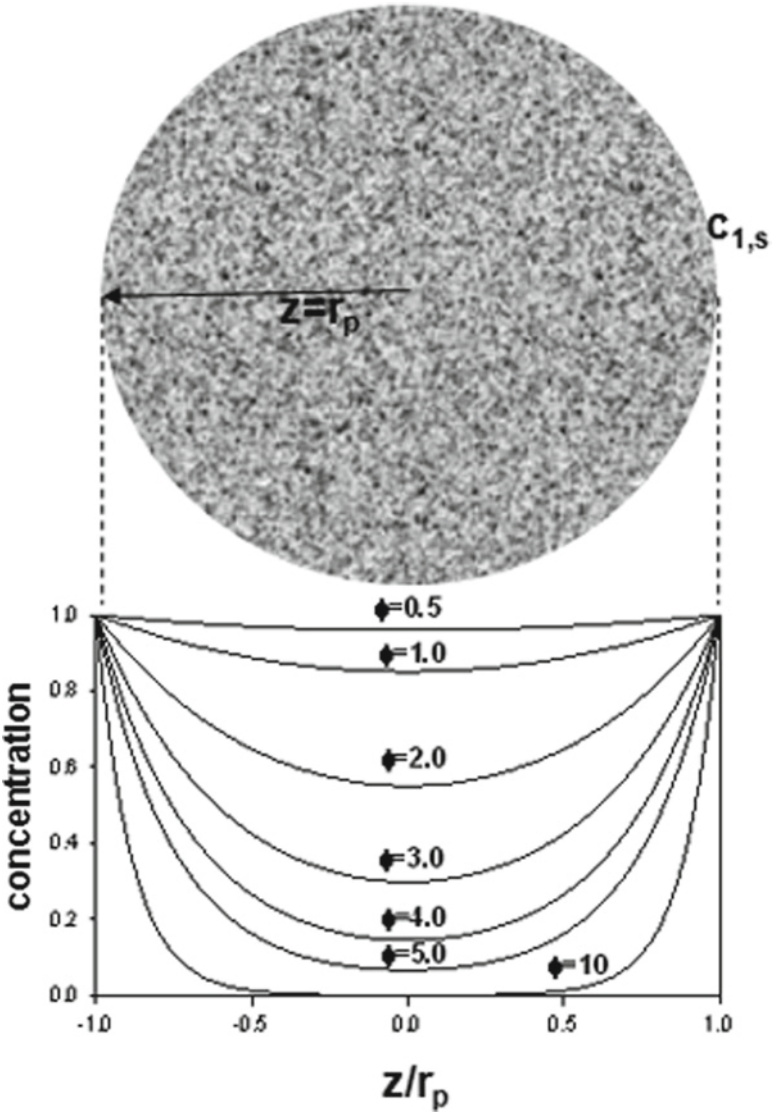

Fig. 8.6 Concentration profiles in porous catalysts as function of the Thiele modulus ϕ

The effective reaction rate is smaller compared to the rate, which would occur at constant bulk phase concentration.

To quantify the influence of the transport phenomena on the observable reaction an effectiveness factor is introduced with the following definition:

$$\eta_p = \frac{\text{observed rate of reaction}}{\text{rate of reaction at surface concentration}} = \frac{r_{eff}}{r_s} \tag{8.11}$$

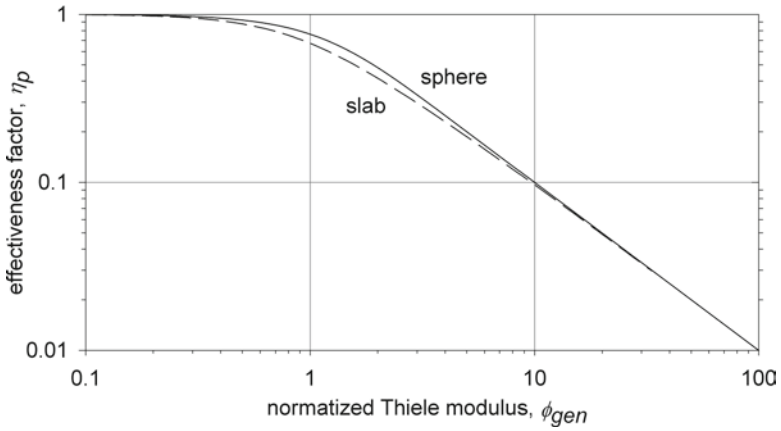

Fig. 8.7 Effectiveness factor as function of the generalized Thiele modulus for different pellet geometries

With Eq. 8.10 the effectiveness factor becomes:

$$\eta_S = \frac{r_{eff}}{k_r c_{1,s}} = \frac{3}{\phi_S}\left(\frac{1}{\tanh\left(\phi_S\right)} - \frac{1}{\phi_S}\right) \tag{8.12}$$

Similar relationships can be developed for different particle shapes like flat plates or cylindrical extrudates [7, 8]. For all shapes the effectiveness factor reaches unity for small values of the Thiele modulus. The reactant concentration in the pellet is constant and identical to the surface concentration. The reaction is controlled by the intrinsic kinetics assuming external transfer phenomena negligible (see Fig. 8.7). This situation is observed for low catalyst activity or very small particles as used in suspension reactors. For large values of the Thiele modulus the dependency of η_p approaches an asymptotic solution given in Eq. 8.13.

$$\eta_p = \frac{m}{\phi}; \tag{8.13}$$

with: m = 1, 2, 3 for slab, cylinder, sphere, respectively

This situation occurs for very fast reactions or large particles. The concentration in the particle center becomes zero for $\eta_p < 0.2$.

The observation that the slope of the asymptotic solution for $\eta_p = f(\phi)$ becomes independent of the pellet geometry can be used to develop a generalized definition for the Thiele modulus, ϕ_{gen} (Eq. 8.14). The effectiveness factor as function of the generalized Thiele modulus is shown for a flat plate and a sphere in Fig. 8.7.

$$\phi_{gen} = \frac{V_p}{A_p}\sqrt{\frac{k_r c_{1,s}^{n-1}}{D_{1,e}}} \cdot \sqrt{\frac{n+1}{2}} \tag{8.14}$$

Both curves coincide for $\phi_{gen} \to \infty$. The maximal differences between the two curves are about 10%.

Since the intrinsic reaction rate is normally unknown, the Thiele modulus cannot be estimated and the corresponding relationships are of limited value for the evaluation of experimental results. For this purpose, a relation between the observed effective rate (r_{eff}) of reaction and the effectiveness factor is more useful. The characteristic diffusion can be easily estimated based on the particle dimension and the efficient diffusion coefficient. The ratio between the effective reaction time ($t_{r,eff}$) and the diffusion time in the pellet is called the Weisz modulus. The definition is given in Eq. 8.15:

$$\psi_{gen}^2 = \frac{\left(V_p/A_p\right)^2}{D_{1,e}} \frac{r_{eff}}{c_{1,s}} \frac{n+1}{2} \tag{8.15}$$

The effectiveness factor as function of the observable Weisz modulus can be calculated with Eq. 8.16 and Fig. 8.7. Based on experimental results the effectiveness factor can be estimated by means of Fig. 8.8. This allows to identify whether the measured kinetics are disguised by internal mass transport phenomena.

$$\psi_{gen}^2 = \frac{\left(V_p/A_p\right)^2}{D_{1,e}} \frac{r_{eff}}{c_{1,s}} \frac{n+1}{2} = \frac{\left(V_p/A_p\right)^2}{D_{1,e}} \frac{r}{c_{1,s}} \frac{n+1}{2} \cdot \eta_s = \frac{n+1}{2} \eta_s \cdot \phi_{gen}^2 \tag{8.16}$$

The decrease of the product selectivity due to transport phenomena is often more important than the reduced catalytic activity. In the following paragraph

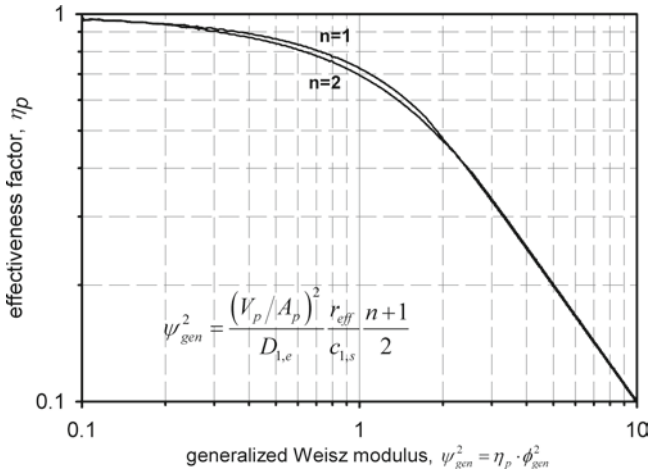

Fig. 8.8 Effectiveness factor as function of the generalized Weisz modulus for different reaction orders

we will discuss the influence of internal diffusion on two important schemes for multiple reactions:

Parallel reactions $A_1 \xrightarrow{k1} A_2$
$A_1 \xrightarrow{k2} A_3$

and

Consecutive reactions $A_1 \xrightarrow{k1} A_2 \xrightarrow{k2} A_3$

Assuming simple power law kinetics and *parallel reactions* the rate equations for the disappearance of the reactant A_1 and the formation of the desired product A_2 are formulated as follows:

$$-R_1 = k_1 c_1^{n1} + k_2 c_1^{n2}; \quad R_2 = k_1 c_1^{n1} \tag{8.17}$$

with k_1 and k_2 the intrinsic rate constants.

The influence of mass transport phenomena can be discussed easily on the basis of the so called point or instantaneous selectivity. The instantaneous selectivity for the product A_2 referred to the reactant A_1 is defined as the ratio of the production rate to the rate of disappearance:

$$s_{2,1} = \frac{R_2}{-R_1} = \frac{k_1 c_1^{n1}}{k_1 c_1^{n1} + k_2 c_1^{n2}} = \frac{1}{1 + \kappa c_1^{(n2-n1)}};$$
$$\kappa = \frac{k_2}{k_1}; \ |\nu_i| = 1 \tag{8.18}$$

As can be seen from Eq. 8.18, there is no influence of the concentration profile within the catalyst pellet for $n_1 = n_2$. In contrary, if $n_1 \neq n_2$, the effective selectivity will be influenced by intraparticle diffusion. Since the influence of internal concentration profiles becomes more pronounced with increasing reaction order, the product selectivity will diminish, whenever the desired reaction has a higher order than the undesired one.

To simplify the discussion on the influence of internal transport processes on *consecutive reactions*, we assume irreversible first order reactions with identical stoichiometric coefficients of $|\nu_i| = 1$. We will also neglect concentration gradients between the bulk phase and the outer surface of the pellet. This leads to: $c_{i,s} = c_{i,b}$. With k_1 and k_2 being the intrinsic rate constants, the rate of reactant disappearance and the production rate of A_2 are as follows:

$$-R_1 = k_1 c_1$$
$$R_2 = k_1 c_1 - k_2 c_2 \tag{8.19}$$

In the kinetic regime the concentrations inside the pellet are identical to the concentration on the catalyst outer surface, and the instantaneous product selectivity corresponds to:

$$s_{2,1} = \frac{R_2}{-R_1} = 1 - \frac{k_2 c_{2,s}}{k_1 c_{1,s}} = 1 - \kappa \frac{c_{2,s}}{c_{1,s}}; \text{ with } \kappa = \frac{k_2}{k_1} \tag{8.20}$$

With increasing conversion, X, decreasing reactant concentration, $c_{1,s}$, in a batch reactor or in a tubular reactor the instantaneous selectivity decreases. The final product yield is obtained by integration of the instantaneous selectivity over the reactant conversion (Eq. 8.21). The results are plotted in Fig. 8.9 for $\kappa = k_2/k_1 = 0.1$ and different Thiele moduli. The yield of the intermediate product increases up to a maximum value and finally tends to zero for $X \to 1$ as shown in Fig. 8.9.

$$Y_{2,1} = \int_0^X s_{2,1} dX' = \frac{1}{1-\kappa}\left[(1-X)^{\kappa} - (1-X)\right] \tag{8.21}$$

The maximum yield depends on the ratio of the two rate constants. With decreasing κ the maximum yield increases and is reached at higher conversions at X_{op}. Both values can be calculated with Eq. 8.22

$$Y_{2,1,\max} = \kappa^{\kappa/(1-\kappa)} \text{ at } X_{op} = 1-\kappa^{1/(1-\kappa)} \text{ for } \kappa \neq 1 \tag{8.22}$$

Under the influence of internal diffusion resistance different concentration profiles for the reactant and the products will develop inside the porous catalyst pellet. The concentration of the reactant decreases with the distance to the outer surface and reaches a minimum in the particle center. In contrast, the concentration of the intermediate product will be maximal in the center and decreases towards the outer surface. As a consequence, the effective formation of A_2 diminishes with increasing

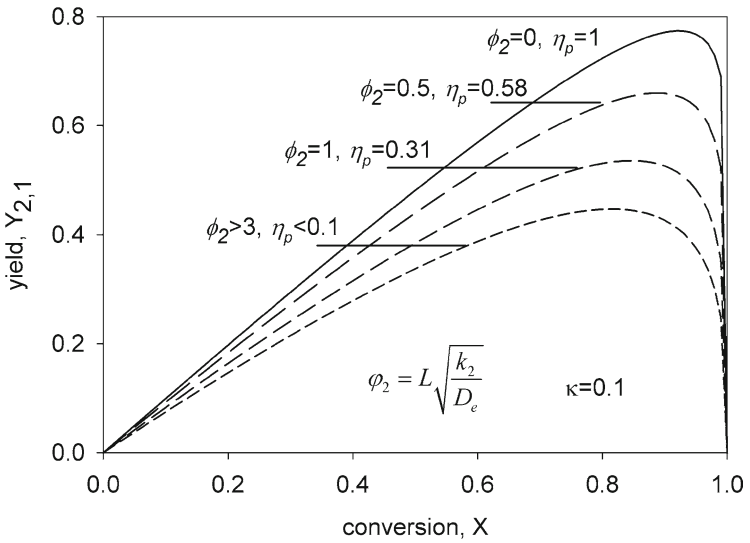

Fig. 8.9 Influence of internal mass transfer resistance on the product yield. First order consecutive reactions: $\kappa = k_2/k_1 = 0.1$

diffusion resistance (increasing Thiele modulus, ϕ), while the rate of the consecutive reaction increases with increasing ϕ. As a result, the instantaneous selectivity as well as the product yield is reduced for all reactant conversions as illustrated in Fig. 8.9. For very strong diffusional resistance in the catalyst pellet characterized by $\phi_2\sqrt{\kappa} > 3$, the instantaneous effective selectivity is given by:

$$s_{2,1,eff} = \frac{1}{1+\sqrt{\kappa}} - \sqrt{\kappa}\,\frac{c_{2,s}}{c_{1,s}};$$

$$\text{for } \phi_2\sqrt{\kappa} > 3, \text{ with } \phi_2 = r_p\sqrt{\frac{k_2}{D_{2,e}}} \tag{8.23}$$

The integral product yield as function of the conversion for different values of the Thiele modulus is shown in Fig. 8.9 for $\kappa = 0.1$. It is obvious that internal diffusion resistances lead to important losses of the desired product. Compared to the obtainable values for intrinsic kinetics the maximum yield is reduced for more than 30% (Eq. 8.24).

$$\left(Y_{2,1,\max}\right)_{\phi 2\sqrt{\kappa}>3} = \frac{\kappa^{\left[0.5\sqrt{\kappa}/\left(1-\sqrt{\kappa}\right)\right]}}{1+\sqrt{\kappa}} \text{ at } X_{op} = 1-\kappa^{\left[0.5/\left(1-\sqrt{\kappa}\right)\right]} \tag{8.24}$$

8.3.1.2 Non-isothermal Pellet

A large number of catalytic reactions are accompanied by thermal effects due to the heat of reaction. For relatively fast reactions compared to the mass and heat transfer phenomena, the development of internal temperature gradients can be expected. Heat and mass transfer balances have to be solved simultaneously to estimate concentration and temperature profiles under steady state conditions. As the reaction rate depends exponentially on temperature the resulting temperature and concentration profiles have to be calculated by numerical methods. The largest possible temperature difference between the outer surface and the center of the catalysts is attained, when the reactant concentration in the center becomes zero. The maximum temperature difference is easily estimated:

$$\left(T_{center} - T_s\right)_{\max} = \left(-\Delta H_r\right)\cdot c_{1,s}\,\frac{D_e}{\lambda_e} \tag{8.25}$$

Obviously, the temperature profile in the pellet depends on the reaction enthalpy and the surface concentration of the reactant, as well as the ratio of the two transport coefficients: the effective diffusion coefficient and the effective heat

conductivity of the pellet. Most of the commonly used inorganic porous supports are characterized by effective heat conductivities in the range of $0.2 < \lambda_e < 0.5$ W/m/K. The effective diffusion coefficients for gases are in the order of 10^{-6} to 10^{-5} m²/s. Therefore, maximum temperature differences inside porous catalyst particle seldom exceed 10 K. For solid/liquid systems temperature effects can be always neglected.

8.3.2 External Mass and Heat Transfer

The first step in heterogeneous fluid solid reactions is the transfer of the reactant from the bulk of the fluid phase to the external surface as indicated in Fig. 8.5. The external mass transfer can be described by the film-model. According to this model a boundary layer or stagnant film of the thickness δ surrounds the particle. The total resistance for external mass transfer is located in the boundary layer as indicated in Fig. 8.10. In analogy to the effectiveness factor defined for internal diffusion in porous catalysts, an external effectiveness factor can be defined as ratio between the effective reaction rate and the observable at bulk conditions. For a nth order reaction we obtain:

$$\eta_{ex} = \frac{k(T_s)}{k(T_b)} \frac{c_{1,s}^n}{c_{1,b}^n} \tag{8.26}$$

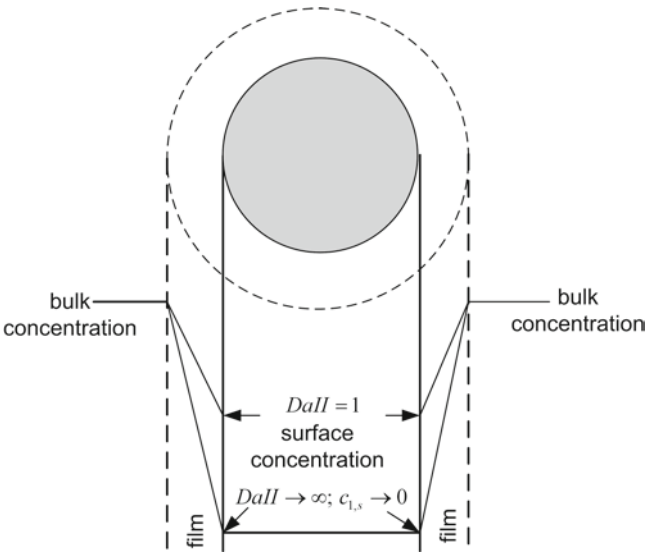

Fig. 8.10 External concentration profile according to the film model

8.3.2.1 Isothermal Pellet

Under isothermal conditions the temperature at the surface is identical to the bulk concentration ($T_s = T_b$) and the effectiveness factor becomes

$$\eta_{ex} = \left(\frac{c_{1,s}}{c_{1,b}} \right)^n \tag{8.27}$$

The molar flux of reactant A_i is proportional to the concentration difference between the fluid bulk ($c_{i,b}$) and the surface ($c_{i,s}$)as given in Eq. 8.28.

$$J_i = k_{fl} \left(c_{i,b} - c_{i,s} \right) \tag{8.28}$$

with k_{fl} the fluid/solid mass transfer coefficient.

At steady state, the external molar flux is equal to the mean rate of transformation ($-R_i$) in the catalyst particle:

$$-R_i = k_{fl} \cdot A_p / V_p \left(c_{i,b} - c_{i,s} \right) = k_{fl} \cdot a_p \left(c_{i,b} - c_{i,s} \right) \tag{8.29}$$

With A_p, V_p the outer surface area and particle volume, respectively. For a spherical pellet the specific surface area becomes:

$$a_p = \frac{A_p}{V_p} = \frac{6}{d_p} \text{ (sphere)} \tag{8.30}$$

For known reaction kinetics the surface concentration of the reactant can be determined on the base of Eq. 8.29. This is demonstrated for a simple irreversible first order reaction with

$$-R_1 = k_r c_{1,s} \tag{8.31}$$

$$c_{1,s} = \frac{k_{fl} a_p}{k_{fl} a_p + k_r} c_{1,b} = \frac{1}{1 + \frac{k_r}{k_{fl} a_p}} c_{1,b} = \frac{1}{1 + DaII} c_{1,b} \tag{8.32}$$

The surface concentration of the reactant A_1 is dependent on the ratio between the characteristic mass transfer time (t_m) and the characteristic reaction (t_r) time. This ratio is called second Damköhler number, DaII.

$$DaII = \frac{t_m}{t_r} = \frac{k_r}{k_{fl} a_p} \tag{8.33}$$

The effective transformation rate can be calculated by replacing the surface concentration of the reactant in Eq. 8.31.

$$-R_{1,eff} = c_{1,s} = \frac{k_r \cdot k_{fl} a_p}{k_{fl} a_p + k_r} c_{1,b} \tag{8.34}$$

The effectiveness factor becomes:

$$\eta_{ex} = \frac{c_{1,s}}{c_{1,b}} = \frac{1}{1 + DaII} \tag{8.35}$$

With increasing characteristic transfer time respectively decreasing characteristic reaction time the concentration at the catalyst surface diminishes and approaches $c_{1,s} \to 0$ for $DaII \to \infty$. Under these conditions the effective observed transformation rate is controlled by the mass transfer. The effective transformation rate becomes:

$$-R_{1,eff} = k_{fl} a_p c_{1,b}; \quad DaII \to \infty \tag{8.36}$$

A similar development can be accomplished for nth order reactions. For irreversible reactions with reaction orders n = 2, ½ and −1 the following expressions for the effectiveness factors result:

$$\begin{aligned}
&n = 2: \ \eta_{ex} = \left(\frac{\sqrt{1 + DaII} - 1}{2 DaII} \right)^2 \\
&n = \frac{1}{2}: \eta_{ex} = \left[\frac{2 + DaII^2}{2} \left(1 - \sqrt{1 - \frac{4}{\left(2 + DaII^2\right)^2}} \right) \right]^{1/2} \\
&n = -1: \ \eta_{ex} = \frac{2}{1 + \sqrt{1 - 4 DaII}}; \ \text{for } DaII < 0.25 \\
&\text{with } DaII = \frac{k_r c_{1,b}^{(n-1)}}{k_{fl} a_p}
\end{aligned} \tag{8.37}$$

The effectiveness factor as function of DaII are reproduced in Fig. 8.11.

The results shown in Fig. 8.11 can be summarized as follows:

- For the same value of the Damköhler number the effectiveness factor diminishes with increasing reaction order.
- For reactions with a formal negative order (e.g. reactions with educt inhibition) the effectiveness factor can become higher than one.
- For large values of the Damköhler number the effectiveness factor is inversely proportional to $DaII$ ($\eta_{ex} \sim 1/DaII$).
- With increasing rate of the intrinsic reaction (increasing $DaII$) the observed reaction order changes from n to unity and the effective rate constant corresponds to the volumetric mass transfer coefficient ($k_{eff} \xrightarrow{DaII \to \infty} k_{fl} a_p$).

Whereas the results shown in Fig. 8.11 are quite instructive, they are of limited use for estimating the importance of mass transfer influence from experimental data, since the intrinsic kinetics is mostly unknown. But, based on Fig. 8.11 and Eq. 8.27 we can plot the effectiveness factor as function of the

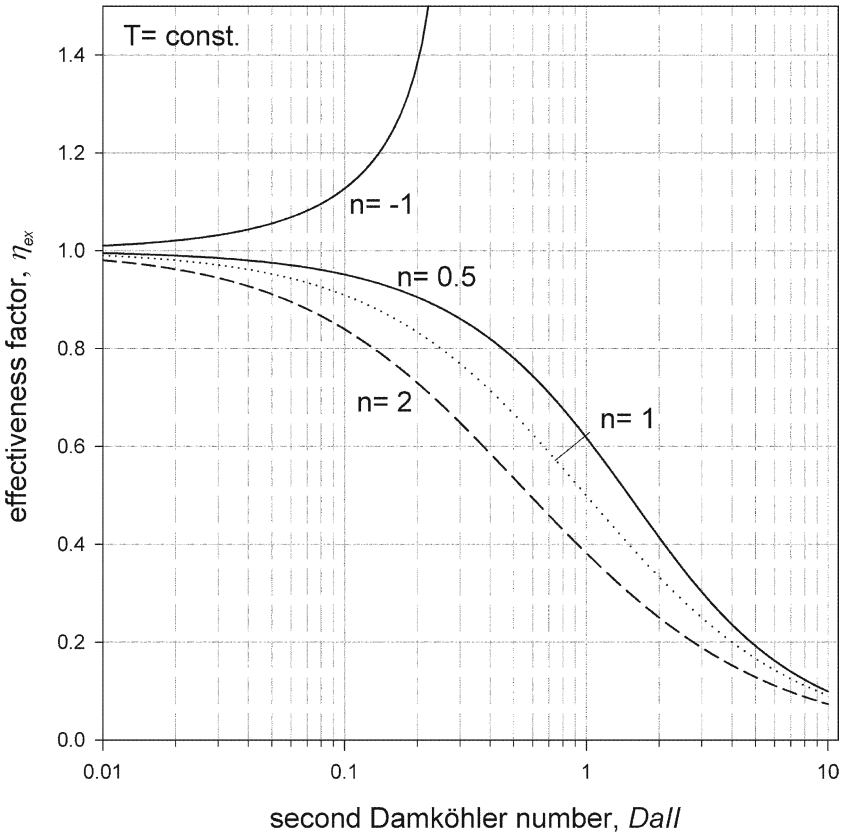

Fig. 8.11 Isothermal external effectiveness factor as function of the Damköhler number for different reaction orders

ratio between the observed reaction rate and the estimated maximum mass transfer rate.

$$\frac{r_{p,eff}}{k_{fl}a_p c_{1,b}} = \eta_{ex}\frac{k_r c_{1,b}^{(n-1)}}{k_{fl}a_p} = \eta_{ex} DaII \tag{8.38}$$

This relation, plotted in Fig. 8.12, allows estimating the influence of external mass transfer on the basis of measured data. We deduce from Fig. 8.12 that the ratio between maximum mass transfer rate and observed reaction rate must be at least 50 for characterizing correctly the intrinsic properties of the catalyst.

In the case of a complex reaction network with parallel and consecutive reactions, external transport phenomena may also deteriorate the yield and selectivity of the desired product. This will be demonstrated for simple irreversible consecutive and irreversible parallel reactions.

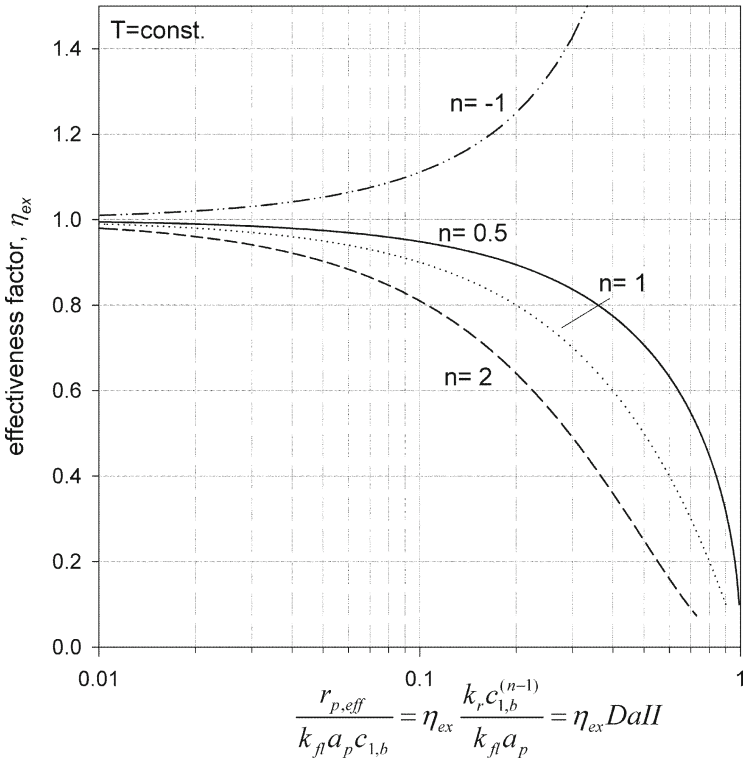

Fig. 8.12 Effectiveness factor as function of observable variables

In the absence of mass transfer influences the transformation rate of the reactant and the production rate of the (desired) intermediate product are given by Eqs. 8.39 and 8.40.

$$A_1 \xrightarrow{k1} A_2 \xrightarrow{k2} A_3 \tag{8.39}$$

$$-R_1 = k_1 c_{1,b}$$

$$R_2 = k_1 c_{1,b} - k_2 c_{2,b} \tag{8.40}$$

The instantaneous selectivity for the intermediate is obtained by dividing its production rate by the rate of the reactant transformation.

$$s_{2,1} = \frac{R_2}{-R_1} = 1 - \frac{k_2 c_{2,b}}{k_1 c_{1,b}} \tag{8.41}$$

Anticipating mass transfer phenomena lead to:

$$k_{fl} a_p \left(c_{1,b} - c_{1,s}\right) = k_1 c_{1,s} \tag{8.42}$$

$$k_{fl} a_p \left(c_{2,s} - c_{2,b}\right) = k_1 c_{1,s} - k_2 c_{2,s} \tag{8.43}$$

Solving the equations for the surface concentrations $c_{1,s}$ and $c_{2,s}$, we obtain the following relations for the instantaneous selectivity:

$$\left(s_{2,1}\right)_{eff} = \frac{R_{2,s}}{-R_{1,s}} = 1 - \frac{k_2 c_{2,s}}{k_1 c_{1,s}}$$

$$\left(s_{2,1}\right)_{eff} = \frac{1}{1 + DaII_2} - \frac{k_2}{k_1} \frac{\left(1 + DaII_1\right) c_{2,b}}{\left(1 + DaII_2\right) c_{1,b}} \tag{8.44}$$

with $$DaII_1 = k_1 / \left(k_{fl} a_p\right);\ DaII_2 = k_2 / \left(k_{fl} a_p\right).$$

Under initial conditions respectively at the reactor entrance of a packed bed reactor the product concentration is zero and the instantaneous selectivity becomes:

$$\left(s_{2,1}\right)_{eff} = \frac{1}{1 + DaII_2} = \frac{1}{1 + k_2 \Big/ \left(k_{fl} a_p\right)} \tag{8.45}$$

Obviously, the effective selectivity of the intermediate products depends on its rate to escape from the surface and the rate of the (destructive) consecutive reaction. Low mass transfer rates compared to the consecutive reaction are detrimental for the selectivity and yield of the intermediate.

For parallel reactions the influence of mass transfer depends on the individual reaction orders:

$$A_1 \xrightarrow{k1} A_2;\ R_2 = k_1 c_1^{n1} \tag{8.46}$$

$$A_1 \xrightarrow{k2} A_3;\ R_3 = k_2 c_1^{n2} \tag{8.47}$$

The ratio between the products A_2 and A_3 depends on the rate constants and the reactant concentration.

$$\frac{R_2}{R_3} = \frac{k_1}{k_2} c_1^{(n1-n2)} \tag{8.48}$$

As the concentration gradient around the catalyst leads to a lower reactant concentration at the surface compared to the bulk, the observed alteration of rate ratio depends on the individual reaction order:

$$\frac{\left(R_{2,s} \big/ R_{3,s}\right)}{\left(R_{2,b} \big/ R_{3,b}\right)} = \left(\frac{c_{1,s}}{c_{1,b}}\right)^{(n1-n2)} \tag{8.49}$$

As $c_{1,s} < c_{1,b}$ we see that diffusion intrusion leads to

- A reduced selectivity for A_2, if $n_1 > n_2$
- An increased selectivity for A_2, if $n_1 < n_2$
- No change of the selectivity for $n_1 = n_2$

8.3.2.2 Non-isothermal Effect

Temperature differences between the bulk of the fluid and the solid surface may become important for fast highly exo- or endothermic gas phase reactions. Depending on the kinetics and the activation energies, the effective transformation rate and/or the product selectivity will be altered.

To evaluate the differences between the temperature at catalyst surface (T_s) and the temperature of the surrounding fluid (T_b), we set up the energy balance for the particle.

$$\left(-\Delta H_r\right)\cdot r_{p,eff} = h \cdot a_p \left(T_s - T_b\right) \tag{8.50}$$

with h, the heat transfer coefficient.

The temperature difference will increase with increasing reaction rate and reaches a maximal value, if the rate is entirely controlled by external mass transfer. Under these conditions the effective rate is given by $r_{p,eff} = k_{fl} a_p c_{1,b}$ (Eq. 8.36). Replacing the $r_{p,eff}$ in Eq. 8.50 and rearranging leads to:

$$\left(T_s - T_b\right)_{\max} = \left(-\Delta H_r\right)\frac{k_{fl}}{h} c_{1,b} \tag{8.51}$$

Accordingly, the maximal temperature difference between surface and fluid depends on the reaction enthalpy, the reactant concentration in the bulk of the fluid and the ratio of the mass and heat transfer coefficient. Invoking the Chilton–Colburn analogy between heat and mass transfer allows estimating the ratio of the two coefficients:

$$\frac{h}{\rho \cdot c_p}\mathrm{Pr}^{2/3} = k_{fl} Sc^{2/3} \tag{8.52}$$

with $Sc = \dfrac{\upsilon}{D_m}$ the Schmidt number, and $\mathrm{Pr} = \dfrac{\upsilon}{\lambda / \left(\rho c_p\right)}$ the Prandtl number.

Following the analogy, we can estimate the ratio of the two transport coefficient from the physical properties of the fluid:

$$\frac{k_{fl}}{h} = \frac{1}{\rho c_p}\left(\frac{\mathrm{Pr}}{Sc}\right)^{2/3} \tag{8.53}$$

For the maximal temperature we finally obtain:

$$\left(T_s - T_b\right)_{\max} = \frac{\left(-\Delta H_r\right)c_{1,b}}{\rho c_p}\left(\frac{\mathrm{Pr}}{Sc}\right)^{2/3} = \Delta T_{ad}\left(\frac{\mathrm{Pr}}{Sc}\right)^{2/3} \tag{8.54}$$

with ΔT_{ad} the adiabatic temperature rise.

Typical values for the Prandtl and Schmidt numbers are given in the following table.

From Table 8.1 it is evident that important temperature differences can be expected for gas phase reactions and in a lesser extent in organic liquids.

Table 8.1 Typical range of Prandtl and Schmidt numbers

Fluid	Prandtl number (Pr)	Schmidt number (Sc)
Gas	0.7 < Pr < 1.1	0.6 < Sc < 1.1
Water	Pr = 7	Sc = 1,200
Organic liquids	10 < Pr < 1,000	300 < Sc < 2,000

8.3.3 Internal and External Mass Transport in Isothermal Pellets

If the efficient reaction rate is high enough, the reactant concentration drops significantly across the external boundary layer as indicated in Fig. 8.10. In this case the surface concentration is lower compared to the bulk of the fluid phase ($c_{1,s} < c_{1,b}$). At first we will neglect eventual heat effects and assume equal temperatures in the fluid and the catalyst particle ($T = T_s = T_b$). To determine the concentration profile in the particle, we first have to calculate the concentration at the external surface. This will be done based on the mass balance for the reactant A_1. At steady state, the molar flux of A_1 from the bulk to the external surface must be equal to the effective rate of transformation (see Eq. 8.55).

$$J_1 = k_{fl}\left(c_{1,b} - c_{1,s}\right) = \frac{-R_{1,p,eff}}{a_p} \tag{8.55}$$

For a simple irreversible first order reaction we obtain:

$$k_{fl}\left(c_{1,b} - c_{1,s}\right) = \frac{\eta_p k_r c_{1,s}}{a_p} \tag{8.56}$$

with η_p the internal effectiveness factor.

Solving Eq. 8.56 for the unknown surface concentration:

$$c_{1,s} = \frac{c_{1,b}}{1 + \eta_p k_r \Big/ \left(k_{fl} a_p\right)} \tag{8.57}$$

If we introduce the ratio between the characteristic diffusion time in the pellet t_D and the external mass transfer time t_m we will get a clearer physical interpretation of the relationship. The mentioned ratio is known as the mass Biot number Bi_m.

$$Bi_m = \frac{t_D}{t_m} = \frac{L_c^2}{D_e} k_{fl} a_p \tag{8.58}$$

with L_c the characteristic length of the pellet.

Introducing the Biot number in Eq. 8.57 yields:

$$c_{1,s} = \frac{c_{1,b}}{1 + \eta_p \dfrac{k_r L_c^2}{D_e} \cdot \dfrac{1}{Bi_m}} = \frac{c_{1,b}}{1 + \eta_p \dfrac{\phi^2}{Bi_m}} \tag{8.59}$$

The overall effectiveness factor is defined as the ratio between the effective transformation rate and the rate at constant bulk concentration.

$$\eta_{ov} = \frac{-R_{1,eff}}{-R_{1,b}} = \frac{-R_{1,eff}}{k_r c_{1,b}} = \frac{\eta_p c_{1,s}}{c_{1,b}} \tag{8.60}$$

In combination with Eq. 8.59 we obtain:

$$\eta_{ov} = \frac{\eta_p}{1 + \eta_p \dfrac{\phi^2}{Bi_m}} = \frac{1}{\dfrac{1}{\eta_p} + \dfrac{\phi^2}{Bi_m}} \tag{8.61}$$

For a catalyst in form of a flat plate the effectiveness factor is given by $\eta_p = \tanh\phi_L / \phi_L$ and the overall effectiveness factor can be expressed as a function of the Thiele modulus and the Biot number.

$$\eta_{ov} = \frac{\tanh\phi}{\phi\left(1 + \dfrac{\phi \cdot \tanh\phi}{Bi_m}\right)} \tag{8.62}$$

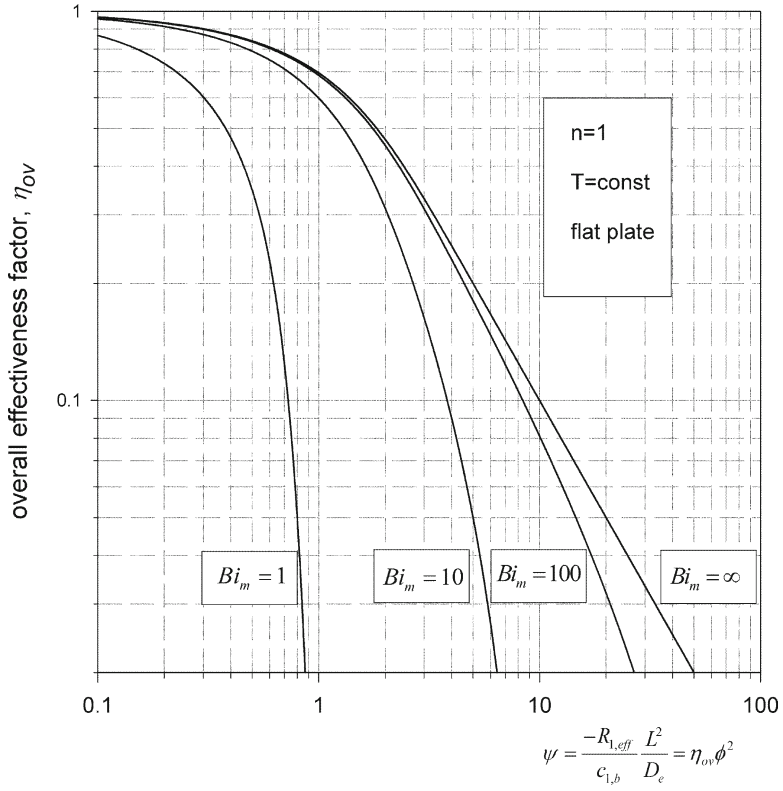

Fig. 8.13 Overall effectiveness factor as a function of the Weisz modulus for different mass Biot numbers (isothermal, irreversible first order reaction in a porous slab

The relationship shown in Eq. 8.62 suffers from the fact that the Thiele modulus must be specified to estimate the catalyst efficiency. This is, in general, not possible as the intrinsic kinetics is not known. It is therefore more convenient to relate the overall effectiveness factor to the Weisz modulus which is only based on observable parameters.

The catalyst efficiency decreases strongly at small mass Biot numbers as seen in. Figure 8.13. This is due to the reduced reactant concentration on the external pellet surface. In contrast, external mass transfer influences can be neglected at $Bi_m > 100$. In practice, catalytic particles are in the range of several millimeters and the mass Biot numbers are in the order of 100–200. Hence, the overall effectiveness factor is nearly entirely determined by the intraparticle diffusion.

8.3.4 *Implication of Mass Transfer on the Temperature Dependence*

As pointed out, the influence of mass transfer on the observed reaction rate depends on the ratio between the characteristic reaction time and the characteristic time for mass transfer. By increasing the temperature, the intrinsic reaction rate increases more strongly than the rates of inter- and intraparticle mass transfer. Consequently, the Thiele modulus and the second Damköhler number augment with increasing temperature and transport phenomena become more and more important and will finally control the transformation process. In addition, the temperature dependence of the observed reaction rate will change as indicated in Fig. 8.14.

At low temperatures the process is controlled by the intrinsic chemical kinetics and the rate constant increases exponentially following Arrhenius law:

$$k = k_0 \exp\left(\frac{-E}{RT}\right) \tag{8.63}$$

with k_0 the frequency factor and E the true activation energy.

The temperature dependence of the diffusion process can be also represented by an Arrhenius equation:

$$D_e = D_{e,0} \exp\left(\frac{-E_D}{RT}\right); \text{ with } 5 < E_D < 10\,\text{kJ/mol} \tag{8.64}$$

This is not a theoretical dependence of D_e, but the approximation is useful for the following discussions. At strong influence of internal diffusion on the reaction rate, the effectiveness factor was found to be inversely proportional to the Thiele modulus (e.g. Eq. 8.13). Accordingly, the effective rate constant is given by

$$k_{eff} = \frac{k}{L\sqrt{k/D_e}} = \frac{1}{L}\sqrt{k \cdot D_e} \tag{8.65}$$

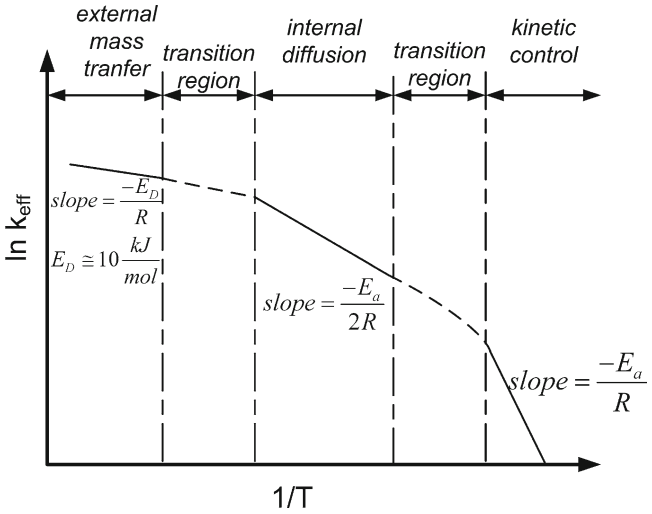

Fig. 8.14 Arrhenius plot for heterogeneous catalytic reactions. Transition from the kinetic regime to mass transfer controlled regime

For the temperature dependence follows:

$$k_{eff} = \frac{\sqrt{k_0 D_{e,0}}}{L} \exp\left(-\frac{E + E_D}{2 \cdot RT}\right) \tag{8.66}$$

Normally $E \gg E_D$, since diffusion is not very temperature sensitive, so the observed apparent activation energy is about one-half the true value when pronounced internal concentration profiles are present.

Further temperature increase will diminish the reactant concentration on the outer pellet surface as the influence of external mass transfer becomes important. Finally, interface mass transfer will be the rate controlling step and the surface concentration drops to zero. Under those conditions, the apparent activation energy corresponds to E_D.

Besides the apparent activation energy, the effective reaction order changes during the transition from kinetic to diffusion control. A first order will be observed under external mass transfer control. The effective reaction order observed approaches $n_{app} = (n+1)/2$ for severe influence of intraparticle diffusion.

8.4 Supported Liquid Phase Catalysts

The biphasic liquid/liquid system described in Section 8.2 combines homogeneous catalysis leading to high product selectivity with an easy separation and recycling of the catalyst. The disadvantage of the biphasic system is its relative low interfacial

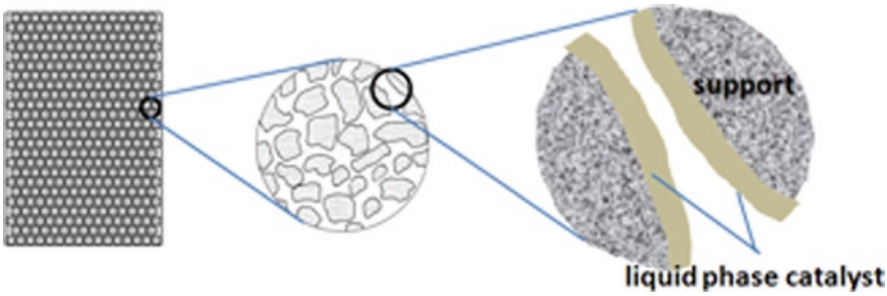

Fig. 8.15 Schematic presentation of the concept of supported liquid phase catalysis

area which must be continuously generated by vigorous stirring of the multiphase mixture. Mass transfer between the different phases may lead to a poor use of the reaction phase. As fast reactions mainly take place within a thin film near the interface the overall reactor efficiency drops to very low values.

A possibility to overcome this drawback consists in immobilizing the liquid on a highly porous support. In this way a thin liquid layer is formed on the solid support leading to the desired high gas/liquid interface. This so called Supported Liquid Phase Catalyst (SLPC) combines homogeneous catalysis with the advantages of a heterogeneous fluid/solid system. SLP catalysts can be used like traditional heterogeneous contacts in packed bed reactors or even in fluidized beds. A schematic representation is shown in Fig. 8.15.

The idea of using SPLCs is not new. In fact, Moravec et al. [17], described the use of supported sulfuric acid on porous silica gel and carbon to polymerize olefins in the gas and liquid phase in 1939.

The vanadium catalysts for SO_2 oxidation are probably the most important industrially used SLPCs. The catalysts consist of sulfate and pyrosulfate compounds of vanadium and alkali metals, which are supported on porous materials like silica. Under reaction conditions (700–800 K) the active component is a melt forming a thin layer on the surface of the support [18].

8.4.1 Supported Liquid Phase Catalysts with Metal Complexes

Important studies on the use of supported liquid phase hydroformylation catalysts were carried out by Scholten and Herman [19–29]. They mainly used rhodium catalysts ($RhHCO(PPh_3)_3$) dissolved in liquid triphenylphosphine supported on different porous materials. The degree of pore filling was found to be important for the observed catalytic activity and the reaction kinetics [27, 29]. The nature of the support plays a further important role. The ligands and/or the catalytic complex can be adsorbed on the surface thus changing the metal/ligand ratio [28, 30]. This in turn may have an important influence on the activity and selectivity.

The main drawback of SPL catalysts is the loss of solvent due to evaporation in a continuously operated catalytic reactor. This problem can be overcome by using ionic liquids as solvent [31–34]. Ionic liquids are molten salts and their partial pressure is low under conditions commonly used for hydroformylation and hydrogenation reactions. As generally observed for SLPC, the catalytic activity and product selectivity depends on the pore filling and the nature of the porous support [35].

8.4.2 Liquid Distribution in Porous Supports

The amount of liquid catalyst effectively used for the catalytic reaction depends on the manner in which the liquid is distributed in the porous support and the diffusion resistance in the porous network. The liquid distribution is determined by the balance of cohesive forces in the liquid and adhesive forces between the liquid and the solid surface. The process is governed by the thermodynamic principle that the total free surface energy must increase for any perturbation of the distribution ($dG^s > 0$). The Gibbs free energy of the SLP system is composed of three types of interfaces formed:

$$G^s = A \cdot s_L \cdot \gamma_{SL} + A \cdot \left(1 - s_L\right) \cdot \gamma_{SG} + A_{LG} \cdot \gamma_{LG} \tag{8.67}$$

With A, the total area of the support, A_{LG}, the gas/liquid interfacial area, s_L, the fraction of A covered by the liquid, γ, the surface tension.

Whereas the theoretical prediction of the liquid distribution in the porous material is very complicated and therefore difficult to obtain, some general principles can be established [36].

(a) Negative adhesion tension, $\gamma_{SG} - \gamma_{SL} > 0$ (contact angle >90°): The solid surface cannot be wetted by the liquid. G^s attains a minimum value when the solid and liquid phases are completely separated. Molten metals on ceramic supports show this behavior.
(b) Positive adhesion tension, $\gamma_{SG} - \gamma_{SL} < 0$ (contact angle <90°): By wetting the surface of the solid free energy is released and serves to increase the gas/liquid interface A_{LG}. In consequence, the liquid tends to spread over the whole surface and fills up small pores. This situation corresponds to SLP catalysts.

The total liquid mass in the wettable porous material is distributed between capillary liquid and adsorbed liquid. The change in chemical potential by forming a liquid in a cylindrical pore of radius r_c from free liquid can be determined with Kelvin's equation:

$$\Delta\mu_{rc} = -\frac{2\gamma_{LG}V_m}{r_c}\cos\theta_c \tag{8.68}$$

with V_m, the molar volume of the liquid and θ_c, the liquid/solid contact angle.

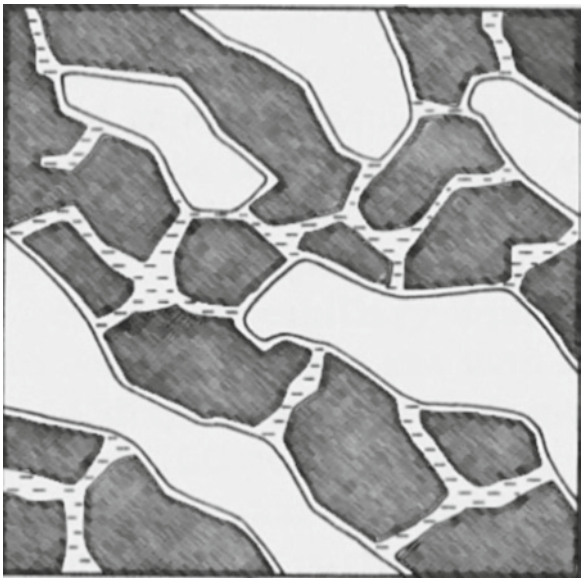

Fig. 8.16 Liquid distribution in a porous material. Liquid enclosed as capillary liquid in pores with $r_c \leq r_{c,m}$ and as an adsorbed layer with thickness $\delta_{L,m}$

When an adsorbed layer of thickness δ_L is formed, the chemical potential changes by [36]:

$$\Delta\mu_{\delta L} = -\frac{\Delta E \cdot V_m}{N_A \cdot \delta_L^3} \tag{8.69}$$

Where ΔE is the difference in average molar interaction energy between liquid/solid and liquid/liquid atomic pairs respectively, and N_A is the Avogadro number. At equilibrium follows: $\Delta\mu_{rc} = \Delta\mu_{\delta L}$. This allows calculating the largest pores with a radius $r_{c,m}$ which contain capillary liquid in equilibrium with an adsorbed liquid layer of the thickness $\delta_{L,m}$. Maximum pore radius and layer thickness will increase with the total liquid volume. The liquid distribution is schematically shown in Fig. 8.16.

8.4.3 Mass Transfer and Reaction in SLPC

The apparent catalyst activity and the reaction kinetics in SLPC are strongly influenced by the relative liquid loading of the porous material. The liquid loading α is defined as the fraction of the pore volume occupied by the liquid:

$$\alpha = \frac{V_L}{\varepsilon \cdot V_p} \tag{8.70}$$

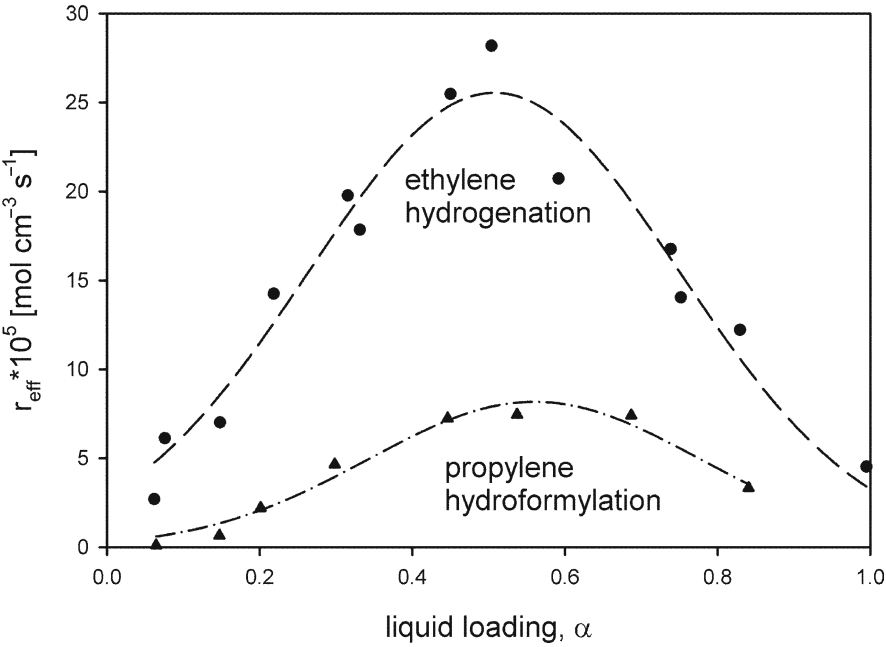

Fig. 8.17 Reaction rate of the ethene hydrogenation and the hydroformylation of propene as function of loading over different SLPC (See text for details, data taken from [30])

With V_L, V_p the liquid and particle volume, ε, the particle porosity. In consequence, the liquid loading varies between $\alpha = 0$ to $\alpha = 1$.

Typical experimental results of the effective reaction rate as function of the liquid loading (α) of SLP catalysts are shown in Fig. 8.17 for two different catalysts [30]. For the first catalyst a support with a low BET-surface area of 7.5 m^2/g was impregnated with RhCl(CO) $(PPh_3)_3$ as active compound dissolved in PPh_3 and dioctylphthalate. The hydrogenation of ethene was used as model reaction. The course of the curve with a pronounced maximum suggests that the effective reaction rate is influenced by two counteracting phenomena: At low loadings, the reaction rate increases with α due to the growing amount of the homogeneous catalyst. But the accessibility of the gaseous educt diminishes at high loadings with liquid, due to increasing diffusion resistances in the porous network and eventual pore blocking. The observed behavior was qualitatively confirmed for the hydroformylation of propene over RhH(CO) $(PPh_3)_3$ dissolved in dimethylglycolphthalate. The BET-surface of the support was found to be in the order of 60 m^2/g. This corresponds to an order of magnitude higher values compared to the first SLPC. In both cases the observed reaction rate passes through a maximum at loadings of $0.4 < \alpha < 0.6$.

Different models are proposed to explain the experimental observations, at least qualitatively [36–40]. Abed and Rinker [37] explained the experimental findings on

the base of gas and liquid diffusion in the SLPC. The authors assumed homogeneous distribution of liquids in the pores. Based on steady-state diffusion experiments with liquid loaded pellets, they described the effective gas diffusion with the following relationship:

$$\frac{D_{eff}^{G}}{D_{1,2}} = C_2 \left(1-\alpha\right)^2 \tag{8.71}$$

Where D_{eff}^{G} is the effective gas-phase diffusivity, $D_{1,2}$ is the binary molecular diffusivity of A_1 in A_2 in a free space, C_2 is one of the dusty gas constants which only depends on the structure of the solid support.

The diffusivity in the liquid is described in a similar manner and shown in Eq. 8.72.

$$\frac{D_{eff}^{L}}{D_1^{L} H} = C_2 \alpha^2 \tag{8.72}$$

The inclusion of the Henry coefficient H in Eq. 8.72 is required to obtain the molar flux in the liquid based on gas phase concentrations. Finally, an overall effective diffusivity is introduced which consists of the sum of the two effective diffusivities defined above:

$$D_{eff} = D_{eff}^{G} + D_{eff}^{L} = C_2 D_{1,2} \left(1-\alpha\right)^2 + C_2 D_1^{L} \alpha^2 \tag{8.73}$$

The mass balance for an infinite slab catalyst and simple irreversible first order reaction is given as:

$$D_{eff} \frac{d^2 c_1}{dz^2} - k'' H \varepsilon c_1 = 0 \tag{8.74}$$

With the boundary conditions:

$$z = 0 \qquad c_1 = c_{1,s}$$

$$z = L \qquad \frac{dc_1}{dz} = 0$$

With L the half-thickness of the slab, $c_{1,s}$ the reactant concentration at the outer surface and ε the porosity of the support. Solving Eq. 8.74 leads to the well-known effectiveness factor as function of the Thiele modulus.

$$\eta_{SLPC} = \frac{\tanh(\phi_{SLPC})}{\phi_{SLPC}} \quad \text{(infinite slab)} \tag{8.75}$$

The Thiele modulus is defined as

$$\phi_{SLPC} = L \sqrt{\frac{k'' H \cdot \varepsilon \cdot \alpha}{D_{eff}}} \tag{8.76}$$

It follows that ϕ_{SLPC} and as a consequence the effectiveness factor will change with the degree loading. With Eqs. 8.73 and 8.76 we obtain after rearrangement:

$$\phi_{SLPC} = L\sqrt{\frac{k'' H \cdot \varepsilon}{C_2 D_{1,2}}} \cdot \sqrt{\frac{\alpha}{(1-\alpha)^2 + \left(D_1^L H / D_{1,2}\right)\alpha^2}} \tag{8.77}$$

By defining a "molecular" Thiele modulus ϕ_m based on the intrinsic reaction rate in the liquid and the free gas phase diffusion, a parameter is obtained which is independent of the loading. After introducing a liquid/gas diffusivity ratio D′ the following relation results:

$$\phi_{SLPC} = \phi_m \cdot \sqrt{\frac{\alpha}{(1-\alpha)^2 + 2\alpha + \alpha^2 (1+D')}}$$
$$\text{with } \phi_m = L\sqrt{\frac{k'' H \cdot \varepsilon}{C_2 D_{1,2}}}; \quad D' = \frac{D_1^L H}{D_{1,2}} \tag{8.78}$$

The maximum reaction rate (r_{max}) per particle volume is reached for negligible diffusion resistance. The concentration inside the porous pellet is identical to the concentration at the outer surface and $\alpha = 1$.

$$r_{\max} = k'' H \varepsilon c_{1,s} \tag{8.79}$$

In contrast, the observed effective rate is influenced by the degree of loading (α) and the effectiveness factor (η_{SLPC}).

$$r_{eff} = k'' H \varepsilon c_{1,s}\, \alpha \cdot \eta_{SLPC} \tag{8.80}$$

The effectiveness factor depends on the Thiele modulus as shown in Eq. 8.75.

$$r_{eff} = k'' H \varepsilon c_{1,s} \alpha \cdot \frac{\tanh(\phi_{SLPC})}{\phi_{SLPC}} \tag{8.81}$$

Finally we define a global effectiveness factor based on the maximum rate:

$$\eta_{SLPC,0} = \frac{r_{eff}}{r_{\max}} = \alpha \cdot \frac{\tanh(\phi_{SLPC})}{\phi_{SLPC}} \tag{8.82}$$

If we express ϕ_{SLPC} by Eq. 8.78 we see that the global effectiveness factor depends on the molecular Thiele module (ϕ_m), the diffusivity ratio (D′) and the loading of the porous pellet (α). As the liquid diffusivity is roughly four orders of magnitude

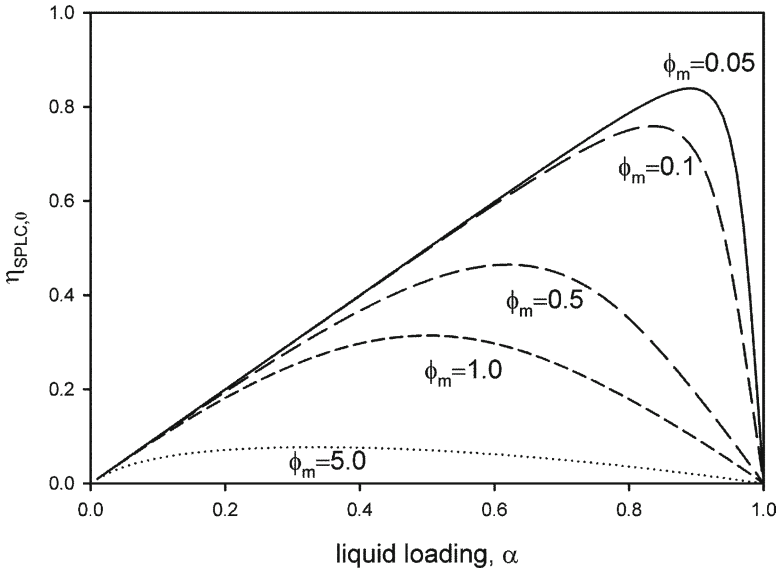

Fig. 8.18 The dependence of the global effectiveness factor on liquid loading and molecular Thiele modulus ($D' \ll 1$)

lower compared to the diffusivity in the gas phase, D' can mostly be neglected, thus the effective reaction rate mainly depends on the molecular Thiele modulus and the liquid loading. In Fig. 8.18 the variation of the global effectiveness factor, which corresponds to a referred effective reaction rate, is shown as function of the liquid loading and the Thiele modulus (ϕ_m).

For all values of ϕ_m the effectiveness factor as function of the loading passes through a maximum. This corresponds essentially to published experimental results (see Fig. 8.17). For comparable characteristic reaction times and diffusion times ($\phi_m \approx 1$) the maximum effective rate is attained at loadings of $\alpha \approx 0.5$.

With decreasing intrinsic reaction rate, corresponding to decreasing Thiele modulus, the mass transfer resistance diminishes and the maximum effective rate is shifted to higher loadings as indicated in Fig. 8.18. Finally, for very low intrinsic reaction rates, the reaction will occur uniformly within the supported liquid and the optimal loading approaches unity ($\phi_m \approx 0$; $\alpha \approx 1$).

Although the presented model is able to gain some basic understanding on the influence of liquid loading on the observed chemical reactions in SLPC, more sophisticated models are necessary for a more quantitative description of the experimental findings.

8.5 List of Symbols

a	m^2/m^3		Specific interfacial area
A_p	m^2		Surface area of particle
c*	mol/m^3		Equilibrium concentration at interface
c_i	mol/m^3		Concentration of compound Ai
cp	kJ/(kg K)		Heat capacity
D_e	m^2/s		Effective diffusion coefficient
d_h	m		Hydraulic diameter
D_i	m^2/s		Molecular diffusion coefficient
d_p	m		Particle diameter
E	kJ/mol		Activation energy
E_a	kJ/mol		Apparent activation energy
h	$W/(m^2 K)$		Heat transfer coefficient
k_{fl}	m/s		Mass transfer coefficient
k_L	m/s		Mass transfer coefficient in liquid phase
k_r	Variable units		Reaction rate constant
$k_{r,0}$	Variable Units		Frequency factor
L_c	m		Characteristic length
n	–		Reaction order
r	$mol/(m^3 s)$		Reaction rate
R	J/(mol K)		Gas constant
r_{eff}	$mol/(m^3 s)$		Effective (observed) rate
R_i	$mol/(m^3 s)$		Transformation rate
$s_{k,i}$	–		Instantaneous selectivity of A_k referred to A_i
T	K		Temperature
t_m	s		Characteristic mass transfer time
t_r	s		Characteristic reaction time
V_I, V_{II}	m^3		Volume of phase I, II
V_p	m^3		Particle volume
V_R	m^3		Reactor volume
X	–		Conversion
$Y_{k,i}$	–		Yield of A_k referred to A_i
ΔH_r	kJ/mol		Reaction enthalpy
Greek symbols			
λ		W/(m K)	Heat conductivity
η		–	Effectiveness factor
ρ		kg/m^3	Density
δ_{II}		m	Stagnant layer thickness (film model)

(continued)

(continued)

Dimensionless numbers		
Bi		Biot-number
DaII		Second Damköhler number
Ha	–	Hatta number
Pr		Prandtl number
Sc		Schmid number
Ψ		Weisz modulus
ϕ	–	Thiele modulus

References

1. Cornils B, Herrmann WA, Horváth IT, Leitner W, Mecklenburg S, Olivier-Bourbigou O, Vogt D (eds) (2005) Multiphase homogeneous catalysis, vol 1. Wiley, Weinheim
2. Manassen J (1973) In: Basolo F, Burwell RL (eds) Catalysis progress in research. Plenum, London 177
3. Joó F (2001) Aqueous organometallic catalysis. Kluwer, Dordrecht
4. Bahrmann H, Bach H (2010) Oxo synthesis. In: Ullmann's encyclopedia of industrial chemistry. Wiey, Weinheim
5. Wiebus E, Cornils B (2006) Biphasic systems: water-organic. In: Cole-Hamilton DJ, Tooze RP (eds) Catalyst separation, recovery and recycling. Springer, Dordrecht
6. Trambouze P, Euzen JP (2002) Les réacteurs chimiques. TECHNIP, Paris
7. Levenspiel O (1999) Chemical reaction engineering. Wiley, New York
8. Baerns M, Hofmann H, Renken A (2002) Chemische Reaktionstechnik, 3rd edn. Wiley, Weinheim
9. Wachsen O, Himmler K, Cornils B (1998) Catal Today 42:373
10. Wiese KD, Möller O, Protzmann G, Trocha M (2003) Catal Today 79–80:97–103
11. Burgi R, Tauscher W, Streiff F (1981) Chem Ing Tech 53:39–42
12. Jancic SJ, Zuiderweg FJ, Streiff F (1984) AIChE Symp Series 238:139
13. Schneider G (1990) Inst Chem Eng Symp Ser 121(Fluid Mixing 4):109
14. Streiff FA, Jancic SJ (1984) German Chem Eng 7:178
15. Nienow AW (2010) Stirred tank reactors. In: Ullmann's encyclopedia of industrial chemistry. Wiley, Weinheim
16. Zlokarnik M (2001) Stirring. Wiley, Weinheim
17. Moravec RZ, Schelling WT, Oldershaw CF (1939) 1939. Brit Patent 511:566
18. Balzhinimaev BS, Ivanov AA, Lapina OB, Mastikhin VM, Zamaraev KI (1989) Faraday Discuss R Soc Chem 87:133
19. Gerritsen LA, Herman JM, Klut W, Scholten JJF (1980) J Mol Catal A Chem 9:157
20. Gerritsen LA, Herman JM, Scholten JJF (1980) J Mol Catal A Chem 9:241
21. Gerritsen LA, Klut W, Vreugdenhil MH, Scholten JJF (1980) J Mol Catal A Chem 9:265
22. Gerritsen LA, Klut W, Vreugdenhil MH, Scholten JJF (1980) J Mol Catal A Chem 9:257
23. Gerritsen LA, Van Meerkerk A, Vreugdenhil MH, Scholten JJF (1980) J Mol Catal A Chem 9:139
24. Herman JM, van den Berg PJ, Scholten JJF (1986) Chem Eng J 32:101
25. Herman JM, van den Berg PJ, Scholten JJF (1987) Chem Eng J 34:133
26. Herman JM, van den Berg PJ, Scholten JJF (1987) Chem Eng J 34:123
27. Herman JM, Verwater HJC, Rocourt AP, van den Berg PJ (1987) Chem Eng J 34:117
28. Pelt HL, van der Lee G, Scholten JJF (1985) J Mol Catal A Chem 29:319

29. Pelt HL, Verburg RPJ, Schölten JJF (1985) J Mol Catal A Chem 32:77
30. Hoffmeister M, Hesse D (1990) Chem Eng Sci 45:2575
31. Mehnert CP, Cook RA, Dispenziere NC, Afeworki M (2002) J Am Chem Soc 124:12932
32. Mehnert CP, Mozeleski EJ, Cook RA (2002) Chem Commun 8:3010
33. Riisager A, Eriksen KM, Wasserscheid P, Fehrmann R (2003) Catal Lett 90:149
34. Riisager A, Wasserscheid HR, Fehrmann R (2003) J Catal 219:452
35. Riisager A, Fehrmann R, Haumann M, Wasserscheid P (2006) Eur J Inorg Chem 4:695
36. Villadsen J, Livbjerg H (1978) Catal Rev 17:203
37. Abed R, Rinker RG (1973) J Catal 31:119
38. Rony PR (1968) Chem Eng Sci 23:1021
39. Rony PR (1969) J Catal 14:142
40. Rony PR, Roth JF (1975) J Mol Catal 1:13

Chapter 9
Chemoselective and Enantioselective Hydrogenations on Immobilized Complexes

Agnes Zsigmond, Ferenc Notheisz, Petr Kluson, and Tomas Floris

Abstract Homogeneous catalysts, which are mixed with the reactants at the molecular level, typically show the highest activity and selectivity as they offer chemically well-defined active sites and are not limited by heat and mass transport. However, an inherent disadvantage of the homogeneous catalysis is the need to separate the catalyst from a product after the reaction. Therefore, solid or immobilized homogeneous catalysts are preferred in industry. In this contribution we pay attention to chemoselectivity, regioselectivity and enantioselectivity in the synthesis of fine chemicals by means of hydrogenation reactions with immobilised homogeneous complexes. Preferential hydrogenation of one functional group in a molecule over another is the chemoselective process, while regioselective hydrogenation is the preferential formation of one constitutional isomer of the product in a reaction in which other isomers may also be formed, and the stereoselective hydrogenation is the formation of an excess of one stereoisomer over others. Homogeneous and heterogeneous catalytic transfer hydrogenations (CTH) were additionally introduced as alternative methods to the classical hydrogenation processes. They utilise a different hydrogen source from molecular hydrogen and can find their use for reduction of any type of groups.

9.1 Introduction

Catalysis is a key principle for selective transformations in the manufacture of specialty chemicals. Through the use of catalysts milder reaction conditions can be achieved and undesired side products might be suppressed. Homogeneous catalysts, which are mixed with the reactants at the molecular level, typically show the highest activity and selectivity as they offer chemically well-defined active sites and are not limited by heat and mass transport. However, an inherent disadvantage of the homogeneous catalysis is the need

A. Zsigmond (✉), F. Notheisz, P. Kluson, and T. Floris
Department of Organic Chemistry, University of Szeged, Dóm tér 8, 6720 Szeged, Hungary
e-mail: azsig@chem.u-szeged.hu

P. Barbaro and F. Liguori (eds.), *Heterogenized Homogeneous Catalysts for Fine Chemicals Production*, Catalysis by Metal Complexes 33,
DOI 10.1007/978-90-481-3696-4_9,

to separate the catalyst from a product after the reaction. This frequently requires complex operations and it is associated with a loss of catalyst which is often unacceptable due to the high price, negative impact on product quality and also from environmental reasons. Therefore, solid or immobilized homogeneous catalysts are preferred in industry.

In the production of chemical specialities the parameter of selectivity of a particular catalyst is probably its most important property. Chemoselectivity, regioselectivity and enantioselectivity play an important role in the synthesis of most fine chemicals. Preferential hydrogenation of one functional group in a molecule over another is called chemoselective hydrogenation, while regioselective hydrogenation is the preferential formation of one constitutional isomer of the product in a reaction in which other isomers may also be formed. At the same time stereoselective hydrogenation is the formation of an excess of one stereoisomer over others. Stereoselectivity is sub-divided into enantioselectivity and diastereoselectivity according to the formation of enantiomers or diastereomers. Three approaches might be adopted for obtaining the enantiometrically pure compound. These are resolution of a racemic mixture, stereoselective synthesis starting from a chiral building block or transformation of a prochiral substrate into a chiral product by asymmetric catalysis. The last approach comprises an amplification of the chirality: One molecule of the chiral catalyst produces thousands of molecules of the chiral product from the starting material, which is optically inactive. Homogeneous catalytic transfer hydrogenation (CTH) is our last focus. It is an alternative method to the classical hydrogenation using variable molecules as a source of hydrogen. Typically unsaturated hydrocarbons such as cyclohexene, cyclohexadiene, limonene, etc., can play the role of hydrogen donor.

9.2 Chemoselectivity in Hydrogenation on Immobilized Complexes

The chemoselective hydrogenation of C=C and/or C=O of compounds containing both these bonds has attracted attention in the recent years [1]. The hydrogenation of C=C double bond is relatively easy, because of both thermodynamic and kinetic reasons. Thermodynamics favors the hydrogenation of C=C double bond over C=O with 35 kJ/mol and kinetically the reactivity of C=C bond for the hydrogenation is much higher than those of the C=O bond. However, the chemoselective hydrogenation of the C=O bond of α,β-unsaturated carbonyl compounds to allylic alcohols becomes more and more important since allylic alcohols are valuable intermediates in the pharmaceutical, agrochemical and cosmetics industry [2].

9.2.1 Chemoselective Hydrogenation of Unsaturated Carbonyl Compounds

Different homogeneous catalysts were used for the chemoselective hydrogenation of α,β-unsaturated aldehydes [3]. Water-soluble Ru complexes, such as $[\{RuCl_2(TPPMS)_2\}_2]$,

(TPPMS = (3-sulfonatophenyl) diphenylphosphane sodium salt), were applied in the hydrogenation of α,β-unsaturated aldehydes under homogeneous conditions, and various Ru-hydride complexes were established as active catalytic species depending on the pH [4]. At pH < 6 the species $[HRuCl(TPPMS)_3]$ was the dominant Ru(II)-complex and it catalyzed the slow but very selective hydrogenation of the C=C bond in the molecule of cinnamaldehyde. At pH > 8 the $[H_2Ru(TPPMS)_4]$ complex was found to be an active and selective catalyst for the C=O reduction. Consequently, changing the pH of the solution it could shift the equilibrium between the two Ru species and invert the selectivity of the hydrogenation of cinnamaldehyde [3, 4]. With the aim of developing active and chemoselective heterogenized catalysts the anchored $[\{RuCl_2(TPPMS)_2\}_2]$ and $[RuCl_2(PPh_3)_3]$ complexes were prepared [5] using the method developed by Augustine [6–8]. In all cases phosphotungstic acid (PTA) was used as anchoring material, and zeolite Y as a support. The heterogenized complexes were characterized by spectroscopic methods and applied as catalysts in the hydrogenation of α,β-unsaturated aldehydes. The hydrogenation of crotonaldehyde and cinnamaldehyde were studied under slightly different conditions based on the results obtained under homogeneous conditions [4]. For the C=O reduction, as mentioned basic conditions were applied (0.05 mmol PPh_3 together with 0.04 mmol Et_3N) while the C=C hydrogenation was expected under acidic condition (0.02 mmol Et_3N and 0.03 mmol PPh_3). The experimental observations can be seen in the hydrogenation of trans-cinnamaldehyde (in Tables 9.1 and 9.2) using the two different conditions (see also Fig. 9.1).

As Table 9.1 shows both the soluble and the heterogenized catalysts are well active in the hydrogenation of trans-cinnamaldehyde under basic conditions. Both heterogenized catalysts reveal higher TOF than the homogeneous catalysts. The product distributions are about the same as those of the homogeneously catalyzed reactions.

Under acidic conditions selective hydrogenation of the C=C double bond is expected (Table 9.2). Indeed, the C=C selectivity is very high providing the saturated aldehyde – the major product on all catalysts. The selective C=C bond hydrogenation is definitely more pronounced on sulfonated catalysts, with all other products amounting less than 30%. This is in contrast to the selectivity of the same catalyst in basic conditions where the C=O hydrogenation is dominant [4]. The same

Table 9.1 The hydrogenation of *trans*-cinnamaldehyde under basic conditions with soluble and heterogenized Ru(II)-phosphane complexes

			Product distribution (%)			
Catalyst	Time (h)	Conversion (%)	S_{ald}	S_{alc}	U_{alc}	TOF
$[H_2Ru(TPPMS)_4]$	1.5	29	12	0	88	7.7
	3	68	7	0	93	–
$[H_2Ru(TPPMS)_4]$/PTA/Y	3	15	12	0	88	33
	6	36	12	0	88	–
$[H_2Ru(PPh_3)_4]$	3	94	6	12	83	13
	6	96	5	20	75	–
$[H_2Ru(PPh_3)_4]$/PTA/Y	3	92	3	11	86	11
	6	96	3	13	84	–

Reaction conditions: 10 mg hom. or 300 mg het. complex, 3 ml ethanol, 6 μl Et_3N, 13.5 mg PPh_3, 50 μl substrate, 338 K, 0.4 MPa H_2 and 3 h reaction time

Table 9.2 Product distribution in the hydrogenation of *trans*-cinnamaldehyde in acidic condition with soluble and heterogenized Ru(II)-phosphane catalysts

Catalyst	Time (h)	Conversion (%)	Product distribution (%)			TOF
			S_{ald}	S_{alc}	U_{alc}	
$[H_2Ru(TPPMS)_4]$	1.5	39	63	9	28	10
	3	55	62	10	28	–
$[H_2Ru(TPPMS)_4]$/PTA/Y	3	31	58	20	22	67
	6	56	60	20	20	–
$[H_2Ru(PPh_3)_4]$	3	26	41	7	52	3
	6	35	42	8	50	–
$[H_2Ru(PPh_3)_4]$/PTA/Y	3	42	54	10	36	5
	6	48	52	15	33	–

Reaction conditions: 10 mg hom. or 300 mg het. complex, 3 ml ethanol, 3 µl Et_3N, 7.8 mg PPh_3, 50 µl substrate, 338 K, 0.4 MPa H_2 3 h reaction time

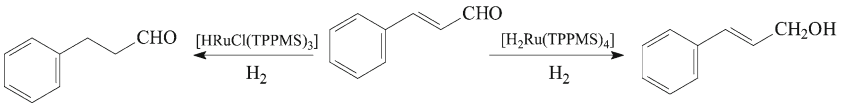

Fig. 9.1 Selective hydrogenation of *trans*-cinnamaldehyde

results were observed [5] in the hydrogenation of crotonaldehyde. The heterogenized catalyst $[H_2Ru(PPh_3)_3]$/PTA/Y was used in three subsequent runs in the hydrogenation of cinnamaldehyde. The catalyst did not lose its activity significantly and the product distributions were very similar from run to run (Table 9.3). In other words the selectivity did not change considerably. It increased slightly in favour of the formation of the unsaturated alcohol. The conversion decreased to some extent, which can be caused by the physical loss of the catalyst. In aqueous/organic biphasic conditions [4] the hydrogenation of cinnamaldehyde catalyzed by water-soluble Ru(II)-phosphane complex at pH = 3 produced a 51:49 mixture of cinnamyl alcohol and 3-phenylpropanal at 0.1 MPa of H_2 pressure. However, with increasing H_2 pressure this ratio increased, and at 1 MPa it reached the ratio 93:7. This dramatic pressure effect on the selectivity can be explained by the different pressure dependence on the rate of C=C and C=O hydrogenations.

The increase in H_2 pressure changes the molecular distribution of Ru among its various hydride species. However, it is also possible that some other Ru complexes, e.g. $[RuH(H_2)(TPPMS)_4]^+$, also take part in the hydrogenation reaction. Under 0.4 MPa H_2 pressure, in ethanolic solution and at acidic conditions, a product ratio of cinnamyl alcohol : 3-phenylpropanal = 36:54 was obtained [5] in the hydrogenation of cinnamaldehyde with the heterogenized catalyst $[HRuCl(PPh_3)_3]$/Y. Based on the results obtained in aqueous biphasic systems, the effect of H_2 pressure on the selectivity of catalysts was also studied (Fig. 9.2). Indeed, these measurements showed a remarkable pressure effect on the selectivity. For comparison, experiments were also carried out under the same conditions with the soluble $[HRuCl(PPh_3)_3]$ catalyst (Fig. 9.2). An increase in hydrogen pressure causes a substantial increase in the

Table 9.3 The product distribution for three subsequent runs of the hydrogenation of cinnamaldehyde on $[H_2Ru(PPh_3)_3]$/PTA/Y catalyst in basic condition (reaction time 1 h)

			Product distribution (%)		
Runs	Time (h)	Conversion (%)	S_{ald}	S_{alc}	U_{alC}
1. run	1	33	5	10	85
2. run	1	28	3	12	85
3. run	1	26	2	12	86

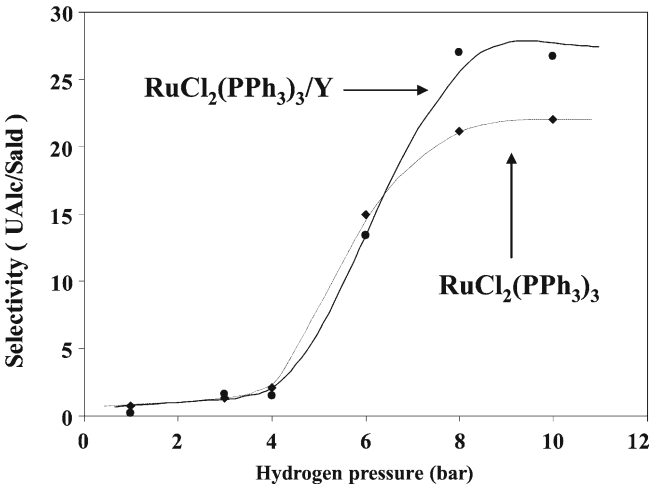

Fig. 9.2 The effect of H_2 pressure on the selectivity of the hydrogenation of cinnam-aldehyde catalyzed by $[HRuCl(PPh_3)_3]$ (▼) and $[HRuCl(PPh_3)_3]$/PTA/Y (▲) catalysts

selectivity towards the formation of the unsaturated alcohol (both the soluble and the heterogenized catalysts). This also implies, though does not prove unequivocally, that the same ruthenium-hydride complexes, $[HRuCl(PPh_3)_3]$ and $[H_2Ru(PPh_3)_4]$ known from the solution phase hydrogenations of cinnamaldehyde act as catalytic species on the surface of the support.

As a result, the selectivity in this system can be affected not only by manipulating the basicity of the solution phase, but also by varying the hydrogen pressure. In conclusion, the heterogenized catalysts show about the same activity as their homogeneous counterparts and at the same time their selectivity towards the formation of the unsaturated alcohol product is found to be approximately as twice as high as the corresponding homogeneous catalysts. In addition, it is possible to use these heterogenized catalysts in three subsequent runs, without any significant loss of activity, and even with a slight increase in selectivity.

Chemoselective hydrogenation of α,β-unsaturated carbonyl compounds was also reported on anchored $RuCl_2(PPh_3)_3$ complex to the inner surface of MCM-41 and MCM-48 mesoporous supports [9]. The authors used the post-synthesis grafting

method for the organic modification of the inner surfaces of MCM-41 and MCM-48. The most important aspect of their work was the detailed characterization in order to get evidences of the metal complex formation and its anchoring to the inner surface of the mesoporous material. For the organic modification the MCM-41 and MCM-48 materials were treated with dichlorodiphenylsilane (Ph_2SiCl_2) to passive the external surface, consequently the anchoring was expected to happen on the inner surface [10]. The desired trialkoxyorganosilane (3-aminopropiltrimetoxy silane, *N*-[3-(trimetoxysylilpropil)]-ethylenediamine) was added to the MCM-41 or MCM-48 at 195 K then the materials were slowly warmed up to room temperature. Then it was further stirred for additional 24 h in inert atmosphere and washed with dry dichloromethane and dried under vacuum. This process yielded organofuncionalized mesoporous materials, which were designated as NH_2-MCM-41/48 and EN-MCM-41/48 respectively. The $RuCl_2(PPh_3)_3$ complex was anchored onto the inner surface by a dative bond from the nitrogen atom on the NH_2 modified zeolite and an additional bond which was formed by ligand exchange in the case of ethylenediamine modification.

The catalytic hydrogenation reactions of different olefins and α,β-unsaturated aldehydes were carried out in high pressure autoclave between 0.34 and 2.76 MPa of H_2 pressure in propan-2-ol solution, adding potassium tert-butoxide as a base. The solid catalysts were filtered after the reactions and recycled several times.

The authors [9] have applied all possible spectroscopic methods to characterize the anchored catalysts. The XRD spectra were recorded before and after the anchoring of the complex and the results showed evidence that the mesoporous materials did not change after the complex anchoring. The FTIR and the ^{31}P CP MAS NMR spectra were also taken for all the materials and the comparison of these spectra showed convincingly the anchoring of the complex. The authors also used SEM and TEM images in order to prove that the mesoporous matrices have retained their morphological integrity (both, the shape and size) after functionalization and after immobilization of the complexes.

The prepared catalysts were used in the chemoselective hydrogenation of α,β-unsaturated aldehydes and the activity and the chemoselectivity of the heterogeneous catalysts were compared to the homogenous ($RuCl_2(PPh_3)_3$-ethylenediamine) composite system.

Table 9.4 clearly shows that under the experimental conditions both C=C and C=O double bonds were hydrogenated and major products were aldehydes or unsaturated alcohols. However, the consequent hydrogenation did not take place, and thus saturated alcohols were not formed. The Table 9.4 also shows that RuP-NH_2-MCM-41 catalyst is not really active in the hydrogenation of α,β-unsaturated aldehydes and the main product is the saturated aldehyde. Almost no activity was observed in the C=O bond hydrogenation. However, the ethylenediamine containing catalysts reveal high activities towards the C=O double bond hydrogenation and the main product is the unsaturated alcohol.

The selectivity was increased by increasing the substitution of β-carbon, but it did not change with increasing substitution of α-carbon. Comparing the TOFs of the heterogeneous and the homogeneous catalysts the later exhibited the higher

Table 9.4 Chemoselective hydrogenations of α,β-unsaturated aldehydes on heterogenized ($RuCl_2(PPh_3)_3$-ethylenediamine) catalysts

Catalyst	Substrate	Conversion (%)	Unsaturated alcohol	Aldehyde	TOF (h^{-1})
RuP-NH_2-MCM41	Cinnamaldehyde	45	0	100	300
RuP-NH_2	Cinnamaldehyde	64	0	100	500
RuP-EN-MCM41	Acrolein	85	44	56	600
RuP-EN-MCM41	Crotonaldehyde	81	63	37	600
RuP-EN-MCM41	Cinnamaldehyde	74	76	24	550
RuP-EN-MCM41	2-Methyl-cinnamaldehyde	67	74	26	500
RuP-EN-MCM48	Cinnamaldehyde	76	79	N21	550
RuP-EN-SiO_2	Cinnamaldehyde	72	76	24	550

Reaction conditions: 100 mg catalyst, 9 mmol substrate, S/C = 100/1, 373 K, 1.38 MPa H_2 pressure, 4 h

values, which was rationalized by the restricted interaction of the metal complex and the substrate molecules under the heterogeneous conditions.

At the same time all the supported catalysts, the MCM-41, MCM-48 and the silica supported ones, showed similar activity and selectivity, explained by the similar interaction between the substrate molecules and the catalyst active sites. However, there are available literature data [11] showing that the metal complexes built inside the MCM-41 can have increased activity and selectivity as well. These expected special effects are the main reasons to prepare these types of catalysts.

The results pointed out strongly for the necessity of the ethylenediamine moiety in the complex, since the reactions proceeded via the "metal–ligand bifunctional mechanism" proposed by Noyori et al. [12]. The NH_2- or NH- moieties are crucial for the high catalytic activity, since these moieties have a unique hydrogen-bonding ability to activate the carbonyl bond. The stability of the heterogeneous catalysts were evaluated to filter out the catalyst from the reaction mixture and to analyze the liquid by ICP-AES. Only negligible leaching was observed and at the same time the catalysts were recycled four times in the hydrogenation of cinnamaldehyde without any significant loss of activity or selectivity. However the catalyst anchored to fumed silica showed significant leaching which further caused decrease in activity in every recycling step. The filtered catalyst was also checked by XPS for the stability, indicating that neither the ligand nor the metal changed its chemical environment during the reaction [12]. The influence of the reaction time on the activity and selectivity was also studied. It was found that both the chemoselectivity and conversion were increasing with increasing reaction time and reached a maximum at ~4 h reaction time. However, the C=C hydrogenation remained constant during the course of the reaction, which meant the unsaturated alcohol became the major product as the reaction proceeded.

In case of cinnamaldehyde the minimum of 373 K was necessary to get the maximum conversion and chemoselectivity. At lower temperature the saturated

aldehyde was formed predominantly, meanwhile at ~373 K the unsaturated alcohol became the major product. By increasing the temperature up to 393 K no further change in activity as well as chemoselectivity was observed [9].

The pressure of molecular hydrogen has a pronounced effect on the hydrogenation of cinnamaldehyde and a minimum pressure of 1.38 MPa is required for the maximum conversion both the heterogeneous and the homogeneous catalysts. However, the chemoselectivity does not depend on the H_2 pressure, the chemoselectivity of the hydrogenation on C=O bond is very high even at lower H_2 pressure regime.

Macroreticular anion exchange resins, Amberlite IRA-900 and Amberlite IRA-96, were used [13] to bind the monosulfonated triphenylphosphine ligand via noncovalent electrostatic interactions. The resin-phosphine system was found to be very efficient at promoting the immobilization of [Rh-2(mu-OMe)(2)(cod)(2)] [13]. The resulting stable Rh/TPPMS immobilized catalyst was tested in the hydrogenation of unsaturated oxosteroids (4-androstene-3,17-dione and 3 beta-acetoxypregna-5, 16-dien-20-one). These immobilized catalysts could selectively reduce the C=C bonds leading to the preferential formation of the alpha-diastereoisomer, as in the homogeneous systems. Furthermore, these new immobilized rhodium catalysts showed good performance, easy separation and recycling without loss of activity after at least three reaction cycles.

9.2.2 Chemoselective Hydrogenation of Alkenes and Alkyne

Chemoselective hydrogenation of one C=C double bond in the presence of other carbon-carbon double or triple bonds represents an important example of selective hydrogenations. Preferential hydrogenation of one C=C double bond in the presence of another C=C double bond is called regioselective hydrogenation, because the products are isomers. Meanwhile, the same hydrogenation in the presence of a triple bond is called chemoselective hydrogenation, because the products are different compounds.

Palladium-Salen complexes have been reported to reveal catalytic activity for the hydrogenations of alkenes. Moreover, it was observed in the liquid phase that this catalyst activated hydrogen in a very similar way like the enzyme hydrogenase [14]. The selective hydrogenation of cycloocta-1,5-diene was been studied on immobilized Pd-Salen and Rh-Salen complexes in the liquid phase [15].

The encapsulated Pd-Salen catalyst was prepared by the method called the “flexible ligand“ and it was characterized by XRD [15]. The X-ray powder pattern did not show any significant difference before and after the complex formation, which means that the zeolite framework was not affected by the intrazeolitic complex formation. According to the results the free ligands are flexible enough to diffuse into the zeolite supercages, where the metal cations can be found. After the complex formation the resulting complexes are too rigid and too bulky to diffuse out of the supercages. The uncomplexed free ligand should be removed by Soxhlet extraction with acetone and the resulting catalyst can be characterized by solid-state

UV-VIS and FT-IR spectroscopy. Comparing the spectra of the free ligand and the encapsulated catalyst it can be stated that most of the free ligand was removed by the extraction process together with only a little amount of the metal complex. The actual Pd content of the catalyst was determined as 1.6 w% of Pd which corresponded to 0.15 mmol Pd/g of zeolite.

The prepared catalysts were applied [15] in the liquid phase hydrogenation of cycloocta-1,5-diene, which was hydrogenated relatively fast under the conditions applied in the study to cyclooctene and further to completely saturated compound on the Pd complex. The hydrogenation on the corresponding Rh complex was much slower but at the same time it was much more chemoselective for the formation of the partially hydrogenated product, cyclooctene [15]. This observation was indicated by the experimental fact that the yield of cyclooctane did not increase with increasing the reaction time. This is a very interesting observation regarding the chemoselective hydrogenation of the multiple double bond. The influence of the concentration of Pd-Salen complex can be deduced from the catalytic results, since the catalytic activity passes through a maximum curve. The increase of initial activity with increasing Pd content can be rationalized by increasing the active species. However, if too many complexes are in the supercages the reaction rate will decrease because of the partial blockade of diffusion pathways in the zeolite. Consequently the observed reaction rate is decreasing due to the mass transfer limitation. Changing the zeolite from FAU to EMT and keeping the Pd content constant, it did not cause any significant change indicating that the accessibility of the reactant molecules were comparable in the two cases.

The Pd complex of chiral Salen type of ligand (*R,R*)-*N,N*,-bis-(3,5-di-*tert*-butylsalicylidene)-1,2-cyclohexanediamine, Fig. 9.3) was also encapsulated in the large supercages of FAU and EMT zeolite [15]. The catalyst spectral characterization showed a convincing evidence for the encapsulation of the desired complex. However, the attempt to perform enantioselective hydrogenation failed, indicating that even the encapsulation was successful, the resulting catalyst, however, did not show the reactivity of the original homogeneous complex (Figs. 9.4).

Among the different solid supports, to which complexes can be attached, polymers derived from the ring opening metathesis (ROM) of norbornene and 7-oxanorbornene derivatives are particularly attractive [16]. These supports can be prepared highly functionalised from monomers using ruthenium carbene [17]. The obtained polymers (ROMP-gel) can have high loading and significant swelling in different solvents [18].

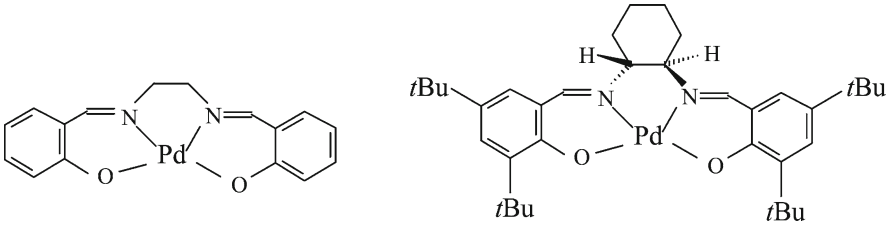

Fig. 9.3 The structure of Pd-Salen and its chiral version

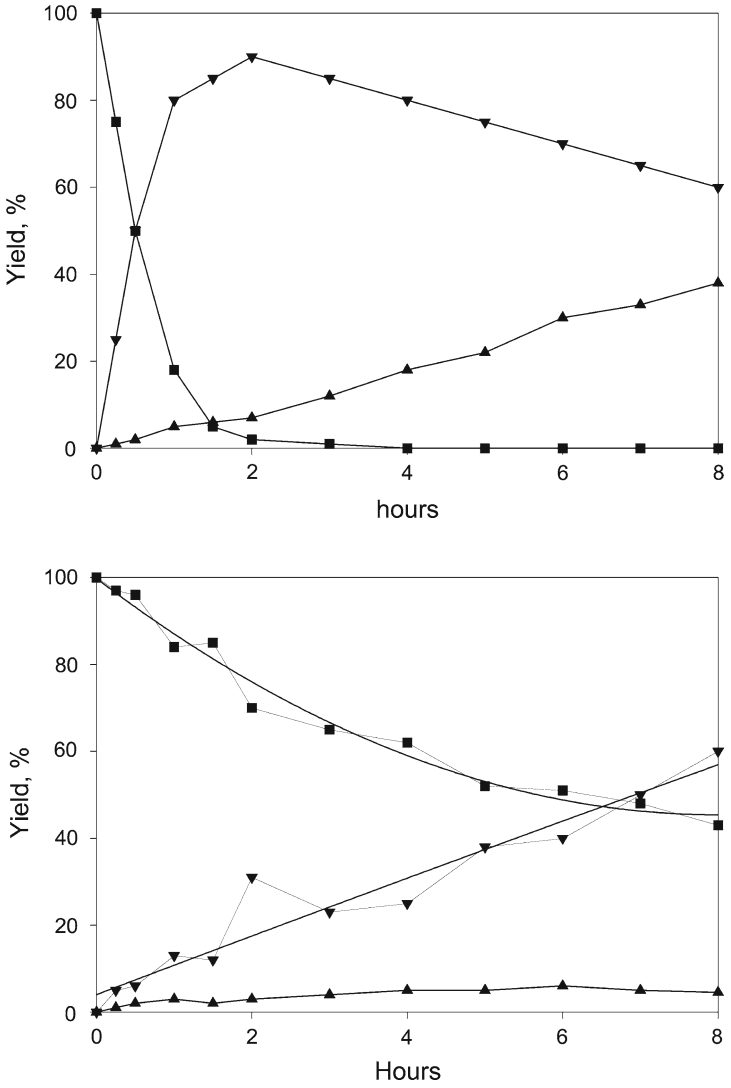

Fig. 9.4 The catalytic activity and selectivity of the hydrogenation of 1,5-cyclooctadiene on encapsulated Pd-Salen (upper) and Rh-Salen(lower) complexes

Tris(triphenylphosphine)rhodium(I)chloride, the Wilkinson's catalyst, is widely used for the selective hydrogenations of not conjugated olefins. It hydrogenates well the sterically unhindered alkenes meanwhile for the more substituted ones, e.g. for the tetrasubstituted alkenes, it has no activity at all. To combine the good selectivity of the Wilkinson's catalyst with the easy separation of the heterogeneous catalyst it was anchored on different supports [17]. However, it has not been demonstrated yet that the supported catalyst can be used in parallel synthesis.

Ionic liquids are usually not soluble in most organic solvents, but they have high affinity to metal complexes [17]. Therefore they can be efficiently used in a two phase system (organic solvent/ionic liquid) where the reagents are soluble in organic solvents while the metal complex retains in ionic liquid. Reaction rates and selectivities for hydrogenations are often improved in such systems. In this very interesting approach the authors [18] used the ROMP methodology to prepare a novel supported Wilkinson's catalyst allowing the fine tuning of the polymer support in order to obtain the best chemical environment for the catalysis. The authors investigated the use of different ROMP polymers containing triarylphosphine, imidazolium units and the mixture of these two. The ROMP-gel supported tris(triphenylphosphine) was prepared as previously reported [19], while the imidazolium hexafluorophosphate monomer was obtained in three steps from commercially available starting materials. Addition of the second generation of Grubbs' catalyst to the corresponding monomers afforded the ROMP-gels. The Wilkinson's catalyst was anchored to the ROMP-gel by heating the suspension of the polymer with the complex for 18 h in dichloromethane solution. In the case of tris(triphenylphosphine) containing polymers the attachment of the complex was achieved by ligand exchange. In the case of the imidazolium containing polymer the possibility of ionic attachment was investigated [16]. The activity of the prepared supported rhodium catalyst was screened by selective hydrogenation of different terminal alkenes. When the catalysts were compared it turned out that the anchored Wilkinson complex made by the ligand exchange showed much higher activity than the one with the attempt to anchor by ionic forces. These results clearly showed that the ionic moiety did not have the desired rate enhancing effect on the catalytic hydrogenation. The ROMP-gel supported Wilkinson complex was further hydrogenated to avoid the unnecessary competition of the backbone double bond with the possible substrates and the loosely bonded rhodium complexes was also removed by extensive washing. The resulted catalyst was characterized by ICP-AES method containing 0.66 mmol/g rhodium complex. To compensate the rate reduction by diffusion, relatively large amount of catalyst was used in the case of bulky substrates, e.g. steroids, and efficient stirring was applied. Using these conditions different alkene/alkyne starting materials were hydrogenated selectively with high yields and purity.

As it can be seen from Table 9.5 the immobilized catalyst is selective and it allows the chemoselective hydrogenation of alkenes in the presence of more hindered alkenes.

In addition a chemoselective hydrogenation of ring alkenes is possible in the presence of *trans*-disubstituted alkenes. Also alkenes can be reduced in the presence of different functional groups such as carbonyl, ester, amides and nitro groups. In all cases the products are obtained in good or excellent yield and purities, which further implies that the ROMP-gel supported Wilkinson's complex can be applied in specific cases for production of small amounts of specific compounds.

The chemo- and stereoselective hydrogenations of different alkynes were reported on the Ru sulfonated triphenyl phosphine complex, immobilized on ion-exchange resins [20]. Since the ion-exchange resins are available in a large variety

Table 9.5 Selective hydrogenation of alkenes on ROMP-gel supported $RhCl(PPh_3)_3$ catalyst

Starting material	Products	Yield (%)	Purity (%)
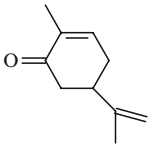	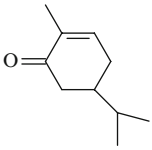	94	95
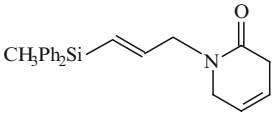	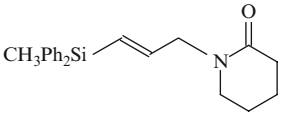	98	90
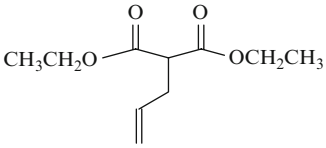	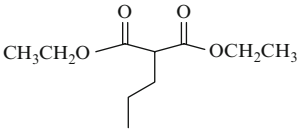	100	95
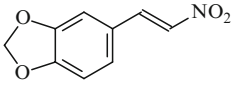	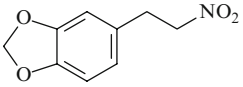	68	95

Reaction conditions: 0.04 g substrate, 0.04 g polimer, solvent mixture: THF : ethanol = 1: 1.2

and different ionic phosphines and other ligands are also known, this approach offers the synthesis of heterogenized catalysts for different purposes. The hydrogenations of different starting materials were studied on the above heterogenized catalyst, using the H-Cube flow reactor [20]. According to the earlier observations of the authors in water/toluene biphasic system at 323 K and 1 bar total pressure the $[RuCl_2(m\text{tppms})_2]_2$ complex selectively hydrogenates diphenylacethylene and other disubstituted alkynes to *Z*- or *E*-alkenes, depending on the pH of the aqueous phase [21, 22].

The hydrogenation of diphenylacethylene, 1-phenyl-1-propyne and 1-phenyl-1-butyne were studied on immobilized $[RuCl_2(m\text{tppms})_2]_2$ catalysts placed into a CatCard cartridge using H-Cube reactor under mild conditions. The hydrogenation of diphenylacethylene in different toluene/ethanol solvent mixture showed that the conversion was independent in a wide range of the composition of the solvent phase, and thus additional experiments were performed in the 1:1 mixture of toluene/ethanol [21, 22].

The hydrogenation of diphenylacethylene on $[RuCl_2(m\text{tppms})_2]_2$ /DEAE-Molselect resulted *cis*-stilbene as a major product. The conversion was increased with increasing temperature, however, the selectivity dramatically dropped meanwhile (Fig. 9.5). At optimum temperature (323 K) *cis*-stilbene was obtained with 83% selectivity. Similar conversion and selectivity was found using different

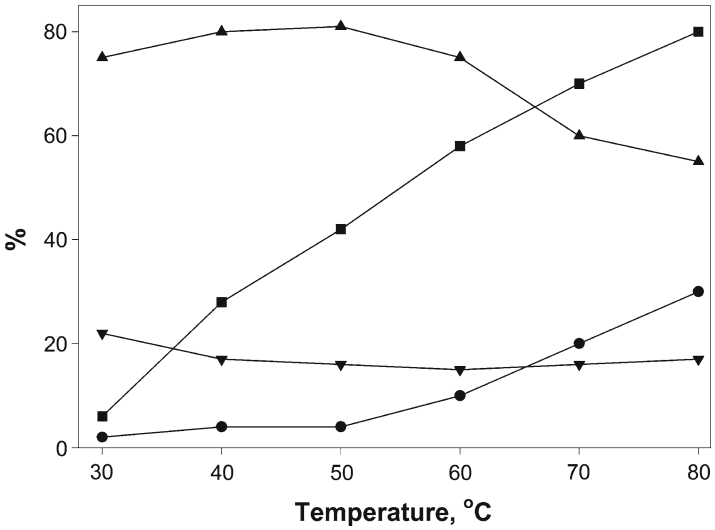

Fig. 9.5 The effect of temperature on the conversion in the hydrogenation of diphenylacethylene on anchored [$RuCl_2$(*m*tppms)$_2$] catalyst

supports, such as QAE-Shepadex or Lewatit Monoplus support. The effect of flow rate was also studied and it was found that the higher flow rate resulted to lower conversion. However, when the flow rate was small enough good conversion could be reached, meanwhile the selectivity was always very high (more than 80% of *cis*-stilbene), independently on the flow rate. The hydrogenation of 1-phenylprop-1-ene and 1-phenylbut-1-ene was also studied on DEAE-Molselect supported [$RuCl_2$(*m*tppms)$_2$]$_2$ catalyst and the result was similar to the results obtained for diphenylacethylene. In all cases the *cis*-alkenes were the major products with more than 75% selectivity. However, at higher temperature more *trans*-alkenes and alkanes were forming as well [21, 22].

The effect of hydrogen pressure on the hydrogenation of diphenylacethylene, 1-phenylprop-1-ene and 1-phenylbut-1-ene was also studied. It was found that the pressure of hydrogen had only little effect on the conversion, higher pressure led to higher conversion but meanwhile the selectivity was decreasing, because of the formation of alkanes. The immobilized catalyst was recycled in three subsequent runs and neither the yield, nor the products distribution were changed, which means that the immobilization on ion-exchange resin resulted in a recyclable catalyst [46, 47]. The immobilized [$RhCl_2$(mtppms)$_2$]$_2$ catalyst was found to be less selective than the Ru analogue, because the Wilkinson type of the complex was active for the saturation of C=C double bond, forming alkanes. As a conclusion, it was found that the immobilization on ion-exchange resin was fast and simple, resulting in a recyclable catalyst. However, the catalyst must be physically and chemically robust under the condition of the catalysis. Very fine powder or supports which may swell in organic solvent can damage the catalyst cartridge [21, 22].

Using the same catalytic system hydrogenation of α,β-unsaturated aldehydes was also studied. In their earlier work on the hydrogenation of α,β-unsaturated aldehydes [4, 5] the authors found that in water/chlorobenzene two-phases system depending on the pH of the water phase the reaction yielded either the saturated aldehyde or the unsaturated alcohol. In other words the selectivity was shifted from the selective C=C hydrogenation to the selective C=O hydrogenation by changing the pH. On the anchored $[RuCl_2(m\text{ttpms})_2]_2$ on Lewatit MonoPlus, the hydrogenation of *trans*-cinnamaldehyde resulted in a selective C=C hydrogenation at 333 K and 8 MPa hydrogen pressure. At the same time, using the same conditions, the $[RuCl(m\text{ttpms})_3]$ anchored on DEAE-Molselect was a good catalyst for the hydrogenation of acetophenone to phenylethanol. The isomerization of 1-octene-3-ol was also observed on the anchored $[RuCl_2(m\text{ttpms})_2]_2$ on Lewatit MonoPlus resulting octan-3-one with 78% selectivity. The reaction did not proceed without hydrogen, in addition of isomerisation, hydrogenation also took place.

These reactions demonstrate well that the heterogenized complexes can reveal similar activity and selectivity as the homogeneous counterparts and the carefully selected supports can be used in continuous flow systems, which is important from the industrial point of view.

9.2.3 Chemoselective Hydrogenation of Diketones

Large variety of organic substrates containing the CO group is very important in synthesis since they can be transformed into several valuable functionalities. Partial or total hydrogenation of carbonyl groups gives an important example of these reactions, getting the corresponding alcohols or alkanes. However preparative methods that may drive these reactions selectively have been seldom optimized in the past. The first time when partial hydrogenation was observed in the presence of conventional reducing agent such as $LiAlH_4$ or $NaBH_4$, followed by hydrogenolysis [23]. Ketols are important starting materials because they have two different functional groups in the same molecule. The hydrogenation of 1,3-diketones is a possibility for the preparation of ketols (Fig. 9.6).

Several attempts have been made to hydrogenate diketones over different metal complexes in organic solvents. However, significant formation of diols reduces the chemoselectivity towards the ketol formation. Therefore, it is still a challenge to develop highly chemoselective catalytic systems for the hydrogenation of diketones to ketols.

Noyori and coworkers developed homogeneous asymmetric transfer hydrogenation system employing complexes of the type $[RuCl_2(P\text{-}P)(1,2\text{-diamine})]$ where (P-P) is chiral biphosphine [24]. Currently Ru is the most widely used metal for this reaction [25] but similar reactivities have been observed using Ir [26] and Rh complexes [27].

A heterogenized ruthenium phenanthroline metal complex anchored in organo-functionalized MCM-41 [Ru(Phen)2Cl-NH-MCM-41] was used for the chemoselective

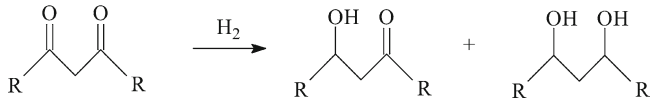

Fig. 9.6 Hydrogenation of 1,3-diketones

hydrogenation of 1,3-diketones to ketols using water as the reaction medium [28]. It was found in the hydrogenation of acetylacetone over neat and heterogenized [Ru(Phen)2Cl-NH-MCM-41] complexes at 120°C and 2.0 MPa H_2 pressure that the homogeneous [$Ru(Phen)_2Cl_2$] catalyst hydrogenated almost completely the starting material in 8 h, while the complete hydrogenation on the heterogenized catalyst took place only in 10 h. This is probably due to the restricted mass transfer and thereby slower interaction between the reactant molecules and the active metal atoms. At the same time the slightly higher chemoselectivity towards ketol formation in heterogeneous catalyst (99%) as compared to homogeneous catalyst (96%) was observed.

When $RuCl_3$ was used as a catalyst under homogeneous conditions quite low selectivity towards ketol formation (51%) was observed compared to $Ru(Phen)_2Cl_2$ complex (96%) indicating that steric hindrance around metal atoms plays an important role in obtaining a higher ketol selectivity.

To find out whether the reaction was truly heterogenized the reaction was carried out in aqueous layer obtained after hot filtration followed by by-product extraction in dichloromethane. No reaction was observed. However, when the reaction was carried out using the original liquor, obtained after hot filtration, as such without extraction very insignificant conversion (~3%) was obtained. Further, the filtered liquor was analyzed by AAS and the Ru content was found less than 0.9 wt% of the total Ru present in the solid catalyst. These results showed that reaction was truly heterogeneous.

The encapsulated catalyst can be effectively recovered by filtration and reused for the hydrogenation reaction. The catalyst showed slightly lower yield at the time of third recycle, which was due to the partial leaching of ruthenium from the complex as it was confirmed by chemical analysis of aqueous layer obtained after the work-up.

Different 1,3-diketones (e.g. 1-phenylpentan-1,3-dione) were also hydrogenated. All the substrates show high conversions and high ketol selectivities (98–99%). Data on the regioselectivity of hydrogenation of 1-phenylpentan-1,3-dione was not published [28] (Fig. 9.7).

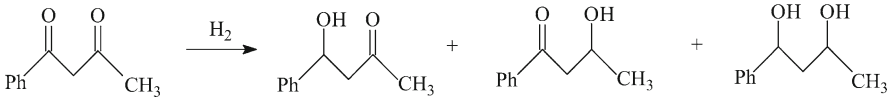

Fig. 9.7 The product distribution of the hydrogenation of 1-phenylpentan-1,3-dione

9.2.4 Selective Hydrogenation of Sorbic Acid

Sorbic acid can be hydrogenated to a number of products, but only two of them are useful as starting materials in fragrant compounds synthesis, namely the *cis*-hex-3-enoic acid and the *trans*-hex-2-enoic acid. *Cis*-hex-3-enoic acid is the starting material of the *cis*-hex-3-ene-1-ol, which is very intensively used in the fragrance industry [29] (Fig. 9.8).

Those catalysts which are chemoselective hydrogenates only one C=C bond, regioselectively producing hex-3-enoic acid isomers, and stereoselectively leading only to one diasteromer, to *cis*-hex-3-enoic acid. Few years ago the [Cp*Ru(sorbic acid)]CF_3SO_3 complex was discovered as an active and highly selective catalyst for the hydrogenation of sorbic acid to *cis*-hex-3-enoic acid [29]. This catalyst was able to hydrogenate the sorbic acid with very high selectivity (96%) under relatively mild conditions (1 MPa, 333 K). However, this catalyst was used only in homogeneous and two-phase hydrogenations. The two-phase hydrogenation may be considered as a type of immobilization but in this case the recycling of the catalyst was not possible. The catalyst provided only a few possibilities to be attached to a solid support. On the other hand the immobilization by means of the hydrogen bonds to silica via the triflate group was possible. This catalyst ([Cp*Ru(sorbic acid)]CF_3SO_3) was anchored to the silica surface by hydrogen bonds of the surface OH groups (Fig. 9.9) [30].

The [Cp*Ru(sorbic acid)]CF_3SO_3 complex was prepared by the method described in the literature [29]. The silica surface was pre-treated with water to reach the maximum amount of surface OH groups and the solution of the complex was filtered to the silica. This solution was stirred typically for 3 h and the solid was washed with ether several times to remove the weakly bonded complex. The immobilized catalyst was dried under vacuum for 12 h and stored under Ar. The theoretical loadings of Ru complex was 2 wt% of the obtained catalyst.

The prepared catalyst was characterized by FT-IR spectroscopy and a significant increase was observed in the -OH vibration at 1,200 cm^{-1}, which could prove the immobilization of the complex by hydrogen bonds. A strong C-F vibration was also observed, which showed the attachment of the triflate groups on the surface. The hydrogenation

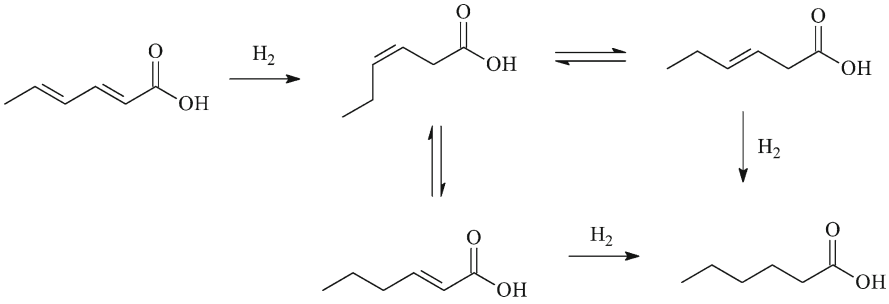

Fig. 9.8 The product distribution in the hydrogenation of sorbic acid

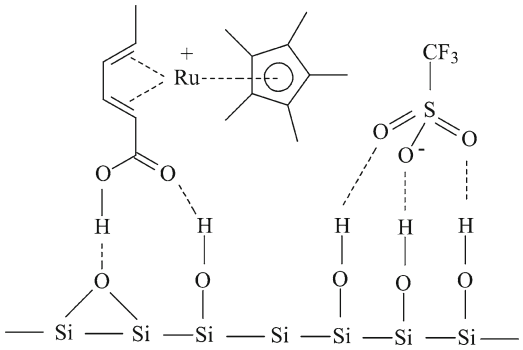

Fig. 9.9 The immobilization of [Cp*Ru(sorbic acid)]CF_3SO_3 via hydrogen bonds

Table 9.6 Comparison of catalyst activity and selectivity in the hydrogenation of sorbic acid to *cis*-hex-3-enoic acid

System	TOF (h^{-1})	Selectivity (%)
Homogeneous	21	98
Two phase	16	94
Heterogeneous	13	96

Reaction conditions: 2 MPa H_2 pressure, 323 K, solvent MTBE

of sorbic acid to *cis*-hex-2-enoic acid was carried out in the range of 0.35–5 MPa and between 323 and 358 K. It was found that neither the pressure nor the temperature change had any effect on the selectivity and the activity of the catalyst [30]. The solvent effect was also studied and the methyl *tert*-butyl ether was found to be the best tested solvent. The leaching of the catalyst was typically 0.5% except the drastic conditions (5 MPa, 358 K) when it was about 6%. Comparison of the catalyst activity and selectivity in homogenous and two phase reactions can be seen in Table 9.6.

The homogenous reaction revealed the highest activity as expected, but the selectivity was about the same in all three cases. The recycling of the catalyst was not successful but the immobilized catalyst was much easily handled than the homogenous ones [30].

9.2.5 Selective Hydrogenation of Imines

Although there are many excellent examples of highly active and selective catalyst for hydrogenation of olefins or ketones, however, the hydrogenation of imines is still a challenge in terms of the turnover frequency (reaction rate) and the lifetime of the catalysts. This is due to the fact that the CN bonds have certain

properties, such as their preferred mode of bindings and the strong donor character of the nitrogen, which makes the homogenous reaction unfavorable. One of the best transition metal complexes for ketone hydrogenation is the Ru(II)-diphosphine/1,2-diamine complex, developed by Noyori [12]. This system was found to be active in the chemoselective hydrogenation of C=O bond over C=C bond and the reduction of imines.

Compared with organic polymers as supports for immobilization of metal complexes inorganic materials have several advantages such as their rigid structure, and superior thermal and mechanical stability under the catalytic conditions. The pure silica, e.g. SBA15, is a good candidate to be a support because of its long range order, large monodispersed mesoporous particles (up to 50 nm), and thicker walls, which all makes it thermally and hydrothermally more stable than the classical MCM type of materials.

A novel heterogeneous catalyst was prepared by direct grafting a chiral 1,2-diamino-cyclohexane based Ru triphenylphosphine complex onto the surface of mesoporous silica SBA-15 [31]. The prepared catalyst [RuCl2(dach)(PPh3)2-SBA15] was applied in the chemoselective hydrogenation of ketones over the olefin functional groups and the hydrogenation of imines.

The surface functionalization of SBA-15 was carried out by a post synthesis method. The SBA-15 was first treated with chlorotriethoxypropylsilane, then with (*S,S*)-diaminocyclohexane in the presence of triethylamine in dichloromethane solution under argon [31]. The support was treated with the solution of $RuCl_2(PPh_3)$ complex in dichloromethane at room temperature for 12 h in Ar. The prepared catalyst was characterized by spectroscopic methods: XRD, FT-IR, NMR and elemental analysis. The XRD patterns were the same which was reported for SBA-15 material and they did not change with the complex immobilization. The FT-IR spectra of the anchored and not anchored complex were compared and found to be very similar which proved its successful heterogenisation. ^{1}H-^{31}P coupled NMR spectra of the anchored complex $[RuCl_2(dach)(PPh_3)_2$-SBA15] revealed a slight shift comparing with the spectra of the neat complex. The SEM image of the anchored complex showed well distributed hexagonal particles organized in a rope-like structure. This means that the mesoporous material retained the morphological characteristic after the functionalization with organic molecules, however, some agglomeration occurred.

The prepared catalyst was applied in the asymmetric hydrogenation of ketones and the result can be seen in Table 9.7. 2-Methylnaphtyl ketone was successfully hydrogenated [31] at 343 K and 2.7 MPa of hydrogen pressure. The main product was 1-(2-naphtyl)ethanol obtained with 90% yield and with ee of 76% in 20 h. Some other ketones were hydrogenated successfully using the same reaction conditions with high activity in terms of TOF and very good selectivity. Similar conditions were applied in the hydrogenation of α,β-unsaturated ketones and imines and the results can be seen in Table 9.8. The chemoselective hydrogenation of (E)-1,3-diphenyl-2-en-1-one to the corresponding allyl alcohol occurred with high activity (TOF 2519) and excellent selectivity >99%. In the case of cyclohex-2-en-1-one the major product was cyclohexanone and the selectivity of the corresponding allyl alcohol was only 10%.

Table 9.7 Chemoselective hydrogenation of the C=O bond in α,β-unsaturated ketones on [Ru(dach)$(PPh_3)_2(Cl_2)$]-SBA15 catalyst

Substrate	Time (h)	Conversion (%)	Selectivity (%)	TOF
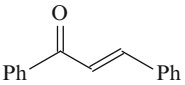	14	98	99	1,800
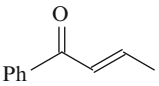	10	95	99	2,400
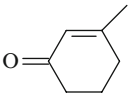	20	70	90	900
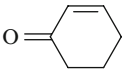	22	100	10	1,150

Reaction conditions: 348 K and 2.7 MPa H_2, 10 mmol substrate. Substrate/catalyst/base: 256440/1/20 in 40 ml propan-2-ol

Table 9.8 Hydrogenation of imines to secondary amines on [Ru(dach)$(PPh_3)_2(Cl_2)$]-SBA15 catalyst

Substrate	Time (h)	Conversion (%)	TOF
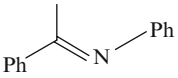	18	98	350
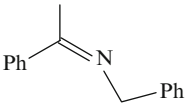	20	97	300
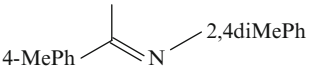	24	60	150
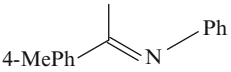	20	90	300

Reaction conditions: 348 K and 2.7 MPa H_2, 2.5 mmol substrate. Substrate/catalyst/base: 6410/1/30 in 20 ml propan-2-ol.

However, when a methyl group is present in the third position the major product is the corresponding allyl alcohol.

As seen in Table 9.8 the catalyst was active in the hydrogenation of imines to secondary amines. In this case no enantioselectivity was observed as when using the homogeneous analogues. When the hydrogenation was completed the catalyst was filter off from the reaction mixture, washed with propan-2-ol and dried in vacuum. After this treatment it was ready to reuse and after three subsequent runs

the activity did not decrease significantly/conversions 90%, 89% and 74% were observed. The Ru amine complex immobilized on SBA-15 was found to be very active for the hydrogenation of ketones and chemoselective hydrogenation of α,β-unsaturated ketones. It revealed a good activity in the hydrogenation of imines as well and its activity was comparable to the activity of the homogeneous analogues. At the same time the anchored catalyst could be filtered out from the reaction mixture easily and recycle several times [31].

9.3 Enantioselective Hydrogenations on Immobilized Complexes

9.3.1 Asymmetric Catalysis

Some 150 years ago Louis Pasteur (1822–1895) concluded that certain organic molecules can exist in one of two forms, called optical isomers – that is, having the same structure, and differing only in being mirror images of each other. In his days these structures were referred to as "left-handed" and "right-handed" forms of the same molecule [32]. The molecular chirality often occurs in organic chemistry – any molecule which has a carbon atom bonded to four different atoms or groups of atoms exists in a pair of chiral forms – enantiomers. Pairs of enantiomers reveal identical chemical properties, and their physical properties such as melting temperature, boiling temperature, and solubility in different solvents are also the same. They do differ, however, in their effect on polarized light. When polarized light is shone through a solution, one enantiomer will rotate the plane of polarization clockwise and the other will rotate it through the same angle anticlockwise. It is well known that living systems, having a high degree of chemical specificity, can discriminate between the two forms, metabolizing one and leaving the other untouched and free to rotate light. Pairs of enantiomers often reveal very different biochemical effects [33–35] (Fig. 9.10).

For example, the smell of lemons is caused by a compound called *S*-limonene, which is chiral. Its non-identical mirror image, called *R*-limonene, smells of oranges. The common painkiller ibuprofen exists as a pair of enantiomers – one is the active ingredient and the other form has no medicinal effect at all. The drug we buy is actually a mixture of the two as the method of manufacture makes both forms (Fig. 9.11). They are difficult to separate and the non-active isomer represents no harm. Another common example is the artificial sweetener aspartame (Nutrasweet™) – its mirror image tastes bitter, or the very tragic case with administration of a racemic mixture of thalidomide (Contergan™) to pregnant women in 60s in the last century. The *R* isomer was an effective sedative, the *S* isomer revealed teratogenic effects. [35–38].

Synthesis of fine chemicals with chiral centres requires involvement of stereoselective reactions from the beginning. Due to identical physical properties standard separation methods usually fail. The synthesis may either start with an optical pure

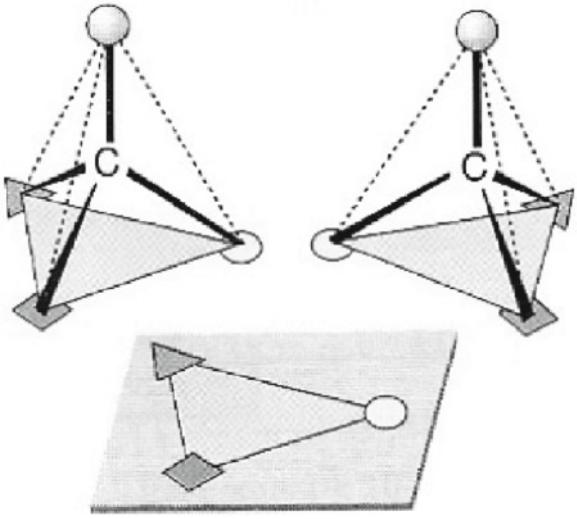

Fig. 9.10 Stereoselectivity in occupying a biological receptor site – only one of the enantiomers reveals the pertinent complementarities

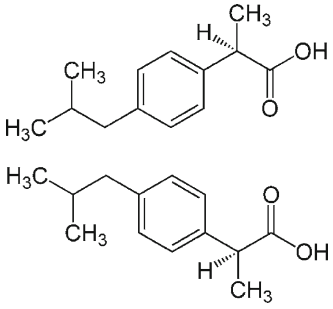

Fig. 9.11 Two optical isomers of ibuprofen

compound or with a racemic mixture which is then transformed to the optical pure product. Asymmetric catalysis represents a very valuable tool for the research and industry of optically pure fine chemicals. The major advantage comprises a multiple enantioresolution on a single chiral active centre, when a number of individual enantiomers are formed with help of only a small amount of a chiral catalyst [39–41].

Enantioselective catalysis, using homogeneous chiral metallic organocomplexes is a dynamic field of physical and organic chemistry, even granted with the Nobel Prize in 2001 for invention of active chiral complexes for stereoselective hydrogenations (Ryoji Noyori, William S. Knowles) [42–44]. There is only one major drawback of the active homogeneous complexes regarding their practical utilisation – the absence or complications with their separation and repeated use. No doubts asymmetric catalysis is a multidimensional task. The solely stereochemical point of view is not certainly enough complete and the high effectiveness (enantioresolution) could be

only achieved by combination of the three dimensional molecular structures of the catalyst and the reactant with optimised kinetics. For maximum multiplication of chirality a specific system capable to discriminate between enantiomers, functional groups or geometry of achiral molecules is needed [45].

In catalysis several approaches might be chosen either using principles of homogeneous and heterogeneous catalysis or their combinations. There have been quite a few heterogeneous catalysts described in the past for asymmetric hydrogenations, e.g. those based on supported nickel catalyst modified with chiral tartrates or on supported platinum with cinchona type of optically active alkaloids (Fig. 9.12). Neither of these systems could have been considered as competing with the chiral homogeneous organometals. Achieved enantioselectivities were incomparable lower and the undesired and tedious separation procedures could not be avoided anyway e.g. [46–56].

On the other hand it is quite common that the attained optical resolution (enantioselectivity) with a chiral organometallic complex is reported on a similar level as the optical purity of the catalyst. Some effort has been spent in the recent years to immobilise effectively the homogeneous catalysts while keeping their activity, enantioselectivity and stability on the original level and providing their simple separation and possibility of the repeated use as "extra values" [57–60].

In the next paragraphs we shall report on heterogenisation of chiral homogeneous complexes and their use in asymmetric reactions. Special attention will be paid to the group of techniques using heteropolyacid of the Keggin's type as a linker between the complex and the support – inorganic oxide. In the next section an attractive alternative comprising utilisation of ionic liquids for selective accommodation of the chiral catalytic complex is profoundly discussed. This pseudo-immobilisation approach has a potential to reach comparable kinetic characteristics as the standard homogeneous experiment, and providing most of advantages of the heterogenized catalysts. Both strategies (immobilization on solids and confinement in ionic liquids) will be carefully discussed with help of case studies offering enough illustrative experimental examples. For the sake of simplicity most of these examples will involve diphosphine chiral ligand (2,2′-bis(diphenylphosphino)-1,1′-binaphtyl)

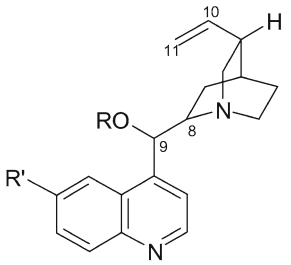

R = H, R'=H (8*S*, 9*R*) cinchonidin
R = H, R'=H (8*R*, 9*S*) cinchonin
R = H, R'=OMe (8*R*, 9*S*) chinidin
R = H, R'=OMe (8*S*, 9*R*) chinin

Fig. 9.12 The family of optically active cinchona alkaloids

known as BINAP used in asymmetric hydrogenation of β-ketoesters. In parallel historical development of the field of asymmetric hydrogenations with chiral organometallic complexes is followed with special attention to the keystones of these two immobilization techniques.

9.3.2 Catalytic Organometallic Complexes

Organometallic compounds of transition metals represent multitask and multipurpose tools of organic synthesis and catalysis applied in fine chemistry. Their structure is often complicated either with multiple central atoms, bonds involving more electrons or with ion-dipole interactions. Structure related properties such as electron deficient behaviour, Lewis acidity of metal centres, nucleophilic character or basicity of substituents may further influence their practical utilisation [e.g. 61–73].

Complexity of these structures and the involved interactions are the reasons of their unique reactivity. Central atoms typical reveal two to six coordination sites. Some of the non-reactive sites are occupied with neutral or negatively charged additional ligands. Electron character and geometry of these ligands may further modify the original properties. Obviously proper selection of the chiral ligands represents a key point in the definition of the suitable catalytic system. The most common organometals, especially those used in asymmetric catalysis are shown in Fig. 9.6 together with their generally used abbreviated names [74–78].

Despite hydrogenation, which is the dominating field, such complexes have been reported for epoxidations, isomerisations, hydroboration, oxidations, hydroformylations, carbomethylation and many other reactions with formation of the C–C bond (cycloadition, aldol condensation, Diels-Alder reaction, cross-coupling, etc.). Design of the chiral ligands capable of coordination with transition metals, mostly with Rh or Ru, has developed to an independent and self-confident segment of organometallic chemistry during the recent years. It exploits all the current knowledge on behaviour of hundreds of chiral ligands mostly based on diphosphine, diamine, aminoalcohols or non-symmetric *P,N* ligands and their combinations. In spite of an enormous number of such possible ligand combinations the BINAP ligand (2,2′-bis(diphenylphosphino)-1,1′-binaphtyl) might be referred to as the most universal and in the effectiveness usually surpassing its cognates. For many specific cases also other ligands must not be omitted. The most frequent are: DIOP, DiPAMP, DuPHOS, BOX, TADDOL SALEN, XYLIPHOS, PHANEPHOS, BIPHEP, BIPNOR, BIPHEMP, SKEWPHOS, CHIRAPHOS, JOSIPHOS and others (Fig. 9.13). References are advised to be checked for their particular applications) [74–78]

9.3.2.1 Ru-BINAP

As early as 1974 Ryoji Noyori designed and synthesized the chiral BINAP ligand (2,2′-bis(diphenylphosphino)-1,1′-binaphtyl) (also see Fig. 9.13). Its successful

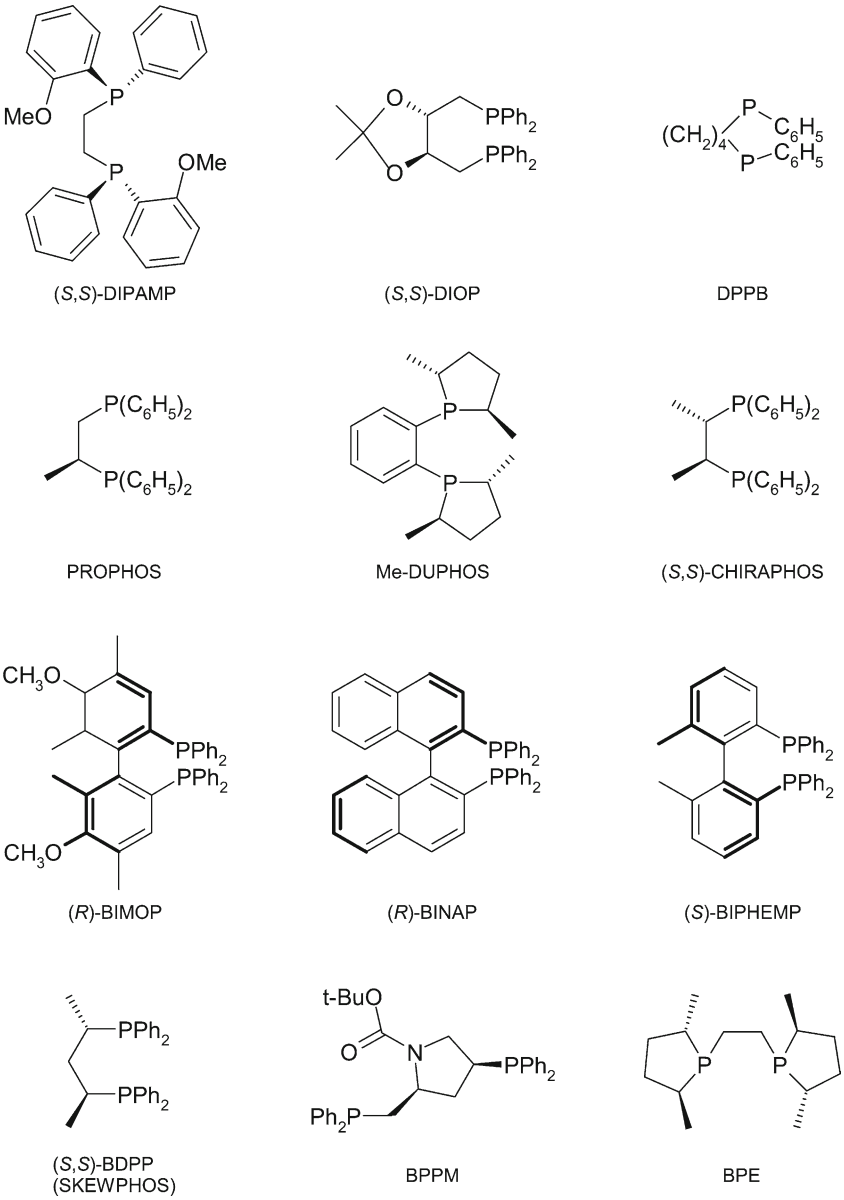

Fig. 9.13 The most common ligands used in the field of asymmetric catalysis

incorporation to the complexes of rhodium and ruthenium marked the revolution in the field of asymmetric catalysis [79–82].

The initial synthesis of the chiral BINAP ligand was not as simple as expected and it held back its first successful application. It came finally 16 years later in 1980 when the chiral Rh-BINAP complex was used in the stereoselective synthesis of optically pure menthol from myrcene [83–89]. The next decade had witnessed a

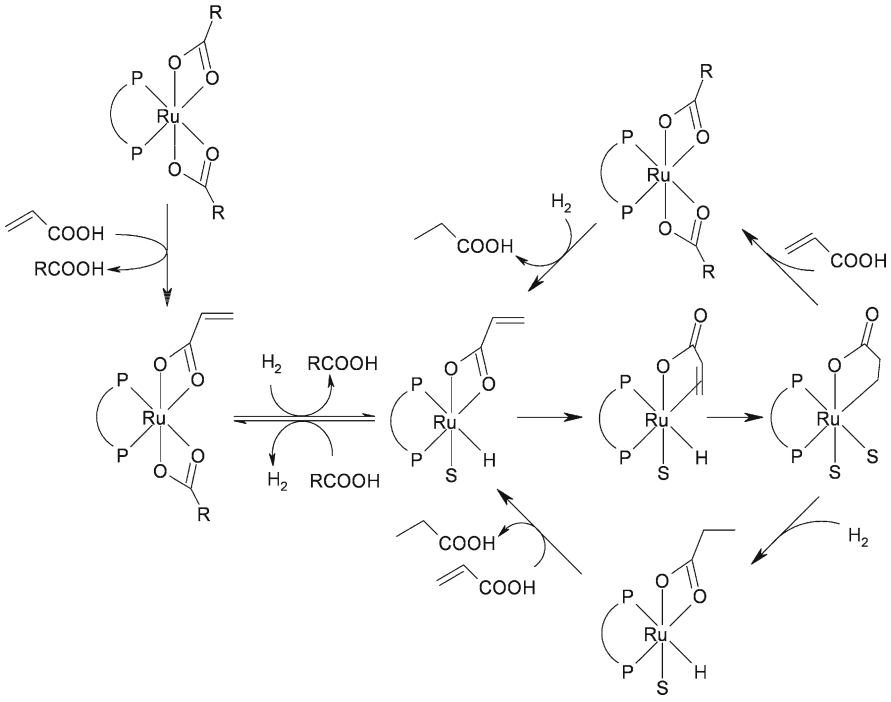

Fig. 9.14 Catalytic cycle of Ru(II) dicarboxylate of BINAP in hydrogenation of α-unsaturated carboxylic acids

steep growth of interest in this complex, but for many new applications rhodium was replaced with ruthenium. Ru(II) complexes of the BINAP dicarboxylate were identified as eminent homogeneous catalysts for hydrogenation of functionalised alkenes and for α,β-unsaturated carboxylic acids (Fig. 9.14) [90–96].

The keystone and the key achievement which cannot be omitted was the hydrogenation step in the synthesis of antiphlogistic Naproxene™ performed with 100% yield and enantioselectivity (*ee*) 97%. Stereoselective hydrogenation step was also involved in the synthesis of isoquinoline alkaloids (synthetic or synthetically modified opioids), unsaturated alcohol citronellol from nerol and geraniol (perfume industry), α-tocoferol, and intermediates of carbapene antibiotics or building blocks of prostaglandins [97].

Already 6 years before Noyori, in 1968, William S. Knowles, working for Monsanto, collected enough experimental proofs that chiral complexes of transition metals were capable to introduce their chirality to optically non-active molecules. Knowles was not an academic person and his goal was to find a practical synthetic route to aminoacid L-DOPA [(S)-3-(3,4-dihydroxy-phenyl)alanine)], already known as an effective drug for suppression symptoms of the Parkinson disease. For this purpose cationic rhodium complex with the chiral DiPAMP ligand was designed (Fig. 9.15) and prepared. The Monsanto technology leading to L-DOPA was historically the first large industrial exploitation of the available knowledge on the chiral homogeneous complexes [83, 90].

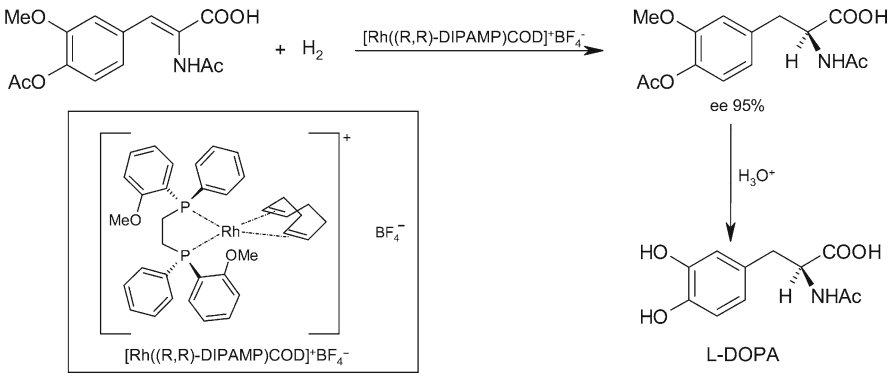

Fig. 9.15 Synthesis of L-DOPA with the asymmetric hydrogenation step

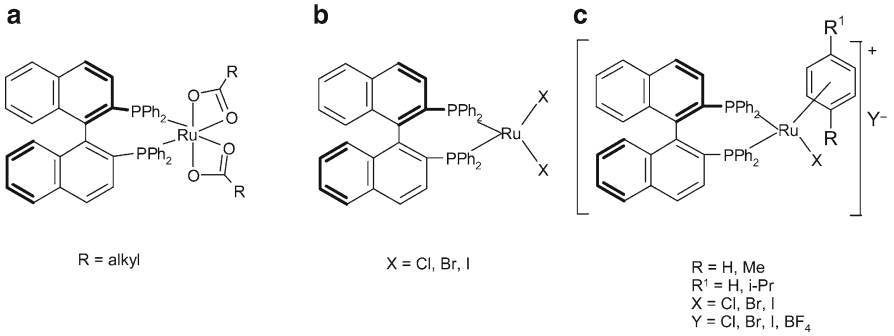

Fig. 9.16 Forms of chiral Ru-BINAP complexes for hydrogenation of: I. functionalised alkenes (**a**) [Ru(OCOR)$_2$(binap)]; II. Carbonyl compounds (**b**) [RuX$_2$(binap)], (**c**) [RuX(arene)(binap)]Y

Let's return back to Ru-BINAP, originally designed by Noyori, and its structurally affinitive complexes [42–44]. Carboxylate ligands of the ruthenium complex might be simply exchanged in the environment of strong acid for other anions. The most common are complexes with halogen of an empirical formula [RuX$_2$(binap)] (X = Cl, Br, I) [98, 99].

From commercially simply available precursors [RuCl$_2$(benzene)]$_2$ or [RuCl$_2$(*p*-cymene)]$_2$ and the BINAP ligand a cationic complex with a structure [RuX(arene)(binap)]Y (X = halogen, Y = halogen or BF$_4$) could be obtained. Both types of complexes with halogenides have been repeatedly shown as excellent catalysts for hydrogenation of substances with a carbonyl function (Fig. 9.16) [98, 99].

For the sake of completeness it cannot be forgotten that also complexes [RuCl$_2$(nitril){(R)-binap}], [Ru$_2$Cl$_4${(R)-binap}$_2$NEt$_3$], [RuCl$_2$(PhCN){(R)-binap}], [RuCl$_2$(FurCN){(R)-binap}] and [RuCl$_2$(C$_6$F$_5$CN){(R)-binap}] were produced and

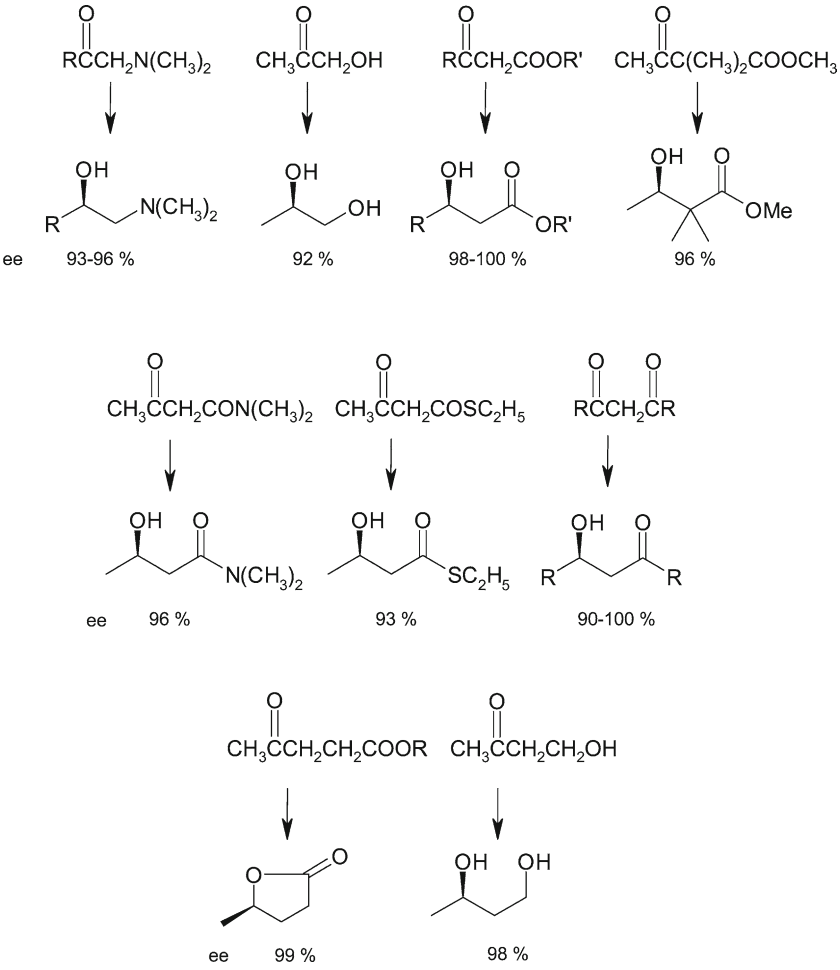

Fig. 9.17 Examples of substances with carbonyls in β or γ positions suitable for hydrogenation with chiral Ru-BINAP

successfully tested [74, 75, 98–104]. In the context of this communication it should be emphasized that Ru-BINAP complexes with halogenides are notably active for hydrogenations of molecules with a keto group in β- or γ-positions in respect to the carboxyl function or its derivatives (Fig. 9.17)

Probably the most frequently reported molecule being hydrogenated with help of chiral Ru-BINAP has been methyl acetoacetate, a typical representative of β-ketoesters. The reaction yields optical isomers of methyl-3-hydroxybutanoate (MHB) (Fig. 9.18). This reaction is anticipated, especially later in this text, as a model transformation to discuss the effects of various types of surface immobilisation of the chiral ruthenium BINAP complex [105–109].

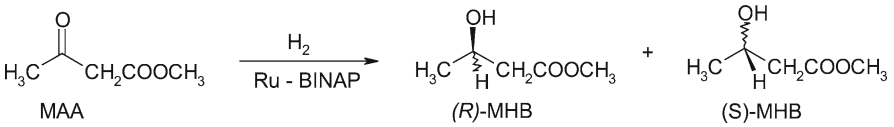

Fig. 9.18 A simplified reaction scheme of hydrogenation of MAA

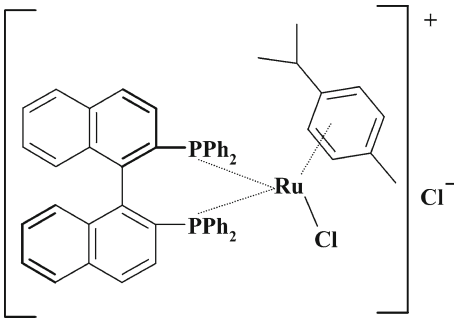

Fig. 9.19 [RuCl((*R*)-BINAP)(p-cymene)]Cl catalytic complex

9.3.3 Immobilisation of Ru-BINAP

Extraordinary catalytic properties of Ru-BINAP (Fig. 9.19) have speeded up an endeavour to immobilise it for its better recollection after the reaction and for the possibility of its repeated use. This generally not difficult task is complicated, because the essential parameter of enantioselectivity is critically sensitive to even minor variations of the complex structure [110–126].

9.3.3.1 Immobilisation in Polymers

In the middle of 90s one of the "pathfinders" Pierre A. Jacobs anchored [RuCl((R)-binap)(p-cymene)]Cl inside of the elastomer of the poly(dimethylsiloxane) type (PDMS) [125]. The initially accomplished data were not "breathtaking". The parameter of enantioselectivity did not pass over the level of 70% in the MAA hydrogenation (in comparison with 98% in the homogeneous set-up). Better results were then achieved (ee 92%) when 4-methylbenzensulfonic acid was added to the PDMS membrane as a source of Brønsted acid sites. Few years later (in 1998) the BINAP ligand was covalently bound to the functionalized polystyrene [126]. The ee achieved was not very high again (70–80%), but it was important that it remained constant for several repeated catalytic cycles and with 100% conversion. In the beginning of new millennium the Ru-BINAP inventor Ryoji Noyori minimized

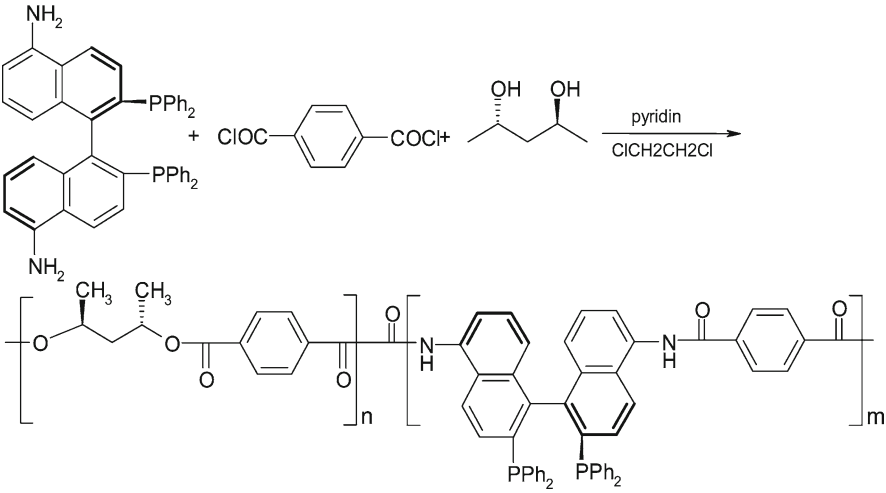

Fig. 9.20 The BINAP ligand built in the polyester chain

[127] the effect of mass transport resistance inside of the swelled polymer matrix by using a combination of two transport solvents propan-2-ol and dimethylformamide. This relatively insignificant modification brought an increase of ee to 97% in hydrogenation of 1-acetylnaphtalene. Roughly in the same period (2 years earlier, in 1999) a new strategy for incorporation the BINAP ligand to the polymer matrix (polyester) was published by making [128] use of copolymeration of 5,5′-diamino-(R)-binap, (S,S)-pentan-2,4-diol and chloride of terephtalic acid (Fig. 9.20). Finally the polymer complexated with ruthenium precursor. The catalyst was utilised in the popular hydrogenation step of the NaproxeneTM synthesis (ee 90% at 95% conversion).

Similarly, starting with the same ligand, (5,5′-diamino-(*R*)-binap), well soluble BINAP-containing dendrimer was prepared. After complexing with Ru it revealed the *ee* nearly 93% in the hydrogenation step of the synthesis of ibuprofen. Due to the presence of water soluble dendrimer the catalyst was simply precipitated from the reaction mixture and repeatedly used with comparable kinetic scores (Fig. 9.21). Poly(BINAP)/DPEN/Ru for hydrogenations of aryl(methyl)ketons (*ee* 84%) and BINOL-BINAP (BINOL = 1,1′-binaphtyl-2,2′-diol) for acetophenone hydrogenation (*ee* 84%) should be also mentioned as important keystones [129–132].

Another remarkable catalyst was reported by Lemaire [133, 134] who immobilised the 6,6′-bis(aminomethyl)-binap ligand in the reaction with diisocyanates under the formation of polyuretane chains. The best results were achieved with the poly-NAP-Ru complex produced in copolymeration with toluene-2,6-diisocyanate (Fig. 9.22). The remarkable ee of 99% in hydrogenation of MAA was reported in four consecutive hydrogenation cycles.

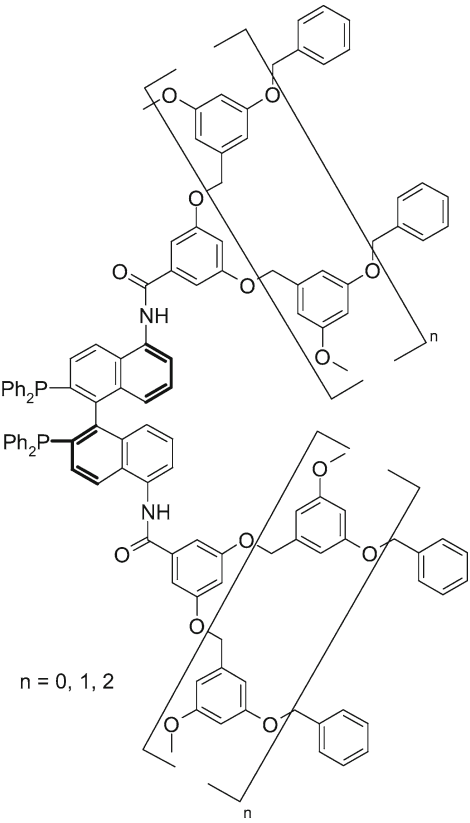

Fig. 9.21 The BINAP containing dendrimer

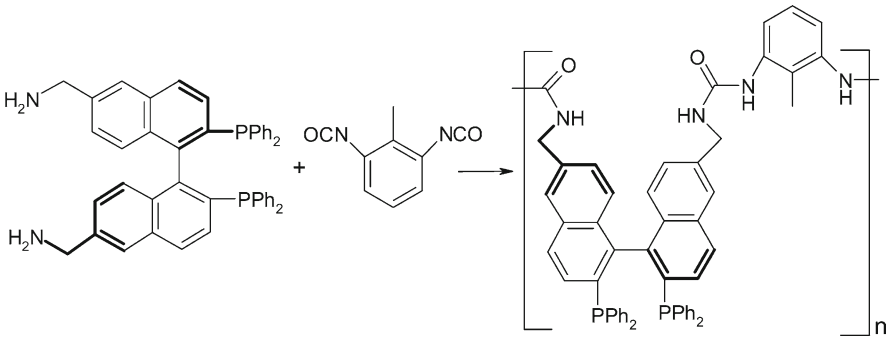

Fig. 9.22 6,6′-Bis(aminomethyl)binap incorporated in the polyuretane chain

9.3.3.2 Inorganic Supports

Inorganic supports had been seen initially as more elementary and simply feasible (accessible) matrixes for immobilisation of Ru-BINAP in comparison with polymers. Despite many attempts and extended optimisation studies have been performed, likely

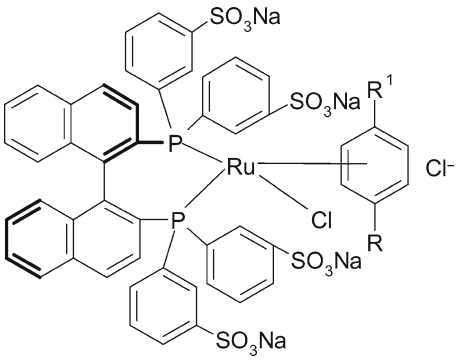

Fig. 9.23 Water soluble complex [RuCl(arene)(binap($SO_3Na)_4$)]Cl, (R, R_1 = H, alkyl)

due to a number of interfering effects, satisfactory and comparable kinetic characteristics as in the homogeneous arrangement have never been achieved. Despite this reality some of the anchoring strategies deserve attention and will be treated in details.

One of the first successful attempts (1995) [135] comprised entrapping of water soluble [RuCl(binap($SO_3Na)_4$)(C_6H_6)]Cl (Fig. 9.23) in the form of a thin film deposited over porous hydrophilic glass spheres. The catalyst was applied in the "popular" hydrogenation step of the NaproxeneTM production in the two phase reaction environment water/ethylacetate, but only with 70% enantioselectivity. This approach was later modified with using ethyleneglycol film with the same complex and the ee increased up to 96%.

It must be emphasized that with the complexes supported on inorganic solids it is always essential to test carefully the heterogenized catalyst on the possible leaching. Ru-BINAP is highly active even at very low concentrations and it must be avoided that "homogeneous data" are reported instead.

It is not surprising that various zeolites were also considered as primary candidates for anchoring the complex. The "pioneer" of the polymer – BINAP immobilisation Pierre Jacobs also followed this direction. In 1997 he put to use electrostatic interactions of acid β-zeolite with the [RuCl((*R*)-binap)(*p*-cymene)]Cl complex. Such a physically bound catalytic system provided 95% enantioselectivity in the hydrogenation of MAA. Also Jacobs used layered hydroxides and sulphonated Ru-BINAP for successful hydrogenation of geraniol to citronellol [136, 137].

9.3.3.3 Immobilisations with Heteropolyacid Spacers

It must be emphasized that the most prominent immobilisation technique regarding inorganic solids as supports and the organic complex ligands have been based on utilisation of heteropolyacid spacers (Fig. 9.24).

The "father-founder" of this method Robert Augustine [138] attempted (1998) to anchor a series of Ru and Rh complexes, namely DIPAMP, BPPM, DPPB, PROPHOS, Me-DUPHOS and BINAP on various inorganic supports, namely montmorillonite, active charcoal, alumina or lanthanum(IV) oxide. The spacers acting there as a tethering agent were acids of the Keggin's type such as

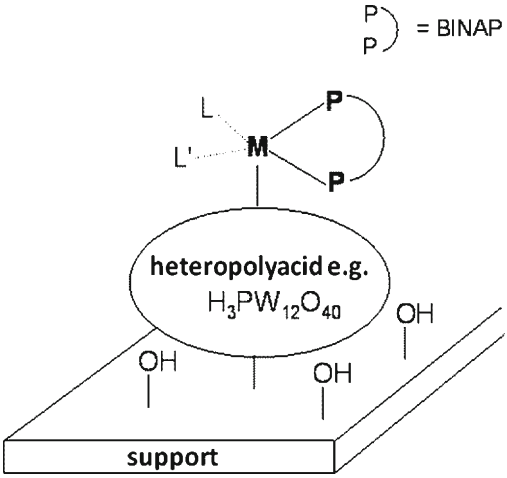

Fig. 9.24 Schematically shown the anchorage of the Ru-BINAP complex over a solid support by means of a spacer

$H_3PW_{12}O_{40}{\cdot}nH_2O$, and other polyoxometalates on the basis of P/Mo, Si/W and Si/Mo. The nature of involved interactions has not been fully understood yet. Van der Waals forces, electron interactions or even covalent or ionic bonds between the spacer and the transition metal in the complex were suggested [138–140].

Aside from the mechanism some of the reported practical systems revealed high conversions and satisfactory enantioselectivities. If leaching is rigorously excluded then this approach represents a simple and cheap alternative. More attention will be paid to this issue in the next chapters devoted to the case study on the effectiveness of various modifications of this immobilization technique.

9.3.4 Case Study of the Immobilisation of Ru-BINAP on Inorganic Supports

In this chapter special attention will paid to the discussion of experimental data from asymmetric hydrogenation of MAA over (*R*)-Ru-BINAP immobilised on various inorganic supports. Before proceeding to this particular topic, notes on preparation of Ru-BINAP, its catalytic cycle with MAA, and other specifics of this asymmetric hydrogenation are briefly introduced.

9.3.4.1 Preparation or Other Sources of Ru-BINAP

The most commonly used method for preparation of chiral Ru-BINAP is that introduce by Kazushi Mashima already in 1994 [106]. The synthesis starts with optically pure BINAP ligand [(*R*)-2,2′- bis(diphenylphosphino)-1,1′-(binaphtyl)] and a dimeric complex $[RuCl_2(p\text{-cymene}]_2$ (Fig. 9.25).

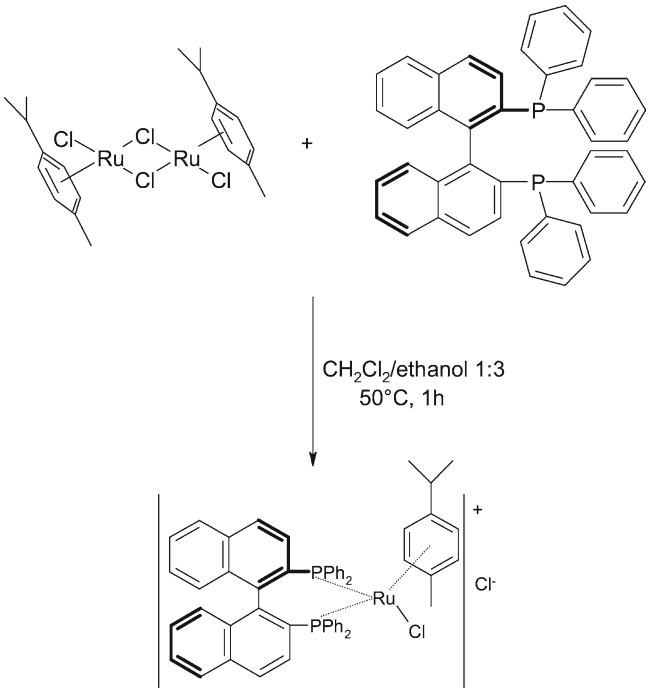

Fig. 9.25 Synthesis of [RuCl((*R*)-binap)(*p*-cymene)]Cl

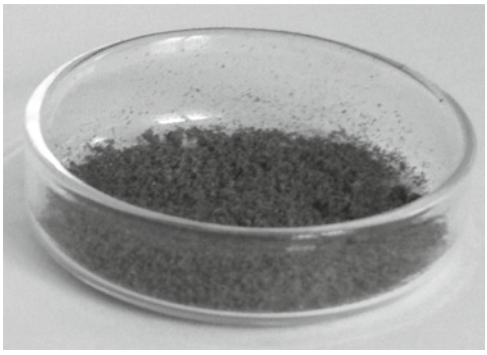

Fig. 9.26 Crystals (ochre colour) of freshly prepared Ru-BINAP

Both precursors are simply available commercially [106]. The complexation must be carried out isolated from the laboratory environment in the Schlenk apparatus under argon. The synthesis usually proceeds with high yields of about 98% and the general appearance of the product is crystallic with ochre colour (Fig. 9.26). If stored the complex must be strictly kept under inert atmosphere to minimise its contact with air and air moisture.

Nowadays the chiral complex is also simply available commercially from several suppliers. It is, however, advised, one to be careful because quality may differ significantly. Quality variations in time (of the supply) had been experienced

repeatedly even from one supplier. Currently it is possible to purchase the complex of the quality specified as the "Noyory (*R*) type" (Aldrich), for which constant properties might be expected. Nevertheless, everyone who wishes to take the research with Ru-BINAP in asymmetric reactions seriously should consider "in house" production of the complex time to time, analyse it properly and use it as a reference when data with the commercial sample deviate too much from expectations or previous experiments. This approach has been repeatedly proved as efficient, and finally very much time saving, indeed [109, 141–143].

9.3.4.2 The Ru-BINAP/MAA Catalytic Cycle

The catalytic action (role) of the [RuCl((*R*)-binap)(*p*-cymene)]Cl complex in the asymmetric hydrogenation of MAA (methyl-3-oxobutanoate, methylace-

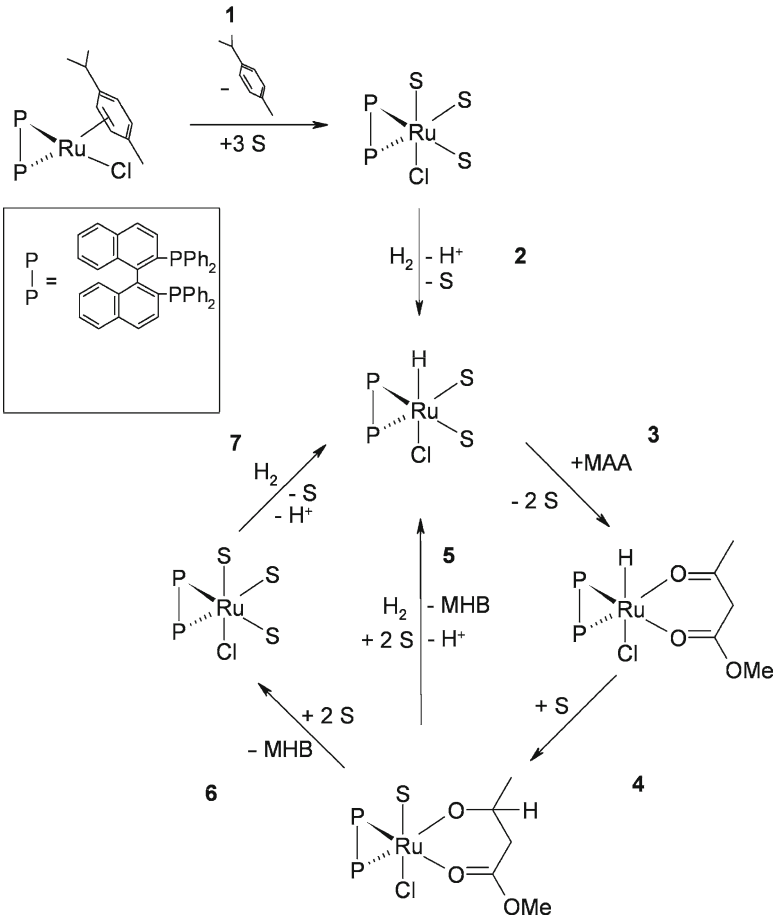

Fig. 9.27 The catalytic cycle of enantioselective hydrogenation of MAA with Ru-BINAP

toacetate) to the isomers (*R*)-(−) or (*S*)-(+)-methyl-3-hydroxybutanoates (MHB) was first introduced by Ivo Vankelecom, Ari Wolfson and Pierre Jacobs in 2003. Their interpretation was more or less generally accepted, since that time it has been widely used and it might be extended to any β-ketoesters (Fig. 9.27) [105].

The essential role of the used solvent (S) is clearly evident from the scheme of the reaction cycle. The first inevitable step comprises retraction of the *p*-cymene ligand which leads to the appearance of three available coordination sites for the solvent (step 1). Next heterolytic dissociation of gaseous hydrogen takes place yielding a hydride form of the complex (step 2). To this structure, through the two carbonyl groups, β-ketoester is coordinated (step 3). It is essential that this coordination is strictly "superintended" by the configuration of the chiral BINAP ligand. Obviously, this step is that one determining the resulting enantioresolution (step 4). In the next step (5) one hydrogen atom is transferred from the solvent molecule and the half-hydrogenated state is being constituted. Direct hydrogenation (or alternatively proton transfer from the protic solvent) participates on the transformation of the half-hydrogenated state (step 6). Finally the catalytic cycle terminates with disengaging the product and restoration of the active hydride form of the complex (step 7) [105]. Hydrogenation of MAA may proceed in a range of solvents differing in their polarity and solvent powers toward individual components of the reaction mixture.

Solvents of the first choice are alcohols. They, however, complicate the reaction course with temporary appearance of acetals (Fig. 9.28) [109, 141, 142].

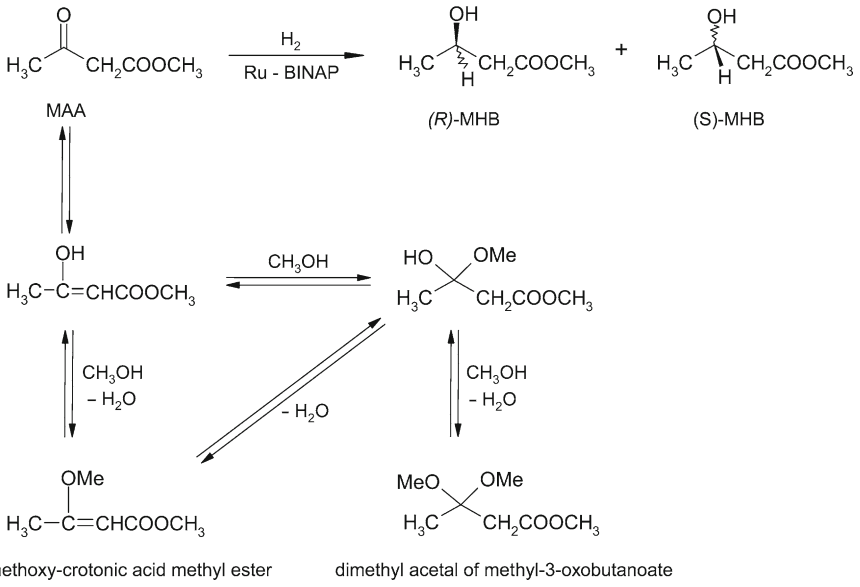

Fig. 9.28 Hydrogenation of MAA in methanol – acetal formation

9.3.4.3 Homogeneous Arrangement

Data that must be presented first introduce optimization of the homogeneous experiment because this reaction system is in the next chapters referred to as the "standard one". Kinetic data obtained with the immobilized Ru complex are compared with characteristics of this system [142]. For this comparison a set of kinetic parameters is used: TOF90 (turn-over-frequency; the number of reaction turns per single catalytic centre and per time unit) [h^{-1}], ee90 [%] enantioselectivity (optical yield) of the reaction at 90% conversion, S90 [%] is the selectivity of methyl-3-hydroxybutanoate formation in respect to other reaction intermediates (acetals) at 90% conversion of MAA. The relations for their evaluation were defined as:

$$ee_{90}\left[\%\right]=\frac{\left[R-(+)-MHB\right]-\left[S-(-)-MHB\right]}{\left[R-(+)-MHB\right]+\left[S-(-)-MHB\right]}\cdot 100 \tag{9.1}$$

$$S_{90}\left[\%\right]=\frac{\left[MHB\right]-\left[\sum\left(acetal\right)\right]}{\left[MHB\right]+\left[\sum\left(acetal\right)\right]}\cdot 100 \tag{9.2}$$

$$TOF_{90}\left[h^{-1}\right]=\frac{n_0\left(MAA\right)-n\left(MAA\right)}{n_{CAT}\cdot t} \tag{9.3}$$

Where [*R*-(−)-MHB] and [*S*-(+)-MHB] denote for weight % of methyl-(*3R*)-(−)-hydroxybutanoate and methyl-(*3S*)-(+)-hydroxybutanoate, [MHB] represents weight % of methyl-3-hydroxybutanoate, [Σ(*acetal*)] weight % of the sum of individual products of acetalisation, *n0*(*MAA*) is the initial amount of MAA [mol] at t = 0, *n*(*MAA*) is the amount of MAA at its 90% ($n(MAA) = 0.1*n_0(MAA)$), n_{CAT} is the amount of the catalyst and t represents time [h]. As already introduced the reaction solvent accepts an active role in the hydrogenation as the proton donor. Solvents of a first choice are obviously alcohols promoting formation of acetals [141–143]. Kinetic data on comparison of a series of solvents including alcohols are provided in Table 9.9. It is evident that all alcohols contribute to very high optical yields and TOFs.

Reasonably high values of the *ee* parameter were also achieved in some aprotic solvents (dichloromethane *ee* ~ 97%, acetonitrile *ee* ~ 89%, tetrahydrofuran *ee* ~ 84%), however with much lower reactivities of the Ru-BINAP complex. Data in the Table 9.9 are in a good agreement with the mechanism of the Ru-BINAP catalytic action [105]. The solvents assist in the hydride insertion from the complex to the molecule of MAA (by means of an exchange of hydride for another molecule of a solvent) and it also participates on releasing the hydrogenated product from the coordination sphere of the complex by the proton transfer. Generally all tested alcohols may provide hydrogen proton, aprotic solvents apparently not. In the latter case acetals cannot be formed from principle reasons, on the other hand reaction rates are lower (necessity of protonation of the substrate from the gaseous phase – hydrogen).

Table 9.9 Role of a solvent in MAA stereoselective hydrogenation over Ru-BINAP

Solvent[a]	TOF_{90} (h^{-1})	S_{90} (%)	ee_{90} (%)
Methanol	3,150	84	98
Ethanol	3,050	92	98
Propan-1-ol	2,000	95	97
Propan-2-ol	1,600	94	96
Ethyleneglycol	750	96	87
2-Methylpropan-1-ol	50	92	47
Tetrahydrofuran	150	100	84
Dichloromethane	200	100	96
Acetonitrile	150	100	89
No solvent	0	0	0

[a]343 K, 5 MPa, 17 ml methanol, 2 g MAA, S/C = 1,500 (mol/mol)

Clear similarities with methanol and ethanol are due to their very close values of dissociation constants (pK_a(methanol) = 15.5; pK_a(ethanol) = 15.9). The pK_a values for propanols are already higher (pK_a(propan-1-ol) = 16.1; pK_a(propan-2-ol) = 17.1) and together with steric reasons to Ru (especially for propan-2-ol) they contribute to lower TOFs and enantioselectivities. With more branched alcohols these effects are even more pronounced [144]. In definition of the "standard" experiment conditions the optimum reaction temperature must also be identified [141–143]. Under the conditions listed below the Table 9.9, the highest TOF was recorded at 338 K, however, at this level, the selectivity drop was already observed. It must be noted that above 343 K the Ru-BINAP complex is being decomposed and reddish precipitate occurs that might be assigned to the appearance of metallic ruthenium. On the other hand below 313 K the reaction is very slow. Also the pressure of hydrogen affects the reaction progress.

With increasing pressure the TOF parameter also increases up to 7 MPa. This trend could be attributed to higher concentration of hydrogen in the liquid phase and thus to the more rapid substrate protonation and the improved formation of the hydride of the complex. Above the level of 7 MPa the complex lower stability might already be seen. To summarise – optimum conditions of the "standard" experiment were found at 333 K and hydrogen pressure 5 MPa in methanol.

A characteristic kinetic course of the MAA asymmetric hydrogenation is shown in Fig. 9.29. In order to limit acetals in the environment of alcohol reaction conditions were also optimised toward suppression of this intermediate. The curve for acetal in Fig. 9.29 reveals a clear maximum. As MAA disappears this intermediate disappears as well.

A characteristic kinetic course of the MAA asymmetric hydrogenation is shown in Fig. 9.29 In order to limit acetals in the environment of alcohol reaction conditions were also optimised toward suppression of this intermediate. The curve for acetal in Fig. 9.29 reveals a clear maximum. As MAA disappears this intermediate disappears as well. Longer reaction time may thus naturally contribute to its elimination. On the other hand, especially from practical and technology reasons this is

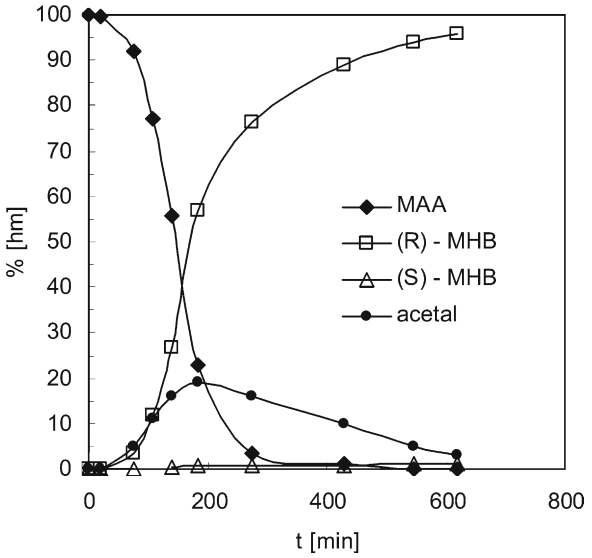

Fig. 9.29 A typical course of the MAA hydrogenation in methanol with Ru-BINAP (333 K, 5 MPa, methanol, S/C = 1500)

Table 9.10 Role of water in methanol

Solvent[a]	TOF_{90} (h^{-1})	S_{90} (%)	ee_{90} (%)
MeOH	370	94	98
MeOH + 1% H_2O	440	99.9	98
MeOH + 3% H_2O	600	99.9	99
MeOH + 5% H_2O	440	99.9	93
MeOH + 7% H_2O	340	99.9	90
MeOH + 10% H_2O	270	99.9	87

[a]333 K, 5 MPa, 17 ml methanol, 2 g MAA, S/C = 1,500 (mol/mol)

not the most suitable approach. The rational solution is based on addition of small amounts of water [142]. Water is one of the products occurring due to the formation of acetals (Fig. 9.28). Diacetal of methyl-3-oxobutanoate is associated with parallel surrendering of two water molecules. Addition of H_2O tends to a shift of the reaction equilibrium and suppression of the acetals appearance. The amount of water must be, however, relevant to its amount generated in the reaction. Table 9.10 covers trends on the water content. It is noteworthy that besides the "acetal effect" up to 3 wt% water also contributes to enhancing *ee* and TOF. Above 10% the complex is already deactivated. MAA hydrogenation only in water does not proceed.

The explanation might be sought in partial elimination of acetals and also in the presence of another protic solvent contributing to the protonation of the substrate (pK_a(MeOH) = 15.5; $\varepsilon_{(MeOH)}$ (dielectric constant) = 32.6; $pK_a(H_2O)$ = 15.74; $\varepsilon_{(H2O)}$ = 78) [144, 145].

9.3.4.4 Immobilisation of Ru-BINAP

For immobilisation purposes three approaches were chosen. Besides the direct heterogenisation of the complex on a solid support described by Pierre Jacobs [136, 137], two modifications of the approach developed by Robert Augustine were utilised [138–140].

Immobilisation with Heteropolyacid – Approach A

The principle of this method is expressed schematically in Fig. 9.30. The [RuCl((*R*)-binap)(*p*-cymene)]Cl complex is supported on the surface of a solid matrix via the heteropolyacid of Keggin's type. The whole process must be carried out strictly under inert atmosphere in the Schlenk apparatus and it starts with a special treatment of the solid support. It is repeatedly washed out with water, calcined, outgassed and the system is then purged thoroughly with argon and evacuated. In the next step degassed ethanol is brought into the contact with the support followed by addition of heteropolyacid. The mixture must be stirred for a long time (~10 h), then it is filtered, washed with methanol and finally dried. The support treated in this way is finally transferred again back to the Schlenk system and outgassed. First ethanol then the mixture of ethanol and [RuCl((*R*)-binap)(*p*-cymene)]Cl are introduced to the apparatus with help of argon overpressure and stirred for the next 10 h together with the support. Surpass of

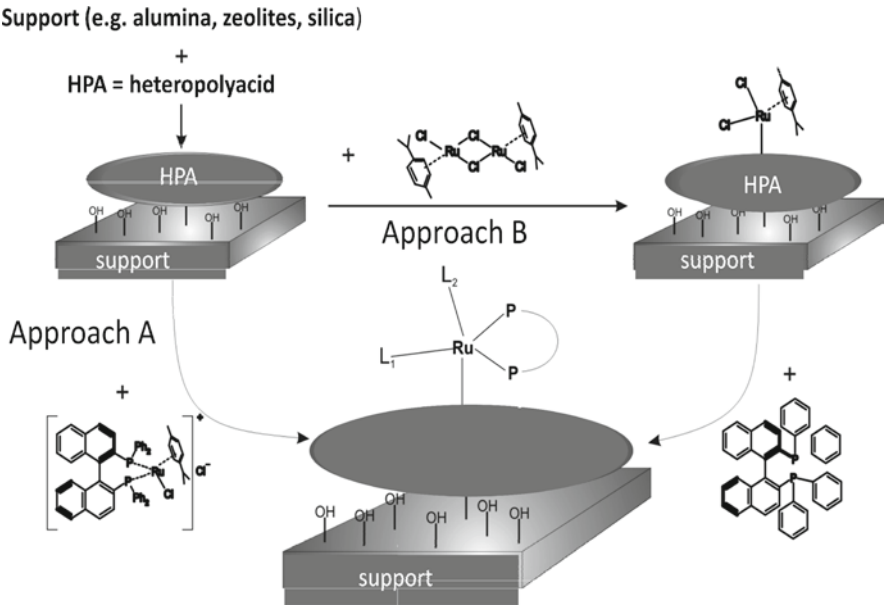

Fig. 9.30 A scheme of the heterogenization approaches of Ru-BINAP via the spacer

the liquid phase is removed, the remaining suspension repeatedly washed with ethanol until the withdrawn solvent reveals no colour [138–140]. The resulting yellow-brownish product is dried in vacuum with argon and used in the MAA hydrogenation.

Immobilisation with Heteropolyacid – Approach B

The initial treatment of a support together with heteropolyacid was performed identically as in the previous case. Then it was brought into the contact (in the Schlenk apparatus) with the ethanol solution of dimeric $[RuCl_2(p\text{-cymene})]_2$. The mixture was stirred for 10 h, then the liquid phase was removed and the suspension washed carefully with ethanol. To this product, again in the Schlenk system, BINAP ligand (2,2′-bis(diphenylphosphino)-1,1′-binaphtyl) in ethanol/dichloromethane was introduced. The mixture was purged with argon, stirred, and heated under reflux for 2 h. The product was treated finally as in the case of approach A [138–140].

Direct Immobilisation

The direct immobilisation resembles methods usually used in heterogeneous catalysis and known as impregnations (Fig. 9.31). The support was first treated repeatedly with argon and evacuated in the Schlenk system to remove all possible traces of oxygen. Then the complex in ethanol was also transferred there and the mixture stirred for 10 h. The final catalyst was treated as previously [136, 137]. Supports used in all three methods are summarised in Table 9.11 together with the values of their specific surface areas. Special attention was paid to the series of alumosilicates with a variable ratio Al/Si [141, 142].

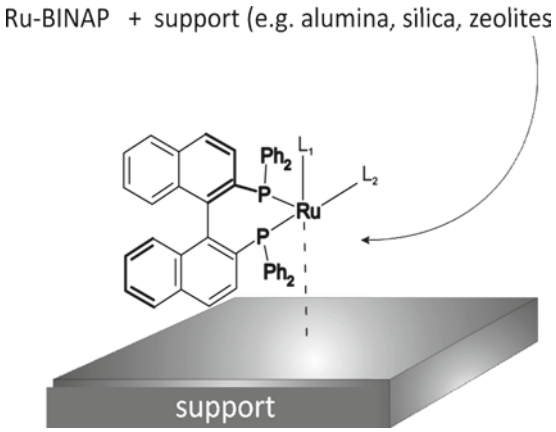

Fig. 9.31 Direct immobilisation

Table 9.11 Inorganic supports used for immobilisation of Ru-BINAP

Support	Si/Al[a]	S_g (m^2 g^{-1})[b]
Beta-9	9	680
Beta-12.5	12.5	680
Beta-13.5	135	680
Beta-19	19	710
Beta-25	25	725
USY/6.8	6.8	730
USY/15	15	780
Montmorillonite	3.4	240
Mordenite	10	500
X	1.2	650
ZSM-5	25	344
γ-Al_2O_3	–	188
Silicagel	–	268

[a]From XRF
[b]BET method with nitrogen at 77 K

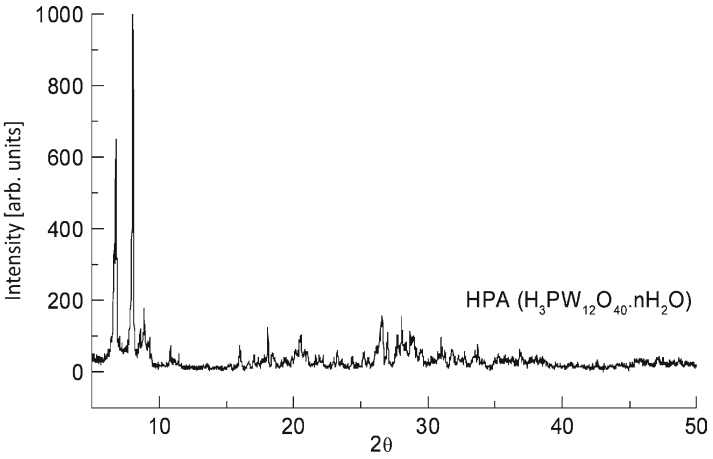

Fig. 9.32 XRD pattern of $H_3PW_{12}O_{40}{\cdot}nH_2O$

Notes on the Heteropolyacid and Ru-BINAP Contents

The spacer used – heteropolyacid of the Keggin's type – $H_3PW_{12}O_{40}.nH_2O$ (HPA) is characteristic by its variable water content [146]. In the hydrate form it reveals very good crystallinity (Fig. 9.32). However, this property is not retained when it is impregnated on the surface of an inorganic matrix. It loses its crystal character and changes to an amorphous surface film (e.g. Fig. 9.33) [142].

HPA in the impregnated form is stable up to ~773 K, above this level it decomposes. It is very important to assess independently the amount of anchored HPA and Ru-BINAP as a function of the preparation process. For such purposes XRF analysis

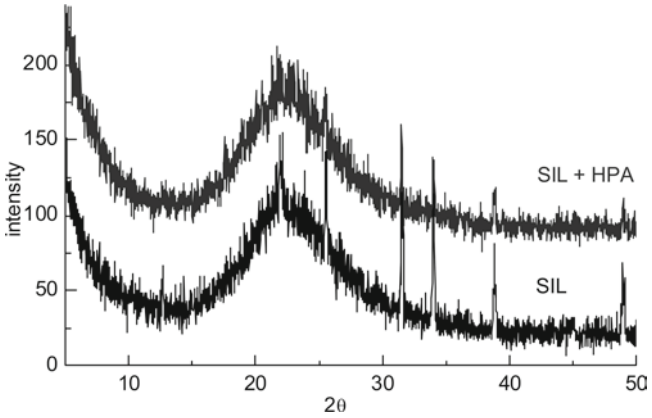

Fig. 9.33 XRD patterns of silica and silica impregnated with HPA

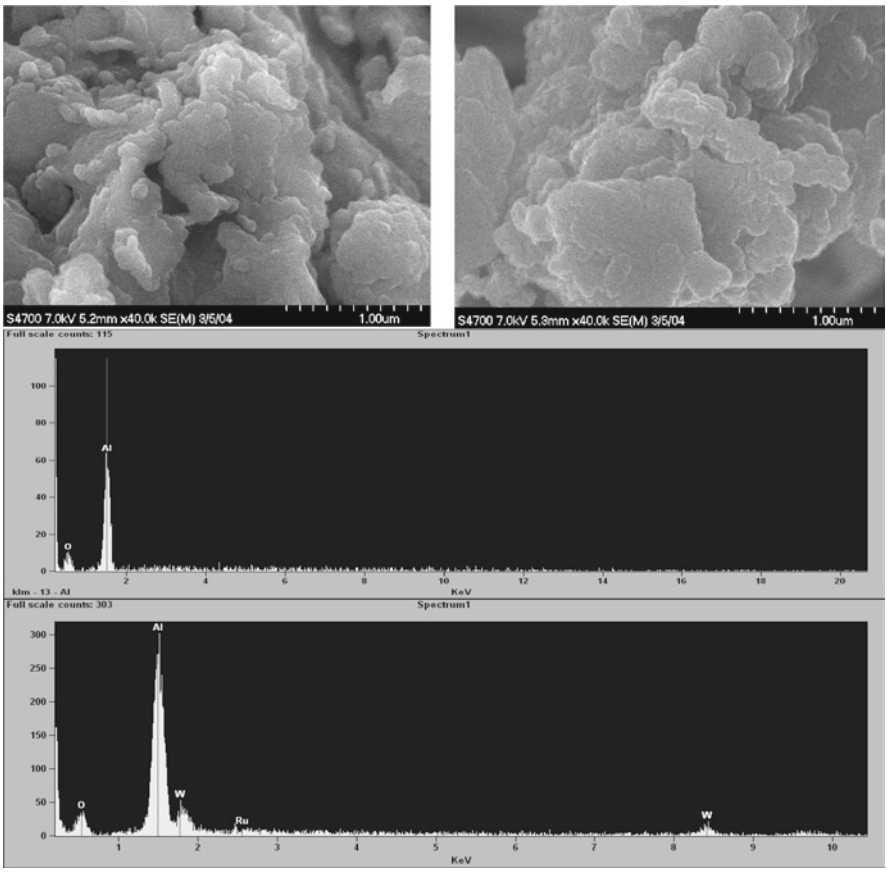

Fig. 9.34 SEM images/EDX spectra of Al_2O_3 and Al_2O_3/HPA with Ru-BINAP

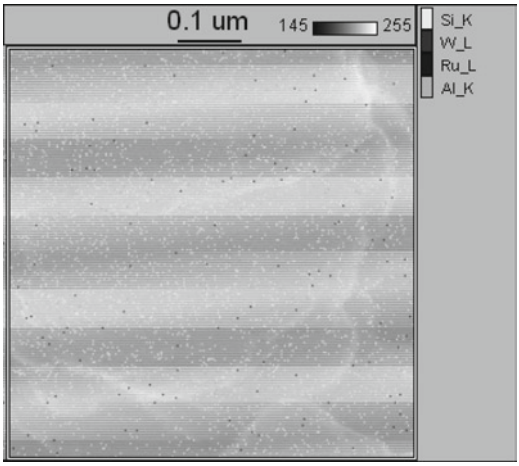

Fig. 9.35 SEM/EDX surface map for alumina impregnated with $H_3PW_{12}O_{40}{\cdot}nH_2O$ and [RuCl((*R*)-binap)(*p*-cymene)]Cl complex

is well suited together with SEM microscopy associated with energy dispersed X-ray screening. In Fig. 9.34 SEM images and EDX spectra are shown together for alumina and alumina/HPA with supported Ru-BINAP [142].

The same technique SEM/EDX may also provide valuable information on surface distribution of ruthenium. As it is seen in Fig. 9.35. the [RuCl((*R*)-binap)(*p*-cymene)] Cl as well as $H_3PW_{12}O_{40}.nH_2O$ are distributed homogeneously over the surface of alumina without any specific locations of their much higher appearance [142].

Because of the presence of Ru and W atomic absorption spectroscopy (AAS) is another tool for evaluating the amount of HPA and the complex on the studied surfaces by analysing their contents before immobilisation in preparation solutions, and before and after the washing process. The same information for Ru-BINAP could be extracted from elementary analysis (EA) focused on determination of carbon and chlorine.

Data on the content of Ru-BINAP are given in Table 9.12. It is evident that the SEM-EDX outputs fluctuate due to the "surface character" of this analysis. AAS and EA from their principles and because of complexity of the analysed samples do not also provide accurate results. Obviously the best suited is XRF reflecting the contents in the whole volume of a sample. With exception of EA the same information could be obtained for the content of HPA (Table 9.13).

9.3.4.5 MAA Hydrogenation with Immobilised Ru-BINAP

Various supports were impregnated with [RuCl((*R*)-binap)(*p*-cymene)]Cl by means of the approach without HPA. These samples were used in stereoselective hydrogenation of MAA in methanol under conditions. The evaluated kinetic parameters are given in Table 9.14. It is seen that some of the produced samples were well active

Table 9.12 Ru-BINAP surface content

	Method/content of the complex (wt%)			
Support[a]	SEM-EDX	XRF	AAS	EA
Al_2O_3[b]	5.9	5.1	4.4	4.5
Al_2O_3[c]	15.8	4.2	–	4.7
Silicagel	0.9	0.8	0.6	0.8
Montmorillonite A[b]	8.2	6.3	5.5	5.5
Montmorillonite B[d]	13.2	9.9	7.7	8.9
Beta 9[e]	3.2	2.8	2.4	3.7
Beta 13.5	2.7	1.6	1.5	3.9
ZSM-5	4.8	0.6	0.4	2.7
USY 15	0.7	0.5	0.6	0.4

[a]Support + $H_3PW_{12}O_{40}{\cdot}nH_2O$ + [RuCl((*R*)-binap)(*p*-cymene)]Cl
[b]Approach A – in equilibrium
[c]Approach B
[d]Approach without HPA
[e]NH_4 form of zeolite beta

Table 9.13 HPA surface content

Support[a]	Method/content of the complex (wt%)		
Al_2O_3[b]	–	8.8	9.2
Al_2O_3[c]	11.9	17.8	16.8
Silicagel	0.7	<	0.8
Montmorillonite A[b]	3.7	2.4	3.8
Montmorillonite B[d]	4.2	2.9	4.7
Beta 9[e]	2.9	1.2	3.1
Beta 13.5	2.7	1.3	2.7
ZSM-5	2.2	0.9	2.9
USY 15	0.8	1.2	1.6

[a]Support + $H_3PW_{12}O_{40}{\cdot}nH_2O$ + [RuCl((*R*)-binap)(*p*-cymene)]Cl
[b]Approach A
[c]Approach B
[d]Approach without HPA
[e]NH_4 form of zeolite beta.

and even selective. Unfortunately no specific role of a particular type of a support could be evaluated. It applies even for the zeolites in which no dependence on their modulus was identified [142].

These rather irregular trends were caused by very significant leaching of the complex. Obviously the reactions proceeded under conditions of a pseudo-homogeneous arrangement. The leached amounts are summarised in Table 9.15 (AAS) and it is seen that the ability of the supports to retain effectively the active complex under the conditions of the hydrogenation experiment was very poor. High observed TOFs values for some of the samples could be attributed to the acidic character of the support. It does not act as a matrix for immobilisation, but as a reaction additive providing acid sites.

Table 9.14 Reaction parameters with directly supported Ru-BINAP

	Direct immobilization		
Support[a]	TOF_{90} (h^{-1})[b]	ee_{90} (%)[b]	S_{90} (%)[c]
Beta/12.5	40	97	8
Beta/13.5	30	79	1
Beta/25	190	6	41
USY/6.8	140	67	2
USY/15	120	82	41
Montmorillonite/25	170	4	14
Mordenite/10	90	30	65
X/1.2	7	6	97
ZSM-5/25	70	24	2
γ-Al_2O_3	150	3	96
Silicagel	70	22	39

[a]0.3 g of a support + ~2 μmol of [RuCl((R)-binap)(p-cymene)]Cl
[b]303 K, 5 MPa, 300 mg of Ru-BINAP, 1 g MAA, 17 ml of a solvent
[c]wt% of acetals

Table 9.15 Leached amounts of Ru-BINAP – direct immobilisation

	Direct immobilisation	
Support[a]	Ru-BINAP (μmol)[b]	Ru-BINAP (%)[c]
Beta/12.5	0.6	27.4
Beta/13.5	0.7	35.2
Beta/25	1.4	75.7
USY/6.8	2	97.8
USY/15	1.6	83.5
Montmorillonite/25	1.1	51.6
Mordenite/10	2.1	99.4
X/1.2	1.4	72.1
ZSM-5/25	1.3	65.3
γ-Al_2O_3	0.3	17.1
Silicagel	0.9	48.6

[a]0.3g of a support + ~2 μmol([RuCl((R)-binap)(p-cymene)]Cl
[b]303 K, 5 MPa, 300 mg of a catalyst, 1 g of MAA, 17 ml of a solvent
[c]wt% of the original amount

It is interesting to compare these outputs with data from the MAA hydrogenation with Ru-BINAP heterogenised with help of $H_3PW_{12}O_{40}{\cdot}nH_2O$ by means of the "approach A" (Table 9.16).

All the three evaluated kinetic parameters are relatively high for most of the samples. However, if the leaching of the complex is studied (Table 9.17) it is seen that the effective heterogenisation of Ru-BINAP has not been again achieved ("approach A").

No doubts the leached amounts are considerably lower than previously (Table 9.15), but in many cases they are still high enough for running the reaction in the pseudo-homogeneous mode.

Table 9.16 Reaction parameters with Ru-BINAP immobilised by "approach A"

	Approach A[a]		
Support	TOF_{90} (h^{-1})[b]	ee_{90} (%)[b]	S_{90} (%)[c]
Beta/12.5	70	84.0	68
Beta/13.5	130	99.0	60
Beta/25	20	53.0	72
USY/6.8	100	97.7	3
USY/15	90	96.5	7
Montmorillonite/25	30	94.0	78
Mordenite/10	140	98.0	87
X/1.2	30	93.0	74
ZSM-5/25	20	98.0	88
γ-Al_2O_3	3	88.0	94
Silicagel	120	98.0	79

[a]One step approach with HPA
[b]303 K, 5 MPa, 300 mg of a catalyst, 1 g of MAA, 17 ml of a solvent
[c]wt% of acetals

Table 9.17 Leached amounts of Ru-BINAP – "approach A"

	Approach A[a]	
Support	Ru-BINAP (μmol)[b]	Ru-BINAP (%)[c]
Beta/12.5	6.2	11.7
Beta/13.5	9.9	16.5
Beta/25	3.9	5.9
USY/6.8	12.2	25.3
USY/15	11.3	37.3
Montmorillonite/25	8.7	17.1
Mordenite/10	19.3	44.2
X/1.2	9.5	14.8
ZSM-5/25	9.9	10.2
γ-Al_2O_3	9.9	8.6
Silicagel	13.7	8.0

[a]One step approach with HPA
[b]303 K, 5 MPa, 300 mg of a catalyst, 1 g of MAA, 17 ml of a solvent
[c]wt% of the original content

Especially in this case some of the published data must be accepted with precaution. There have been quite a few papers describing utilisation of an organometallic complex immobilised in this way and successfully used in a hydrogenation reaction. Whenever very high enantioselectivities are reported for such systems it is advised to ask for the data on the complex leaching. In many cases the reaction were performed in fact homogeneously with only some promoting effect of the inorganic solid.

Typical for such systems is the data fluctuation because the leached amounts differ sample to sample, and also the additive role of every type of a support is different. Despite the "approach A" via the HPA is more effective for anchoring the

Table 9.18 Reaction parameters with Ru-BINAP immobilised by "approach B" reported together with data from three homogeneous experiments

	Approach B[a]		
Support	TOF_{90} (h^{-1})[b]	ee_{90} (%)[b]	S_{90} (%)[c]
Beta/12.5	25	77.2	99
Beta/13.5	26	97.2	35
Beta/25	24	25.6	4
USY/6.8	24	51.2	0.5
USY/15	18	20.4	2
Montmorillonite/25	23	96.2	6
Mordenite/10	28	93.1	98
X/1.2	7	4.2	100
ZSM-5/25	7	13.1	18
γ-Al_2O_3	10	74.7	44
Silicagel	6	24.8	32
(R)-Ru-BINAP[d] – homo	45	97.0	69
(R)-Ru-BINAP[e] – prehydro	67	97.0	76
(R)-Ru-BINAP[f] – add. H_2O	87	99.0	99.9

[a]Two step approach with HPA
[b]303 K, 5 MPa, 300 mg of a catalyst, 1 g of MAA, 17 ml of a solvent
[c]wt% of acetals
[d]303 K, 5 MPa, 17 ml of methanol, 2 g of MAA, S/C = 1,500 (mol/mol)
[e]303 K, 5 MPa, 17 ml of methanol, 2 g of MAA, S/C = 1,500 (mol/mol), prehydrogenation
[f]303 K, 5 MPa, 17 ml of methanol + 3% H_2O, 2 g of MAA, S/C = 1,500 (mol/mol).

Ru-BINAP complex than the direct impregnation, from the practical point their utilization is not advisable [142].

The third tested methodology ("approach B") based on the two step immobilization of the complex precursors was expected [142] to yield similarly unstable catalyst regarding the strength of the surface anchorage of Ru-BINAP. Surprisingly the catalysts prepared in this way revealed much better functionality than in the two previous cases. The kinetic data are summarized in Table 9.18, this time together with kinetic outputs of the three "standard" homogeneous experiments.

The first of them comprises the complex with no additional treatment, the second involves the complex treated in hydrogen in the autoclave for 60 min before the reaction (without MAA), and the third comprises also traces of water.

Direct comparison of TOFs is of course questionable, but if we focus on the parameters of *ee* and S we may identify highly effective samples among the series of the catalysts.

Regarding the former parameter (*ee*) the catalysts samples based on Beta/13.5, Montmorillonite/25, and Mordenite/10 might be referred to as excellent and competitive. The selectivities S were very high for Beta/12.5 and X/1.2 based catalysts. In most cases the leached amounts were very low, definitely below the level for

Table 9.19 Leached amounts of Ru-BINAP – "approach B"

	Approach B[a]	
Support	Ru-BINAP (μmol)[b]	Ru-BINAP (%)[c]
Beta/12.5	1.0	1.6
Beta/13.5	0.6	1.9
Beta/25	0.1	0.6
USY/6.8	0.8	2.4
USY/15	0.3	0.3
Montmorillonite/25	0.1	0.5
Mordenite/10	5.0	3.6
X/1.2	0.3	0.3
ZSM-5/25	0.2	6.3
γ-Al_2O_3	0.8	0.8
Silicagel	0.3	0.4

[a]Two step approach with HPA
[b]303 K, 5 MPa, 300 mg of a catalyst, 1 g of MAA, 17 ml of a solvent
[c]wt% of the original content

considering more serious involvement of the homogeneous portion of Ru-BINAP on the reaction (Table 9.19).

The best supports in this respect (and in combination with the "approach B" methodology) were Beta 13.5 or Montmorillonite 25. Also the less stable catalyst with Mordenite 10 was still incomparably much less vulnerable to leaching than in the two other used methods [142].

It might be concluded at this point that catalysts supported on Beta 13.5, Montmorillonite 25 and Mordenite 10 with help of $H_3PW_{12}O_{40}.nH_2O$ and the two step method with precursors of Ru-BINAP are competitively effective for stereoselective hydrogenation of MAA to the "standard" homogeneous systems.

Attention was also paid to the possibility of their repeated use. The most important parameter of enantioselectivity was reduced for ~8% after four full reaction runs. This result is considered as quite promising.

9.3.5 Ionic Liquids as Immobilisation Media

Another attractive alternative for immobilising homogeneous complexes comprises utilisation of ionic liquids (IL) as the phase accommodating selectively the catalyst. This is a very progressive approach and no surprise there have been quite a few research groups during the recent years studying the corresponding phenomena [e.g. 147–153].

In the next chapters we are going to remind first the major properties of ionic liquids, then we shall focus on the description of practical catalytic systems with Ru-BINAP homogeneous complexes confined (immobilised) in the ionic liquid phase including a case study with MAA and some characteristic ILs.

9.3.5.1 Reminding Notes on Ionic Liquids

Historically the first described ionic liquid was ethanolammonium bromide in 1888 followed by ethylammonium nitrate in 1914 (Fig. 9.36) [154, 155]. Since that time hundreds of structurally different ionic liquids have been prepared including those with centres of asymmetry [156–162], or very recently ionic liquids as parts of polymer clusters [163].

Ionic liquids are organic salts, usually in the liquid form at temperatures below 100°C. Many of them reveal melting points at ~20°C, but there are quite a few ILs melting even below 0°C [147–155, 164–169]. Ions of standard inorganic salts are typically small and symmetric. On the other hand ionic liquids are composed of large ions with a low degree of the overall molecular symmetry. Due to this fact their charge is delocalized by resonation over the whole molecular volume (Fig. 9.37). Very high coloumbic interactions are behind their impressive electrical and mechanical stabilities, thermal and pressure resistivity (up to ~5 MPa and 300°C), and extremely low tension of vapours. Low flammability, very good electrical conductivity, high thermal capacity and unusual phase behaviour might be added to the previous list of exceptional properties.

No doubts these features qualify them for a broad band applications ranging from "green solvents" due to their negligible volatility, over templates for synthesis of nanoparticles (some of them tend to form organised ionic clusters), liquid electrolytes in solar cells and fuel cells, to liquid adhesives, special lubricants, chromatography mobile phases, incombustion additives, etc. Till now more than

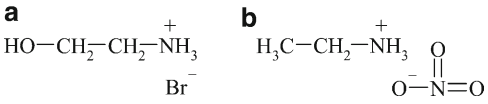

Fig. 9.36 (**a**) Ethanolammonium bromide and (**b**) Ethylammonium nitrate

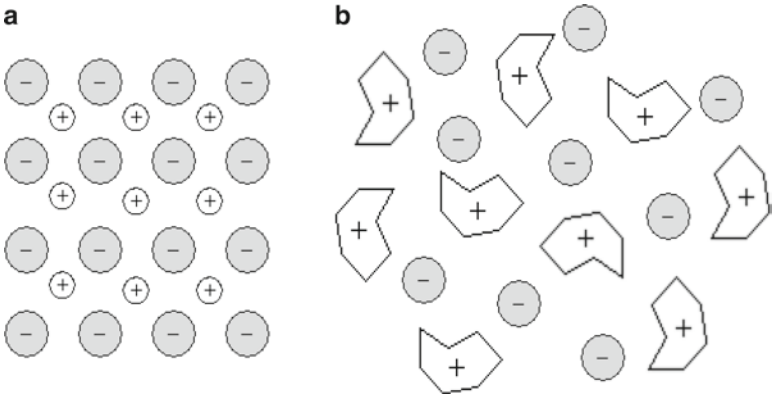

Fig. 9.37 (**a**) A typical inorganic salt and (**b**) an ionic liquid

1,000 structurally different ILs have been described, commercially available are about 300 of them. Initially majority of the reported ILs were composed of substituted heterocyclic pyridinium or imidazolium cations and halogenide or tetrahalogenideAl anions [147–155, 164–168].

These compounds were, however, unstable in presence of even traces of water. The next generation of ILs based on hexafluorophosphate or tetrafluoroborate anions were already much less sensitive to water and thus allowed their much wider utilisation [41, 170–172]. We have witnessed a very steep interest in the research corresponding with ionic liquids during the last decade. In 1999 there were 300 published papers devoted to ILs, in 2008 this number reached the level of 3,000! Currently majority of ILs reported for practical use are those referred to as aprotic. These ionic molecules could be prepared by a quaternisation reaction of the cation precursor followed by anionic metathesis. The most typical representatives of this group of ILs are introduced in Fig. 9.38a,b). Protic ionic liquids are formed upon a

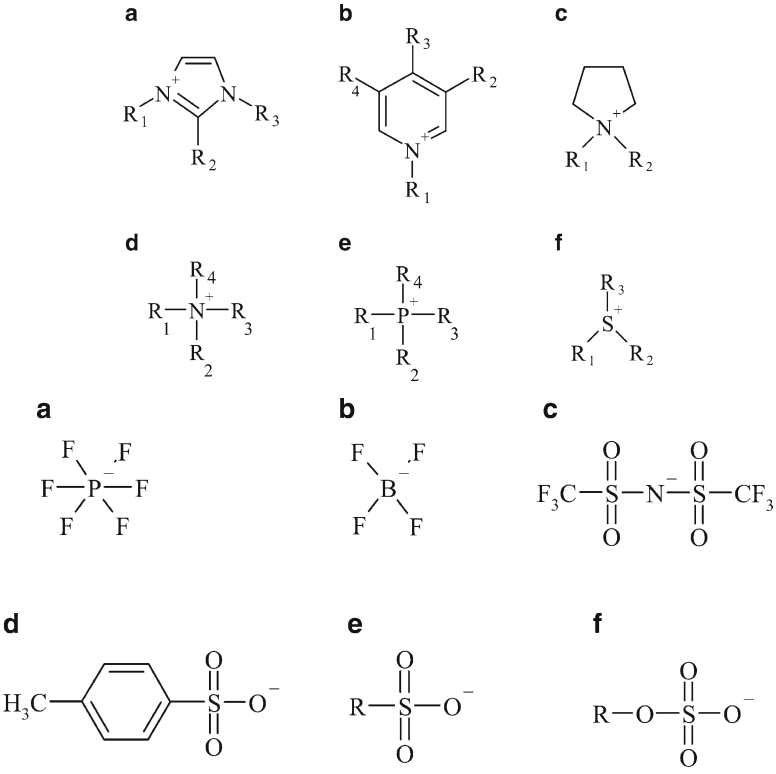

Fig. 9.38 (**a**) Characteristic molecular structures of cations of aprotic ILs. ( ) 1-alkyl-3-alkylimidazolium (R_2 = alkyl/H), (**b**) 1-alkylpyridinium (R_2, R_3, R_4 = alkyl/H), (**c**) 1,1′-dialkylpyrrolidinium, (**d**) mono/di/tri/tetra-alkylammonium, (**d**) mono/di/tri/tetra-alkylphosphonium, (**f**) mono/di/tri-alkylsulphoniumFig. 9.38b Characteristic molecular structures of anions of aprotic ILs. (**a**) hexafluorophosphate, (**b**) tetrafluoroborate, (**c**) bis(trifluoromethylsulfonyl)imide, (**d**) tosylate, (**e**) alkylsulphonate, (**f**) alkylsulphate

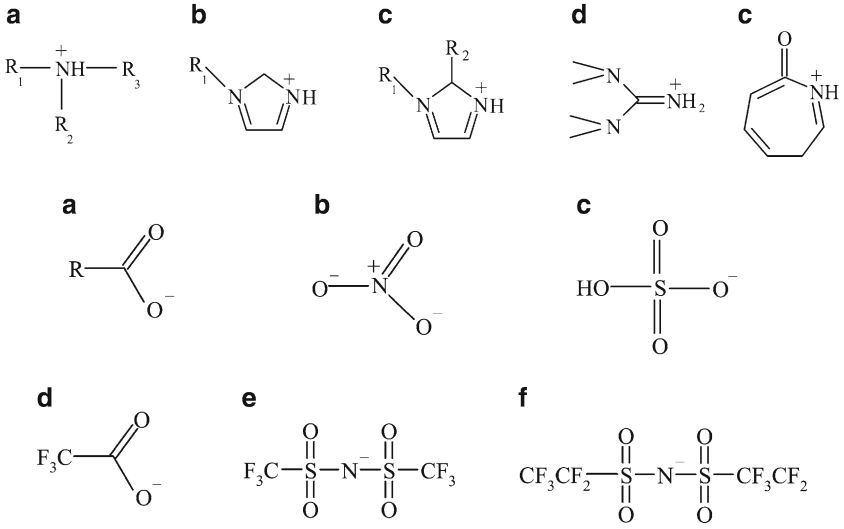

Fig. 9.39 (**a**) Typical structures of cations of protic ILs. (**a**) mono/di/tri-alkylammonium, (**b**) 1-alkylimidazolium, (**c**) 1-alkyl-2-alkylimidazolium, (**d**) 1,1′,3,3′-tetramethylguanidinium, (**e**) caprolaktamFig. 9.39b Typical structures of anions of protic ILs. (**a**) carboxylate, (**b**) nitrate, (**c**) hydrogensulfate, (**d**) trifluoroacetate, (**e**) bis(trifluoromethylsulphonyl)imide, (**f**) bis(perfluoroethylsulphonyl)imide

contact of Brønsted acid and Brønsted base. Their key property is the availability of proton in the cation part and their very high polarity. The proton may interact with the environment via its transfer or hydrogen bridging. Besides functioning as solvents, protic ILs may also act as the source of proton in catalytic reactions, or they may provide this proton for non-bonding interactions [41, 164–172]. Typical cations and anions of protic ILs are summarised in Fig. 9.39a,b.

9.3.5.2 Ionic Liquids in Homogeneous Asymmetric Catalysis

The subject of this contribution, feasible and effective immobilisations of homogeneous complexes, might be also addressed with help of various ionic liquids. Structurally different ILs may reveal variable phase behaviour in the same or slightly modified reaction systems and thus allowing the performance of the reactants` transformation under completely different conditions [169]. There are also many other accompanying phenomena, such as trace impurities of ILs, or variations of the catalytic complex structure, that may reveal a tremendous impact on the practical course of the reaction in the IL environment.

The first ever reported utilisation of an ionic liquid [173] as a solvent for a homogenous catalyst containing transition metal was described by Nobel laureate Yves Chauvin in 1990 (Nobel prize in 2005). The particular reaction was the dimerisation of propene to isomers of hexane catalysed by Ni complexes in the

environment of ionic liquids. Later attention was paid to the asymmetric hydrogenation of α-acetamidoacrylic acid with the Rh complex in ionic liquids (Fig. 9.40). The reaction was carried out in the two phase arrangement [bmim][SbF_6]/propan-2-ol (3/8) with the [Rh(cod){(−)-diop}][PF_6] complex and the product, (*S*)-N-acetylphenylalanine, was obtained with an optical yield 64%. It was important that the complex was simply separable after the reaction and successfully recycled.

In the next 2 years many interesting works had appeared, such as that of Jairton Dupont [36] on hydrogenation of 2-phenylacrylic acid in the two phase system [bmim][BF_4]/propan-2-ol with [$RuCl_2$(cod)(binap)(NEt_3)]. The noteworthy point was that comparable optical yields as in the pure homogeneous system were obtained, but dropping in the repeated cycles. The popular hydrogenation of 2-(6′-methoxy-2′-naphtyl) of acrylic acid leading to Naproxene™ in the same biphasic system and over chiral Ru-BINAP was also reported (100% conversion, *ee* 80%, Fig. 9.41)

In 2001 a clear message was sent out by Ari Wolfson [174] that ionic liquids reveal the evident stabilisation effect on the otherwise very sensitive chiral catalyst. It was shown that no inerts were necessary and that the manipulation with the IL phase confining the catalyst was much simpler. The complex Rh-MeDuPHOS in [bmim][PF_6] catalysed very efficiently asymmetric transformations of enamides (methylesters of α-acetamidoacrylic and α-acetamidocinnamic acids) with *ee* on the level of original homogeneous experiments and preserving this level up to five consecutive reaction cycles (*ee* 96% in the first run, *ee* 94% in the fifth run for methylester of α-acetamidocinnamic acid).

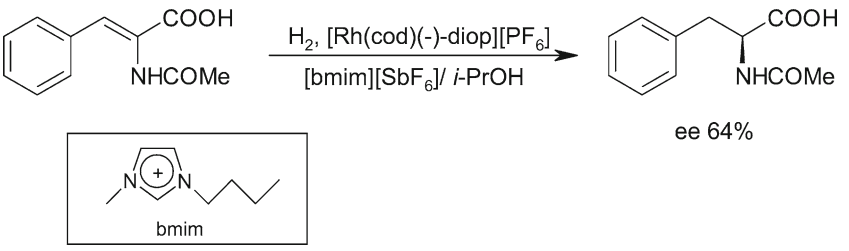

Fig. 9.40 Asymmetric hydrogenation of α-acetamidoacrylic acid in the two phase arrangement ionic liquid/alcohol

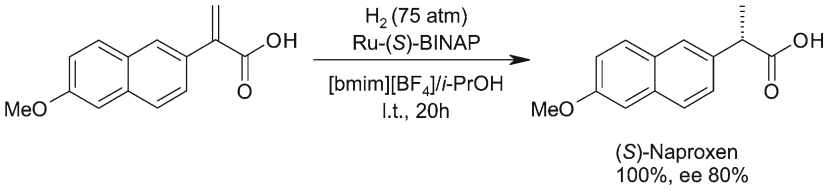

Fig. 9.41 Naproxene synthesis in the biphasic system ionic liquid/alcohol

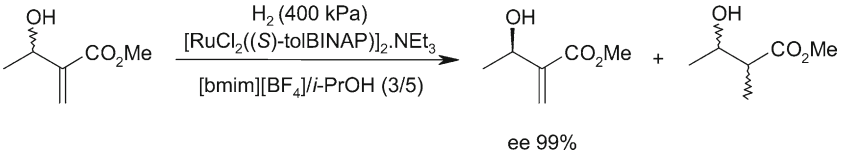

Fig. 9.42 Enantioresolution of (±)-methyl-3-hydroxy-2-methylenbutanoate

Another interesting feature, the effect of hydrogen pressure in presence of traces of water (for [bmim][PF_6]/H_2O system), should be mentioned [175]. At lower pressure of hydrogen the effect of water was negligible, at higher pressures (~5 MPa) optical yields evidently increased. An opposite effect was described for the enantiomeric resolution of the racemic mixture of (±)-methyl-3-hydroxy-2-methylenbutanoate with [$RuCl_2$((*S*)-tolbinap)]$_2NEt_3$ in [bmim][BF_4]/propan-2-ol (Fig. 9.42). Only at lower pressure (400 kPa) of hydrogen a pure optical isomer (*ee* 99%) was obtained (yield 29%).

Successful and still continuing attempts have been also made to eliminate completely organic solvents for extraction of the product in the biphasic or monophasic systems. They might be replaced with supercritical carbon dioxide in which transition metal complexes are virtually insoluble. This new strategy [176–178] was first demonstrated for the extraction of 2-methylbutanoate acid as the reaction product obtained with *ee* 91%.

As repeatedly emphasized in the part devoted to inorganic supports – the complex leaching, if not properly examined, may completely blur the data interpretation. Surprisingly also the biphasic system with ILs is quite sensitive to this phenomenon [142, 169]. It was observed that with the IL/propan-2-ol phase yields and *ee* often decreased with increasing the number of repeated reaction cycles. It might be attributed to the successive leaching of the complex from the IL phase to alcohol. In 2003 Ivo Vankelecom tested [179] the approach we might perhaps call "the principle of secondary heterogenisation". The immobilisation phase for Ru-BINAP, the ionic liquid, was also immobilized in the polymer matrix of poly-diallyldimethylammonium chloride. The system was used for MAA hydrogenation with great expectations, since it had a potential to eliminate the problem of leaching completely (absence of the IL phase in the standard liquid form). Unfortunately comparable kinetic results with the biphasic system of the same composition (without the polymer matrix) were not achieved.

In recent years [179–183] ionic liquids have been considered to be altered with supercritical media (fluids, SCF). Polarity of a particular SCF could be varied by varying slightly temperature or pressure in the vicinity of its critical point. Such variations are reflected in changes of solubilites of individual components of a reaction mixture. In 1995 Mark J. Burk reported [179] successful hydrogenations of amidoacrylic acids with Rh-EtDuPHOS in supercritical carbon dioxide ($scCO_2$). The results were comparable with homogeneous systems containing only the complex and the organic solvent. In the next years many other attempts has been made to utilise SCFs in stereoselective reactions. We must accentuate it was again Ryoji

Noyori [181] who tested Ru-BINAP performance in the environment of $scCO_2$ (1996). Partially hydrogenated complex [$Ru(OCOCH_3)_2(H_8$-binap)] was utilised for stereoselective transformation of α,β-unsaturated carboxylic acids with achieved *ee*s about 80%. More information of these interesting reaction systems could be found in a number of papers devoted to this topic.

9.3.5.3 Reaction Arrangements with ILs

At this point attention will be paid to three general reaction arrangements regarding the phase behaviour of ILs accommodating the homogeneous catalyst.

Monophasic Arrangement

The "pure" monophasic reaction arrangement [169, 175, 177, 184–188] is not suitable in cases when one of the reactants is gaseous, such as hydrogen in hydrogenations, due to typically low solubility of gases in highly viscous and polar ionic liquids. However, "a secondary solvent" (organic co-solvent) may completely change this undesired situation toward much better solubility of the reaction gas. This is a common approach especially in cases when the particular IL is well miscible with the chosen co-solvent. In such an environment adequate solubility of gaseous as well as non-polar reactants is effectively achieved. The catalytic complex dissolved in the IL phase is homogeneously distributed over the whole reaction mixture with no significant resistance to the mass transfer. It is indeed very similar to the "standard" homogeneous experiment without the IL phase. However, in this case it allows the product to be simply removed by another solvent which is immiscible with the IL phase confining the active metal complex.

To this monophasic arrangement also the system in which a very thin layer of IL surrounding the catalytic complex could be assigned. In fact it is already a biphasic system as treated in the next paragraph however, visually it appears as monophasic. The IL film helps to protect the complex due to the increased mass transfer resistance for oxygen, but it is still thin enough to allow the effective transport of hydrogen. Many of the reported monophasic reaction systems with ILs and homogeneous catalytic complexes are believed to be of this type [169, 184–188]. In the case of asymmetric hydrogenations the achieved enantioselectivities are usually comparable with those from the "standard" homogeneous experiment without IL. Suppression of reaction rates is also typically insignificant and the repeated use of the complex is of course possible.

Reactions in the Two-phase System

The two-phase system of ionic liquids with organic or inorganic solvents is usually understood [147–149, 179, 184, 185, 189–194] as an attractive option to the commonly used system of organic solvent with water. No doubts the already

mentioned low solubility of gases in ionic liquids suppresses the reaction progress. On the other hand the presence of the separate IL phase is apparently very positive in terms of the protection and preservation of the highly sensitive catalytic complex. Especially air oxygen acts as the catalytic poison affecting bonds among the central atom and the reactive ligands. Often any manipulation must be confined inside of special equipments such the Schlenk apparatus. Very low solubility of oxygen in most ionic liquids contributes significantly to its effective protection in the IL phase. It is well separated from the organic phase by the phase boundary, and in principle it allows the possibility of its straightforward repeated use, generally much simpler manipulation and storage, durability, and preservation of its long-term catalytic activity. Composition of the organic phase is usually designed to fulfil also the role of the extraction solvent for the product. It must be accentuated that this biphasic system reveals generally lower reaction yields and reaction rates than achieved in the "standard" homogeneous experiment or even in the monophasic arrangement. Existence of the liquid-liquid phase boundary is the reason, but in spite of this there have been many practical reactions in which this approach represented a feasible option with evident positives.

Reversibly Biphasic Arrangement

The reversibly biphasic arrangement comprises most of positive attributes of the two previous systems. If practically works it might be referred to as the system ideally suited for carrying out the asymmetric reaction, even repeatedly, with the metallic complex confined in the IL phase. This arrangement [177, 184, 189, 190, 193, 195–197] is based on utilisation of solvent mixtures with IL revealing a clear temperature dependence of the phase behaviour. The system may exhibit the reversible biphasic change at specific and for each system characteristic thermodynamic conditions (temperature). At lower temperature two phases appear, by increasing the temperature the miscibility increases up to the point when only one-phase system exists.

This upper temperature level is also the temperature at which the reaction is performed. When achieving the desired conversion the temperature is lowered. Then the product is naturally separated from the catalytic phase, which is selectively confined in the IL and now appearing as the separate phase again. Temperature dependent phase behaviour of most ILs in the presence of main organic solvents has not been yet adequately described, which is obviously the major obstacle of wider applications of this reversibly biphasic arrangement.

MAA Hydrogenation

The originally presented model system with MAA stereoselectively transformed to the optical isomers of MHB over the chiral Ru-BINAP catalyst might be also modified with ILs to achieve any of the three above described arrangements [143, 147, 169, 174, 175, 191, 197, 198]. Among others, well suited for such purposes are two types of imidazolium

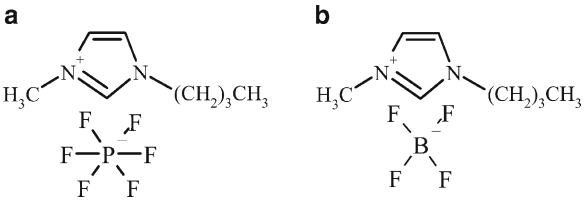

Fig. 9.43 (**a**) 1-Butyl-3-methylimidazolium hexafluorophosphate, (**b**) 1-Butyl-3-methylimidazolium tetrafluoroborate

ionic liquids (Fig. 9.43a,b), namely bmimPF_6 (1-butyl-3-methylimidazolium hexafluorophosphate) and [bmim][BF_4] (1-butyl-3-methylimidazolium tetrafluoroborate).

The "pure" monophasic experiment is not advisable because of low solubility of hydrogen, but in the presence of well miscible co-solvent – methanol, the stereoselective reaction proceeds with high optical yields and comparable rates as in methanol without IL (the "standard" model experiment). The product is then isolated with help of diethylether. Very effective is also the reversibly biphasic model composed of bmimPF_6 and ethanol or bmimBF_4 and propan-2-ol. Both systems are strictly biphasic at 20°C, by increasing the temperature to 60°C they become monophasic. Biphasic arrangements were also described in the presence of water or polar organic solvents such as hexane, etc.

9.3.6 MAA Hydrogenation with Ru-BINAP/IL – the Case Study

In this part practical examples on the utilisation of various ionic liquids and their specific role for immobilisation of Ru-BINAP in MAA hydrogenation are treated together with some other phenomena which are believed important.

9.3.6.1 Structurally Different ILs

In this chapter four different ionic liquids were employed, each of them structurally resulting from combinations of the four appearing ionic pairs for the purpose of the Ru-BINAP effective reaction confinement [143, 199].

Depending on the choice of ions, the ionic liquids may reveal very different properties [147–155, 164–168]. Upon a contact with a particular IL the metallic centre of the catalytic complex is re-coordinated with the Lewis anions of the IL. Alternatively metathesis of the complex and the migration of the IL's anions might be taken into account together with various steric effects. It leads to conformation modifications of an active centre and/or to blocking the substrate access. All these factors could significantly contribute to the magnitude of the achieved parameter of enantioselectivity.

The performed reactions were carried [143] out separately in pure methanol, in methanol combined with 1-butylimidazolium bis(trifluoromethylsulfonyl)imide (bmimTf_2N), 1-butylimidazolium hexafluorophosphate (bmimPF_6), triethylhexylammonium bis(trifluoromethylsulfonyl)imide [N6222][Tf_2N]) and triethylhexylammonium hexafluorophosphate ([N6222][PF_6]) (Table 9.20). Turn-over frequencies (TOF), selectivities (S) to MHB and enantioselectivities (ee) to the (R) isomer were evaluated as principal kinetic parameters. The TOF, ee and the selectivity were always determined at 90% conversion. The ee and the S parameters were defined as previously (Section 9.3.4.5).

It is seen (Table 9.20) that the bistriflamides based ILs revealed much less negative effect on the reaction rate than the hexafluorophosphates. This is an important finding due to the broadband utilisation of [bmim][PF_6] in reactions of this type. The TOF was in average three times lower with the [Tf_2N] anion in comparison to the standard experiment in methanol, and nearly six times lower in the case of the [PF_6] anion.

It is seen (Table 9.20) that the bistriflamides based ILs revealed much less negative effect on the reaction rate than the hexafluorophosphates. This is an important finding due to the broadband utilisation of [bmim][PF_6] in reactions of this type. The TOF

Table 9.20 The ionic pairs' effect[a]

IL	TOF_{90} (h^{-1})	ee_{90} (%)	S_{90} (%)
MeOH	1,091	98.0	79.4
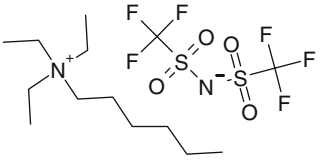 [N6222][Tf2N]	386	92,5	86.9
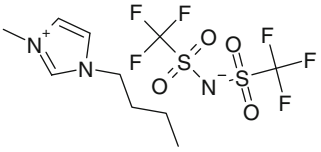 [bmim][TF2N]	335	96.7	91.3
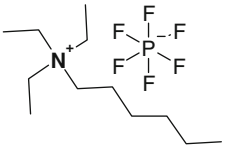 [N6222][PF6]	209	54.5	86.4
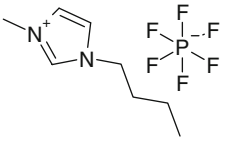 [bmim][PF6]	164	78.3	87.6

[a]Reaction conditions: 2 g MAA, 17 ml solvent IL-MeOH 1/1 wt., S/C = 1580, 333 K, 50 bar H_2

was in average three times lower with the [Tf_2N] anion in comparison to the standard experiment in methanol, and nearly six times lower in the case of the [PF_6] anion. There are two major reaction rate limiting factors: hydrogen solubility and/or structural modifications of the active catalytic centre with the anionic pair (Fig. 9.38a,b). Both factors are considered as similarly important [143, 199]. Solubility of hydrogen is generally low in the ionic liquid phase. It is believed that each Ru-BINAP molecule is selectively entrapped by the IL molecules.

The effect of anion's type of the IL predominated the effect of the cation's type as illustrated in the Figs. 9.44 and 9.45. The reaction proceeded in general faster

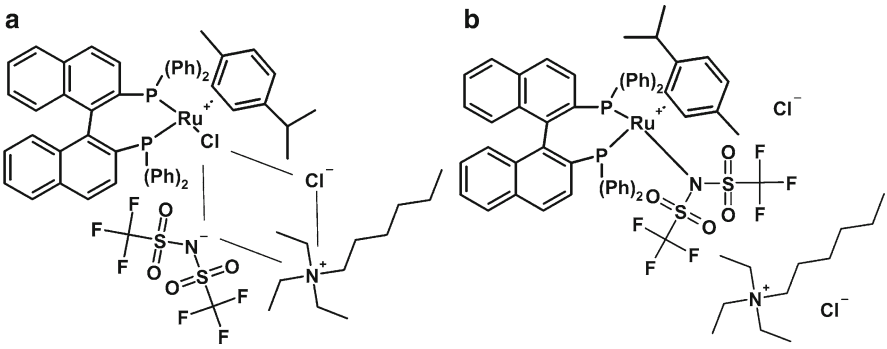

Fig. 9.44 "Weak" catalyst-IL ionic pairs interaction (**a**) and catalyst-IL ionic pairs re-coordination (**b**)

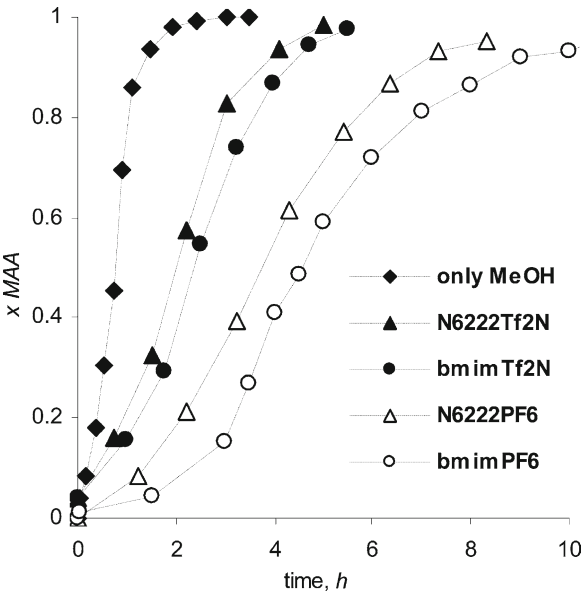

Fig. 9.45 Effect of IL's pairs on the conversion of MAA

with the quaternary ammonium based ILs, in comparison with the imidazolium based ILs. Unlike the TOFs the *ee* values achieved with the $[TF_2N]^-$ based ILs were quite high, especially with [bmim][TF_2N] (Table 9.20). It should be emphasized that its value was nearly comparable with the *ee* evaluated for the standard methanol experiment. On the other hand these parameters (for the PF_6 anion based ILs) were rather low.

It is important to note that $J(^{14}N,^{13}C)$ and $J(^{14}N,^{1}H)$ couplings from NMR analysis could be clearly observed due to the symmetry of the N_{6222} cation. The NMR data displayed almost no change of the corresponding spectra depending on the anion's type (both 1H NMR and 13C NMR). Hence, it should be also noted that the extended positive charge delocalization of the imidazolium's cation may play a certain role in the catalytic course when compared to the aromatic-less ammonium IL, and considering the aromatic nature of the BINAP and *p*-cymene ligands [143].

As might be seen in Fig. 9.46 the parameter of enantioselectivity typically revealed an increasing tendency with the progress of the reaction and this phenomenon was even more pronounced with reactions in the IL/methanol phase. Some interpretation might be sought in terms of formation of the highly unstable enolic intermediate in the presence of pure methanol as discussed earlier. The enol form is much less stereospecific than MAA and thus a lower ratio of the *(R)* to *(S)* isomers could be expected. By analogy to this explanation the hydrogenation of acetals might be also considered. Obviously highly reversible enol and acetals formation is significant especially at low MAA conversion. At higher conversions

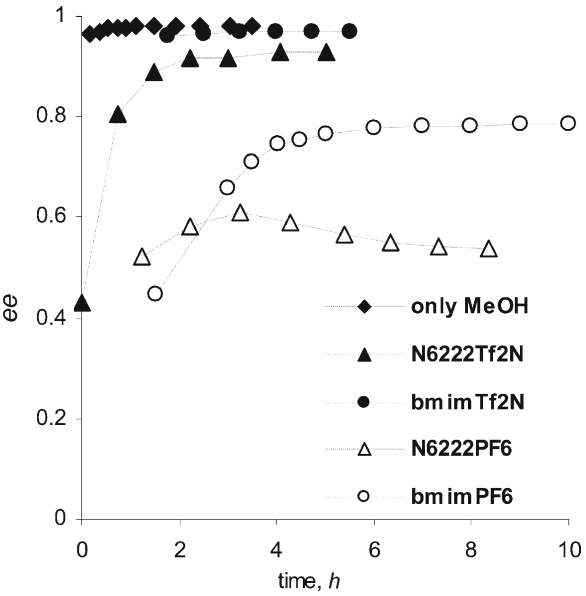

Fig. 9.46 Effect of ionic pairs on the enantioselectivity

concentration of enols is lower and thus *ee* increases. When the ionic liquid is present in the methanol phase the reaction rate is much lower as already described and also the enol and acetal intermediates are formed at much lower extent. This in turn may cause indirect suppression of the magnitude of *ee*. In other words the lower S_{90} at more rapid reactions may indicate much higher *ee*. The maximum of acetals formation was in all cases higher in the presence of imidazolium cation. It might be attributed to the hydrogen acidic properties of imidazolium. In spite of the lower acidity of IL in comparison with methanol the imidazolium based ILs are more acidic than ammonium ILs.

9.3.6.2 Varying a Structure of a Particular IL

It must be emphasized that even minor variations of a structure of a particular IL accommodating the Ru-BINAP complex may reveal a tremendous impact on the achieved kinetic parameters. Ideally suited to demonstrate [143, 199, 200] this phenomenon are quaternary ammonium salts ionic liquids, namely n-alkyl-triethylammonium bis(trifluoromethane sulfonyl) imides ($[N_{R222}][Tf_2N]$, R = 6, 7, 8, 10, 12, 14) differing in the length of their alkyl chain (Fig. 9.47).

As previously, the major component – organic solvent, in this case methanol, improves hydrogen solubility and it allows simple extraction of the produced isomers of methyl 3-hydroxybutyrate (MHB). The reaction product was extracted with water transferring also methanol and leaving the Ru-BINAP complex dissolved and protected in the IL phase [143, 199, 200].

Before discussing the "reflection" of the molecular structure of $[N_{R222}][Tf_2N]$ attention is paid to the identification of the amount of the quaternary ammonium salt IL capable to accommodate the catalyst and to preserve it for the repeated use. As it is seen in Table 9.20 a series of experiments with different content of $[N_{6222}][Tf_2N]$ varying from ~0.2 wt% to 100 wt% was carried out. It was evident that very high values of *ee* to (*R*)-MHB in the range 92.5% to ~97% were achieved with all contents of IL in methanol.

The highest *ee* was observed [143, 200] for the experiment with pure methanol (98%), the lowest (85%) for the experiment with pure $[N_{6222}][Tf_2N]$. In this latter case, however, all the three kinetic parameters were not evaluated at 90% conversion level of MAA but only at x = 21%. The very low TOF can be attributed to the limited solubility of hydrogen in the pure IL phase.

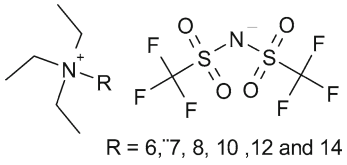

Fig. 9.47 N-alkyl-triethylammonium bis(trifluoromethane sulfonyl) imides ($[N_{R222}][Tf_2N]$, R = 6,7,8,10,12,14)

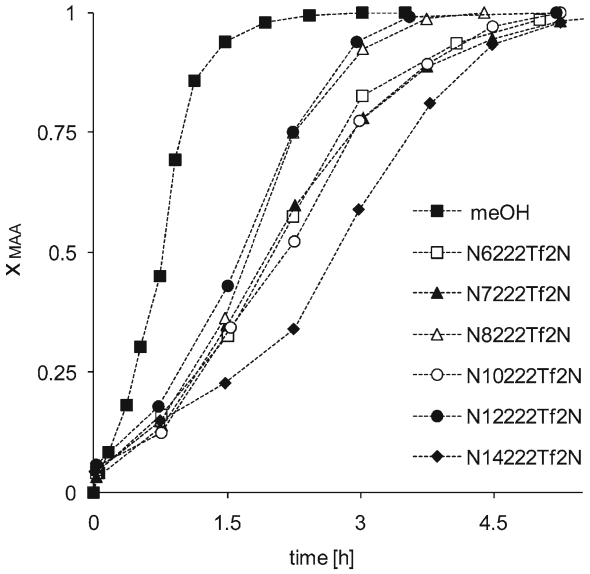

Fig. 9.48 Conversion vs. time dependency with $[N_{R222}][Tf_2N]$, R = 6,7,8,10,12,14

On the other hand even only the 25 wt% content of methanol represented already the amount capable to guarantee sufficient supply of dissolved hydrogen for the reaction. Longer reaction times to achieve the 90% conversion level in experiments with higher contents of $N_{6222}Tf_2N$ improved the process selectivity *S* due to parallel reactions of acetals (Fig. 9.22). The most important result of this part comprises the eventual possibility to use less than 0.2 wt% of $[N_{6222}][Tf_2N]$ to accommodate effectively the catalytic amount of *(R)*-Ru-BINAP, while keeping nearly its activity observed in pure methanol and also with only insignificant decline of *ee* [143, 199, 200]. Molecular structures of the ionic pairs of the $[N_{R222}][Tf_2N]$ type of IL are shown in Fig. 9.38 It is evident that the linear length of the alkyl chain might be intentionally modified with a potential effect reflected in the course of the reaction (Fig. 9.48). For this screening $[N_{R222}][Tf_2N]$ was mixed with methanol using the one to one weight ratio. Surprisingly rather irregular trends with changing the length of the alkyl chain were observed (Fig. 9.49). The highest reaction rates (Table 9.21) were achieved in the system with $[N_{12222}][Tf_2N]$ and $[N_{8222}][Tf_2N]$. Systems with $[N_{6222}][Tf_2N]$, $[N_{7222}][Tf_2N]$ and $[N_{10222}][Tf_2N]$ were much slower. Interestingly in the case of $[N_{12222}][Tf_2N]$ the attained enantioselectivity was approximately on the same level as in experiments with pure methanol (*ee* 97.5% vs. *ee* 98% in methanol) [143, 169, 199, 200].

The same reaction system was also exploited to demonstrate the possibility of the *(R)*-Ru-BINAP repeatable use (Table 9.22, ee_{sr} *sr* as the "second run"). The catalyst re-run is, from principle of this experimental arrangement, impossible in pure methanol.

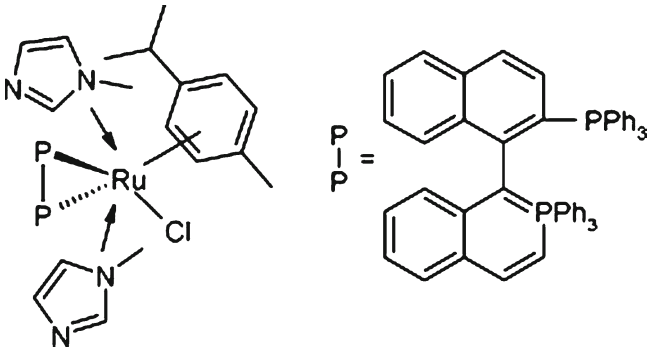

Fig. 9.49 A sketch expression of the competitive re-coordination of impurities on the ligand atom of the complex

Table 9.21 Effect of the $N_{6222}Tf_2N$ amount[a]

$[N_{6222}][Tf_2N]$ (wt%)	TOF_{90} (h^{-1})	ee_{90} (%)	S_{90} (%)
0	1100	98.0	79
0.2	850	96.9	79
1.8	800	96.3	78
12.5	600	95.7	85
25	500	95.0	86
50	400	92.5	87
75	250	92.8	93
100	7.0[b]	85.0[b]	100[b]

[a]Reaction conditions: 2 g MAA, 17 ml solvent IL-meOH, S/C = 1580, 333 K, 5 MPa H_2
[b]x = 21%

Table 9.22 Effect of the variable alkyl chain in $[N_{R222}][Tf_2N]$[a]

IL[b]	TOF_{90} (h^{-1})	ee^{90} (%)	S^{90} (%)	ee_{sr}^{90} (%)
MeOH	1,100	98.0	79	–
$[N_{6222}][Tf_2N]$	390	92.5	87	54.0
$[N_{7222}][Tf_2N]$	370	95.4	92	73.3
$[N_{8222}][Tf_2N]$	490	96.1	92	82.1
$[N_{10222}][Tf_2N]$	380	95.9	91	83.6
$[N_{12222}][Tf_2N]$	500	97.5	93	93.9
$[N_{14222}][Tf_2N]$	330	96.4	90	88.4

[a]Reaction conditions: 2 g MAA, 17 ml solvent, S/C = 1580, 333 K, 5 MPa H_2
[b]IL/meOH 1/1 wt

The very impressive level of ee_{sr} revealed the system with $[N_{12222}][Tf_2N]$, reminding its excellent performance in the first run and the deviation of the runs did not exceed 3.5%. On the other hand the achieved level of ee_{sr} with $[N_{6222}][Tf_2N]$ was rather poor. The increasing tendency of ee_{sr} with prolongation of the alkyl chain was evident, peaking for $[N_{12222}][Tf_2N]$ and falling again slightly for $[N_{14222}][Tf_2N]$. The very specific role of the alkyl chain length (the optimum experimentally indicated for R = 12 in $[N_{R222}][Tf_2N]$) is not fully clear at the moment and it is a subject of further research.

9.3.6.3 Elimination of Impurities in the IL Immobilising Phase

Ionic liquids suitable for the Ru-BINAP immobilisation are either commercially readily available or they are not difficult to prepare fresh from commonly available precursors. In both cases a problem of their purity is encountered. Presence of even trace impurities may either suppress or promote the reaction progress, and most importantly, the parameter of enantioselectivity. Sometimes the role of a particular ionic liquid is discussed profoundly, whereas the problems usually arise only from the presence of trace impurities. A complex treatment of the reaction system should be accepted whenever a genuine role of an ionic liquid as the immobilisation phase for the organometal is being sought [143, 199, 200]. As an example [RuCl((*R*)-BINAP)(p-cymene)]Cl is typically very sensitive to trace amounts of amines such as 1-methylimidazole and/or halogenides both from the preparation of commonly used [bmim][PF_6] (Fig. 9.49). It is prepared in two steps – quaternisation and ion exchange. The unreacted components might be retained in the forming ionic liquid. Usually FTIR and FT-Raman spectra reveal clearly their presence, e.g. typically a broad band near 2,600 cm^{-1} (FTIR) assigned to the contribution of the NH-N stretching from 1-methylimidazole [143, 199, 200].

9.3.6.4 Halide Effect

The rather introductory notes in the previous chapter (Section 9.3.6.3) were focused on eliminating trace impurities to avoid their interfering effect when discussing the role of a particular IL for immobilising Ru-BINAP. At this point attention will be paid to contaminants which may reveal a positive role on the catalytic performance of the organometallic complex. It has been described that the catalytic activity of the BINAP complex might be strongly suppressed by the presence of with origin in the preparation of ILs. On the contrary a positive halide effect in the transition metal catalysis was repeatedly reported; for details see [143, 199].

The precursor of [N_{R222}][Tf_2N] (Section 9.3.6.4), quaternary ammonium bromides, were prepared by quaternization of n-alkylbromides with triethylamine affording high yields (92–99%) toward alkylbromide. [N_{R222}][Tf_2N] were then synthesized by metathesis of [N_{R222}][Br] and [Li][Tf_2N], purified over charcoal and neutral alumina with ~99% yields. The role of trace impurities originating from the IL's preparation was tested with the corresponding alkylbromides. Amazingly small concentrations of [N_{6222}][Br] or [N_{12222}][B]r in methanol (1 wt%) offered remarkable positive effect on *ee* and TOF as evidenced in Table 9.23 (Note: All experiments in Table 9.23 were carried out without IL).

With this knowledge other potential impurities were introduced to the reaction system (also Table 9.23). However, in these cases such significant impacts as for alkylbromides were not already observed.

Finally [N_{6222}][Br] was added to the reaction system with 50 wt% of [N_{6222}][Tf_2N] and 50 wt% of methanol. The results (Table 9.24) are provided for comparison together with the already reported data for the runs in pure methanol, in 1 to 1 mixture of methanol and [N_{6222}][Tf_2N] without traces of [N_{6222}][Br] and for the

Table 9.23 Effects of reaction impurities[a]

Contaminant[b]	TOF_{90} (h^{-1})	ee^{90} (%)	S^{90} (%)
–	1,100	98.0	79
n-$C_6H_{13}Br$	60	98.5	86
n-$C_{12}H_{25}Br$	920	98.3	84
$N(et)_3$	–	Racemic	–
$[N_{6222}][Br]$	1,200	99.1	89
$[N_{12222}][Br]$	1,100	99.1	87
$[N_{6222}][Tf_2N]$	670	97.4	87
$[N_{12222}][Tf_2N]$	630	97.2	86
$[Li][Tf_2N]$	670	96.8	86

[a]Reaction conditions: 2 g MAA, 17 methanol, S/C = 1580, 333 K, 5 MPa H_2
[b]3,500 ppm wt

Table 9.24 Additional effects of reaction impurities[a]

Solvent	TOF_{90} (h^{-1})	ee^{90} (%)	S^{90} (%)	ee_{sr}^{90} (%)
MeOH	1,100	98.0	79	–
$[N_{6222}][Tf_2N]$	390	92.5	87	54
$[N_{6222}][Tf_2N]$[b]	1,250	98.3	94	85

[a]Reaction conditions: 2 g MAA, 17 ml solvent IL/meOH 1/1 wt., S/C = 1580, 333 K, 5 MPa H_2
[b]1% wt. $[N_{6222}][Br]$

repeated runs. As might be seen the system modified in this way revealed even better kinetic characteristics than the reactions in pure methanol! It is evident that the very positive effect of $[N_{6222}][Br]$ was preserved even for the systems with IL [143, 199, 200]. As already stated the evaluated kinetic parameters surpassed slightly their values determined in pure methanol. This finding blurred the initially accepted general presumption that the lower catalytic activity of Ru-BINAP in the IL/methanol phase was caused by the limited hydrogen solubility. If this was true addition of no more than 1 wt% of $[N_{6222}][Br]$ could not improve the reaction appearance significantly. It is rather believed that the positive role of this additive might be interpreted by means of its exclusive coordination to the Ru-BINAP complex.

The role of the cation-bromide ionic pairs was studied further. The reaction course was significantly influenced when various bromides (see Table 9.25) were introduced at low concentrations in methanol (19/1 molar excess to the catalyst). In the presence of the inorganic cation -K^+ the *ee* raised from 98.0% to 98.7%. Nevertheless, when changing the structure of quaternary ammonium cations the values of *ee* stayed amazingly constant ~99.3%. The byproducts (acetals) were suppressed in the KBr presence (S parameter 95% vs. 80%) but no considerable selectivity enhancement was achieved (82–86%) with variations of the organic ammonium cation structure [143, 169, 199, 200].

The cation structure modifications were reflected in the substantial reaction rate increase. Compared with the standard methanol system, in the presence of KBr the TOF increased nearly two times. The TOF was 3–4.5 times higher with the structure

Table 9.25 Role of the quaternary ammonium bromides[a]

Additive[b]		TOF_{90} (h^{-1})	ee^{90} (%)	S^{90} (%)
	–	1,100	98.0	79
	Q^+Br^-			
Q =	K	2,300	98.7	95
	N_{4444}	3,600	99.3	85
	N_{12222}	4,200	99.3	82
	N_{bz222}	3,200	99.3	86
	N_{16111}	5,100	99.3	83
	N_{6222}	3,200	99.2	85

[a]Reaction conditions: 2 g MAA, 17 ml meOH, S/C = 1580, 333 K, 5 MPa H_2
[b]Q^+Br^-/C = 19

variations of the cation. Interestingly the TOF_{90} ratio 1.33 in the case of $[N_{12222}][Br]$ and $[N_{6222}][Br]$ additives was similar to the TOF_{90} ratio 1.2 observed in the performed in the mixture IL $[N_{12222}][Tf_2N]$ and $[N_{6222}][Tf_2N]$ with methanol (1/1 wt.).

9.4 Transfer Hydrogenations on Immobilized Metal Complexes

Catalytic transfer hydrogenations have the potential to be safe and innocuous industrial alternatives to avoid application of explosive hydrogen in the hydrogenation process. It was again Ryori Noyori [201] who first reported the Ru-(1*S*,2*S*)-N-(*p*-toluenesulfonyl)-1,2-diphenylethylene-diamine (TsDPEN) complex as a highly active and selective catalyst for the transfer hydrogenation of carbonyl and imino compounds. No doubts for industrial applications this complex must be immobilized on a solid support. The heterogenized catalyst allows an easy of separation from products by filtration and the expensive complex can be recycled [202]. The most often used support is silica because of its thermal stability, neutral behaviour and high mechanical strength. Silica can also be prepared with different pores sizes and morphology [203]. Siliceous mesocelluar foam (MCF) reveals a unique 3-dimensional pore structure with 20–50 nm pores which are interconnected with windows of smaller openings (9–26 nm). This ultralarge and uniform pores' size allows the encapsulation of the active complex without steric hindrance.

Such types of silica were applied as supports to immobilize the chiral organoruthenium complex and the activity of the heterogenized catalysts were evaluated in asymmetric transfer hydrogenation. The chiral ligand was covalently grafted onto the silica gel by the surface silanol groups. In route "A" 4-ethyl benzenesulfonyl-chloride-fuctionalized silica was stirred with (1*S*2,*S*)-1,2-diphenylethylene diamine [*S,S*-DPEN] in dichloromethane solution. In route "B", the unfunctionalized silica gel was stirred with phenethyltrimetoxisilane in toluene for 24 h, followed by sulfonation using chlorosulfonic acid in chloroform. This sulfonic acid reacted with oxalyl cloride and *N,N*-dimethylformamide (DMF) in dichloromethane resulting in

the immobilized 4-ethyl benzenesulfonic acid on silica gel [204]. This material was mixing with [*S,S*-DPEN] in dichloromethane using triethylamine as a base provided the desired [*S,S*-TsDPEN] grafted in silica gel. The ligand 3, – the third catalyst, was also prepared by the route "B", the only difference was that MCF was used as a support [205]. The immobilized ligands were characterized by spectroscopic methods, especially the Raman spectroscopy was found very useful to confirm the structure of the desired product. The ligand immobilized on MCF was also characterized by N_2 adsorption measurement. A comparison with the original support showed a significant pore size reduction. This observation could be attributed to the fact that the complex was attached inside the pore instead on the external surface of MCF. The immobilized Ru-TsDEN complex was produced by mixing the immobilized ligand (1, 2, 3) with the di-μ-chlorobis(*p*-cymene)chlororuthenium(II) in a mixture of dichloromethane and triethylamine at room temperature for 1 h. The immobilized Ru complex on silica was designated as 4, 5, 6, respectively.

Preparation of alkaloid salsolidine (Fig. 9.50) was chosen to evaluate the activity of the immobilized complexes [202] 4, 5, 6 (Table 9.26) Results of this transfer hydrogenation reaction on different Ru-TsDEN catalysts are provided in Table 9.26.

For the transfer hydrogenation formic acid – triethyl amine complex (5 : 2) was used as a hydride source and with the catalyst 4 excellent activity (yield 94%) and moderate enantioselectivity (78%) was achieved. This catalyst was recycled in two times with the same activity and selectivity, however in the third run it lost its activity. As it is seen in Table 9.26 the best was the catalyst 6, which was possible to recycle in 6 subsequent runs with the highest 91% *ee* and full conversion. Its enantioselectivity was the same as of the homogenous Ru-TsDEN but the activity was somewhat lower. It can be attributed to the formation of a side product during the immobilization, which is also a ligand for the Ru complex. In order to improve further the catalyst activity and enantioselectivity some other combination of formic acid – triethyl amine complex was used in different solvents [202]. However these alternative conditions did not improve the activity and selectivity, in some cases inferior results were even obtained. To check the leaching the metal content was determined after

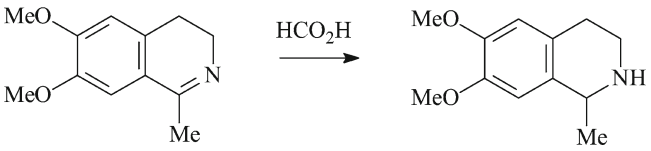

Fig. 9.50 Enantioselective synthesis of salsolidine

Table 9.26 Enantioselective synthesis of salsolidine using different immobilized Ru-TsDEN catalysts

Ru catalyst	Yield (%)	ee (%)	Successive runs
4	94–95	78–81	2
5	95–97	86–87	3
6	95–100	90–91	6

Table 9.27 Asymmetric transfer hydrogenation of ketones

Ketone	Solvent	Temperature	Yield (%)	ee (%)
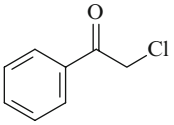	CH_2Cl	r.t.	94–100	97–98
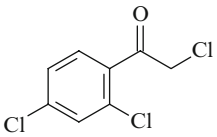	CH_2Cl	r.t.	97–99	90–92
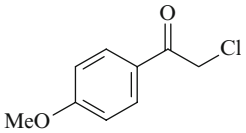	CH_2Cl	r.t.	88–94	97
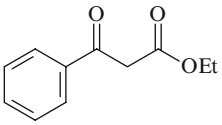	i-PrOH	45°C	90–95	96–97
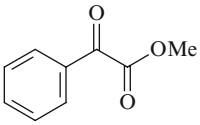	i-PrOH	r.t.	95–98	71–73

each run. Typically 2–5 ppm Ru was found in the reaction mixture. Elemental analysis after the 6 run showed 17% loss of Ru and 7% loss of ligand. The catalyst 6 was further examined in the asymmetric transfer hydrogenation of ketones in 12-h runs. 2-Chloroacetophenone was converted into the chiral 2-chlorophenethanol with 94–100% yield and 97–98% *ee*.

In all reactions presented in Table 9.27 the catalyst no. 6 was used in six subsequent runs without any significant loss in activity and enantioselectivity. In summary the TsDEN ligand was successfully anchored onto the silica surface. Among the studied supports the MCF showed superior performance over the traditional silica. The Ru-TsDEN complex immobilized on MCF demonstrated an excellent activity, enantioselectivity and reusability in the asymmetric transfer hydrogenation of imines and ketones [202].

Reduction of carbonyl functionality via transition metal catalyzed transfer hydrogenation using a suitable stable H donor is a valuable synthetic tool and it could be used as an alternative to the hydrogenation with molecular hydrogen [206]. In transfer hydrogenations several organic molecules such as hydrocarbons, secondary alcohols formic acid and its salts can be used as hydrogen sources. Transition metals

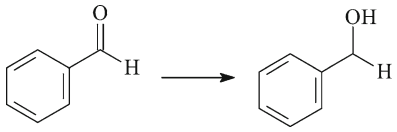

Fig. 9.51 $RuCl_3$ catalyzed transfer hydrogenation of aryl aldehydes

Table 9.28 Optimization of the reaction conditions of the transfer hydrogenation of the *p*-anisaldehyde

Catalyst concentration (mol.%)	Temperature (°C)	Solvent	Time (h)	Yield (%)
5.0	100	DMF/DMA	10	81
5.0	80	DMF	10	84
5.0	60	DMF	10	21
2.5	100	DMF/DMA	10	80
2.5	80	DMF	10	81
2.5	80	DMF	8	83
2.5	60	DMF	12	29
2.0	80	DMA	12	41
2.0	80	DMF	8	80
2.5	60	DMF	8	63

such as Rh, Ir, Ni, Pd and for carbonyl reduction Ru–complexes and propanol in the presence of base can catalyze the reduction [207]. The solution of (*N,N*)-dimethylformamide (DMF) and (*N,N*)-dimethylacetamide (DMA) with $RuCl_3$ has also been demonstrated to catalyze the hydrogenation of simple olefins [208].

Aryl aldehydes were successfully transfer hydrogenated with the aid of resin supported formate in the presence of catalytic amount of $RuCl_3$ H_2O in DMF or DMA solution (Fig. 9.51), since aryl alcohols are important compounds [209]

To try to find the optimum conditions for the reaction the transfer hydrogenation of *p*-anisaldehyde was studied to use Amberlite resin formate as a hydrogen source. Different conditions were applied and the obtained results are collected in Table 9.28.

Starting with 5 mol% of $RuCl_3$ H_2O at 100°C in DMF during 10 h the alcohol yield was 81%. To reduce the amount of catalyst by half the yield did not change, but further reduction in the amount of catalyst reduced the yield, as well. To check the catalyst efficiency {Ru(II)dichloro(p-cymene)} complex was used as well and the results were comparable. On the basis of this comparison it was assumed that the Ru(III) salt was in situ reduced to Ru(II) and this form it was going to catalyse the hydrogenation of aldehydes [211]. The Amberlite formate was prepared by ion exchange starting with the chloride form of the resin and exchange with formic acid. Different aryl aldehydes were studied using the optimum reaction conditions and the result were also similar (Table 9.29), giving the corresponding alcohol with high yields.

Table 9.29 Reduction of aryl aldehydes using resin-supported formate and catalytic $RuCl_3 \cdot 3H_2O$

Substrate	Temperature (°C)	Time (h)	Yield (%)
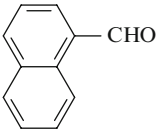	80	8	91
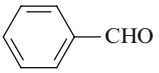	80	8	74
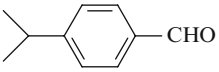	85	9	83
	85	8	83
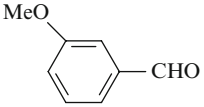	80	8	70
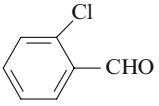	90	7	78
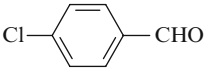	85	8	70
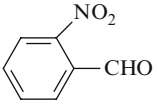	80	8	96
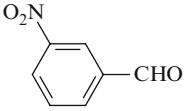	90	9	84
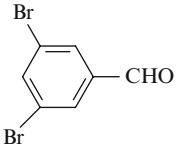	85	8	72
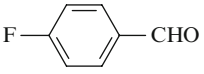	90	8	79

(continued)

Table 9.29 (Continued)

Substrate	Temperature (°C)	Time (h)	Yield (%)
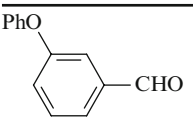	90	8	81
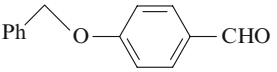	90	8	86
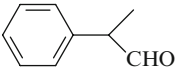	80	8	79
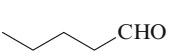	80	12	94
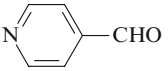	80	8	83
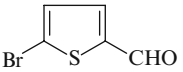	80	8	76
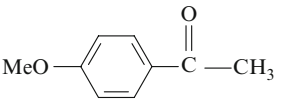	85	8	89

The potentially reducible groups such as nitro or halogens were not effected by the reduction meanwhile the different substituents (electron donating or withdrawing) on the aromatic ring did influence neither the reaction rate nor the yield. Aliphatic aldehydes can be reduced also with a high yield.

Hetero-aryl aldehydes can be reduced as well and the ortho substituents do not affect the reaction rate. However the aryl ketones can not be reduced using similar reaction condition. This chemoselectivity might be advantageous when both of these functional groups are present. The authors [211] compare the reactivity of the aryl ketones and aryl aldehydes running the transfer hydrogenation in a reaction mixture with both functionalities. After 8 h of the reaction time ketones were recovered completely meanwhile the corresponding alcohol in a high yield was isolated from the aldehydes. The heterogeneous Amberlite resin makes possible to remove the catalyst by simple filtration, which is a definite advantage using the formate salt in the homogenous phase.

Another advantage of this reaction is that the reaction conditions are mild without any base, consequently the alcohols form with high yields without any side products. The transfer hydrogenation of 1,2-diketones was also studied under similar reaction conditions. Meanwhile the reduction of aryl ketones did not hap-

pen the transfer hydrogenation of benzoin to benzil proceeded with an excellent yield. This transfer hydrogenation could be a very good method to produce hydroxyketones from the 1,2- diketones without their over-reduction to diols [211]. Novel catalysts for reduction reactions were prepared by immobilization of binuclear Rh(II) and Ru(II, III) teraacetate complexes with metal–metal bond on original chitosan and succinamide chitosan derivatives [212]. Obtained metal complex systems catalyzed the transfer hydrogenation of carbonyl group of cyclohexanone and acetophenone in the liquid phase under mild conditions (82.4°C, Ar). Propan-2-ol was a hydrogen donor and the reaction was promoted by KOH in the propan-2-ol solution. The preparation procedure (solvent, time of the complex deposition, size of chitosan corpuscles) strongly influenced the activity of the prepared catalysts. The metal complex structures formed on the carrier surface were examined by IR- and electronic spectroscopy [210]. The synthesis, characterization and catalytic application of covalently anchored heterogeneous Ru(II) catalyst system, derived from a chiral (1R,2S)-(+)-cis-1-amino-2-indanol was reported for asymmetric transfer hydrogenation of simple ketones [211].

The metal complex was anchored over mesoporous solid support, such as SBA-15, which was synthesized by literature process with a slight modification [212]. The modification of the support was done using 4-chloromethylphenyltriethoxysilane in toluene solution, to obtained Bz-SBA-15 material. The modified support was treated with a mixture of treiethylamine and (1*R*.2*S*)-(3)-cis-1-amino-2-indanol to obtained the modified and functionalized SBA-15. The obtained material was refluxed in a dry propanol solution of $[Ru^{II}Cl_2(benzene)]_2$ or $[Ru^{II}Cl_2(p\text{-}cymene)]_2$ to result the heterogeneous Ru-1 or Ru-2 catalyst. The obtained catalyst were carefully characterized using powder X-ray diffraction, N_2 sorption, solid-state ^{13}C CP MAS NMR, FT-IR and TEM. From the XRD characterization it was possible to see that the ordered mesoporosity and the stuctural stability of the support have retained after incorporation of organometallic complexes [212]. The N_2 adsorption-desorption studies showed high surface are and considerable pore size distribution, which is in general agreement with previous reports on mesoporous SBA-15. The ^{13}C CP MAS NMR, FT-IR study showed definite evidence for anchoring the Ru-complex on the support, which was futher confirmed by UV-VIS analysis. The prepared catalyst was used for the enantioselective transfer hydrogenation of range of simple prochiral ketones and the results are collected in Table 9.30. As Table 9.30 shows the prochiral ketones were hydrogenate with moderate to good conversions and enantioselectivity under mild reaction conditions. It was futher observed that the substrate having electron withdrawing groups in the para position of the aromatic ring showed higher conversion, but a decreased enantiomeric excess, which is exactly the opposite to the substrate having electron donating groups in the para position, as it was expected. The comparative studies showed that the Ru-1 is catalytically more active and enantiomerically less selective than the Ru-2. Acetophenone has given a maximum of 56% conversion and 62% ee for Ru-1 and 18% conversion and 77% ee for Ru-2. The recyclability of the catalysts was effective up to the second recycling step, after an immediate deactivation was observed [212].

Table 9.30 Asymmetric transfer hydrogenation of simple prochiral ketones

Substrate	Product	Conversion (%)	ee (%)
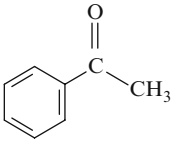	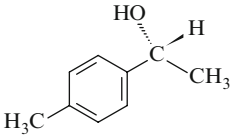	56 Ru-1 18 Ru-2	62 Ru-1 77 Ru-2
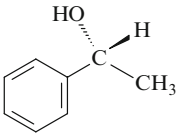	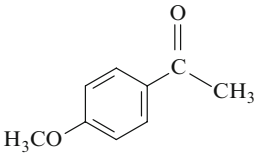	60 Ru-1 35 Ru-2	50 Ru-1 60 Ru-2
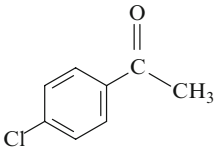	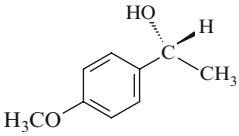	60 Ru-1 34 Ru-2	52 Ru-1 62 Ru-2
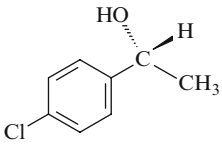	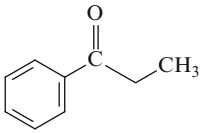	33 Ru-1 19 Ru-2	60 Ru-1 64 Ru-2
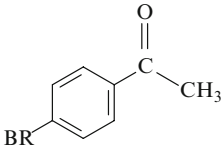	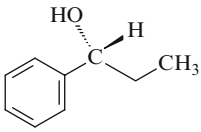	52 Ru-1 21 Ru-2	53 Ru-1 64 Ru-2
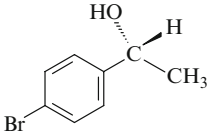	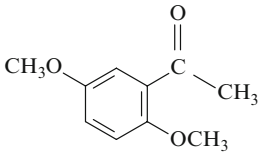	49 Ru-1 14 Ru-2	54 Ru-1 70 Ru-2
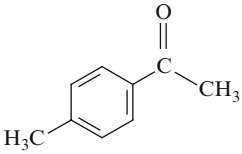	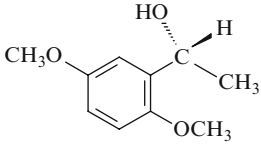	43 Ru-1 14 Ru-2	44 Ru-1 51 Ru-2

Acknowledgments Authors wish to express their thanks to the Czech – Hungarian bilateral project Mobility Contact "Advanced Catalytic Reactions for Fine Chemicals" No. MEB 040802.

References

1. Gallezot P, Richard D (1998) Catal Rev-Sci Eng 40:81–126
2. Fache E, Mercier C, Pagnier N et al (1993) J Mol Catal A Chem 79:117–131
3. James BR, Morris RH (1978) J Chem Soc. Chem Commun 21:929–930
4. Joó F, Kovács J, Bényei A et al (1998) Angew Chem Int Ed 37:969–970
5. Zsigmond A, Balatoni I, Bogár K et al (2004) J Catal 227:428–435
6. Augustine RL, Tanielyan SK, Mahata N et al (2003) Appl Catal. A 256:69–76
7. End N, Schoning KU (2004) Top. Curr Chem 242:241–271
8. Augustine RL, Tanielyan SK, Anderson S et al (1999) Chem Commun 13:1257–1258
9. Ghosh A, Kumar R (2005) Microporous Mesoporous Mater 87:33–44
10. Sephard DS, Zhou W, Maschmeyer T et al (1998) Angew Chem Int Ed 37:2719–2723
11. Thomas JM, Raja R (2004) J Organomet Chem 689:4110–4124
12. Noyori R, Ohkuma T (2001) Angew Chem Int Ed 40:40–73
13. Nunes RMD, Fernandes TF, Carvalho GA et al (2009) J Mol Catal A Chem 307:115–120
14. Guoyu Y, Ailing S, Wenfeng Z, Hainin Z, Denggao J (2007) Catal Lett 118:275–279
15. Ernst S, Disteldorf H, Yang X (1998) Microporous Mesoporous Mater 22:457–464
16. Arstad E, Barrett AGM, Tedeschi L (2003) Tetrahedron Lett 44:2703–2707
17. Buchmeiser MR (2000) Chem Rev 100:1565–1604
18. Barrett AGM, Hopkins BT, Kobberling J (2002) Chem Rev 102:3301–332
19. Barrett AGM, Hopkins BT, Kobberling J (2002) J Org Letters 4:1975–1977
20. Horvath HH, Papp G, Csajagi C et al (2007) Catal Commun 8:442–446
21. Horvath HH, Joo F (2005) React Kinet Catal Lett 85:355–360
22. Zsigmond A, Undrala S (2007) Notheisz, Papp G, Joo F. Catal Lett 15:163–168
23. Burke SD, Danheiser RL (1999) Handbook of reagents for organic synthesis. Wiley, New York
24. Ohkuma T, Ooka H, Hashiguchi S et al (1995) J Am Chem Soc 117:2675–2676
25. Baratta W, Herdtweck E, Siega K et al (2005) Organometallics 24:1660–1669
26. Choualeb A, Lough AJ, Gusev DG (2007) Organometallics 26:5224–5229
27. Schrock RR, Osborn JA (1970) Chem Commun 9:567–568
28. Deshmukh AA, Kinage AK, Kumar R (2008) Catal Lett 120:257–260
29. Steines S, Englert U, Driessen-Hoelscher B (2000) Chem Commun 3:217–218
30. Leitmannova E, Cerveny L (2007) J Mol Catal A Chem 261:242–245
31. Sahoo S, Kumar P, Lefebvre F et al (2007) J Mol Catal A Chem 273:102–108
32. Bronowski J (1973) The ascent of man. British Broadcasting Corporation Publishers Series, London
33. Cerna I, Kluson P, Drobek M et al (2007) Chem Listy 101:994–1001
34. Noyori R (1994) Asymmetric catalysis in organic synthesis. Wiley-Interscience, New York
35. Von Moos R, Stolz R, Cerny T et al (2003) Swiss Med Weekly 133:77–87
36. Monteiro AL, Zinn FK, De Souza RF et al (1997) Tetrahedron Asym 8:177–179
37. Pino P, Consiglio G (1979) Fundam Res Homogen Catal 3:519–536

38. Fan Q-H, Chen Y-M, Chen X-M et al (2000) Chem Commun 789–790
39. Noyori R (1994) Tetrahedron 50:4259–4292
40. Akutagawa S (1995) Appl Catal A 128:171–207
41. Fry SE, Pienta NJ (1985) J Am Chem Soc 107:6399–6400
42. Noyori R (2001) Les Prix Nobel, 186 (http://nobelprizes.com/nobel/)
43. Knowles WS (2001) Prix Nobel, 160 (http://nobelprizes.com/nobel/)
44. Sharpless KB (2001) Prix Nobel, 225 (http://nobelprizes.com/nobel/)
45. Onitsuka K, Ajioka Y, Matsushima Y et al (2001) Organometallics 20:3274–3282
46. Sugimura T (1999) Catal Surv Jpn 3:37–42
47. Shimazu S, Ro K, Sento T, Ichikuni N, Uematsu T (1996) J Mol Catal A 107:297–303
48. Blaser HU (1991) Tetrahedron Asym 2:843–849
49. Keane MA (1994) Can J Chem 72:372–380
50. Nitta Y, Imanaka T, Teranishi S (1983) J Catal 80:31–39
51. Osawa T, Mita S, Iwai A et al (2000) J Mol Catal A Chem 157:207–216
52. Yasumori I, Yokozeki M, Inoue Y (1981) Faraday Discuss Chem Soc 72:385–396
53. Osawa T, Harada T (1984) Bull Chem Soc Jpn 57:1518–1521
54. Izumi Y, Imaida M, Fukawa H et al (1963) Bull Chem Soc Jpn 21
55. Keane MA (1994) Langmuir 10:4560–4565
56. Bennett A, Christie S, Keane MA et al (1991) Catal Today 10:363–370
57. Tani K, Yamagata T, Otsuka S et al (1989) Org Synth 67:33–43
58. Noe CR, Weigand A, Pirker S et al (1997) Monatsh Chem 128:301–316
59. Noe CR, Weigand A, Pirker S (1996) Monatsh Chem 127:1081–1097
60. Carrea G, Colonna S, Meek AD et al (2004) Tetrahedron Asym 15:2945–2949
61. Benhamza R, Amrani Y, Sinou D (1985) J Organomet Chem 288:C37–C39
62. Jessop PG, Morris RH (1992) Coord Chem Rev 121:155–284
63. Brunner H, Muschiol M, Wischert T et al (1990) Tetrahedron Asym 1:159–162
64. Osawa T, Harada T, Tai A et al (1997) Stud Surf Sci Catal 108:199–206
65. Keane MA, Webb G (1992) J Catal 136:1–15
66. Tani K, Yamagata T, Otsuka S et al (1982) J Chem Soc, Chem Commun 600–601
67. Tani K, Yamagata T, Akutagawa S et al (1984) J Am Chem Soc 106:5208–5217
68. Otsuka S, Tani K (1985) Asymmetric Synth 5:171–191
69. Genet JP (2003) Acc Chem Res 36:908
70. Noyori R, Kitamura M (1989) Modern Synthetic Methods 5:115
71. Noyori R (2003) Adv Synth Catal 345:15–32
72. Sharpless KB (1985) Chemtech 15:692–700
73. Sharpless KB (2002) Angew Chem. Int Ed 41:2024–2032
74. Abdur-Rashid K, Faatz M, Lough AJ et al (2001) J Am Chem Soc 123:7473–7474
75. Shao L, Takeuchi K, Ikemoto M et al (1992) J Organomet Chem 435:133–147
76. Chauvin Y, Commereuc D, Stern R (1978) J Organomet Chem 146:311–318
77. De Araujo MP, Valle EMA, Ellena J et al (2004) Polyhedron 23:3163–3172
78. Hobbs CF, Knowles WS (1981) J Org Chem 46:4422–4427
79. Noyori R, Ohta M, Hsiao Y et al (1986) J Am Chem Soc 108:7117–7119
80. Kitamura M, Tokunaga M, Noyori R (1992) J Org Chem 57:4053–4054
81. Takaya H, Ohta T, Inoue S-I (1995) Org Synth 72:74–85
82. Ohta T, Takaya H, Noyori R (1990) Tetrahedron Lett 31:7189–7192
83. Pu L (1998) Tetrahedron Asym 9:1457–1461
84. Halpern J (1983) Pure Appl Chem 55:99–106
85. Knowles WS (2003) Adv Synth Catal 345:3–13
86. Miyashita A, Yasuda A, Takaya H et al (1980) J Am Chem Soc 102:7932–7934
87. Miyashita A, Takaya H, Souchi T et al (1984) Tetrahedron 40:1245–1253
88. Brown KJ, Berry MS, Waterman KC et al (1984) J Am Chem Soc 106:4717–4723
89. Takaya H, Mashima K, Koyano K et al (1986) J Org Chem 51:629–635
90. Knowles WS, Sabacky MJ (1968) Chem Commun 22:1445–1446
91. Osborn JA, Jardine FH, Young JF et al (1966) J Chem Soc A Inorg Phys Theoret 1711–1732

92. Richards CJ, Locke AJ (1998) Tetrahedron Asym 9:2377–2381
93. Korpiun O, Mislow K (1967) J Am Chem Soc 89:4784–4786
94. Knowles WS, Sabacky MJ, Vineyard BD (1970) Ann N Y Acad Sci 172:232–237
95. Morrison JD, Burnett RE, Aguiar AM et al (1971) J Am Chem Soc 93:1301–1303
96. Knowles WS, Sabacky MJ, Vineyard BD (1977) (Monsanto Co., USA). Int. Pat. Appl.: US 75-602484/4005127; Chem Abstr AN 1977:190463
97. Perry MC, Burgess K (2003) Tetrahedron Asym 14:951–956
98. Taber DF, Silverberg LJ (1991) Tetrahedron Lett 32:4227–4230
99. Hoke JB, Hollis LS, Stern EW (1993) J Organomet Chem 455:193–196
100. Ikariya T, Ishii Y, Kawano H et al (1985) J Chem Soc. Chem Commun 13:922–924
101. King SA, Thompson AS, King AO et al (1992) J Org Chem 57:6689–6691
102. Kawano H, Ishii Y, Ikariya T et al (1987) Tetrahedron Lett 28:1905–1908
103. Abdur-Rashid K, Lough AJ, Morris RH (2001) Organometallics 20:1047–1049
104. Ohkuma T, Koizumi M, Doucet H et al (1998) J Am Chem Soc 120:13529–13530
105. Wolfson A, Vankelecom IFJ, Geresh S et al (2003) J Mol Catal A Chem 198:39–45
106. Mashima K, Kusano K-H, Sato N et al (1994) J Org Chem 59:3064–3076
107. Pavlov VA, Starodubtseva EV, Vinogradov MG et al (2000) Russ Chem Bull 49:725–728
108. Wolfson A, Vankelecom IFJ, Geresh S et al (2004) J Mol Catal A Chem 217:21–26
109. Bartek L, Drobek M, Kuzma M et al (2005) Catal Commun 6:61–65
110. Cornils B, Herrmann WA (1996) Appl Homogen Catal Organomet Compounds 2:575–601
111. Palmer MJ (1999) Will M 10:2045–2049
112. Sellner H, Faber C, Rheiner PB et al (2000) Chem-Eur J 6:3692–3705
113. Itsuno S, Frechet JMJ (1987) J Org Chem 52:4140–4142
114. Herrmann WA, Cornils B (1996) Appl Homogen Catal Organomet Compounds 2:1167–1197
115. Wynberg H (1982) Chemtech 12:116–121
116. Annis DA, Jacobsen EN (1999) J Am Chem Soc 121:4147–4154
117. Nagel U, Kinzel E (1986) J Chem Soc Chem Commun 14:1098–1099
118. Pugin B (1996) J Mol Catal A Chem 107:273–279
119. Mollmann E, Tomlinson P, Holderich WF (2003) J Mol Catal A Chem 206:253–259
120. De Vos DE, Jacobs PA (2000) Catal Today 57:105–114
121. De Vos DE, Sels BF, Jacobs PA (2001) Adv Catal 46:1–87
122. Sabater MJ, Corma A, Domenech A et al (1997) Chem Commun 14:1285–1286
123. Adima A, Moreau JJE, Man MWC (1997) J Mater Chem 7:2331–2333
124. Vankelecom IFJ, Tas D, Parton RF et al (1996) Angew Chem. Int Ed 35:1346–1348
125. Tas D, Thoelen C, Vankelecom IFJ (1997) Chem Commun 23:2323–2324
126. Bayston DJ, Fraser JL, Ashton MR et al (1998) Org Chem 63:3137–3140
127. Ohkuma T, Takeno H, Honda Y et al (2001) Adv Synth Catal 343:369–375
128. Q-h F, C-y R, C-h Y et al (1999) J Am Chem Soc 121:7407–7408
129. Fan Q-H, Chen Y-M, Chen X-M et al (2000) Chem Commun 9:789–790
130. Fan QH, Deng GJ, Lin CC et al (2001) Tetrahedron Asym 12:1241–1247
131. Yu H-B, Hu Q-S, Pu L (2000) Tetrahedron Lett 41:1681–1685
132. Ohkuma T, Doucet H, Pham T et al (1998) J Am Chem Soc 120:1086–1087
133. Lamouille T, Saluzzo C, ter Halle R et al (2001) Tetrahedron Lett 42:663–664
134. Lemaire M, Ter Halle R, Schulz E, Colasson B, Spagnol M, Saluzzo C, Lamouille T (2000) (Rhodia Chimie, Fr.; Centre National de la Recherche Scientifique (C.N.R.S.)). Int Pat Appl: WO 2000-FR82/2000052081; Chem Abstr AN 2000:628204
135. Wan KT, Davis ME (1995) J Catal 152:25–30
136. Van Brussel W, Renard M, Tas D, Rane VH, Parton R, Jacobs PA (1997) (K.U. Leuven Research & Development, Belg.; Van Brussel, Willy; Renard, Michel; Tas, Diedrik; Rane, Vilas Hare; Parton, Rudy; Jacobs, Pierre A.). Int Pat Appl: WO 96-BE108/9714500; Chem Abstr AN 1997:380998
137. Tas D, Jeanmart D, Parton RF et al (1997) Stud Surf Sci Catal 108:493–500
138. Tanielyan SK, Augustine RL (1998) Chem Ind 75:101–1107
139. Barnard FJCh, Rouzaud J, Stevenson SH (2005) Org Process Res Dev 9:164–167

140. Augustine RL, Goel P, Mahata N et al (2004) J Mol Catal A Chem 216:189–197
141. Bartek L, Kluson P (2004) Chem Listy 98:157–167
142. Bartek L, Kluson P – unpublished results
143. Floris T, Kluson P, Pelantova H et al (2009) Appl Catal. A 366:160–165
144. Reichardt C (1988) Solvents and solvent effects in organic chemistry, 2nd edn. VCH Verlagsgesellschaft, Weinheim
145. Senapati S, Chandra A (2001) J Phys Chem B 105:5106–5109
146. Zhu K, He H, Xie S et al (2003) Chem Phys Lett 377:317–321
147. Welton T (2004) Coord Chem Rev 248:2459–2477
148. Welton T (1999) Chem Rev 99:2071–2084
149. Wasserscheid P, Gordon CM, Hilgers C (2001) Chem Commun 13:1186–1187
150. Welton T (2008) Green Chem 10:483
151. Welton T (2004) Phys Chem Chem Phys 6:3280–3285
152. Hintermair U, Gutel T, Slawin AMZ et al (2008) J Organomet Chem 693:2407–2414
153. Ochsner E, Etzold B, Junge K et al (2009) Adv Synth Catal 351:235–245
154. Gabriel S (1888) Ber Deutsch Chem Ges 21:566
155. Walden P (1914) Bull Acad Sci St. Petersburg 405–422
156. Earle MJ, McCormac PB, Seddon KR (1999) Green Chem 1:23–25
157. Chen X, Li X, Hu A et al (2008) Tetrahedron Asym 19:1–14
158. Ni B, Headley AD et al (2006) Tetrahedron Lett 47:7331–7334
159. Luo SP, Xu DQ, Yue HD (2006) Tetrahedron Asym 17:2028–2023
160. Ding J, Armstrong DW (2005) Chirality 17:281–292
161. Jodry JJ, Mikami K (2004) Tetrahedron Lett 45:4429–4431
162. Ishida Y, Miyauchi H, Saigo K (2002) Chem Commun 2240–2241
163. Ghatee MH, Zolghadr AR (2008) Fluid Phase Equilib 263:168–175
164. Pârvulescu VI, Hardacre C (2007) Chem Rev 107:2615–2665
165. Wilkes JS, Zaworotko MJ (1992) J Chem Soc Chem Commun 965–966
166. Weyershausen B, Lehmann K (2005) Green Chem 7:15–19
167. Wilkes JS (2002) Green Chem 4:73–80
168. Greaves TL, Drummond CJ (2008) Chem Rev 108:206–237
169. Ohta T, Takaya H, Kitamura M, Nagai K, Noyori R (1987) J Org Chem 52:3174–3176
170. Wasserscheid P, Keim W (2000) Angew Chem. Int Ed 39:3772–3789
171. Baudequin C, Baudoux J, Levillain J et al (2003) Tetrahedron Asym 14:3081–3093
172. Boon JA, Levisky JA, Pflug JL et al (1986) J Org Chem 51:480–483
173. Chauvin Y, Gilbert B, Guibard I (1990) J Chem Soc. Chem Commun 23:1715–1716
174. Guernik S, Wolfson A, Herskowitz M et al (2001) Chem Commun 22:2314–2315
175. Berger A, de Souza RF, Delgado MR et al (2001) Tetrahedron Asym 12:1825–1828
176. Liu F, Abrams MB, Baker RT et al (2001) Chem Commun 5:433–434
177. Brown RA, Pollet P, McKoon E et al (2001) J Am Chem Soc 123:1254–1255
178. Jessop PG, Stanley RR, Brown RA et al (2003) Green Chem 5:123–128
179. Wolfson A, Vankelecom IFJ, Jacobs PA (2003) Tetrahedron Lett 44:1195–1198
180. Burk MJ, Feng S, Gross MF et al (1995) J Am Chem Soc 117:8277–8278
181. Xiao J, Nefkens SCA, Jessop PG (1996) Tetrahedron Lett 37:2813–2816
182. Uemura T, Zhang X, Matsumura K et al (1996) J Org Chem 61:5510–5516
183. Jessop PG, Ikariya T, Noyori R (1999) Chem Rev 99:475–493
184. Sheldon R (2001) Chem Commun 23:2399–2407
185. Finotello A, Bara JE, Narayan S et al (2008) J Phys Chem B 112:2335–2339
186. Olivier-Bourbigou H, Magna L (2002) J Mol Catal A Chem 182:419–437
187. McLean AJ, Muldoon MJ, Gordon CM et al (2002) Chem Commun 17:1880–1881
188. Anthony JL, Maginn EJ, Brennecke JF (2002) J Phys Chem B 106:7315–7320
189. Talaty ER, Raja S, Storhaug VJ et al (2004) J Phys Chem B 108:13177–13184
190. Chaudhari RV, Bhanage BM, Deshpande RM et al (1995) Nature 373:501–503
191. Gordon CM (2001) Appl Catal A 222:101–117
192. Cammarata L, Kazarian SG, Salter PA et al (2001) Phys Chem Chem Phys 3:5192–5200

193. Wolfson A, Vankelecom IFJ, Jacobs PA (2005) J Organomet Chem 690:3558–3566
194. Crosthwaite JM, Muldoon MJ, Aki SNVK et al (2006) J Phys Chem B 110:9354–9361
195. Driessen-Hölscher B (1998) Adv Catal 42:473–505
196. Horvath I, Rabai J (1994) Science 266:72–75
197. Suarez PAZ, Dullius JEL, Einloft S et al (1996) Polyhedron 15:1217–1219
198. Wagner M (2004) Chim Oggi 22:17–21
199. Floris T, Kluson P, Muldoon MJ et al (2009) Catal Lett doi:10.1007/s10562-009-0233-3
200. Floris T, Kluson P, unpublished results
201. Hashiguchi S, Fujii A, Takehara J et al (1995) J Am Chem Soc 117:7562–7563
202. Xiaohua H, Jackie Y (2007) Chem Commun 18:1825–1827
203. Ying JY (2006) Chem Eng Sci 61:1540–1548
204. Badley RD, Ford WT (1989) J Org Chem 54:5437–5443
205. Schmidt-Winkel P, Lukens WW Jr, Zhao D et al (1999) J Am Chem Soc 121:254–255
206. Samec JSM, Bäckvall J-E, Andersson PG et al (2006) Chem Soc Rev 35:237–248
207. Noyori R, Hashiguchi S (1997) Acc Chem Res 30:97–102
208. Halpern J, Harrod JF, James BR (1966) J Am Chem Soc 88:5150–5155
209. Basu B, Mandal B, Das S et al (2008) Beilstein J Org Chem 4:53
210. Isaeva V, Sharf V, Nifant'ev N et al (1998) Stud Surf Sci 118:237–243
211. Parambadath S, Singh AP (2009) Catal Today 141:161–167
212. Zhao D, Feng J, Huo Q et al (1998) Science 279:548–552

Chapter 10
Oxidations Mediated by Heterogenized Catalysts

Paulo Forte and Dirk De Vos

Abstract Metal complex oxidation catalysts can be heterogenized with the aim of improving the practicality of their use. This review discusses general factors that are decisive for the best immobilization strategy, such as nature of the metal and of the oxidant. The general approach is illustrated with specific recent examples.

10.1 Introduction

The immobilization of homogeneous catalysts is presently one of the most endeavouring areas of heterogeneous catalysis. It offers as advantages the retainment of the catalyst's structure – ideal in the cases where the catalytic action is well studied and already solidly applied even in industrial processes – its stabilization and that of its activity and, in many cases, ease of fabrication and even interchangeability of the immobilized catalyst. All these characteristics permit the use of fixed-bed reactors, lowering process costs and waste. The importance of oxidation reactions and their catalysis has increased greatly in the last decades. The oxidation of hydrocarbons and other organic molecules, as a result of the need to minimize waste and maximize efficiency in the petrochemical, base chemical and fine chemical industries, is one of the examples to showcase its relevance. In light of this, the immobilization of oxidation catalysts, though a challenging field, has attracted numerous research contributions over the last years. The importance of this field is much more evident in a time when environmental viability issues come into play almost as prominently as economic ones. Considering factors such as disposal, toxicity or environmental harmfulness of processes and their constituents is now of as much importance as their cost. The overall objective is, like in all areas dealing with homogeneous catalyst immobilization, to achieve optimal separation, recovery and

P. Forte and D. De Vos (✉)
Centre for Surface Chemistry and Catalysis, Department M2S, Katholieke Universiteit Leuven, Kasteelpark Arenberg 23, 3001 Leuven, Belgium
e-mail: Dirk.DeVos@biw.kuleuven.be

P. Barbaro and F. Liguori (eds.), *Heterogenized Homogeneous Catalysts for Fine Chemicals Production*, Catalysis by Metal Complexes 33,
DOI 10.1007/978-90-481-3696-4_10, © Springer Science+Business Media B.V. 2010

recyclability of the often toxic and expensive catalysts through their heterogenization, whilst preferably enhancing their activity. When dealing with oxidation catalysis, which usually involves the use or formation and manipulation of oxometal complexes and other metal–oxygen bonds, the inhibition of undesired interactions between catalyst molecules will lead to the enhancement of their stability and thus prevent their deactivation, either by oxidative degradation or by the formation of μ-oxo-bridged dimers or other oligonuclear entities.

In this chapter, the techniques for immobilization of oxidation catalysts are discussed and some of the latest and most relevant literature is reviewed. The focus will be on metal-catalyzed, synthetically relevant reactions of organic compounds in the liquid phase using environmentally and economically acceptable oxidants. The latter include molecular oxygen, hydrogen peroxide and certain organic peroxides. Chiral catalysts are not discussed in extenso. The role of each factor, such as the type of solid support or the metal complex and the matters of stability and heterogeneity are also presented.

10.2 General Considerations

10.2.1 Immobilization Methods

The choice of immobilization method is intimately related with the kind of complex and the reaction to be performed [1, 2]. Generally speaking, the choice of immobilization procedure is not affected by the fact that the reaction to perform is an oxidation reaction and all the common immobilization methods, such as adsorption, physical entrapment, electrostatic immobilization, are liable to be employed. However, the mechanism of the reaction has to be understood to a full extent to achieve a catalytic system that is stable throughout all the reaction steps. This means that the immobilization of the metallic centre has to be assured for all the oxidation states it goes through during the catalytic cycle. Also to be taken into account is the formation of charged intermediates, polar or even coordinating by-products and/or products of the reaction which can also cause the degradation of the system either by deactivation of the catalyst or leaching.

10.2.1.1 Adsorption

This is the most time- and cost-effective procedure for immobilization of a homogeneous catalyst. The adsorption is usually effected by van der Waals interactions between groups such as aromatic systems [3, 4], by interactions between H-bond donors and acceptors and others. The scope of this technique, however, is quite limited: the surface of the supports is most of the time of polar nature, limiting the application to the immobilization of catalysts with polar ligands. The adsorptive interactions

are rather weak, and can be disrupted by solvent effects or competition from oxidation products or polar oxidants.

The range of supports that are used with this technique is broad. Both amorphous and crystalline materials, such as silica and zeolites, are examples of supports that are suitable to form non-covalent bonds, e.g. H-bonds, with the molecular catalyst to be immobilized [4–6].

10.2.1.2 Electrostatic Immobilization

The immobilization by electrostatic interactions is a simple and fast approach to the fabrication of heterogenized catalytic systems [7]. The ease of application of the catalyst to the support and even its exchange by playing with solvent polarity and ion affinity make this an attractive technique, when the conditions for its application are met. The scope of this technique is limited by its own nature as only charged catalysts are liable to be immobilized in this manner. While in the fields of hydrogenation, hydroformylation or even cross-coupling the sulfonation of phosphine ligands is a generally applicable concept to make complexes ionic [8], there are only few cases within oxidation catalysis in which sulfonation of a ligand will result in a charged active complex. One such example is the use of bathophenanthroline [10] as a ligand for Pd in alcohol oxidations, or of sulfonated phthalocyanines containing Fe or Mn [9]. On the other hand, quite a few oxoanions that are active catalysts for oxidations are themselves already negatively charged. Also, the weak nature of the interaction with the support hinders somewhat the range of applications because of possible competition with ionic reaction substrates or even oxidants like hypochlorite.

As is obvious, charged supports are the choice for this immobilization method. Ion-exchange resins, zeolites, clays or layered double-hydroxides, are all susceptible of being used as supports. One case worth mentioning is the immobilization of molybdenum oxychloride via electrostatic interactions with Nafion [11], an organic cation-exchange resin with a fluorinated hydrocarbon backbone, which confers a strongly electron-withdrawing nature to this support and, consequently, the possibility of activation of the catalyst by enhancement of its Lewis acid character.

10.2.1.3 Physical Entrapment

This is a technique that works on the encapsulation of the catalyst inside pores of the support, rather than relying on the physicochemical interaction between the surface of the support and the catalyst. As a distinguishing advantageous characteristic in comparison with the other techniques, encapsulation presents the fact that the homogeneous catalyst, when immobilized, will not suffer a change in its structure, which could possibly be detrimental to its function. Also, the chemistry of the complex is unaltered, which might not be the case when there is chemical interaction with the support surface either by the ligand or the metal centre. Another advantage is the impossibility of catalyst deactivation by oligomerization, since

each catalyst molecule is encased in a well-defined cage from which, by definition of encapsulation and because of the complex's size, there is no exit and, therefore, no interaction with neighbouring homologues. Because the encapsulation requires a complex of a well-defined size, the range of applications is limited. Another disadvantage is the low mobility of substrates inside the support's channels and pores, when occupied with the metal complex, potentially causing a diffusion limitation. However, as a counterpart, if the entrapped complex is stable throughout the reaction, there is no leaching possible. This, coupled with the already mentioned retainment of the catalyst structure, makes this technique very useful for the immobilization of metal complexes with bulky ligands such as porphyrins, phthalocyanines [12], bipyridine [13–15], tetradentate Schiff bases, etc.

The supports for this immobilization approach are often crystalline and contain cages. Such supports are zeolites, mesoporous silica or coordination polymers, among others. There are two ways of constructing such a catalytic system: build the catalyst inside the support or the support around the catalyst. The first strategy is termed the ship-in-a-bottle approach, in which each component of the complex is inserted in turn into the support's cages. The ligands, which themselves may be formed inside the supports' pores and cages, will be made to react with the metal, already immobilized by adsorption or ion exchange, forming the complex, which will then be too bulky to leave the confinement. As the conditions usually applied for complex synthesis are relatively mild, the formation of the complex inside the support does not affect the solid's structure and/or chemistry. Examples of the application of such a method include the formation in situ of phthalocyanines or porphyrins [16] or the insertion of the whole ligand, as in the case of bipyridine [14].

The other approach, often termed envelopment, consists in the construction of the solid support's framework around the already formed complex which acts as a template. An advantage of this method in relation to the ship-in-a-bottle one is the ability to immobilize well studied complexes without any tampering with the structure while at the same time avoiding contamination with unreacted components. A drawback of the method is in the relatively harsh conditions of the support's synthesis, which implies that only metallic complexes that are stable in those conditions can be employed in this case. For instance, most zeolites are prepared between pH values of 11–14, and at temperatures up to 200°C, and few metal complexes survive these conditions, with the highly aromatic and robust phthalocyanines as an example [17]. Even then, it is not always easy to control the amount of complex that can be incorporated per weight of support.

10.2.1.4 Covalent Binding

The immobilization of the catalyst via covalent bonding is, chemically speaking, the option that yields the most stable systems. Because the immobilization method relies on the chemical modification of the ligand to incorporate a linking group that attaches to the support it is also a very ubiquitous technique: virtually all metal complexes are, in principle, liable to such modification and therefore suitable to be

immobilized in this manner [18–24]. However, the chemical modification premise is also its greatest disadvantage. Regardless of whether the modification is being applied to the ligand before complex formation or to the complex itself, the inherent costs and possibly unfavourable reaction conditions of the chemical modification have to be weighed in against the advantages when considering such a process. Like in other immobilization methods, the complexity of the system also offers some drawbacks and care has to be taken to optimize certain parameters, especially regarding the potential loss of catalytic activity by di-or oligomerization reactions due to an inadequate surface coverage.

In an analogous manner as in the case of immobilization by physical entrapment, the complex can either be fitted with the linker group and made to react with and attached to the preformed support; or it can be functionalized in such a manner that the linker contains a monomer unit of the support and the latter is formed in situ, "enveloping" the attached complex [25]. The latter is termed the sol-gel procedure, while the first is usually named 'grafting' of the catalyst onto the support. Suitable polymerizable units are obviously vinyl groups, but also Si-based functional groups such as silicon alkoxides or silicon chlorides.

10.2.1.5 Framework Substitution

In rare cases, a metal catalyst, typically a cation, can be immobilized by isomorphous substitution in a framework [26]. This first implies that the general conditions for this process are met: the introduced ion needs to have a similar size and an equal or smaller charge than the original ion, thus minimizing framework lability or charge build-up. The technique has especially been applied with silicate or aluminosilicate zeolites, and with aluminophosphates. The most prominent successful example is that of Titanium silicalite-1 (TS-1), which is isostructural with the widely applied acid catalyst H-ZSM-5, with which it shares the MFI topology. In TS-1, part of the Si^{4+} of the silicalite framework has been replaced with Ti^{4+}. The active site of TS-1 has been much debated, but there is little doubt that at least 2 and likely 3 of the original -O-Si links are still on place, firmly withholding the Ti in the structure. Moreover, in the typical TS-1 reactions, like epoxidation, phenol hydroxylation or ammoximation, the valence state of the Ti is constant at + 4, which minimizes the strain on the lattice. The Ti approach has been extended to other zeolites with larger pores, such as Ti-Beta and Ti-Al-Beta [27], or Ti-MCM-22 [28], and to mesoporous materials like Ti-MCM-41 or Ti-SBA-15 [29]. The difference with an amorphous Ti-Si mixed oxide gradually fades away if one moves from the zeolites to the mesoporous materials. Another well-discussed class of substituted materials are the microporous aluminophosphates, which come with numerous topologies such as AFI, AEL etc. The Al^{3+} in these materials can be replaced by Cr^{3+}, by V^{4+} or by Co^{2+}. While the charge balance is respected for Cr, it is perturbed for V and Co. The consequences need to be considered case per case. Thus, as it turns out, the frameworks of AlPO-5 and AlPO-11 are flexible enough to accommodate both Co^{2+} and Co^{3+}, and CoAPO-11 is a truly heterogeneous catalyst for

alkane oxidation [30]. However, as will be discussed below, more severe issues of leaching can be encountered with V- and Cr-containing molecular sieves.

10.2.1.6 Supported Ionic Liquid Phases

In keeping with the intense research in the field of ionic liquids (IL) and their applications, also the immobilization of homogeneous catalysis seems to take advantage of these materials' unusual characteristics [31]. Most usually, a coating of IL is deposited on the surface of the support, by either non-covalent – adsorption or electrostatic interaction – or covalent binding of a primary monolayer and a subsequent layer of the liquid, yielding a supported IL phase (SILP), analogous to the already established family of supported aqueous phase catalysts. In this manner, the also well-established chemistry of biphasic IL-solvent systems is improved with the great increase in surface area relative to volume and the subsequent elimination of the issue of difficult diffusion of the substrate inside the IL phase. The ionic liquid phase's properties, such as polarity, presence of certain functional groups, etc., can be easily adjusted in order to tune the interactions with the metal complex and the substrate and, at the same time, maintain the aspects which make them such good supported liquid phases, such as negligible volatility or the stable interactions with the support. This factor, coupled with the ease of fabrication and, by means of solvent play, the easy switch of the immobilized liquid phase, makes this an interesting method for the optimization of the use of fixed-bed reactors.

The virtually inexistent vapour pressure of these solvents makes SILP catalysts ideally suited for gas-phase reactions: positive arguments are the inalterability of the IL phase in relation to the substrate phase, in terms of concentration of catalyst, and the ease of separation of the products from the supported phase. Catalysis in liquid phase is also viable using this type of catalytic system, provided that all constituents are tuned to avoid leaching of the ionic liquids and/or the catalyst into the mobile phase [32].

10.2.2 Oxidants

In principle, the factors that rule the choice of oxidant for an immobilized catalyst are no different than those for the corresponding homogeneous system. As usual, there are three major aspects in play: chemical, environmental and economical reasons will determine the chosen oxidant. Approaching the matter from the chemical point of view, an oxidant is more useful the better its selectivity is and the larger its active oxygen content is. Molecular oxygen and hydrogen peroxide, cheap reactants with innocuous reaction products, are the best choices for active oxygen content, but their selectivity is many times not good and their reactions sometimes difficult to control. Efficiency of H_2O_2 utilization is a particular concern. Other oxidants commonly used are alkyl hydroperoxides (ROOH), the reduction products

of which are not as innocuous as in the previous examples, but by far not as hazardous as for certain inorganic oxidants like Jones' reagent or pyridinium chlorochromate, or potassium permanganate. Other, rather environmentally harmful organic oxidants are sometimes used, such as iodosylbenzene or *N*-methylmorpholine-*N*-oxide, but mainly for study purposes, as the general tendency is to eliminate environmental risks as much as possible.

10.2.3 Metal Catalysts

The type of metal catalyst and the oxidant will have a preponderant role in the development of the oxidation reaction. Pathways such as radical formation or formation of oxometal species are determined by the metallic centre, its oxidation state and the reactivity of the oxidant.

10.2.3.1 Peroxide Oxidants

This type of oxidants can react by either homolytic or heterolytic scission of the O–O bond. The latter can proceed via peroxo- or oxometal complexes as active species. The activation of a peroxide by the metal in the formation of a peroxometal complex requires a metal species in its highest oxidation state and one that is both a strong Lewis acid, to activate the peroxide, and a weak oxidant, to avoid one electron oxidation of the peroxide. In fact, the oxidation state of the metal species does not change during the catalytic cycle and its action is ensured only by the Lewis acid character. The most electron-deficient ions of the left-hand side of the transition metal part in the Periodic Table, such as Mo(VI), W(VI), Re(VII), Ti(IV) or V(V) are the ones that best fit this description.

The oxometal pathway requires a two-electron oxidation of the metal species. The formation of the oxometal complex occurs by heterolytic scission of the O–O bond and transfer of one oxygen atom from ROOH or H_2O_2. Examples include some Mn(III) and Fe(III) compounds.

Metals that easily undergo one-electron redox processes, like Cu (I/II), Mn (II/III), Fe (II/III), V(IV/V), are more prone to the homolytic activation of the peroxide to form free radical intermediates.

10.2.3.2 Molecular Oxygen

Oxidation by molecular oxygen often involves free radical pathways and the formation of ROOH intermediates [33, 34]. These reactions may proceed selectively though with the aid of a coreductant. In the case these coreductants are aldehydes or alcohols, these systems mimic monoxygenases and are called Mukaiyama systems [35]. In immobilized systems, however, these can be detrimental because of the formation

of polar groups, such as acids, which can cause leaching of the catalyst by competitive binding to the supported metal complex.

Some late transition metal ions catalyse the oxidation of alcohols via ß-hydride elimination from a metal alkoxide. The closing of the cycle most likely involves the insertion of molecular oxygen into the M–H bond and formation of H_2O_2. A typical metal is palladium. The oxidation of olefins to ketones using dioxygen as the terminal oxidant follows a similar pathway. Many new versions of this classical 'Wacker' chemistry are now around [36].

10.2.4 Supports

When choosing a support for the immobilization of a homogeneous catalyst, two major aspects have to be considered: the stability of the system and its chemical efficiency. The attached metal complex must be well dispersed throughout the surface of the support – for a better activity of the catalyst and better diffusion conditions – and this system must be able to endure the reaction conditions, both chemically and physically, to be able to achieve its maximum of efficiency. In order to ensure good reaction conditions, other parameters also have to be analysed, such as surface charge, polarity and acid–base properties for good interaction with reactants and substrates, and particle and pore size for good diffusion of the reaction constituents.

10.2.4.1 Organic Supports

Organic polymer supports present a high degree of tunability, due to the ability to adjust the amount of cross-linking, the nature of the backbone, the nature of the side chains, and the presence of a spacer between the support and the complex [37, 38]. Their ease of synthesis aids this customizability in the sense that the desired polymer can be made with simple organic synthetic techniques. The most usual polymer types contain a polystyrene or polyacrylate backbone. The most usual methods of immobilization used with these kinds of supports are electrostatic immobilization – when the polymer is functionalized with a charged group, as in the case of ion-exchange resins [7] – or covalent binding, when the functionalization is with polar, complexating groups that bind the metal. In this latter case, there exists also the possibility to construct the polymer around the complex, "enveloping" it, as already seen when discussing the various immobilization methods. In this aspect, the customizable side of these supports also plays a role, in the possibility to control the number and positioning of the complexes.

This kind of material presents as its major disadvantage its limited temperature range, when compared with inorganic supports and its possible instability in oxidative conditions. In these conditions, the most appropriate would be the use of a backbone that prevents such undesired degradation reactions, such as polybenzimidazole,

polyimide or polydimethylsiloxane [38, 39]. Another drawback is the possibility of swelling, which happens to some of these supports when using certain solvents.

10.2.4.2 Inorganic Supports

This type of materials is by far the most widely used in immobilization of homogeneous catalysts. In opposition to the previously seen organic supports, these are chemically and thermally stable, being able to endure the high temperatures usually used in the industry and resisting the oxidative conditions. Also an advantage relative to the previous case is the absence of swelling, which makes them suited for reactions in fixed-bed continuous-flow reactors. There are several major classes of inorganic supports, including silica, alumina, titania, but also microporous materials like zeolites.

The silica-based supports can be either amorphous or pseudocrystalline and ordered with mesopores. They present high surface areas and, in the case of the latter, well defined and stable uniform mesoporous cavities. Both are easily available commercially. The preferred method of immobilization is covalent binding, taking advantage of the surface silanol groups. Also possible is adsorption by hydrogen bond formation with said groups. The combination of one of these methods with an ionic liquid layer makes them also prime materials for the fabrication of SILPs.

Zeolites, with their crystalline frameworks and well defined cavities are more usually used for the physical entrapment of homogeneous catalysts. Examples of ion pair formation between the support and charged metal complexes by ion exchange are also abundant: the negatively charged zeolites, as well as clays, can immobilize cationic metal complexes.

Other commonly used supports are the negatively charged layered double hydroxides (LDH) [40] - which immobilize anionic metal complexes - , crystalline microporous aluminophosphates and hydroxyapatites, alumina and titania.

10.2.4.3 Metal-Organic Frameworks

Metal-organic Frameworks (MOFs) are a quickly developing class of coordination polymers, i.e. hybrid materials in which the metal centres are connected by rigid organic linkers, forming a lattice [41, 42]. In the case of their application to immobilization of homogeneous catalysts, the complexes can be part of the structure of the solid material. In this way, the metal centres that perform the catalysis are always accessible in a rigid structure [43]. However, because a change in the metal species or in the ligand of the catalytic complex implies a change in the structure of the solid, its stability must be tested in addition to the catalytic activity. To increase rigidity, the metal centres are usually fully coordinated, which somehow counteracts their activity, as open coordination sites are needed for activation of oxidants or reagents. Therefore materials have been developed with two types of metal function: one metal functions as the node points of the structure, while the other metal is fully integrated in the polycipital linker, and thus procures the activity.

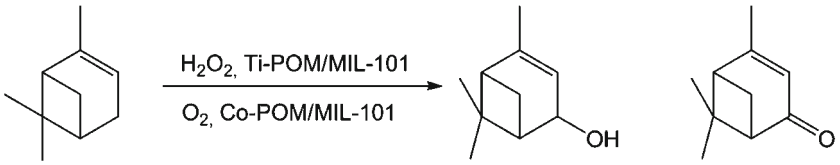

Scheme 10.1 Oxidation of α-pinene to verbenol and verbenone

A fine example of the encapsulation strategy is found in the entrapment of heteropolyacids like $[PW_{11}CoO_{39}]^{5-}$ and $[PW_{11}TiO_{40}]^{5-}$ in the metal-organic framework MIL-101. MIL-101 is an exceptionally stable framework formed from Cr^{3+} and terephthalate as the organic linker. Its unusual architecture contains two cage types with diameters of 2.9 and 3.4 nm, to which the access is controlled by windows with a free aperture of 1.2 and 1.5 nm respectively. As proposed in the original report by Férey [44], Keggin ion type structures, with a typical diameter of 1.3 nm, are only expected to have access to the largest cages. Even a simple adsorption seems sufficient to ensure irreversible retention of the polyanion by the MOF structure; about 1 polyoxometallate (POM) anion per large MIL-101 cage cannot be removed by desorption with acetonitrile. Note nevertheless that the MIL-101 framework is essentially neutral; encapsulation of the anionic polyoxometallates implies that some charge-compensating cations, e.g. Na^+ or H^+, must be absorbed along with the Keggin anions. It has also been proposed that the polyoxometallate is retained by electrostatic interactions with Cr^{3+} in the structure, which implies that some the fluoride anions bound to Cr should be displaced. Composites of MIL-101 and $[PW_{11}CoO_{39}]^{5-}$ or $[PW_{11}TiO_{40}]^{5-}$ were evaluated as catalysts for the oxidation of bulky reactants like α-pinene and caryophyllene [45]. Both with O_2 and H_2O_2 as the oxidants, α-pinene was oxidized via free radical reactions to its allylic oxidation products verbenol and verbenone (Scheme 10.1):

Using the Co-POM and O_2, the activity and selectivity were essentially stable over five reaction cycles; but the Ti-POM/MIL-101 in the presence of H_2O_2 and at elevated temperature suffered from structural degradation of the MOF framework.

10.2.5 Leaching

In immobilized oxidation catalysis this is a major issue, due to the nature of the constituents: oxidants, products, byproducts and even intermediates. These compounds will, by consequence of their oxygen content, have a strong affinity to coordinate the metal centre. While this can prove to be a positive aspect – if required conditions are met – in the case of the oxidants to facilitate the reaction, this coordination may nevertheless disrupt the metal-support interaction in some way. Deactivation of the catalyst can occur, when coordinated to unwanted ligands, and, if this coordination affects the complex's or the metal's immobilizing interactions with the support, leaching will ensue.

The proof of heterogeneity of an immobilized homogeneous catalyst is the lack of catalytic activity of the solution obtained by filtration of the heterogeneous system [46]. This proof can only be properly obtained when the filtration is performed at the reaction conditions to test the, sometimes synergetic, effects of temperature, presence of oxidants, of coordinating compounds or solvent in the stability of the immobilized catalyst. For this reason, to ensure that all the system's constituents are present, it is important that the heterogeneity test must be performed before completion of the reaction.

Leaching can be minimized or prevented by choosing the correct immobilization method. As seen, methods that rely on the physicochemical interaction with the support, like covalent binding or even adsorption, can always be liable to suffer degradation by leaching through the severing of the bond between the catalyst and the support, whereas a physical entrapment of the complex will make this impossible unless there is disruption of the complex itself. On the other hand, the reaction components can also be tweaked to reach a set of conditions that minimize leaching. Among these adjustments, as the presence of complexating side-products can cause leaching, a lower loading of the catalyst lowers the conversion of the reagents and so the formation of detrimental interactions can be avoided [30]. Also, the choice of solvent or other reaction components, like acids or bases, will be important to ensure the heterogeneity of the system, as some solvents, like acetic acid, or bases, like alkoxides, can complex metal centres or even damage the interaction with the support.

10.3 Two-Electron Reactions

These form the largest class of selective oxidation reactions in the liquid phase. Their catalysis does not necessarily involve two electron reduction of the metal centre, but can also be accomplished by Lewis acid action, or by two consecutive one-electron transfers and regenerations of the metal centre.

10.3.1 Epoxidations

The epoxidation of olefins is a very useful and consequently very well studied reaction. Hence, the range of catalysts and oxidants used to perform this reaction is broad.

10.3.1.1 Manganese and Iron

Manganese and *iron*'s chemistry are to some extent similar, and so are the methods for their immobilization. The mechanism of epoxidations catalyzed by these metals often involves the formation of oxometal complexes, via a two-electron oxidation of the metal centre, following activation of peroxides. Their homogeneous complexes,

when in the most oxidized oxometal state, usually go through a process of deactivation by dimerization or bimolecular reaction which is avoided when the catalyst is immobilized, leading to higher activities.

The range of immobilization methods for these complexes is broad. The extended π system of porphyrin or phthalocyanine complexes offers the possibility of adsorption on the surface of such supports as carbon [47]. The positive charge of these complexes also allows for the formation of ion pairs with negatively charged supports. A usual immobilization method is also covalent binding: Mn(II)-porphyrin, -phthalocyanine or -Schiff-base complexes were immobilized onto SiO_2 by grafting and sol-gel procedures [25, 48]. The coordinative anchoring of a tethered Lewis base such as pyridine or imidazole to the axial position of planar complexes offers an interesting alternative, in terms of catalyst activity. However, these planar complexes present a selectivity limitation, strongly preferring *cis*-olefins over *trans*-olefins. Immobilization by axial coordination on a planar complex is also less stable than covalent binding.

The bulky character of these complexes, as well as of other, non-planar, Mn and Fe complexes, makes them also good candidates for entrapment inside cages of crystalline supports, such as zeolites or even MOFs [49]. This method will prevent the deactivation by dimerization of the catalyst; the enhanced peroxide activation, which before led to decomposition of the oxidant in a bimolecular complex, now is taken advantage of for epoxidation reactions. In case the ligands are small, the formation of dimeric complexes is also possible, inside more spacious cavities of some supports like faujasite zeolites [50]. However, for entrapped planar complexes like porphyrins or phthalocyanines, the large size of the complexes is also their biggest disadvantage: a poor access of the substrate to the active site accounts for many reports of low activity, when compared with the homogeneous counterparts [51, 52].

Mn(II)-salen complexes were also used in supported ionic liquid phase materials to perform epoxidations. These reactions afforded better results than the homogeneous counterparts and no leaching was observed [53]. The same kind of Mn(II) complexes were immobilized in a Zn-based metal-organic framework. In this case, as is the norm with catalyst immobilization with these materials, the complex is part of the structure of the support, which means that each site's neighbourhood is well defined and its position rigid, which offers stability against bimolecular deactivation pathways [54].

10.3.1.2 Titanium

Immobilized *titanium* complexes are also used for epoxidation reactions. Their preferred method of immobilization is covalent binding on the surface of silica, by direct attachment of the metal atom to surface silanol groups, forming Si–O–Ti bonds. The supports' ligands act as electron acceptors, increasing the Lewis acidity of the metal. These materials are prepared by reaction with a Ti complex. At contrast with the framework substituted material TS-1 which prefers H_2O_2, most of the immobilized Ti complexes have an alkyl hydroperoxide as the oxidant of choice.

The relatively unhindered complex and the large porosity of the material accounts for high activities with bulky substrates. Alternatively, modification of the silica surface with alkoxy triazine functions and subsequent complexation of Ti affords a possibility to tune the loading of the catalyst and its surroundings, adjusting its hydrophobicity [55].

10.3.1.3 Cobalt

Cobalt, usually employed for one-electron reactions, was nonetheless used for the epoxidation of olefins with the aid of isobutyraldehyde as co-reductant [6]. Co(salophen) complex immobilized by adsorption on a montmorillonite clay performed the reaction with 92% conversion and 84% selectivity.

The oxidation of cyclohexene by a Co-salen complex adsorbed on SBA-15, a mesoporous silica material, was studied by Luque et al. [56], who, by performing the reaction under microwave conditions, achieved the oxidation of cyclohexene to the epoxide, the enol or the enone. The selectivity was dependent on factors like microwave power, catalyst loading and reaction time. Although relatively moderate conversions were achieved when tuning the system for epoxidation of the alkene, a yield of 89% and 99% conversion was achieved for the preparation of the enone. This method afforded high conversions and selectivities for each of the oxidation reactions in mild conditions, when compared with other works (Scheme 10.2).

10.3.1.4 Molybdenum

Homogeneous *molybdenum* catalyzed epoxidation of olefins with alkyl peroxides is a very efficient and well established method, used in industry [57–59]. Molybdenum has a strong affinity for organic ligands, which is why its immobilization usually involves binding to organic polymers, functionalized with groups such as 1,2-diols, carboxylic acids, nitroxides, amines, etc. [60–62]. The binding to organic polymers implies however a temperature limitation due to degradation of the support. To overcome this, polybenzimidazole and other, previously mentioned, thermally resistant polymers have been used. Polybenzimidazole has the advantages of good thermal resistance and good affinity towards the Mo complexes [39]. The catalysts' predilection for binding to organic nucleophilic groups can also be a disadvantage: side-products such as diols can bind strongly to the metal, causing its deactivation.

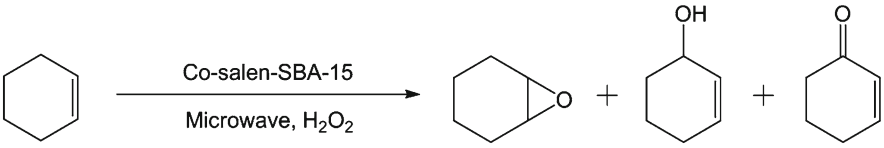

Scheme 10.2 Oxidation of cyclohexene to the epoxide, enol and enone, with H_2O_2 and a Co-salen catalyst on mesoporous silica SBA-15 under microwaves

10.3.1.5 Ruthenium

Planar *ruthenium* complexes, e.g. with porphyrins as the ligand, catalyze epoxidations via Ru(V) oxo species or Ru(IV) oxo radicals, using alkylperoxides or *N*-oxides as oxidants, and leading to moderate selectivities [63–65]. Immobilization of these catalysts is done by covalent binding of the macrocycle or coordinative binding at an axial position of the complex. Entrapment of the catalyst was also reported. The site isolation of the macrocycles plays an important role in the activity of the catalyst as well as in its oxidative resistance.

10.3.1.6 Tungsten

The most commonly used *tungsten* epoxidation catalysts are negatively charged, heteronuclear peroxotungsten complexes [18, 66–69]. For this reason, their most favoured method of immobilization is by ion exchange [69]. This is helped by the fact that, throughout the catalytic cycle, the complex maintains a negative charge. Inorganic anion exchangers, like layered double hydroxides (LDH), are a typical choice for supporting these catalysts. The exchange can purposefully be made incompletely, to allow the ability to have hydrophilic or hydrophobic environments by choosing the proper co-anion (e.g., NO_3^- or an organic fatty carboxylate or sulfate [70]). This is a very stable system, with no leaching, given the proper conditions. For some highly substituted olefin substrates, these catalysts were shown to have improved performance in the presence of catalytic amounts of halide [71, 72]. In this manner, the reaction proceeds via halohydrin formation by oxidative halogenation and subsequent epoxide ring closure with release of the catalytic halogen. In this case, the oxygen atom of the epoxide originates from the solvent. The ring-closing step is complete in highly substituted olefins, but the halohydrin is usually the main product starting from mono- or disubstituted olefins.

These anionic tungsten-based catalysts can also be immobilized in quaternary ammonium-functionalized organic polymers [69]. These need to be purged of the presence of chloride, a common counter-balancing anion for these materials, since halogenations reactions can occur with the substrates. The thermal instability of these supports in comparison with the inorganic materials inspired researchers to a combination of both: an inorganic support functionalized with quaternary groups, linked via hydrocarbon spacers. Here, the activity in solvent-free systems is influenced by the spacer probably due to a balance of hydrophobicity that enables a better interaction with the active site. In this manner, a phosphotungsten complex was immobilized by electrostatic interaction with a film of covalently supported imidazole groups on silica [68]. These, in turn were quaternized to imidazolium groups by the acid character of the inorganic compound resulting in a system very similar, formally, to a SILP. The application of this catalyst in the epoxidation of a broad range of alkenes, yielded better conversions and selectivities than the homogeneous phosphotungstic acid in almost all cases. The system showed good stability and negligible leaching was observed.

The easy formation of heteronuclear compounds between peroxotungsten species and phosphorus groups is also a sound strategy in immobilization of the tungsten

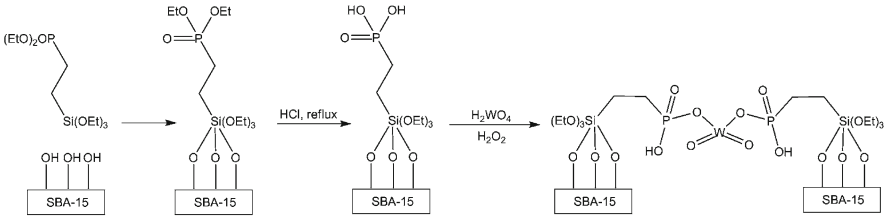

Scheme 10.3 Synthesis and proposed structure of the SBA-15-immobilized phosphonate tungsten complex

epoxidation catalysts. The approach was already presented by Hoegaerts et al. [18]. They reacted $POCl_3$ with an aminopropyl group, immobilized on silica. This results in a surface-attached phosphoramide, which can form covalent bonds with oxotungsten compounds. A variant of this approach was presented recently, as shown in Scheme 10.3 [66]. In a first step, a phosphonate moiety is anchored to a siliceous SBA-15 surface by reaction of diethylphosphatoethyltriethoxysilane. Hydrolysis of the phosphonate ester results in free phosphonic acid groups. Addition of a mixture of H_2O_2 and tungstic acid leads to anchoring of phosphotungstate species.

These immobilized tungstates can be used as selective epoxidation catalysts, e.g. for the 95% selective epoxidation of geraniol to its 2,3- and 6,7-epoxides; [18] or in the presence of an excess of the H_2O_2 oxidant, an olefin like cyclopentene can be further oxidized to ring-opened products like glutaraldehyde [66].

Another immobilization technique is the formation of peroxotungsten-containing supported ionic liquid phases (SILPs), taking advantage of the charged nature of these complexes [66]. These are stable catalytic systems, even in liquid phase reactions, with no measurable leaching.

10.3.2 Dihydroxylation

10.3.2.1 Manganese and Iron

The dihydroxylation of alkenes can be catalyzed by *manganese* or *iron* complexes in a follow-through action of these catalysts' epoxidation of olefins. Bipyridine complexes of manganese entrapped in Brönsted acidic zeolites can catalyze the opening of the epoxide ring to form *trans*-1,2-cyclohexanediol from cyclohexene [15]. Usually the *trans*-diols are obtained, although one case has been reported in which the immobilization of a Mn catalyst specifically triggered the direct *cis*-dihydroxylation of olefins [73].

10.3.2.2 Osmium

The most studied dihydroxylation catalyst is *osmium*. Tetraoxo osmium complexes can catalyze the *cis*-hydroxylation of olefins with a number of oxidants like H_2O_2,

organic hydroperoxides, *N*-oxides, etc., whose function in the catalytic cycle is to reoxidize Os(VI) to Os(VIII). A review on this subject, by Kobayashi and Sugiura [3], was published recently.

The immobilization of these catalysts by coordinative attachment to N-sites in functionalized organic polymers – e.g. pyridine or imidazole moieties – leads to leaching of the metal due to the hydrolysis of the Os(VI) intermediate that is required in the catalytic cycle and which implies the detachment from the support [74]. Also because of the cycle's intermediates, more specifically their neutral nature, the immobilization by ion-pair formation is not the best choice. Although reports have described its successful use in this case, no explanation was given for the retention of said intermediates, which leads to conclude that this technique, while applied without loss of activity, may not be the most suited.

In this case, the knowledge of the catalytic cycle offered an insight on an efficient immobilization method. The cycle involves two main steps: the attack of the Os(VIII) *cis*-dioxo complex to the olefin and the hydrolytic release of the newly-formed *cis*-diol and consequent reoxidation of Os(VI) to Os(VIII) [74, 75]. Knowing that this last step becomes increasingly difficult with increasing substitution [76] and that the metal can be reoxidized to *cis*-dioxo Os(VIII) while still possessing an attached *cis*-diolate group, it becomes clear that it is possible to immobilize the metal complex by addition of the OsO_4 to a supported tetrasubstituted olefin. The *cis*-diolate group will not detach and the metal is thus coordinatively bonded to the support. The reoxidation reaction follows, to generate the active species which will then react with the olefinic substrate, be reduced to Os(VI) and regenerated again with the exit of the product while still attached to the support. This is a highly selective and active technique with a broad scope of non-tetrasubstituted substrates.

10.3.3 Oxyfunctionalization of Alkanes

10.3.3.1 Manganese and Iron

Manganese and *iron* can catalyze the oxidation of alkanes via similar metaloxo intermediates as used for the epoxidation of olefins. The reaction of the oxometal species with a C–H bond leads, after hydrogen atom abstraction, to the formation of a carbon radical and immediate recombination with the metal-bound OH group results in an alcohol.

The porphyrin or phthalocyanine complexes of Mn and Fe can be seen as attempts to mimic the activity of cytochrome P450, one of nature's preferred oxidation catalysts [12]. The immobilization of these catalysts by encapsulation in zeolites like zeolite Y is done by synthesis of the ligand in situ and posterior complexation with the metal atom. This last step is the one that offers more complications, as the metal may not be completely chelated and residues of the "free" metal may interfere with the catalytic action of the complex, e.g. by catalyzing unproductive decomposition of the

peroxide. To avoid this, a rather stable complex of the same metal is used as the metal source, e.g. a metallocene, and metal ions will only gradually be released from the metallocene precursor complex to be chelated by the phthalocyanine. As previously mentioned, the isolation of these catalysts inside the cages of the support will enhance drastically their activity by impeding their bimolecular deactivation. The complex's activity can also be enhanced by enhancing the Lewis acidity of the metal centre. This can be achieved by the placement of electron-withdrawing groups, e.g. -Cl or -NO_2, on the periphery of the macrocycle [17, 48, 77]. A noteworthy example is the encapsulation on a Mn(II)-porphyrin catalyst in a metal-organic framework and its use in the oxidation of cyclohexane which afforded good conversions [49].

10.3.3.2 Ruthenium

An interesting immobilization method was used to support *ruthenium*-porphyrin [63–65] catalysts on an organic polymer. The complex, covalently attached to monomeric units of the support, served as template to the latter's polymerization, in a process already discussed. The nuance is that the complex was modified to include, coordinated in an axial position, a co-template, which is removed after the formation of the support. This co-template, e.g. diphenylaminomethane, was such that its shape was reminiscent of the intended substrate's shape, in this case diphenylmethane, so that the final material contains a pocket designed for the selective entrance of that substrate.

10.3.4 Oxidation of Alcohols

10.3.4.1 Palladium

Palladium complexes are some of the most studied catalysts for the oxidation of alcohols. Recently, N-heterocyclic carbenes (NHC) have come increasingly to the foreground. These important ligands possess strong σ-donor character and their Pd(II) complexes are very well studied. NHC ligands were covalently grafted on the surface of mesoporous silica and used to immobilize palladium through the formation of Pd-NHC complexes. These were, in turn, reduced to NHC-stabilized Pd nanoparticles (Scheme 10.4). Their use in the catalysis of the oxidation of benzyl alcohol with oxygen afforded almost quantitative conversions and a recyclability of up to eight times [78].

10.3.4.2 Copper

Although *copper*, with its favoured oxidation states of +1 and +2, is used mostly for catalysis of one-electron oxidations, a case has been shown of a binuclear Cu

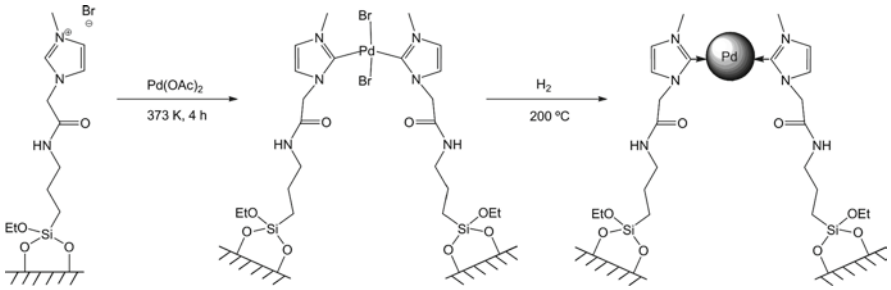

Scheme 10.4 Immobilization of Pd in NHC-modified silica

complex catalyzing the two-electron oxidation of catechol to orthoquinone [13]. In this case, the complex, two units of Cu(II)-*bis*-bipyridine or *bis*-phenantroline bridged by a hydroxyl group, $[(bpy)_2Cu\text{-}OH\text{-}Cu(bpy)_2]^{3+}$, is immobilized by encapsulation on mesoporous silica. The catechol binds to both the copper atoms with its oxygen atoms and, aided by a base and formally donating one proton to the hydroxyl group, breaks the connection between the cuprous atoms, releasing water and generating two lone $(bpy)_2Cu(I)$ complexes. Next, the hydroxyl bridge is regenerated by molecular oxygen and the oxidation of an additional molecule of substrate, completing the catalytic cycle. However, the formation of the Cu(I) complexes causes a certain amount of leaching, due to the change of size of the catalyst and the choice of immobilization method and support. The use of zeolite Y, with its smaller pores and stronger electrostatic interactions with the complexes, which stabilize the cupric complex in place allows the regeneration of the bridged complex and guarantees a successful completion of the catalytic cycle.

10.3.4.3 Ruthenium

Ruthenium is a very versatile catalyst and effects the oxidation of alcohols with molecular oxygen in the form of the lone Ru^{3+} ion. Allyllic or benzylic primary alcohols are oxidized to the corresponding aldehydes with negligible formation of acids and aliphatic alcohols. This is a very selective catalyst, capable of reacting only with the hydroxyl moiety of a molecule that can contain other groups liable to be oxidized. Despite its charged nature, this catalyst's immobilization is more commonly done by incorporation into the structure of layered double hydroxides, such as hydrotalcite [80]. In this case, the presence of cobalt in the structure is thought to play a key role in the stabilization of the Ru(V)-oxo species. Framework substitution of Ca^{2+} ions on the outer surface of hydroxyapatite or adsorption on the surface of alumina are other used methods [81, 82]. In these cases, given the basic nature of the supports, the reaction is thought to proceed via formation of an alkoxymetal complex and subsequent elimination of the carbonyl compound, leaving a metal-hydride complex which is reoxidized by O_2.

The tetraoxide of this metal, RuO_4^-, was also immobilized in an imidazolium SILP prepared by sol-gel method [83]. When compared with other similar catalytic systems, RuO_4^- presented moderate activities but the advantage of a controlled oxidation of benzyl alcohol to benzaldehyde. Leaching was not observed.

10.3.4.4 Cobalt

Cobalt(II) Schiff base complexes, as catalysts for the oxidation of alcohols to the corresponding carbonyl species, have been immobilized onto organic polymer supports in an innovative fashion, taking advantage of the efficiency of reactions of azides, be it the Copper-catalyzed [3 + 2] cycloaddition to alkynes – termed "click reaction" – or the phosphine-mediated nucleophilic attack to a carboxylic acid – the Staudinger ligation [79]. This immobilization method could be carried out either before or after the formation of the complex. These immobilized catalysts were used in the oxidation of alcohols with excellent yields and in mild conditions. Moreover, their reutilization was proved effective, with no deactivation after five runs and no leaching to the liquid phase. This implies that even complex organic linkers can possess sufficient oxidation stability (Scheme 10.5).

10.3.4.5 Molybdenum

The aerobic oxidation of alcohols catalyzed by charged polyoxometallates such as *molybdovanadates* was carried out in SILP supports [32]. The anion-exchanged ionic liquid $[C_4MIM]_5[PMo_{10}V_2O_{40}]$ was deposited on the surface of an imidazolium-modified

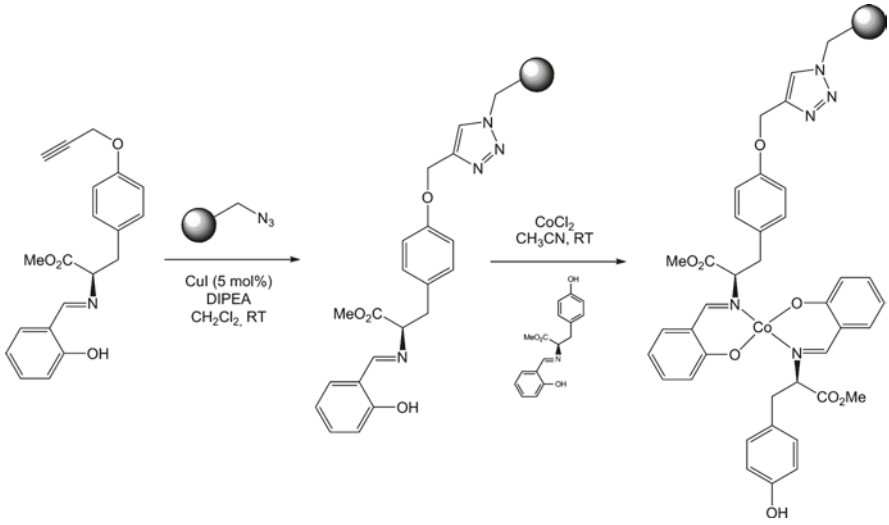

Scheme 10.5 Immobilization of the ligand via Click reaction and subsequent Co(II) Schiff base complex formation

silica support. These systems offered excellent conversions (>90%) for a broad range of substrates, showing good selectivity for the oxidation of secondary alcohols in the presence of olefins, primary alcohols and other functional groups, and no leaching is observed, as the catalyst could be reutilized up to five times with negligible loss of activity.

10.3.4.6 Manganese

In some cases, a homogeneous catalyst even can be turned into a heterogeneous one without using a true support. Ion pairing of a cationic catalyst with a well-matching anion can indeed also result in a solid material that is insoluble in common solvents used for the catalytic reaction. This was recently illustrated in a study using the oxidation catalysts based on *manganese* and the cyclic triamine ligand 1,4,7-methyl–1,4,7-triazacyclononane (tmtacn; = L). In combination with H_2O_2 and with a suitable carboxylic acid as co-catalyst, these Mn-tmtacn complexes catalyze the selective epoxidation of olefins like 1-hexene and the oxidation of alcohols like 2-hexanol with high turnover frequencies and efficiencies based on H_2O_2 [84]. Successful heterogenization attempts include encapsulation of the dimeric Mn-tmtacn complexes in the cages of a zeolite Y, or covalent attachment to a silica matrix. As an alternative approach, Veghini et al. [85] found that when a solution of $[LMn(\mu\text{-}O)_3MnL][PF_6]_2$ was mixed with the heteropolyacid $H_4[SiW_{12}O_{40}]$, a solid precipitate was formed, with as formula $[LMn(\mu\text{-}O)_3MnL]_2[SiW_{12}O_{40}]$. The catalytic activity for 2-octanol oxidation was to some extent preserved in the solid material, but the activity decrease necessitated the use of higher molar catalyst percentages than when the homogeneous counterpart was used. It is unclear whether this is due to the non-porous nature of the solid compound. Some leaching of Mn was found by elemental analysis; however it appeared that there was no activity in the filtrate, giving evidence for truly heterogeneous catalysis.

10.4 One-Electron Reaction

These reactions proceed mostly via the formation of radical species, the metal being the initiator.

10.4.1 Oxidative Coupling of Phenols

The oxidative coupling of phenols is catalyzed by unchelated *copper*(II) ions which are immobilized by ion exchange on the surface of a charged support, for example mesoporous silica [86–89]. In the presence of a base, the coupling of the phenols takes place via the formation of a phenolate radical with consequent reduction of the metal to Cu(I). Two of these radicals combine to yield the 4,4′-dihydroxybiphenyl molecule. This is a very stable technique that affords a leach-free catalysis due to the absence of competing components in the reaction mixture for the metal's charge.

10.4.2 Oxyfunctionalization of Alkanes (Radical Pathway)

10.4.2.1 Cobalt

At low conversions, in the presence of molecular oxygen, *cobalt* catalyzes the autoxidation of alkanes. The hydroperoxides formed by reaction of the oxygen with the alkane are easily broken by cobalt's II/III redox pair, initiating radical chain reactions [30]. At high conversions, however, there is deactivation by cluster formation with autoxidation side-products such as acids. Also at high conversions, the presence of the formed Co(II) may terminate the radical reaction. Another mechanism of Co action for the oxidation of alkanes is reaction of Co(III) directly with the alkane. This happens in the presence of acetic acid as solvent [90]. Because the reaction in that case does not proceed via the normal radical pathway, unusual regioselectivities are expected. These factors will influence the choice of immobilization method for this metal.

Framework substitution of the metal in aluminophosphates is the most studied system for this type of metal catalysis. The metal is protected against deactivation by cluster formation and readily accessible to the substrates. The conversion, however, must be kept low, to safeguard that all the ions are inserted in the lattice and that there are none in the counter-ion layer, which would be detrimental because of the formation of clusters and termination of the radical reactions [30]. The formation of acids, which occurs at high conversions, is prejudicial to the metal's immobilization, causing dissolution of the Co ions.

10.4.2.2 Ruthenium

One-electron oxidations of alkanes with oxygen can also be performed with the help of light and suitable immobilized photocatalysts. To this aim, SiO_2 was first functionalized with styryltrimethoxysilane; and a vinyl-functionalized *ruthenium* complex was reacted this support in the presence of AIBN in $CHCl_3$. Radical coupling ensues, with a C_4H_6 bridge between the functionalized surface and the Ru compound. UV-irradiation resulted in elimination of the p-cymene, and coordination of the Ru by a surface oxygen atom (Scheme 10.6):

In the presence of dioxygen and UV-light, cyclohexane oxidation proceeded at a constant rate for at least 6 h, with almost equal production of cyclohexanone and cyclohexanol [91] (Scheme 10.7).

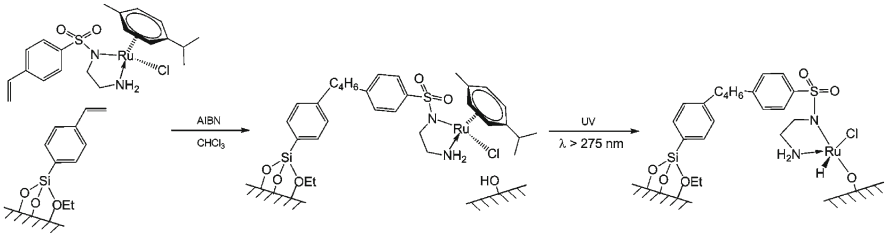

Scheme 10.6 Photoinduced synthesis of coordinatively unsaturated SiO_2-supported Ru complexes

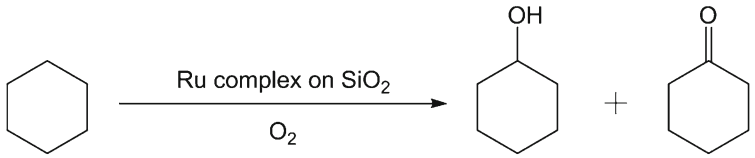

Scheme 10.7 Photo-oxidation of cyclohexane to cyclohexanol and cyclohexanone

10.5 Conclusion

This concise overview gives a fair impression of the variety of approaches that have been pursued in the immobilization of homogeneous oxidation catalysts. Over the past few years, new supports and immobilization techniques have come to the foreground, such as the supported ionic liquid phases, or the use of metal-organic frameworks. It is quintessential to have a clear view on the metal complex in all its oxidation states of the catalytic cycle before proposing an immobilization strategy. Even then, one always has to weigh the economical and environmental cost of the immobilization against the use of a homogeneous catalyst and subsequent removal of the dissolved catalyst.

References

1. De Vos DE, Sels BF, Jacobs PA (2001) Adv Catal 46:1
2. Alaerts L, Wahlen J, Jacobs PA, De Vos DE (2008) Chem Commun 15:1727
3. Kobayashi S, Sugiura M (2006) Adv Synth Catal 348:1496
4. Huang G, Liu SY, Guo YA, Wang AP, Luo J, Cai CC (2009) App Catal A Gen 358:173
5. Bahramian B, Ardejani FD, Mirkani V, Badii K (2008) App Catal A Gen 345:97
6. Jiang J, Ma K, Zheng Y, Cai S, Li R, Ma J (2009) App Clay Sci 45:117
7. Barbaro P, Liguori F (2009) Chem Rev 109:515
8. Shaughnessy K (2009) Chem Rev 109:643
9. Sorokin A, Meunier B (1994) J Chem Soc Chem Commun 1799–1800
10. ten Brink G, Arends IWCE, Sheldon RA (2000) Science 287, 1636–1639
11. Singh B, Jain SL, Khatri PK, Sain B (2009) Green Chem 11:1941
12. Parton R, Vankelecom IFJ, Casselman M, Bezoukhanova C, Uytterhoeven JB, Jacobs PA (1994) Nature 370, 541–544
13. Lee C-H, Lin H-C, Cheng S-H, Lin T-S, Mou C-Y (2009) J Phys Chem C 113:16058
14. Mori K, Kagohara K, Yamashita H (2008) J Phys Chem C 112:2593
15. Knops-Gerrits P-P, De Vos D, Thibault-Starzyk F, Jacobs PA (1994) Nature 369:543
16. Nakamura M, Tatsumi T, Tominaga H (1990) Bull Chem Soc Jpn 63:3334
17. Balkus KJ, Eissa M, Levado R (1995) J Am Chem Soc 117:10753
18. Hoegarts D, Sels BF, De Vos DE, Verpoort F, Jacobs PA (2000) Catal Today 60:209
19. Moghadam M, Mirkhani V, Tangestaninejad S, Mohammdpoor I, Kargar H (2008) J Mol Catal A Chem 288:116
20. Zhao J, Wang W, Zhang Y (2008) J Inorg Organomet Polym 18:441
21. Gao B, Zhang G, Li Y, Du R (2009) Polym Adv Tech 20:1183
22. Mureseanu M, Parvulescu V, Ene R, Cioatera N, Pasatoiu TD, Andruh M (2009) J Mater Sci 44:6795

23. Shamim T, Gupta M, Paul S (2009) J Mol Catal A Chem 302:15
24. Masteri-Farahani M (2010) J Mol Catal A Chem 316:45
25. Stamatis A, Giasafaki D, Christoforidis KC, Deligiannakis Y, Louloudi M (2010) J Mol Catal A Chem 319:58
26. Bellussi G, Rigutto M (1994) Stud Surf Sci Cat 85, 177–213
27. Camblor MA, Constantini M, Corma A, Gilbert L, Esteve P, Martinez A, Valencia S (1996) Chem Commun 1339–1340
28. Wu P, Tatsumi T, Komatsu T, Yashima T (2001) J Phys Chem B 105, 2817–2905
29. Luan Z, Maes E, van der Heide P, Zhao D, Czernuszewicz RLK (1999) Chem Mater 11, 3680–3686
30. Vanoppen DL, De Vos DE, Genet MJ, Rouxhet PG, Jacobs PA (1995) Angew Chem Int Ed 34:560
31. Gu Y, Li G (2009) Adv Synth Cat 351:817
32. Bordoloi A, Sahoo S, Lefebvre F, Halligudi SB (2008) J Catal 259:232
33. Mallat T, Baiker A (2004) Chem Rev 104:3037
34. Mishra GS, Alegria ECB, Martins LMDRS, Silva JJRFd, Pombeiro AJL (2008) J Mol Catal A Chem 285:92
35. Mukaiyama T, Yorozu K, Takai T, Yamada T (1993) Chem Lett 22, 439–442
36. Stahl S (2004) Angew Chem Int Ed 43:3400
37. Bergbreiter D (2002) Chem Rev 102:3345
38. Mandoli A, Lessi M, Pini D, Evangelisti C, Salvadori P (2008) Adv Synth Catal 350:375
39. Leinonen S, Sherrington DC, Sneddon A, McLoughlin D, Corker J, Canevali C, Morazzoni F, Reedijk J, Spratt SBD (1999) J Catal 183:251
40. Sels BF, De Vos DE, Jacobs P (2001) Catal Rev Sci Eng 43:443–488
41. Farrusseng D, Aguado S, Pinel C (2009) Angew Chem Int Ed 48:7502
42. James SL (2003) Chem Soc Rev 32:276
43. Ma LQ, Abney C, Lin WB (2009) Chem Soc Rev 38:1248
44. Férey G, Mellot-Draznieks C, Serre C, Millange F, Dutour J, Surblé S, Margiolaki I (2005) Science 309:2040
45. Maksimchuk NV, Timofeeva MN, Melgunov MS, Shmakov AN, Chesalov YA, Dybtsev DN, Fedin VP, Kholdeeva OA (2008) J Catal 257:315
46. Sheldon RA, Arends IWCE, Dijksman A (2000) Catal Today 57:157
47. Parton RF, Neys PE, Jacobs PA, Sosa RC, Rouxhet PG (1996) J Catal 164:341
48. Zucca P, Sollai F, Garau A, Rescigno A, Sanjust E (2009) J Mol Catal A Chem 306:89
49. Alkordi MH, Liu YL, Larsen RW, Eubank JF, Eddaoudi M (2008) J Am Chem Soc 130:12639
50. De Vos DE, Meinershagen JL, Bein T (1996) Angew Chem Int Ed 35:211
51. Faria AL, Leod TOCM, Barros VP, Assis MD (2009) J Braz Chem Soc 20:895
52. Halma M, Castro KADF, Prévot V, Forano C, Wypych F, Nakagaki S (2009) J Mol Catal A Chem 310:42
53. Lou L-L, Yu K, Ding F, Zhou W, Peng X, Liu S (2006) Tetrahedron Lett 47:6513
54. Cho S-H, Ma B, Nguyen ST, Hupp JT, Albrecht-Schmitt TE (2006) Chem Commun 2563–2565
55. Ballesteros R, Perez Y, Fajardo M, Sierra I, del Hierro I (2008) Micro Meso Mater 116:452
56. Luque R, Badamali SK, Clark JH, Fleming M, Macquarrie DJ (2008) App Catal A Gen 341:154
57. Deubel DV, Sundermeyer J, Frenking G (2000) J Am Chem Soc 122:10101
58. Haas GR, Kolis JW (1998) Organometallics 17:4454
59. Joergensen KA (1989) Chem Rev 89:431
60. Campestrini S, Conte V, Di Furia F, Modena G, Bortolini O (1988) J Org Chem 53:5721
61. Thiel WR, Eppinger J (1997) Chem Eur J 3:696
62. Saraiva MS, Filho NLD, Nunes CD, Vaz PD, Nunes TG, Calhorda MJ (2009) Micro Meso Mater 117:670
63. Che CM, Huang JS (2009) Chem Commun 3996–4015
64. Nestler O, Severin K (2001) Org Lett 3:3907
65. Zhang JL, Che CM (2002) Org Lett 4:1911

66. Le Y, Yang X, Dai W-L, Gao R, Fan K (2008) Catal Commun 9:1838
67. Liu P, Wang C, Li C (2009) J Catal 262:159
68. Sofia LTA, Krishnan A, Sankar A, Raj NKK, Manikandan P, Rajamohanan PR, Ajihtkumar TG (2009) J Phys Chem C 113:21114
69. Venturello C, Alneri E, Ricci M (1983) J Org Chem 48:3831
70. Sels BF, De Vos DE, Jacobs PA (1996) Tetrahedron Lett 37:8557
71. Sels BF, De Vos DE, Buntinx M, Pierard F, Kirsch-De Mesmaeker A, Jacobs PA (1999) Nature 400:855
72. Sels BF, De Vos DE, Buntinx M, Jacobs PA (2003) J Catal 216:288
73. De Vos DE, Wildeman Sd, Sels BF, Grobet PJ, Jacobs PA (1999) Angew Chem Int Ed 38:980
74. Severeyns A, De Vos DE, Jacobs PA (2002) Top Catal 19:125
75. Severeyns A, De Vos DE, Fiermans L, Verpoort F, Grobet PJ, Jacobs PA (2001) Angew Chem Int Ed 40:586
76. Wai JSM, Marko I, Svendsen JS, Finn MG, Jacobsen EN, Sharpless KB (1989) J Am Chem Soc 111:1123
77. Parton RF, Bezoukhanova C, Grobet PJ, Jacobs PA (1994) Stud Surf Sci Cat 83:371–378
78. Hou Y, Ji X, Liu G, Tang J, Zheng J, Liu Y, Zhang W, Jia M (2009) Catal Commun 10:1459
79. Jain S, Reiser O (2008) ChemSusChem 1:534
80. Matsushita T, Ebitani K, Kaneda K (1999) Chem Commun 265–266
81. Yamaguchi K, Mori K, Mizugaki T, Ebitani K, Kaneda K (2000) J Am Chem Soc 122:7144
82. Yamaguchi K, Mizuno N (2003) Chem Eur J 9:4353
83. Ciriminna R, Hesemann P, Moreau JJE, Carraro M, Campestrini S, Pagliaro M (2006) Chem Eur J 12:5220
84. De Vos DE, Sels BF, Reynaers M, Rao YVS, Jacobs PA (1998) Tetrahedron Lett 39:3221–3224
85. Veghini D, Bosch M, Fischer F, Falco C (2008) Catal Commun 10:347
86. Fujiyama H, Kohara I, Iwai K, Nishiyama S, Tsuruya S, Masai M (1999) J Catal 188:417
87. Kohara I, Fujiyama H, Iwai K, Nishiyama S, Tsuruya S (2000) J Mol Catal A Chem 153:93
88. Okamura J, Nishiyama S, Tsuruya S, Masai M (1998) J Mol Catal A Chem 135:133
89. Tadokoro H, Nishiyama S, Tsuruya S, Masai M (1992) J Catal 138:24
90. Belkhir I, Germain A, Fajula F, Fache E (1998) J Chem Soc Faraday Trans 94:1761
91. Tada M, Akatsuka Y, Yang Y, Sasaki T, Kinoshita M, Motokura K, Iwasawa Y (2008) Angew Chem Int Ed 47:9252

Chapter 11
Heterogeneous Initiators for Sustainable Polymerization Processes

Matthew D. Jones

Abstract One of the main challenges facing the twenty-first century is the need to produce chemicals from renewable resources. The dwindling supplies of fossil fuels coupled with instability in supply mean that technologies that were once deemed too expensive are now becoming more economically viable options. The majority of man-made polymers are derived from crude oil based monomers. However, in recent years a tremendous effort has been channeled into the preparation of polymers from sustainable chemicals. Two classic examples are polylactide (derived from corn starch) and polycarbonates (prepared directly from CO_2). This chapter serves as an introduction into these two polymers and reviews the literature associated with heterogeneous catalyst for the polymerizations, concentrating on approaches describing the heterogenization of homogeneous catalysts.

11.1 Introduction

The area of heterogeneous catalysts for carbon–carbon coupling processes and polymerizations is enormous and growing rapidly year-on-year [1–4]. This is largely due to the significant advantages that heterogeneous catalysts can offer. Specifically, these are higher selectivities and the potential to be recycled, thus possibly reducing costs. This chapter will focus upon the applications of heterogenizing homogeneous catalysts for sustainable "green" polymerizations, which in the modern era are becoming an ever important area of contemporary polymerization science. Heterogeneous catalysts are also a key tool in the chemist's armory to achieve Paul Anastas' so called "12 Principles of Green Chemistry", which are summarized as follows [5–7]:

1. Prevent waste.
2. Be atom efficient.

M.D. Jones (✉)
Department of Chemistry, University of Bath, Claverton Down Bath BA2 7AY, UK
e-mail: mj205@bath.ac.uk

P. Barbaro and F. Liguori (eds.), *Heterogenized Homogeneous Catalysts for Fine Chemicals Production*, Catalysis by Metal Complexes 33,
DOI 10.1007/978-90-481-3696-4_11,

3. Avoid production of toxic/harmful by-products.
4. Products should be designed efficiently.
5. Avoid the use of solvents where possible.
6. Reduce energy requirements and environmental impact of any process.
7. Use renewable feedstocks.
8. Avoid unnecessary protection chemistry whenever possible.
9. Catalytic reagents are superior to stoichiometric reagents.
10. The final products are not harmful to the environment.
11. Develop real-time analytical methods to allow the detection of hazardous materials.
12. All materials should minimize the risk of explosion or harm to health/environment.

Without doubt one of the global challenges for the twenty-first century is the development of sustainable and low carbon technologies [8, 9]. With the rise in oil prices in recent years, technology that was too costly is now becoming more and more cost effective and has helped to ignite research in this area [5, 10–15]. Concurrently, organizations and governments (for example SuSChem organization in Europe) have published action plans supporting the use of renewable materials in chemical synthesis [8, 16, 17]. There are various barriers holding this technology back, one of the main ones being the high cost involved in processing the renewable feedstocks into chemicals – as this technology is competing with well established and proven technology developed over the last century for the petrochemical industry. The heterogenization of homogeneous catalysts to facilitate separation of products, potential enhancements in selectivity or conversion and recovery of the catalysts are well established for small molecular catalysis [18–27]. However, the technology is far less advanced in the area of heterogenization of homogeneous catalysts for polymerization processes, catalyst recovery and recycling for polymerizations are extremely rare in the literature [28]. Hence, this chapter will discuss the use of heterogeneous catalysts for polymerization processes and specifically review the current state-of-the-art in "heterogenizing homogeneous catalysts" for sustainable polymerizations.

11.1.1 Constrained Geometry

The concept of constraining catalysts inside "organized arrays" is well advanced and common place for small molecular catalysis [24]. In-fact there are many elegant approaches where simply heterogenizing a homogeneous catalyst inside a pore can dramatically improve the selectivity of the reaction in question [19–22, 24]. In recent years similar approaches have been utilized to great effect in polymerization processes, however they are dwarfed by the examples for small molecular catalysis. For constrained polymerizations there are two main approaches [29]:

1. Perform the polymerization in a confined channels, e.g. zeolites or mesoporous silica.
2. The second approach is to polymerize monomers that are already ordered.

This chapter is concerned with the polymerization of monomers in confined channels (e.g. SBA-15, MCM-41 etc.). This was made possible by workers at Mobil corporation who, in 1992, synthesized a new family of silica-based molecular sieves, designated as M41S type materials [30, 31]. The pore sizes are in the mesoporous (20–100 Å) regime. Synthesis of the materials involves ordered arrays of surfactant molecules ($\{C_nH_{2n+1}(CH_3)_3N^+\}\{X^-\}$ where X is the counter-anion, typically a halide ion) which act as a "template" for the silica to polymerize around. Members of this family show several remarkable features that make them ideal for catalytic supports for organometallic moieties:

- Well defined pore size and morphology
- Fine adjustments of pore size/dimensions possible
- High thermal and hydrolytic stability
- Very high degree of pore ordering over micrometer length scales

The concept of encapsulation of a catalyst inside a porous material is summarized in Fig. 11.1.

Mesoporous materials have a further advantage over microporous media in the fact that they can accommodate the inclusion of larger molecules. Therefore, mesoporous materials are perceived to be a more attractive option for polymerizations where mass transport and diffusion effects will be important considerations. Examples of polymerizations in MCM-41 include, but are by no means limited to (i) radical polymerization of methylmethacrylate [32]; (ii) radical polymerization of acrylonitrile [33]; (iii) production of poly(phenolformaldehyde) [34]; (iv) polyethylene and other polyolefins [35]; (v) ring opening metathesis polymerization of norbornene [36]; (vi) ring opening polymerization of cyclic esters [37].

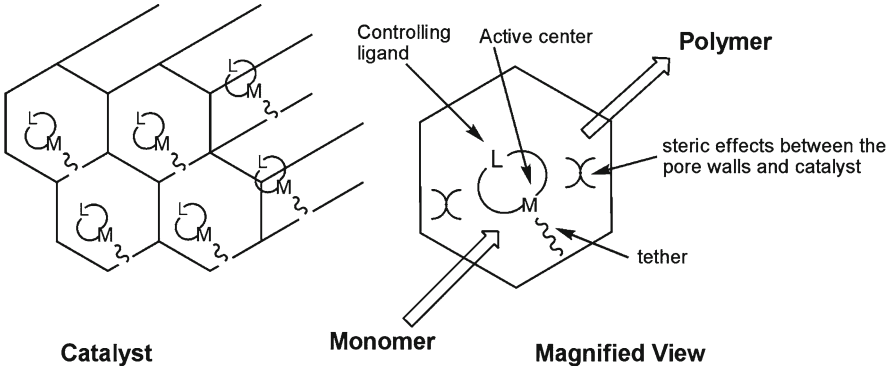

Fig. 11.1 Illustration of the confinement effect in heterogeneous polymerization catalysis

11.1.2 Aims

One of the earliest systems for the polymerization of α-olefins is the well-known and studied Ziegler-Natta catalyst (both of whom shared the Nobel Prize for Chemistry in 1963) which is based on titanium or zirconium and the ill-defined MAO (methylaluminoxane) [38, 39]. This has been subject to many reviews and is a staple example in many undergraduate University courses on heterogeneous catalysts around the world. A more up-to date example of the heterogenization of homogeneous catalysts is that of the anchoring of Grubbs' (won the Nobel Prize for Chemistry in 2005 for his work on olefin metathesis) catalyst to silica. In this example, Grubbs' olefin metathesis catalyst was derivatized to be capable of being anchored onto silica to produce a well-defined supported system (Fig. 11.2) [40]. Heterogenizing well-defined and characterized homogeneous catalysts arguable produces single-site heterogeneous catalysts and consequently uniform reactivity. This perhaps succinctly encompasses the rationale for this area of science.

Olefin metathesis is a powerful method to interconvert olefin hydrocarbons in organic and polymerization chemistries. A problem of this technology is in the lifetime and efficiency of the homogeneous catalysts. One strategy to counteract this drawback is to heterogenize the homogeneous catalyst on a support, for example silica. These catalysts were shown to be active for the RCM (ring closure metathesis) of diethyl-diallyl malonate at 60°C in benzene [40]. As is important in all heterogeneous systems hot filtration experiments were performed to ascertain whether the catalyst is truly heterogeneous and not due to minute quantities of the active catalyst leaching into solution. In this example the catalysis was proven to be heterogeneous and not due to small impurities leaching into solution. In-fact the residue was analyzed via ICP-MS and less than 5 ppb of ruthenium was detected in

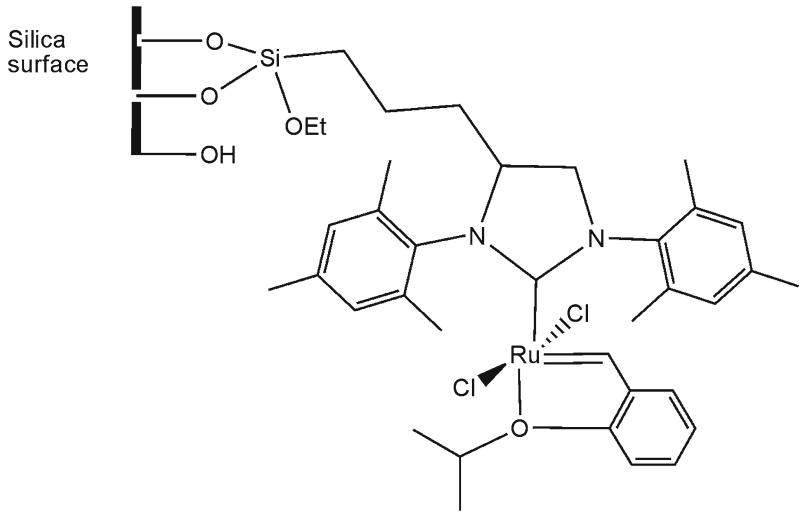

Fig. 11.2 Heterogenization of Grubbs' ruthenium olefin metathesis catalyst (Adapted from [40])

the product [40]. The catalysts could also be recycled many times without significant loss of activity.

In this chapter we will examine current approaches for the heterogenization of homogeneous catalysts for sustainable polymerizations. Specifically, we will review recent work in the following two areas:

Production of Polylactide (PLA) – the monomer used for the polymerization (3,6-dimethyl-1,4-dioxane-2,5-dione or lactide) can be produced from lactic acid which is formed by the fermentation of corn starch. Examples for the related polymerization of ε-caprolactone will also be discussed.

Production of Polycarbonates (PC) from CO_2 – the green credentials of this polymerization lies in the utilization of the greenhouse gas CO_2 and producing a useful product (applications as a thermoplastic) which will "lock" away the CO_2 for many generations.

11.2 Polylactide

Polylactide can be prepared from the ring-opening polymerization (ROP) of the cyclic ester monomer lactide via a coordination-insertion mechanism, Fig. 11.3 [41–45]. Polylactide (PLA) and its co-polymer polylactic-co-glycolic acid (PLGA) are renowned polymers for use in medical and pharmaceutical applications, primarily due to their biocompatibility [46]. These polymers are also FDA (Food and Drug Administration) approved. Such polymers have been used for wound dressings, surgical fibres, stents and have been extensively applied in the area of tissue engineering [46, 47]. As well as biomedical uses PLA is used in the packaging industry due to it biodegradable properties [48]. Currently, the initiator for this polymerization used in industry is based on tin and the complete extraction of tin residues from the PLGA co-polymer is practically impossible. Due to toxicity issues associated with tin there is an exigent need for more effective and efficient initiators for the production under green conditions (in the absence of solvent and using biologically benign initiators) of these polymers for high-value biomedical applications [49]. Studies have shown that residual metal content in the polymer can have a significant impact on cell growth, for example zirconium residues, compared to tin residues, have been found to be favorable for the production of collagen on the copolymers [50]. This phenomenon is of great importance in the application of these polymers in biomaterials. One approach that is receiving considerable attention in the literature is the immobilization of homogeneous initiators on supports, which then fulfill this goal and have the added potential of being recyclable. This approach is ubiquitous in small molecule catalysis, but less so in polymerization catalysis [24].

There are numerous examples in the literature for the use of homogeneous initiators for this polymerization based on, but not limited to, Ti(IV), Zr(IV), Hf(IV), Al(III), Y(III), Zn(II), La(III), Mg(II), Ca(II) [51–61]. However, a small handful of groups have made use of heterogeneous initiators for the ROP of cyclic esters and the few

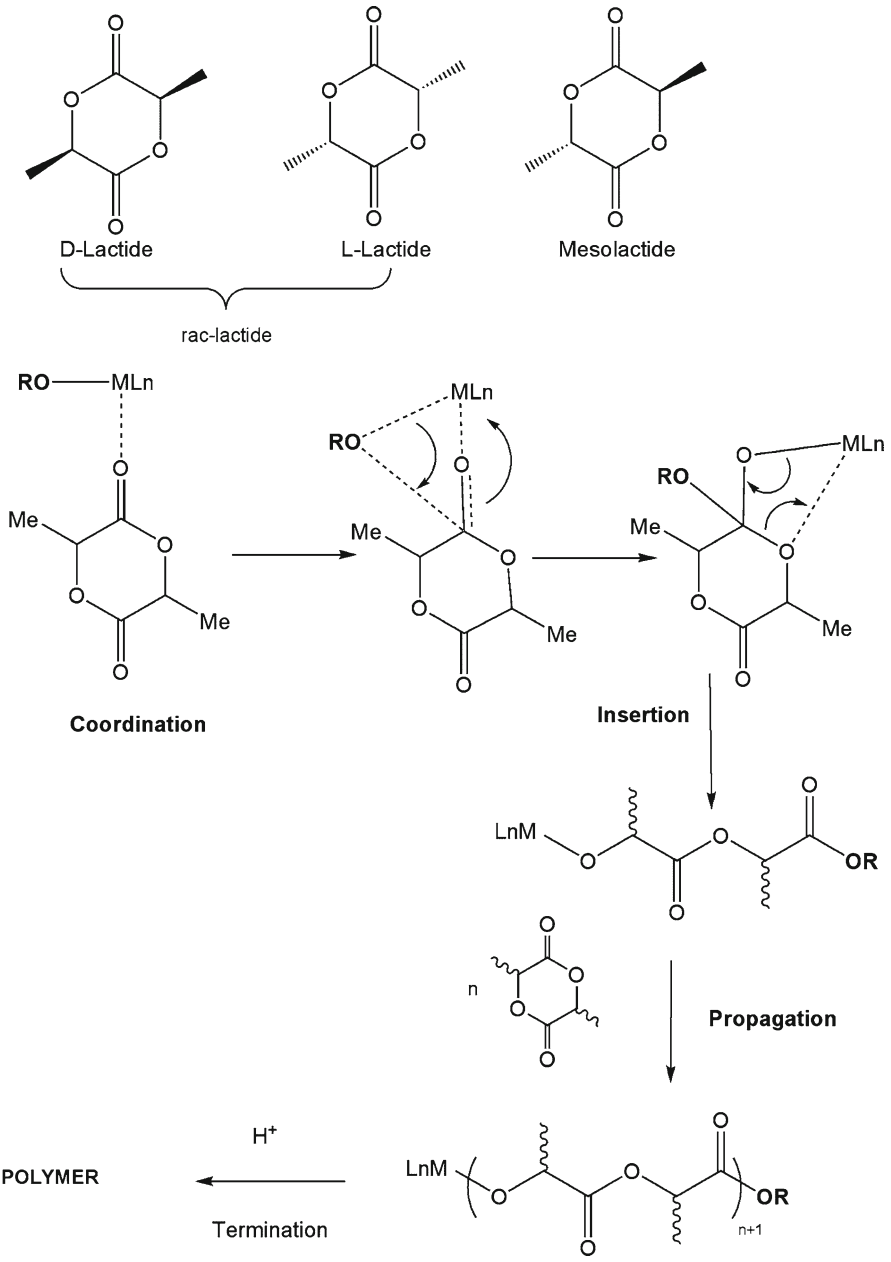

Fig. 11.3 The monomers used in the process and the mechanism of the polymerization of lactide

examples are summarized: Aida et al. have made use of the Lewis acidity of Al-MCM-41 with an alcohol initiator (MeOH, BuOH, BnOH) for the ROP of δ-valerolactone and achieved high conversion with very low PDIs (1.07–1.28), this

material was separated from the reaction mixture and used again for the polymerization [37, 62]. Noteworthy, they observed no reaction for the pure silicate material MCM-41. Furthermore, use of a microporous material zeolite-Y (pore diameter = 8 Å), under identical conditions to Al-MCM-41 (pore diameter = 27 Å) resulted in no polymer formation. C.W. Jones et al. have immobilized Coates' Zn-β-diiminate initiators to SBA-15 (pore diameter 105 Å) [41, 42]. SBA-15 is hexagonally ordered silica with remarkable thermal stability [63]. C.W. Jones observed that the surface silanols can contribute to premature chain transfer processes; attempts to avoid such terminating processes were undertaken in this work, via capping the unreacted silanol moieties [64]. The same group has also supported sulfonic acid groups to silica and has shown promising results for the polymerization of ε-caprolactone [65]. Hamaide et al. have developed silica based yttrium complexes for the polymerization of ε-caprolactone [66, 67] and Jérôme et al. have anchored Y(III) [68]. These examples will be discussed in more detail in the following sections.

11.2.1 Heterogenization of Zn(II)

Perhaps one of the most promising (in terms of activity and selectivity) initiators for the production of PLA was described by Coates and co-workers, Fig. 11.4 [41, 42, 45]. These Zn-β-diiminate initiators were able to produce PLA with very low polydispersities (typically less than 1.10) and with excellent stereocontrol (heterotactic PLA was produced with P_r = 0.94, P_r is the probability of heterotactic enchainment and is determined from ^{1}H homonuclear decoupled NMR spectroscopic experiments). It was also observed that this family of initiators produces PLA in a living manner. Interestingly, these systems are also capable of acting as initiators for the alternating polymerization of CO_2 and epoxides [69]. In 2004 C.W. Jones and co-workers developed two methods for the heterogenization of these promising initiators, Fig. 11.4 for the ROP of L-lactide [28, 64]:

The first method (Method 1, Fig. 11.4) involved the synthesis of complex **1** and reacting in toluene with the silica surface. Two different silica materials were utilized in this work, namely SBA-15 with a pore diameter 105 Å and controlled pore glass (CPG) with an average pore diameter of 246 Å respectively. SBA-15 is a well-defined, hexagonal mesoporous silica material with straight mesopores that are connected through small, random micropores. However, for industrial applications these materials are not ideal due to the one dimensional nature of the support. Hence, in this study C.W. Jones utilized a second silica material CPG, which has a much lower surface area 80 $m^2\ g^{-1}$ (c.f. 803 $m^2\ g^{-1}$ for SBA-15 used in this work) and this material has pores that are interconnected randomly. The second method (Method 2, Fig. 11.4) involved the synthesis of complex **2** which was reacted with a thiol-functionalized silica material with AIBN (2,2′-azobis(2-methylpropionitrile)). Finally, the excess silanol groups on the surface can be capper with hexamethylsilazane. To confirm that the complexes are covalently anchored to the support the solids were analyzed via Raman spectroscopy. For example, the initiator prepared using method 2 showed a disappearance of the peak at 2,575 cm^{-1} which

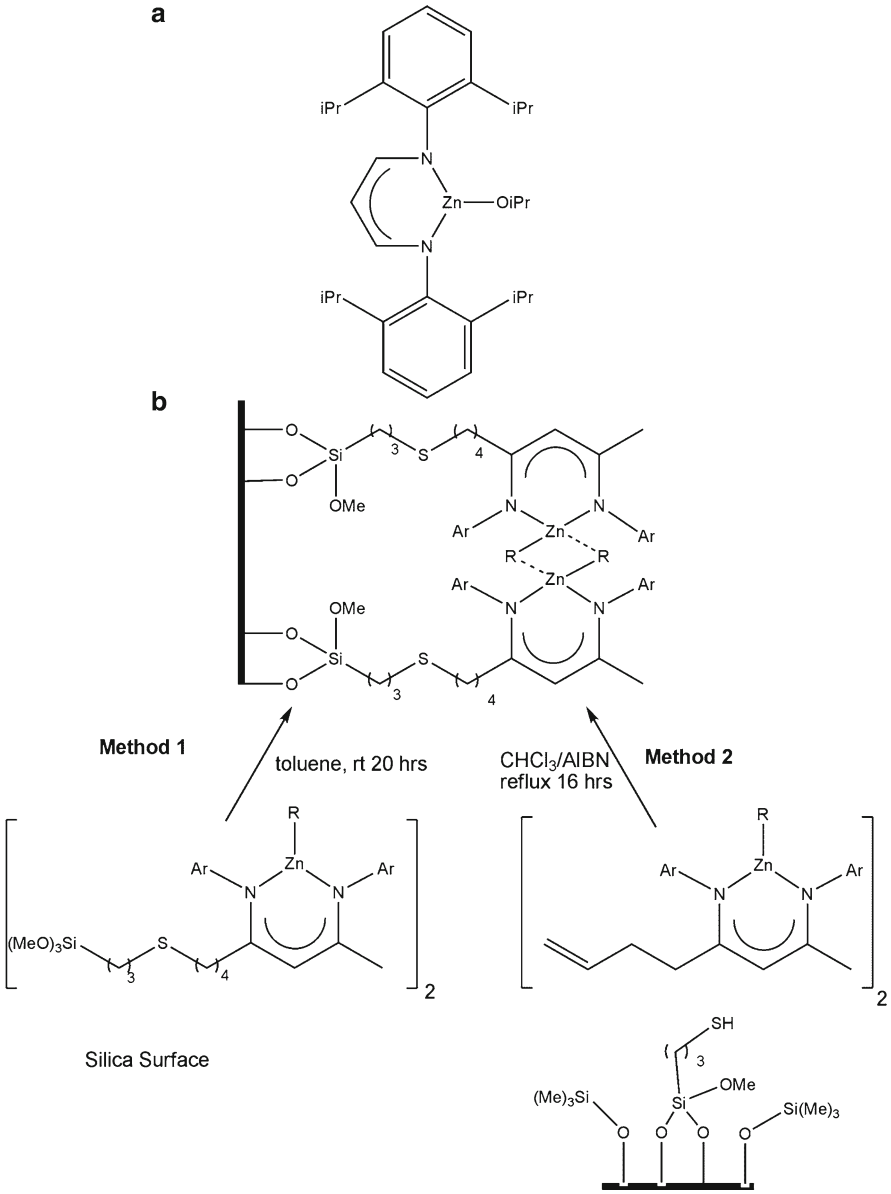

Fig. 11.4 Homogeneous and heterogeneous initiators based on Zn(II), adapted from [41] and [64]. (**a**) – Coates' homogeneous Zn-β-diiminate initiator, and (**b**) – C.W. Jones' heterogeneous analogue. Ar = 2,6-diisopropylphenyl and R = O^{i}Pr

corresponds to the S–H bond when compared to the tethered S–H material. For method 1 the Raman spectrum for the homogeneous initiator was compared to the heterogeneous spectrum for confirmation of reactivity.

In a typical polymerization procedure the heterogeneous initiators and L-lactide were stirred in either dichloromethane or toluene for the desired length of time, under argon. Selected results are summarized in Table 11.1. Initiators labeled **3** were prepared via method 1 and those labeled **4** and prepared via method 2, Fig. 11.4. Initiators **1** and **2** are the Zn(II) homogeneous precursors employed in the synthesis of the heterogeneous systems, Fig. 11.4.

Both of the homogeneous systems were highly active for the polymerization of L-lactide, with almost complete conversion after 30 min. Two methods of heterogenization and two supports were employed. The molecular weights of the PLA produced by the heterogeneous initiators are considerably lower than those predicted by analysis of the monomer-to-initiator ratio. The polymerizations were performed in dichloromethane as this was shown to produce PLA with higher molecular weights and narrower polydispersities, compared to toluene. The CPG anchored systems afforded PLA with higher molecular weights and narrower polydispersities; this was assigned to the increased porosity facilitating mass transport and diffusion of the monomer to the active center [64]. To investigate this process further C.W. Jones and co-workers determined the molecular weight as a function of conversion, for initiator **3** on SBA-15 (without capping the excess silanol moieties with hexamethylsilazane). After 30% conversion the resulting M_n of the polymer was ~ 2,300 g/mol. It was seen that the molecular weight of the polymer is independent of the reaction time after the first 2 h, conversion increases with time but the molecular weight remains relatively constant.

Jones (M.D.) has heterogenized a series of Zn(II) complexes to commercially available Davisil silica with a pore diameter of 60 Å, Fig. 11.5 [70]. To dry silica (60 Å Davisil Grade 635) 3-aminopropyltrimethoxy silane (AMPS) was added to form the heterogenised amine SiO_2-AMPS, as shown in Fig. 11.5.

Table 11.1 Summary of the results of C.W. Jones et al. for the polymerization of L-lactide

Initiator[a]	Capping[b]	[Mon]/[Init]	Time[c]	Conv.[d]/%	M_n[e]	PDI[e]
1	–	180	0.5	94	27,500	1.18
2	–	100	0.5	96	15,630	1.09
3, SBA-15	Yes	58	18	48	4,725	1.38
3, SBA-15	No	58	24	59	2,375	1.09
3, CPG	Yes	103	17	51	4,860[f]	1.28
3, CPG	No	103	24	68	2,595	1.12
4, SBA-15	Yes	58	20	41	1,745	1.47
4, CPG	Yes	132	21	53	3,480	1.35

[a]See Fig. 11.4 for the numbering of the initiators
[b]Capping of the excess silanols groups on the silica surface
[c]Time in hours
[d]Determined from ^{1}H NMR spectroscopic analysis
[e]Determined from GPC measurements
[f]Bimodal distribution. The polymerizations were carried out in CH_2Cl_2 at 45°C

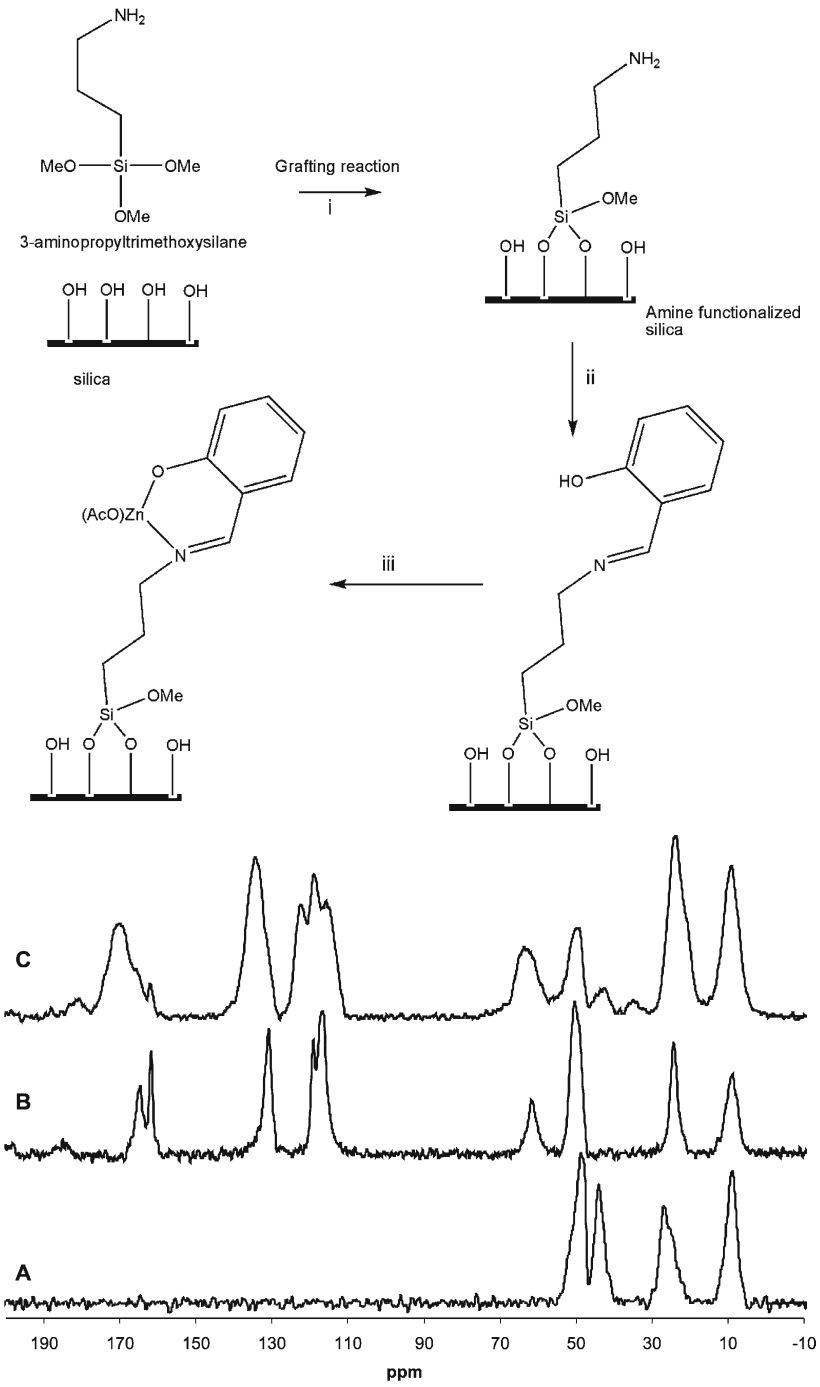

Fig. 11.5 Preparation of the heterogeneous Zn(II) initiator for the ROP of *rac*-lactide. (i) $(MeO)_3Si(CH_2)_3NH_2$/toluene (SiO_2-AMPS); (ii) salicylaldehyde/MeOH (SiO_2-AMPS-SAL); (iii) $Zn(OAc)_2.2H_2O$/MeOH (SiO_2-AMPS-SAL-Zn). Lower Figure shows the solid-state $^{13}C\{^1H\}$ CP/MAS NMR spectra of (**a**) aminopropyl functionalized silica, (**b**) salicylaldehyde functionalized silica and (**c**) the Zn(II) initiator. The figure has been adapted from [70]

$^{13}C\{^{1}H\}$ CP/MAS solid-state NMR spectroscopy revealed four peaks centered at 9, 27, 44 and 49 ppm respectively. Dipolar dephasing experiments indicated that the resonance at 49 ppm arises from Si-OCH_3 [71]. This material was reacted with salicylaldehyde, using standard literature procedures to form SiO_2-AMPS-SAL as a bright yellow solid [72–74]. The NMR resonance at 44 ppm had almost completely disappeared and a new resonance at 62 ppm (CH_2-N) was observed, together with new resonances for the aryl carbons and the imine (CH=N) at 165 ppm. This material was treated with $Zn(OAc)_2.2H_2O$ to form SiO_2-AMPS-SAL-Zn, as a pale yellow solid. There is significant broadening in the $^{13}C\{^{1}H\}$ CP/MAS NMR spectrum of SiO_2-AMPS-SAL-Zn, indicative of more disorder being present, compared to the precursor materials. A new peak at 170 ppm was observed, which is assigned to the carbonyl of the acetate group, the peak at 23.5 ppm is asymmetric and encompasses the CH_2 of the tether and CH_3 of the acetate.

In this case it was deemed that capping the excess silanol groups on the surface was not necessary as high molecular weight PLA was obtained. These heterogeneous initiators and homogeneous analogues were tested for the ROP of *rac*-lactide under solvent free conditions (130°C, with a monomer-to-initiator ratio of 300:1). Initially, two control polymerizations were run to evaluate, (i) the free ligand and (ii) unfuntionalized silica as possible initiating species. In both cases no polymer was produced, therefore any polymer produced in subsequent experiments must be due to the Zn(II) center. For example, in the homogeneous case when the chloro-salicylaldehyde derivate was employed a conversion of 80% was achieved and from the GPC M_n = 41,200 g/mol, PDI of 1.43 and there was no evidence of any stereoselectivity in the polymerization. However, the heterogeneous initiator produced a 76% yield, M_n 19,000 g/mol, PDI of 1.08 and importantly the PLA had a P_r of 75%. There are numerous examples in the literature of so-called "confinement" effects (Section 12.1.1) of heterogenizing active centers in pores to boost enantioselectivity in small molecular catalysis [19–23, 27]. The arguments employed to explain the enhancement in selectivity are again valid in this case as both the stereoselectivity and the polydispersity are dramatically improved upon heterogenization.

In a more simple example $ZnMe_2$ can be easily anchored to MCM-41, $^{13}C\{^{1}H\}$ CP/MAS solid-state NMR spectroscopy clearly indicates the presence of the metal alkyl at –10 ppm. To generate the catalytically active center the polymerization is preformed with an equivalent of isopropyl alcohol to generate the alkoxide initiator in-situ, which is common place in the ROP of lactide [75]. A homogeneous silsesquioxane model initiator was also prepared, Fig. 11.6. Both the homogeneous and heterogeneous systems were active for the ROP of *rac*-lactide (low conversions ~10% after 24 h, no stereocontrol was detected and molecular weights of ~2,000 g/mol were observed) [76].

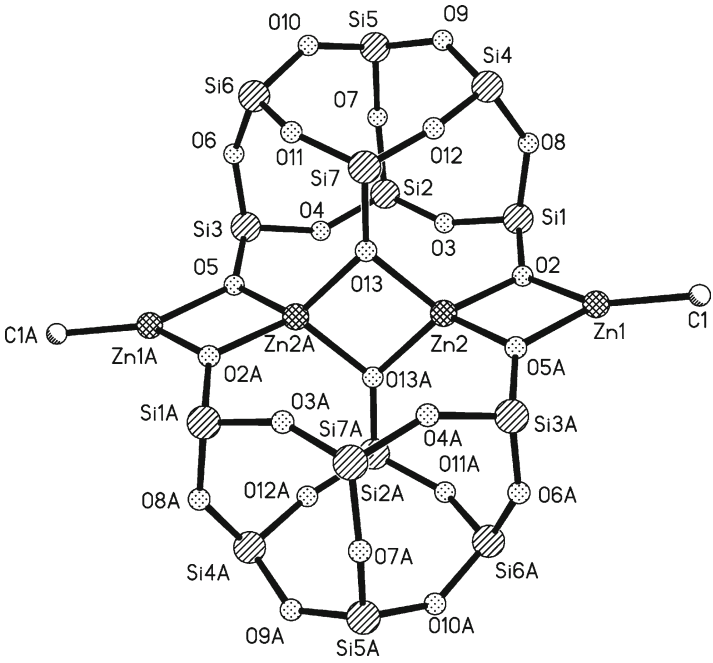

Fig. 11.6 Homogeneous Zn-Me initiator as a model for the heterogeneous Zn(II) initiators (Reproduced from [76])

11.2.2 Heterogenization of Ti(IV) and Zr(IV)

One of the classical examples of the heterogenization of Ti(IV) on silica was that of Aida's work, Fig. 11.7, for the polymerization of ethylene to produce highly crystalline polyethylene (PE) [35]. This pioneering foray into the field demonstrated the possibility of using ordered mesoporous silica as extruders for the nanofabrication of highly crystalline polymeric materials. The initiator was simply prepared by the heterogenization of $TiCp_2(O^iPr)_2$ on MCM-41, using the method of Thomas and co-workers [77]. Recently, similar approaches as that described by Aida have been utilized for the production of PLA under melt conditions.

Examples of the production of PLA in mesoporous materials have focused on the heterogenization of $Ti(O^iPr)_4$ or $TiCl(O^iPr)_3$ onto silica by M.D. Jones et al. and Chung et al. [78–80] For example, M.D. Jones utilized a 60 Å pore diameter silica support for Ti(IV) [78]. The initiators were prepared by simply stirring a slurry of the silica support the metal alkoxide $\{Ti(O^iPr)_4\}$. These materials were characterized by $^{13}C\{^1H\}$ CP/MAS solid-state NMR spectroscopy, Fig. 11.8, which shows a broad resonance centered at 80 ppm and a sharper resonance at 67 ppm for the methine carbon and a resonance at 24 ppm for the methyl group or the isopropoxide moiety. Much attention has been directed towards understanding and appreciating the binding of $Ti(O^iPr)_4$ on the silica surface [81, 82].

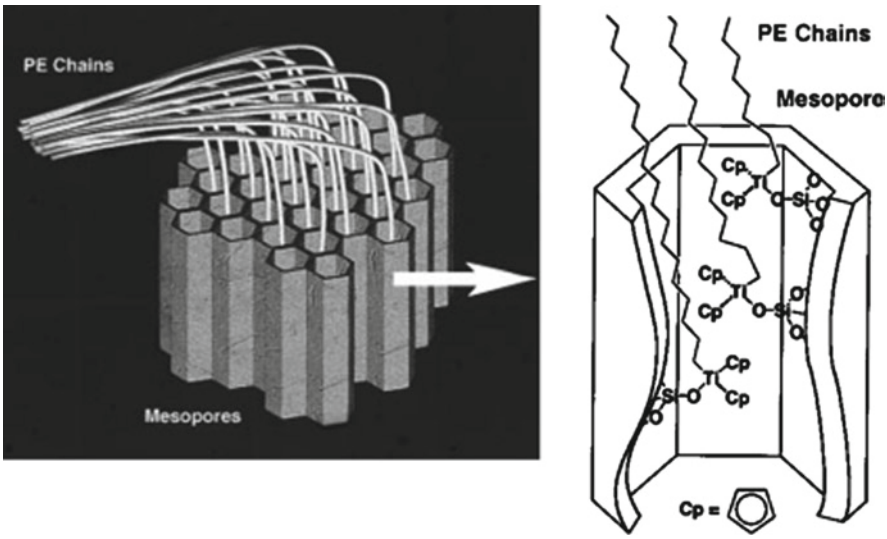

Fig. 11.7 Schematic representation of Aida's heterogeneous Ti(IV) initiator for the polymerization of ethylene (Reproduced with permission directly from [35])

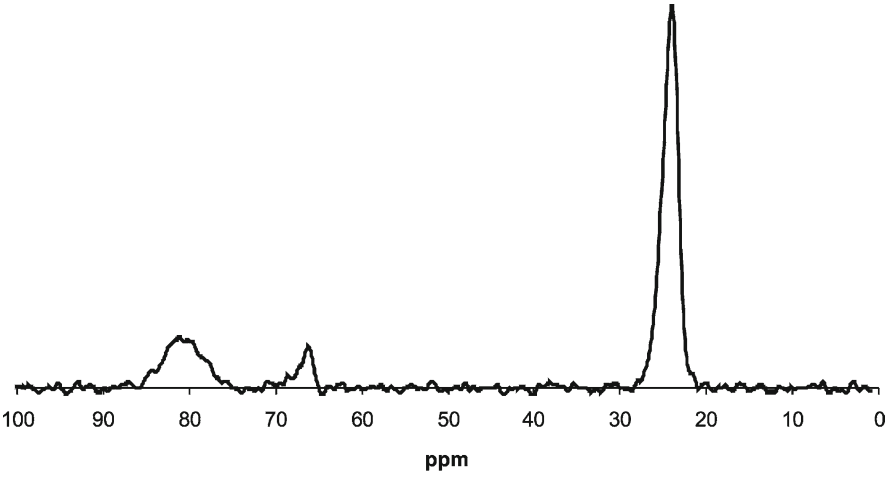

Fig. 11.8 $^{13}C\{^{1}H\}$ CP/MAS solid-state NMR spectrum of $Ti(O^{i}Pr)_4$ heterogenized onto silica

The Ti-SiO_2 materials were tested for the polymerization of *rac*-lactide (conditions: 2 g of *rac*-lactide and 100 mg of the heterogeneous initiator, the loading of the initiators as shown by ICP-AES was approximately 3 wt% of metal.) For the Ti-SiO_2 material a 70% conversion was achieved in just 2 h (M_n = 46,100 g/mol, M_w = 52,500 g/mol and PDI = 1.14), the polymer was shown to be atactic by ^{1}H homonuclear decoupled NMR spectroscopy (N.B. ^{1}H homonuclear decoupled NMR spectroscopy is the method of choice to determine the tacticity of the polymers, the

method and assignments are beyond the scope of this chapter the reader is directed to the following references for more details) [41, 83, 84]. Results from MALDI-TOF mass spectrometry showed that the repeat unit was 144 g/mol and that only a small series originating from transesterification with a repeat unit of 72 g/mol was observed and no cyclic polymer (resulting from intramolecular backbiting) was detected. If the pore diameter of the silica is reduced to 40 Å then the conversion drops but the polymerization is still well controlled (40%, M_n = 46,100 g/mol M_w = 52,500 g/mol and PDI = 1.14). Importantly, the pure silica material was inactive for the polymerization. ICP-AES of the resulting polymer indicates that there is 15 ppm of titanium remaining in the final polymer after work-up, compared to 1,250 ppm for a model homogeneous system (based on silsesquioxane) under a similar monomer-to-initiator ratio in the homogeneous phase. Silsesquioxanes have been used since the early 1990s as realistic models for silica surfaces. In this case an isobutyl variant was utilized and reacted with $Ti(O^iPr)_4$, the single crystal X-ray structure for the resulting product is shown in Fig. 11.9. This structure is analogous to those prepared by Feher [85] Crocker [86] and Johnson [87, 88], with bond lengths and angles in the appropriate range for complexes of this type. For the homogeneous initiator PDIs in excess of 2 were achieved, indicating that the simple method of heterogenizing has a dramatic influence of the degree of control of the polymerization.

Chung et al. employed a similar strategy in this case they used the heterogeneous initiators for the ROP of L-lactide, the starting titanium species was $TiCl(O^iPr)_3$. In this study molecular weights of 29,500 and 30,300 g/mol were obtained after 72 h under melt conditions. Interesting, they also observed an increase in the melting point T_m of the polymer compared to polymer produced from the parent Ti-isopropoxide complex. Again transesterification was reduced due to the immobilization of the initiators on the support. It was hypothesized that constraining of the

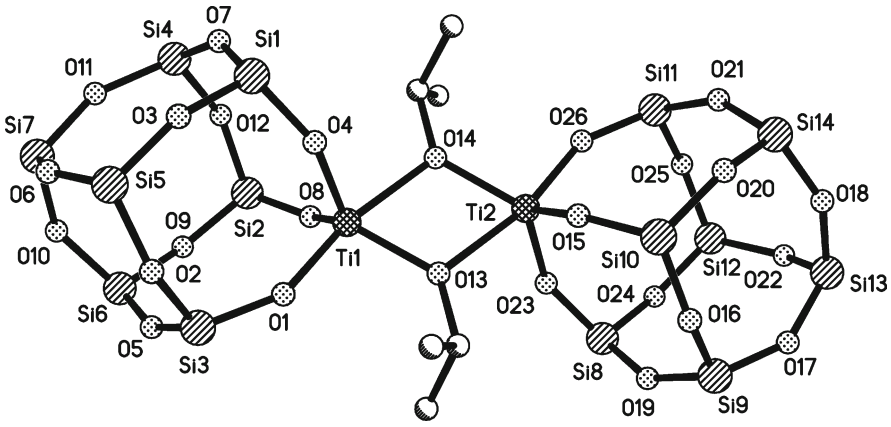

Fig. 11.9 Molecular structure of a homogeneous Ti-isopropoxide initiator as a model for the heterogeneous Ti(IV) initiators (Reproduced from [78] by permission of the Royal Society of Chemistry)

initiator inhibits the propensity for intramolecular "backbiting", via a similar mechanisms as that proposed by Aida in 1999 for the polymerization of polyethylene [35].

Examples of the heterogenization of Zr(IV) for the ROP of lactones are rare, when $Zr(O^nBu)_4$ was anchored onto silica by Hamaide 100% conversion of the polymerization of ε-caprolactone was observed after 3.5 h. However, M.D. Jones heterogenized $Zr(O^iPr)_4$ using the same method as for $Ti(O^iPr)_4$ above, but failed to produce PLA under melt conditions [78].

11.2.3 Heterogenization of Sn(II)

Tin octanoate is the current initiator used in industry for the ROP of lactide. One of the first heterogenizations of a homogeneous initiator for the ROP of lactide was the work of Pinnavaia and co-workers in 1996 [89]. In this example they prepared a tin-substituted HMS silica by the reaction and aging of tetraethylorthosilicate, tin (IV) isopropoxide, dodecylamine, ethanol and water, which were aged for 18 h and finally calcined. This material was tested for the ROP of L-lactide, under melt conditions 130°C. After a reaction time of 72 h a conversion of 82% was achieved with a molecular mass of 36,000 g/mol (PDI = 1.1). The same group also heterogenized titanium, iron, yttrium and lanthanum, with limited success. For example the titanium heterogeneous initiator was active but only a 15% conversion was achieved in the same time frame. Importantly, when they used the host HMS material no conversion was observed, therefore they concluded that the polymerization is metal catalyzed. They also conclude that the Sn-HMS initiator combines the reactivity of the Lewis acidic tin center with the selectivity of the ordered/regular mesoporous material to afford PLA with reasonably high molecular weight and low polydispersity. It is proposed that the ordered pore structure improves the polymer properties with respect to the homogeneous system by constraining the catalysis and minimizing side reactions such as "back-biting" and intermolecular transesterification which tend to manifest themselves by an increase in PDI.

Further examples of the heterogenization of homogeneous tin initiators have arisen from the laboratory of Biesemans [90, 91]. Her group has performed elegant mechanistic studies into the ROP of ε-caprolactone. For example, dibutyltin dichloride (Bu_2SnCl_2) has been shown to be a promising ROP initiator and can be heterogenized onto polystyrene beads and is a recyclable catalyst for the ROP of ε-caprolactone. The support for the work is Amberlite XE-305 (which is a cross-linked polystyrene bead with a diameter in the range 500–850 μm) using standard literature procedures to form $[P\text{-}H]_{1\text{-}t}[P\text{-}(CH_2)_nSnBuCl_2]$ (P = polymer and n = length of the carbon chain of the tether.) The initiators have been characterized via a combination of ^1H and ^{119}Sn HR-MAS solid-state NMR spectroscopy. For example when n = 6 in the ^{119}Sn NMR spectrum a resonance at $\delta = 120$ ppm was observed [90–92]. A combination of 2D ^1H-^{13}C HSQC and ^1H-^{119}Sn 2D techniques have been employed to fully characterize the materials. A summary of the polymerization results is given in Table 11.2 [91]:

Table 11.2 Summary of the results of Biesemans et al. for the polymerization of ε-caprolactone with heterogenized tin initiators

Entry	t	n	Time/h	T (°C)	Conv./%	M_n[a]	PDI[a]
1	0.32	6	72	100	58	8,200	4.40
2	0.32	6	72	70	10	1,150	4.80
3	0.11	6	72	100	>99	17,000	2.42
4	0.32	6	5	100	75	1,400	5.18
5	0.26	11	5	100	59	1,200	1.93
6[b]	0.26	11	5	100	59	1,300	1.77
7	0.26	11	7	100	72	1,100	1.89

[a]Determined from GPC measurements

[b]This is a repeat with the same material used in entry 5. The polymerizations were performed in toluene at the given temperature and time ($[CL]_0$ 4.51 mol L^{-1}, $[CL]_0/[^nPrOH]_0 = 10$, $[^nPrOH]/[Sn]_0 = 20$). t is a measure of the degree of functionality of the support

From analysis of the ^1H NMR spectrum of the resulting polymer the propyl end group was observed. Reasonable conversions were obtained, however the PDIs of the resulting polycaprolactone (PCL) were high and bimodal distributions were observed. Analogous homogeneous systems produced PCL with low PDIs typically less than 1.10. It was shown that it was possible to recycle the catalyst with no loss of activity and minimal amounts of PCL appear to be trapped in the bead pores after isolation of the catalyst.

11.2.4 Heterogenization of Al(III)

Aida et al. have used Al-MCM-41 type materials to polymerize ε-caprolactone and δ-valerolactone [37, 62]. It was observed using Al-MCM-41 (Si/Al = 17, surface area 1,010 m^2 g^{-1} and pore diameter 27 Å) was much faster than pure silica MCM-41 for the ROP of δ-valerolactone. When the surface was capped by silylation no activity was observed implying that the surface acidity is critical for the polymerization. Addition of alcohol to the polymerization resulted in a well-controlled process with narrow PDIs (~1.15), and the alcohol was observed as the end group of the polymer. The group also prepared Ti-MCM-41, however they found this to produce polyesters with a multimodal distribution of molecular weights.

It is possible to anchor $Al(O^iPr)_3$ to silica surfaces [66, 67, 78]. Jones et al. have shown from ^{27}Al solid-state MAS NMR spectrum it is clear that several active sites are present as three main resonances (at 0, 30 and 50 ppm) were detected. For the Al-SiO_2 system the polymerization is far less active that Ti-SiO_2 (10% conversion in 24 h, M_n = 3,600 M_w = 4,100 and PDI = 1.13). Importantly, in stark contrast to Ti-SiO_2 the polymer was shown to be almost totally isotactic stereoblock PLA. This is one of the only examples of the use of a heterogeneous initiator for the stereoselective polymerization of *rac*-lactide. MALDI-TOF mass spectrometry indicated the presence of the O^iPr end group indicating that the aluminium is the active center and not the silica surface.

11.2.5 Heterogenization of Sc(III) and Y(III)

The ROP of cyclic esters has been shown to be catalyzed via $Sc(OTf)_3$ in a quasi-living fashion under homogeneous conditions. Recently, Takasu and co-workers have heterogenized $Sc(OTf)_3$ onto polystyrene resins, Fig. 11.10, and these have been found to be active initiators for the ROP of ε-caprolactone in toluene or ionic liquids [93, 94]:

A summary of the polymerization results are given in Table 11.3:

Using $Sc(OTf)_3$ heterogenized onto polystyrene low PDIs were obtained, analogous to the homogeneous system. The heterogeneous catalysts appear to be less active than their homogeneous counterparts as longer times were necessary to achieve analogous conversions. It was possible to recycle this catalyst; however there was loss in activity when using BnOH as the initiator. Analysis of the recovered catalyst indicated no change in the Sc or S loadings after the polymerization. Improve reusability was observed when employing ethanol as the initiator, a yield of 84% and Mn 5,800 g/mol with a PDI of 1.10 c.f. 86%, 6,200 g/mol and 1.12 for the fresh system. The PS-Sc system was also shown to be active in ionic liquids.

Jérôme and coworkers have heterogenized Y(III) alkoxides onto porous silica [68]. This was simply achieved by grafting $Y[N(SiMe_3)_2]_3$ onto the porous silica (in this example 17 nm pore diameter silica was utilized) surface followed by the addition of ^{i}PrOH to form the active Y-alkoxide species. This initiator was found to produce PCL in near quantitative yields with a M_n (from GPC) slightly lower than

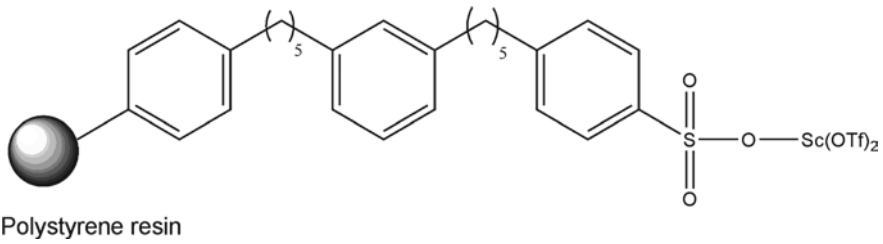

Fig. 11.10 Heterogeneous Scandium based initiator (Adapted from [93])

Table 11.3 Summary of the results of Takasu et al. for the polymerization of ε-caprolactone with heterogenized $Sc(OTf)_3$

	Catalyst	Initiator	$[M]_0/[I]_0$	T/°C	Time/hr	Conv./%	M_n [a]	PDI[a]
1.	$Sc(OTf)_3$	EtOH	40	35	21	98	6,100	1.16
2.	PS-Sc	EtOH	40	35	72	86	6,200	1.12
3. 1st	PS-Sc	BnOH	20	50	10	83	3,000	1.15
4. 2nd	PS-Sc	BnOH	20	50	10	57	2,700	1.12
5. 3rd	PS-Sc	BnOH	20	50	10	38	1,800	1.18

[a]Determined from GPC measurements. The polymerizations were performed in toluene at the given temperature and time ($[CL]_0$ 3 mol/L, 1 g of CL was used for each experiment, catalyst 1 mol%)

the theoretical value and it was possible to vary the conditions to obtain low PDIs. It was shown that it was also possible to recycle these systems with minor loss in activity and no Yttrium was detected in the resulting PCL.

11.2.6 Heterogenization of Rare Earth Elements

Using an analogous procedure as with Y(III), Boisson and co-workers have grafted Nd(III) onto the silica (Grace 332 or 432 grade silica) using the neodymium hexamethyldisilazane precursor [95]. Again the alkoxide was generated in-situ by the addition of an equivalent of ^{i}PrOH or BnOH. Quantitative conversions were obtained with predictable molecular weights and low PDIs. These systems have the following three main advantages:

1. Grafting is carried out under mild conditions.
2. High yields were obtained in a short time (30 min).
3. The polymer produced is well-defined.

Neodymium and Samarium have been grafted onto alumina by Hamaide and co-workers. They observed enhanced activity of these systems for the ROP of ε-caprolactone compared to analogous Al(III) and Zr(IV) systems [67]. There are numerous examples of the use of lanthanide homogeneous initiators for the ROP of cyclic esters [51], however examples of heterogeneous systems are rare.

11.2.7 Heterogenization of Initiators for Metal Free Polymerization

Perhaps one of the most attractive routes into PLA is the use of so called "metal-free" initiators for the polymerization. This field has been pioneered by Hendrick and Waymouth, who have prepared many elegant organo-initiators for the controlled production of PLA [96–98]. Pertinent to this chapter are the studied of C.W. Jones et al. who has prepared an *n*-propylsulfonic acid-functionalized porous and non-porous silica and tested these for the polymerization of ε-caprolactone, Fig. 11.11 [65]. Initially the silica surface is treated with 3-mercaptopropyltrimethoxysilane to generate the thio-functionalized silica, the excess silanols moieties are capped with HMDS and finally the thiol is oxidized to the sulfonic acid. Four different silica materials were utilized SBA-15, Cab-o-Sil M5, CPG240 and MS-3000, Table 11.4 summarizes the polymerization results.

The heterogeneous systems appear to offer a greater degree of control over the polymerization than the homogeneous TsOH, as indicated by the lower PDIs. The SBA-15 system was seen to be the most active and this also appears to be the

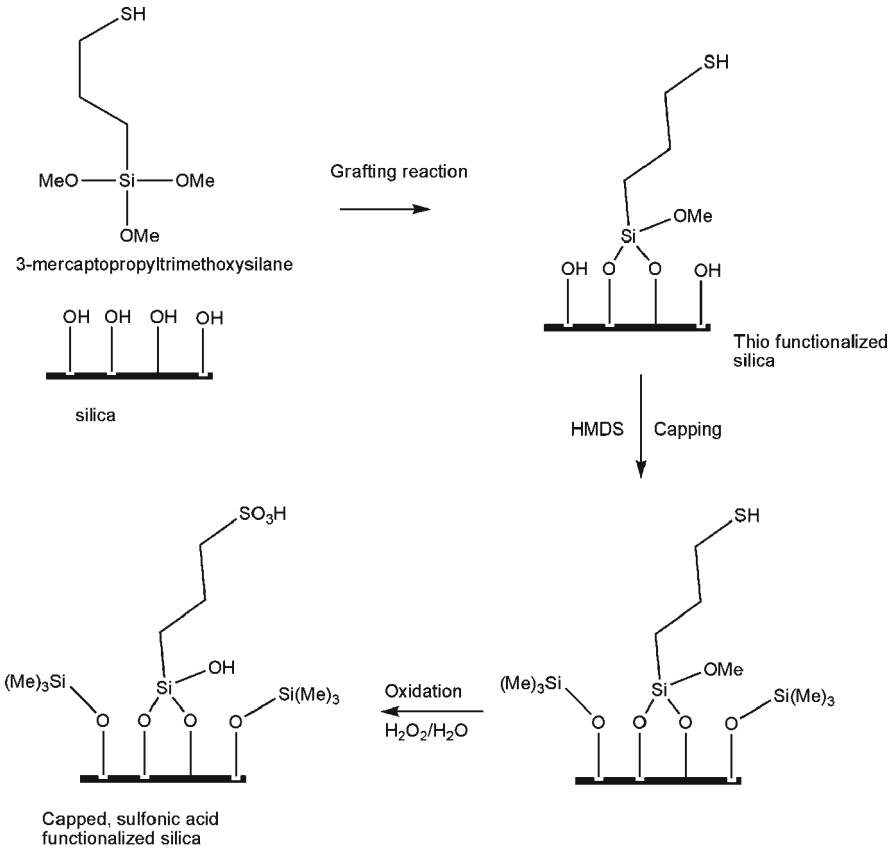

Fig. 11.11 Preparation of heterogenized sulfonic acid initiator for polyester production (Adapted from [65])

Table 11.4 Summary of the results of C.W. Jones et al. for the polymerization of ε-caprolactone with heterogenized sulfonic acid initiators

Initiator	Mol.% cat	Time/h	Conv.[a]/%	M_n [b]	PDI[b]
TsOH (homogeneous)	0.30	5.5	82	9,470	1.61
SBA-SO_3H	0.30	27	96	6,210	1.1
SBA-SO_3H-Cap	0.30	101.5	95	5,270	1.18
CPG-SO_3H	0.30	116	70	5,080	1.2
CPG-SO_3H-Cap	0.30	116	38	2,410	1.49
Cab-SO_3H	0.30	60	84	4,770	1.16
Cab-SO_3H-Cap	0.30	136.5	84	5,900	1.18

[a]Determined from GC analysis

[b]Determined from GPC measurements. A monomer-to-initiator ratio of 43:1 was employed. The polymerizations were performed in toluene at 52°C

most controlled system. However, the heterogeneous systems are slower than the homogeneous analogue and the majority of metal-catalyzed processes in the literature [99]. The heterogeneous systems do offer advantages since the obtained molecular weights were closer to those of the theoretical molecular weights implying a greater living character. Elemental analysis of the resulting polymer indicated that the sulfur contents were very low (~65 ppm). Hence, recycling experiments were also attempted with the heterogeneous initiators. It was hypothesized that the main stumbling block to this process would be the blocking of the pores, therefore the recovered initiators were Soxhlet extracted with both THF and CH_2Cl_2 (solvents known to readily dissolve polyesters) prior to reuse. Unfortunately, using this approach it proved difficult to reuse the initiator and only oligomeric products were produced after several days of polymerization using the recycled initiators.

11.3 Polycarbonate Production

Polycarbonates are emerging as promising engineering thermoplastics due to their good impact strength, thermal resistance and transparency. Polycarbonates are commonly produced from the copolymerization of epoxides (the two most common being cyclohexene oxide and propylene oxide) with carbon dioxide (Fig. 11.12) [100]. The first example of this copolymerization was demonstrated by Inoue and co-workers in 1969 [101]. In this case the initiator was derived from a 1:1 mixture of $Zn(Et)_2$ and H_2O. Since this early foray into this polymerization there have been numerous examples in the literature for the use of homogeneous initiators for this process, typically these are based on Cr(III), Al(III), Zn(II), Mn(III) or Co(III) [100]. The most common coordinating ligands are salan, salen and other Schiff base system [100]. For this process to become industrially viable homogeneous polymerization initiators are not ideal as the polymerization mixtures become very viscous, even at low conversions. One way to alleviate this problem is to perform the reaction in a non-solvent so that the polymer precipitates out of solution before it can add to the viscosity. The use of a homogeneous catalyst with this precipitation methodology tends to lead to reactor fouling and/or poor polymer morphology control. However, the use of a heterogeneous catalyst tends to alleviate if not circumvent these processing issues and are therefore highly industrially desirable.

It should be noted that the copolymerization of epoxides and CO_2 is the not the only method to produce polycarbonates. An approach that is currently receiving attention in the literature is the oxidative carbonylation of bisphenol A [102, 103]. Catalysts for this process are typically heterogenized Pd(II) or bimetallic Pd(II)/Co(II) systems, however this process is beyond the scope of this chapter.

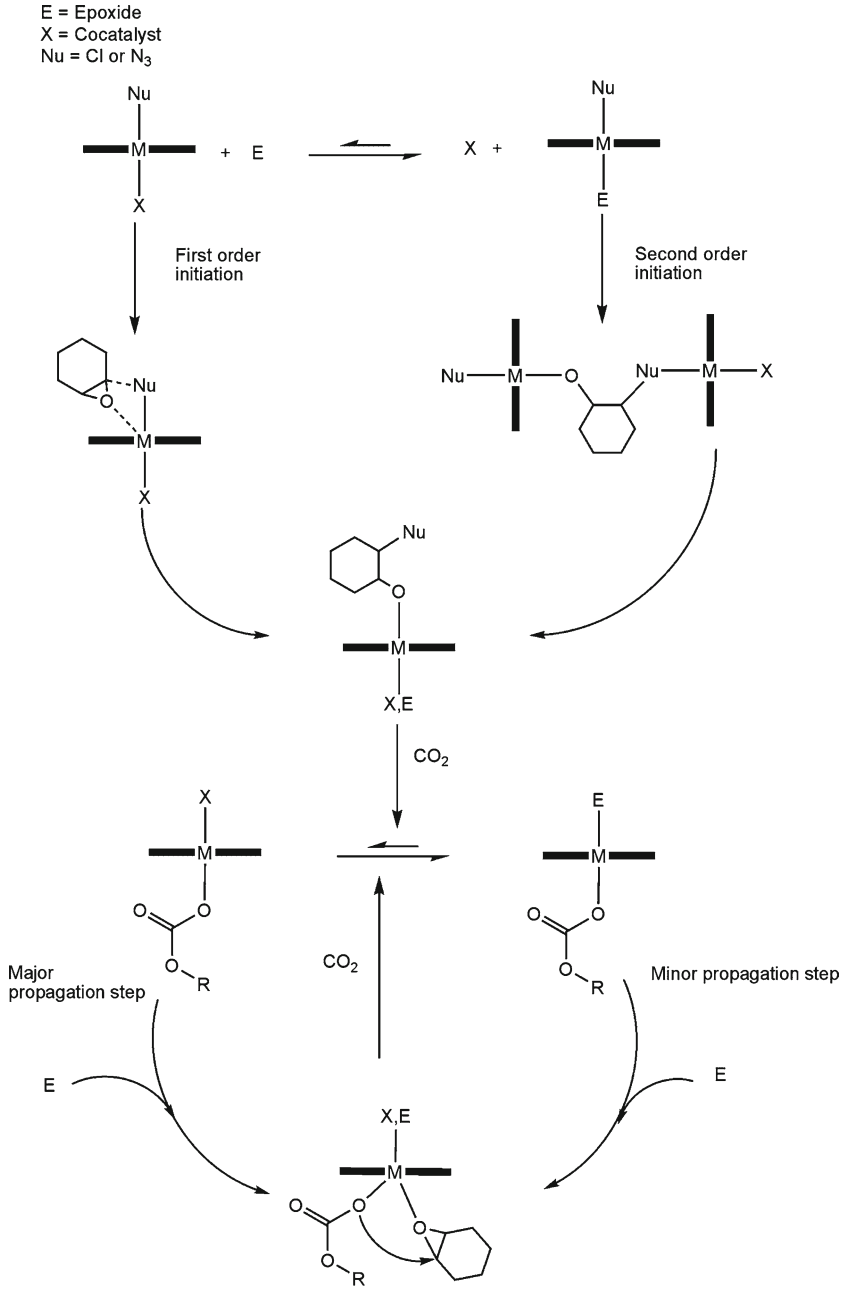

Fig. 11.12 Mechanism for the ring opening of epoxides with carbon dioxide, adapted from [100], M = metal, e.g. chromium

11.3.1 Supercritical CO_2

Two of the earliest examples of the formation of polycarbonates utilized supercritical CO_2 as the solvent and the reagent, eliminating the need for toxic and volatile organic solvents and thus enhancing the green credentials of the polymer further. The first system was prepared by Darensbourg et al. involved the preparation of a heterogeneous Zn(II) material by the reaction of ZnO with glutaric acid to produce Zn(glutarate) as an insoluble white solid [104]. This material was shown to copolymerize CO_2 with propylene oxide. Molecular weights in the range of 4,000–29,400 g/mol were achieved with relatively large distributions; PDIs in excess of 3 were typically obtained. When the temperature was increased the cyclic carbonate by-product was observed to be produced. In 2001 Holmes and coworkers heterogenized a homogeneous Cr(III) porphyrin catalyst onto an argogel support, Fig. 11.13 [105]:

The heterogenized Cr(III)-porphyrin was shown to be active the copolymerization, with narrow PDIs obtained. It was also possible to recycle the catalyst, although there was loss in activity upon reuse, Table 11.5. The polymers were observed to have a mild colouration, which implies a minor degree of leaching occurs. Similarly narrow PDIs were obtained with the analogous homogeneous catalyst [106].

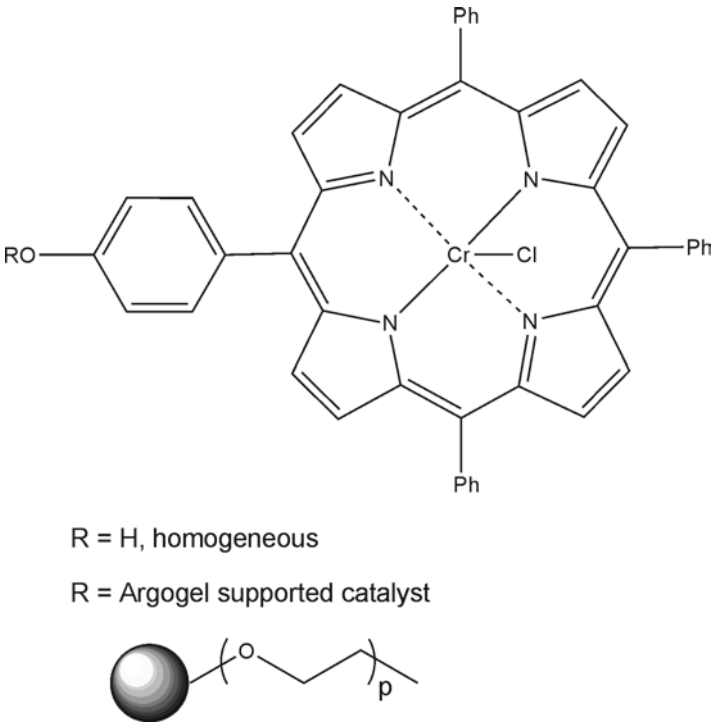

Fig. 11.13 Cr(III) catalyst for the copolymerization of CO_2 and cyclohexene oxide (Adapted from [105] and reproduced by permission of the Royal Society of Chemistry)

Table 11.5 Summary of the results of Holmes and co-workers for the copolymerization of CO_2 and cyclohexene oxide

Entry	Cycle	Yield	M_n[a]	PDI[a]
1	1	56	3,600	1.3
2	2	40	3,000	1.4
3	3	25	2,300	1.1
4	1	55	4,000	1.4
5	2	50	3,500	1.2
6	3	6	1,500	1.3
7	1	64	5,000	1.2
8	2	64	3,700	1.1
9	3	47	2,000	1.1
10	4	7	1,400	1.1

[a]Determined from GPC measurements. Conditions: P = 170 bar, T = 90°C, volume fraction of monomer 25%, 100 mg of catalyst used

11.3.2 Zn(II) Base Initiators

As with the ROP of lactones the heterogenization of Zn(II) has proved popular and there are several well-designed examples in the literature [28, 107]. An early example was the work of Kim who made use of the so-called double-metal-cyanide (DMC) catalysts, amongst others. The catalysts are prepared by the reaction of $K_3Co(CN)_6$ and $ZnCl_2$ in water/alcohol. These have been shown to very active catalyst for the copolymerization of CO_2 with epoxides. These systems are beyond the scope of this chapter since they are not truly heterogenized homogeneous catalysts; however there are numerous examples in the literature of these systems [108–110].

An example of heterogenizing a homogeneous catalyst is again by C.W. Jones et al. [28, 64]. In this work the two approaches for heterogenization of Zn(II), as discussed in Section 11.2.1, were also utilized for the copolymerization. However, a third heterogenization method was also employed Fig. 11.14, for the preparation. In this approach instead of forming pre-coordinated Zn(II) complexes and then heterogenizing to silica, the ligand was first bound to silica followed by addition of the Zn(II) metal centre, Fig. 11.14:

Again two supports were utilized, namely CPG and SBA-15 and the heterogeneous materials (prepare via the three methods) and the homogeneous systems were tested for the copolymerization of CO_2 and cyclohexene oxide, Table 11.6:

Analogous homogeneous initiators afforded a TON of c.a. 200, M_n ca. 11,000 g/mol and PDIs typically less than 1.10. All the modified heterogeneous systems have activity less than the homogeneous system. The SBA-15 heterogeneous systems (entries 1–3, Table 11.6) have approximately a sixth of the activity of the homogeneous system. The heterogeneous systems also have increased ether linkages and consequently reduced carbonate linkages compared to the heterogenized system. The relatively poor performance of the systems prepared using method III was attributed to the difficulty in generating the Zn-OMe catalyst in-situ on the solid support. It is hypothesized that the MeOH can react with the silica surface, limiting the amount available for the desired transformation, an excess of MeOH was not an

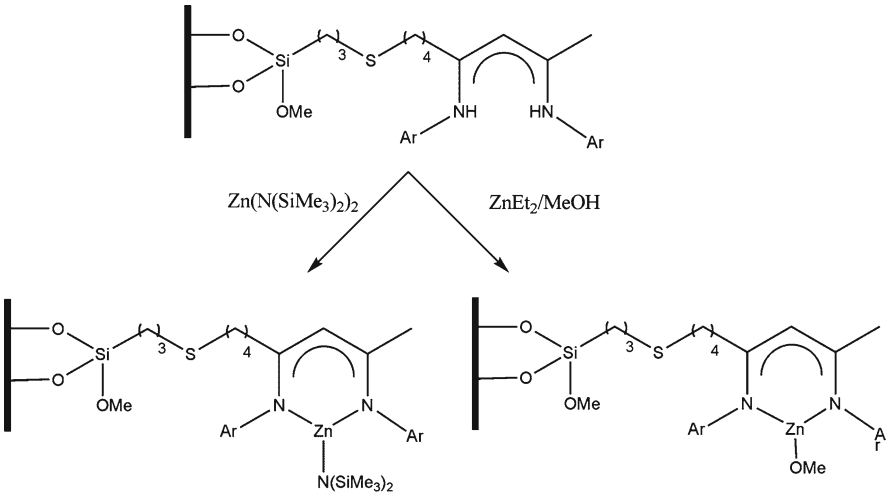

Fig. 11.14 Homogeneous and heterogeneous initiators based on Zn(II) for the copolymerization of CO_2 and epoxides (Adapted from [28])

Table 11.6 Summary of the results of C.W. Jones et al. for the copolymerization of CO_2 and cyclohexene oxide

Entry	Catalyst[a]	[Monomer]:[Cat]	TON[b]	Carbonate linkages[c]	M_n[d]	PDI[d]
1	I-OMe	1,457	72	73	15,500	1.31
2	II-OMe	1,467	70	61	14,700	1.48
3	III-OMe	1,546	40	33	25,200	1.89
4	I-OMe	2,000	126	78	16,600	1.29
5	II-OMe	2,800	102	69	15,900	1.40
6	III-OMe	3,400	48	41	23,400	1.62

[a]See Figs. 11.4 and 11.14 for the numbering of the initiators I-OMe indicates that the catalyst was prepared via method one and that the R group = OMe, II using method two and III method three

[b]TON = turn-over-number

[c]Determined from ^{1}H NMR spectroscopic analysis

[d]Determined from GPC measurements. The polymerizations were performed in neat cyclohexene oxide, T = 50°C, P = 100 psi. Entries 1–3 use SBA-15 as the support and 4–6 are the Zn(II) catalysts heterogenized on CPG

option since this led to demetalation of the ligand. A perceived problem of the use of SBA-15 was that the pores could become full and then blocked by the growing polymer chain and thus inhibiting mass transport of the monomer to the active metal center. To investigate this further the Zn(II) systems were supported on the much larger pore size material CPG, which should have much more efficient mass transport properties. As predicted higher activity was observed (Table 11.6, entries 4–6) with a higher percentage of the desirable carbonate linkages. However, a drawback of this system is the low surface area of the CPG results in a lower metal loading, therefore to achieve the desired TONs a larger amount of material is required.

As with the lactide polymerization discussed in Section 11.2.1 silica can be simply treated with alkyl-zinc species to generate active catalysts. A classic example of this approach is the work of Duchateau and co-workers [107]. In this example $ZnEt_2$ is easily anchored to silica, the loading of was determined by ICP-MS and was found to be 1.82 mmol per gram of SiO_2. A silsesquioxane model compound was also prepared. In this work silsesquioxanedisilanol was utilized instead of the triol in the work of M.D. Jones [76]. This produced complexes which contain four Zn(II) centers all of which have one alkyl group coordinated, Fig 11.15:

The model compound, the heterogeneous system and $Zn(OTf)_2$ were tested for the copolymerization of cyclohexene oxide and CO_2, Table 11.7.

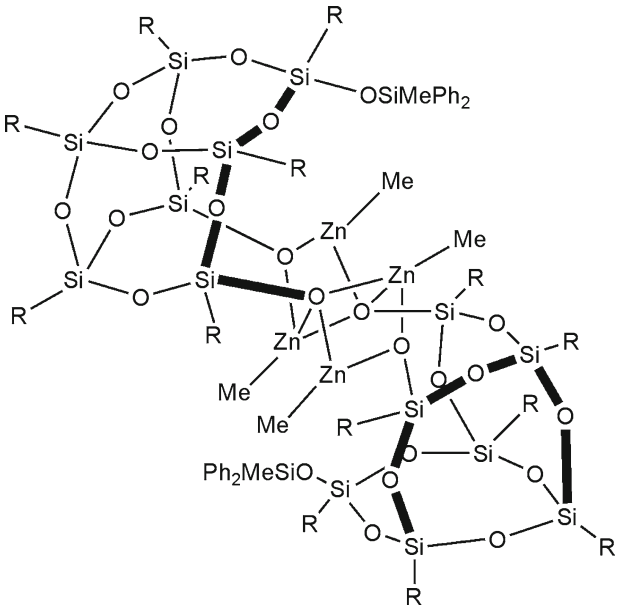

Fig. 11.15 Model homogeneous silsesquioxane complex for the copolymerization of cyclohexene oxide and CO_2 (Adapted from [107], R = c-C_5H_9)

Table 11.7 Summary of the results of Duchateau et al. for the copolymerization of CO_2 and cyclohexene oxide

Catalyst	T/°C	CHO conversion %[a]	TOF[b]	M_n[c]	PDI[c]
$[Zn(OTf)_2.THF]_2$	80	19	15.4	25,800	18.4
Model	80	34	10.1	10,600	10.8
Model	120	44	13.5	11,600	10.0
SiO_2-$ZnEt_2$	120	6	0.7	9,000	5.3
SiO_2-$ZnEt_2$	120	6	0.6	8,400	5.0

[a]The conversion of cyclohexene oxide was determined via ^{1}H NMR spectroscopy
[b]TOF = turn-over-frequency
[c]Determined from GPC measurements. The polymerizations were performed at, P = 80 bar, catalyst loading 200 μmol, 35 ml of toluene, 15 ml of cyclohexene oxide

The homogeneous systems were seen to be more active with significantly higher TOFs, however the PDIs are significantly lower using the heterogeneous catalyst.

11.4 Conclusions and Future Challenges

This chapter has detailed several approaches for the use of heterogeneous systems for the ROP of cyclic esters and copolymerization of epoxides and CO_2. It has been shown that significant enhancements in the polymerization can be achieved by heterogenization. However, significant challenges remain for this technology to become industrially relevant and to rival established homogeneous protocols. Namely, (i) stereocontrol in the polymerization of *rac*-lactide; (ii) the ability for the systems to be efficient under the industrially preferred melt (temperatures in excess of 130°C) conditions; (iii) it is difficult to predict how immobilized catalyst will behave, in most examples the heterogenized systems behave subtly different to their homogeneous counterparts. The ability to formulate structure–activity relationships is of paramount importance in the future development of the materials discussed, this will be achieved by preparing *single-site fully characterized* heterogeneous systems; (iv) perhaps the most significant challenge is that only a handful of systems are able to be recycled without significant loss in activity. A key issue that is preventing widespread use of heterogenized systems in the fact that these catalysts are prone to metal leaching, it is imperative that the cause of such leaching is understood so that it can be controlled.

References

1. Hlatky GG (2000) Chem Rev 100:1347–1376
2. Lu J, Toy PH (2009) Chem Rev 109:815–838
3. Wight AP, Davis ME (2002) Chem Rev 102:3589–3613
4. Yin LX, Liebscher J (2007) Chem Rev 107:133–173
5. Anastas PT, Kirchhoff MM (2002) Acc Chem Res 35:686–694
6. Anastas PT, Kirchhoff MM, Williamson TC (2001) Appl Catal General 221:3–13
7. Anastas PT, Zimmerman JB (2003) Environ Sci Technol 37:94A–101A
8. Gallezot P (2007) Green Chem 9:295–302
9. Schlaf M (2006) Dalton Trans 39:4645–4653
10. Clavier H, Grela K, Kirschning A et al (2007) Angew Chem Int Ed Engl 46:6786–6801
11. Coperet C (2004) New J Chem 28:1–10
12. Eissen M, Metzger JO, Schmidt E et al (2002) Angew Chem Int Ed Engl 41:414–436
13. Furstner A, Ackermann L, Beck K et al (2001) J Am Chem Soc 123:9000–9006
14. Kiss AA, Dimian AC, Rothenberg G (2006) Adv Synth Catal 348:75–81
15. Ragauskas AJ, Williams CK, Davison BH et al (2006) Science 311:484–489
16. Poliakoff M, Fitzpatrick JM, Farren TR et al (2002) Science 297:807–810
17. Mours M (2008) ChemSusChem 1:59–62
18. Baleizao C, Gigante B, Das D et al (2004) J Catal 223:106–113

19. Corma A, Garcia H (2006) Adv Synth Catal 348:1391–1412
20. Corma A, Garcia H, Moussaif A et al (2002) Chem Commun 10:1058–1059
21. Jones MD, Raja R, Thomas JM et al (2003) Top Catal 25:71–79
22. Jones MD, Raja R, Thomas JM et al (2003) Angew Chem Int Ed Engl 42:4326–4331
23. Raja R, Thomas JM, Jones MD et al (2003) J Am Chem Soc 125:14982–14983
24. De Vos DE, Dams M, Sels BF et al (2002) Chem Rev 102:3615–3640
25. Rechavi D, Lemaire M (2002) Chem Rev 102:3467–3493
26. Xia QH, Ge HQ, Ye CP et al (2005) Chem Rev 105:1603–1662
27. Thomas JM, Raja R (2008) Acc Chem Res 4:708–720
28. Yu KQ, Jones CW (2003) Organometallics 22:2571–2580
29. Tajima K, Aida T (2000) Chem Commun 24:2399–2412
30. Beck JS, Vartuli JC, Roth WJ et al (1992) J Am Chem Soc 114:10834–10843
31. Kresge CT, Leonowicz ME, Roth WJ et al (1992) Nature 359:710–712
32. Ng SM, Ogino S, Aida T et al (1997) Macromol Rapid Commun 18:991–996
33. Wu CG, Bein T (1994) Science 264:1757–1759
34. Johnson SA, Khushalani D, Coombs N et al (1998) J Mater Chem 8:13–14
35. Kageyama K, Tamazawa J, Aida T (1999) Science 285:2113–2115
36. Gimenez J, Nunes CD, Vaz PD et al (2006) J Mol Catal A Chem 256:90–98
37. Kageyama K, Ogino S, Aida T et al (1998) Macromolecules 31:4069–4073
38. Bochmann M (1996) J Chem Soc Dalton Trans 3:255–270
39. Britovsek GJP, Gibson VC, Wass DF (1999) Angew Chem Int Ed Engl 38:428–447
40. Allen DP, Van Wingerden MM, Grubbs RH (2009) Org Lett 11:1261–1264
41. Chamberlain BM, Cheng M, Moore DR et al (2001) J Am Chem Soc 123:3229–3238
42. Cheng M, Attygalle AB, Lobkovsky EB et al (1999) J Am Chem Soc 121:11583–11584
43. Chmura AJ, Chuck CJ, Davidson MG et al (2007) Angew Chem Int Ed Engl 46:2280–2283
44. Chmura AJ, Davidson MG, Frankis CJ et al (2008) Chem Commun 11:1293–1295
45. Ovitt TM, Coates GW (2002) J Am Chem Soc 124:1316–1326
46. Albertsson AC, Varma IK (2003) Biomacromolecules 4:1466–1486
47. Rezwan K, Chen QZ, Blaker JJ et al (2006) Biomaterials 27:3413–3431
48. Auras R, Harte B, Selke S (2004) Macromol Biosci 4:835–864
49. Khan JH, Schue F, George GA (2009) Polym Int 58:296–301
50. Czajkowska B, Dobrzynski P, Bero M (2005) J Biomed Mater Res A 74A:591–597
51. Arnold PL, Buffet JC, Blaudeck RP et al (2008) Angew Chem Int Ed Engl 47:6033–6036
52. Chisholm MH, Gallucci J, Phomphrai K (2003) Chem Commun 1:48–49
53. Chisholm MH, Gallucci JC, Phomphrai K (2004) Inorg Chem 43:6717–6725
54. Chisholm MH, Gallucci JC, Phomphrai K (2005) Inorg Chem 44:8004–8010
55. Chisholm MH, Phomphrai K (2003) Inorg Chim Acta 350:121–125
56. Chmura AJ, Davidson MG, Jones MD et al (2006) Macromolecules 39:7250–7257
57. Gendler S, Segal S, Goldberg I et al (2006) Inorg Chem 45:4783–4790
58. Ma H, Spaniol TP, Okuda J (2008) Inorg Chem 47:3328–3339
59. Whitelaw EL, Jones MD, Mahon MF et al (2009) Dalton Trans 41:9020–9025
60. Zhong ZY, Dijkstra PJ, Feijen J (2002) Angew Chem Int Ed Engl 41:4510–4513
61. Zhong ZY, Dijkstra PJ, Feijen J (2003) J Am Chem Soc 125:11291–11298
62. Kageyama K, Tatsumi T, Aida T (1999) Polym J 31(11):1005–1008
63. Kruk M, Jaroniec M, Ko CH et al (2000) Chem Mater 12:1961–1968
64. Yu KQ, Jones CW (2004) J Catal 222:558–564
65. Wilson BC, Jones CW (2004) Macromolecules 37:9709–9714
66. Miola-Delaite C, Colomb E, Pollet E et al (1999) Anionic ring opening polymerization of oxygenated heterocycles with supported zirconium and rare earths alkoxides as initiators in protic conditions. Towards a catalytic heterogeneous process. In: International symposium on recent advances in ring opening (metathesis) polymerization (ROMP 99). Mons, Belgium.
67. Pollet E, Hamaide T, Tayakout-Fayolle M et al (2004) Polym Int 53:550–556
68. Martin E, Dubois P, Jerome R (2003) Macromolecules 36:7094–7099
69. Moore DR, Cheng M, Lobkovsky EB et al (2003) J Am Chem Soc 125:11911–11924

70. Jones MD, Davidson MG, Keir CG et al (2009) Eur J Inorg Chem 5:635–642
71. McKittrick MW, Jones CW (2003) Chem Mater 15:1132–1139
72. Rajabi F, Clark JH, Karimi B et al (2005) Org Biomol Chem 3:725–726
73. Jana S, Dutta B, Bera R et al (2007) Langmuir 23:2492–2496
74. Mostafa SI, Ikeda S, Ohtani B (2005) J Mol Catal A Chem 225:181–188
75. Hormnirun P, Marshall EL, Gibson VC et al (2004) J Am Chem Soc 126:2688–2689
76. Jones MD, Keir CG, Johnson AL, Mahon MF (2010) Polyhedron 29:312–316
77. Maschmeyer T, Rey F, Sankar G et al (1995) Nature 378:159–162
78. Jones MD, Davidson MG, Keir CG et al (2008) Dalton Trans 28:3655–3657
79. Kim E, Shin EW, Yoo IK et al (2009) J Mol Catal A Chem 298:36–39
80. Kim E, Shin EW, Yoo IK et al (2009) Macromol Res 17:346–351
81. Fraile JM, Garcia JI, Mayoral JA et al (1995) J Chem Soc Chem Commun 5:539–540
82. Fraile JM, Garcia JI, Mayoral JA et al (2003) J Phys Chem B 107:519–526
83. Chisholm MH, Iyer SS, Matison ME et al (1997) Chem Commun 20:1999–2000
84. Thakur KAM, Kean RT, Zell MT et al (1998) Chem Commun 17:1913–1914
85. Feher FJ, Newman DA, Walzer JF (1989) J Am Chem Soc 111:1741–1748
86. Crocker M, Herold RHM, Orpen AG (1997) Chem Commun 24:2411–2412
87. Maschmeyer T, Klunduk MC, Martin CM et al (1997) Chem Commun 19:1847–1848
88. Quadrelli EA, Davies JE, Johnson BFG et al (2000) Chem Commun 12:1031–1032
89. AbdelFattah TM, Pinnavaia TJ (1996) Chem Commun 5:665–666
90. Deshayes G, Mercier FAG, Degee P et al (2003) Chem Eur J 9:4346–4352
91. Deshayes G, Poelmans K, Verbruggen I et al (2005) Chem Eur J 11:4552–4561
92. Poelmans K, Pinoie V, Verbruggen I et al (2008) Organometallics 27:1841–1849
93. Oshimura M, Takasu A, Nagata K (2009) Macromolecules 42:3086–3091
94. Takasu A, Oshimura M, Hirabayashi T (2008) J Polym Sci Part A Polym Chem 46:2300–2304
95. Tortosa K, Hamaide T, Boisson C et al (2001) Macromol Chem Phys 202:1156–1160
96. Csihony S, Culkin DA, Sentman AC et al (2005) J Am Chem Soc 127:9079–9084
97. Culkin DA, Jeong WH, Csihony S et al (2007) Angew Chem Int Ed Engl 46:2627–2630
98. Pratt RC, Lohmeijer BGG, Long DA et al (2006) J Am Chem Soc 128:4556–4557
99. O'Keefe BJ, Hillmyer MA, Tolman WB (2001) J Chem Soc Dalton Trans 15:2215–2224
100. Darensbourg DJ, Mackiewicz RM, Phelps AL et al (2004) Acc Chem Res 37:836–844
101. Inoue S, Koinuma H, Tsuruta T (1969) J Polym Sci Part B Polym Phys 7:287–292
102. Okamoto M, Sugiyama J (2009) J Appl Polym Sci 114:2226–2234
103. Okamoto M, Sugiyama J, Yamamoto T (2008) J Appl Polym Sci 110:3902–3907
104. Darensbourg DJ, Stafford NW, Katsurao T (1995) J Mol Catal A Chem 104:L1–L4
105. Stamp LM, Mang SA, Holmes AB et al (2001) Chem Commun 23:2502–2503
106. Mang S, Cooper AI, Colclough ME et al (2000) Macromolecules 33:303–308
107. Duchateau R, van Meerendonkt WJ, Huijser S et al (2007) Organometallics 26:4204–4211
108. Darensbourg DJ, Adams MJ, Yarbrough JC et al (2003) Inorg Chem 42:7809–7818
109. Darensbourg DJ, Adams MJ, Yarbrough JC (2001) Inorg Chem 40:6543–6544
110. Robertson NJ, Qin ZQ, Dallinger GC et al (2006) Dalton Trans 45:5390–5395

Chapter 12
Reactivity and Selectivity of Heterogenized Homogeneous Catalysts: Insights from Molecular Simulations

Kourosh Malek and Rutger A. Van Santen

Abstract Immobilized metal complexes on nanoporous materials have recently been proposed as a novel class of heterogeneous enantioselective catalyst for epoxidation of unfunctionalized olefins as well as hydrogenation, alkylation, and nitroaldol reactions. The porous hosted materials affect catalytic performance due to a cooperative interaction among the nanoporous solid, immobilizing linker, and metal complex asymmetry. The effects of mesoporous materials and immobilizing agents on chiral catalysis are not well understood, however, the catalysts confined in nanopores show comparable or even higher conversions and enantioselectivity compared to their homogeneous counterparts. This chapter highlights major scientific problems for fundamental understanding and design of heterogenized homogeneous catalysts. It describes in detail the pivotal role of a sound framework in physical theory and molecular modeling in systematic efforts towards better materials and catalytic performance optimization. The common threads of the various topics addressed is the wide range of scales that has to be considered in establishing relations between structure, physicochemical properties, and catalytic performance. Physical theory and modeling employ a variety of methods, encompassing ab-initio calculations, molecular simulations, and the continuum model of transport and reaction in nanoporous materials. We particularly describe how molecular simulations can be used to investigate the origin of enantioselectivity of an anchored metal complex in nanoporous materials. These

K. Malek (✉)
National Research Council of Canada, Institute for Fuel Cell Innovation,
4250 Wesbrook Mall, V6T 1W5, Vancouver, BC, Canada
and
Department of Chemistry, Simon Fraser University, 8888 University Drive,
V5A 1S6, Burnaby, BC, Canada
e-mail: kourosh.malek@nrc-cnrc.gc.ca

R.A. Van Santen
Schuit Institute of Catalysis, ST/SKA, Eindhoven University of Technology,
Eindhoven, The Netherlands
e-mail: R.A.v.Santen@tue.nl

P. Barbaro and F. Liguori (eds.), *Heterogenized Homogeneous Catalysts for Fine Chemicals Production*, Catalysis by Metal Complexes 33,
DOI 10.1007/978-90-481-3696-4_12, © Springer Science+Business Media B.V. 2010

studies provide new insights into the steric effects that relate to choices of substrate and linker and to the interplay with mesopore confinement. We also bring detailed example of employing molecular simulations to unravel the catalytic properties of metallomacrocyclics for the electrochemical reduction of molecular oxygen in aqueous media. We rationalize the importance of immobilization and show how it relates to the steric communication between the substrate and the metal complex. These fundamental concepts are important for the interpretation of the enantioselectivity of immobilized organometallic catalysts in nanoporous materials.

12.1 Introduction

Nanoporous materials are currently of the utmost importance in major nanotechnological areas in chemistry and chemical engineering such as catalysis, separation and biotechnology [1–5]. These materials are anywhere from nanoporous and composite catalysts, amorphous mesoporous organic or inorganic membranes, to cross-linked protein and enzyme crystals and biological membranes. Selective adsorption, diffusion, and reaction of molecules in the nanoporous materials are of paramount importance in catalysis and separation technologies [6, 7].

Zeolitic nanoporous materials play important roles in catalysis, adsorption, and separation because they consist of a unique porous structure, and high reaction and adsorption selectivity. The use of zeolites, as one of the most important microporous materials, is limited to host small molecules, as a result of small channels and cavities of sizes between 0.8 and 1.5 nm [8]. In contrast to zeolites, mesoporous materials of channel sizes in the range of 2–50 nm permit easy migration of molecules in the host frameworks [9]. Mesoporous materials are the most applicable supports for the immobilization of transition metal complexes [10, 11]. Particularly in this class, FSM (folded sheets mesoporous material) and MCM (mobile composition of matter) materials have attracted great attention mainly due to their uniform pore sizes larger than 2 nm, large pore volumes, and considerable surface areas. Depending on the synthesis method, the pore sizes of these materials can be controlled ranging from about 1.5 nm to about 30 nm [12, 13].

Immobilized metal complexes on micro- and meso-porous materials have recently been proposed as a novel class of heterogeneous selective catalysts [14–36]. Mesoporous materials can be functionalized by incorporating (anchoring) small to large catalyst species on the pore wall or on the pore surface [14, 20]. Four main approaches have been commonly used to immobilize the chiral catalyst: adsorption of chiral modifiers onto an active metal surface; covalent tethering of homogeneous catalysts; electrostatic interaction between a negatively charged framework and a cation; and encapsulation. Two main fabrication methods have been generally used to anchor functional groups onto a mesostructured material: grafting method as a post-synthesis technique and co-condensation reaction in a direct synthesis process. The grafting process is based on the modification of the

surface with organic groups, whereas direct synthesis refers to the co-condensation of precursors in the presence of structure-directing agent (SDA). Both methods produce materials with functional groups in the mesopores. The porous hosted materials affect catalytic performance due to a cooperative interaction among the nanoporous solid, immobilizing linker, and metal complex [14, 15]. Along with hydrothermal stability and excellent selectivity, this attractive strategy has the inherent advantages of heterogeneity, such as easy separation and operation.

Based on density functional calculations (DFT and QM/MM) and molecular dynamics simulations, new insights were provided on the importance of electronic and steric effects for epoxidation reaction of *cis*- and *trans*-methylstyrene catalyzed by anchored oxo-Mn-salen into MCM-41 channels [37, 38]. Calculations showed that how immobilization relates to the linker and substrate choice as well as the interplay with the confined channel. Although a trans-substrate has a higher level of asymmetric induction to the immobilized Mn-salen complex than that to a homogeneous catalyst [39], the reaction path is most likely more favorable for the cis-substrate. The MCM-41 channel reduces the energy barriers and enhances the enantioselectivity by influencing geometrical distortions of Mn-salen complex [38].

Metallomacrocyclics have been extensively used as the electrocatalyst for the electrochemical reduction of oxygen [40–50]. Either in aqueous media or confined on an electrode surface, the electrocatalytic activity of these materials are affected by the nature of the central metal, the ligands, and the conformation of bimetallic molecules. Different factors affect the catalytic activity of these materials such as the nature of the central metal and the ligand, and the particular conformation of bimetallic molecules. The special catalytic activity is due to the binding of O_2 simultaneously to two metal centers [40–45]. Despite unresolved questions about the electrocatalytic reduction activity of O_2 mediated by metallomacrocyclics confined on electrode surfaces, it is well demonstrated that Fe and Co macrocyclic complexes are by far the best catalyst for oxygen reduction reaction (ORR) [50]. Generally, for non-Pt catalysts, elucidating the active site structure is a challenge. Theoretical modeling has applied valuable structural information, facilitating the basic understanding of active site structures [46, 47, 49].

Our focus in this chapter is on providing an overview of the state of affairs in theory and molecular modeling of selectivity and reactivity of heterogenized, homogeneous catalysts. The theoretical framework fulfils an integrating function in this complex interrelated endeavor, linking the various disciplines in molecular heterogeneous catalysis, particularly selectivity and structure–reactivity relationship. At the fundamental level, theory helps to unravel complex relations between chemical and morphological structures and properties, bridging scales from molecular to macroscopic resolutions. Understanding these relations could facilitate the design of novel, tailor-made catalyst materials. We bring detailed examples from asymmetric epoxidation reaction of *cis*- and *trans*-methylstyrene on oxo-Mn-salen in the mesopore of MCM-41, and the catalytic properties of metallomacrocyclics for the electrochemical reduction of molecular oxygen in aqueous media.

12.2 Chiral Metal Complexes Immobilized in Mesoporous Materials

Heterogeneous chiral metal catalysts immobilized in the nanopores of mesoporous materials have been synthesized and applied for asymmetric hydrogenation, epoxidation, alkylation, and nitroaldol reactions [14, 15]. The effects of mesoporous materials and immobilizing agents on chiral catalysis are not well understood, however, the catalysts confined in nanopores show comparable or even higher conversions and enantioselectivity compared to their homogeneous counterparts. Recently, immobilization of chiral Mn-salen catalysts in mesoporous silicas have been investigated for the asymmetric epoxidation of unfunctionalized olefins [51–58]. Mn-salen catalysts can axially immobilized in the nanopores and on the external surface of mesoporous materials through phenoxy and organic sulfonic linkers. For the asymmetric epoxidation of unfunctionalized olefins, the Mn-salen catalysts immobilized in the nanopores generally provide higher chemical selectivity and enantioselectivity than those immobilized on the external surface of supports [14, 39, 51–53]. Concomitantly, the Mn-salen catalysts grafted through flexible propyl sulfonic groups generally give higher chemical selectivity and enantioselectivity than those grafted through rigid phenyl sulfonic groups. This is probably due to the electronic and steric factors of the linkages, which may affect the configuration of the transition state for the asymmetric reactions.

For chiral Mn-salen catalysts immobilized in the nanopores of supports, an increase in conversion, chemical selectivity, and enantioselectivity was observed with increasing the axial linkage lengths [15]. The porous hosted materials affect catalytic performance due to a cooperative interaction among the nanoporous solid, immobilizing linker, and Mn-salen complex [14, 15, 37–39, 50–53]. Along with hydrothermal stability and excellent enantioselectivity, this attractive strategy has the inherent advantages of heterogeneity, such as easy separation and operation. Mesoporous materials are the most applicable supports for the immobilization of Mn-salen complexes [14, 15, 50]. For Mn-salen catalysts immobilized on the external surface of the support, on the other hand, the conversion and chemical selectivity increases, but the enantioselectivity remains unchanged.

The difficulty in the diffusion of reactants and products in nanopores may reduce the reaction conversions. To improve the conversion, the nanopores of the mesoporous materials are modified with organic groups [15]. In general, asymmetric reactions in nanopores, compared to those on the surface and in homogeneous media, can improve the enantioselectivity for some asymmetric transformations. When the nanopore size of the support or the tether length is tuned to a suitable value, the chiral catalysts in the nanopores can show higher enantiselectivity yield. Moreover, hydrophobic modification of the inner wall of mesoporous silica is believed to result in improving catalytic activity and enantioselectivity [14, 15].

12.2.1 Molecular Modeling of Enantioselectivity of Immobilized Mn-Salen Complexes

In a heterogeneous catalyst, reactant molecules diffuse through the pore network, collide with pore walls and react on active sites on these walls. This implies that the topology of the pore network and the morphology of pores affect the molecular movement and the accessibility of the active sites. Hence the diffusivities of the components and therefore the conversion and product distributions of the reaction depend on the catalyst geometry. The correlation between the chemical heterogeneity and diffusion still remains poorly understood. It is not feasible, if not impossible, to make exact predictions for the effective properties of composite materials with the simple models of morphology. Both continuum and discrete models have been applied to provide and describe the theoretical approaches for estimating the effective properties of random heterogeneous materials. As described above, continuum models represent the classical approach to describing and analyzing transport processes in materials of complex and irregular morphology. Thus, the effective properties of materials are defined as averages of the corresponding microscopic quantities. The shortcoming of discrete models such as random network models, Bethe lattice models etc. compared to continuum models, is the demand for large computational effort to represent a realistic model to describe the material and simulate its effective properties. It is of course a challenging problem to generate a realization of a heterogeneous material, for which limited microstructure information is available.

Mn-salen complexes have been successfully anchored in the mesopores of MCM-41 through the complexation of manganese by oxygen atoms of a linkage grafted on the surface of MCM-41 [14, 15, 51–58]. It has been shown that these heterogeneous catalysts give different excess enantioselectivity (ee) values for asymmetric epoxidation of *cis*-β-methylstyrene than their homogeneous counterparts [14, 15, 51–53]. The choice of *cis*- or *trans*- (*Z* or *E*) olefin as the substrate is another important issue worthy of further investigation [58]. Despite the numerous experimental and computational studies on various homogeneous Mn-salen-based catalysts, the exact mechanism of the Mn-salen complex reaction remains under extensive debates [59–67]. Although the origin of the enantioselectivity of Mn-salen complexes has been extensively investigated by first-principle calculations [60–62], the mechanism of epoxidation of olefins by a heterogeneous immobilized Mn-salen catalyst cannot be trivially inferred from that occurring with homogeneous catalysts. The mechanism of enantioselective induction is not well known from a microscopic standpoint. A detailed computational study on the immobilized Mn-salen/MCM-41 system can help unravelling the catalytic properties of the immobilized Mn-salen complexes as a function of substrate, nanoporosity, and immobilizing linker. It is necessary to provide an improved understanding of how confinement and stereochemical effects of the nanopores and immobilizing agents influence the choice of enantioselective reaction path.

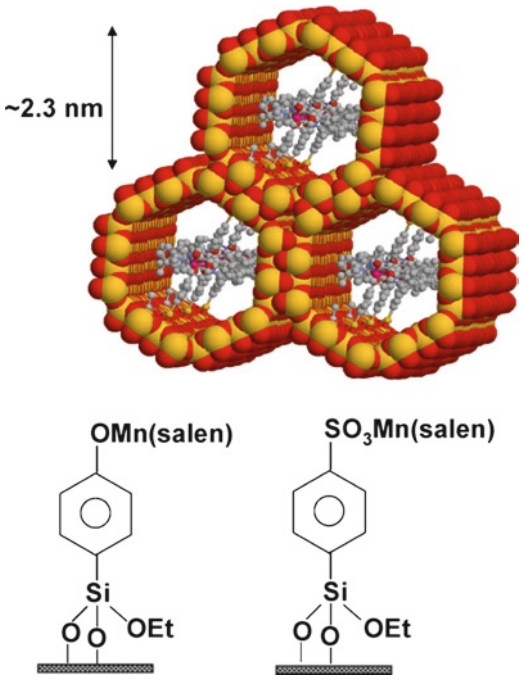

Fig. 12.1 (**a**) Visualized Mn-salen complexes anchored inside a MCM-41 channel using phenoxyl group as the immobilizing linker. (**b**) The models for the immobilized Mn-salen complexes using different axial linkages [38]

12.2.1.1 Molecular Dynamics Simulations

Malek et al. [37, 38] studied the asymmetric epoxidation reaction of cis- and trans-methylstyrene on oxo-salen, confined in the mesopore of MCM-41 using molecular dynamic simulations (Fig. 12.1). The calculations based on full-atomistic molecular dynamic simulations provided new insights into the importance of electronic and steric effects of the salen ligand, substrate, immobilizing linker, and MCM-41 channel. The calculation demonstrated the influence of the confined framework, substrate (*cis*- vs *trans*-) and immobilizing linker on the conformation of the immobilized Mn-salen complex. To translate this into practice, the continuous chirality measure (CCM) was adopted to quantitatively evaluate the distortion of Mn-salen complex [68–72]. The chirality of the complex was evaluated and compared to that of a free complex in vacuo and that of a free complex within the MCM-41 mesopore. Malek et al [37] performed independent simulations in the presence of a docked *cis*- and *trans*-β-methyl styrene as the substrate, where the steric interactions were analyzed by means of Mn-salen complex dynamics.

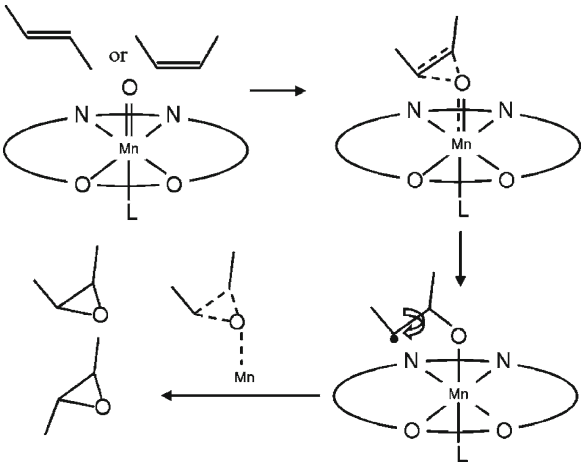

Fig. 12.2 General mechanism scheme for asymmetric epoxidation of olefins using Mn-salen complexes; L = axial linker [37]

The oxo-Mn intermediate (Fig. 12.2) carries the activated oxygen that will be attached to the olefin double bond. Oxo-Mn-salen complex is used as the model catalyst, attaching to phenoxyl group as the immobilizing linker. In Ref. [37], all simulations were carried out using a fully atomistic model of Mn-salen complex, phenoxyl linker, and MCM-41 channel. MD simulations explain the enantioselectivity of an immobilized Mn-salen complex in MCM-41 in terms of the dynamics of the salen ligand. Due to the interactions with axial linkage and MCM-41, the Mn-salen complex may prefer a distorted conformation. The MD force field has adapted the nonbonding and bonding parameters of Mn and Si from the ESFF force field [73]. ESFF is an ab initio-derived force field, covering all atoms up to Rn in the periodic table. The parameterization in ESFF has been shown to be sufficient for organometallic compounds such as the salen complexes [74]. A typical effective potential is of the form

$$
\begin{aligned}
V = & \sum_{\text{bond}} D_{\text{bi}} \left[1 - \exp\left(-\alpha_i \left(r - r_i^0 \right) \right) \right]^2 \\
& + \sum_{\text{angles}} \frac{K_{ai}}{\sin^2 \theta_i^0} \left[\cos\theta - \cos\theta_i^0 \right]^2 \\
& + \sum_{\text{dihedrals}} k^{\Phi} \left(1 + \cos\left(n \left(\Phi - \Phi^0 \right) \right) \right) \\
& + \sum_{i<j} \frac{A_{ij}}{r_{ij}^{12}} - \frac{B_{ij}}{r_{ij}^{6}} + \sum_{i<j} \frac{\operatorname{erfc}\left(\beta r_{ij} \right)}{4\pi \in_0 r_{ij}} q_i q
\end{aligned}
\tag{12.1}
$$

12.2.1.2 Continuous Chirality Measure (CCM)

A continuous symmetry scale is able to express quantitatively how far a given distorted structure is from ideal symmetry [68–72]. A chiral center is usually determined by a condition that no pair of groups attached to the atom in the center is identical. Chirality is conventionally defined in tetravalent configurations and never for planar structures [68]. The degree of chirality or the disturbance of achirality also depends on the size and chemical nature of the groups attached to a chiral center. If a large group is used as a substituent in the chiral center, then the chirality of the molecule is not so pronounced. In some cases, a pair of identical groups still produces chirality. To explain these observations, a quantitative description of "chirality" is needed. Numerous approaches have been developed to quantifying chirality of an object [68, 69]. The Avnir CCM is one of the best models and has proven a high degree of predictability in many cases [68]. Malek et al. [37], used the CCM method to compute the chirality content of the optimized geometries of the salen complex. The optimized geometry of the Mn-salen complex of different steps along the reaction pathways is used as input for the calculation of CCM. The measure is based on the minimal distance that the atoms of the molecule need to undergo to attain a desired symmetry, namely achirality. The structure of desired symmetry is not a priori and is obtained by optimization techniques for each configuration. The latter is the most time-consuming step in evaluating the chirality content of an object by the CCM approach [69, 70]. In analogy to a recent work by Handgraaf et al. [75], a slightly different approach was used in [37] to calculate the chirality of the complexes. In [37] the minimum distance between the enantiomers is calculated by superimposing the random orientation of the enantiomers on each other. After superimposing two enantiomers by translation to the coordinates of the image to the Mn center, the image enantiomer is randomly rotated (by generating random angles using a spherical coordinate centered at Mn), until the minimum value of CCM is attained. Thus, the numerical optimization procedure is less complicated [75].

12.2.1.3 Effects of Substrate, Linker and Confinement

The triplet and quintet spin states of the oxo-Mn-salen complex are of lower energy relative to the singlet state [38, 65, 76], where puckered and step-like distortions exist for triplet and quintet.

Table 12.1 illustrates the effect of the linker on the relative energies of the different spin states, calculated by Density Functional Theory (DFT) and based on the

Table 12.1 Relative energies (kJ/mol) of spin states for truncated oxo-Mn-salen complex vs axial linkage [37]

Method	Spin state	Mn-salen-Cl	Mn-salen-phenoxyl
B3LYP	Singlet	10	50
B3LYP	Triplet	0	0
B3LYP	Quintet	2	10

Mn triple-basis/B3LYP/6-31G* [37, 38]. In the presence of Chloride (L=Cl), the triplet state is the ground state [37, 38, 65, 76]. Some studies have shown that the triplet state is almost isoenergetic with the single state [60]. Similarly, when the phenoxyl group is introduced, a triplet state becomes the most stable state. In the MD simulations, a step-like structure is believed to be the starting configuration for the Mn-salen complex. We assume that epoxidation reaction for both homogeneous catalysts (i.e., where Cl is the axial ligand) and heterogeneous catalysts (i.e., where phenoxyl group is the axial ligand) occurs on a triplet surface. Nevertheless, the reader should refer to the appropriate literature accounting for spin-crossing along the reaction pathway [77, 78]. DFT calculations suggest that the triplet state has the lowest energy and that a metallocyclic intermediate likely is not involved in the reaction, whereas the presence of a radical intermediate is evident [77]. It appears that the choice of calculation method (DFT vs HF), the basis set for geometry optimization (hybrid B3LYP vs pure BP86), as well as the choice of model system for salen ligand (truncated vs full ligand) cause many of the contradictions reported in the literature [78]. To avoid all such discrepancies, we limited ourselves to a widely accepted reaction mechanism on a triplet surface (Fig. 12.2).

The conformational changes in the complex due to the interactions with the channel wall or interactions with the axial linkage are studied by different simulation setups; free complex in vacuo, free complex attached to linkage in vacuo, free complex inside a MCM-41 channel, and an anchored complex inside a MCM-41 channel [37]. Simulations also have been performed on the ACM system in the presence of *cis*- and *trans*-methylstyrene as the substrate, namely OACM(cis) and OACM(tr), respectively. Due to the interactions with the axial linkage and MCM-41, the Mn-salen complex may prefer a distorted conformation different from that of a homogeneous catalyst. Two main approaching trajectories (side-on vs top-on) have been proposed to explain the degree and type of enantioselective communications between olefin and Mn-salen catalyst [79]. According to the side-on mechanism, the swinging and twisting motions of the phenyl groups and the 3,3 and 5,5 *tert*-butyls, together with the swinging of the cyclohexyl substituent, are the most important distortion features of the Mn-salen complex. It has been suggested that the steric constraints of the framework favor a certain conformation of the Mn-salen complex, so that this conformation is stable at room temperature [74]. The swinging of the cyclohexyl, as well as the twisting motion of the phenyl groups and their substituents, play important roles when the olefin approaches the oxo group (Mn=O) from the oxygen side. It is also important to note that the degree of distortion depends on the initial orientation of the complex in the channel. Although several studies based on the most probable (dihedral) angles have provided insight into a preferable distorted conformation [60, 74], a comprehensive description of the origin of the enantioselectivity is still scarce. Based on CCM technique [68–70], it is now possible to compute the chirality of Mn-salen complexes as a function of twisting and swinging measures. An interesting correlation between the enantiomeric separation efficiency and the degree of chirality of the metal–complex catalyst has been established [70]. Such an analysis in terms of CCM rather than the pure geometry can provide a more accurate assessment of the origin of enantioselectivity [37, 70].

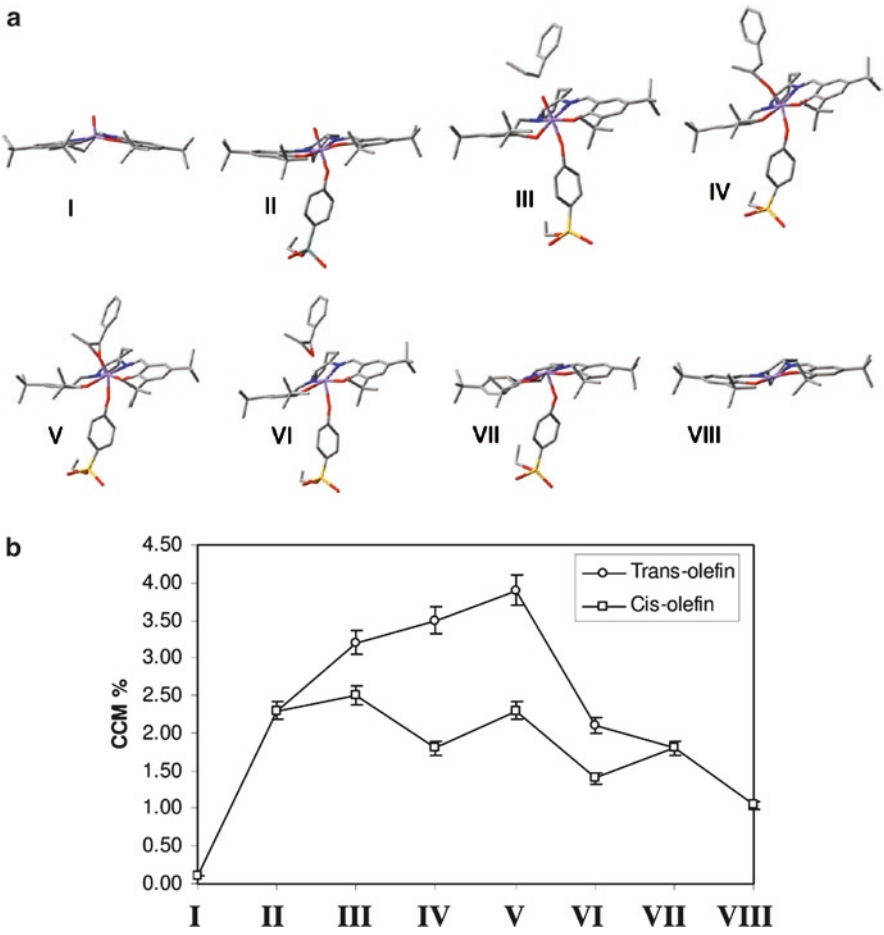

Fig. 12.3 (**a**) Optimized configuration of different steps along the reaction pathway for *cis*-methylstyrene substrate. The MCM-41 channel was removed for clarity. (I) Isolated oxo-Mn-salen; (II) the anchored complex; (III) docked olefin and encounter-complex of catalyst and substrate; (IV) radical intermediate complex of catalyst and substrate; (V) intermediate state; (VI) complex of reacted catalyst and product; (VII) de-oxygenated anchored catalyst; (VIII) isolated de-oxygenated catalyst. (**b**) CCM of Mn-salen along the reaction pathway for *cis*- and *trans*-methylstyrene substrates [37]

Figure 12.3a shows the optimized structures of the Mn-salen complex along the proposed reaction pathway, where the MCM-41 atoms were removed for clarity. The structures contain the isolated oxo-Mn-salen (I), the anchored complex (II), docked olefin and encounter-complex of catalyst and substrate (III), reacting intermediate complexes of catalyst and substrate (IV), reaction intermediate state (V), complex of reacted catalyst and product (VI), deoxygenated anchored catalyst (VII), and isolated deoxygenated catalyst (VIII). Figure 12.3b shows the CCM of the Mn-salen complex along the reaction pathway for *cis*- and *trans*-substrate as illustrated in Fig. 12.3a. A transition from

cup-like to step-like behavior is evident. This transition provides an explanation for the effectiveness and importance of additional ligand as the immobilizing linker. Recent DFT geometry optimizations [38], along with those of Cavallo and Jacobsen [61], show that a homogeneous transition state complex similar to that of V and with chloride as the axial ligand is the most stable species (106 kJ⁄mol lower than III) within the reaction pathway. In the intermediate state, the olefin strongly interacts with the oxo-Mn center at a specific high chiral configuration of the complex. Although this finding, along with Fig. 12.3b, suggest that trans-olefin has a high level of asymmetric induction to the catalyst, it does not trivially lead to a high ee and catalytic yield. Recent experiments [39, 58] confirmed that when cis- is used as the reactant, there is high production of trans-epoxide isomer for the immobilized system compared with the cis-epoxide. This suggests that in the radical intermediate III, the trans-configuration is more favorable because of the less steric hindrances. When the formation of this radical intermediate is the rate-determining step, the influence of cis- or trans-substrate on enantioselectivity is less pronounced.

Because of mass transfer limitations, the catalytic activity of Mn-salen complex is often lower than that of homogeneous Mn-salen catalyst [14, 15]. During the reaction, Mn-salen complex may selectively bind a (stereo)isomer of the products. The more strongly binding component will have the lower diffusion rate, giving a bias to the enantiomeric product generated with the lower probability. Moreover, a strong interaction will give maximum chiral selectivity of the more strongly interacting component because of the lower transition state free energy [51, 56]. The lower diffusivity, originating from nanoporous confinement, can improve chiral recognition (i.e., chirality) and asymmetric induction to the catalyst [58]. The collapse of radical intermediate IV originates a selectivity route that competes with the route based on the product desorptions. Thus, in the overall catalytic process, the enatioselectivity results from two conflicting elementary processes that have opposite effects on the ee. This finding may provide a general reason for the often-observed difference in performance between homogeneous catalysts and their corresponding immobilized catalysts.

12.2.2 DFT Calculations: Reaction Profile and Transition States

Understanding the direct effects of substrate on enantioselectivity requires a detailed DFT-based investigation of electronic and steric communication between stereoisomers (substrate or products) and Mn-salen complex. Before we describe the DFT results, a few remarkable concerns from previously used methodologies in the literature should be addressed. Recently, efforts in developing DFT-based computational techniques have explored ways to improve the utilization of the epoxidation reaction using Mn-salen complexes [60–65]. The central theme for most of those recent studies was to evaluate the accuracy of the computational methods used for epoxidation reactions catalyzed by homogeneous Mn(salen) complexes. The effect of oxo-Mn multiplicity, spin crossing dilemma and its effect on reaction intermediates have been demonstrated accordingly. Up to the present, however, no clear description of either the spin of Mn^{V}-O or the reaction intermediates has been

provided [78]. In the DFT calculations described here, the Pure Quantum Mechanics QM calculations use a reduced model system II (Scheme 12.1) that mimics the full Mn(salen) complex I, along with the Cl or phenoxyl group as the axial linker L.

Density functional calculations were performed with the B3LYP hybrid functional in combination with 6-31G* using GAUSSIAN 03 [80]. A two-layer ONIOM protocol was used to couple the (QM) and Molecular Mechanics (MM) parts in the full Mn-salen-L (Scheme 12.1, L = pheoxyl) calculations as well as for the immobilized Mn-salen catalyst into MCM-41 channel. Based on density functional theory (DFT) and quantum-mechanic/molecular-mechanic (QM/MM) calculations, the effect of applicable linkers and substrates was described in terms of their geometry and electronic properties, and the enantioselectivity of the catalyst was evaluated with respect to the energy surfaces along the epoxidation reaction pathway.

Different sets of DFT calculations are performed on all species along the reaction pathway (Fig. 12.4). For most of the calculations, the truncated salen ligand II (Scheme 12.1) is used as the model ligand, attaching to Cl or phenoxyl group. The complex Mn-salen-Cl refers to the homogeneous catalyst. The Mn-salen-phenoxyl indicates the heterogeneous catalyst, where phenoxyl group is used as an immobilization linker. The effect of MCM-41 mesopore attached to the phenoxyl linker, as well as the effect of *t*-butyl substituents ligands in the full salen ligand I is examined by QM/MM calculations using two-layer ONIOM methodology [38].

Table 12.2 demonstrates that phenoxyl group has more effect on the Mn–O bond length than Cl. An electrophilic linkage, lengthened through introduction of aliphatic chains [58, 81], affects the geometry of the salen ligand in terms of Mn–O bond length and Mn atom motion. This may explain the higher ee observed in the recent experimental studies by a long phenylsulfonic linker [14, 15, 51, 58, 81]. The longer axial linker, however, may decrease the degree of electronic communication between the mesoporous support material and salen ligand, which will have a negative effect on enatioselectivity enhancement by axial linker. It is also important to notice that these local geometrical effects are accompanied by large-scale conformational changes in the ligand. The latter would further increase the enantioselectivity of the catalyst by improving the chirality content of the Mn-salen ligand [37].

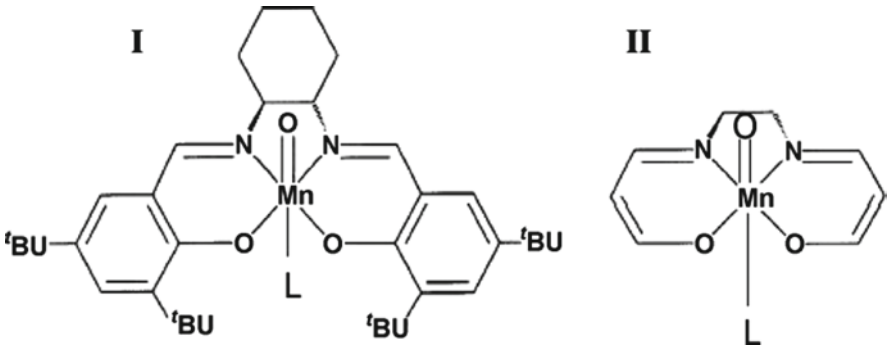

Scheme 12.1 Full (I) and truncated (II) Mn-salen-L models used for DFT calculations (L = pheoxyl)

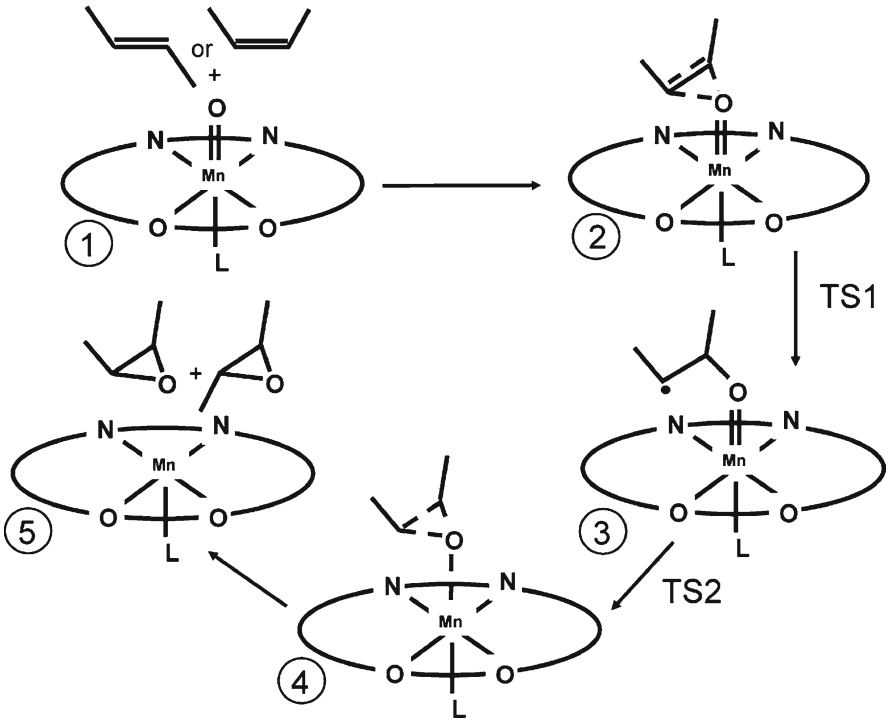

Fig. 12.4 General mechanism scheme for asymmetric epoxidation of olefins using Mn-salen complexes, L = axial linker [38]

Table 12.2 Effect of axial linkage on the geometry of oxo-Mn-salen II for the triplet spin sate using B3LYP method: distances in A°, angles in degrees Bond/angle Mn-salen-Cl [38]

Bond/angle	Mn-salen-Cl (truncated)	Mn-salen-phenoxyl (truncated)
Mn=O (oxo)	1.82	2.11
Mn-O (phenoxyl)	2.34	1.85
Ligand plan ... Mn	0.184	0.555
Mn-O (oxo)-L	56.94	124.93

The energetics of reaction sequence for the transformation of *cis*-methylstyrene (CBMS) and *trans*-methylstyrene (TBMS) T into *cis/trans*-epoxide is illustrated in Fig. 12.5. First, we consider the energy profile for the homogeneous epoxidation reaction of CBMS along the reaction pathway (Fig. 12.4). The reference state at 0 kJ/mol is the epoxide complex 4, in which both of the carbon atoms of the olefin are connected to the oxygen. System 1 is the mixture of CBMS and the catalyst in gas phase without any interaction in between. The state 2 refers to the system in which olefin enters the coordination sphere of complex from the Mn-O center in a side-on approach. The distance between olefin and oxygen in Mn-O was found to be

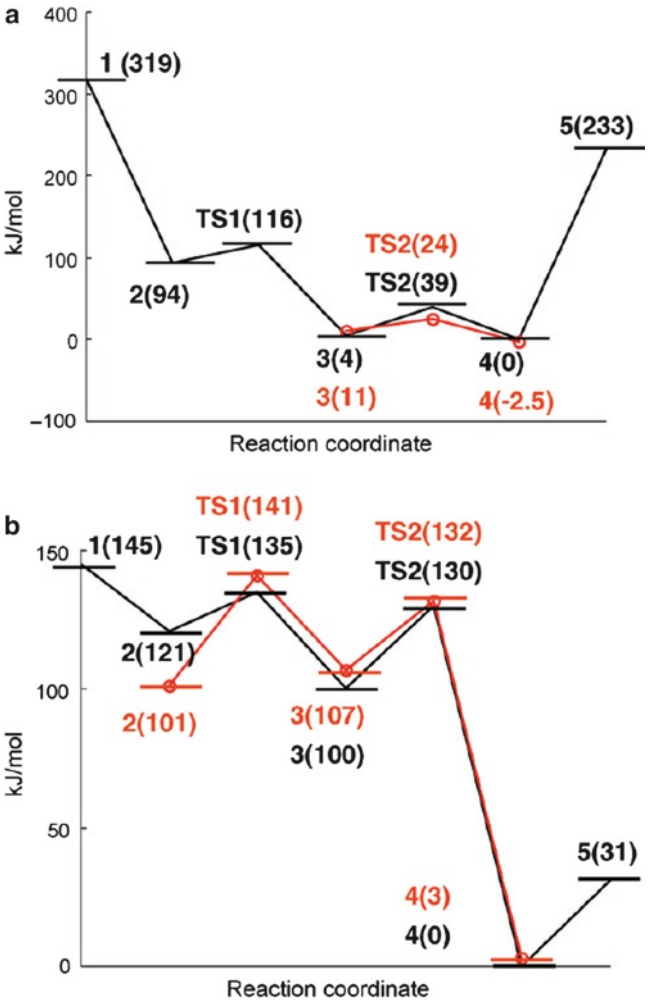

Fig. 12.5 Reaction profiles for the oxygen transfer reaction on the triplet surface for (**a**) homogeneous and (**b**) heterogeneous Mn-salen catalyst. The species are defined as in Fig. 12.4. The (*black*) full line refers to the energy profile for the attack of CBMS, while the (*red*) dotted line is the profile of TBMS attack. The relative energies are shown in parentheses [38]

0.28 nm [61]. This system passes through the transition state TS1 and converts to the radical intermediate 3. The activation energy for this step is around 22 kJ/mol. The radical intermediate 3 is 90 kJ/mol more stable than system 2. The radical 3 can further collapses to yield the epoxide complex through a relatively high activation barrier (35 kJ/mol). Similar calculations were performed for the side-on attack of TBMS onto Mn-O center. Calculations show that the attack of TBMS is overall about 7 kJ/mol less in favor compared to that in CBMS. Moreover, Fig. 12.5a illustrates that the epoxide complex 4 formed by TBMS lies 2.5 kJ/mol below the

epoxide complex formed by CBMS. These findings are in agreement with a general assumption in homogeneous Mn-salen catalyst that TBMS is a less suitable substrate than CBMS. The more stable *t*rans-epoxide complex 4 is in qualitative agreement with the experimental observation that epoxidation of CBMS leads to a thermodynamically more stable *trans*-epoxide [82]. When the axial linkage is replaced by phenoxyl group, the potential energy surface changes considerably. Figure 12.5b shows the energy profile for the epoxidation reaction of CBMS and TBMS catalyzed by immobilized Mn-salen complex. Similar to Fig. 12.4a, the epoxide complex is the reference state at 0 kJ/mol. On the triplet energy surface, the calculations suggest that epoxide formation is clearly more preferred by the immobilized catalyst compared to the homogeneous catalyst. The activation barrier for the formation of adsorbed CBMS radical is overall 8 kJ/mol less than that for the homogeneous salen catalyst. When comparing the epoxide complex 4 for homogeneous and immobilized catalyst, the activation energy for epoxide complex formation is about 5 kJ/mol lowered for the immobilized Mn-salen complex. These observations provide an explanation for the effectiveness and importance of additional ligand as the immobilizing linker. When Mn-salen complex is immobilized by a neutral donor ligand such as phenoxyl group, the energy barrier of the final step of product formation is significantly reduced. Figure 12.5b shows that the epoxide complex formed of CBMS is slightly (3 kJ/mol) more stable than its *trans*-epoxide counterpart, despite of the fact that there is a lower barrier (5 kJ/mol) towards epoxide formation starting from TBMS radical adsorbed on MnO center. The energy profile strongly depends on electron donor/acceptor properties of the axial linker. A different linker such as phenylsulfonic group may convert the reaction pathway towards *trans*-epoxide formation. However, the energy barrier is still in favor for *cis*-substrate.

12.3 Catalytic Activity of Metallomacrocyclics for the Electrochemical Reduction of Oxygen

The last example in this chapter discusses the role of theory and simulation for characterization of active sites in non-precious metal catalysts immobilized on a graphite surface. We present theoretical and computational studies on non-precious electrocatalysts for oxygen reduction reaction (ORR). Development of non-Pt oxygen reduction catalysts is of vital importance for the commercialization of fuel cells [83]. The research on non-precious metal catalysts for ORR has mainly focused on metal macrocyclic complexes. The low activity and a lack of high stability under fuel cell operating conditions are the major disadvantages of metal mactocyclic complexes. Sidik et al [46] reported theoretical and experimental studies of oxygen reduction to peroxide on graphite and nitrogen-doped graphite. They observed an oxygen reduction overpotential for nitrided Ketjenblack at 0.5 V (SHE) and for untreated carbon at 0.2 V. Moreover, reversible potential for the oxidation of H and O_2 reduction intermediates were evaluated. On a pure graphite, the reversible potential for the formation of OOH on site c (Fig. 12.6) was calculated to be 0.311 V. The results from [46]

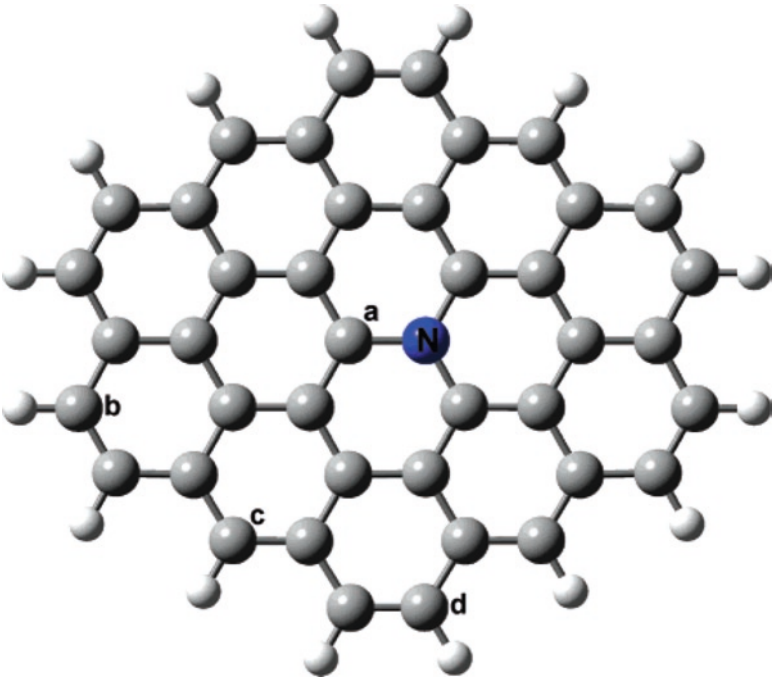

Fig. 12.6 Optimized structure for the N-substituted graphite model, C41NH16. The larger gray circles are carbon atoms, and the smaller white circles are hydrogen atoms [46]. Reproduced from Sidik RA, Anderson AB, Subramanian NP, Kumaraguru SP, Popov BN, O_2 Reduction on Graphite and Nitrogen-Doped Graphite: Experiment and Theory, J Phys Chem B 110:1784–1793 Copyright @ 2006 with permission from ACS

showed that carbon radical sites in adjacent to substitutional N in graphite are active for reduction of O_2 to peroxide in acidic medium, which explains the high catalytic activity observed for nitrided carbon. Interestingly, the weak catalytic effect of untreated carbon is attributed to the weak bonding of OHH intermediate adsorbed to the CH at graphite edge sites. It was concluded that N atoms far from the graphite sheet edges are more active that those closer to the edges. Jain et al. [47] performed extensive DFT calculations to elucidate structure of Fe-based electrocatalysts. They determined energy of nitrogen incorporation in the bulk and in the edge of a graphite sheet. The main finding was that in the absence of hydrogen on the graphite edge, iron bonds with nitrogen a carbon atom. In the presence of hydrogen, however, iron prefers to bond with two nitrogen atoms, Fig. 12.7.

Vayner and Anderson [48] studied the adsorption energies and products of ORR and identified active sites for the system cobalt-graphite-nitride. The calculation demonstrated that a bare graphite edge with one N atom is inactive for 2-electron and 4-eletron ORR, Fig. 12.7. At overepotentials greater than 0.3 V, N is not hydrogenated

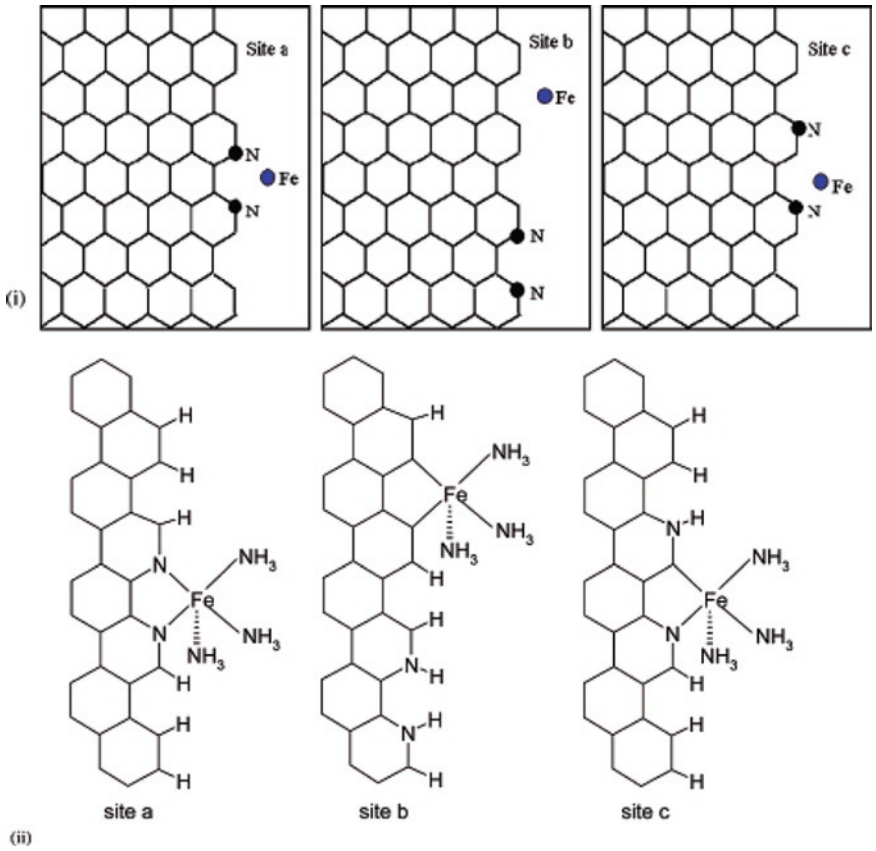

Fig. 12.7 Positions of Fe atoms on the edge of nitrogenated graphene: (i) Fe bond sites a, b, c (ii) models of nitrided grapheme edge being passivated by hydrogen atoms and bonded with Fe. Here Fe is coordinated with three NH3 ligands [47]. Reproduced from Jain M, Chuo S, Siedle A, In Search for Structure of Active Site in Iron-Based Oxygen Reduction Electrocatalysts, J Phys Chem B 110:4179–4185 Copyright @ 2006 with permission from ACS

and is not active for ORR as a result of weak OOH bonds. At lower potentials than 0.3 V, N is hydrogenated and becomes a radical center and the NH edge is not active. Shi and Zhang reported DFT calculations to rationalize the catalytic activity of cobalt- and iron-substituted phthalocyanine and porphyrin systems [49]. They studied the dioxygen and binding mode, energy, charge, and ionization potential (IP) of these catalysts. Particularly, the effect of central metal, ligand, and substituents were investigated. The general trend was that cobalt system can form stable end-on dioxygen adducts while side-on adsorptions did not show enough stability. Consequently, the catalytic activity of phthalocyanine and porphyrin catalysts for ORR is mostly related to the ionization potential and the strength of dioxygen bindings [49].

Besides the computational approaches discussed in above, study of adsorption of reactants, intermediates and products has been widely studied by molecular simulations for understanding catalytic activity and design of non-precious ORR electrocatalysts. In general, the interactions between catalyst and reaction species is determined by calculating the adsorption energies, which is computationally less expensive that computing reaction and activation energies.

12.4 Conclusion and Outlook

The results presented here provide new insights into the important steric effects related to linker choices and the interplay with the mesopore channel for anchored oxo-Mn-salen in MCM-41. The immobilized linker improves the chiral recognition of the catalyst due to the increasing chirality content of the Mn-salen complex. A trans-olefin indicates a high level of asymmetric induction to the Mn-salen catalyst. This, along with the high stability of the intermediate states, suggest that the trans-olefin can be strongly adsorbed on the oxo-Mn center. Unwanted diffusion limitation of the product may lead to a low ee and catalytic yield. This type of analysis can be of use in evaluating enantioselectivity of heterogeneous catalysts. Moreover, QM/MM and DFT calculations provided new insights on the importance of the immobilized linker and the MCM-41 channel DFT calculations indicated that despite of high level of asymmetric induction of trans-substrates to the immobilized Mn-salen complexes, the reaction path is most likely in favour for the cis-substrates. It was suggested that any coordination in the trans-position causes the Mn atom to move into the plane of the ligand. In addition, the Mn–O bond becomes lengthened.

Theoretical procedures have provided quantitative predictions about elementary processes and insights of the oxygen electroreduction mechanism on none-precious Metallomacrocyclics catalysts. Theoretical efforts have been made to relate catalyst molecular structure with ORR electrocatalytic activity. The structure–activity properties includes adsorption energies, activation energy, d-band center, and ionization energy. The task of finding essential structural–catalytic properties for such catalysts is of vital importance for the rational design and development of non-Pt catalyst for fuel cell applications [83].

References

1. Sahimi M, Gavalas GR, Tsotsis TT (1990) Chem Eng Sci 45:1443–502
2. Torquato S (2002) Random hetergeneous materials. Springer, New York
3. Sahimi M (2003) Heterogeneous materials, Part I and Part II. Springer, Heidelberg
4. Sahimi M (1993) Rev Mod Phys 65:1393–1534
5. Rajabbeigi N, Elyassi B, Tsotsis TT, Sahimi M (2009) J Mem Sci 335:5–12
6. Dubbeldam D, Snurr RQ (2007) Mol simul 33:305–325

7. Maginn EJ, Bell AT, Theodorou DN (1993) J Phys Chem 97:4173–4181
8. Kärger J, Ruthven DM (1992) Diffusion in zeolites and other microporous solids. Wiley, New York
9. Breck DW (1974) Zeolite molecular sieves. Wiley, New York
10. Barrer RM (1982) Hydrothermal chemistry of zeolites. Academic, London
11. Szostak R (1998) Molecular sieves-principles of synthesis and identification, 2nd edn. Blackie, London
12. Zhao D, Feng J, Huo Q, Melosh N, Fredrickson GH, Chmelka BF, Stucky GD (1998) Science 279:540
13. Zhao D, Huo Q, Feng J, Chmelka BF, Stucky GD (1998) J Am Chem Soc 20:6024
14. Yang Q, Liu J, Zhang L (2009) C Li. J Mater Chem 19:1945–1955
15. Yang Q, Han D, Yang H, Li C (2008) Chem Asian J 3:1214–1229
16. Noyori R (2002) Angew Chem Int Ed 41:2008–2022
17. Trost BM (2004) Proc Natl Acad Sci USA 101:5348–5355
18. (a) Knowles WS, Sabacky MJ, Vineyard BD (1968) Chem Commun (London) 1445–1446; (b) Knowles WS, Noyori R (2007) Acc Chem Res 40:1238–1239
19. Ohkuma T, Ishii D, Takeno H, Noyori R (2000) J Am Chem Soc 122:6510–6511
20. Yan YJ, Zhang XM (2006) J Am Chem Soc 128:7198–7202
21. Zhang WC, Zhang XM (2006) Angew Chem Int Ed 45:5515–5518
22. Sandoval CA, Ohkuma T, Utsumi N, Tsutsumi K, Murata K, Noyori R (2006) Chem Asian J 1:102–110
23. Sandoval CA, Ohkuma T, Muniz K, Noyori R (2003) J Am Chem Soc 125:13490–13503
24. Wang WB, Lu SM, Yang PY, Han XW, Zhou YG (2003) J Am Chem Soc 125:10536–10537
25. Jacobsen EN, Pfaltz A, Yamamoto H (eds) (1999) Comprehensive asymmetric catalysis, vol 1. Springer, Berlin
26. Noyori R (ed) (1994) Asymmetric catalysis in organic synthesis. Wiley, New York
27. Ojima I (ed) (1999) Catalytic asymmetric synthesis. Wiley, New York
28. Mariz R, Luan X, Garri M, Linden A, Dorta R (2008) J Am Chem Soc 130:2172–2173
29. Ohkuma T, Tsutsumi K, Utsumi N, Arai N, Noyori R, Murata K (2007) Org Lett 9:255–257
30. Ohkuma T, Utsumi N, Tsutsumi K, Murata K, Sandova C, Noyori R (2006) J Am Chem Soc 128:8724–8725
31. Balskus EP, Jacobsen EN (2007) Science 317:1736–1740
32. Wiesner M, Revell JD, Wennemers H (2008) Angew Chem Int Ed 47:1871–1874
33. Yamaguchi T, Matsumoto K, Satio B, Katsuki T (2007) Angew Chem Int Ed 46:4729–4731
34. Blaser HU, Schmidt E (eds) (2004) Asymmetric catalysis on industrial scale. Wiley, Weinheim
35. Zhong L, Gao Q, Gao JS, Xiao JL, Li C (2007) J Catal 250:360–364
36. Burgemeister K, Franci G, Gego VH, Greiner L, Hugl H, Leitner W (2007) Chem Eur J 13:2798–2804
37. Malek K, Jansen APJ, Li C, van Santen RA (2007) J Catal 246:127–135
38. Malek K, Li C, van Santen RA (2007) J Mol Catal A Chem 271:98–104
39. Zhang H, Wang YM, Zhang L, Gerritsen G, Abbenhuis HCL, van Santen RA, Li C (2008) J Catal 256:226–236
40. Lalande G, Guay D, Dodelet JP, Majetich SA, McHenry ME (1997) Chem Mat 9:784–790
41. Fournier J, Lalande G, Cote R, Guay D, Dodelet JP (1997) J Electrochem Soc 144:218–226
42. Wang H, Cote R, Faubert G, Guay D, Dodelet JP (1999) J Phys Chem B 103:2042–2049
43. Wei G, Wainright JS, Savinell RF (2000) J New Mat Electrochem Syst 3:121–129
44. Cote R, Lalande G, Guay D, Dodelet JP, Denes G (1998) Electrochem Solid State Lett 145:2411–2418
45. Zagal JH (1992) Coord Chem Rev 119:89–136
46. Sidik RA, Anderson AB, Subramanian NP, Kumaraguru SP, Popov BN (2006) J Phys Chem B 110:1784–1793
47. Jain M, Chuo S, Siedle A (2006) J Phys Chem B 110:4179–4185
48. Vayner E, Anderson AB (2007) J Phys Chem C 111:9330–9336

49. Shi Z, Zhang J (2007) J Phys Chem C 111:7084–7090
50. Zagal JH, Paez M, Tanaka AA, dos Santos JR, Linkous C (1992) J Electroanal Chem 339:13–30
51. Li C (2004) Catal Rev 46:419
52. Xiang S, Zhang Y, Xin Q, Li C (2002) Chem Commun 22:2696
53. Zhang H, Xiang S, Li C (2005) Chem Commun 1209
54. Piaggio P, McMorn P, Langham C, Bethel D, Bulman-Page PC, Hancock FE, Hutchings GJ (1998) New J Chem 22:1167
55. Piaggio P, McMorn P, Murphy D, Bethel D, Bulman-Page PC, Hancock FE, Sly C, Kerton OJ, Hutchings GJ (2000) J Chem Soc Perkin Trans 2:2008
56. Corma A (2004) Catal Rev Sci Eng 46:369
57. McGarrigle EM, Gilheany DG (2005) Chem Rev 105:1563
58. Zhang H, Zhang Y, Li C (2006) J Catal 238:369
59. Linker T (1997) Angew Chem Int Ed 36:2060
60. Jacobsen H, Cavallo L (2001) Chem Eur J 7:800
61. Cavallo L, Jacobsen H (2000) Angew Chem Int Ed 39:589
62. Khavrutskii IV, Musaev DG, Morokuma K (2003) Inorg Chem 42:2606
63. Linde C, Akermark B, Norrby PO, Svensson M (1999) J Am Chem Soc 121:5083
64. Cavallo L, Jacobsen H (2004) Inorg Chem 43:2175
65. El-Bahraoui J, Wiest O, Feichtinger D, Plattner DA (2001) Angew Chem Int Ed 40:2073
66. Dominguez I, Fornes V, Sabater MJ (2004) J Catal 228:92
67. Ayala V, Corma A, Iglesias M, Sanchez F (2004) J Mol Catal 221:201
68. Alvarez S, Alemany P, Avnir D (2005) Chem Soc Rev 34:313
69. Lipkowitz K, Schefzick S (2002) Chirality 14:677
70. Alvarez S, Schefzick S, Lipkowitz K, Avnir D (2003) Chem Eur J 9:5832
71. Zabrodsky H, Peleg S, Avnir D (1992) J Am Chem Soc 114:7843
72. Zabrodsky H, Avnir D (1995) J Am Chem Soc 117:462
73. Shi S, Yan L, Yang Y, Fisher-Shaulsky J, Thacher T (2003) J Comput Chem 24:1059
74. Mollmann E, Tomlinson P, Holderich WF (2003) J Mol Catal 206:253
75. Handgraaf JW, Reek JNH, Bellarosa L, Zerbetto F (2005) Adv Synth Catal 347:792
76. Avery KA, Mann R, Norton M, Willock DJ (2003) Topics Catal 25:89
77. Cavallo L, Jacobsen H (2003) J Phys Chem 107:5466
78. Sears JS, Sherill CD (2006) J Chem Phys 124:144314
79. Chang S, Galvin JM, Jacobsen EN (1994) J Am Chem Soc 116:6937
80. Frisch MJ, Trucks GW, Schlegel HB, Scuseria GE, Robb MA, Cheeseman JR, Montgomery JA Jr, Vreven T, Kudin KN, Burant JC, Millam JM, Iyengar SS, Tomasi J, Barone V, Mennucci B, Cossi M, Scalmani G, Rega N, Petersson GA, Nakatsuji H, Hada M, Ehara M, Toyota K, Fukuda R, Hasegawa J, Ishida M, Nakajima T, Honda Y, Kitao O, Nakai H, Klene M, Li X, Knox JE, Hratchian HP, Cross JB, Bakken V, Adamo C, Jaramillo J, Gomperts R, Stratmann RE, Yazyev O, Austin AJ, Cammi R, Pomelli C, Ochterski JW, Ayala PY, Morokuma K, Voth GA, Salvador P, Dannenberg JJ, Zakrzewski VG, Dapprich S, Daniels AD, Strain MC, Farkas O, Malick DK, Rabuck AD, Raghavachari K, Foresman JB, Ortiz JV, Cui Q, Baboul AG, Clifford S, Cioslowski J, Stefanov BB, Liu G, Liashenko A, Piskorz P, Komaromi I, Martin RL, Fox DJ, Keith T, Al-Laham MA, Peng CY, Nanayakkara A, Challacombe M, Gill PMW, Johnson B, Chen W, Wong MW, Gonzalez C, Pople JA (2004) Gaussian 03, ReVision, B01. Gaussian, Wallingford, CT
81. Zhang H, Li C (2006) Tetrahedron 62:6640
82. Finnley NS, Pospisil PJ, Chang S, Palicki M, Konsler RG, Hansen KB, Jacobsen EN (1997) Angew Chem 109:1798
83. Eikerling MH, Malek K, Wang Q (2008) Catalyst layer modeling: structure, properties, and performance. In: Zhang JJ (ed) PEM fuel cells catalysts and catalyst layers – fundamentals and applications. London, Springer

Chapter 13
Instrumental Techniques for the Investigation of Heterogenised Catalysts: Characterisation and In situ Studies

John Evans and Moniek Tromp

Abstract To design and optimise efficient supported catalysts, the detailed structural and electronic properties as a function of performance are required. This chapter describes characterisation methods which can be applied ex situ (before and after catalysis) as well as in situ or operando (during catalysis, under process conditions). We focus on spectroscopic techniques, i.e. IR, NMR and XAS, the combination which will shown to be specially good for supported organometallic systems, providing complementary insights in structural and electronic properties of support, ligand and reactant coordination to the metal site and the metal site itself. Selected organometallic systems are chosen to demonstrate the strengths and limitations of the individual and combined techniques.

13.1 Introduction

Heterogenised catalysts are a class of material with a suite of desired characteristics:

- Gaining over homogeneous catalysts in specific activity by achieving a higher density of reaction sites by
  - Avoiding aggregation of unsaturated reactive sites by immobilisation
  - Achieving a higher loading through high area supports
- Gaining over homogeneous catalysts by achieving a gain in activity and selectivity by
  - Providing a synergy with support sites
  - Creating shaped cavities providing selection for reagents, products or transition states

J. Evans (✉) and M. Tromp
School of Chemistry, University of Southampton, Southampton SO17 1BJ, UK
e-mail: J.Evans@soton.ac.uk

P. Barbaro and F. Liguori (eds.), *Heterogenized Homogeneous Catalysts for Fine Chemicals Production*, Catalysis by Metal Complexes 33,
DOI 10.1007/978-90-481-3696-4_13, © Springer Science+Business Media B.V. 2010

- Gaining over homogenous catalysts by achieving ease of catalyst product separation by
  - Creating solid-phase materials
  - Creating mesoscale materials isolable by ultrafiltration
- Gaining over heterogeneous catalysts by
  - Presenting a homogeneity of active sites with the same activity and selectivity
  - Providing more precise tuning of active sites
  - Providing stereochemical selection

However, achieving all of these gains is difficult. Activity can be lost due to deleterious reactions between the reaction centre and the support, and the support can reduce diffusion rates to the reaction centre. More often than not, a homogeneous precursor may be more reactive than its heterogenised counterpart with often a significant change in selectivity, either to one's advantage or disadvantage.

In principle then, full characterisation should probe the reaction site, the nature of the support, especially its near surface, and identify the spatial relationships of sites and supports. The supports that are available are either organic polymers or inorganic solids, generally oxide based or carbons. High specific area can emanate either from small particle size or high porosity. Small particle sizes are often accompanied by low crystallinity, e.g. for silica [1], although this is not universal; MgO smokes [2] and TiO_2 [3] may demonstrate considerable crystallinity in the bulk of the particles. However, the near surface regions can display an amorphous region and/or sectioning through crystal planes [4], and the surface planes require terminations for charge balance. Whether as vacancies or extra atoms (typically protons attached to surface oxygens), these create local defects with differing Brønsted or Lewis acidity [5, 6]. Even in relatively ordered materials, such as mesoporous solids [7, 8] and hybrid materials [9], at the atomic level, the surfaces of the supports are glassy in nature. The most common exceptions are zeolites and other zeotypes which provide a choice of reaction centres of repeating lattice points [10–12], but as yet they provide a restricted band of pore sizes that limit the size of the reaction centre that can be accommodated within them [12], although this challenge is being tackled [13, 14].

As a result the proportion of cases where a supported metal centre can be identified by x-ray diffraction is small. There are examples of single hydroxyl sites in crystalline oxide-hydroxides [15] and also identification of the sites of metal ions [16] and small metal clusters [17] located in zeolites, but these remain exceptions. For the mainstream these materials have low degrees of order and thus present a characterisation not dissimilar to a solution of a homogeneous catalyst, and so we will expect to utilise the same types of characterisation techniques that have good chemical speciation and can be applied to solid and liquid samples (NMR, EPR, IR, Raman, uv-visible absorption spectroscopy, x-ray absorption spectroscopy).

However, the supports give an extra level complexity over and above a liquid phase case when rapid averaging of any dissimilar (solvation) sites would be achieved by Brownian motion. The spatial complexity of a support is generally

considered to offer a wider variety of local sites as compared to those in a solution [18]; they are also considered to be maintained for a substantial time frame. Hence spectroscopies will be sampling a variety of local sites which may not be readily discriminated. Their relative positioning on a variety of length scales within a chemical reactor may also be a factor in the macroscopic properties of the catalytic system and this requires an imaging component to the battery of techniques [19].

In this chapter we will examine the applicability of techniques for characterising these complex materials, both as stand-alone items (ex situ) or under reaction conditions (in situ), recognising that these may not afford the same result due to rapid structural changes [20]. This will show that no single technique has universal application, and most materials require combinations of techniques to derive a reasonably full description. Hence the compatibility of combined techniques is also of concern. Examples of thorough studies by combining techniques will also be illustrated. Finally, some pointers for the future will be given, showing routes to migrate through the classes of characterisation of the chemical reactions of catalysts.

Characterisation of the chemical reactions in catalysts can in principle be carried out in four ways.

(i) Ex situ structural studies may be performed on catalysts before and after a catalytic reaction. The spectroscopic measurements can be optimised to achieve the highest spectral quality and thus provide the greatest insight that the technique can provide. However the remoteness of this from the reaction conditions may limit the relevance to the catalytic processes since changes in structure can be induced by the catalytic substrates.

(ii) In situ, or operando, methods can be rendered more relevant by direct monitoring of the metal centres under the steady state of the presence of the reagents of the catalysed reaction and the appropriate temperature and pressure. This can create significant problems for the design of a reaction cell that will allow the spectroscopy to be carried out, or the compromise in conditions like concentration. For example direct observation of the rhodium centres in a hydroformylation reaction carried out in Sc-CO_2 [21] did require matching the small sample volume to the x-ray beam size [22]. Although some compromises may be necessary, long averaging times may be employed during steady state experiments to achieve good spectral quality. However, the acquisition time is then much slower than the turnover rate and thus the most stable species are observed. These may be the predominant species prior to the rate determining step in a catalytic cycle, or may be a sequestered form of the metal which may be quite distinct from active species within the cycle.

(iii) If the acquisition time of the in situ method is reduced to sub-seconds, then the creation of active sites may be observed [23] and, if the time resolution is faster than the turnover of the reaction, steps along the cycle can be probed. There are more severe compromises in terms or data quality due to the greatly reduced acquisition times, which must be offset by averaging of repeat experiments. A disturbance from equilibrium must be synchronised with the characterisation measurements, either by a temperature of pressure change, pulsing of reagents or energy source. The ultimate time resolution for this class of experiments is

activation by a picoseconds laser and subsequent measurements on a ps timescale both to identify short lived transients and to derive the kinetics of primary steps in a catalytic reaction.

(iv) By increasing the time resolution by a factor of about 10^3, then the observations will be faster than molecular vibrations (~10–200 fs). The experiments then move from kinetics to dynamics. Molecular motion studies are the realm of ultrafast photon lasers and free electron lasers.

13.2 Laboratory Spectroscopies

13.2.1 Vibrational Spectroscopies

Infrared spectroscopy had an early impact on the characterisation of supported metal complexes through the identification of $Rh(CO)_2$ units after exposure of Rh/Al_2O_3 with CO [24], a similar in situ cell having been previously reported [25]. However, it was only once XAFS measurements had been carried out that it was clear that this dicarbonyl was indeed a grafted coordination complex [26]. The high dynamic dipole and interaction force constants of υ(CO) bands together with their sensitivity to local electron density means they provide excellent fingerprints for supported metal complexes. For example, the IR spectrum provides a good fingerprint to differentiate between complexes of the types $[Os_3(CO)_{11}(PPh_2R)]$ (**1**), $[Os_3H_2(CO)_{10}(PPh_2R)]$ (**2**) and $[Os_3H_2(CO)_9(PPh_2R)]$ (**3**) [27]. Thus the model complexes where R = Et afford closely analogous spectra to the silyl bearing derivatives {R = $CH_2CH_2Si(OEt)_3$} and those tethered to Aerosil silica {R = CH_2CH_2SIL}. Complexes of the type (**3**) are 46 electron species and formally present an Os=Os bond supported by two bridging hydrides. This un-saturation can be correlated with the ability to catalyse the hydrogenation of ethene [28]. Fingerprinting IR studies show a decomposition pathway of the tethered complex under ethene/H_2 that is parallel to that observed in solution, that is the incorporation of the C_2 unit to form a face bridging ethylidyne complex $[Os_3(\mu\text{-}H)_3(\mu_3\text{-}CCH_3)(CO)_8(PPh_2CH_2CH_2SIL)]$ (**4**). However, there is another pathway resulting from the direct interaction of the osmium cluster with surface silanol groups to give some broad υ(CO) bands, similar to those observed when the grafted complex $[Os_3(H)(O\text{-}SIL)(CO)_{10}]$ (**5**), derived from $[Os_3(CO)_{12}]$, is heated. The identification of (**5**) could be made from its IR fingerprint [29] compared to close silyl analogues [30].

Other chromophores can also provide valuable qualitative evidence for surface species. For example, the ruthenium version of (**5**) was also identified by its carbonyl fingerprint initially [31], but Raman spectroscopy was also employed. The υ(M-M) bands are very intense and occur at lower energy than the absorptions of the oxide support. The υ(MH) modes of bridging hydride in this structure also occurs in a window outside the main oxide support (~1,400 cm^{-1}), and they have the feature of sharpening considerably at liquid nitrogen temperatures. So this mode too could be identified, this time by IR spectroscopy [32]. Terminal hydrides

typically present stretching vibrations between 2,000 cm^{-1}, and so these can also be observed in a window region of oxide supports. For example, the Zr-H mode in [$HZr(O\text{-}SIL)_3$] could be distinguished from surface Si-H sites by its frequency (1,635 cm^{-1}) [33]; its identity was confirmed by deuterium substitution.

When the chemistry of the supported complexes deviates significantly from that in solution identification becomes more difficult. The information content of an infrared spectrum can be enhanced by isotopic substitution. Partial substitution creates isotopomers and the patterns created by them can be distinctive if the resolution is high enough. Thus, under oxidative conditions $Rh_4(CO)_{12}$ could be shown to oxidise to vibrationally isolated $Rh^I(CO)_2$ sites on oxides such as alumina and titania [34]. These units afford three isotopomers: $Rh^I(^{12}CO)_2$, $Rh^I(^{12}CO)(^{13}CO)$ and $Rh^I(^{13}CO)_2$. Each possess symmetric and antisymmetric υ(CO) modes giving a characteristic pattern of six bands, the intensities of which are dependent upon the isotopic ratio and the OC-Rh–CO bond angle.

Almost all of the measurements described were carried out ex situ, the exceptions being the adsorption of CO on supported metals [24, 25]. These latter experiments were performed in transmission mode on a powder sprayed onto an IR transparent window (e.g. CaF_2). A pressed disc is a common method of sample presentation for in situ studies of supported metal catalysts. Whilst this can afford good quality spectra this method has some risks for catalytic studies. The applied pressure can condense particles together which can create voids, restrict diffusion and extrude water from the merged surfaces. An alternative method is diffuse reflectance infrared Fourier transform spectroscopy (DRIFTS). This is an optically more complicated method to collect an acceptable proportion of the radiation scattered from the catalyst particles, but it does allow for in situ studies avoiding inter particle diffusion constraints. A recent design presents a thorough analysis of the flow dynamics within the cell [35].

Although these have not been applied to heterogenised catalysts as yet, there are pointers to show techniques that could be applied to this area of chemistry. Rapid scanning spectrometers can provide sub-second time resolution, and this has been applied to the study of CO/NO conversion catalysed by Rh/Al_2O_3 [36, 37]. The equilibria were disturbed by a temperature ramp [36] or gas pulsing [37]. In these cases the IR beam was crossed with an x-ray beam to provide simultaneous IR and XAFS spectra. Although these materials began with nanoparticulate metal, proportions were converted into coordination sites during some gas switching experiments, i.e. between $Rh(CO)_2$ and Rh(NO) surface bound units.

Complex spectra can make it difficult to identify changes during chemical reaction due to a highly structured background. This has been tackled using 2D correlation IR spectroscopy [38, 39]. Here correlated and anticorrelated changes in spectrum are presented as a two-dimensional contour plot to identify bands common to species and those altering during reaction sequences. This was applied to coking occurring during xylene isomerisation on the acid zeolite H-MFI. Interestingly, coke formation could be correlated to particular hydroxyl groups, namely silanols at pore defects. By combining IR spectroscopy with in situ thermo-gravimetry, quantification of water and the various surface silanol sites in a variety of silicas has been achieved [40].

The two-dimensional approach has also been combined with a pressure-jump experiment to monitor the probe molecule acetonitrile on an acidic mordenite [41]. The linkages between the υ(CN) of the probe molecule and the υ(OH) of the adsorption sites could be identified.

Identifying primary reaction steps after photochemical activation of organometallics is currently the domain of solution chemistry [42]. The homogeneous medium presented by the solvent host provides good optical transmission and a single reaction centre. The diversity of sites within a conventional support host would broaden out the local kinetics as well as provide light scattering difficulties. Fast (ns-ps) or ultrafast (fs) experiments will probably require modelling the supported catalyst on a flat surface [43].

13.2.2 Nuclear Magnetic Resonance (NMR)

The tethering of a complex to a support can convert the NMR spectra observed from those typical of a solution to those of the solid state. The rapid isotropic tumbling in solution which removes dipolar coupling and averaged our chemical shift anisotropy is largely absent. If the length of the tether to the surface gives significant flexibility then these effects can be mitigated, but for short chain lengths and grafted complexes the effects are very important and so the method of study must take account of them. Thus the ^{31}P spectrum acquired with cross polarisation (CP) from the ^{1}H nuclei of the tethered phosphinidene complex $[Ru_3H_2(\mu_3\text{-}PCH_2CH_2SIL)(CO)_9]$ displays a powder pattern showing chemical shift anisotropy typical of local axial symmetry [44]. With magic angle spinning (MAS), the isotropic chemical shift could be identified from spinning side bands since its position is independent of spinning rate. The chemical shift is within 2 ppm of its precursor, $[Ru_3H_2\{\mu_3\text{-}PCH_2CH_2Si(OEt)_3\}(CO)_9]$ in solution. Thus, as expected, the CP-MAS ^{31}P NMR spectra of the saturated triosmium clusters (**1**) and (**2**) closely matched those of their soluble analogues, although the spectrum of the supported unsaturated complex (**3**) was more problematical [45].

The developments in solid state NMR since that period have provided some excellent examples of ex situ measurements providing considerable structural detail. For example, the salt $[Pd\{PPh_2(CH_2)_3PPh_2\}(S_2C\text{-}NEt_2)]BF_4$ adsorbed on silica presented several viable NMR nuclei for study (^{1}H, ^{13}C, ^{31}P, ^{11}B, ^{19}F, ^{29}Si) [46]. These demonstrated the integrity of the complex on the silica surface. However, also looking for heteronuclear correlations between the cation, anion and silica surface provided evidence for a surface model involving hydrogen bonding of a BF_4^- unit to the silica surface forming the base of anion–cation–anion–cation sandwich. Correlations were observed between several nuclei pairs, including Si to F of the anion the protons on the carbons of both ligands to silicon and between ^{31}P and ^{19}F, showing proximities between all of these components.

1- and 2-D NMR have been invaluable aspects of the characterisation of Schrock-type alkylidenes onto silica surfaces, generally treated to afford isolated silanols as reaction centres. For example, a series of surface complexes of the type

[Mo(=CHCMe$_2$R′)(≡NAr)(OR)$_2$(OSIL)] have been reported, which are efficient precursors to the metathesis of acyclic alkenes [47]; both ^{1}H and ^{13}C spectra confirm the presence of the alkylidene unit. These complexes are much less effective as catalysts for ring closing metathesis, suggesting that the ring closing step is retarded by the silica surface. By a thorough combination of experimental analysis and DFT calculations, the mobility of silica-bound alkylidene complexes of Re, Ta, Mo and W has been investigated [48]. The observed dipolar couplings and chemical shift anisotropies are reduced to varying extents by local molecular motion, and these motions contribute to an axial order parameter and an asymmetry parameter estimating the deviation from axial symmetry at the ^{13}C nucleus of the alkylidene. These results indicate that the molybdenum alkylidenes have high order parameters, indicating relative rigidity. This could be correlated with the reduced activity for ring closing metathesis catalysis [47].

The carrier alkylidene catalysts can only be generated once there is exposure of the precursor, generally stabilised by a bulky carbene ligand, and the alkene substrate. The major surface species obtained by grafting [W(=CHBu^t)(≡NAr)(2,5-Me$_2$NC$_4$H$_2$)$_2$] onto silica was shown to be [W(=CHBu^t)(≡NAr)(2,5-Me$_2$NC$_4$H$_2$)(OSIL)] [49]. In the presence of di-^{13}C-labelled ethene, a 2D ^{1}H-^{13}C HETCOR NMR spectrum provided compelling evidence for the conversion of the alkylidene to both trigonal bipyramidal and square planar isomers of the metallacyclobutane complex [[W(CH$_2$CH$_2$CH$_2$)(≡NAr)(2,5-Me$_2$NC$_4$H$_2$)(OSIL)], as well as the parent methylidene complex. This in situ steady state experiment provided rich detail about the component of the catalytic cycle due to the closeness in stability of the key intermediates.

The next stage up from an ex situ reaction is a sealed tube within the MAS rotor. An example of this is provided by the study of methane activation by a zinc modified H-MFI zeolite [50]. New bands were observed in the ^{1}H and ^{13}C spectra that demonstrated the formation of methyl-zinc reaction centres. However, there are limitations to this approach and moving towards in situ catalytic reactors was an important step. Also, there are difficulties to be overcome linking fixed reagent lines into a cell rotating at several kHz at the magic angle in an NMR magnet. One approach was to replace the rotation by a series of 120° hops [51], and this has been used to track the formation of polyethene on a supported polymerisation catalyst made from cp$_2$ZrCl$_2$/MAO/SiO$_2$. Spectra were recorded in 30 min over a time period of 32 h.

At a similar time, an in situ methodology linking MAS NMR with on-line gas analysis was also reported [52, 53]. Although the applications have substantially been on solid acid catalysis, a combination of in situ techniques has been developed (IR, NMR, EPR) which are very applicable to heterogenised catalysts [54, 55]. One variant combined uv-visible spectroscopy with continuous flow MAS NMR to identify carbenium ions on a H-ZSM-5 zeolite sample [56], but could equally be applied to supported coordination compounds. Time resolution has been included by stopped-flow addition of liquid reagents (steps of 18 min) [57] or by periods of laser heating (60 s) [58]. A new approach to improving time resolution has been to link laser-hyperpolarised ^{129}Xe with ^{13}C NMR [59]. The xenon spectra could be

acquired in ~10 s during the adsorption of methanol on the H-CHA zeolite, and from this the kinetics of methanol adsorption could be measured. This timescale is of considerable interest for catalytic science.

Magnetic resonance imaging techniques can also be applied to in situ catalysis studies providing spatial resolution in the region of ~250–500 μm. Examples include monitoring the isomerisation and hydrogenation of oct-1-ene by ^{13}C DEPT within a trickle-bed reactor containing 1% Pd/Al_2O_3 [60]. In this way a chemical mapping of the reactor was achieved at different flow rates. An alkene (methylstyrene) hydrogenation catalysed by $Pd/Mn/Al_2O_3$ has also been monitored by ^{1}H NMR on both single pellet and multi-pellet reactors. Chemical speciation could show that hydrogenation was complete before the end of the reaction bed. Multinuclear MRI can also be used to probe the elements of the catalyst itself [61]. Examples included and alumina monolith (^{27}Al NMR) and phosphate promoted $Co\text{-}Mo/Al_2O_3$ hydrodesulfurisation catalysts (^{31}P NMR of the impregnated and dried pellets) [62]. These examples show that this technique too has applicability to heterogenised metal catalysts.

13.3 National Facility Spectroscopies

13.3.1 X-Ray Absorption Fine Structure (XAFS) Spectroscopies

13.3.1.1 General

As the name already indicates, x-ray absorption fine structure spectroscopy (XAFS) is a characterisation technique which provides materials properties by measuring the absorption of x-rays of the material as a function of x-ray energy [63]. By increasing the energy the penetration depth of x-rays through electron clouds and materials increases. The absorption of x-rays increases significantly at energies which correlate to the ionisation energies of core electrons (Fig. 13.1), i.e. the so-called absorption edges which are thus element specific. Figure 13.1 shows a typical XAS spectrum.

At x-ray energies around the absorption edge, up to about 50 eV above, the excited photoelectron is able to occupy valence orbitals i.e. the lowest unoccupied molecular orbitals (LUMOs). This part of the spectrum is called the x-ray absorption near edge structure (XANES) and is very sensitive to the electronic properties and geometry of the central atom under investigation. As any spectroscopy technique, dipole transitions dominate the spectrum. Electronic properties like the effective oxidation state of and charge transfer effects within the sample are reflected in the position of the absorption edge as well as possible pre-edge features present. The absence or presence of pre-edge features is indicative of the geometry of the material or molecule. An increased energy resolution of the XANES region as can be achieved by emission techniques in addition the absorption, i.e. high energy resolution fluorescence detection (HERFD) XAS, sharpening all features as displayed in Fig. 13.2 [64, 65].

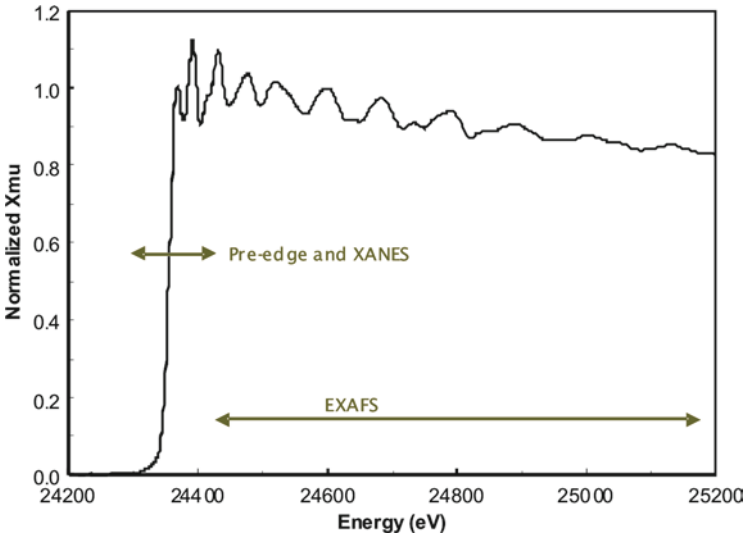

Fig. 13.1 Pd K edge XAS spectrum of a Pd foil

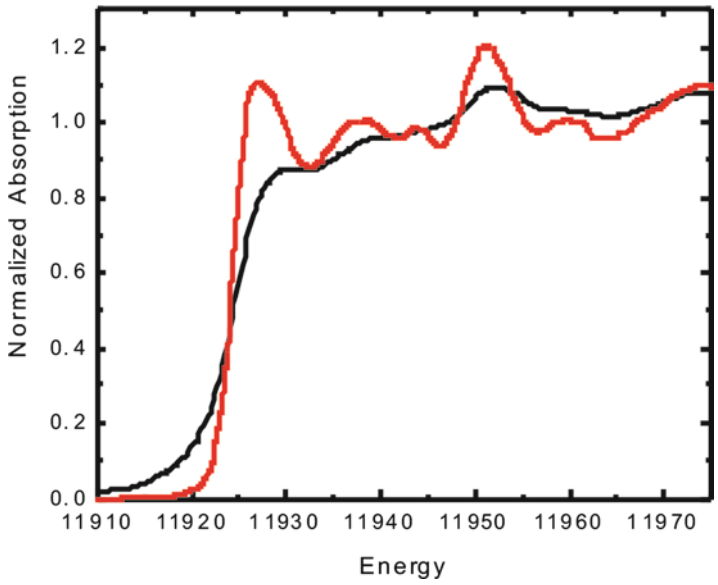

Fig. 13.2 Au L_3 edge XANES spectrum obtained in transmission (*solid black line*) and HERFD mode (*red line*) (Reprinted with permission from [65])

The XAS spectrum displays the absorption probability as a function of energy. The excited photoelectron can be considered a wave; at higher x-ray energies the photoelectron is given extra energy to travel through the material and interact with neighbouring atoms. The total sum of outgoing and backscattered waves gives the

extended x-ray absorption fine structure (EXAFS). Constructive, in-phase, interference of waves increases the overall signal while destructive, out-of-phase, waves lower or diminish the total scattering pattern observed. The specific shape of the wavefunctions, i.e. backscattering amplitudes, is characteristic of the atomic number and can thus be used to identify the neighbouring atoms. The exact frequency of the wave is roughly determined by the distance between central (absorber) atom and scatterer, whereas the intensity is determined by the number of neighbouring atoms and the static and thermal disorder. EXAFS can thus provide detailed structural information of the material under investigation.

The main advantageous of XAS as a characterisation technique is that the techniques does not require long range ordering of the material and can thus be applied to amorphous systems and solutions, including supported organometallic species. Moreover, XAS can be applied in situ or operando, at real process conditions, and in a time-resolved manner [66]. The main disadvantage of XAS as a characterisation techniques is that it probes and average of all structures present in the system under investigation, which can severely complicate the analysis. Therefore, often additional techniques are applied simultaneously with XAS to provide complementary information on the system and thus facilitate the data analysis. At the same time, new developments are underway, again based on emission techniques as mentioned with HERFD, which promise selective EXAFS, e.g. spin-selective, oxidation state selective, in the near future [67–69].

The standard XAS data acquisition method is based on a double crystal monochromator selecting the required x-ray energies from a white synchrotron light source by rotating the two crystals (Braggs Law). The absorption of the sample is measured as a function of energy in either transmission, using ionisation chambers, or fluorescence, using a fluorescence detector. The acquisition time for a full EXAFS spectrum is from minutes to hours, depending on the type of element (and thus x-ray energies) and concentration. Whereas higher concentrated samples are best measured in transmission, low concentrated samples require fluorescence or electron yield detection methods, the latter being very surface sensitive. Developments in monochromators, increasing the scanning rate of the monochromator and associated mechanics now allow spectral acquisition times to go down to milliseconds under favourable circumstances [70]. This acquisition is generally called Quick EXAFS (QEXAFS).

Another method to increase the time resolution of XAS data acquisition is based on energy dispersive optics, i.e. ED-XAS, EDE or DEXAFS. In this case a curved crystal (in either Bragg of Laue geometry) focuses all energies in a small spot on the sample. A position sensitive detector placed behind the sample (transmission mode) enable a full EXAFS spectrum to be obtained in one shot, thereby decreasing the data acquisition times to milliseconds [66, 71].

13.3.1.2 Organometallic Systems

XAS studies have been applied to organometallic systems for several years now, although not in abundance. This has likely to do with the unfamiliarity of the

technique in the field as well as the complicated data-analysis of the compounds, which often display anti-phase behaviour of individual wavefunctions thereby diminishing the total EXAFS obtained [72]. Careful analysis can however result in reliable results and electronic and structural information important for catalysis can be obtained.

In homogeneous catalysis often the structure of the catalyst as obtained with single crystal x-ray diffraction is taken as a start for explaining reaction mechanisms. The problem however, is that the crystal structure is not necessarily the structure of the homogeneous catalyst in its active medium, i.e. solution. This has been clearly demonstrated for bidentate diphosphine Pd systems with a coordinated allyl moiety [73]. Whereas the increase in allylic substitution selectivity as a function of P-Pd-P bite angle was always addressed to differences in electronic and steric properties of the allylic moiety, EXAFS results in solution demonstrated that in fact the coordination of the allylic moiety in solution was not always the same as in the crystal structure and for small bite angle the unsubstituted site of the allyl can bend away from the Pd hence making it both electronically and sterically more favourable to attack.

An in situ study of hydroformylation in supercritical CO_2 has shown that very dilute systems can be investigated with Third Generation beamlines (ID26 of the ESRF) [22] . This study by Rh K-edge XAFS showed that Rh oligomers were present unless the added phosphine, PEt_3, was in excess. Investigating realistic concentrations for active catalysts can be very import. For example, studies on the Herrmann palladacycle for the catalysis of the Heck reaction at concentrations between 50 and 5,000 ppm demonstrated the likely existence of a monomer-dimer equilibrium [74].

To obtain more insights in catalyst properties, characterise reaction intermediates and derive structure–performance relationships as well as reaction mechanisms, homogeneous as well as heterogeneous catalysts have been studied using time-resolved spectroscopy with either QEXAFS or EDE.

The aforementioned (PP)Pd(X) catalysts have been studied for their deactivation using a combined EDE and UV-Vis using stopped flow methods of rapid mixing [75]. The formation of Pd dimers, trimers and colloidal particles could be observed by the increase in PdPd coordination number in EXAFS, with the disappearance of PdP and PdC contributions. At the same time dimers, trimers and colloidal were identified with UV-Visible spectroscopy, nicely correlating with the EDE results. Similar studies were performed for Cu catalysed CN bond formation [76] and activation of alkene oligomerisation catalysis of nickel by aluminium alkyl promoters [23], and important and new insights in reaction intermediates have been obtained.

Although EDE is easier to apply in homogeneous solution because of the small beamsize of the EDE beam, significant developments have been done over the last 10 years for heterogeneous catalysis. By carefully packing a sample bed, reliable EDE spectra can be obtained. The initial EDE studies were performed using a microreactor system studying three way catalytic systems, mainly Rh supported nanoparticles for their reactivity in CO and NO type reactions. In a further step a set-up was developed combining in situ EDE measurements with DRIFTS. The Rh supported systems investigated with this combined approach have recently been

extensively described [37, 77–79] and reviewed by us [20, 80]. Whereas the EDE gives very detailed information on the changing Rh sites and particles sizes, the DRIFTS provides information from the side of the adsorbing species, i.e. NO or CO. The combination provides a detailed image of the changing metal-adsorbate sites upon changing environment, whereas simultaneously applied mass spectrometry gives kinetic catalysis information at the same time.

All these examples indicate that also surface organometallic species can be addressed well using XAS techniques. Indeed ex situ XAFS measurements were carried out on supported samples already mentioned in relation with other techniques, including $[M_3H(O\text{-}SIL)(CO)_{10}]$, M = Ru [31] and Os [81], $[Ru_3H_2(\mu_3\text{-}PCH_2CH_2SIL)(CO)_9]$ [44] and $HZr(O\text{-}SIL)_3$ [33]. This provided additional evidence to the vibrational and NMR evidence obtained, in particular about the presence of metal–metal bonds and the local coordination sites. When the supported complexes are in the form of rigid clusters, then back-scattering from longer ranges is possible and this can provide good evidence for the shape of the cluster complex, as in the case for polyoxometalates supported on hydrotalcite clays [82].

So far all experiments have been done using normal scanning XAS, mostly because many of the supported organometallic systems have relatively low concentrations of metal which require relatively long XAS data acquisition times. At the same time, as with the unsupported complexes, high quality EXAFS data is required to be able to perform a reliable EXAFS analysis. Several examples of supported organometallic systems have been reported in literature and a few examples are described here.

The heterogenisation of tripodal polyphosphine Rh catalysts was studied using a combination of techniques, i.e. IR, Rh K-edge EXAFS, and CP MAS ^{31}P NMR studies. The metal products after hydrogenation of ethene and propene were studied by EXAFS. No evidence of the formation of Rh-Rh sites or the loss of tripodal ligand was found, indicating that the catalytic active sites are isolated Rh atoms and remained so during and after catalysis, as in homogeneous phase [83]. This study included an in situ aspect using an intense source on an insertion device beamline (ID26 of the ESRF).

Several supported organometallic complexes have been studies with EXAFS by the Basset and Copéret groups. In a full study of oxide supported alkene polymerisation catalysts prepared from cyclopentadienyl zirconium alkyl complexes [84], XAFS and solid state NMR were combined to identify the surface species formed from $[(C_5Me_5)Zr(CH_3)_3]$ and alumina (pretreated at 500°C). EXAFS analysis provided evidence for an oxide supported $[Zr(C_5Me_5)(CH_3)_2(O\text{-})]$ unit and underlying aluminium atoms from the alumina surface, suggesting a high degree of uniformity of the attachment site. Similar protonolysis of M–C bonds was also demonstrated for the alkane metathesis catalysts derived from $[Ta(=CHBu^t)(CH_2Bu^t)_3]$ (**8**) and $[(C_5Me_5)Ta(CH_3)_4]$ on silica [85]. Again, solid-state NMR was very informative at identifying the organometallic ligand types, with Ta L(III) EXAFS analysis providing information about the surface attachment site via the Ta-O and Ta…Si distances.

When the organic ligands have been stripped away, for example, after hydrogenation of the grafted version of (**8**) to yield $[Ta(H)(O\text{-}SIL)_3]$ (**9**), then solid state NMR, IR and XAFS can still be combined to good effect [86]. Hydrogenation is

shown to afford an isolated Ta(III) centre, without reduction to the metal. These electrophilic centres activate the C–H bonds of saturated alkanes, including the hydrogenolysis of cycloalkanes. XAFS and NMR studies showed that (**9**) and cyclopentane, first generated a surface pentyl group replacing the hydride, but at higher temperatures, this underwent a dehydrogenation reaction to create a new cyclopentadienyl centre [87].

Recently a new grated ruthenium hydride has been reported, which required prefunctionalising a silica surface provide $SiHMe_2$(O-SIL) sites [88]. Reaction of [Ru(1,5-C_8H_{12})(1,3,5-C_8H_{10})] under H_2 with this centre affords a low coordinate Rh-H site, which has been shown to be stabilised by Ru–Si and Ru–O bonds by Ru K-edge EXAFS analysis. This grafted coordination complex requires the Si-H site; without it metallic ruthenium is created with different catalytic properties for alkene hydrogenation.

13.4 Concluding Comments

The set of spectroscopic characterisation techniques as described here, i.e. (i) IR, (ii) NMR, and (iii) XAS, are a well placed combination of complementary methods providing (i) information on the support used (e.g. surface groups present) and on ligands and reactants attached to either the catalyst metal centre or support providing information on the anchoring of the organometallic complex to the support and reaction intermediates formed respectively, (ii) information on the anchoring of complexes on the surface as well as formation of different reaction intermediates and products, (iii) structural and electronic properties of the metal site. The information from different sides of the total supported catalyst system enables one to build up a complete picture of the catalyst and its reactivity before, during and after its performance, insights which help to design and optimise catalysts. Strength and limitations of all techniques are described. The time-resolution currently feasible is different for all techniques. NMR cannot be performed in subseconds or below, whereas with the right light source femtosecond IR or XAS might be achievable. In practice however, studying real catalytic systems under processing conditions, identifying reaction intermediates, is practically limited to milliseconds by the diffusion of reactants and products to and from the catalytically active sites and support and requires computational modelling for further insights.

References

1. Anderson JR (1975) Structure of metal catalysts. Academic, New York
2. Hacquart R, Jupille J (2009) J Cryst Growth 311:4598–4604
3. Testino A, Bellobono IR, Buscaglia V, Canevali C, D'Arienzo M, Polizzi S, Scotti R, Morazzoni F (2007) J Am Chem. Soc 129:3564–3575
4. Gao Y, Elder SA (2000) Mater Lett 44:228–232

5. (a) Sindorf DW, Maciel, GE (1983) J Am Chem Soc 105:1487; (b) (1983) J Phys Chem 87:5576
6. Carneiro JT, Savenije TJ, Moulijn JA, Mul G (2010) J Phys Chem C 114:327–332
7. Tüysüz H, Lehmann CW, Bongard H, Tesche B, Schmidt R, Schüth F (2008) J Am Chem Soc 130:11510–11517
8. Nandi M, Sarkar M, Sarkar K, Bhaumik A (2009) J Phys Chem C 113:6839–6844
9. Kuschel A, Sievers H, Polarz S (2008) Angew Chem Int Ed 47:9513–9517
10. Barrer RM Zeolite synthesis: an overview, pp 221–244 in ref 11
11. Basset JM, Gates BC, Candy J-P, Choplin A, Leconte M, Grignard F, Santini C (1988) Surface organometallic chemistry: molecular approaches to surface catalysis, NATO ASI Series C231. Kluwer, Dordrecht
12. Rabo JA, New directions in molecular sieve science and technology, pp 245–270 in ref 11
13. Sun JL, Bonneau C, Cantin A, Corma A, Diaz-Cabanas MJ, Moliner M, Zhang DL, Li MR, Zou XD (2009) Nature 458:1154–U90
14. Corma A, Diaz-Cabanas M, Martinez-Triguero J, Rey F, Ruis J (2002) Nature 418:514–517
15. Corma A, Fornes V, Diaz U (2001) Chem Comm 2642–2643
16. Castaldi P, Santona L, Enzo S, Melis P (2008) J Hazard Mater 156:428–434
17. Martinez-Inesta MAM, Lobo RF (2007) J Phys Chem C 111:8573–8579
18. Evans J (1981) Chem Soc Rev 10:159–180
19. Hannemann S, Grunwald JD, van Vetgen N, Baiker A, Boye P, Schroer AG (2007) Catal Today 126:54–63
20. Evans J, Tromp M (2008) J Phys Condens Matter 20:184020
21. Sellin MF, Bach I, Webster JF, Montilla F, Rosa V, Avilés T, Poliakoff M, Cole-Hamilton DJ (2002) Dalton Trans 4569–4576
22. Fiddy SG, Evans J, Neisius T, Sun X-Z, Jie Z, George MF (2004) Chem Comm 676–677
23. Abdul Rahman MBB, Bolton PR, Evans J, Dent AJ, Harvey I, Diaz-Moreno S (2002) Faraday Discuss 122:211–222
24. Yang AC, Garland CW (1957) J Phys Chem 61:1504–1512
25. Eischens RP, Francis SA, Pliskin WA (1956) J Phys Chem 60:194–201
26. (1985) J Am Chem Soc 107:3139–3147
27. Brown SC, Evans J (1978) Chem Comm:1063–1064
28. Brown SC, Evans J (1981) J Mol Catal 11:143–149
29. Besson B, Morawek B, Smith AK, Basset JM, Psaro R, Fusi, A, Ugo R (1980) Chem Comm :569–571
30. Dornelas L, Choplin A, Basset JM, Hsu LY, Shore S (1985) New J Chem 9:155–157
31. Theolier A, Choplin A, Dornelas L, Basset JM, Zanderighi G, Sourisseau C (1983) Polyhedron 2:119–121
32. Alexiev VD, Binsted N, Evans J, Greaves GN, Price RJ (1987) Chem Commun 6:395–397
33. Corker J, Lefebvre F, Lécuyer C, Dufaud V, Quignard F, Choplin A, Evans J, Basset JM (1996) Science 271:966–969
34. Evans J, McNulty GS (1984) Dalton Trans 587–594
35. Meunier FC, Goguet A, Shekhtman S, Rooney D, Daly H (2008) Appl Catal A 340:196–202
36. Newton MA, Jyoti B, Dent AJ, Fiddy SG, Evans J (2004) Chem Comm :2382–2382
37. Dent AJ, Evans J, Fiddy SG, Jyoti B, Newton MA, Tromp M (2007) Angew Chem Int Ed 46:5356–5358
38. Thibault-Starzyk F, Vimont A, Fernandez C, Gilson JP (2000) Chem Commun 1003–1004
39. Thibault-Satzyk F, Vimont A, Gilson JP (2001) Catal Today 70:22–241
40. Gallas JP, Goupil JM, Vimon A, Lavalley JC, Gil B, Gilson JP, Miserque O (2009) Lngmuir 25:5825–5834
41. Chenevarin S, Thibault-Satzyk F (2004) Angew Chem 43:1155–1158
42. Butler JM, George MW, Schoonover JR, Dattelbaum DM, Meyer TJ (2007) Coord Chem Rev 251:492–514
43. Backus EHG, Eichler A, Kleyn AW, Bonn M (2005) Science 310:1790–1793

44. Alexiev VD, Binsted N, Cook SL, Evans J, Price RJ, Clayden NJ, Dobson CM, Smith DJ, Greaves GN (1988) Dalton Trans 2649–2654
45. Alexiev VD, Clayden NJ, Cook SL, Dobson CM, Evans J, Smith DJ (1986) Chem Commun 12:938–941
46. Wiench JW, Michon C, Ellern A, Hazendonk P, Iuga A, Angelici RJ, Pruski M (2009) J Am Chem Soc 131:11801–11810
47. Rendón N, Berthoud R, Blanc F, Gajan D, Maishal T, Basset JM, Coperét C, Lesage A, Emsley L, Marinescu SC, Singh R, Schrock RR (2009) Chem Eur J 15:5083–5089
48. Blanc F, Basset JM, Coperét C, Sinha A, Tonzetich ZJ, Schrock RR, Solans-Monfort X, Clot E, Eisenstein O, Lesage A, Emsley L (2008) J Am Chem Soc 130:5886–5900
49. Blanc F, Berthoud R, Coperét C, Lesage A, Emsley L, Singh R, Kreickmann T, Schrock RR (2008) Proc Natl Acad Sci USA 105:12123–12127
50. Kolyagin YG, Ivanova II, Ordomsky VV, Gedeon A, Pirogov YA (2008) J Phys Chem 112:20065–20069
51. Keeler C, Xiong J, Lock H, Dec S, Tao T, Maciel GE (1999) Catal Today 49:377–383
52. Hunger M, Seiler M, Horvath T (1999) Catal Lett 57:199–204
53. Haw JF (1999) Topics Catal 8:81–86
54. Hunger M, Weitkamp J (2001) Angew Chem Int Ed 40:2954–2971
55. Hunger M (2008) Progr NMR Spectrosc 53:105–127
56. Hunger M, Wang W (2004) Chem Commun:584–585
57. Wang W, Xu M, Buchholz A, Arnold A, Hunger M (2003) Magn Reson Imaging 21:329–332
58. Mildner T, Ernst H, Freude D, Kärger WU (1999) Magn Reson Chem 37:S38–S42
59. Xu S, Zhang W, Liu X, Han X, Bao X (2009) J Am Chem Soc 131:13722–13727
60. Sederman AJ, Mantle MD, Dunckley CP, Huang Z, Gladden LF (2005) Catal Lett 103:1–8
61. Koptyug IV, Lysov AA, Kulikov AV, Kirillov VA, Parmon VN, Sagdeev RZ (2004) Appl Catal A 267:143–148
62. Koptyug IV, Lysova AA, Sagdeev RZ, Parmon VN (2007) Catal Today 126:37–43
63. Koningsberger DC, Prins R (eds) (1988) X-ray absorption, principles, applications, techniques of EXAFS, SEXAFS and XANES. Wiley Interscience, New York
64. Safonova OV, Trmp M, van Bokhoven JA, de Groot FMF, Evans J, Glatzel P (2006) J Phys Chem B 110:16162–16164
65. van Bokhoven JA, Louis C, Miller JT, Tromp M, Safonova OV, Glatzel P (2006) Angew Chem Int Ed 45:4651–4654
66. Newton MA, Dent AJ, Evans J (2002) Chem Soc Rev 31:83–95
67. de Groot F (2001) Chem Rev 101:1779–1808
68. de Groot F (2005) Coord Chem Rev 249:31–63
69. Glatzel P, Bergmann U (2005) Coord Chem Rev 249:65–95
70. Stötzel J, Lutzenkirchen-Hecht D, Fonda E, De Oliveira N, Briois V, Frahm R (2008) Rev Sci Instrum 79:083107
71. Matsushita T (1981) Phizackerley. Jpn J Appl Phys 20:2223–2228
72. Tromp M, van Bokhoven JA, Arink AM, Bitter JH, van Koten G, Koningsberger DC (2002) Chem Eur J 8:5667–5678
73. Tromp M, van Bokhoven JA, van Strijdonck GPF, van Leeuwen PWNM, Koningsberger DC, Ramaker DE (2005) J Am Chem Soc 127:777–789
74. Fiddy SG, Evans J, Newton MA, Neisius T, Tooze RP, Oldman R (2003) Chem Commun 2682–2683
75. Tromp M, Sietsma JRA, van Bokhoven JA, van Strijdonck GPF, van Haaren RJ, van de Eerden AMJ, van Leeuwen PWNM, Koningsberger DC (2003) Chem Comm 128–129
76. Tromp M, van Berkel SS, van de Hoogenband A, Feiters MC, de Bruin B, Fiddy SG, van Bokhoven JA, van Leeuwen PWNM, Koningsberger DC (2010) Organometallics, DOI:10.1021/om9010643
77. Newton MA, Dent AJ, Jyoti FSG, (2007) Catal Today 126:64–72
78. Newton MA, Dent AJ, Fiddy SG, Jyoti B, Evans J (2007) J Mater Sci 42:3288–3298

79. Dent AJ, Evans J, Fiddy SG, Jyoti B, Newton MA, Tromp M (2008) Faraday Discuss 138:287–300
80. Evans J, Puig-Molina A, Tromp M (2007) MRS Bull 32:1038–1043
81. Cook SL, Evans J, Greaves GN (1983) Chem Commun:1287–1289
82. Evans J, Pillinger M, Zhang JJ (1996) Dalton Trans 2963–2974
83. Bianchini C, Burnaby DG, Evans J, Frediani P, Meli A, Oberhauser W, Psaro R, Sordelli L, Vizza F (1999) J Am Chem Soc 121:5961–597
84. Jezequel M, Dufaud V, Ruiz-Garcia MJ, Carrillo-Hermosilla F, Neugebauer U, Niccolai GP, Lefebvre F, Bayard F, Corker J, Fiddy S, Evans J, Broyer JP, Malinge J, Basset JM (2001) J Am Chem Soc 123:3520–3540
85. Le Roux E, Chabanas M, Baudouin A, de Mallmann A, Coperét C, Quadrelli EA, Thivolle-Cazat J, Basset JM, Lukens W, Lesage A, Emsley L (2004) Sunley GJ 126:13391–13399
86. Vidal V, Théolier T-C, Basset JM, Corker J (1996) J Am Chem Soc 118:4595–4602
87. Rataboul F, Chabanas M, de Mallmann A, Coperét C, Thivolle-Cazat J, Basset JM (2003) Chem Eur J 9:1426–1434
88. Berthoud A, Baudouin A, Fenet B, Lukens W, Pelzer K, Basset JM, Candy JP (2008) Coperét C 14:3523–3526

Index